TSINGHUA-PRINCETON-COMBUSTION INSTITUTE

2023 SUMMER SCHOOL ON COMBUSTION

Combustion Chemistry

Michael Pilling
University of Leeds
July 10−14, 2023

Combustion Chemistry

Michael Pilling

University of Leeds

July 10-14, 2023

Tsinghua-Princeton-Combustion Institute

2023 Summer School on Combustion

Contents

Leeds

Combustion Chemistry

Michael J Pilling, University of Leeds, UK

Tsinghua- Princeton- Combustion Institute

2023 Summer School On Combustion

July 10-14, 2023

UNIVERSITY OF LEEDS

Background 1

- Combustion involves the oxidation of a fuel, ideally leading, for an organic fuel such as octane or ethanol, to the formation of carbon dioxide and water, with the release of heat.

- The overall chemical equation, e.g.

  $$C_2H_5OH + 3O_2 \rightarrow 2CO_2 + 3H_2O$$

  does not describe the detailed way in which the reaction occurs.

- Instead the reaction involves a sequence of <u>elementary</u>, or single step reactions, many of which involve <u>atoms</u> or <u>radicals,</u> which are short-lived species with high reaction rates.

Background 2

This series of lectures examines how the rates of these elementary reactions can be determined experimentally and understood and calculated theoretically; how chemical mechanisms describing the overall sequence of reactions can be constructed and then used to model the chemistry of combustion systems.

Reaction kinetics contributions to combustion models

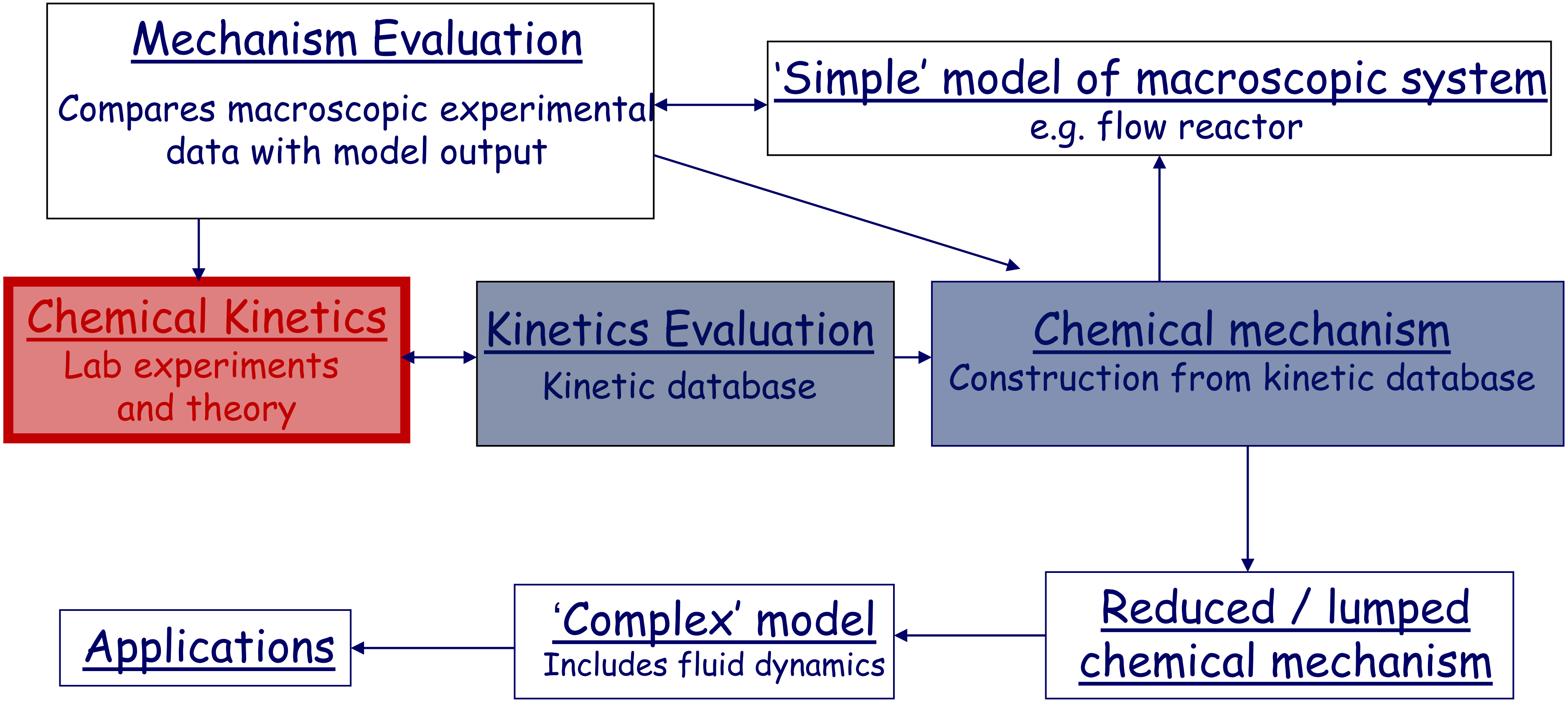

Mechanism Evaluation

Compares macroscopic experimental data with model output

'Simple' model of macroscopic system

e.g. flow reactor

Chemical Kinetics

Lab experiments and theory

Kinetics Evaluation

Kinetic database

Chemical mechanism

Construction from kinetic database

Reduced / lumped chemical mechanism

'Complex' model

Includes fluid dynamics

Applications

Understanding

Similar approaches in atmospheric chemistry, interstellar chemistry.

A similar view
Curran, Proc Comb Inst, 2019, 37, 57

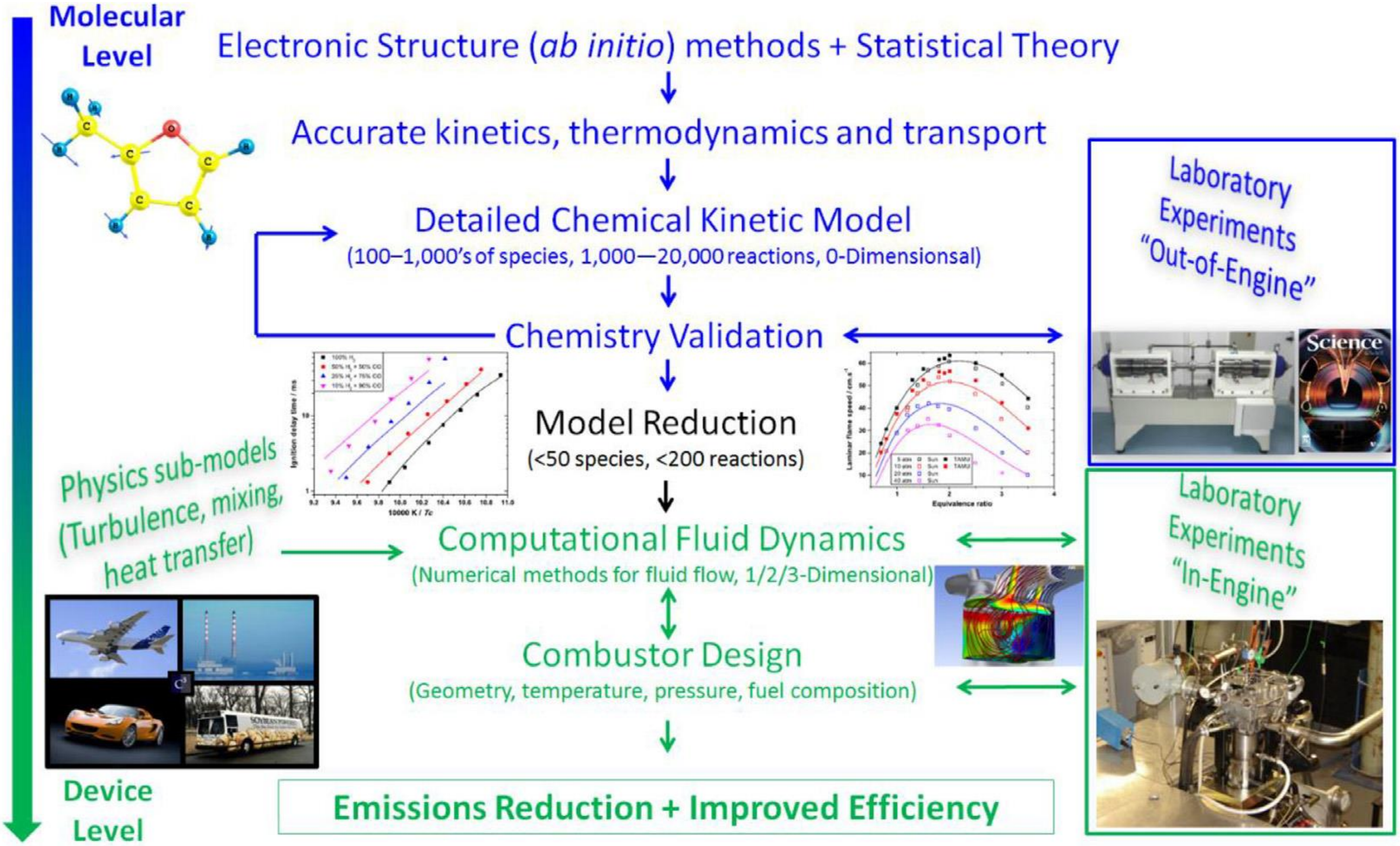

Molecular Level

Electronic Structure (*ab initio*) methods + Statistical Theory

↓

Accurate kinetics, thermodynamics and transport

↓

Detailed Chemical Kinetic Model

(100–1,000's of species, 1,000—20,000 reactions, 0-Dimensionsal)

↓

Chemistry Validation

↓

Model Reduction

(<50 species, <200 reactions)

↓

Computational Fluid Dynamics

(Numerical methods for fluid flow, 1/2/3-Dimensional)

↕

Combustor Design

(Geometry, temperature, pressure, fuel composition)

↓

Emissions Reduction + Improved Efficiency

Physics sub-models (Turbulence, mixing, heat transfer)

Laboratory Experiments "Out-of-Engine"

Laboratory Experiments "In-Engine"

Device Level

Lecture Synopsis

- Background material
  - Chemical mechanisms. Chemical Kinetics. Thermodynamics, Statistical Mechanics, Quantum Theory and Electronic Structure Calculations.
- Experimental methods
  - Pulsed photolysis, shock tubes, flow and static methods. Detection techniques
- Theoretical methods
  - Transition state theory. Microcanonical and canonical systems. Bimolecular and Unimolecular Reactions. Master equation methods
- Kinetic and Thermodynamic databases
- Constructing chemical mechanisms
- A couple of examples
  - Autoignition
  - Soot formation

An example – $H_2 + O_2$ and some definitions

The overall reaction is: $2H_2 + O_2 \rightarrow 2H_2O$

A minimal set of the component elementary reactions is:

1. $H_2 + O_2 \rightarrow H + HO_2$
2. $H + O_2 \rightarrow OH + O$
3. $O + H_2 \rightarrow OH + H$
4. $OH + H_2 \rightarrow H + H_2O$
5. $H + O_2 + M \rightarrow HO_2 + M$
6. H, O, OH → wall
7. $HO_2 + HO_2 \rightarrow H_2O_2 + O_2$

- An elementary reaction is a single step reaction (although we will discuss some issues related to this definition later).
- A complex reaction, such as the $2H_2 + O_2$ reaction, is made of several elementary reactions.
- The set of elementary reactions is called the mechanism of the overall reaction

What do we need to know about these reactions?

- What are the reactants and what are the products? There may be more than one set of products and we need to know the yields of each set. E.g.

  $H + O_2 \rightarrow OH + O$

  $H + O_2 (+ M) \rightarrow HO_2 (+ M)$

- How quickly do the reactions occur? This is described in the rate equation and depends on the concentrations of the species involved and the rate constant. What is M? Pressure dependent reactions.

- What is the enthalpy change of reaction? How much heat is released, or consumed, when the reaction occurs. Heat release is central to combustion.

- The ratio of the rate constants for the forward and reverse reaction (e.g. $H + O_2 \rightarrow OH + O$ and $OH + O \rightarrow H + O_2$) is determined by the equilibrium constant which is related to the Gibbs energy of reaction

Rates of elementary reactions

- The rate of each elementary reaction is determined by the reactant concentrations and the rate coefficient, *k*. *k* depends on *T* and, in some cases, *p*.

  We also need to know the products of the reaction, which in some cases aren't clear.

- Example: $OH + CH_4 \rightarrow H_2O + CH_3$;
- Rate of this reaction =

  $-d[OH]/dt = k[OH][CH_4] = d[H_2O]/dt = d[CH_3]/dt = - d[CH_4]/dt$

- *k* depends on temperature and this is usually expressed in Arrhenius form:

$$k = A\exp(-E_a/RT)$$

or modified Arrhenius form:

$$k = AT^n\exp(-E_a/RT)$$

A is the *A* factor, E_a the activation energy, *n* the temperature exponent and R the gas constant.

- One aim of experimental and theoretical studies of elementary reactions is to determine A, E_a, n

Why does the rate constant depend on temperature? The idea of the transition state

- As OH approaches CH_4, one of the C-H bonds extends and electron density moves from that C-H bond into the newly forming O-H bond. This involves an increase in potential energy.

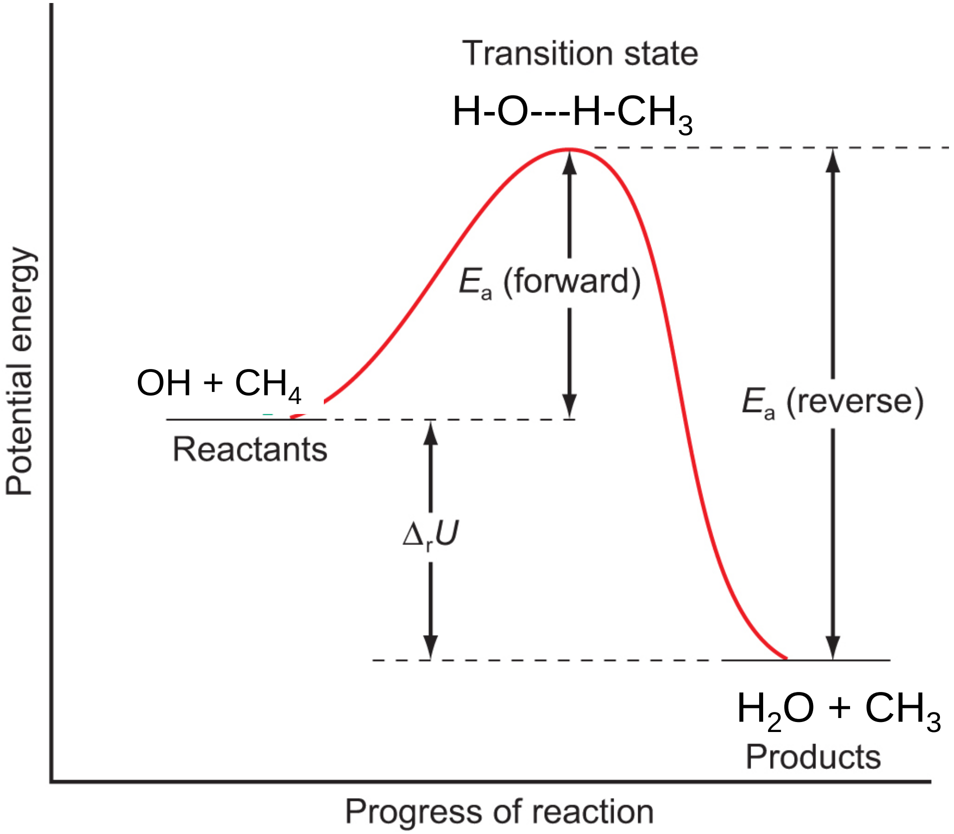

- We need the rate constant and its dependence on *T*:

Kinetics: Experiment, Theory

- We need to be able to incorporate these data in combustion models

Mechanism development:*

- We need some basic understanding of physics and chemistry:

thermodynamics, kinetics, quantum mechanics, statistical mechanics

For a discussion of many of these topics, see Atkins and de Paula, *Physical Chemistry*

* Note that we use the word mechanism in two different ways:

(i) to describe the way in which an elementary reaction occurs

(ii) to describe the chemical mechanism of a complex reaction – the list of component chemical reactions

Basics of chemical kinetics
Definitions

- **Order of reaction** is equal to the exponent of the reactant concentration in the rate equation. For an elementary reaction, this is equal to the stoichiometric number (ν_i) for the reactants in the rate equation e.g.:
  - $O + H_2 \rightarrow H + O_2$, rate = $k[O][H_2]$. Order with respect to O is one, order with respect to H_2 is one, overall order is two.
  - $2CH_3 \rightarrow C_2H_6$, rate = $k[CH_3]^2$. Order with respect to CH_3 is two. Overall order is two.
- **Molecularity** is the number of species involved in forming the transition state e.g.
  - $OH + CH_4 \rightarrow H_2O + CH_3$. Two species involved in forming transition state: bimolecular reaction.
  - $C_2H_6 \rightarrow 2CH_3$. One species involved in forming the transition state: unimolecular reaction.

Relationship between forward and reverse rate coefficients

$$K = \frac{\prod_{products}(a_i^{\nu_i})}{\prod_{reactants}(a_i^{\nu_i})}$$

a is the *activity*. For ideal systems, $a = p/p^{\ominus} = c/c^{\ominus}$ so that K is dimensionless. Other definitions of equilibrium constants are:

$$K_c = \frac{\prod_{products}(c_i^{\nu_i})}{\prod_{reactants}(c_i^{\nu_i})} \qquad K_p = \frac{\prod_{products}(p_i^{\nu_i})}{\prod_{reactants}(p_i^{\nu_i})}$$

These have dimensions if $(\Sigma\nu_i)_{reactants} \neq (\Sigma\nu_i)_{products}$

At equilibrium, forward rate = reverse rate:

$$k_f \prod_{\text{reactants}} (c_i^{\nu_i}) = k_r \prod_{\text{products}} (c_i^{\nu_i}) \qquad \frac{k_f}{k_r} = K_c$$

Detailed balance

Use of thermodynamic databases

Thermodynamic relations: a reminder
1. The Laws of Thermodynamics

- First Law of Thermodynamics:
  The energy, *U*, of an isolated system is constant

$$dU = dq + dw$$

where q is heat absorbed by system and w is work done on system

$$H = U + pV$$

H is enthalpy , p pressure and V volume

- Second Law of Thermodynamics:
  No process is possible in which the sole result is the absorption of heat from a reservoir and its complete conversion into work

$$\mathrm{d}S \geq \frac{\mathrm{d}q}{T}$$

S is the entropy

- Third Law of Thermodynamics:
  The entropy of all perfectly crystalline substances at zero Kelvin is zero.

$$S = 0 \text{ at } T = 0$$

Thermodynamic relations

2. Gibbs Energy

Gibbs energy, *G*:
$$G = H - TS$$

At constant *T*, the change in Gibbs energy, ΔG is given by:

$$\Delta G = \Delta H - T\Delta S$$

Equilibrium occurs at minimum G (at constant T,P)

and the equilibrium constant, *K*, is related to ΔG by:

Note the standard sign

$$\Delta G^{\ominus} = -RT\ln K$$

The equilibrium constant, *K*, can be calculated from tabulated or calculated values of the standard enthalpy *H* and entropy *S*, and hence the reverse rate coefficient(say) determined from the forward rate coefficient and *K*. (The $^{\ominus}$ sign refers to the standard state)

Later in this lecture we will discuss how thermodynamic quantities can be calculated using statistical mechanics. In a later lecture we will discuss tabulations of thermodynamic data that are widely used in combustion.

Thermodynamic relations 3
Heat capacity

- As we shall see, enthalpies of formation are tabulated at 298 K. For combustion applications, we need to be able to determine values at higher *T*.
- Heat capacities

$$C_V = \left(\frac{\partial U}{\partial T}\right)_V \quad ; \quad C_p = \left(\frac{\partial H}{\partial T}\right)_p$$

$$C_p = C_V + R \quad \text{(ideal gas)}$$

- Kirchhoff's Law

$$H(T_2) = H(T_1) + \int_{T_1}^{T_2} C_p \, \mathrm{d}T$$

$$\Delta_r H(T_2) = \Delta_r H(T_1) + \int_{T_1}^{T_2} \Delta_r C_p \, \mathrm{d}T$$

Quantisation of energy

- Using statistical mechanics we can calculate energies and entropies of molecules – a key process in a quantitative understanding of the incorporation of both kinetics and thermodynamics in combustion models - requires us to understand the quantisation of their different forms of energy – electronic, vibrational, rotational and translational.
- The occurrence of energy levels, and their spacing, is a consequence of the wave properties of matter – atomic and molecular particles behave as both particles and waves.
- The next few slides outline the basis of quantisation and of the use of statistical mechanics.

Quantum Mechanics – in 6 slides.

de Broglie relation

$p = h/\lambda$ p = momentum, h = Planck's constant;

λ = wavelength ($h = 6.626 \times 10^{-34}$ J s)

Schrödinger Equation (1 dimension, time independent)

kinetic energy operator V = potential energy, E = total energy

$$\underline{\{-(h^2/8\pi^2 m)(d^2/dx^2) + V(x)\}}\psi = E\psi,$$

Hamiltonian (classically, $H = T + V$)

Wavefunction, ψ

ψ is continuous with continuous slope, single valued, finite everywhere;

$\psi \rightarrow 0$ as $x \rightarrow \infty$.

ψ^2 is the particle probability density; $\int_{-\infty}^{\infty} \psi^2 \mathrm{d}x = 1$

Particle in a one dimensional box

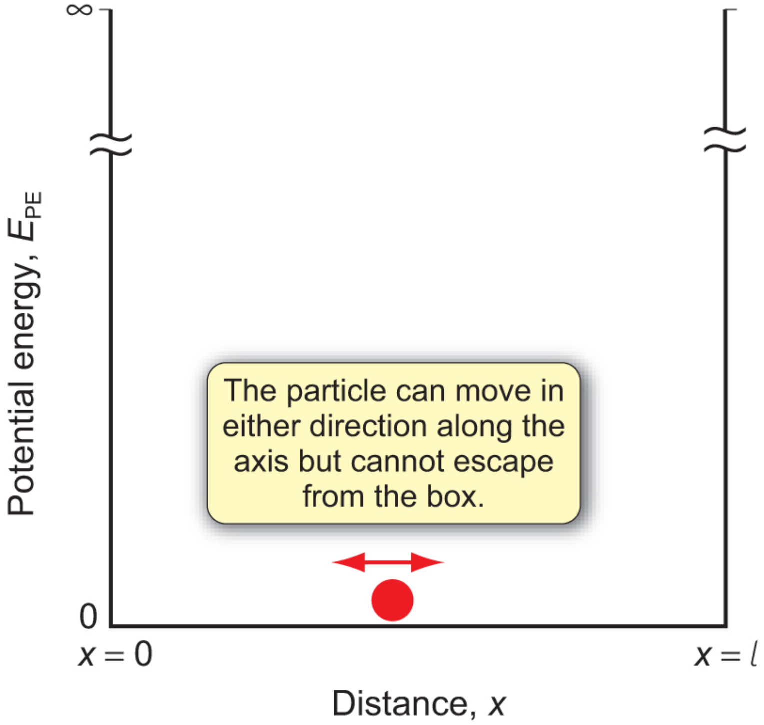

The particle can move in either direction along the axis but cannot escape from the box.

- ψ is zero outside the box and must be zero at x= 0, l
- de Broglie – wavelength of ψ depends on *p* and therefore on kinetic and total energy (*V* is zero): $\lambda = 2l/n$, $n = 1, 2$ …..
- Alternatively, solve the Schrödinger equation:

$$-\frac{h^2}{8\pi^2 m}\frac{\mathrm{d}^2\psi}{\mathrm{d}x^2} = E\psi$$

$$\psi = Ae^{ikx} = Asinkx$$

$$\psi = Asin\left(\frac{n\pi x}{l}\right)$$

$$E = \frac{k^2h^2}{8\pi^2 m} = \frac{n^2h^2}{8ml^2}$$

- *A* is determined from the normalisation property: $\int_0^l \psi^2 \mathrm{d}x = 1$

Wavefunctions and energy levels for a particle in a box

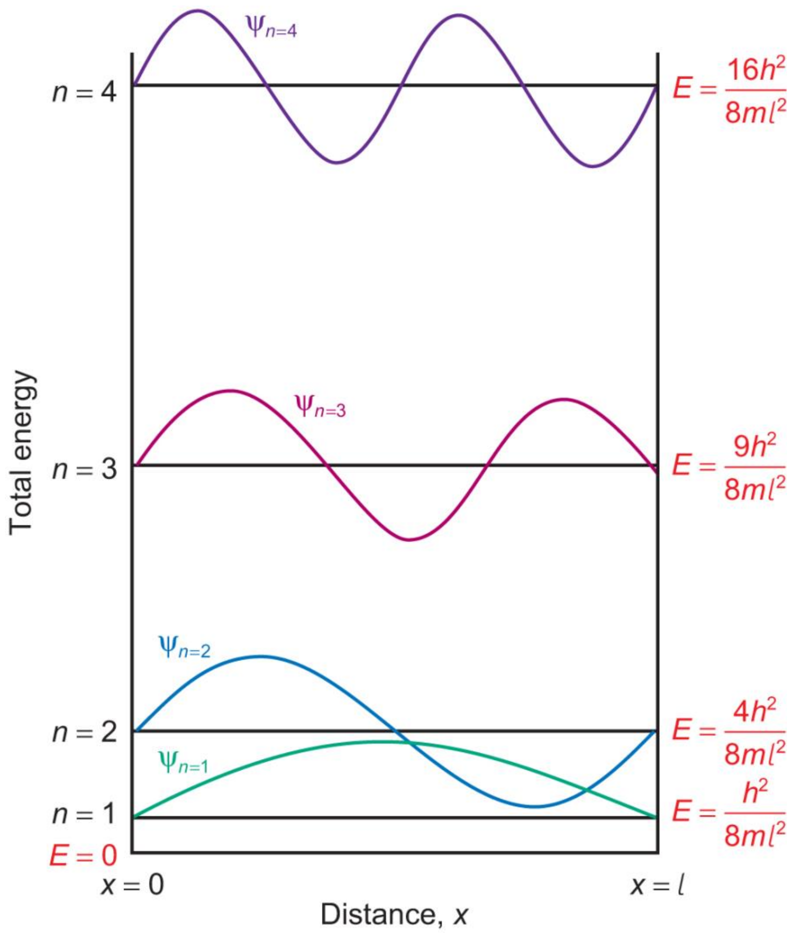

- Note form and properties of wavefunctions:
  - Zero at edges of box
  - Wavelength decreases as E increases (cf de Broglie)
  - Zero kinetic energy is not allowed – there is a so-called *zero point energy*
- Note the form, of the energy levels:
  - Energy is quantised and described by a *quantum number, n:*

$$E = \frac{n^2h^2}{8ml^2}$$

- Note the operation of the *Correspondence Principle:* high mass, l, give large quantum numbers at significant energies – quantisation and wave properties are unimportant for classical systems

Vibrational energy levels and wavefunctions

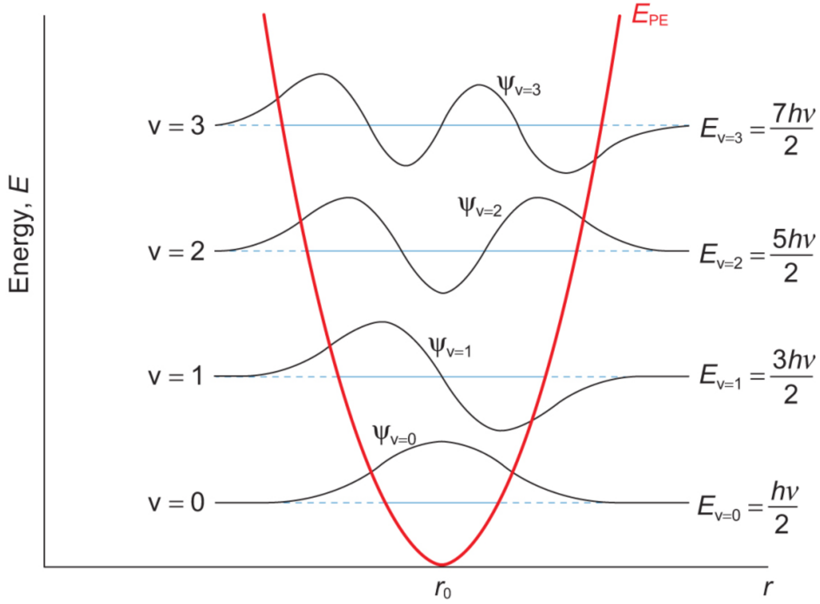

- Model for vibrational motion in a molecule – harmonic oscillator

$$V = \frac{1}{2}k(r - r_0)^2$$

- Wavefunctions are Gaussian functions – they are not simple sine functions because (*E*-V) depends on *r*.
- Note the penetration of the wavefunction into the *non-classical* region where *V > E* : the kinetic energy is negative – *quantum mechanical tunnelling*
- In this region, the wavefunction is no longer oscillatory but decreases to zero at

  $(r - r_0) = \infty$

Quantisation of different types of energy

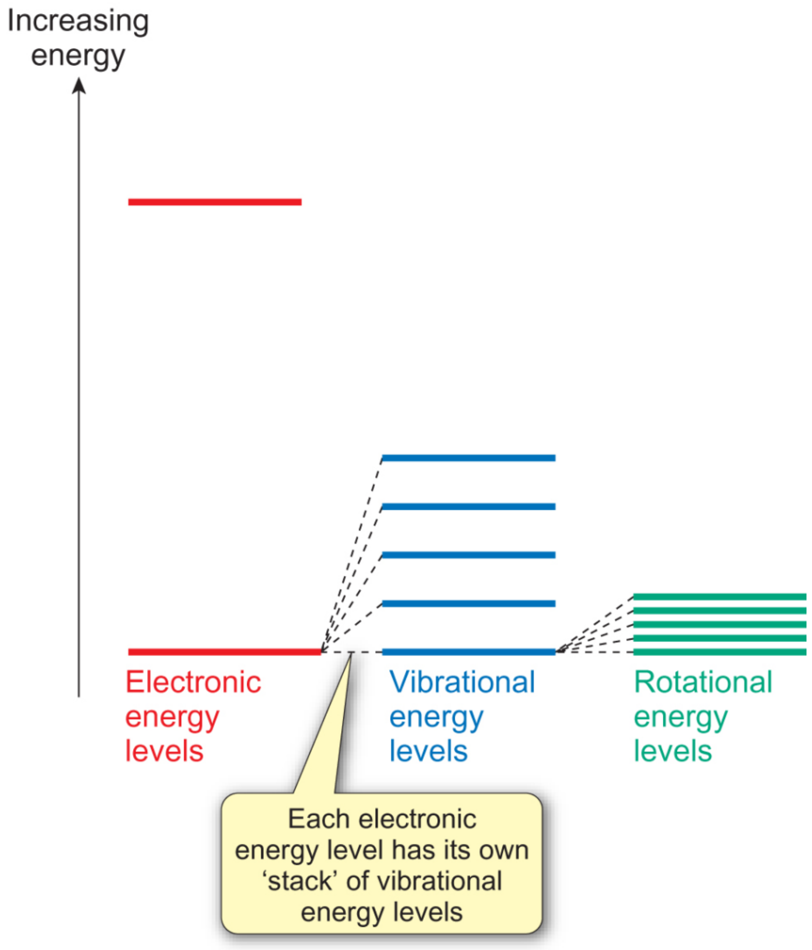

- The spacing of the energy levels is in the order: electronic > vibrational> rotational > translational.
- Most combustion processes involve the ground electronic state, but excited states can be important (e.g. electronically excited oxygen atoms.)

Quantum mechanical tunnelling – an indication of the issues

$$-\frac{\mathrm{d}^2\psi}{\mathrm{d}x^2} = \frac{8\pi^2 m}{h^2}(E-V)\psi$$

For *E-V* = constant a solution of the Schroedinger equation is

$$\psi = A exp(ikx)$$

$$k = \sqrt{\frac{8\pi^2 m(E-V)}{h^2}}$$

For *E* > *V* the solution is oscillatory, as discussed for the particle in a box

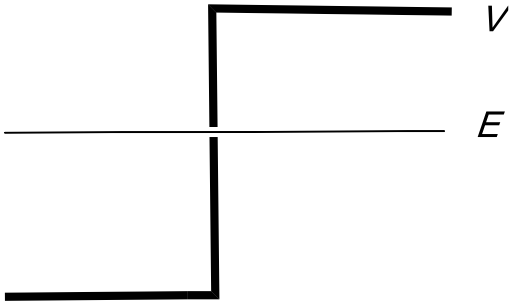

For *V* > *E*, *k* = *iκ*, where

$$\kappa = \sqrt{\frac{8\pi^2 m(V-E)}{h^2}}$$

$$\psi = B exp(-\kappa x)$$

i.e. the wavefuction penetrates into the non-classical region where V > E (and the kinetics energy is negative) and decays exponentially in this region

NB the dependence on mass

Statistical mechanics

- Statistical mechanics is the determination of macroscopic properties (thermodynamic, but also kinetic) from the microscopic properties of the component molecules.
- It relies heavily on a description of the energy levels of molecules and of the distribution of molecules throughout those energy levels.
- We shall examine the thermodynamic properties of canonical ensembles, with fixed numbers of molecules, N , fixed volume, V, and fixed temperature, T.
- We shall base our discussion on the most probable distribution of molecules throughout the energy levels, which is dependent on maximising the entropy (spreading the molecules as widely as possible throughout the energy levels), consistent with a fixed overall energy, defined by the temperature, T. This distribution is the Boltzmann distribution.

Boltzmann distribution 1

- Molecules are arranged through the energy levels subject to a constant total number, N

$$N = \sum N_i$$

and constant total energy, E

$$E = \sum N_i \, \varepsilon_i$$

- N is very large (~ 10^{23}) and the most probable distribution, subject to the above restrictions, dominates.
- If W is the weight of this configuration, its entropy S is

$$S = k \ln W$$

where k is the Boltzmann constant. This distribution is found by maximising W.

Boltzmann distribution 2

- Boltzmann distribution: $\frac{N_i}{N} = \frac{g_i e^{-\beta\varepsilon_i}}{q}$ where $\beta = 1/kT$
- N_i is the number of molecules in energy level i, N is the total number of molecules, g_i is the degeneracy and k is the Boltzmann constant.
- Partition function:

$$q = \sum_{levels,i} g_i \, e^{-\beta\epsilon_i}$$

The partition function is a sum over the energy levels, weighted according to their probability of occupation

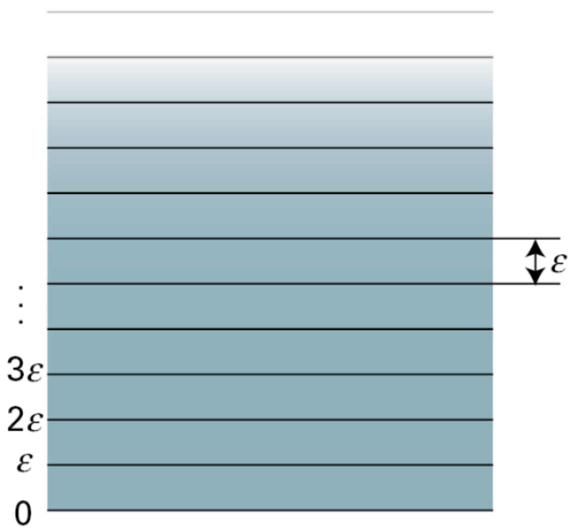

Evenly spaced levels e.g. harmonic oscillator

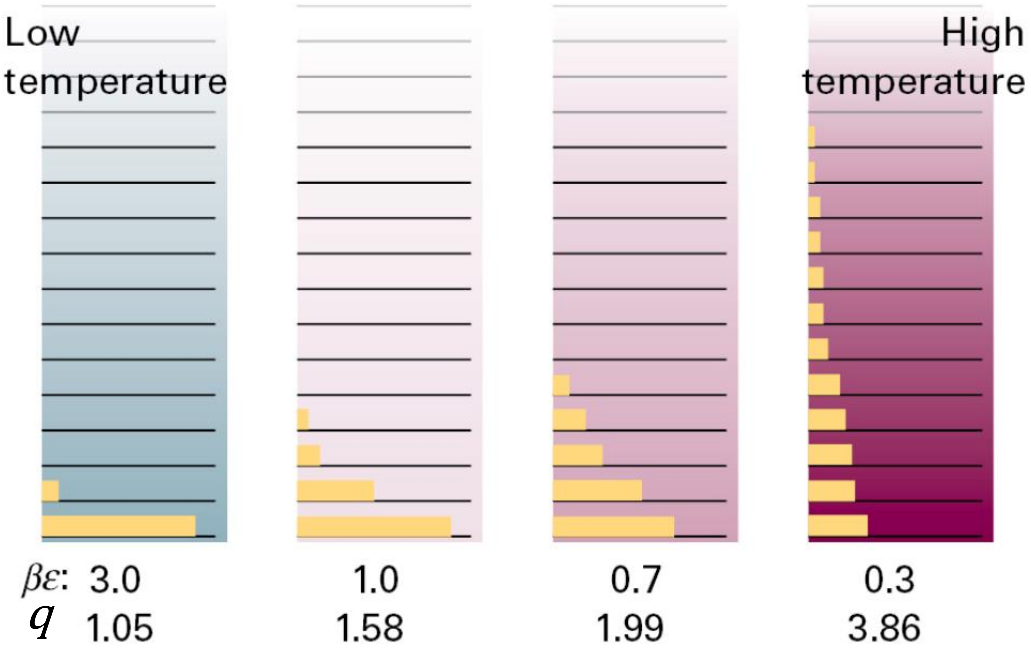

Energy levels

- *h* = Planck's constant = 6.626 x 10^{-34} Js; $\hbar = h/2\pi$, c = speed of light. *kT/hc* = 207.2 cm^{-1} at 298 K.
- Translation. Particle, mass *m*, in cubic box, side *a*, quantum numbers n_x, n_y, n_z. Spacing << *kT*

$$\varepsilon_{n_x,n_y,n_z} = \frac{h^2}{8ma^2}(n_x^2 + n_y^2 + n_z^2)$$

- Rotation, linear molecule, moment of inertia, *I*, quantum number *J*. Spacing <*kT*, except at very low *T*.

$$\varepsilon_J = \frac{J(J+1)h^2}{8\pi^2 I} \qquad B = h/(8\pi^2 Ic)$$

B and ω have units cm^{-1}
They can be determined
spectroscopically and
using quantum mechanics
Degeneracy = 2*J*+1

- Vibration, diatomic molecule, vibrational frequency υ, quantum number v, *k* is the force constant, μ reduced mass.

$$\varepsilon_{\mathrm{v}} = \left(\mathrm{v} + \frac{1}{2}\right)h\upsilon \qquad \upsilon = \frac{1}{2\pi}\sqrt{\frac{k}{\mu}} \qquad \upsilon = \omega c$$

$$V = \frac{1}{2}k(r - r_0)^2$$

Similar expressions for
rotational and vibrational
energy levels for
non-linear and for polyatomic
molecules

Electronic states and energy levels 1. Atoms

- Most of the atoms and molecules we encounter in combustion are in their ground electronic states. There are some exceptions.
- The electronic states of atoms are described by their term symbols. The oxygen atom has three low lying states, $^3P_2$, $^3P_1$, $^3P_0$.

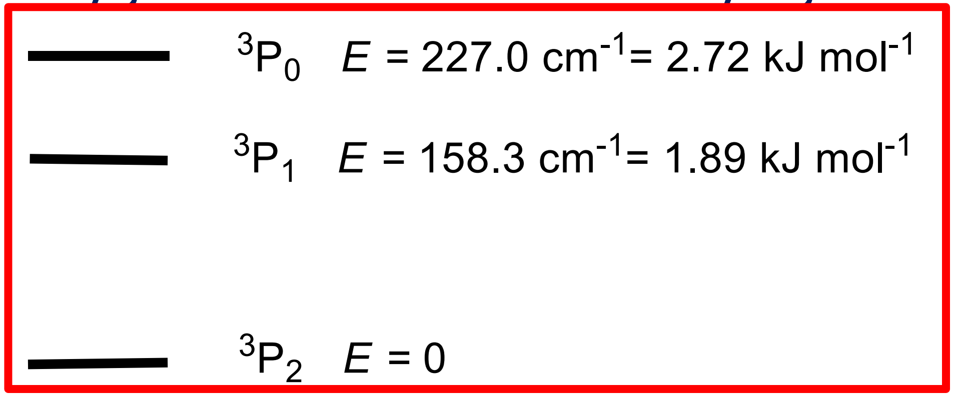

$^3P_0$ $E = 227.0\ \mathrm{cm^{-1}} = 2.72\ \mathrm{kJ\ mol^{-1}}$

$^3P_1$ $E = 158.3\ \mathrm{cm^{-1}} = 1.89\ \mathrm{kJ\ mol^{-1}}$

$^3P_2$ $E = 0$

- Superscript 3 is the multiplicity = 2S + 1, where S is the total spin. In the case of O, S = 1.
- P describes the electronic orbital angular momentum, L. S states have L = 0; P states L= 1; D, L=2 etc.
- The subscript refers to the total angular momentum, J, formed from the quantized vector sum of L and S
- Other atoms: H $^2S_{1/2}$, C $^3P_{0,1,2}$, N $^4S_{3/2}$, S $^3P_{2,1,0}$

Electronic states and energy levels 2. Diatomic Molecules

- Diatomic molecules are described by similar term symbols. Most are in $^1\Sigma$ ground states. The superscript is 2S+1 and the Greek symbol refers to the orbital angular momentum along the internuclear axis, Λ. Σ corresponds to $\Lambda = 0$. So such states have both S and $\Lambda = 0$.
- Both OH and NO have $^2\Pi$ ground states with $S = \frac{1}{2}$ and $\Lambda = 1$. We now need to consider the total angular momentum, Ω, along the internuclear axis. For both OH and NO, we have $\Omega = 3/2$ and 1/2 states; the former is the ground state and the latter lies higher by 139.2 cm^{-1} for OH and 121.1 cm^{-1} for NO

Electronic states and energy levels 2. Polyatomic Molecules

- Most molecules have singlet ground states, i.e. 2S+1=1 and S=0 – there is no net spin.
- Radicals such as CH_3 have a single unpaired electron and are in doublet states, with 2S+1 = 2 and S = $\frac{1}{2}$.
- Methylene, CH_2, is a biradical – we need to consider two electrons. In the ground state, the spin angular momenta of these electrons are parallel, so that the total spin, S = 1 and 2S+1 = 3. This state is termed triplet methylene. The first excited state has paired (ie opposed) spins and S = 0, 2S+1 = 1 – it is a singlet state.
- The singlet lies 37.6 kJ mol^{-1} above the ground state and is much more reactive than it.

Partition functions

$$q = \sum_{levels,i} g_i \, e^{-\beta \epsilon_i}$$

- Translational partition function. *V* = volume, *m* = molecular mass

$$q_{trans} = \left[\frac{2\pi mkT}{h^2}\right]^{3/2} V$$

NB – the term in V:
- Origin
- Q = q/V

- Rotational partition functions (i) linear molecule (ii) non-linear.

  σ = symmetry number

  A, *B*, *C* = rotational constants

$$q_{rot} = \frac{kT}{\sigma hBc}$$

$$q_{rot} = \frac{\sqrt{\pi}}{\sigma}\left\{\frac{\left(\frac{kT}{hc}\right)^3}{ABC}\right\}^{1/2}$$

- Vibrational partition functions (i) diatomic, (ii) polyatomic with α = 3*n* -5 (linear molecule); 3*n* – 6 (non-linear) ω_i is vibrational constant.
- NB. These vibrational partition functions refer to the zero point energy as the energy zero. Harmonic oscillators

$$q_{vib} = \left(1 - e^{-\frac{hc\omega}{kT}}\right)^{-1}$$

$$q_{vib} = \prod_{i=1}^{\alpha}\left(1 - e^{-\frac{hc\omega_i}{kT}}\right)^{-1}$$

Degeneracy

$$\frac{N_i}{N} = \frac{g_i e^{-\beta \varepsilon_i}}{q} \qquad q = \sum_{levels,i} g_i\, e^{-\beta \epsilon_i}$$

- where g_i is the degeneracy - the number of states at energy ε_i.
- For a rotational level, *J*, the degeneracy is 2J+1.
- For an atom, the degeneracy is also 2J+1, so that the degeneracies of the low three lowest states in $O^3P_{2,1,0}$ are 5, 3 and 1, while the lowest state of $H^2P_{1/2}$ is 2.
- For diatomic molecules, the degeneracy depends on Ω, which is constrained to lie along the internuclear axis. For $\Omega > 0$, the degeneracy is 2.
- Note that, as we shall see later, we need to include these electronic degeneracies in calculations of entropies, equilibrium constants and in transition state calculations of rate constants

Partition functions and thermodynamic quantities

- Total molecular energy: $\varepsilon = \varepsilon_{\text{trans}} + \varepsilon_{\text{rot}} + \varepsilon_{\text{vib}} + \varepsilon_{\text{elec}}$
- Total molecular partition function: $q = q_{\text{trans}} q_{\text{rot}} q_{\text{vib}} q_{\text{elec}}$
- The molar thermodynamic energy, U , is obtained from the energy E which is referred to the zero point energy: $U = U(0) + E$; where $U(0)$ is the internal energy at 0 K.

$$U = U(0) - N\left(\frac{\partial \ln q}{\partial \beta}\right)_V = U(0) + NkT^2\left(\frac{\partial \ln q}{\partial T}\right)_V \quad E = \sum N_i\, \varepsilon_i$$

- The entropy is determined from $S = k\ln W$

Gas phase molecules of the same type are indistinguishable and this must be recognised in calculating the molar entropy: $S = \frac{U-U(0)}{T} + R\ln q - R\ln N_A + R$

The $-R\ln N + R$ term derives from the indistinguishability of similar molecules in the gas phase, and is associated with the translational contribution to the entropy. It is omitted if you want to calculate, say, the rotational entropy.

Other thermodynamic functions and equilibrium constants

- The Helmholtz Energy, *A*, is readily calculated from *A* = *U* – *TS*. Note that the total partition function has been defined at constant volume, to define the translational partition function.
- To calculate the Gibbs energy, the system needs to be referred to standard conditions, which define the volume term in the partition function.
- For our purposes, the most useful equilibrium constant is K_c

  For the reaction $\sum \nu_i X_i = 0$

$$K_c = \prod \left(q_{X_i}/V\right)^{\nu_i} \exp\left(-\frac{\Delta\varepsilon_0}{kT}\right)$$

  where $\Delta\varepsilon_0$ is the change in zero point energy in the reaction. Don't forget the electronic contributions to *q (Exercise)*

Exercise: Electronic partition functions

- As we discussed earlier, molecules such as OH and NO have an unpaired electron and also one unit of orbital angular momentum. This results in two states, each with a degeneracy of 2, separated by an energy difference $\Delta\varepsilon$.
- Consider the general case of a two level system, separation $\Delta\varepsilon$ and degeneracies g_1 and g_2:
  - Write down the electronic partition function for this system.
  - Derive an expression for the molar electronic energy, *U*, as a function of temperature.
  - Derive an expression for the contribution of electronic energy to the heat capacity.
  - Sketch the electronic energy and heat capacity vs *T*.

Chemical kinetics

Constructing chemical mechanisms

Interactions between coupled chemical reactions

Constructing coupled differential (rate) equations from chemical mechanisms

1. $H_2 + O_2 \rightarrow H + HO_2$
2. $H + O_2 \rightarrow OH + O$
3. $O + H_2 \rightarrow OH + H$
4. $OH + H_2 \rightarrow H + H_2O$
5. $H + O_2 + M \rightarrow HO_2 + M$
6. H, O, OH → wall
7. $HO_2 + HO_2 \rightarrow H_2O_2 + O_2$

The chemical mechanism is set up together with the associated rate coefficients

The coupled rate equations are then written down for each species

d[X]/dt = Total rate of forming X -Total rate of removing X:

$$\frac{d[\mathrm{H}]}{dt} = k_1[\mathrm{H_2}][\mathrm{O_2}] - k_2[\mathrm{H}][\mathrm{O_2}] + k_3[\mathrm{O}][\mathrm{H_2}] + k_4[\mathrm{OH}][\mathrm{H_2}] - k_5[\mathrm{H}][\mathrm{O_2}][\mathrm{M}] - k_6[\mathrm{H}]$$

$$\frac{d[\mathrm{O}]}{dt} = k_2[\mathrm{H}][\mathrm{O_2}] - k_3[\mathrm{O}][\mathrm{H_2}] - k_6[\mathrm{O}]$$

etc ......

Solve the set of coupled differential equations numerically, subject to initial conditions. E.g. using CHEMKIN – see later

Some kinetics formalities – set of coupled first order reactions

$$\frac{d\mathbf{c}}{dt} = \mathbf{f}(\mathbf{c},\mathbf{k}); \quad \mathbf{c}(t=0) = \mathbf{c}_0$$

c is an *n*-dimensional concentration vector

For a set of first order reactions, we may solve using an eigenvalue approach: $\frac{d\mathbf{c}}{dt} = \mathbf{Mc}$

M is an *n* x *n* matrix of rate constants. The *n* eigenvalues, λ, of **M** are obtained from $\det(\mathbf{M} - \boldsymbol{\lambda}\mathbf{I}) = 0$

We also need the eigenvectors, **x**: $\mathbf{Mx} = \boldsymbol{\lambda}\mathbf{x}$

The time dependent concentrations **c**(*t*) are then given by:

$$\boldsymbol{c}(t) = \boldsymbol{x}e^{\lambda t}\boldsymbol{x}^{-1}\boldsymbol{c}(0)$$

Two simple examples: 1. A → B → C, with rate coefficients k_1 and k_2

Set up the rate equations, with a = [A], etc

$$\frac{da}{dt} = -k_1 a; \quad \frac{db}{dt} = k_1 a - k_2 b$$

$$c = a_0 - a - b$$

$$\mathbf{M} = \begin{pmatrix} -k_1 & k_1 \\ 0 & -k_2 \end{pmatrix}$$

$$\mathbf{c} = \begin{pmatrix} a \\ b \end{pmatrix}$$

$$\det(\mathbf{M} - \boldsymbol{\lambda}\mathbf{I}) = 0$$

$$\begin{bmatrix} -k_1 - \lambda & k_1 \\ 0 & -k_2 - \lambda \end{bmatrix} = 0$$

$$(-k_1 - \lambda)(-k_2 - \lambda) = 0$$

$$\lambda_1 = -k_1; \quad \lambda_2 = -k_2$$

$$a = Ae^{-k_1 t} + Be^{-k_2 t}$$

$$b = Ce^{-k_1 t} + De^{-k_2 t}$$

$$a = a_0 \exp(-k_1 t)$$

$$b = \frac{a_0 k_1}{(k_2 - k_1)}\{\exp(-k_1 t) - \exp(-k_2 t)\}$$

$$c = a_0 - a - b$$

Quasi steady state approximation (QSSA)

Figure (a): $k_1 > k_2$

$$b = \frac{a_0 k_1}{(k_1 - k_2)}\{\exp(-k_2 t) - \exp(-k_1 t)\}$$

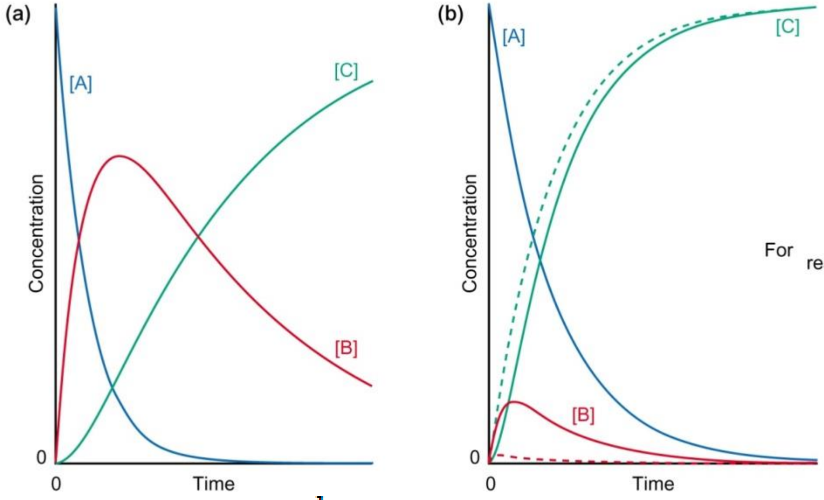

For $\underset{\text{reactant}}{A} \xrightarrow{k_1} \underset{\text{intermediate}}{B} \xrightarrow{k_2} \underset{\text{product}}{C}$

Figure (b): full, $k_2 = 5k_1$
dashed, $k_2 = 50k_1$

Figure (b): $k_1 < k_2$

$$b = \frac{a_0 k_1}{(k_2 - k_1)}\{\exp(-k_1 t) - \exp(-k_2 t)\}$$

For $k_1 << k_2$ and for times long compared with $(k_2)^{-1}$

$$b = \frac{a_0 k_1}{(k_2 - k_1)}\{\exp(-k_1 t)\} \approx \frac{a_0 k_1}{k_2}\{\exp(-k_1 t)\} = \frac{a k_1}{k_2}$$

$$\therefore b \ll a \text{ and } \frac{db}{dt} \ll \frac{da}{dt}$$

- QSSA: $db/dt \approx 0$: rate of forming of B ≈ rate of removing B

On the error in the QSSA

Turanyi et al J. Phys. Chem. 1993,97, 163-172

- Applying the QSSA to a species in a numerical integration introduces an error in the species concentration that propagates as the numerical integration proceeds.
- For a system of rate equations $\frac{\mathrm{d}\mathbf{c}}{\mathrm{d}t} = \mathbf{f}(\mathbf{c},\mathbf{k});\ \ \mathbf{c}(t=0) = \mathbf{c}_0$

  the instantaneous error in concentration in a single species i is:

$$\Delta c_i^s = \frac{1}{J_{ii}} \frac{\mathrm{d}c_i}{\mathrm{d}t}$$

- Here J_{ii} is a diagonal Jacobian element:

$$J_{ik} = \frac{\partial f_i(\mathbf{c},\mathbf{k})}{\partial c_k}$$

- The lifetime, τ, of species i is given by $\tau = -\frac{1}{J_{ii}}$
- So the error in applying the QSSA is least for species with short lifetimes (or slow rates of change).
- Turanyi et al also discussed errors for groups of QSSA species

Pressure dependent association reactions: an example of the application of QSSA

An association reaction involves collisional stabilisation of the adduct:

$$A + B \underset{k_{-a}}{\overset{k_a}{\rightleftharpoons}} AB^* \xrightarrow{k_s[M]} AB.$$ Lindemann, 1922

Apply QSSA:

$$k = \frac{k_a k_s[\mathrm{M}]}{k_{-a} + k_s[\mathrm{M}]}$$

Examples include

$CH_3 + CH_3 \rightarrow C_2H_6$

$OH + C_2H_4 \rightarrow C_2H_4OH$

$$\text{As } [\mathrm{M}] \rightarrow \infty, k \rightarrow k_a = k^\infty$$

$$\text{As } [\mathrm{M}] \rightarrow 0, k \rightarrow \frac{k_a k_s[M]}{k_{-a}} = k_0[\mathrm{M}]$$

Substituting in first equation

$$k = \frac{k_0[\mathrm{M}]k^\infty}{k^\infty + k_0[\mathrm{M}]}$$

Similar treatment for dissociation reactions

Pressure dependence of an association reaction $OH + C_2H_4$

$OH + C_2H_4 \rightleftharpoons C_2H_4OH^*$

$C_2H_4OH^* + M \rightarrow C_2H_4OH + M$

The figure shows experimental data and a fit using a development of Lindemann theory that will be discussed in Topic 3

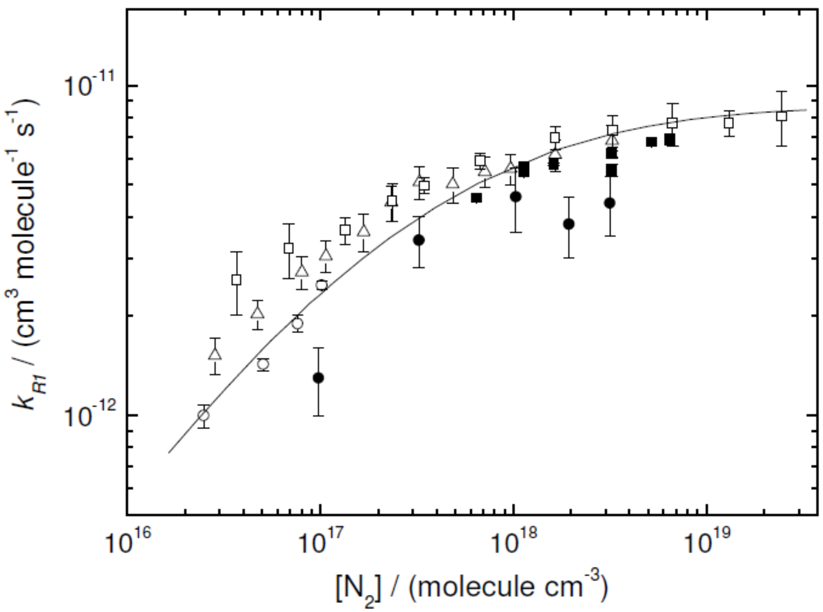

$$k = \frac{k_a\, k_s[\mathrm{M}]}{k_{-a} + k_s[\mathrm{M}]}$$

$$\text{As } [\mathrm{M}] \rightarrow \infty, k \rightarrow k_a = k^\infty$$

$$\text{As } [\mathrm{M}] \rightarrow \infty, k \rightarrow k_a = k^\infty$$

2. $A \rightleftarrows B \rightarrow C$

$$\frac{da}{dt} = -k_1 a + k_{-1} b$$

$$\frac{db}{dt} = k_1 a - (k_{-1} + k_2) b$$

$$\mathbf{M} = \begin{pmatrix} -k_1 & k_1 \\ k_{-1} & -k_{-1} - k_2 \end{pmatrix}$$

$$\mathbf{c} = \begin{pmatrix} a \\ b \end{pmatrix}$$

$$\begin{bmatrix} -k_1 - \lambda & k_1 \\ k_{-1} & -k_{-1} - k_2 - \lambda \end{bmatrix} = 0$$

$$(-k_1 - \lambda)(-k_{-1} - k_2 - \lambda) - k_1 k_{-1} = 0$$

$$2\lambda_{\pm} = -(k_1 + k_{-1} + k_2) \pm \sqrt{(k_1 + k_{-1} + k_2)^2 - 4k_1 k_2}$$

If $k_1 \approx k_{-1} \gg k_2$ binomial expansion gives:

$$\lambda_- \approx -(k_1 + k_{-1} + k_2) \approx -(k_1 + k_{-1})$$

$$\lambda_+ \approx \frac{-k_1 k_2}{(k_1 + k_{-1} + k_2)} \approx \frac{-k_1 k_2}{(k_1 + k_{-1})}$$

The larger magnitude eigenvalue describes the relaxation of A, B to equilibrium. $1/(k_1+k_{-1})$ is termed the relaxation time. The smaller magnitude eigenvalue describes the loss of the equilibrated A,B system to form C. If $k_2 = 0$, the A,B system is conservative. There are still two eigenvalues, $-(k_1+k_{-1})$ and 0. The zero eigenvalue relates to the equilibrium distribution.

Exercise: eigenvalue determination

- Consider the following reaction system:

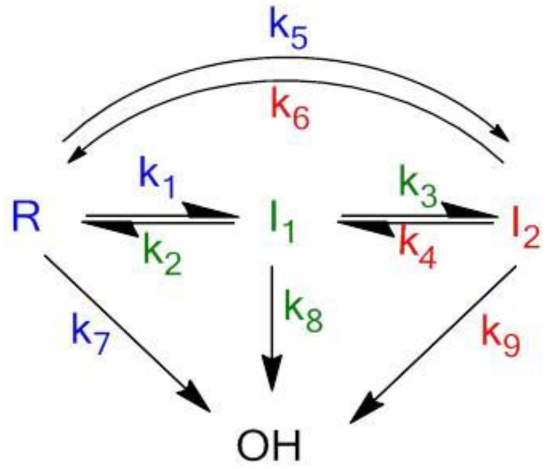

- Set up the rate equations for R, I_1 and I_2 and express in matrix form.
- This results in a 3 eigenvalue system and a cubic equation in λ. However, I_2 is short-lived and the quasi steady state approximation can be applied to it. This allows the matrix **M** to be expressed as a 2x2, for the two variable system, [R] and [I_1], with the rate constants determined from the elimination of [I_2] using the QSSA. Obtain expressions for the two eigenvalues of the system.
- We shall re-examine this reaction system on Friday when we discuss peroxy radical reactions

Chain reactions. 1. straight chain reactions – e.g. $H_2 + Br_2$

- Chain carriers (also called chain centres, i.e. reactive intermediates) are generated in the initiation steps.
- In the propagation steps the chain carriers react with the reactants, produce products and regenerate the chain carriers.
- In the termination steps the chain carriers are consumed

Initiation

$Br_2 + M \rightarrow 2Br + M$ rate = $r_1 = 2k_1[Br_2][M]$

Propagation

$Br + H_2 \rightarrow H + HBr$ $r_2 = k_2[Br][H_2]$

$H + Br_2 \rightarrow Br + HBr$ $r_3 = k_3[H][Br_2]$

Termination

$2Br + M \rightarrow Br_2 + M$ $r_4 = 2k_4[Br]^2[M]$

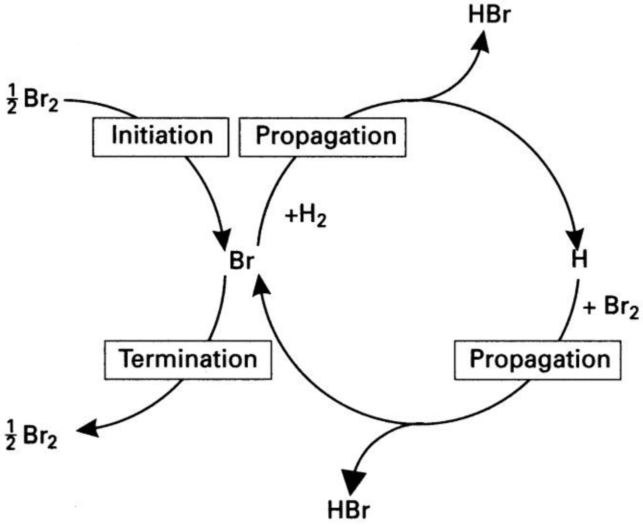

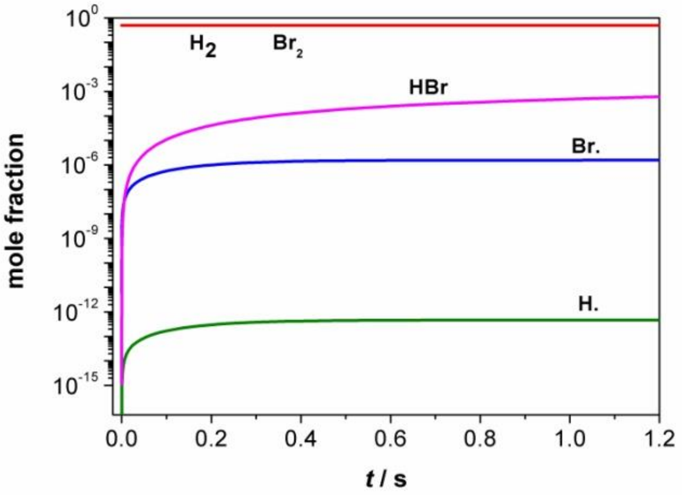

stoichiometric mixture,
T= 600 K, p= 1 atm

Relative rates of reaction after 1s, stoichiometric mixture, T= 600 K, p= 1 atm

$r1 = r4 = 1$ unit

$r2 = r3 = 100$ units

Chain length = 100 (number of propagation cycles per initiation (or termination) event.

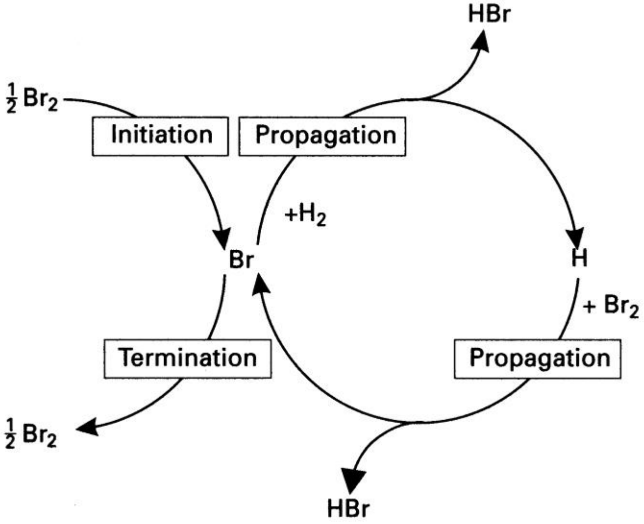

$$d[Br]/dt = 2k_1[Br_2][M] - k_2[Br][H_2] + k_3[H][Br_2] - 2k_4[Br]^2[M] = 0 \quad \text{(QSSA)}$$

$$d[H]/dt = + k_2[Br][H_2] - k_3[H][Br_2] = 0$$

Adding: $2k_1[Br_2][M] = 2k_4[Br]^2[M]$

$$[Br] = \sqrt{\{k_1[Br_2]/k_4\}}$$

From $d[H]/dt = 0$ $\quad [H]/[Br] = k_2[H_2]/k_3[Br_2]$

$$= k_2/k_3$$

(for stoichiometric mixtures)

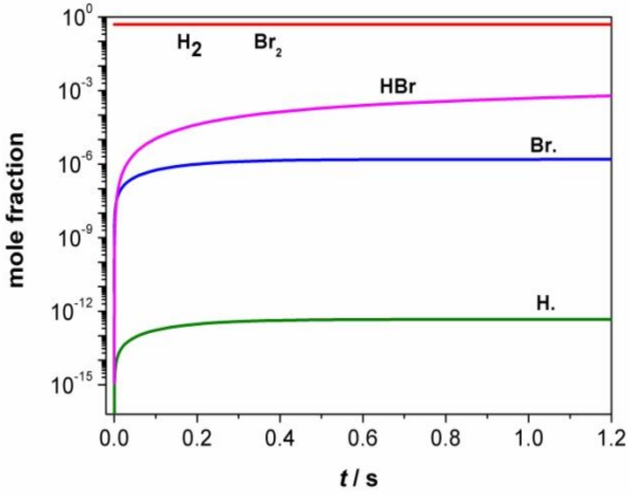

The activation energy of reaction 2 is 82 kJ mol^{-1} and that for reaction 3 is 4 kJ mol^{-1}. The A factors are similar.

At 600 K, the ratio of concentrations is ~1.5×10^{-7}

Chain reactions. 2. branched chain reactions - e.g. $H_2 + O_2$

- In addition to initiation, propagation and termination steps, these reactions have branching steps in which one radical generates 2 radicals, e.g.

$$H + O_2 \rightarrow OH + O$$

- Propagation steps don't change the radical concentration and in determining the time dependence of the radical concentration, *n*, we only need consider the other three reaction types. Considering only linear termination

$$\frac{\mathrm{d}n}{\mathrm{d}t} = i + gn - fn = i + \phi n; \;\; \phi = g - f$$

where *i* is the rate of initiation and g and f are the first order rate constants for branching and termination respectively. Integrating:

$$n = i\{\exp(\phi t) - 1\}/\phi$$

Plots of n/i vs t for negative and positive ϕ

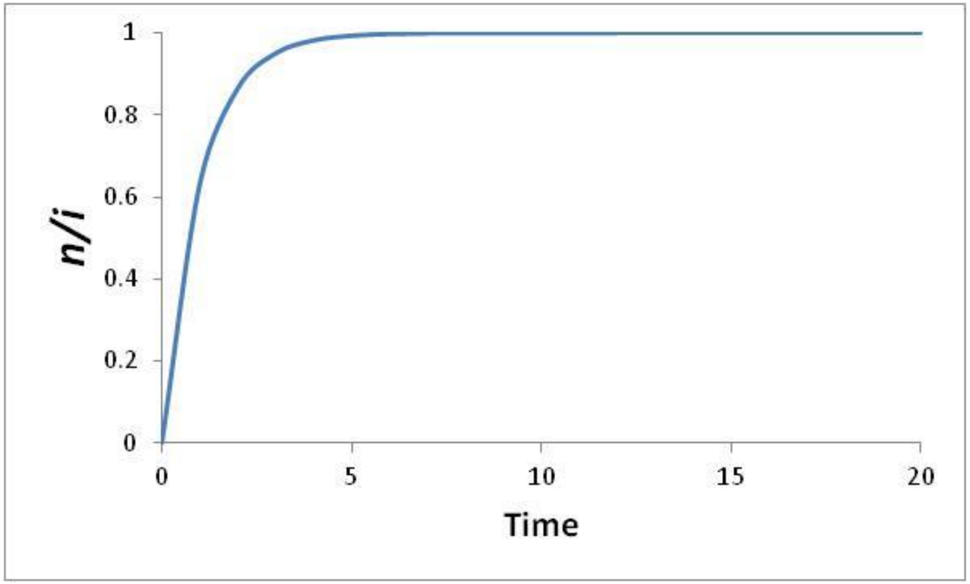

For plot 1, g-f = -1. Termination is faster than branching and n approaches a steady state, $n = i/\phi$, as $\exp(\phi t)$ tends to zero.

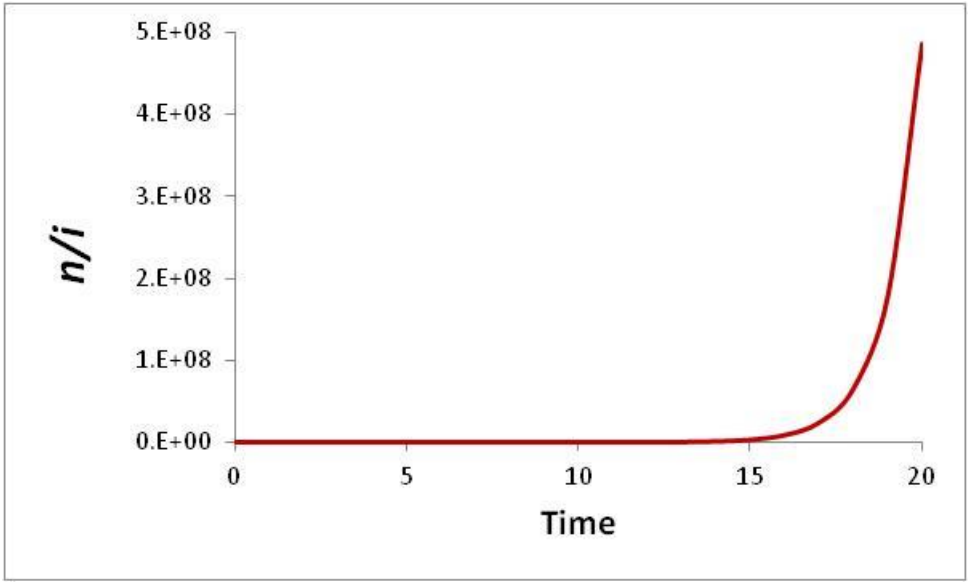

For plot 2, g-f = +1.

Branching is faster than termination and the number of radicals increases exponentially:

$$n = (i/\phi)\exp(\phi t)$$

Explosion of hydrogen–oxygen mixtures

$$2\ H_2 + O_2 \rightarrow 2\ H_2O$$

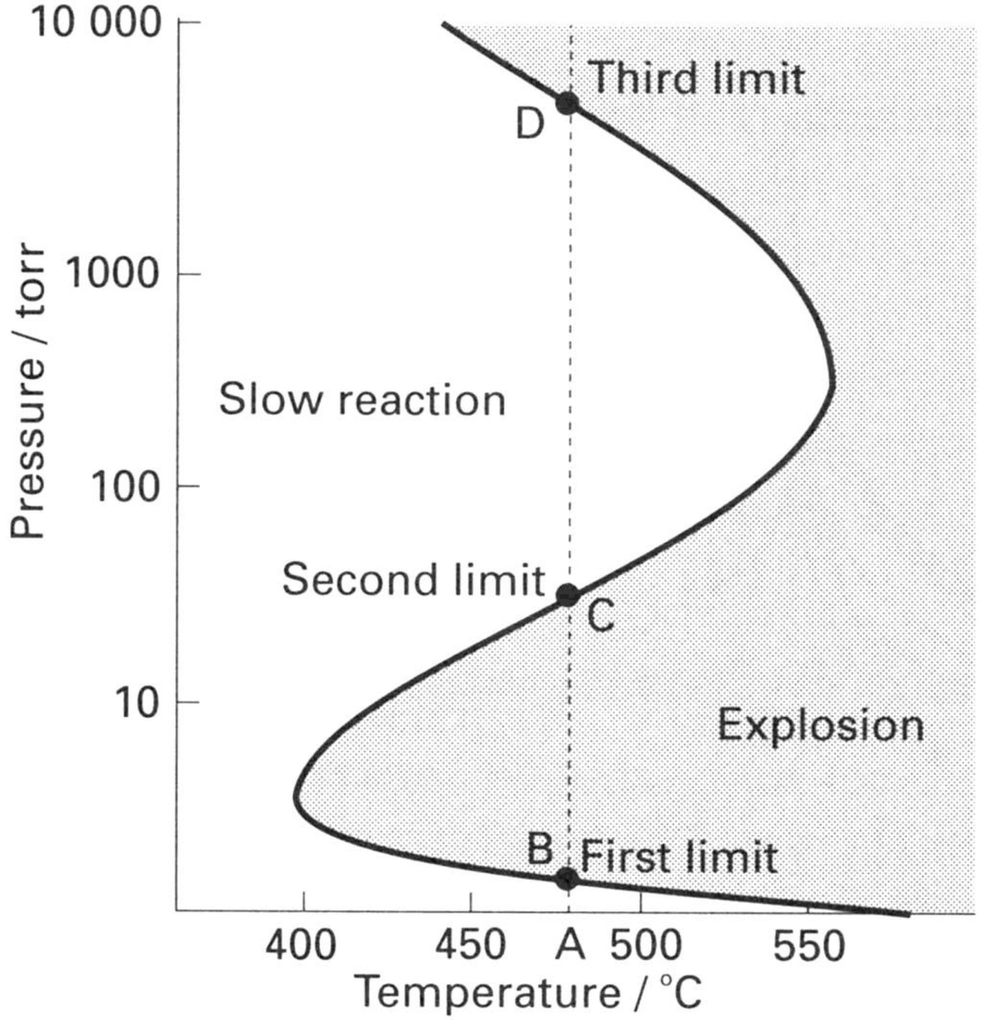

Observations:

The 1st explosion limit depends on the size of the vessel and the quality of the wall.
The 2nd and 3rd limits depend much less strongly on these.

Slightly extended mechanism

1	$H_2 + O_2 \rightarrow .H + .HO_2$	initiation
2	$.OH + H_2 \rightarrow .H + H_2O$	propagation
3	$.H + O_2 \rightarrow .OH + :O$	branching
4	$:O + H_2 \rightarrow .OH + .H$	branching
5	$.H + O_2 + M \rightarrow .HO_2 + M$	termination*
6	$.H \rightarrow$ wall	termination
7	$:O \rightarrow$ wall	termination
8	$.OH \rightarrow$ wall	termination
9	$.HO_2 + H_2 \rightarrow .H + H_2O_2$	initiation *
10	$2\ .HO_2 \rightarrow H_2O_2 + O_2$	termination
11	$H_2O_2 \rightarrow 2\ .OH$	initiation, branching

1	$H_2 + O_2 \rightarrow .H + .HO_2$	initiation
2	$.OH + H_2 \rightarrow .H + H_2O$	propagation
3	$.H + O_2 \rightarrow .OH + :O$	branching
4	$:O + H_2 \rightarrow .OH + .H$	branching
5	$.H + O_2 + M \rightarrow .HO_2 + M$	termination*
6	$.H \rightarrow$ wall	termination
7	$:O \rightarrow$ wall	termination
8	$.OH \rightarrow$ wall	termination
9	$.HO_2 + H_2 \rightarrow .H + H_2O_2$	initiation *
10	$2\ .HO_2 \rightarrow H_2O_2 + O_2$	termination
11	$H_2O_2 \rightarrow 2\ .OH$	initiation

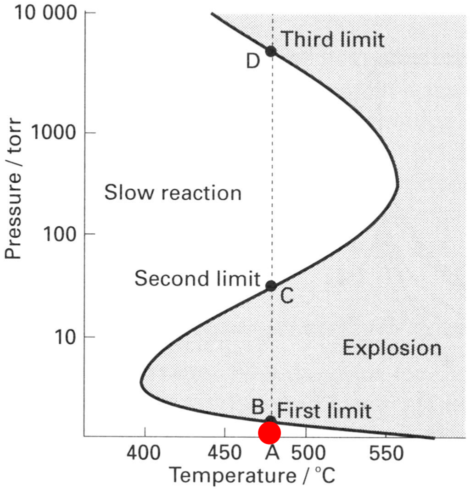

This is a slightly extended version of the mechanism we saw before

Below the 1st explosion limit:

domination of the termination reactions at the wall. Termination by H is the most important

→ no explosion

1	$H_2 + O_2 \rightarrow .H + .HO_2$	initiation
2	$.OH + H_2 \rightarrow .H + H_2O$	propagation
3	$.H + O_2 \rightarrow .OH + :O$	branching
4	$:O + H_2 \rightarrow .OH + .H$	branching
5	$.H + O_2 + M \rightarrow .HO_2 + M$	termination*
6	$.H \rightarrow$ wall	termination
7	$:O \rightarrow$ wall	termination
8	$.OH \rightarrow$ wall	termination
9	$.HO_2 + H_2 \rightarrow .H + H_2O_2$	initiation *
10	$2\ .HO_2 \rightarrow H_2O_2 + O_2$	termination
11	$H_2O_2 \rightarrow 2\ .OH$	initiation

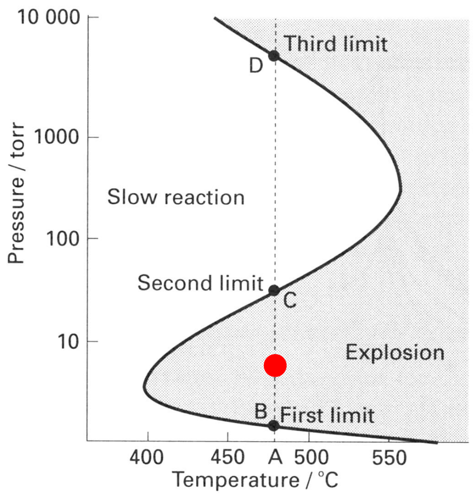

Between the 1st and the 2nd explosion limits:

Propagation step (2). Branching steps (3) and (4).

3 $H + O_2 \rightarrow .OH + :O$
2 $.OH + H_2 \rightarrow .H + H_2O$
4 $:O + H_2 \rightarrow .H + .OH$
2 $.OH + H_2 \rightarrow .H + H_2O$
+ ______________________

$$\mathbf{.H} + O_2 + 3\ H_2 \rightarrow \mathbf{3\ .H} + 2\ H_2O$$

→ **explosion**

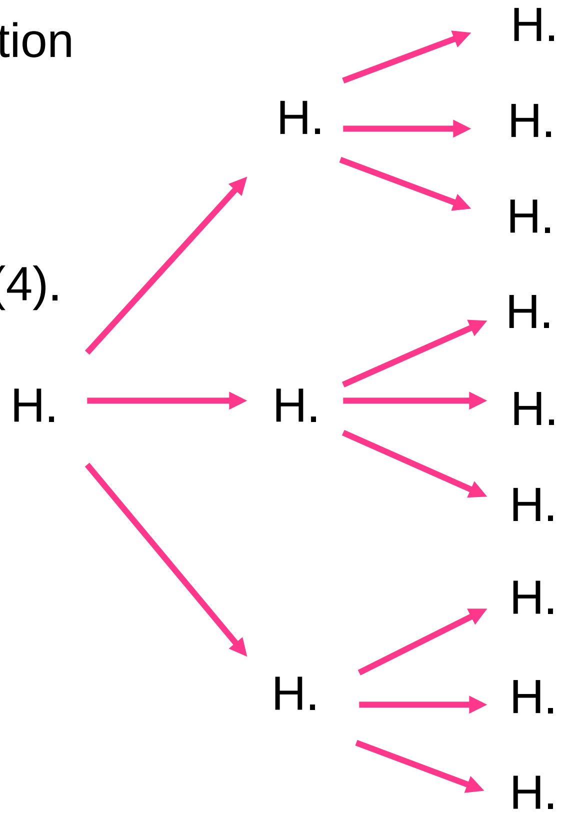

1	$H_2 + O_2 \rightarrow .H + .HO_2$	initiation
2	$.OH + H_2 \rightarrow .H + H_2O$	propagation
3	$.H + O_2 \rightarrow .OH + :O$	branching
4	$:O + H_2 \rightarrow .OH + .H$	branching
5	$.H + O_2 + M \rightarrow .HO_2 + M$	termination*
6	$.H \rightarrow$ wall	termination
7	$:O \rightarrow$ wall	termination
8	$.OH \rightarrow$ wall	termination
9	$.HO_2 + H_2 \rightarrow .H + H_2O_2$	initiation *
10	$2\ .HO_2 \rightarrow H_2O_2 + O_2$	termination
11	$H_2O_2 \rightarrow 2\ .OH$	initiation

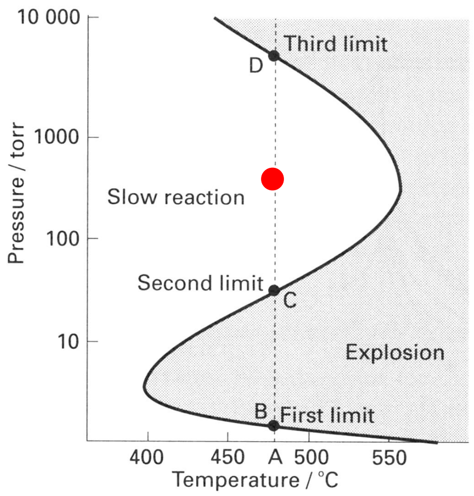

Between the 2nd and the 3rd explosion limits:

5 $.H + O_2 + M \rightarrow .HO_2 + M$ termination*

→ no explosion

1	$H_2 + O_2 \rightarrow .H + .HO_2$	initiation
2	$.OH + H_2 \rightarrow .H + H_2O$	propagation
3	$.H + O_2 \rightarrow .OH + :O$	branching
4	$:O + H_2 \rightarrow .OH + .H$	branching
5	$.H + O_2 + M \rightarrow .HO_2 + M$	termination*
6	$.H \rightarrow$ wall	termination
7	$:O \rightarrow$ wall	termination
8	$.OH \rightarrow$ wall	termination
9	$.HO_2 + H_2 \rightarrow .H + H_2O_2$	initiation *
10	$2\ .HO_2 \rightarrow H_2O_2 + O_2$	termination
11	$H_2O_2 \rightarrow 2\ .OH$	initiation, branching

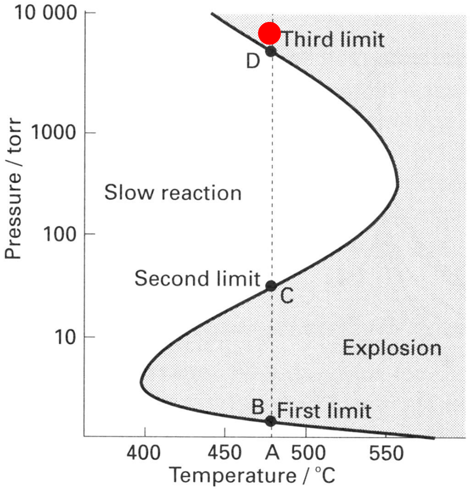

above the 3rd explosion limit

Reactions (9), (10), and (11) become important. While reaction 10 has been classed as a termination, it is a key reaction in this region, because it forms H2O2, which leads to branching

→ explosion

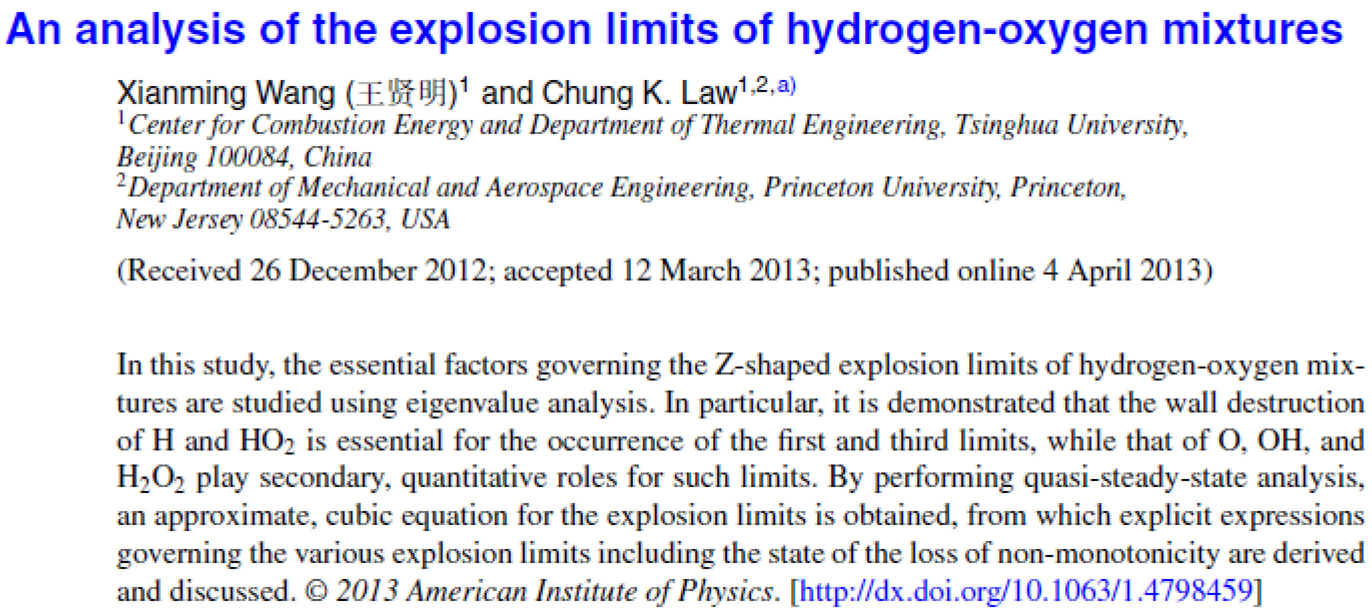

An analysis of the explosion limits of hydrogen-oxygen mixtures

Xianming Wang (王贤明)[1] and Chung K. Law[1,2,a)]
[1]*Center for Combustion Energy and Department of Thermal Engineering, Tsinghua University, Beijing 100084, China*
[2]*Department of Mechanical and Aerospace Engineering, Princeton University, Princeton, New Jersey 08544-5263, USA*

(Received 26 December 2012; accepted 12 March 2013; published online 4 April 2013)

In this study, the essential factors governing the Z-shaped explosion limits of hydrogen-oxygen mixtures are studied using eigenvalue analysis. In particular, it is demonstrated that the wall destruction of H and HO_2 is essential for the occurrence of the first and third limits, while that of O, OH, and H_2O_2 play secondary, quantitative roles for such limits. By performing quasi-steady-state analysis, an approximate, cubic equation for the explosion limits is obtained, from which explicit expressions governing the various explosion limits including the state of the loss of non-monotonicity are derived and discussed. © *2013 American Institute of Physics*. [http://dx.doi.org/10.1063/1.4798459]

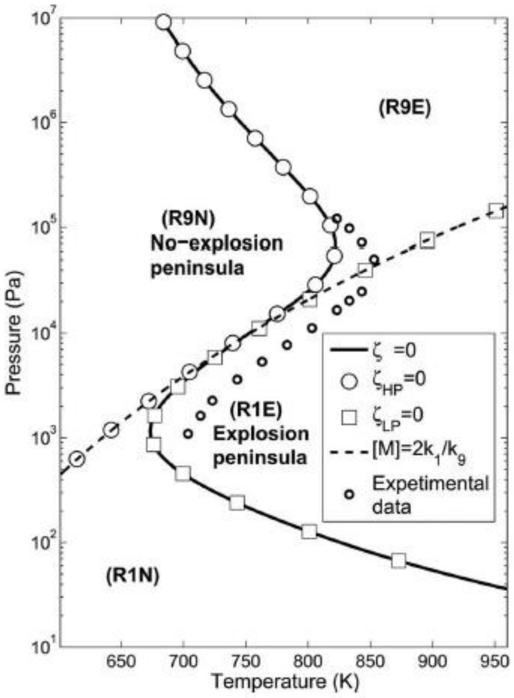

Discusses the explosion limits for H2/O2

Also Liang and Law
Phys.Chem.Chem.Phys.,
2018, 20, 742
An analysis of the explosion limits of hydrogen/oxygen mixtures with nonlinear chain reactions

Topic 2

Measurement of rate coefficients for elementary reactions

Measurement of rates of elementary reactions 1

- Concentrate on reactions of atoms and radicals; say something briefly about reactions that don't involve radicals and are involved in initiation steps
- Need to cover a range of *T* from 1000 to 3000 K for reactions involved in high temperature combustion reactions; 600 – 1000 K for low *T* oxidation in the autoignition regime; 200 - 300 K for reactions of combustion generated pollutants in the lower atmosphere (the troposphere)

Measurement of rates of elementary reactions 2

- Ideally, isolate the individual reaction and study it at the appropriate combustion conditions.
- Not always possible:
  - May have to model the system to extract rate coefficients of interest
  - May need to extrapolate to appropriate T, p. Ideally achieve this with the help of theory (see Topic 3).

Techniques

- Pulsed laser photolysis (laser flash photolysis)
- Shock tubes
- Flow tubes for elementary reactions and whole systems
- Static studies of whole systems

Pulsed laser photolysis

Laser flash photolysis (LFP) / laser induced fluorescence (LIF) for the study of OH + reactant

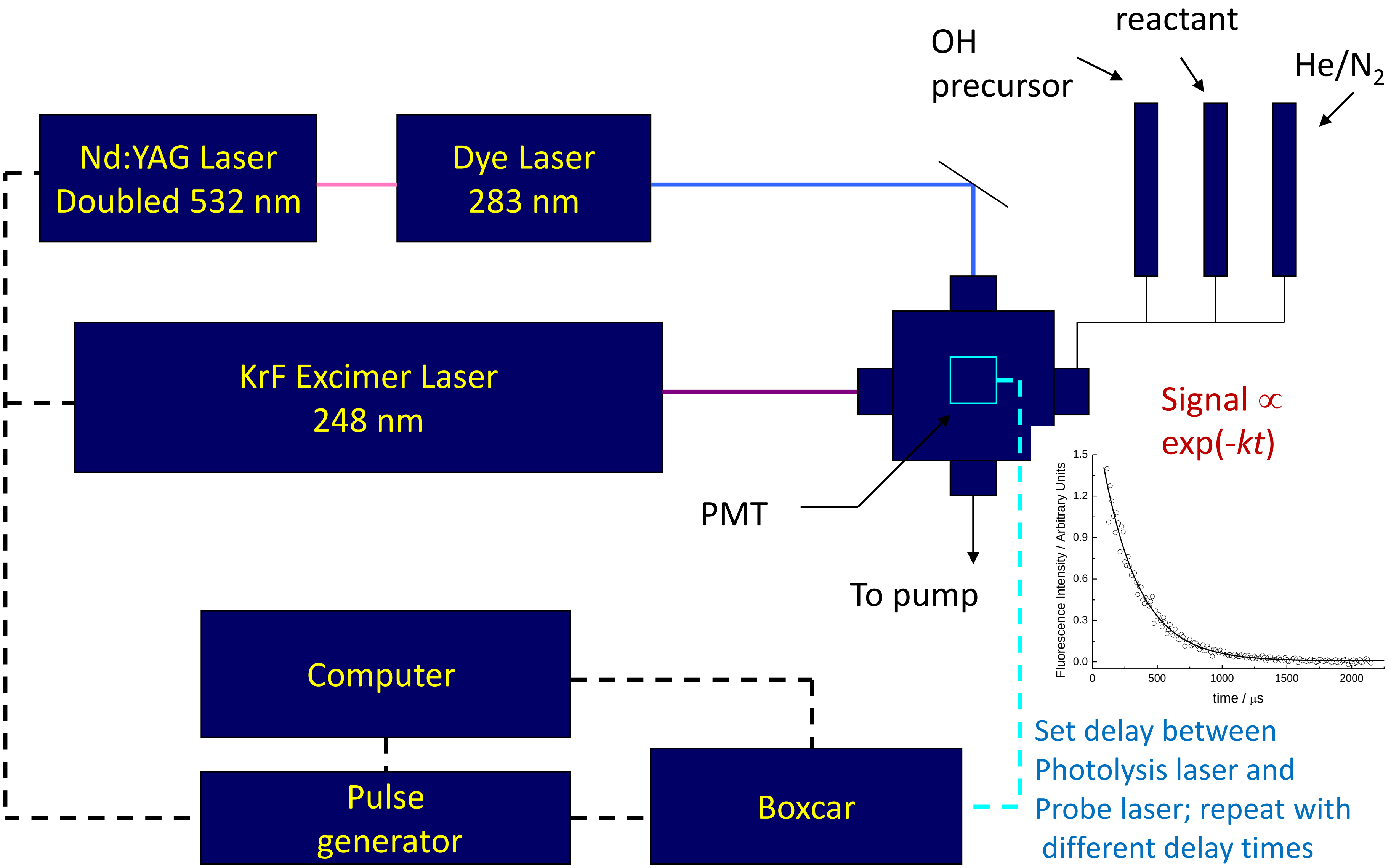

Nd:YAG Laser
Doubled 532 nm

Dye Laser
283 nm

OH
precursor

reactant

He/N_2

KrF Excimer Laser
248 nm

PMT

To pump

Signal ∝ exp(-*kt*)

Computer

Pulse
generator

Boxcar

Set delay between
Photolysis laser and
Probe laser; repeat with
different delay times

Procedure for determining rate coefficients for pseudo first order reactions using LFP for OH + SO_2

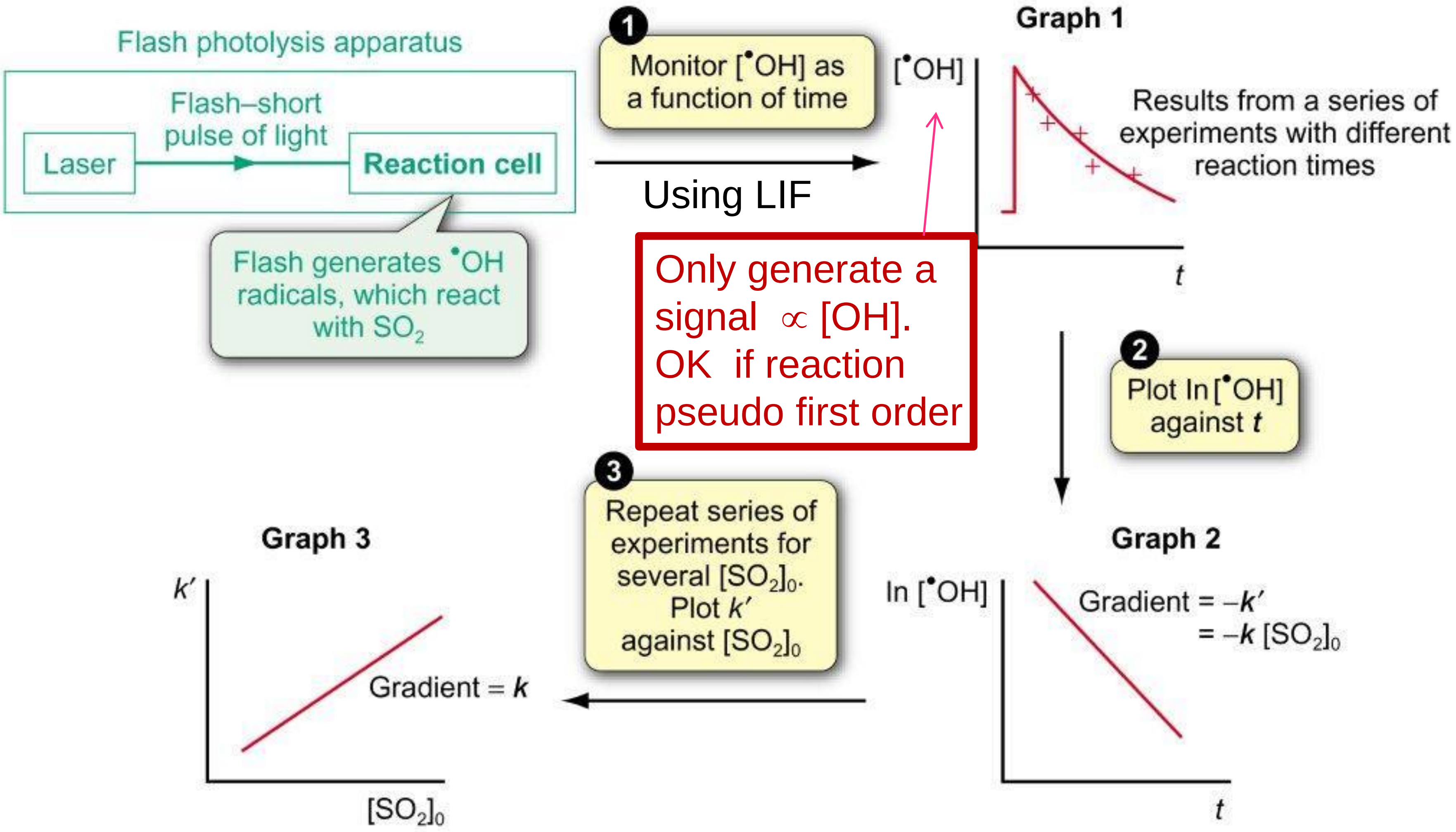

Flash generates $^{\bullet}$OH radicals, which react with SO_2

1 Monitor [$^{\bullet}$OH] as a function of time

Using LIF

Results from a series of experiments with different reaction times

Only generate a signal $\propto$ [OH]. OK if reaction pseudo first order

2 Plot ln [$^{\bullet}$OH] against ***t***

3 Repeat series of experiments for several $[SO_2]_0$. Plot k' against $[SO_2]_0$

$OH + C_2H_2 + M \rightarrow C_2H_2OH + M$
Cleary et al. J. Phys. Chem., 2007, 111, 4043-4055

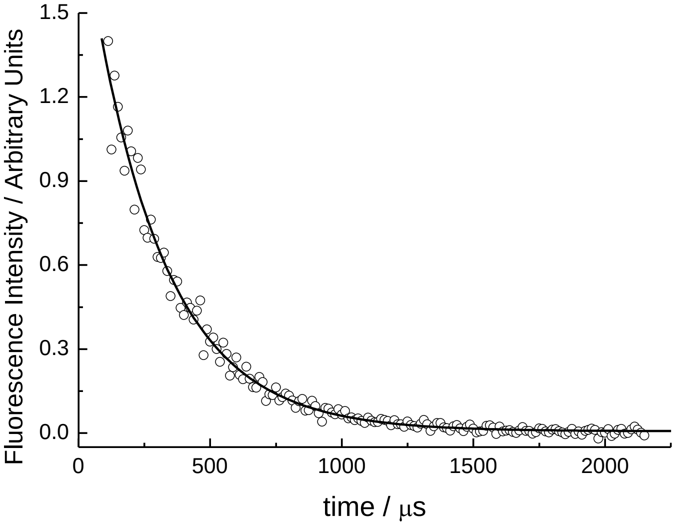

- Pressure dependent (association) reaction.
- Study as a function of temperature and pressure

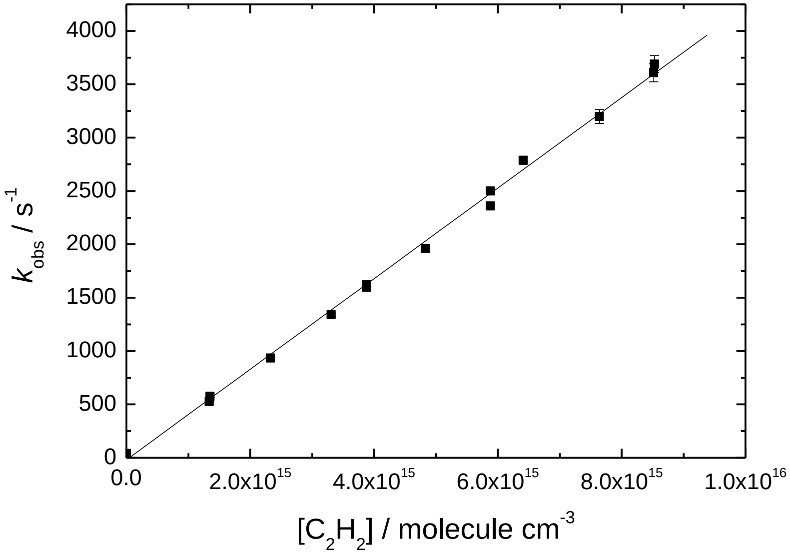

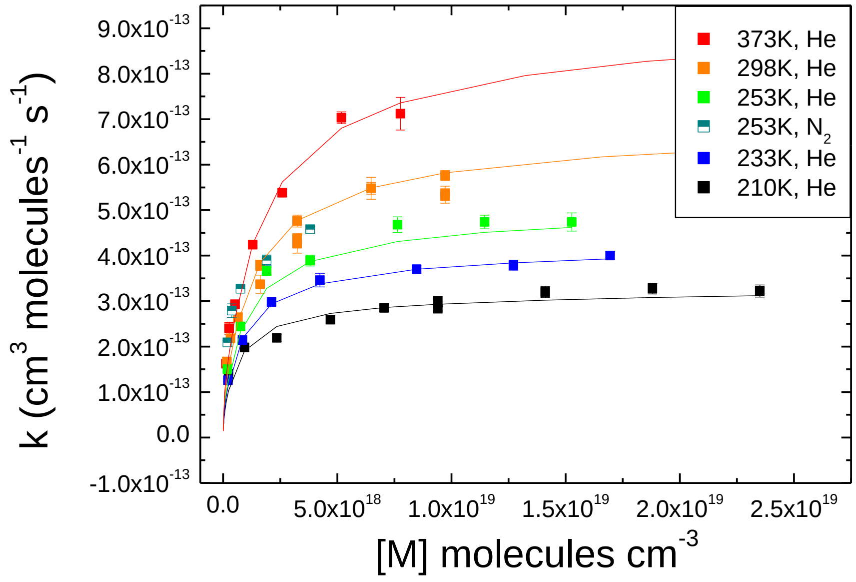

OH + acetone, J N Crowley, JPCA, 2000, **104**,2695

laser flash photolysis, resonance fluorescence/laser induced fluorescence to measure [OH] (relative). Optical measurement of [acetone] before and after reactor.

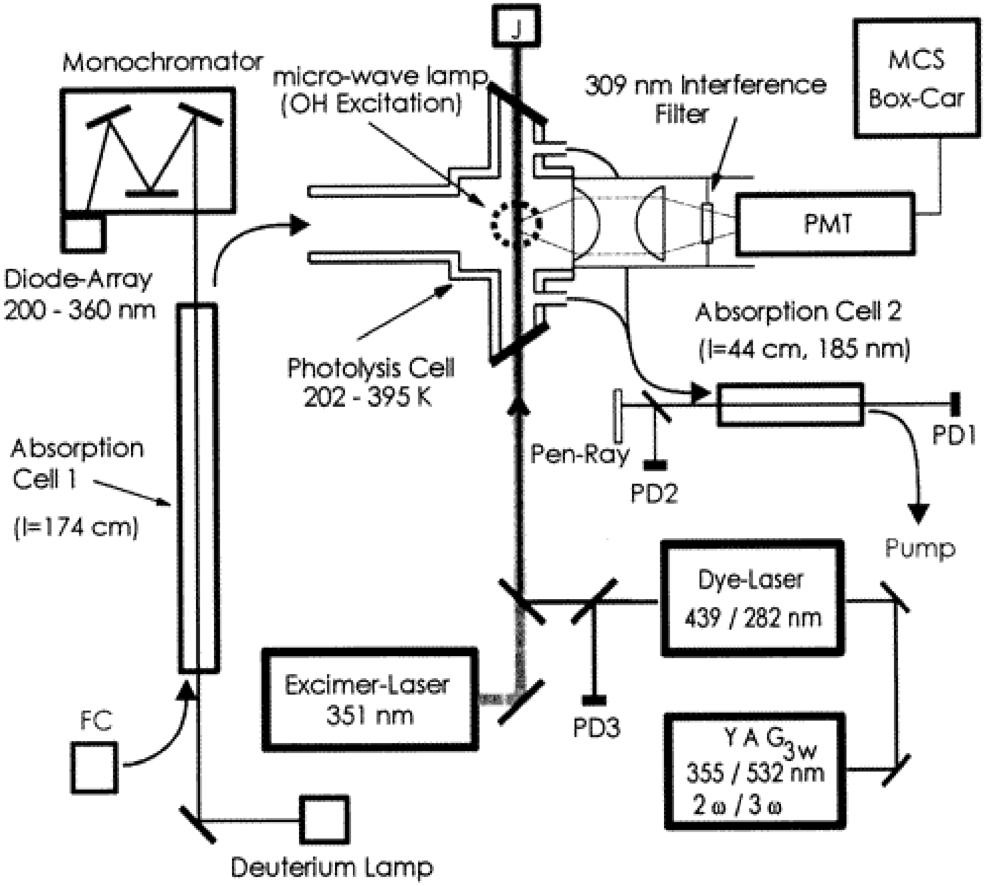

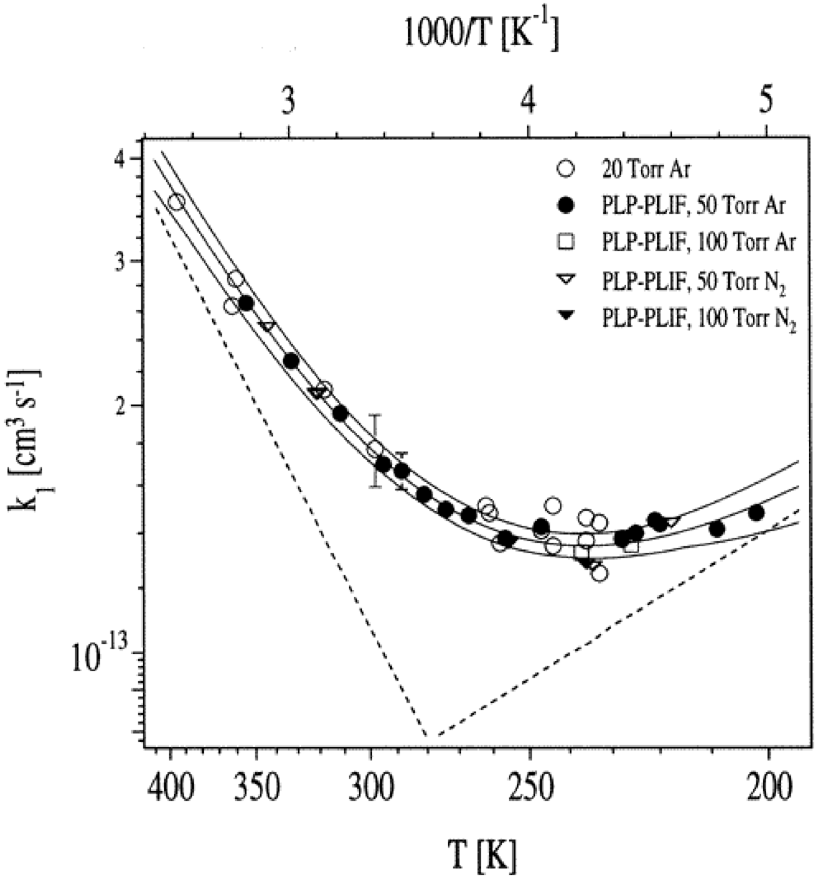

Minimising secondary reactions

- In order to be able to use a simple pseudo first order approach to the analysis of the data, secondary reactions must play a negligible role.
- This involves keeping the initial radical concentration low.
- See Vaghjiani and Ravishankara (Nature, 1991, 350, 406) for a classic experimental analysis of this problem for $OH + CH_4 \rightarrow CH_3 + H_2O$.
- Typical radical decay timescales in pulsed photolysis reactions are ~ 0.1 – 1 ms
- $k(OH + CH_3)$ is ~ 10^{-10} cm^3 $molecule^{-1}$ s^{-1}. The timescale for removal of OH by this reaction is ~ 0.1 s for $[CH_3] = 10^{11}$ cm^{-3} and 1 ms for $[CH_3] = 10^{13}$ cm^{-3} . So it is essential to keep the amount of OH generated in the photolysis pulse low if this secondary reaction is to make a negligible contribution to the observed decay of OH.
- Need a sensitive detection technique – LIF is ideal.

Detection using time of flight mass spectrometry

Blitz et al. Rev. Sci. Inst. 2007, 78, 034103

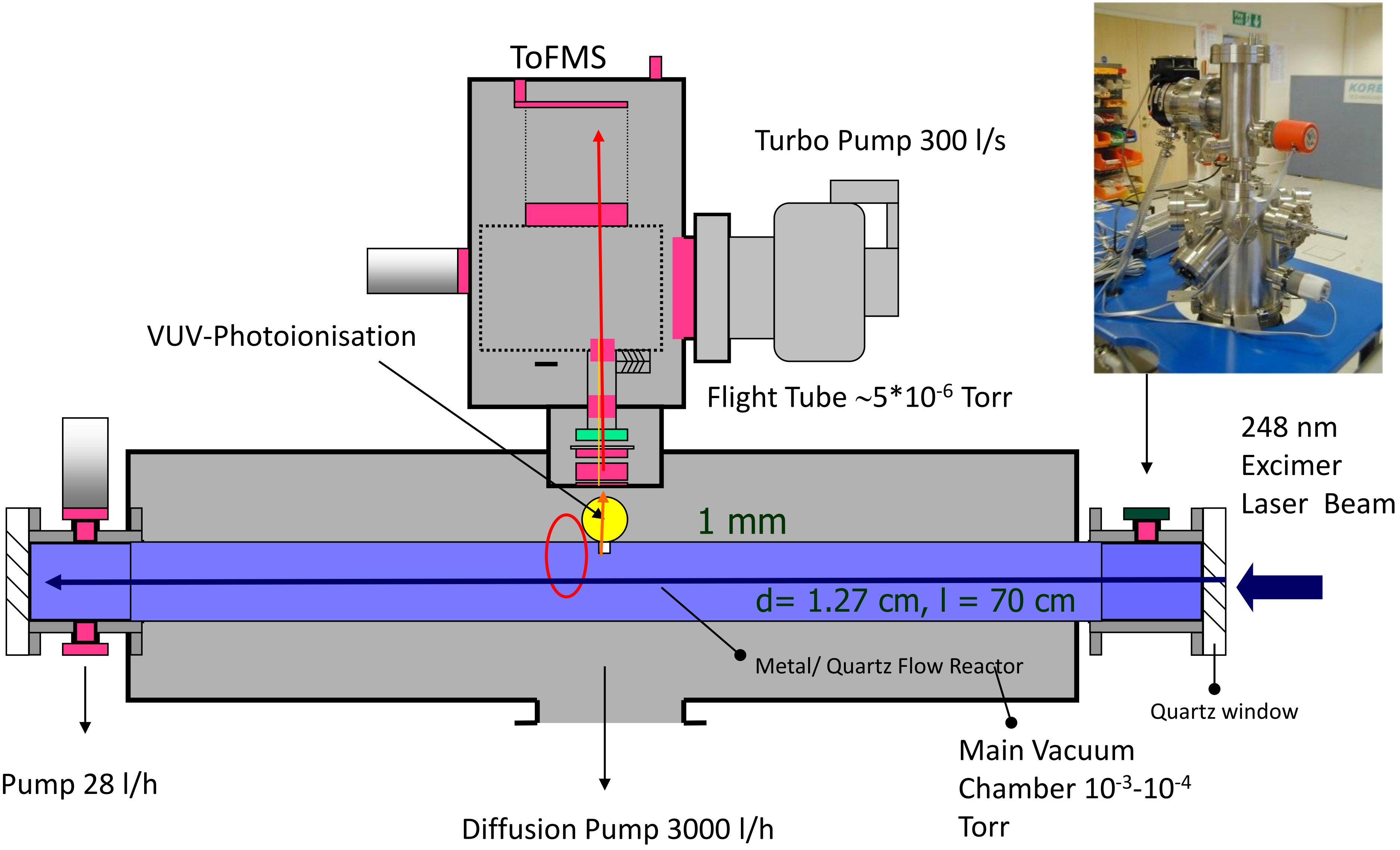

ToFMS

Turbo Pump 300 l/s

VUV-Photoionisation

Flight Tube ~$5*10^{-6}$ Torr

248 nm
Excimer
Laser Beam

1 mm

d= 1.27 cm, l = 70 cm

Metal/ Quartz Flow Reactor

Quartz window

Pump 28 l/h

Main Vacuum
Chamber 10^{-3}-10^{-4}
Torr

Diffusion Pump 3000 l/h

Application of synchrotron radiation for photoionization (SVUV-PIMS) to distinguish isomers in flames

1. ALS, USA

- ALS is tuneable and so it is feasible to distinguish isomers, which have the same mass, through their differing photoionization efficiency curves.
- Traces show m/z=44 for different flames:

acetaldehyde: CH_3CHO

ethenol: $CH_2=CHOH$

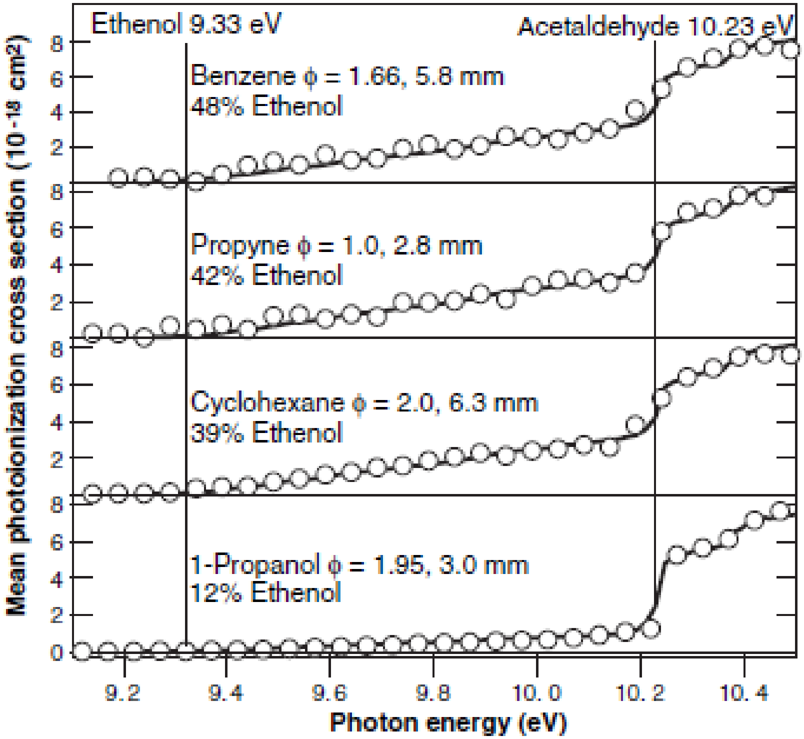

Taatjes et al. *Science* 2005, **308**, 1887

2. NSRL China
Various butanol flames,

- Yang et al.Combust. Flame 148 (2007) 198-209.

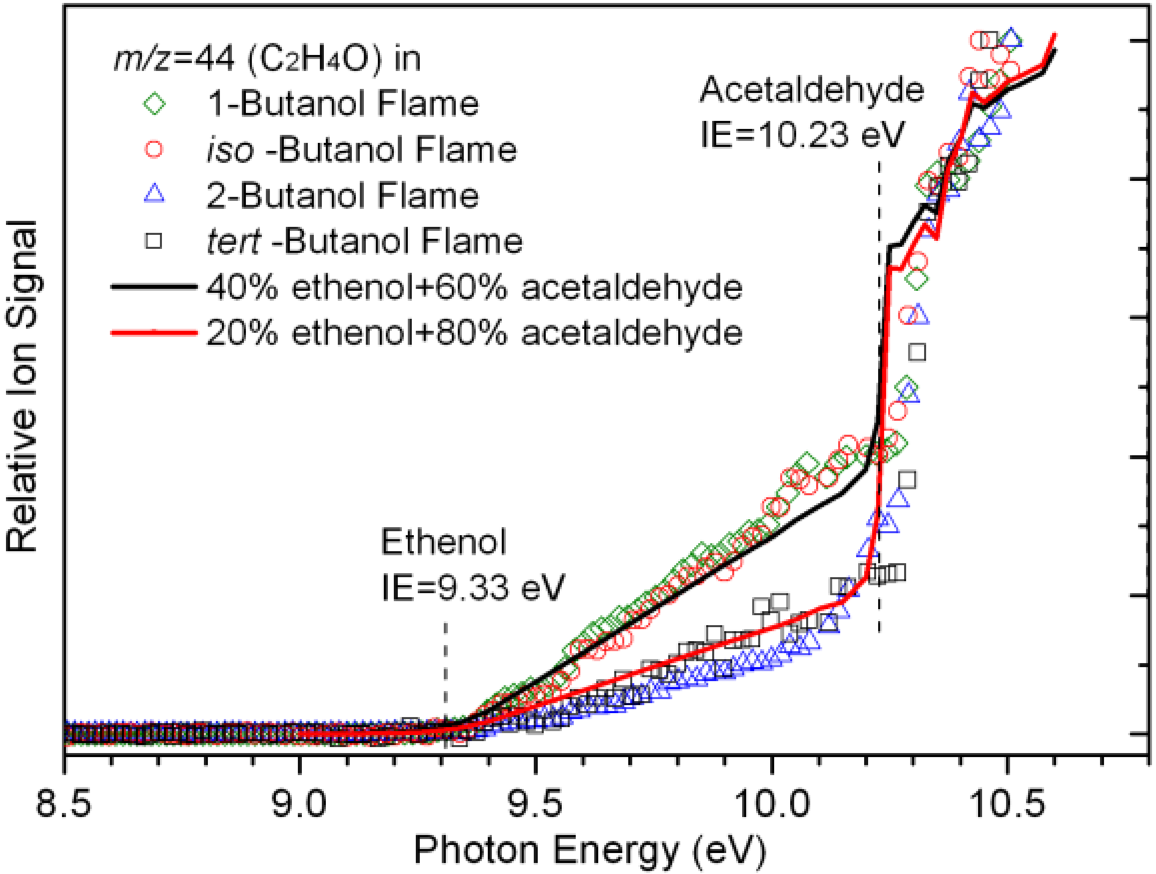

SVUV-PIMS for kinetics
Taatjes et al., PCCP, 2008, 10, 20 – 34

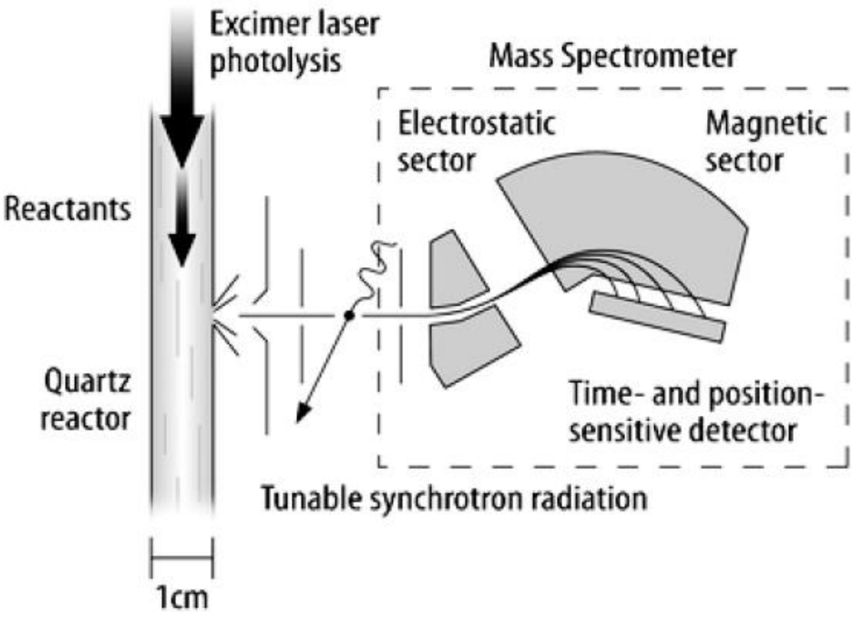

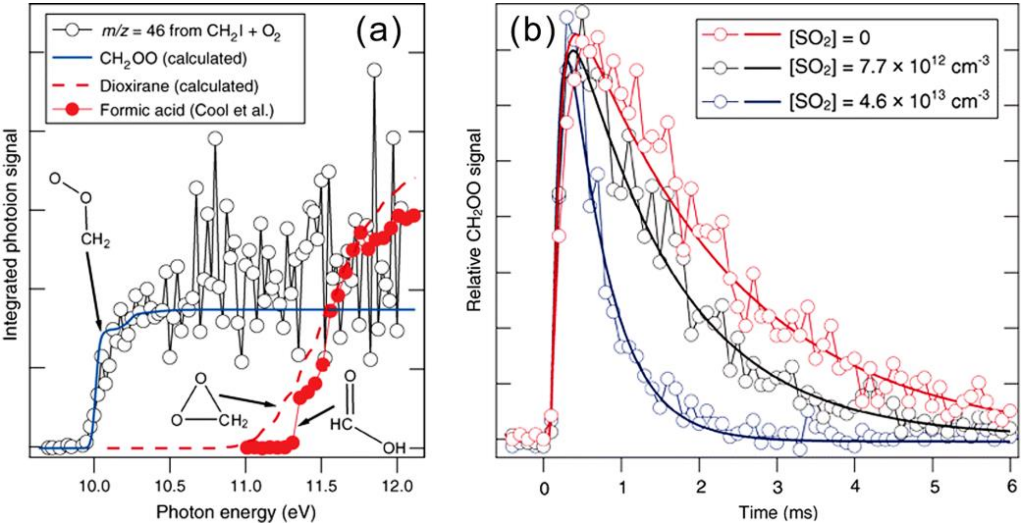

(a) The calculated photoionization spectra of the Criegee intermediate CH_2OO and dioxirane, the experimental photoionization spectrum for formic acid, as well as schematic chemical structures, are shown.

(b) Time-dependent CH_2OO signals for various concentrations of SO_2. Solid lines represent fits to the data traces, including convolution with a measured instrument response function, from which pseudo–first order decay constants are derived Welz et al. Science 335, 204-207

Radical detection using absorption spectroscopy: $C_3H_5 + C_3H_5$

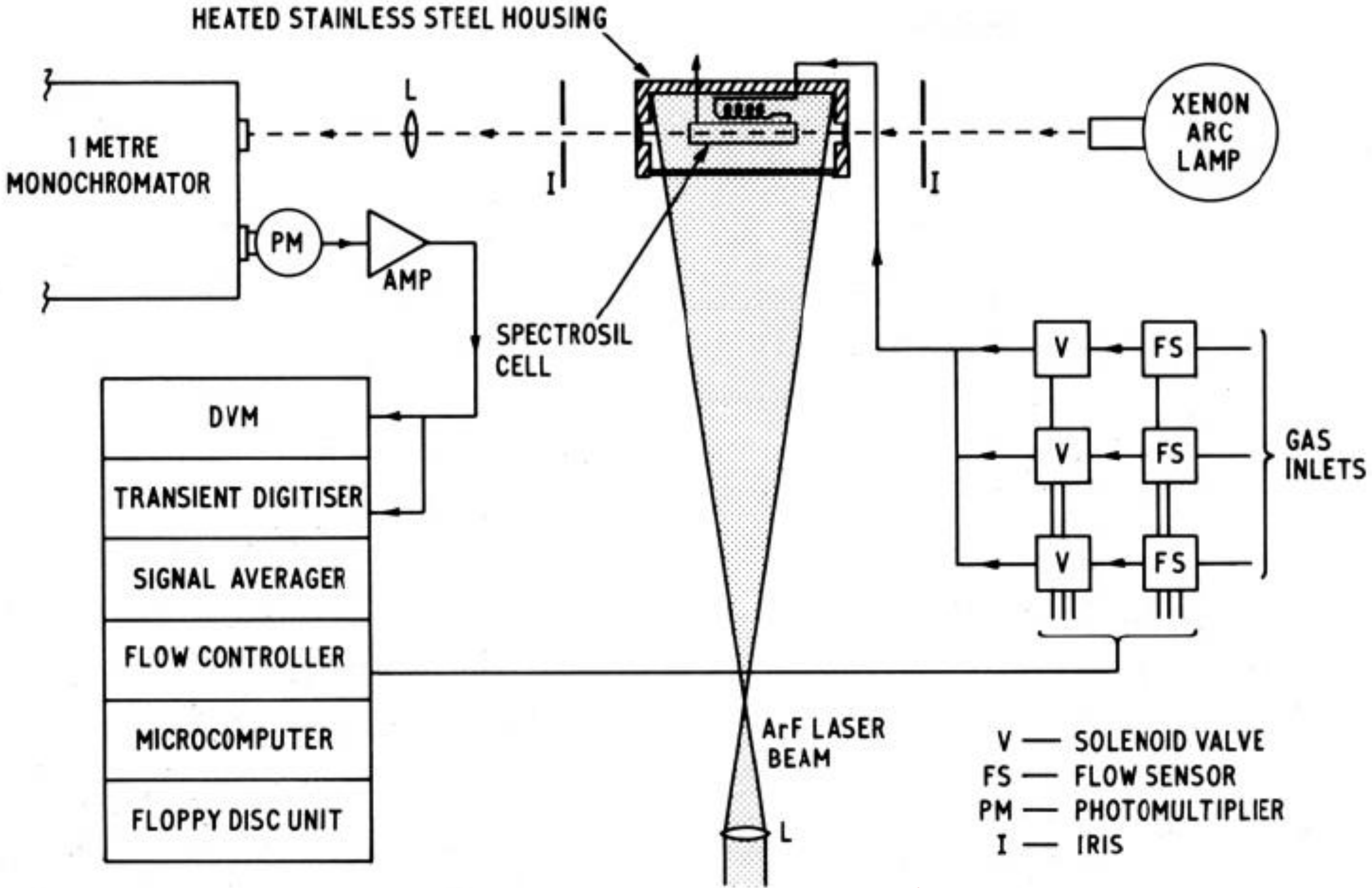

Reaction is second order in the radical – need the absolute concentration to determine *k*.

Tulloch et al. *J. Phys. Chem. l982, 86, 3812-3819*

C_3H_5 + C_3H_5 :Absorption spectroscopy 2

- Reaction is second order in C_3H_5
- Need to know absolute concentration of radical – absorption spectroscopy provides a good route to this. (see J. Phys. Chem. 1985, 89, 2268-2274 for discussion for CH_3)
- $I/I_0 = \exp(-\sigma[C_3H_5]L)$ where I_0 is the incident and I the transmitted light intensity, σ is the absorption cross section and L is the path length.
- Similar method applied to CH_3 + CH_3. See Topic 3 for analysis of multiple determinations using master equation approach.

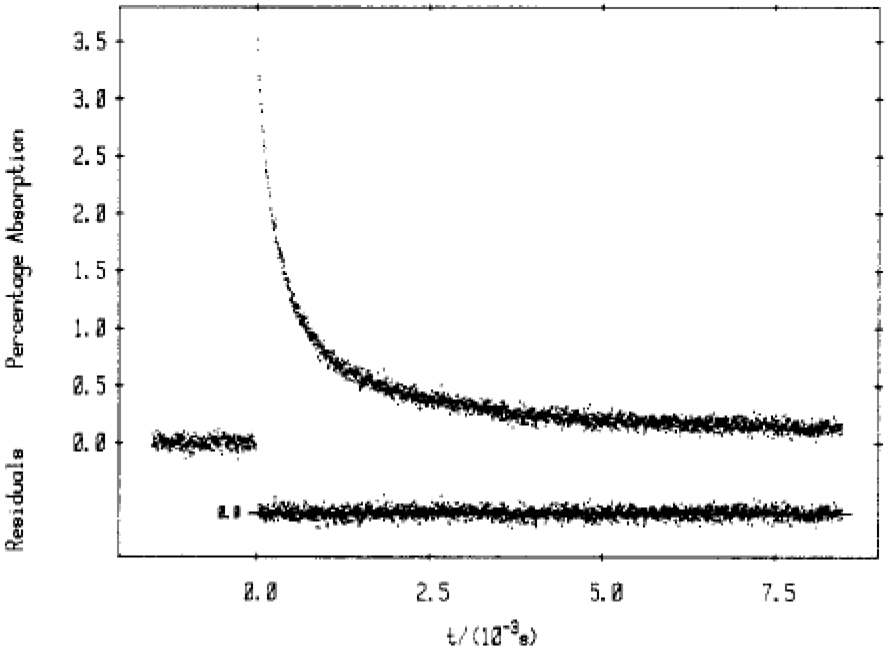

Experimental determination of *k* (CH_3 + H))

- This reaction presents an additional problem – the need to detect two radicals
- Laser flash photolysis producing H and CH_3 with $[H] \ll [CH_3]$
- H by resonance fluorescence, CH_3 by absorption. Need absolute $[CH_3]$, since $k'(H) = k[CH_3]$
- Brouard et al. J. Phys. Chem. 1989, 93, 4047-4059

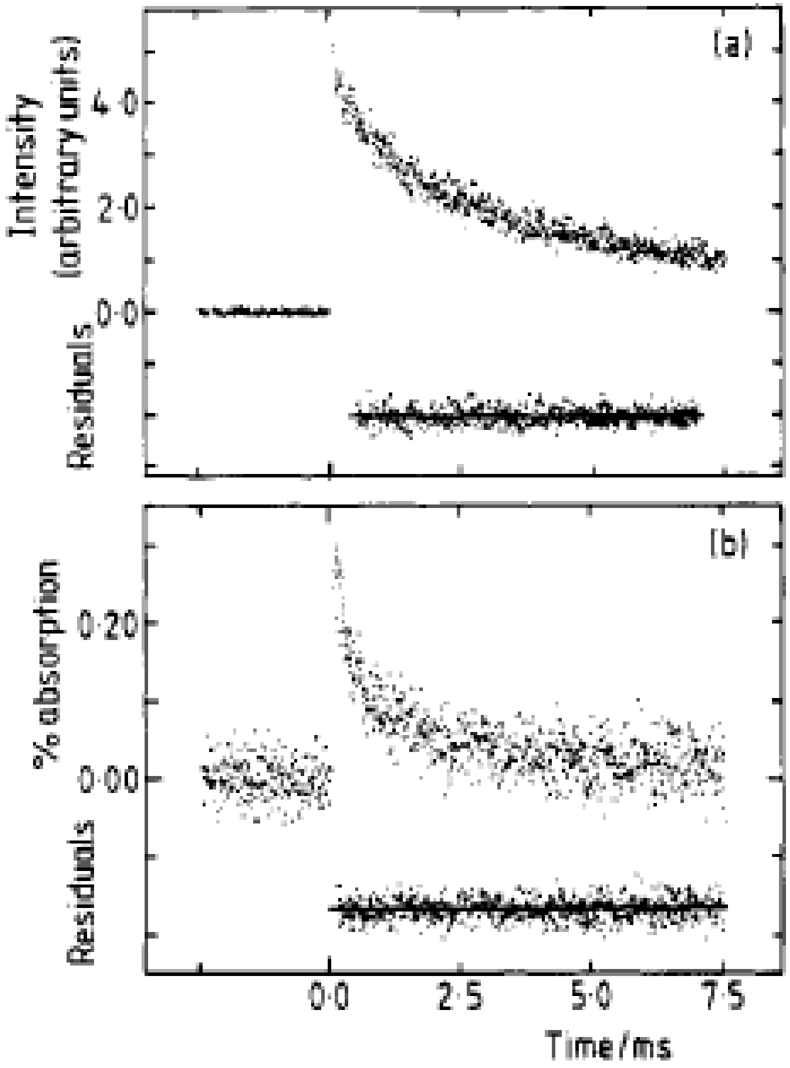

From $1/[CH_3] = 1/[CH_3]_0 + 2k_2t$

Experimental results for CH_3 + H

CH_3 absorption analysed via

$$D(t) = 1 - \exp\{-(\Delta_0^{-1} - \frac{2k_2t}{\sigma L})^{-1}$$

$\Delta_0 = \sigma[CH_3]_0L$

Where $D(t)=\Delta I/I_0$, Δ_0 is the peak optical density, σ is the absorption cross section and L is the path length.

H fluorescence analysed via

$$[H] = [H]_0\left\{1 + \frac{2k_2\Delta_0t}{\sigma L}\right\}^{-\frac{k_1}{2k_2}} \exp(-k_3t)$$

- Where k_2 refers to CH_3 + CH_3 and k_3 to other 1st order loss processes for
- Plot shows rate coefficients vs *p* at 300, 400, 500, 600 K.

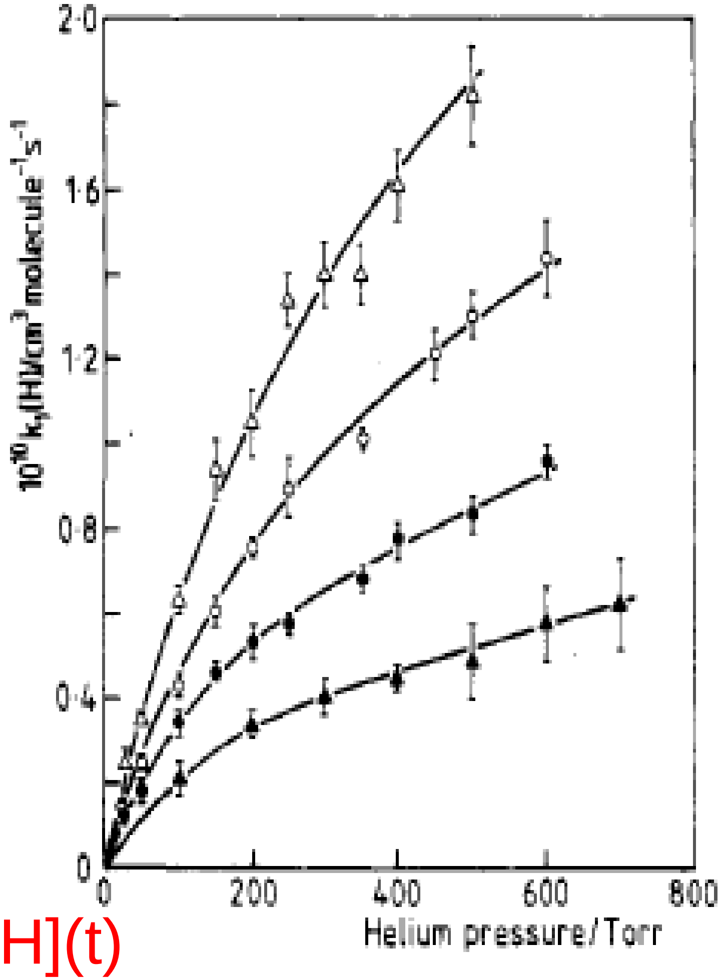

From $d[H]/dt = - k_1[H](t)[CH_3](t) – k_3[H](t)$

CH_3 + H. Parameterisation and determination of k^∞

- Parameterisation using Troe method (next slides)
- Also determined k^∞ using master equation method coupled with inverse Laplace transform (see later)

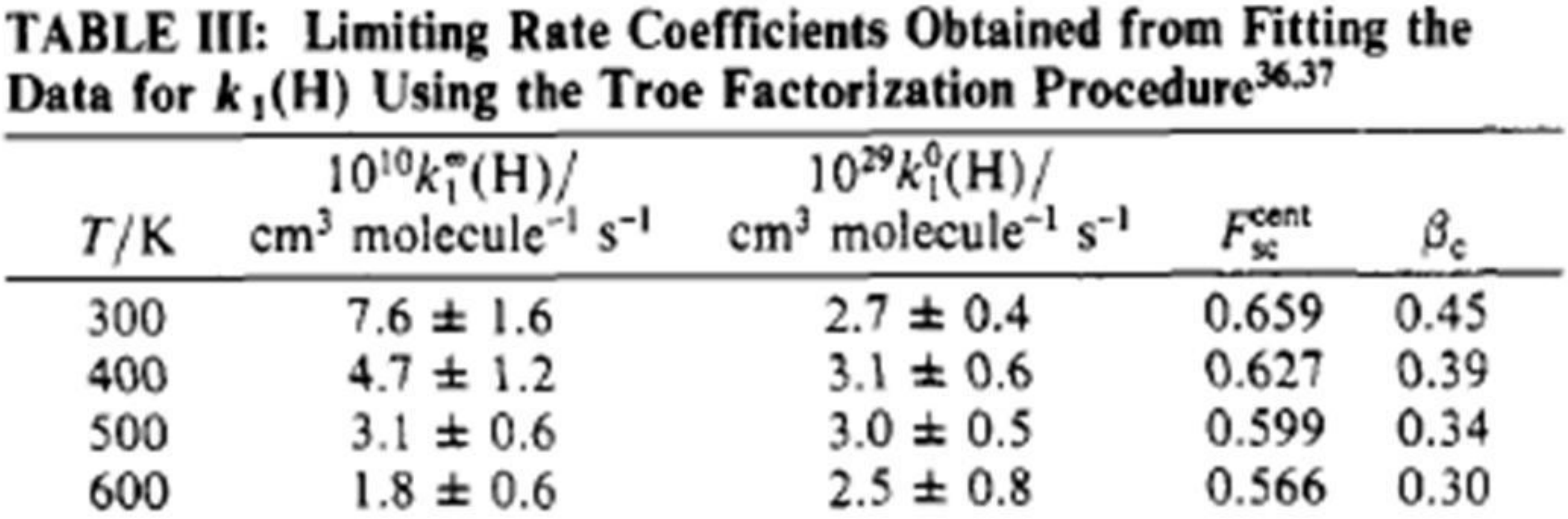

TABLE III: Limiting Rate Coefficients Obtained from Fitting the Data for k_1(H) Using the Troe Factorization Procedure[36,37]

T/K	$10^{10}k_1^\infty$(H)/ cm^3 molecule^{-1} s^{-1}	$10^{29}k_1^0$(H)/ cm^3 molecule^{-1} s^{-1}	F_{sc}^{cent}	β_c
300	7.6 ± 1.6	2.7 ± 0.4	0.659	0.45
400	4.7 ± 1.2	3.1 ± 0.6	0.627	0.39
500	3.1 ± 0.6	3.0 ± 0.5	0.599	0.34
600	1.8 ± 0.6	2.5 ± 0.8	0.566	0.30

Recall earlier slide: Pressure dependent association reactions

$$A + B \underset{k_{-a}}{\overset{k_a}{\rightleftharpoons}} AB^* \xrightarrow{k_s[\mathrm{M}]} AB.$$

$$k = \frac{k_a\, k_s[\mathrm{M}]}{k_{-a} + k_s[\mathrm{M}]}$$

$$\text{As } [\mathrm{M}] \rightarrow \infty, k \rightarrow k_a = k^\infty$$

$$\text{As } [\mathrm{M}] \rightarrow 0, k \rightarrow \frac{k_a k_s[M]}{k_{-a}} = k_0[\mathrm{M}]$$

$$k = \frac{k_0[\mathrm{M}]k^\infty}{k^\infty + k_0[\mathrm{M}]}$$

Similar treatment for dissociation reactions

- This is the Lindemann-Hinshelwood model of pressure dependent unimolecular reactions.
- The treatment is an approximation because (i) k_{-a} depends on the energy of AB* (ii) deactivation of AB* takes place in a number of steps.
- These have the effect of *broadening* the fall-off curve (k vs [M]). These effects have been incorporated in a fitting procedure developed by Troe that is widely used in parameterising rate coefficients for use in combustion modelling

Troe Fitting

Need to represent k(T,P) for Global Models

Standard is Troe Fitting

$$k(T,p) = \frac{k_0[M]k^\infty}{k^\infty + k_0[M]} F \qquad \log_{10} F = \frac{\log_{10} F_{cent}}{1 + \left[\frac{\log_{10}(p^*) + c}{N - d\left(\log_{10}(p^*) + c\right)} \right]^2}$$

$$p^* = k_0[M] / k^\infty \qquad d = 0.14$$

$$c = -0.4 - 0.67 \log_{10} F_{cent} \qquad N = 0.75 - 1.27 \log_{10} F_{cent}$$

Fit k_0 & k^∞ to modified Arrhenius $k_0 = A_0 T^{n_0} \exp(-E_0 / T)$

Fit F_{cent} to:

$$F_{cent} = (1-a)\exp\left(-T/T^{***}\right) + a\exp\left(-T/T^{*}\right) + \exp\left(-T^{**}/T\right)$$

For the most recent formulation of the broadening term, *F*, see
***Zeitschrift für Physikalische Chemie*, 2014; Vol. 228, p 1**

Detection of HCO using cavity ring down spectroscopy (CRDS)

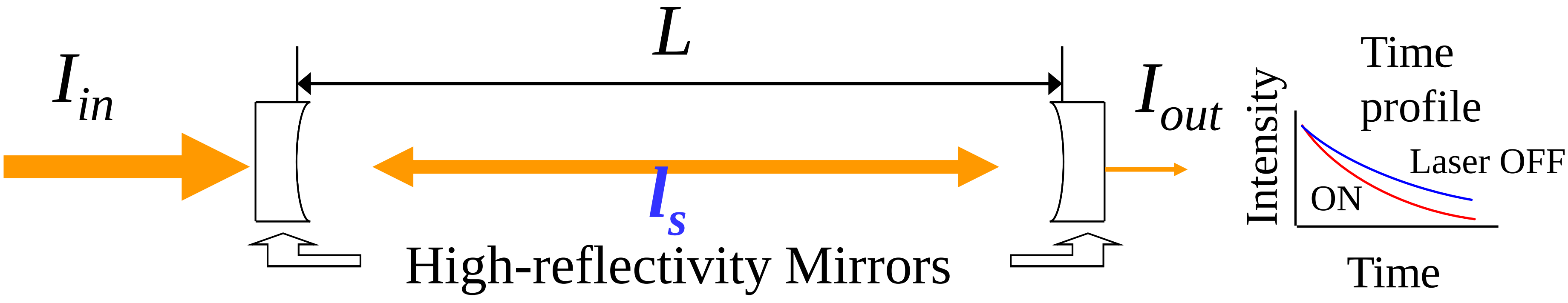

$$(1/k_{OFF}) - (1/k_{ON}) = A\ (\sigma cl)$$

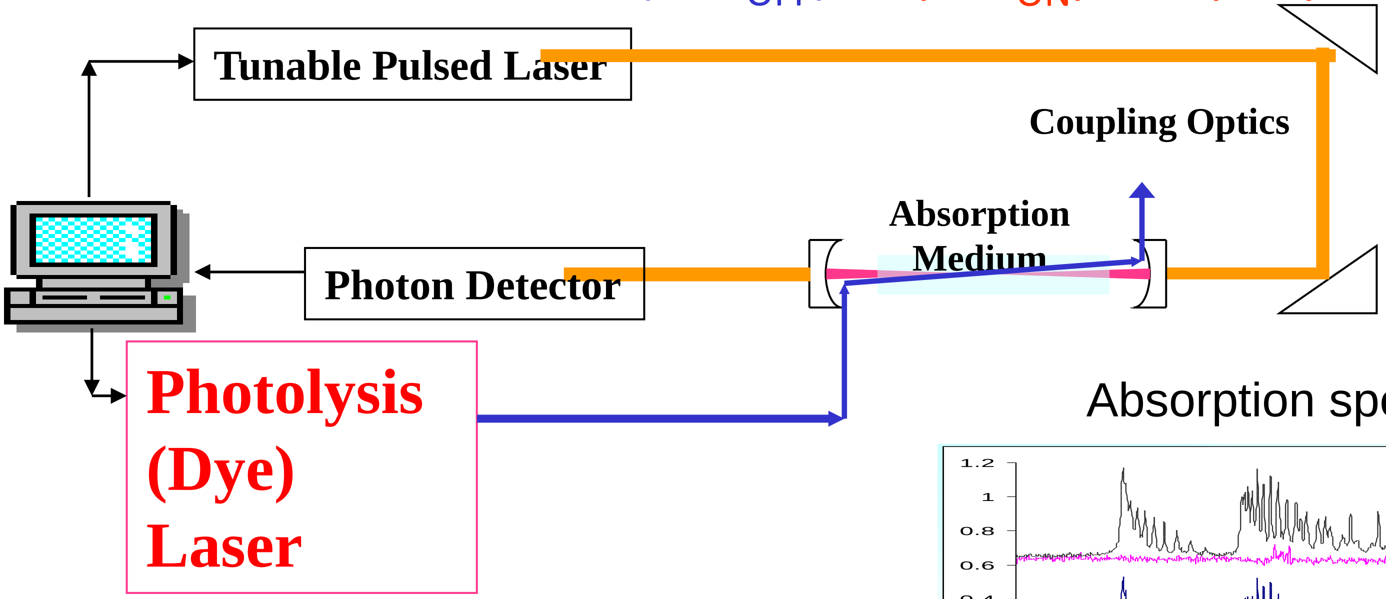

Absorption spectrum of HCO

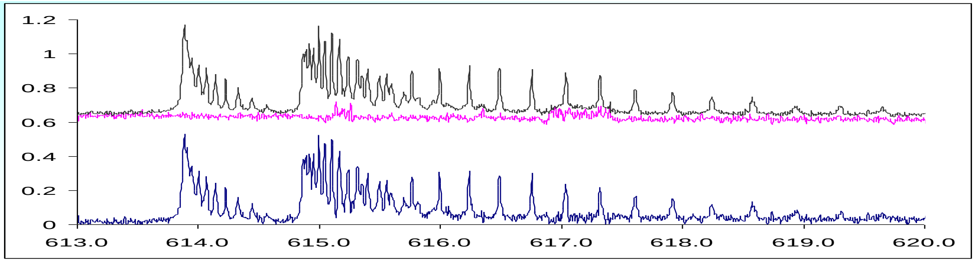

Determination of product yields by Laser Flash Photolysis 1

- Use laser pulse to generate radical on short timescale (~10 ns)
- Observe radical concentration vs time. Obtain kinetics from decay time constant
- Also observe product – calibration gives channel yield for a multichannel reaction:

$$^{1}CH_2 + H_2 \xrightarrow{k_{1a}} {}^{3}CH_2 + H_2$$

$$\xrightarrow{k_{1b}} CH_3 + H$$

- Detection technique: laser induced fluorescence for CH_2 and H
- Need to calibrate signals (used CH_2 reaction with a known yield of H
- Yield of H, α_H vs *T*:

	$^{1}CH_2 + H_2$
T/K	α_H
195	0.71 ± 0.07
298	0.85± 0.08
398	0.92 ± 0.08
500	1.01 ± 0.10

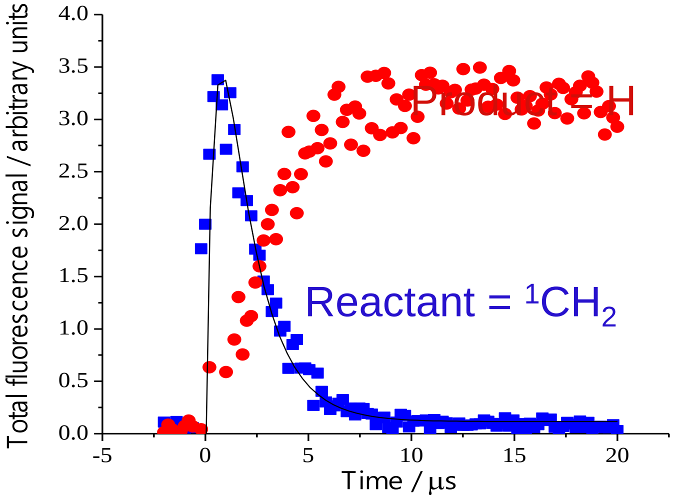

$^{1}CH_2 + H_2 \rightarrow CH_3 + H$

Determination of product yields by Laser Flash Photolysis 2 : $C_2H_5 + O_2$

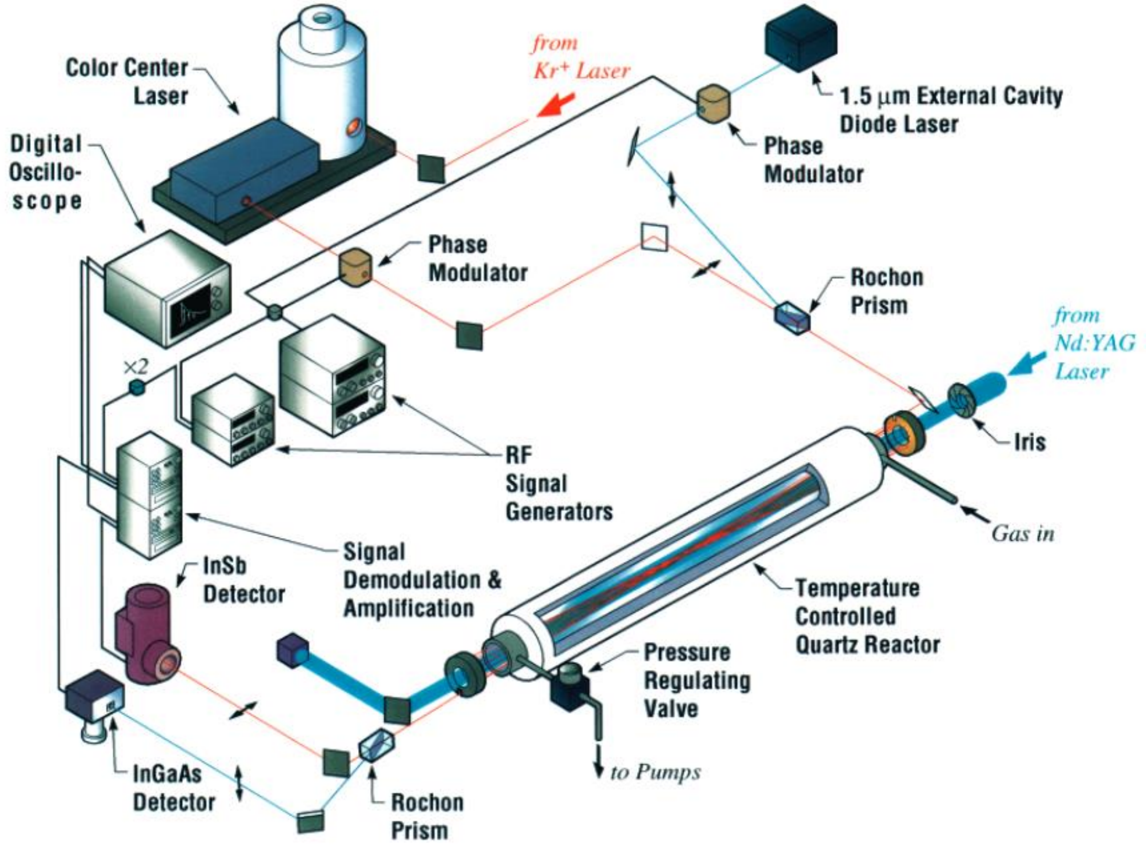

- Taatjes et al. (J. Phys. Chem. A 104 (2000) 11549 – 11560)
- laser photolysis/continuous wave (CW) infrared long-path absorption (LP/CWIRLPA) method

Determination of product yields by Laser Flash Photolysis 2 (contd): $C_2H_5 + O_2$

$$C_2H_5 + O_2 \overset{[M]}{\longleftrightarrow} C_2H_5O_2 \tag{1a}$$

$$\rightarrow C_2H_4 + HO_2 \tag{1b}$$

$$\rightarrow c - C_2H_4O(\text{oxirane}) + OH \tag{1c}$$

- Observed the formation of OH and HO_2, determining the fractional yields.
- Used 100% yield of HO_2 from $CH_2OH + O_2$ to calibrate the system.

$$Cl_2 \xrightarrow{h\nu(355\text{ nm})} 2Cl\bullet \tag{2}$$

$$Cl + CH_3OH \xrightarrow{100\%} CH_2OH + HCl \tag{4}$$

$$CH_2OH + O_2 \xrightarrow{100\%} HO_2 + CH_2O \tag{5}$$

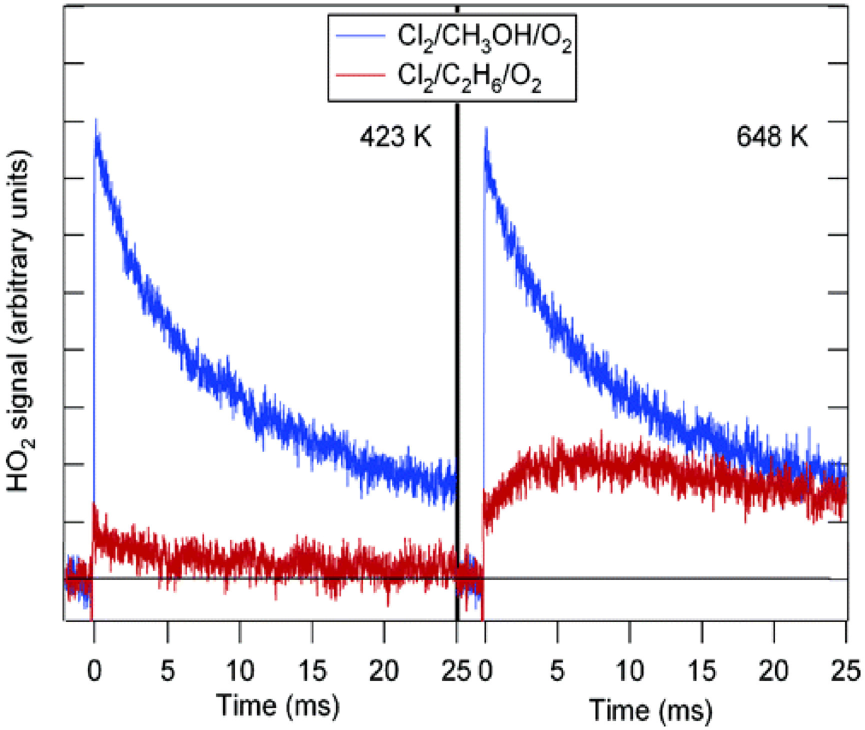

Blue traces, HO_2 from $Cl + CH_3OH$
C_2H_5 produced from $Cl + C_2H_6$
Red trace, HO2 from reaction 1
Growth is formation, decay reaction by HO_2+HO_2

Determination of product yields by Laser Flash Photolysis 2 (contd): $C_2H_5 + O_2$

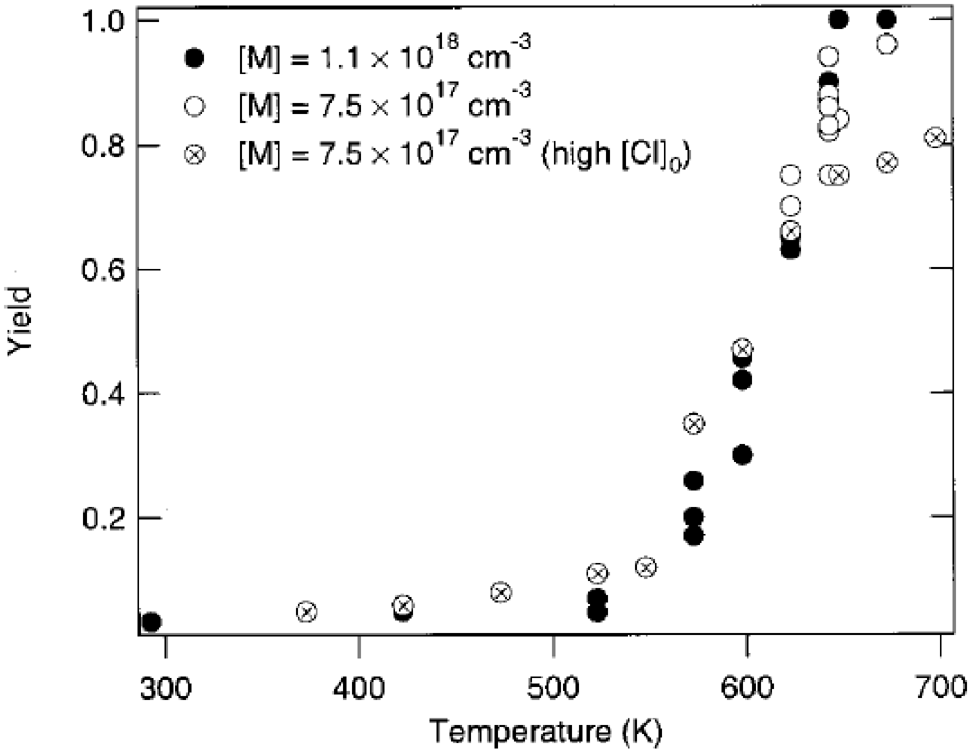

- HO_2 yield↑ as T↑ and p↓
- Two timescales at higher T
- OH yield is small.
- Theoretical interpretation and relevance to autoignition chemistry will be discussed later

Shock tubes

Shock tube - basics

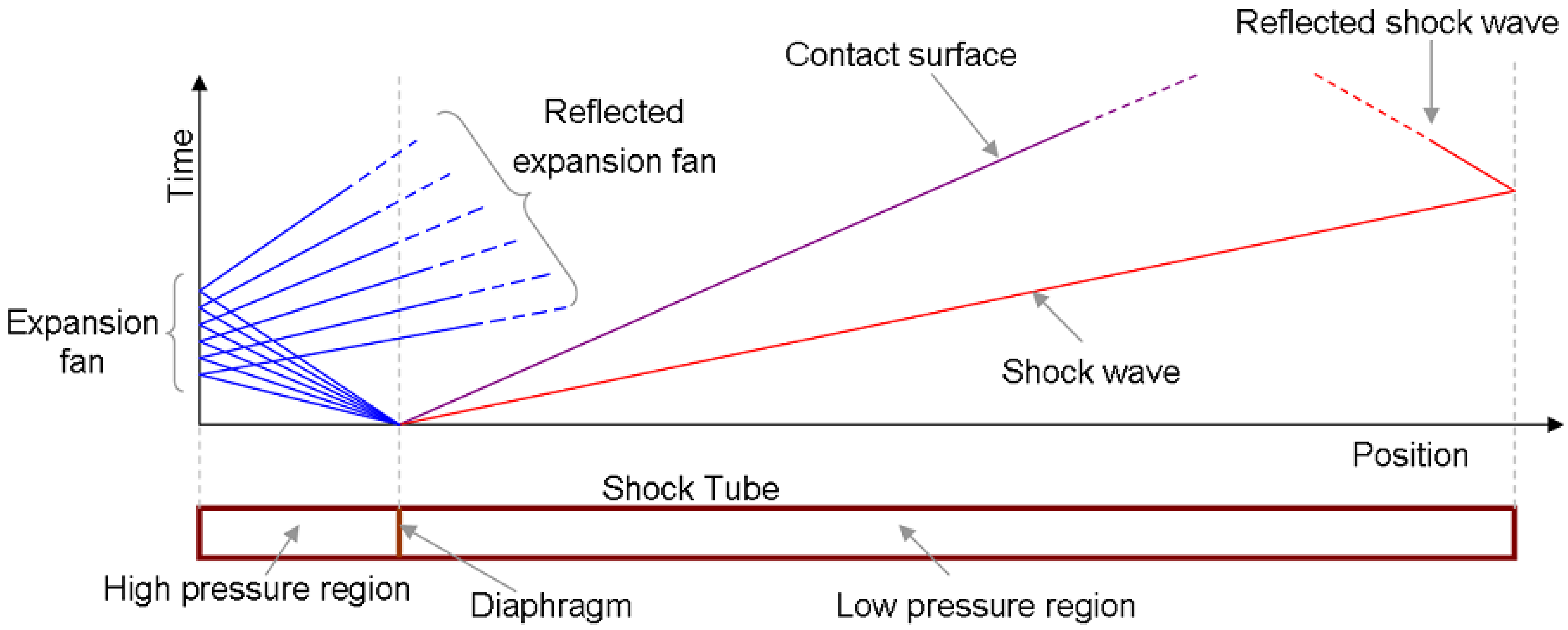

Shock tube:
Hanson lab at Stanford

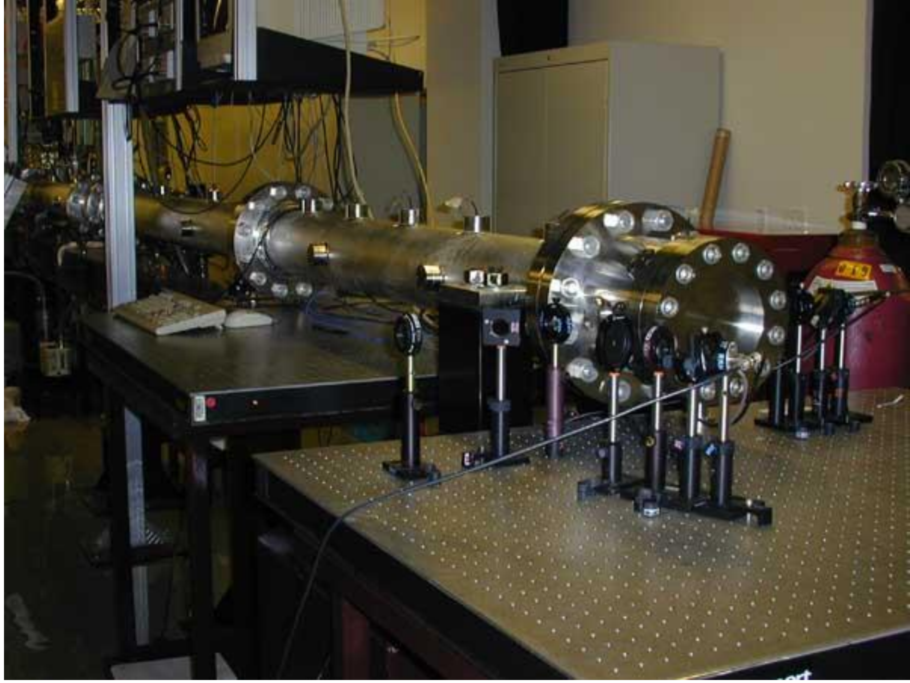

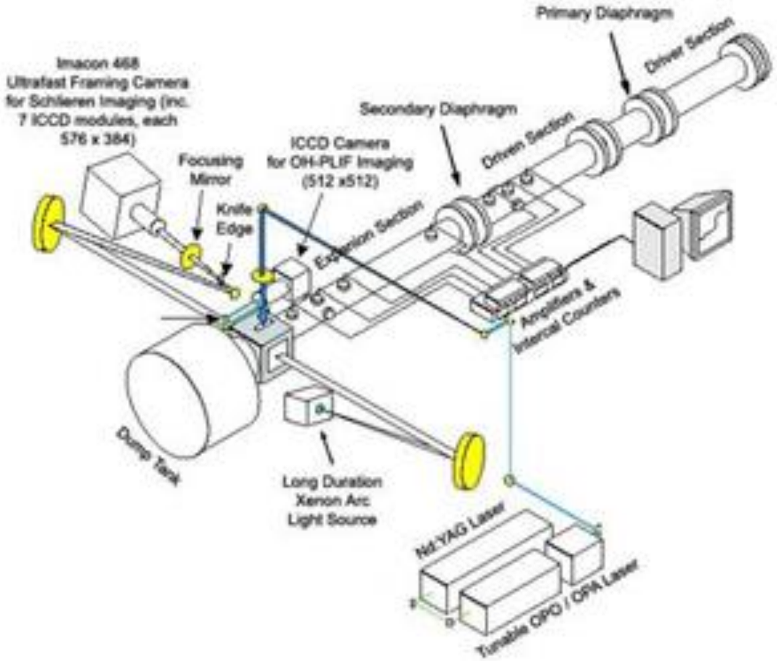

Shock tubes

- Compressive heating of reaction mixture
- Radicals generally formed from thermal dissociation of precursor
- Single shot, so no signal averaging, but impressive optimisation of signal
- Generally need to assess secondary reactions and use numerical chemical model with sensitivity analysis to show viability of measurements.
- Example: Measurement of CH_3 + OH by the Hanson group

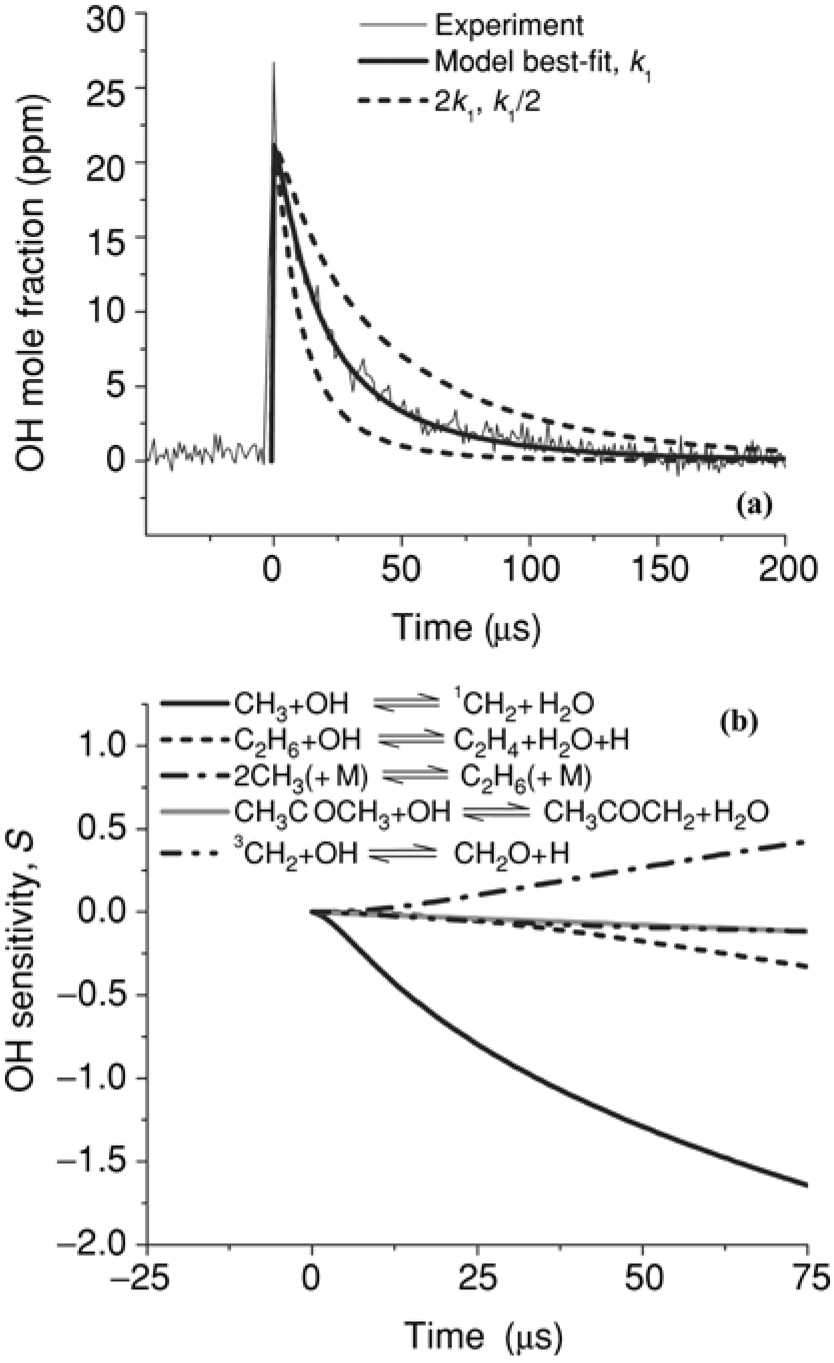

Vasudevan et al, International Journal of Chemical Kinetics (2008), 40(8), 488-495.

OH + HCHO, 934 K to 1670 K, 1.6 atm
Int J Chem Kinet 37: 98–109, 2005

- Behind reflected shock waves. OH radicals shock-heating tert-butyl hydroperoxide
- OH concentration time-histories were inferred from laser absorption using the R1(5) line of the OH A-X (0, 0) band near 306.7 nm.
- Other reactions contribute to the OH time profile, especially CH_3 + OH.
- Rate coefficient determined by fitting to detailed model (GRI-Mech – see Wednesday), with addition of acetone chemistry, deriving from dissociation of OH precursor (t-butylhydroperoxide). Detailed uncertainty analysis

Determination of *k* and uncertainty analysis

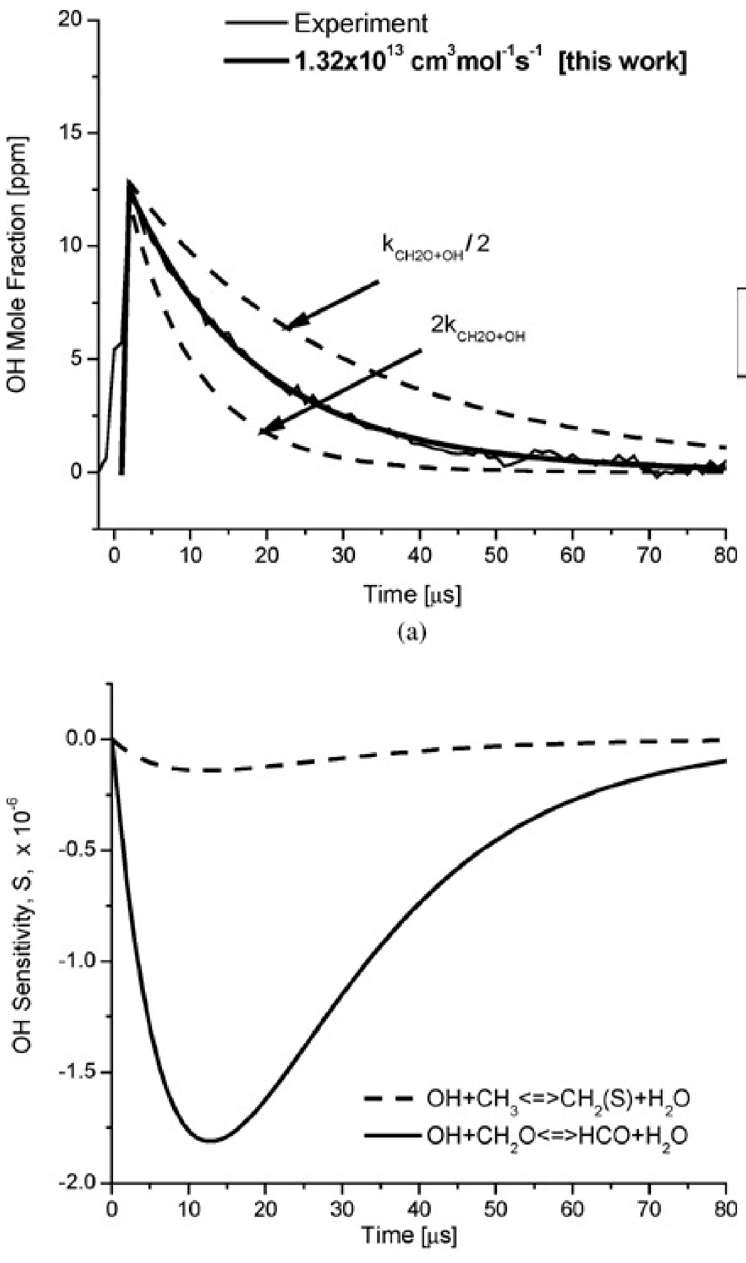

(a)

(b)

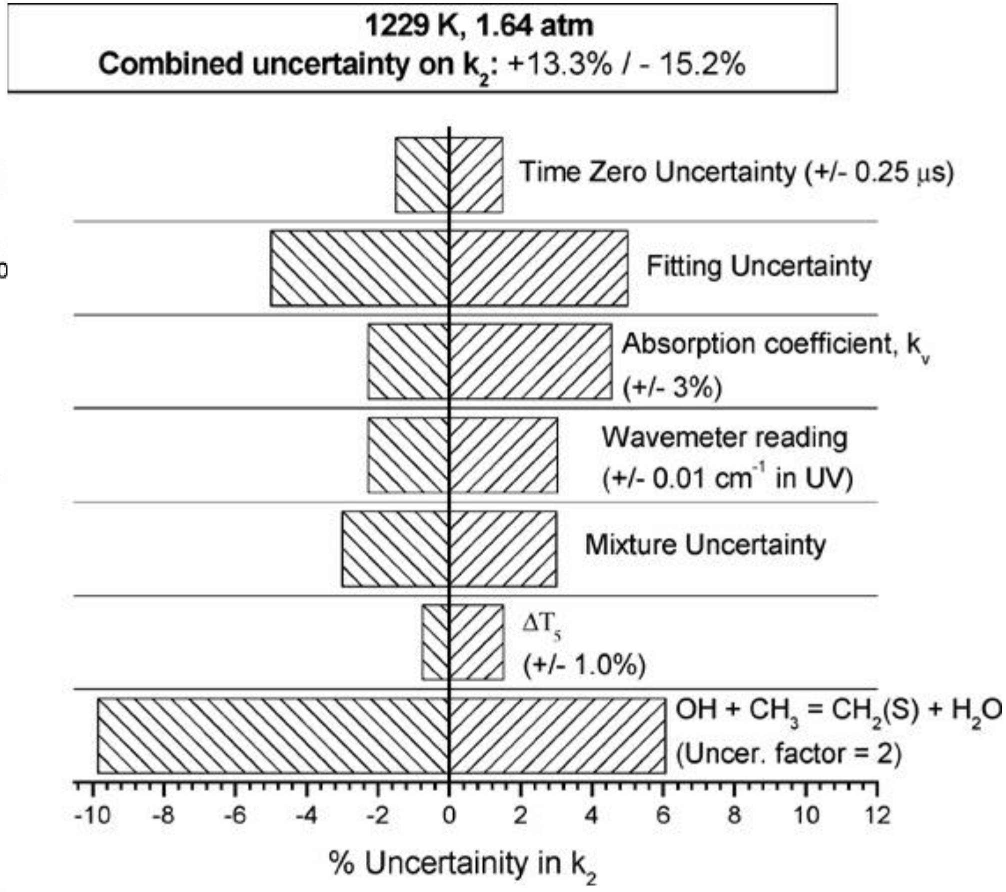

Arrhenius plot for OH + HCHO

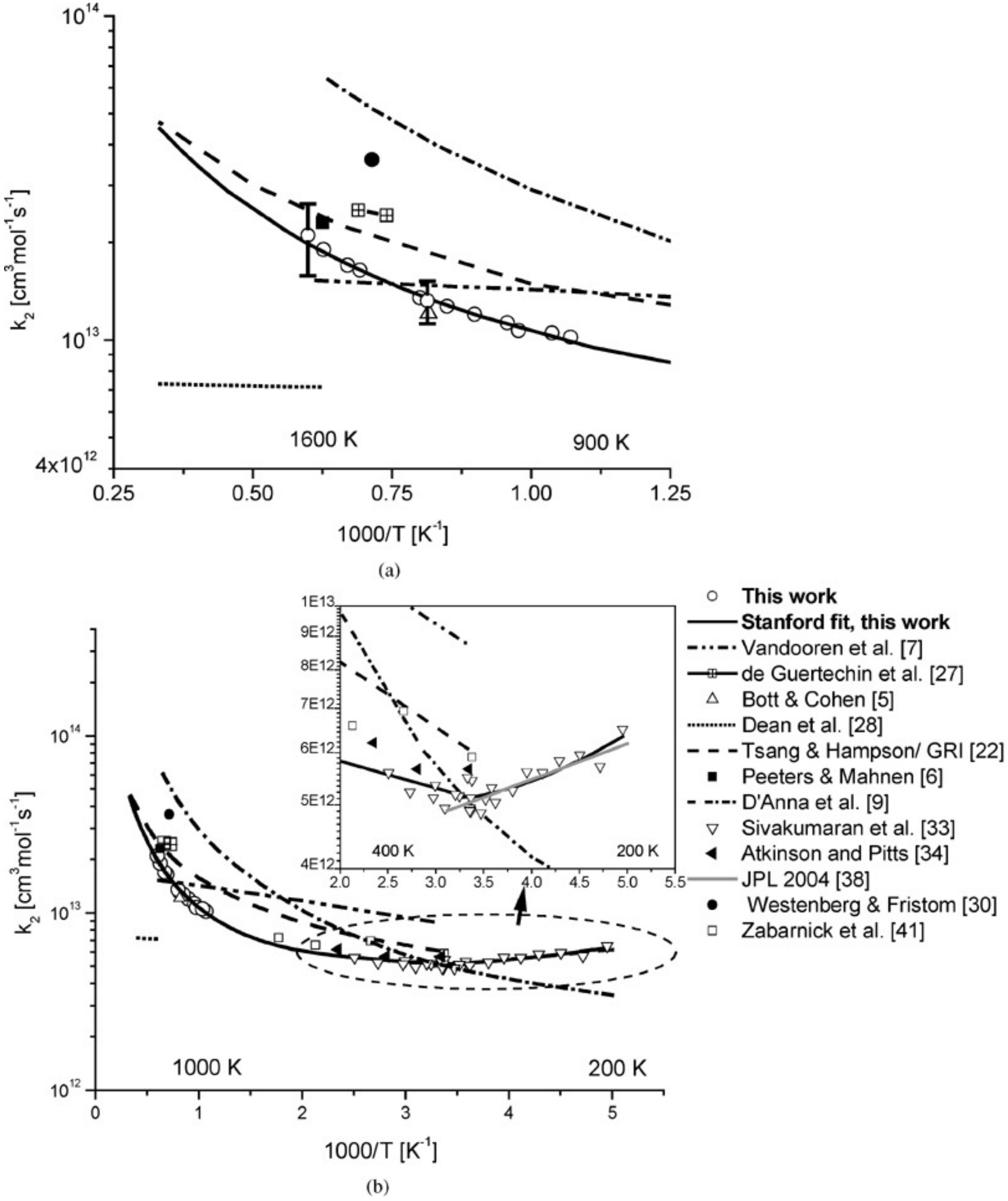

- $k_2 = 7.82 \times 10^7 T^{1.63} \exp(531/T)$ / cm^3 mol^{-1} s^{-1}

OH + Aldehydes

(Wang et al. Proceedings of the Combustion Institute 36 (2017) 151–160)

- Same absorption technique; 976 – 1346 K, 0.6 atm. Some dissociation of aldehyde at higher T. RCHO → RH + CO; RCO + H. Monitor by CO absorption.

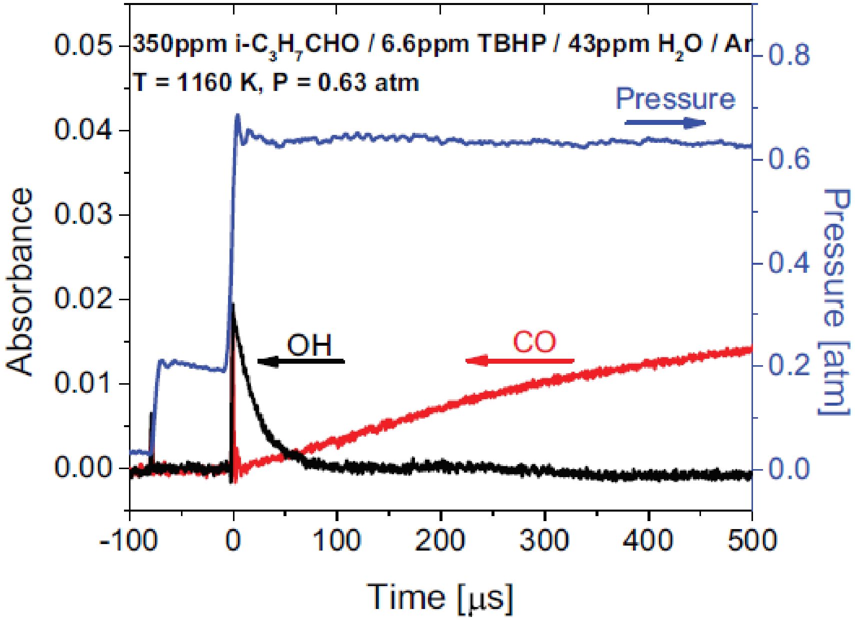

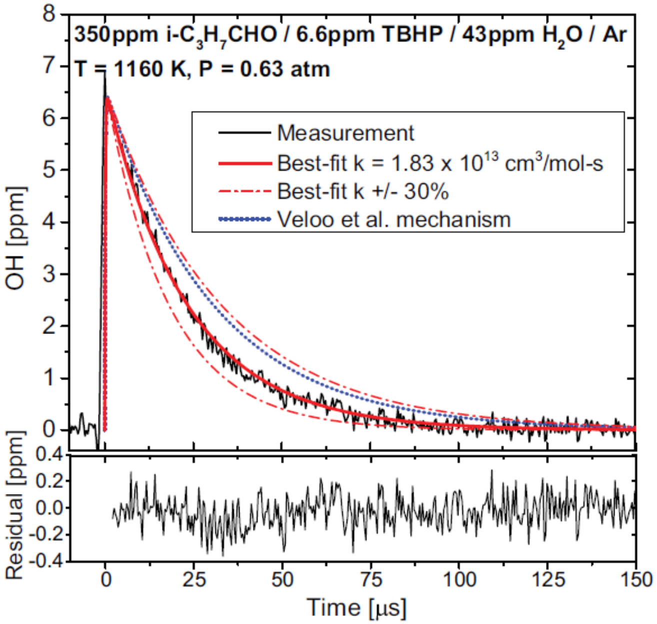

OH + aldehydes contd.

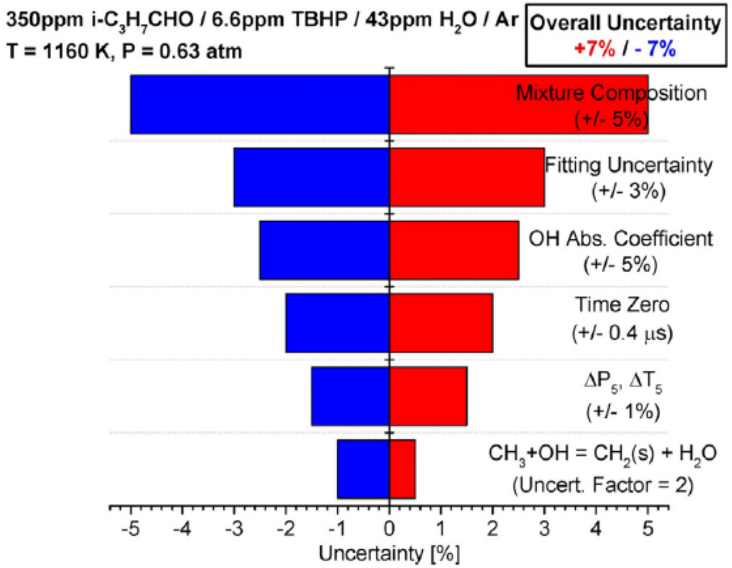

$k_{\mathrm{iC_3H_7CHO+OH}} = 7.70 \times 10^{13} \exp(-1700\ \mathrm{K/T}) \pm 7\%;$

$k_{\mathrm{nC_4H_9CHO+OH}} = 1.03 \times 10^{14} \exp(-1730\ \mathrm{K/T}) \pm 7\%;$

$k_{\mathrm{iC_4H_9CHO+OH}} = 1.02 \times 10^{14} \exp(-1750\ \mathrm{K/T}) \pm 10\%;$

$k_{\mathrm{(CH_3)_3CCHO+OH}} = 7.20 \times 10^{13} \exp(-1670\ \mathrm{K/T}) \pm 8\%;$

$k_{\mathrm{C_2H_5CHCHCHO+OH}} = 6.93 \times 10^{13} \exp(-1340\ \mathrm{K/T}) \pm 8\%;$

$k_{\mathrm{C_6H_5CHO+OH}} = 3.10 \times 10^{13} \exp(-1380\ \mathrm{K/T}) \pm 8\%.$

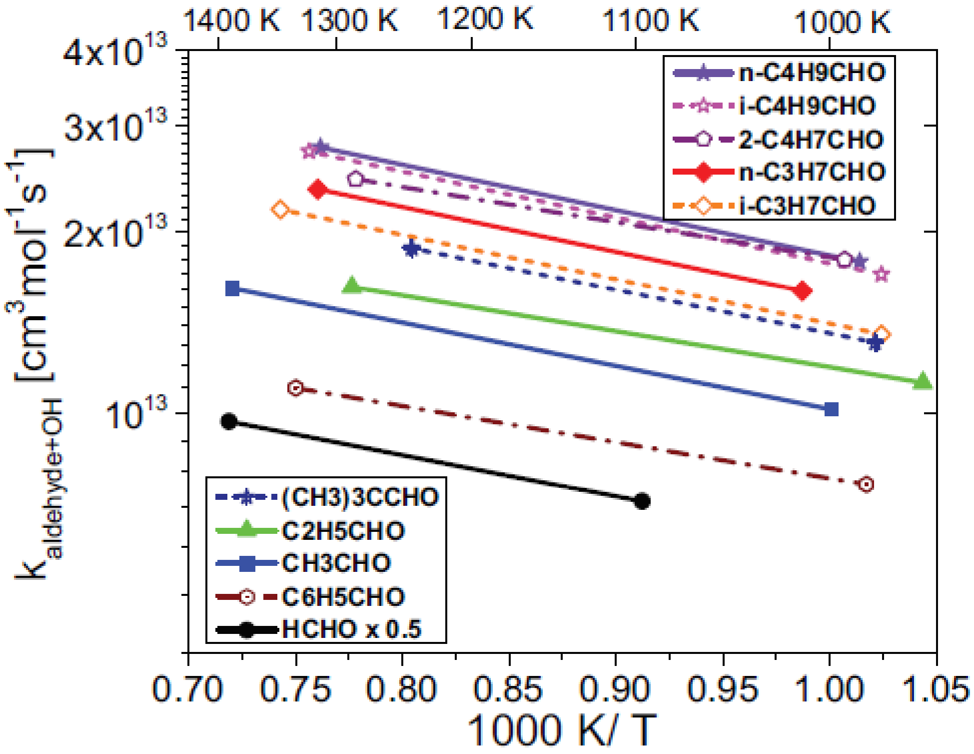

Sub ppm CH_3 detection by cavity enhanced absorption spectroscopy (CEAS)

(Wang et al Proceedings of the Combustion Institute 36 (2017) 4549–4556)

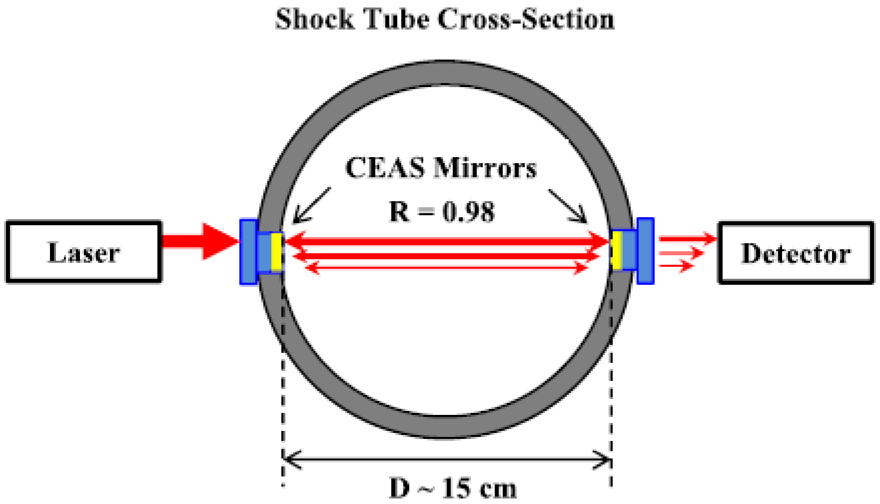

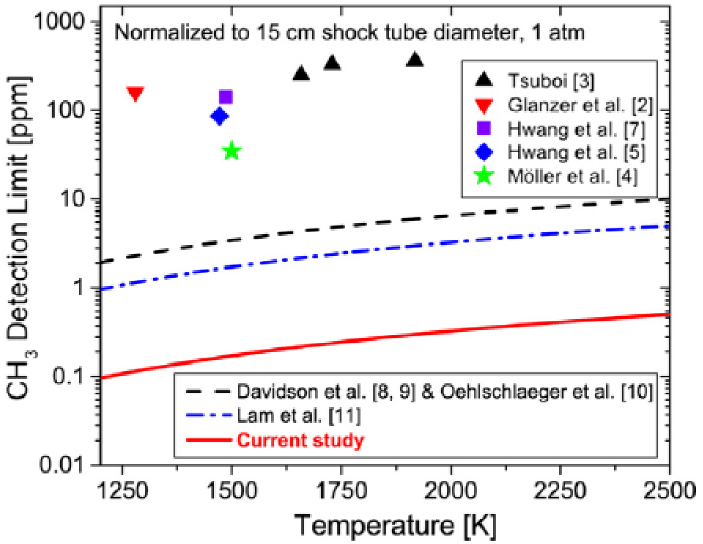

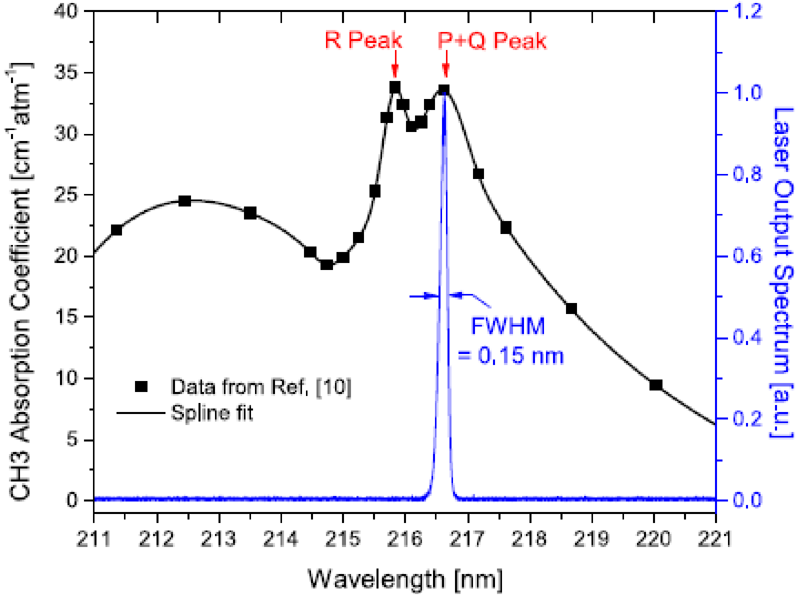

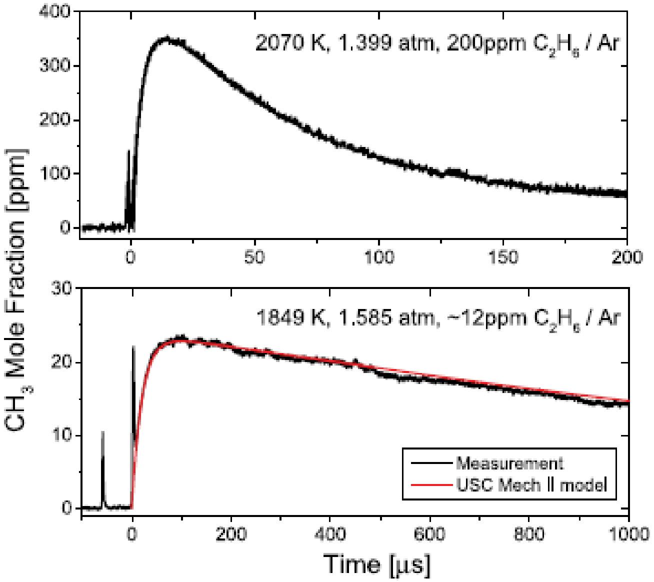

CH3 + H by shock tube
Su and Michael, Proc Comb Inst 2002, 29, 1219

Shock tube study of the thermal decomposition of $C_2D_5I/CH_3I/Kr$ mixtures which generated D atoms and CH_3 radicals. [H] and [D] were monitored by ARAS. A rate constant of $2.20{\cdot}10^{-10}$ cm^3 $molecule^{-1}$ s^{-1} was measured for the reaction $CH_3 + D \rightarrow CH_2D + H$. This rate constant was converted to the high pressure limit for $CH_3 + H \rightarrow CH_4$ using the ratio of 1.6 determined theoretically by Klippenstein, Georgieskii, and Harding. (Proc. Comb. Inst. 2002, **29**, 1229.)

H_2O_2 dissociation in CO_2

Shao et al, Proc Comb Inst10.1016/J.PROCI.2022.08.021

- 1087 – 1234 K; 2 atm, 20% CO_2 in Ar.
- Right hand plot shows low pressure limiting rate constant, compared with literature studies.
- See Topic 7 for need for collisional stabilization data for CO_2

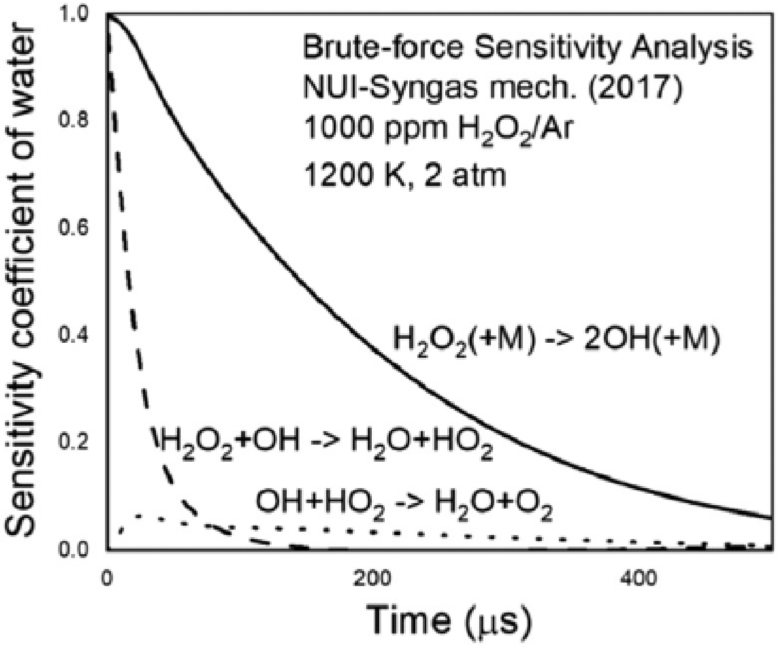

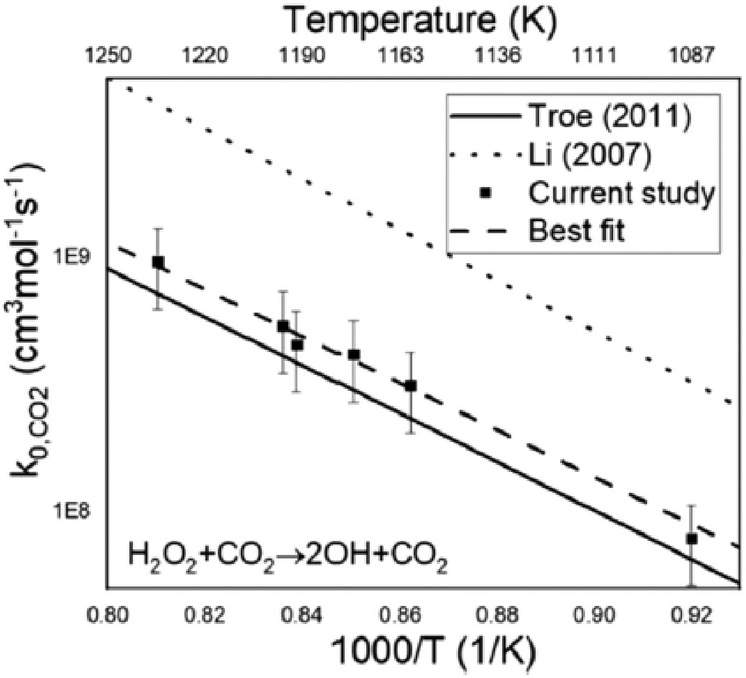

Flow tubes for elementary reactions and whole systems

Combined flow tube and pulsed photolysis: O + OH

Howard and Smith, J. Chem. Soc Faraday Trans. 2, 1981,77,997-1008

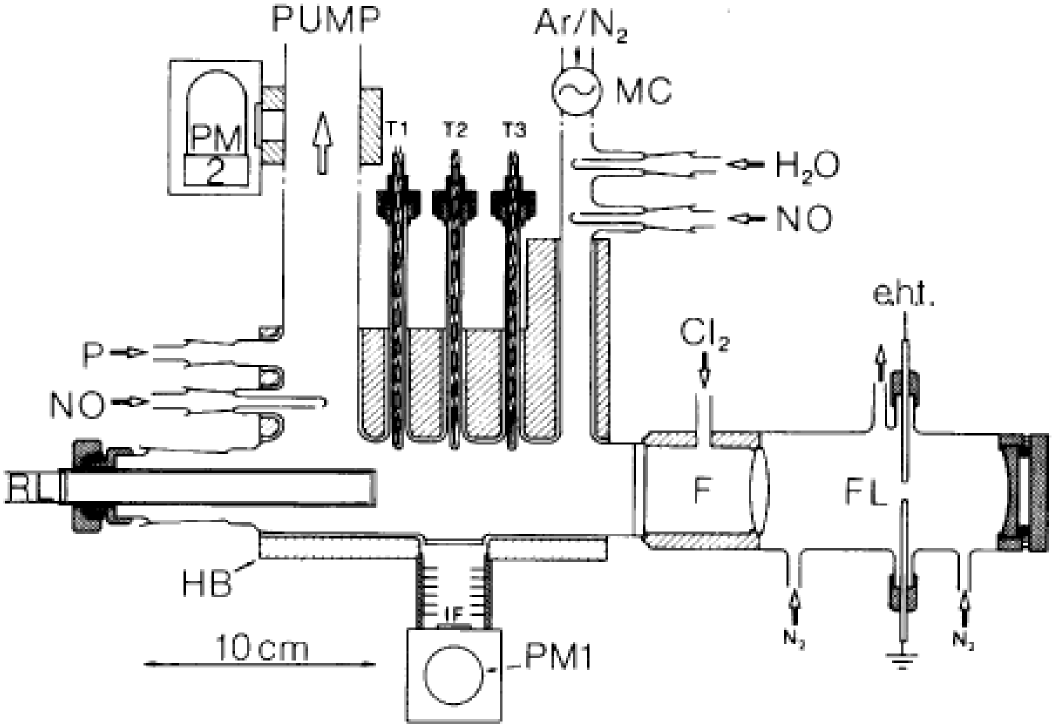

T/K	*k*/cm^3 molecule^{-1} s^{-1}
294	$4.2 \cdot 10^{-11}$
227	$4.5 \cdot 10^{-11}$
190	$5.2 \cdot 10^{-11}$
158	$6.1 \cdot 10^{-11}$

- O generated in discharge, OH by pulsed photolysis, with [O]>> [OH]. [O] generated from N + NO and concentration determined by titration.
- O + OH → O_2 + H. Reverse reaction is key branching step in H_2/O_2
- Data provide key test for theory for H + O_2

Pyrolysis of butanol using molecular beam sampling from a plug flow reactor

Cai et al. (Energy & Fuels, 26, 5550-5568 (2012))

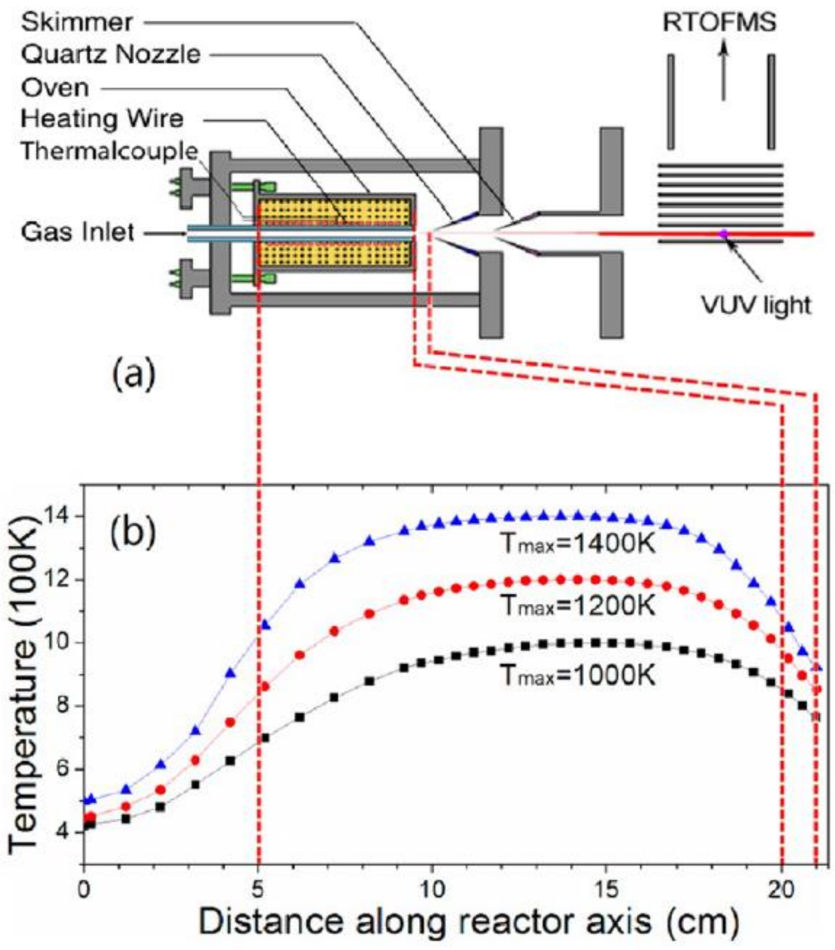

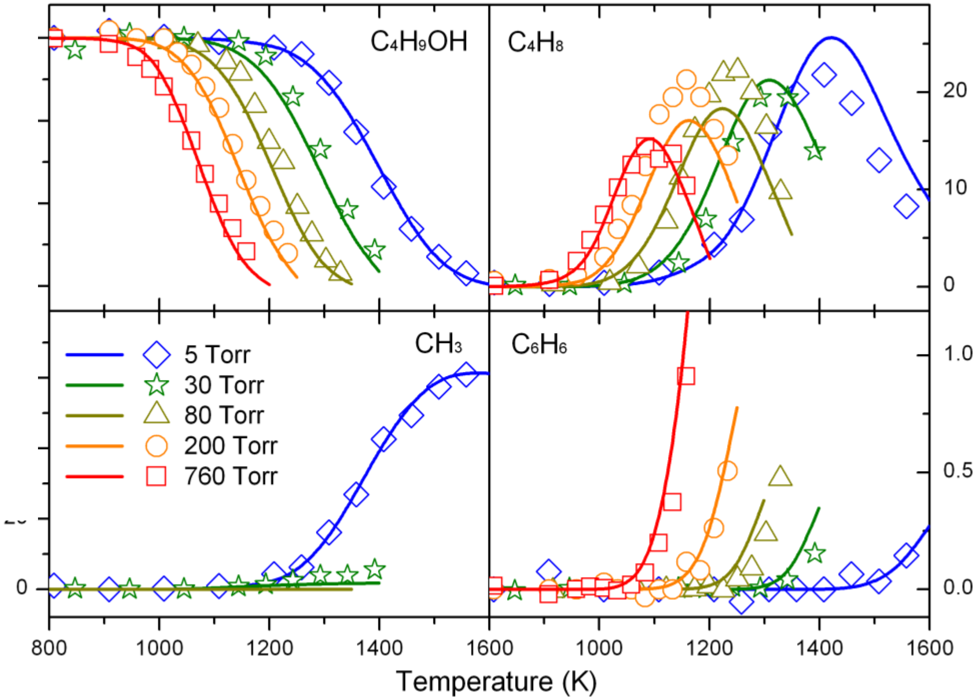

Use of species concentrations in flow reactor to determine rate coefficients: butanol dissociation

Cai et al. (Energy & Fuels, 5550-5568 (2012))

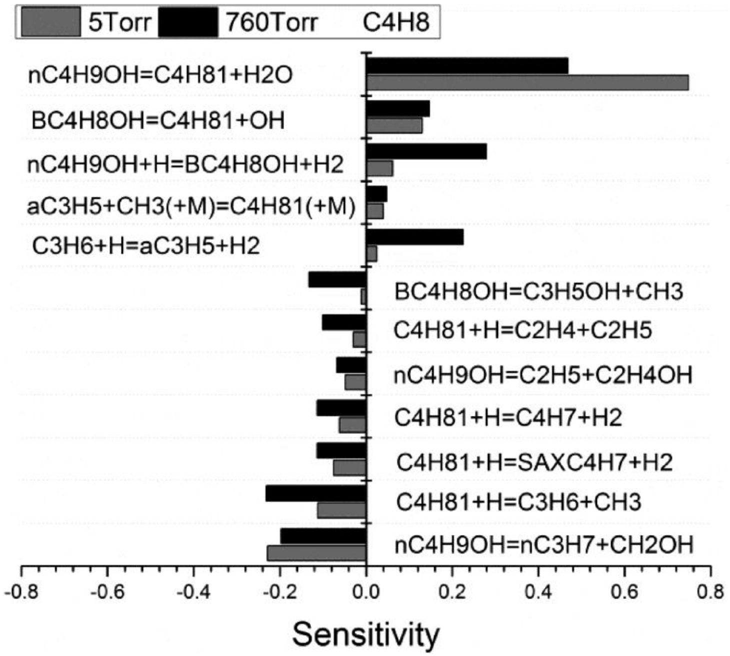

C_4H_8 sensitivity

T_{max} = 1450 K under 5 Torr (gray) and

T_{max} = 1100 K under 760 Torr (black)

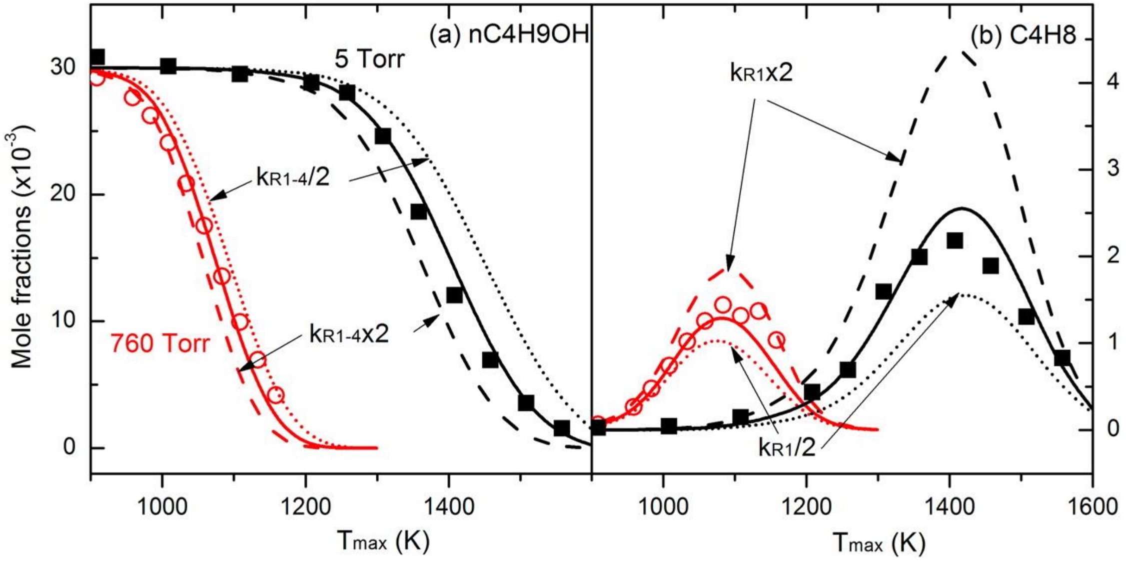

Experimental mole fraction profiles (symbols) and modeling results (lines) of nC_4H_9OH pyrolysis at 5 and 760 Torr.

Decomposition of photoionization curves in a flow tube study of cyclopentene oxidation*J. Phys. Chem. A* 2008, *112*, 13444–13451

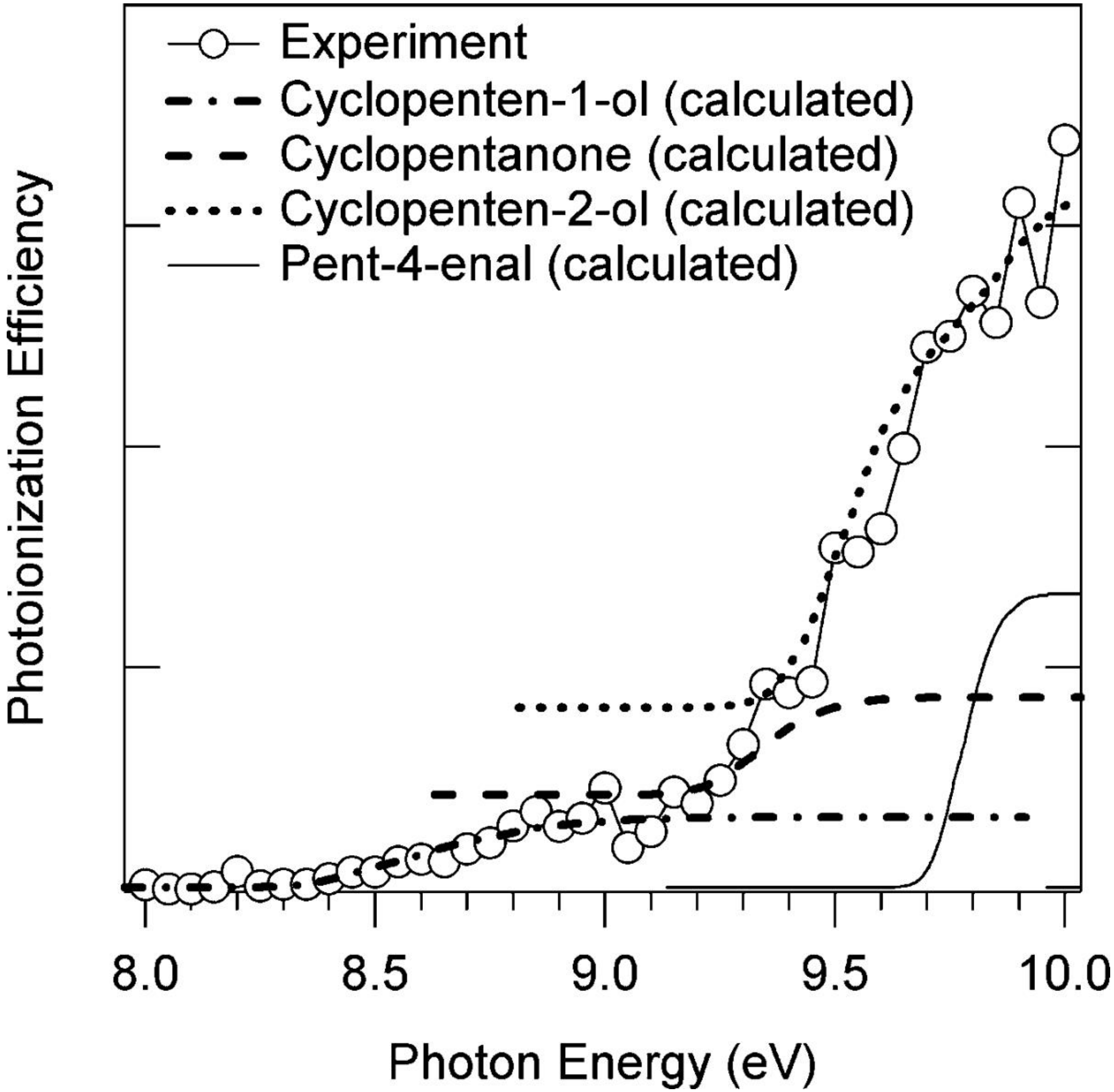

Schematic decomposition of the best fit to the experimental photoionization efficiency spectrum into the substituent calculated photoionization efficiency curves of the three isomers: 1-*c*-C_5H_7OH, *c*-C_5H_8O, and 2-*c*-C_5H_7OH. The isomeric photoionization efficiency curves are scaled by their weighting in the fit to the overall spectrum and vertically displaced for clarity.

Static reactors: Early studies of alkane oxidation kinetics and mechanism by Baldwin, Walker and co-workers

- The techniques rely on end product analysis using gas chromatography. Three techniques were used:
    - Addition of small amounts of alkane, RH, to a slowly reacting $H_2 + O_2$ mixture at ~ 750 K allowed measurements of, e.g. OH, H, HO_2 + RH. $H_2 + O_2$ provides a well-controlled environment containing the radicals. (JCS Faraday Trans 1., 1975, 71, 736)
    - Oxidation of aldehydes (550 – 800 K). Aldehydes act as a source of alkyl radicals, e.g. 2-C_3H_7 from 2-C_3H_7CHO (JCS Faraday Trans 2., 1987, 83, 1509)
    - Decomposition of tetramethylbutane (TMB) in the presence of O_2. System acts as a source of HO_2. (JCS Faraday Trans 1., 1986, 82, 89)

Examples from the H_2 + O_2 system

Reminder Interaction of elementary reactions in $H_2 + O_2$

- There are three ignition (explosion) limits. In each case, there is a competition between a termination reaction (removing radicals, decelerating the rate) and a branching reaction (accelerating the rate)
- First limit – competition between termination at the wall e.g. H → wall (rate ↑as pressure ↓) and $H + O_2 \rightarrow OH + O$.
- Second limit – competition between $H + O_2 + M \rightarrow HO_2 + M$ (rate ↑as pressure ↑) and $H + O_2 \rightarrow OH + O$. HO_2 is an unreactive radical and reacts mainly by $HO_2 + HO_2 + M \rightarrow H_2O_2 + M$.
- Third limit – H_2O_2 dissociates generating OH radicals ($H_2O_2 + M \rightarrow 2OH$) and propagation and branching recommence

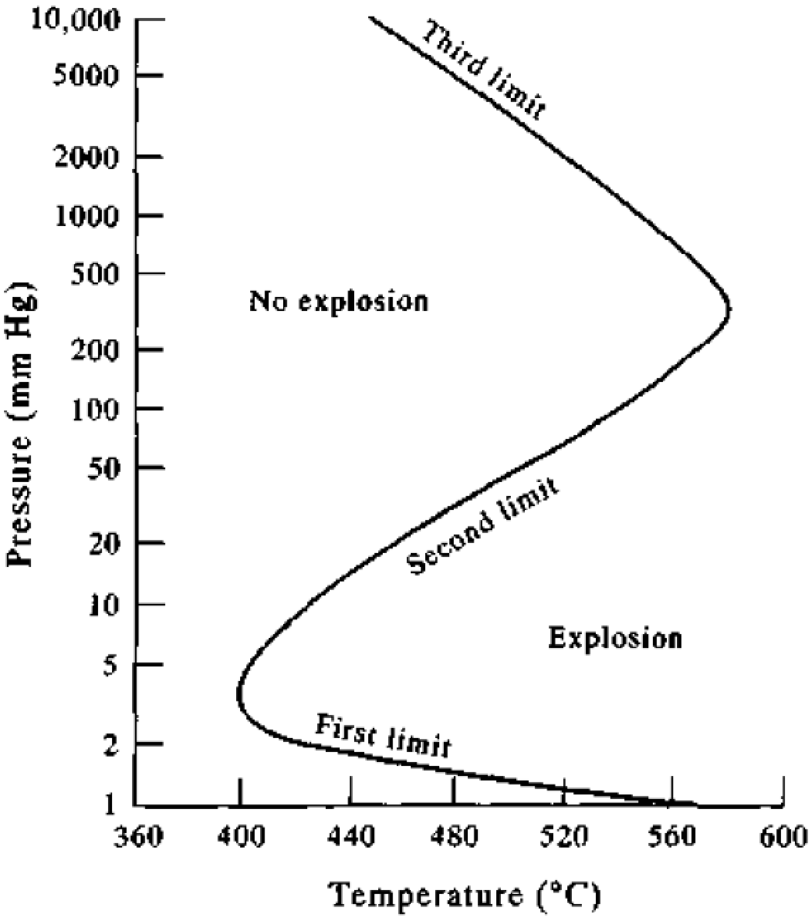

Hydrogen oxygen system

- Review by Miller et al. (Proc Comb. Inst., 2005, 30, 45-88)
- Slide shows sensitivities for ignition delay times (8% H_2, 2% O_2, 90% Ar, 1 bar).
- Note the significance of the H + O_2 branching step, the termination step H + O_2 + M and the H + HO_2 steps

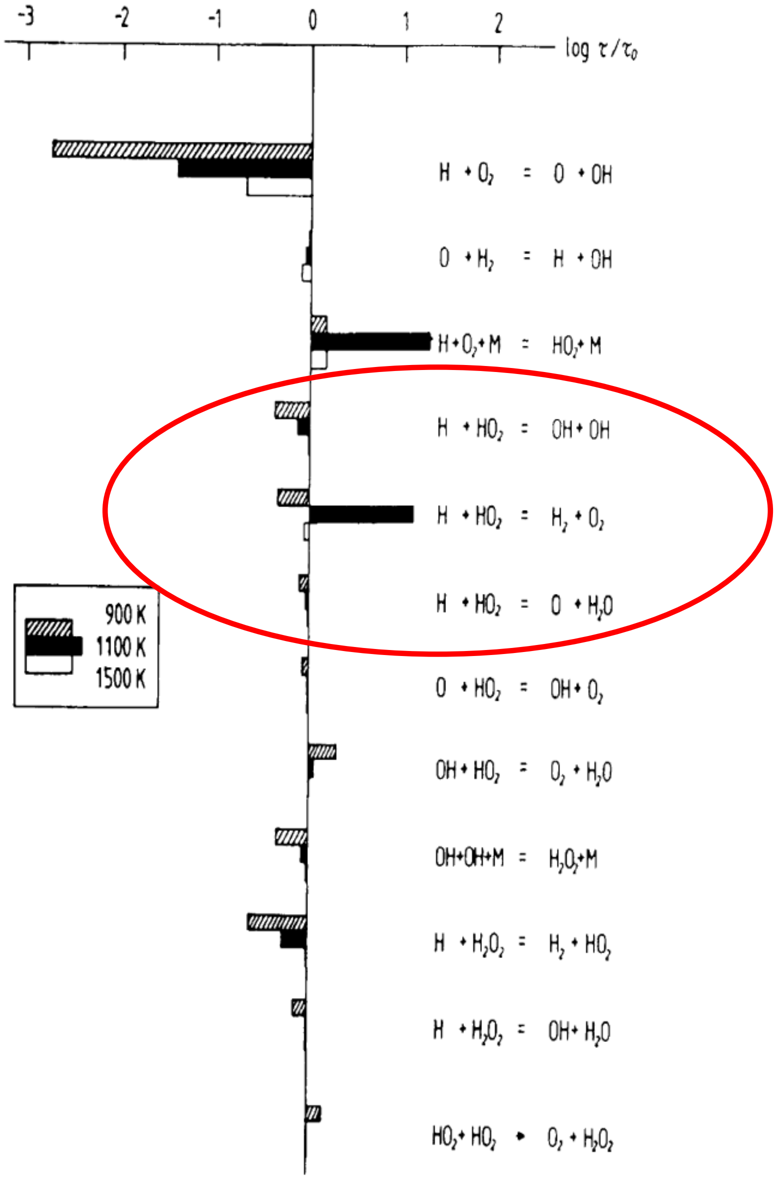

$H + O_2 \rightarrow OH + O$

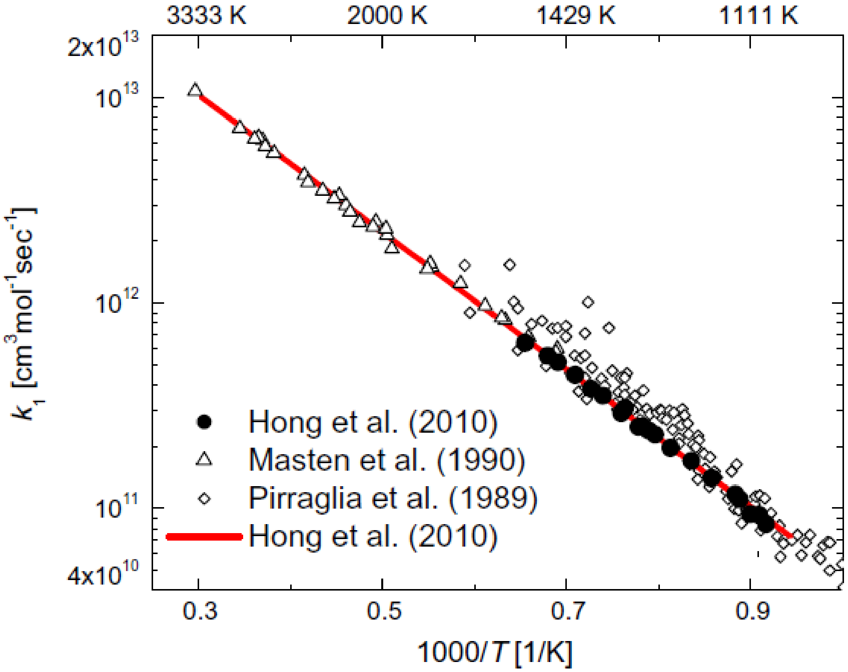

- From Hong et al., shock tube measurements. Comb Flame 2011, 158,633, $k = 1.7\times 10^{-10} \exp(-7670/T)$ (1100 – 3370 K). Uncertainty ± 10%.
- See Burke et al. Int J Chem Kinet, 2012, 44, 444, who support the rate coefficient
- See discussions on evaluation in later lectures.

Reverse reaction: $O + OH \rightarrow H + O_2$

- Studied 150 - 500 K, mainly by discharge flow / laser flash photolysis (see ealier).
- Not of great importance in combustion, but provides additional information on reverse reaction through thermodynamics
- $k = 2.00\times10^{-10}\ T^{-0.352} \exp(113/T)$ cm^3 $molecule^{-1}$ s^{-1} over the range 250–3000 K.
- $\Delta\log k = \pm 0.2$ over the range 250–3000 K.

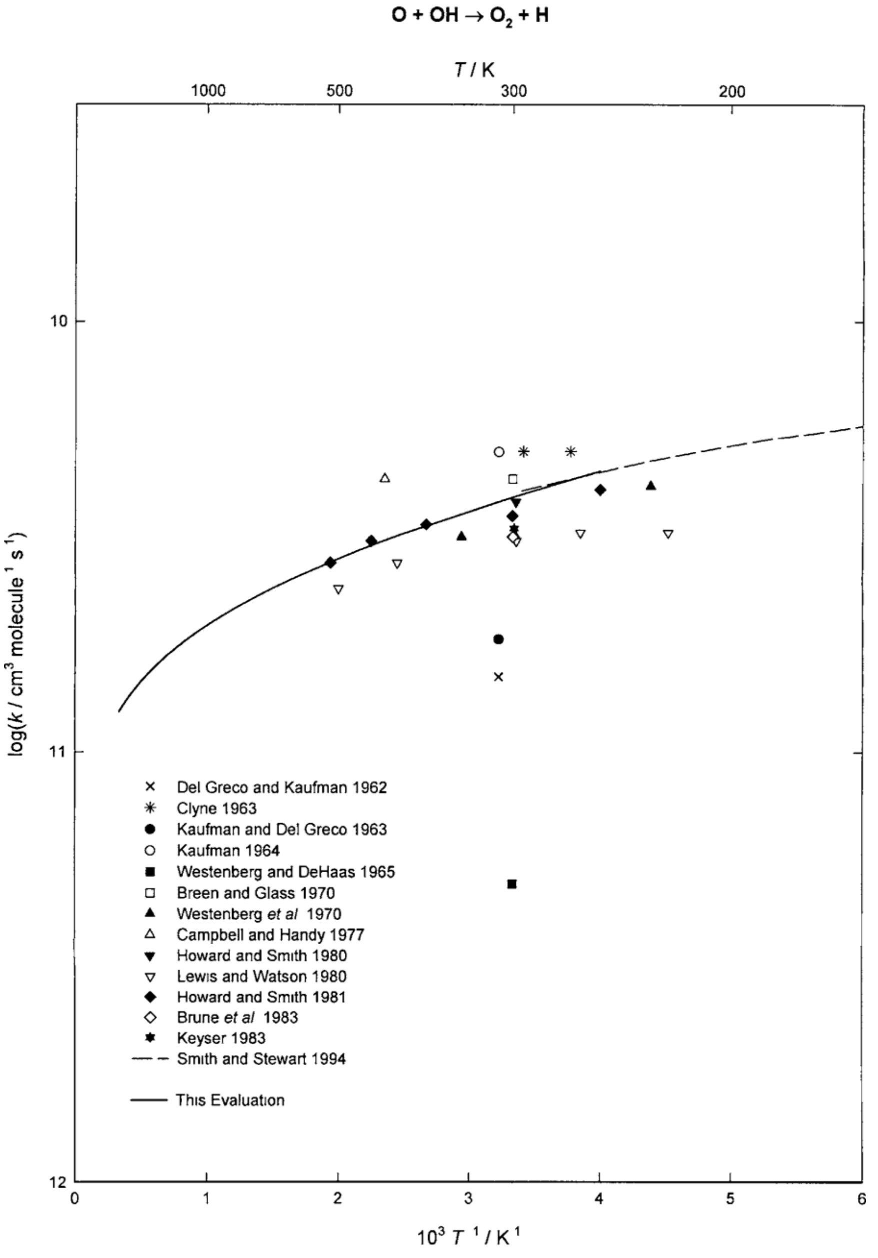

Second branching step
$O + H_2 \rightarrow OH + H$

- Sutherland et al. (21st Symp(Int) Comb, 1986, 929). Used flash photolysis, monitoring O by resonance fluorescence, and shock tube, generating O by flash photolysis of NO and monitoring by ARAS. ()
- Davidson and Hanson (Comb and Flame, 1990, 82, 445) used shock tube, generating O by laser flash photolysis of NO and by pyrolysis of N_2O. O monitored by ARAS. 2120 – 2750 K.
- Javoy et al, (Int J Chem Kinet, 2000, 32, 686 and Expt. Thermal Fluid Sci. 2003, 27, 371). ARAS 2021 – 3356 K.

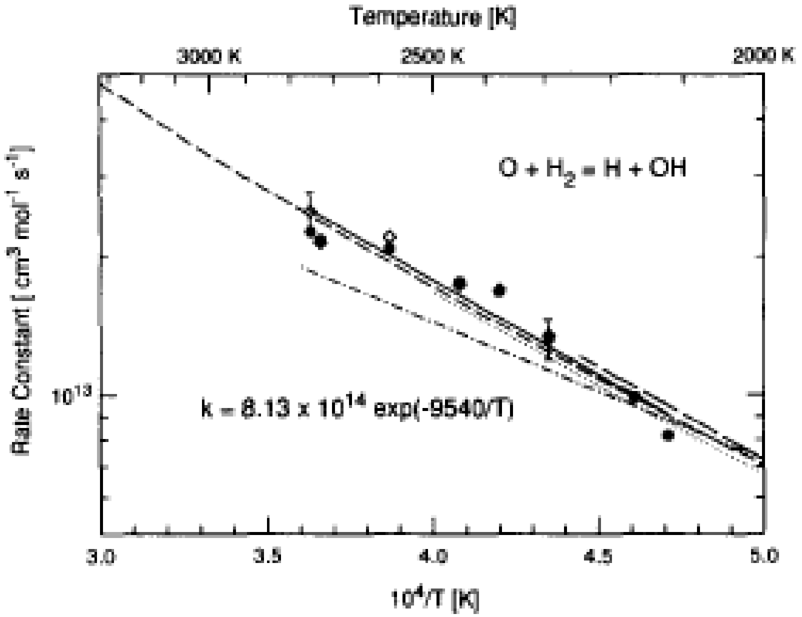

Fig. 2. Arrhenius diagram: $O + H_2 \rightarrow OH + H$. Filled circles—data derived from photolysis method. Open diamonds—data derived from pyrolysis method. Error bars represent ±10%. Solid line—best fit to present data. Dotted line—Sutherland et al. [8]. Dashed line—Nataranjan and Roth [9]. Dot-dashed line—Pamidimukkala and Skinner [10]. Long-dashed line—Shin et al. [11].

Sutherland et al

$H + O_2 + M \rightarrow HO_2 + M$

- Termination step at lower T, converting reactive H into less reactive HO_2. Acts as a route to branching through formation of H_2O_2 through $HO_2 + HO_2$ (and HO2 + RH in hydrocarbon combustion)
- Reaction is at the third order limit except at higher pressures.
- Michael et al. J. Phys. Chem. A 2002, 106, 5297-5313 used flash photolysis at room T for a wide range of third bodies, and a shock tube at higher T for Ar,. O_2 and N_2. Showed that H_2O is an unusually effective third body.
- Detailed analysis of collision frequencies and energy transfer parameters.

$$A + B \rightleftharpoons AB^* \rightarrow AB$$

$$k = \frac{k_0[\mathrm{M}]k^{\infty}}{k^{\infty} + k_0[\mathrm{M}]}$$

$H + O_2 + M \rightarrow HO_2 + M$

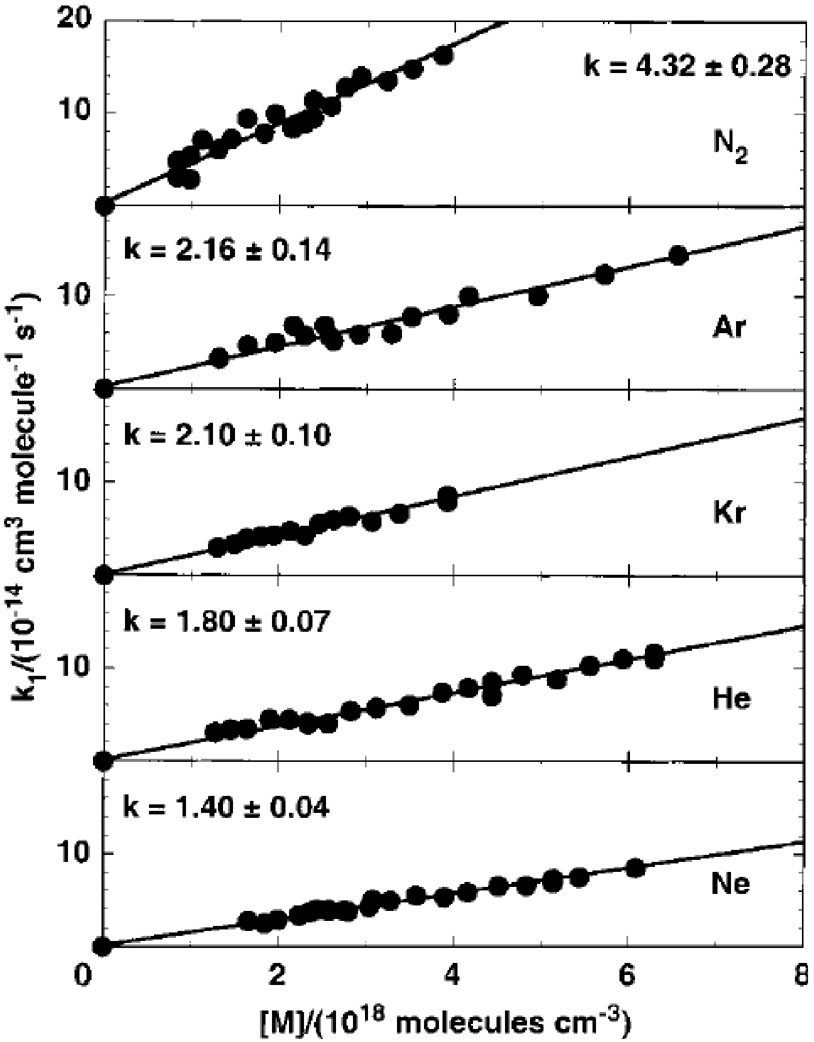

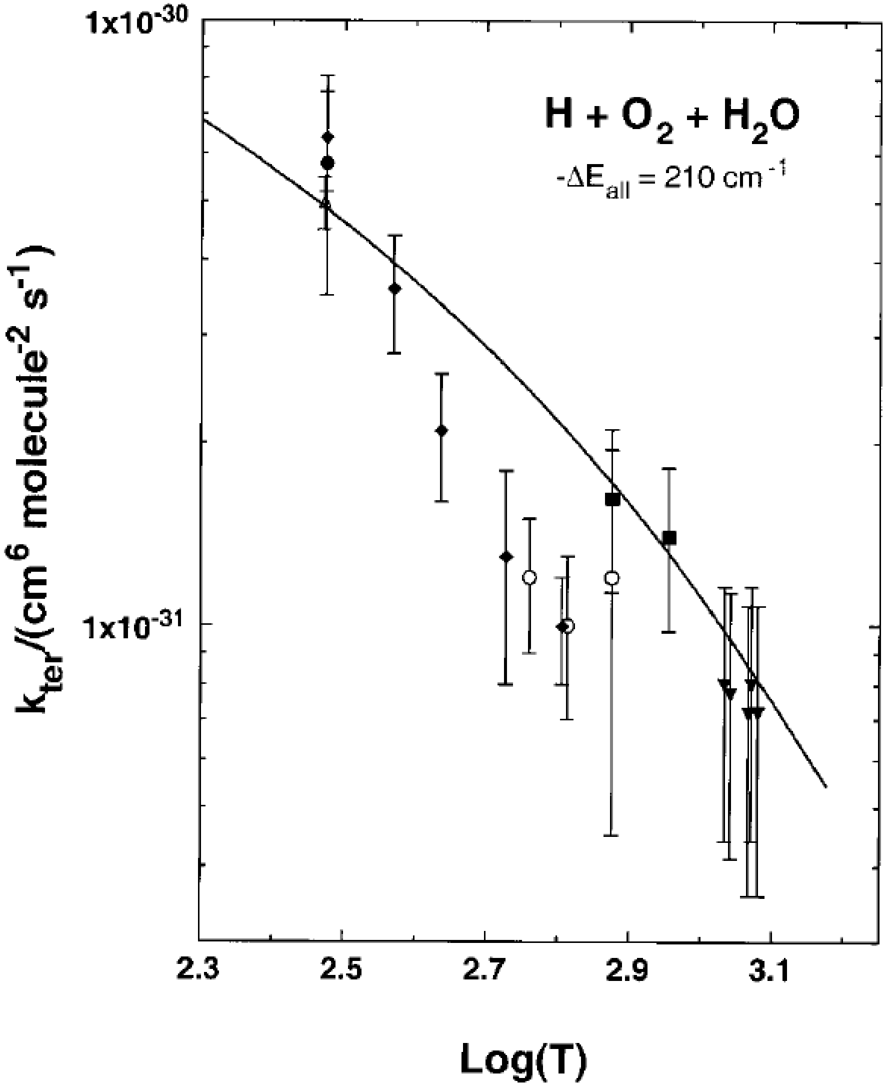

Units of k: 10^{-32} cm^6 $molecule^{-2}$ s^{-1}

High pressure pulsed photolysis / flow reactor

Fernandes et al. Phys. Chem. Chem. Phys., 2008, 10, 4313-4321

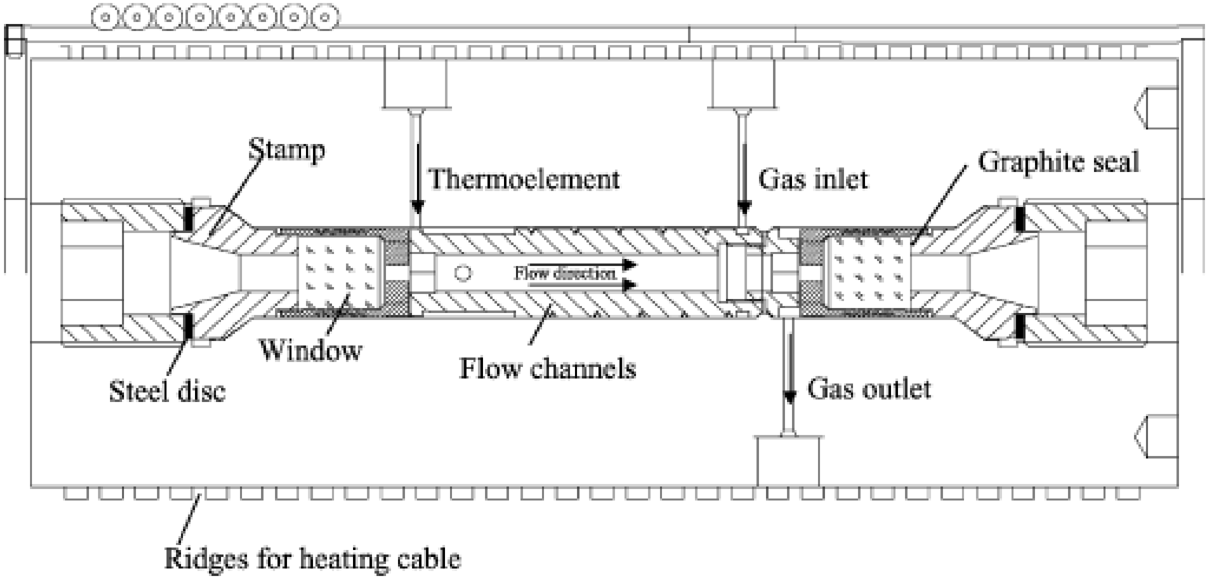

- $H + O_2 + M \rightarrow HO_2 + M$, 300 – 900 K, 1.5 – 950 bar
- H from photolysis NH_3 at 193 nm
- HO_2 detected by absorption spectroscopy at 230 nm.
- At these higher pressures, the reaction moves into the fall-off region

$H + O_2 + M \rightarrow HO_2 + M$

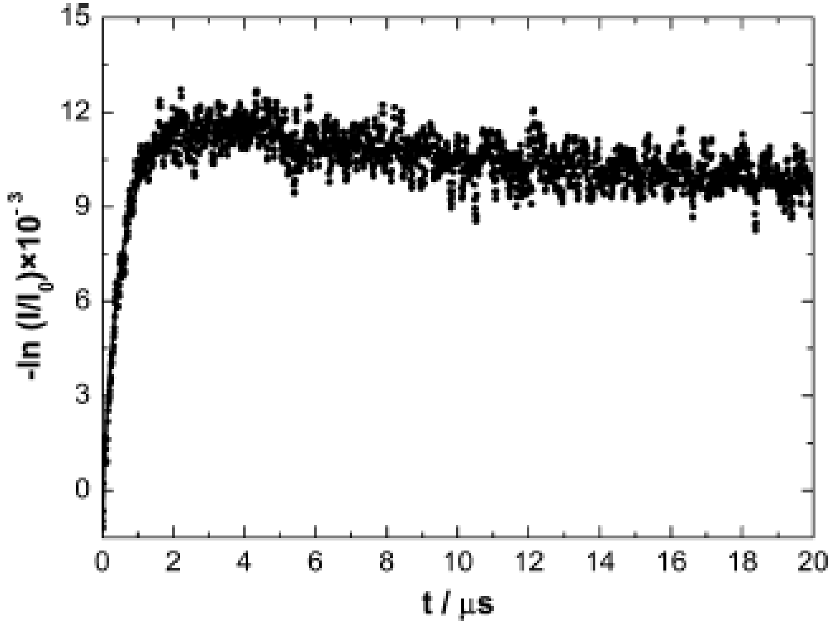

Fig. 2 Absorption–time profile of HO_2 (λ = 230 nm, T = 600 K, p = 300 bar, M = N_2).

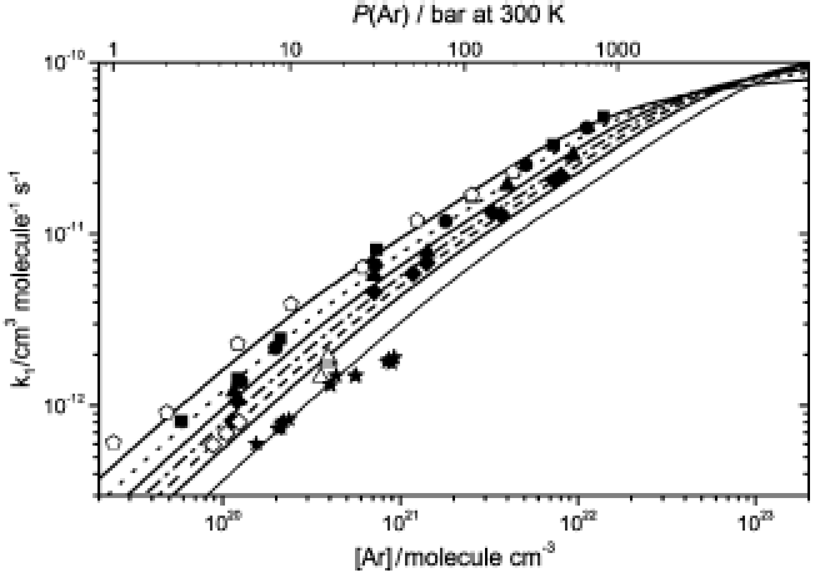

Fig. 5 Falloff curves for the recombination $H + O_2 (+Ar) \rightarrow HO_2 (+Ar)$ (representative upper pressure scale for 300 K; T/K = 300 (■), 400 (●), 500 (▲), and 600 (♦) from this work; 300 (⬠, ref. 19), 820 (◇, ref. 20), 1200 (★, ref. 22), and 1325 (△, ref. 21); the fitted curves at left from top to bottom are for T/K = 300, 400, 500, 600, 700, 820, and 1200, resp.).

$H + O_2 + M \rightarrow HO_2 + M$

- Data for different third bodies and temperatures can be rationalised and placed on the same plot using reduced falloff curves. Requires calculation of high pressure limiting rate coefficient (that isn't accessible to experiment for this reaction.)

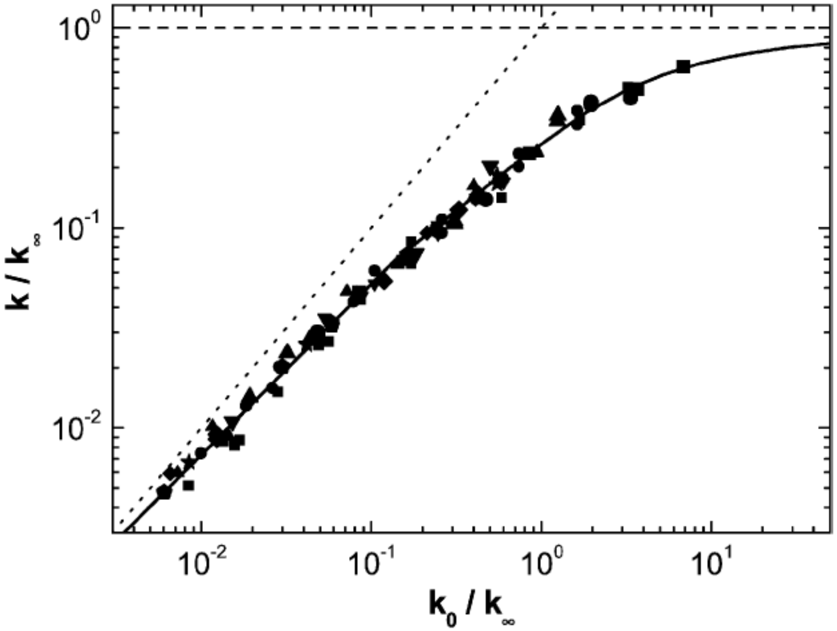

Fig. 7 Doubly reduced falloff curves for the recombination $H + O_2 (+M) \rightarrow HO_2 (+M)$ in the bath gases M = He, Ar, and N_2 (experimental points from this work from Tables 1–3; T/K = 300 (■), 400 (●), 500 (▲), 600 (▼), 700 (♦), 800 (★), and 900 (⬟), see text).

Evaluation: Burke et al, Int J Chem Kinet 2012, 44, 444

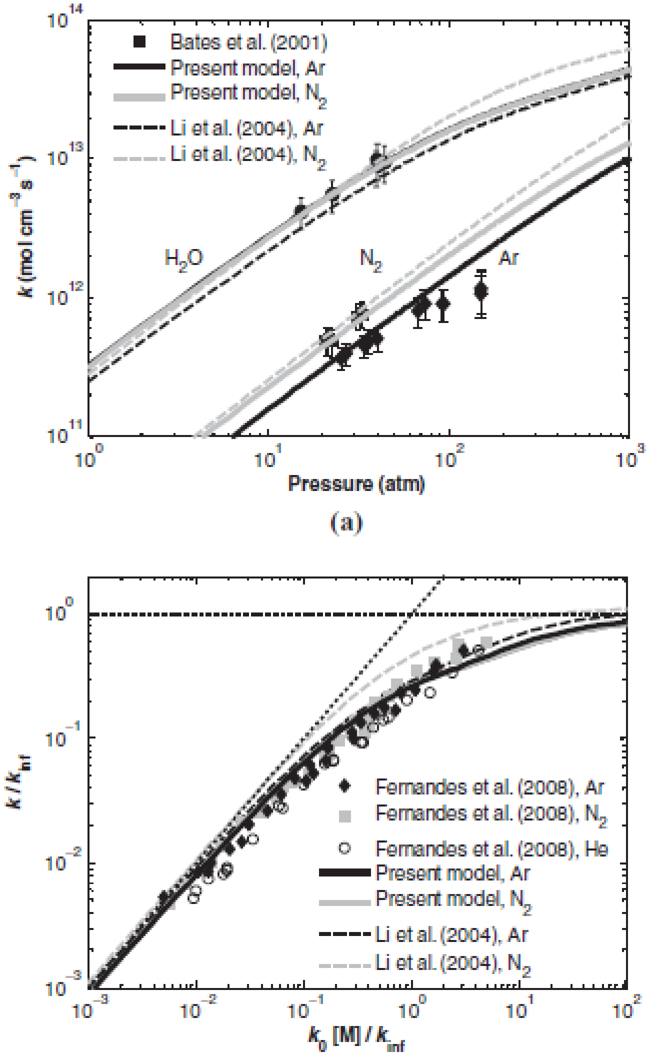

(a)

- See paper for detailed discussion of Troe parameters (next slide), uncertainties etc.

REMINDER

Troe Fitting

Need to represent k(T,P) for Global Models

Standard is Troe Fitting

$$k(T,p) = \frac{k_0[M]k^\infty}{k^\infty + k_0[M]} F \qquad \log_{10} F = \frac{\log_{10} F_{cent}}{1 + \left[\frac{\log_{10}(p^*) + c}{N - d(\log_{10}(p^*) + c)} \right]^2}$$

$$p^* = k_0[M]/k^\infty \qquad d = 0.14$$

$$c = -0.4 - 0.67 \log_{10} F_{cent} \qquad N = 0.75 - 1.27 \log_{10} F_{cent}$$

Fit k_0 & k^∞ to modified Arrhenius $k_0 = A_0 T^{n_0} \exp(-E_0/T)$

Fit F_{cent} to:

$$F_{cent} = (1-a)\exp(-T/T^{***}) + a\exp(-T/T^{*}) + \exp(-T^{**}/T)$$

Alternative generalized polynomial approach: PLOG

Gou, J.A. Miller, W. Sun and Y. Ju, http://engine.princeton.edu, 2011.

$$k(T, p_i) = \sum_{j=1}^{M} A_{ij} T^{nij} \exp\left(-\frac{E_0^{ij}}{RT}\right),$$

$$i = 1, \dots . N, \quad M \geq 1$$

at a set of pressures, p=p_1, p_2,….p_N. M (which determines the order of the polynomial)and N are user specified numbers. The extrapolation is bounded by the two pressure limits, p_1 and p_N.

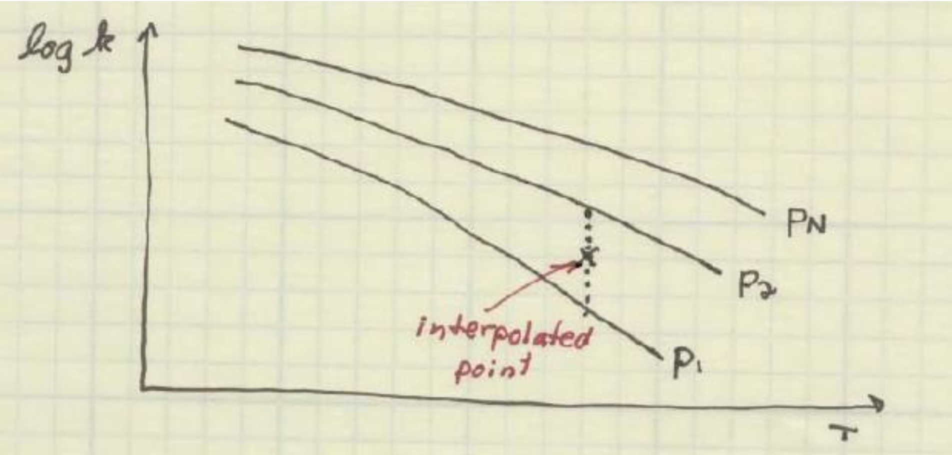

Linear extrapolation of *lgk* vs *lgp* is used to determine *k* at other *p*.

Code available, programmed in CHEMKIN PRO – *see link above*

Chebyshev Polynomials

- Cantera Cantera automates chemical kinetic, thermodynamic, and transport calculations and is widely used in combustion modelling.
- The way in which kinetics are incorporated are discussed in https://cantera.org/science/kinetics.html
- Several methods for incorporating pressure dependent reactions are incorporated, including Troe and PLOG.
- Additionally, Chebyshev polynomials can be used.

$$\log k(T,P) = \sum_{t=1}^{N_T} \sum_{p=1}^{N_P} \alpha_{tp} \phi_t(\tilde{T}) \phi_p(\tilde{P})$$

where a_{tp} are the constants defining the rate, $\phi_n(x)$ is the Chebyshev polynomial of the first kind of degree n evaluated at x

Latest comparison of purely *a priori* theory and experiment, M=Ar

Klippenstein, Proc Comb Inst, 2017, 36, 217

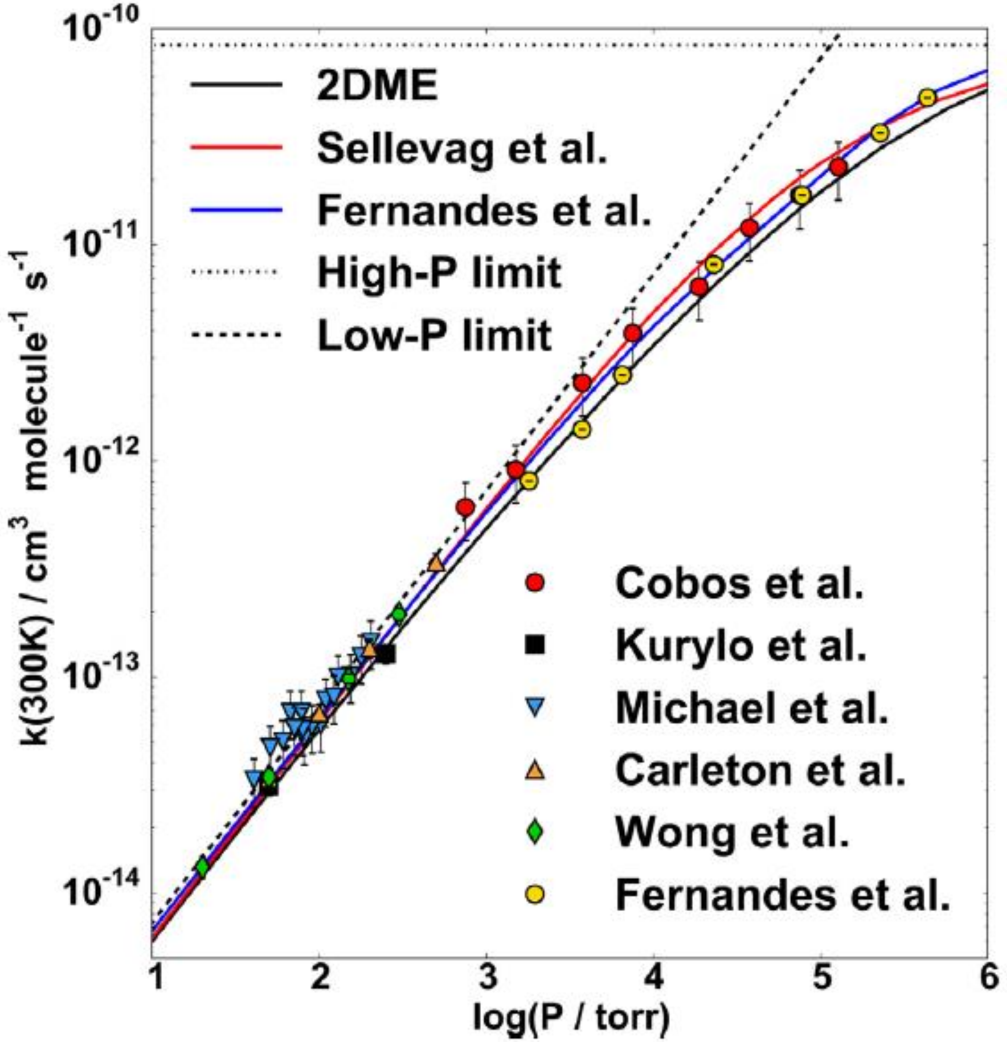

1. solid black line: *a priori* energy transfer based 2DME predictions, coupled with dynamically corrected variable reaction coordinate TST based on a high accuracy well-validated MRCI PES

2: solid red line: fitted master equation results of Sellevag et al. J Phys Chem A 2008, 112, 5085.

3. solid blue line: analytic fit of Fernandes et al. Phys Chem Chem Phys 2008, 10, 4313

$HO_2 + HO_2 \rightarrow H_2O_2 + O_2$

- < 800 K. Flash photolysis, absorption spectroscopy
- Open circles: shock tube, absorption spectroscopy (Kappel et al, Phys Chem Chem Phys, 2002, 4, 4392)
- Reference 5: Hippler et al. J Chem Phys 1990, 93, 1755
- Significant disagreement > 1000 K
- Burke etal. 'Difficult to discern which, if any, (of the high T) determinations is reliable.' More measurements needed under combustion conditions.
- See Topic 3 - Theory

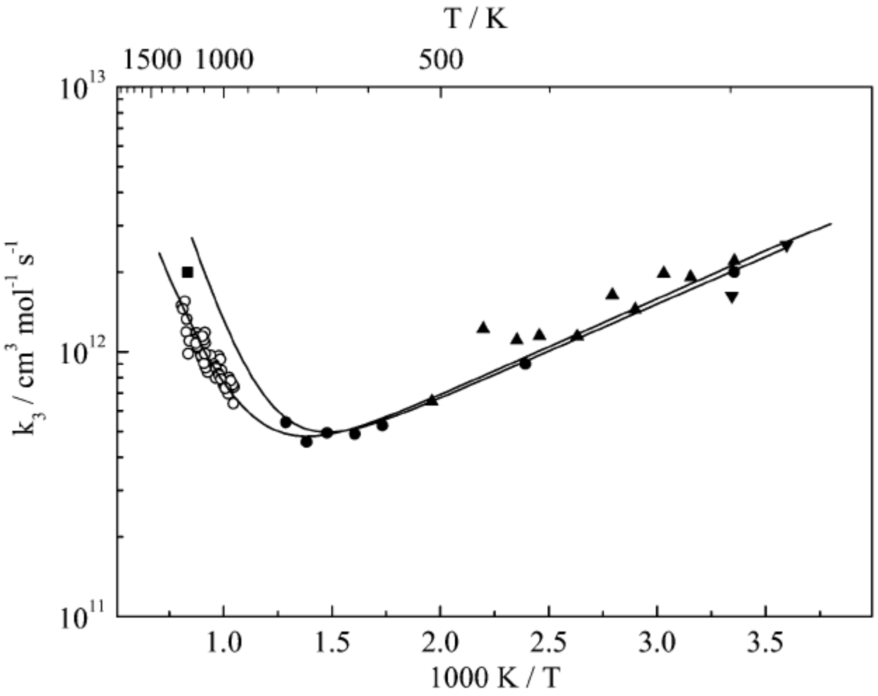

Fig. 10 Rate constants k_3 (■: ref. 2, ▲: ref. 35, ▼: ref. 36, ●: ref. 37, ○ and lower line: this work, upper line: ref. 5).

$H_2O_2 + M \rightarrow 2OH + M$

- Troe, Combustion and Flame 2011, 158, 594-601 The thermal dissociation/recombination reaction of hydrogen peroxide $H_2O_2 \rightleftharpoons 2OH$Analysis and representation of the temperature and pressure dependence over wide ranges.
- Reaction is far from the high pressure limit. To obtain a representation of k(T,p), Troe used the statistical adiabatic channel model to calculate k_∞, using an ab initio surface (Phys. Chem. Chem. Phys. 10 (2008) 3915; J. Chem. Phys. 111 (1999) 2565.
- An important aspect of this work was the use of thermodynamics to relate forward and reverse reactions, using the revised enthalpy of formation of OH – see Wednesday lecture on thermodynamics

Association reaction

- Flash photolysis coupled with saturated LIF.
- Use pressure dependence to separate from O + H_2O channel
- Also problems with secondary reactions (see paper)

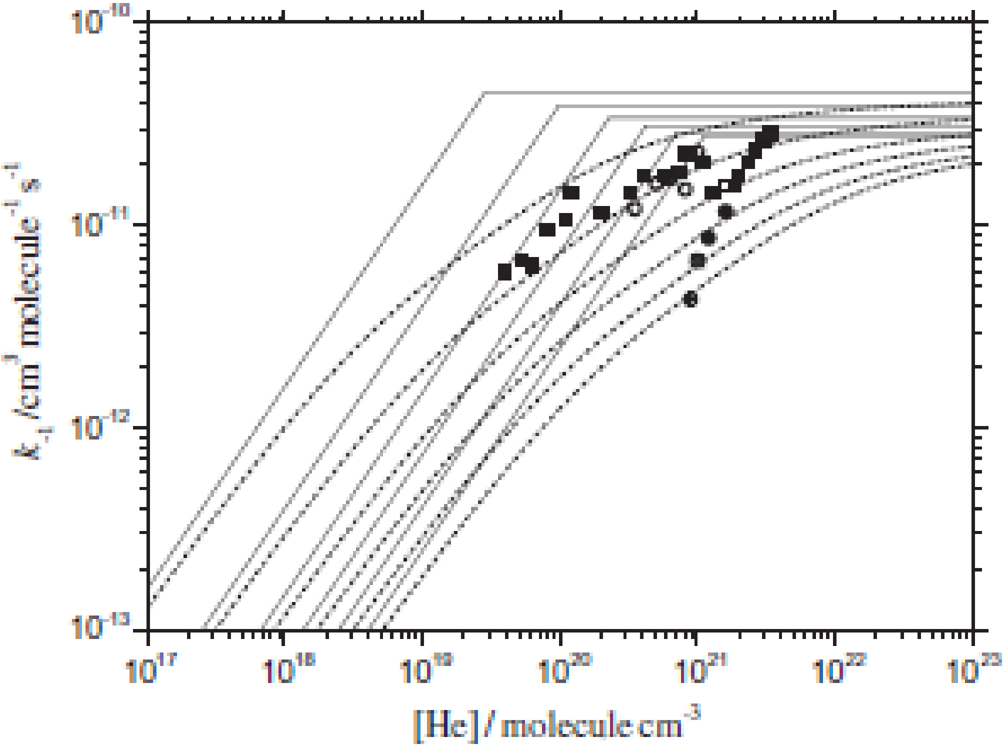

Fig. 3. Experimental recombination rate coefficients k_{-1} and their modelled falloff representation (M = He, experimental points from Refs. [30,31] at $T/K = 210$ (○), 298 (■), 406 (□), 510 (●), 614 (⊚), and 694 (⊕); full lines = modelled limiting low and high pressure rate coefficients from Section 5 of this work; dashed lines = falloff representation by Eq. (3.3) with $F_c = 0.37$ and $N = 1.32$).

Reaction is second order in radical, so absolute concentration is needed

Dissociation reaction

- Flow reactor and static studies at lower T and shock tube measurements above 950 K (see below)

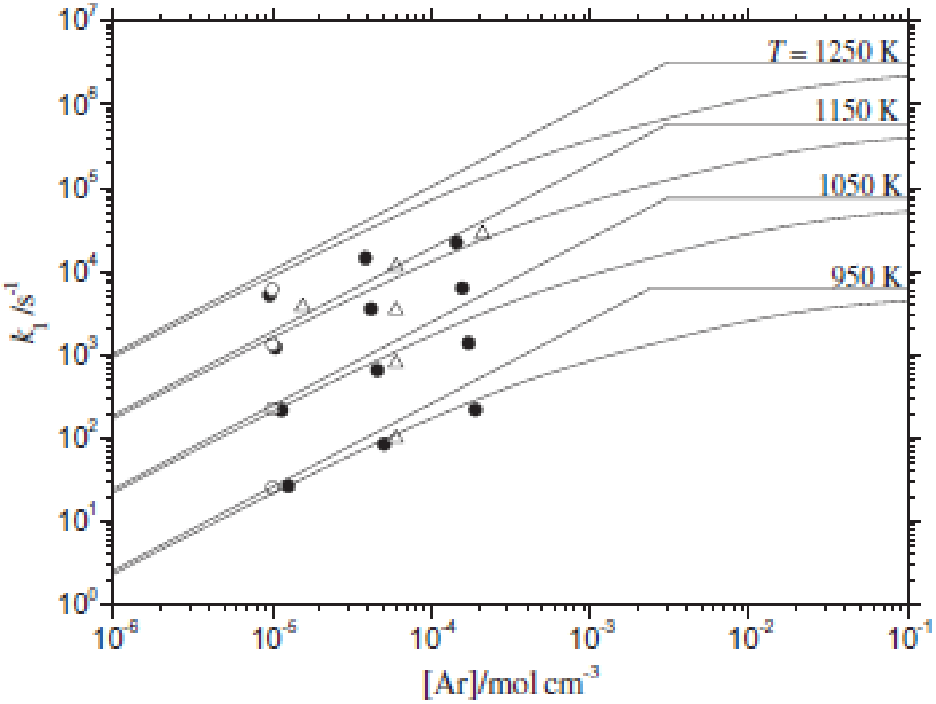

Overall reaction

- Dissociation and association data fitted to Troe expression (see earlier) using theoretical high pressure limit and equilibrium constant

H_2O_2 dissociation
Hong et al. Comb Flame 2011, 158, 633

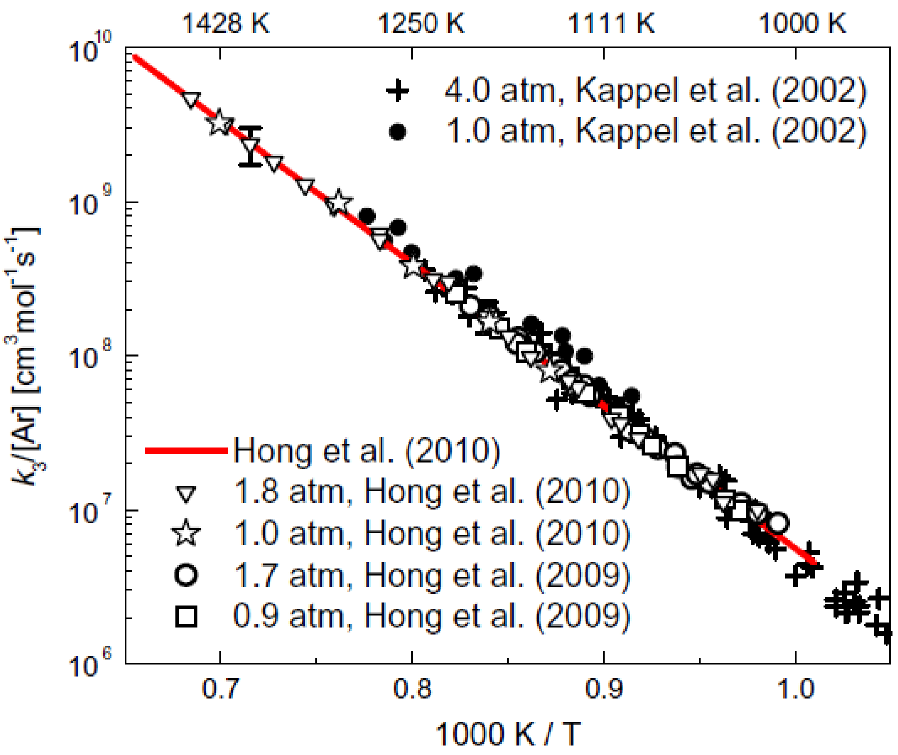

- Data refer to low pressure limit. Used shock tube with laser absorption detection of H_2O and OH

H + HO$_2$ (Burke et al, Int J Chem Kinet 2012, 44, 444)

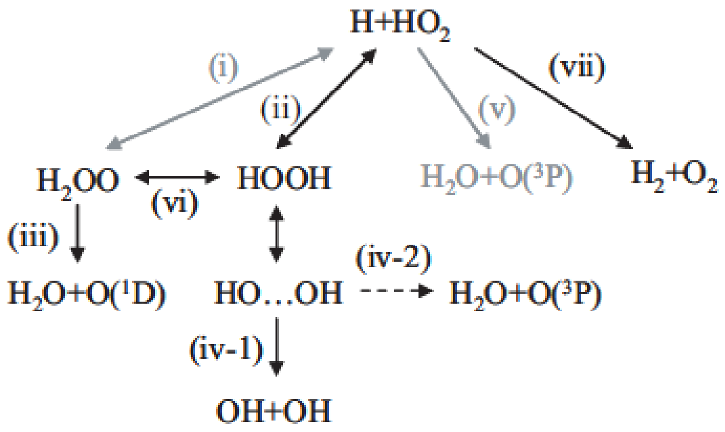

- Theoretical calculations
- Black routes are the major channel; gray less significant
- Plots below show experimental rate constants and an evaluation (see Topic 4)
- See discussion of this reaction in later topics

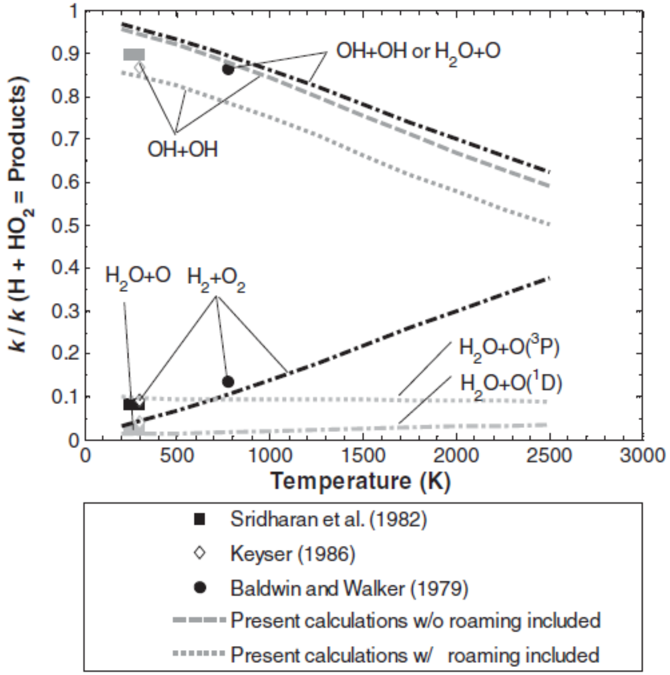

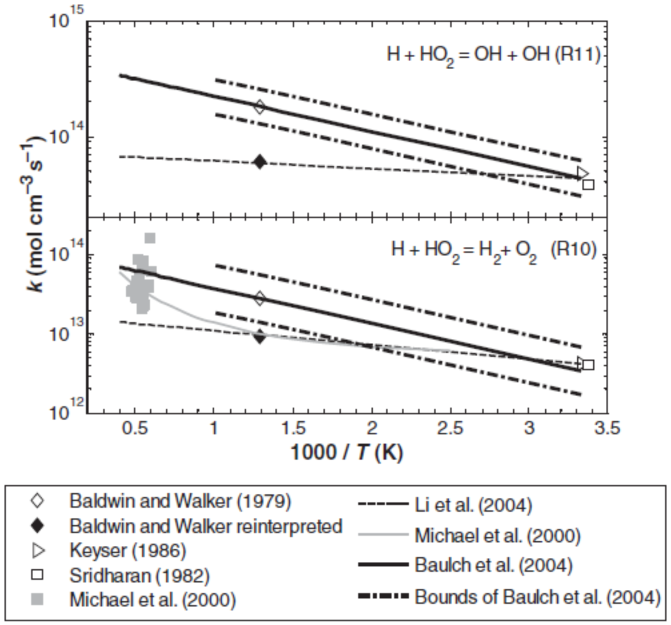

Topic 3
Theoretical basis of Chemical Kinetics

Klippenstein: From theoretical reaction dynamics to chemical modeling of combustion

Proc Comb Inst 2017, 36, 77

- "The accurate prediction of the temperature and pressure dependence of gas phase reactions requires state-of-the- art implementations of a variety of theoretical methods: ab initio electronic structure theory, transition state theory, classical trajectory simulations, and the master equation."
- "Future progress in the fidelity of the chemical modeling of combustion will benefit from more widespread applications of theoretical chemical kinetics and from increasingly intimate couplings of theory, experiment, and modeling."

Numbers of species and reactions in mechanisms for combustion of hydrocarbon fuels (Lu and Law, Prog En Comb Sci, 2009, 35, 192, updated Yuan et al, Science China (Chemistry), 2017, 60, 1391)

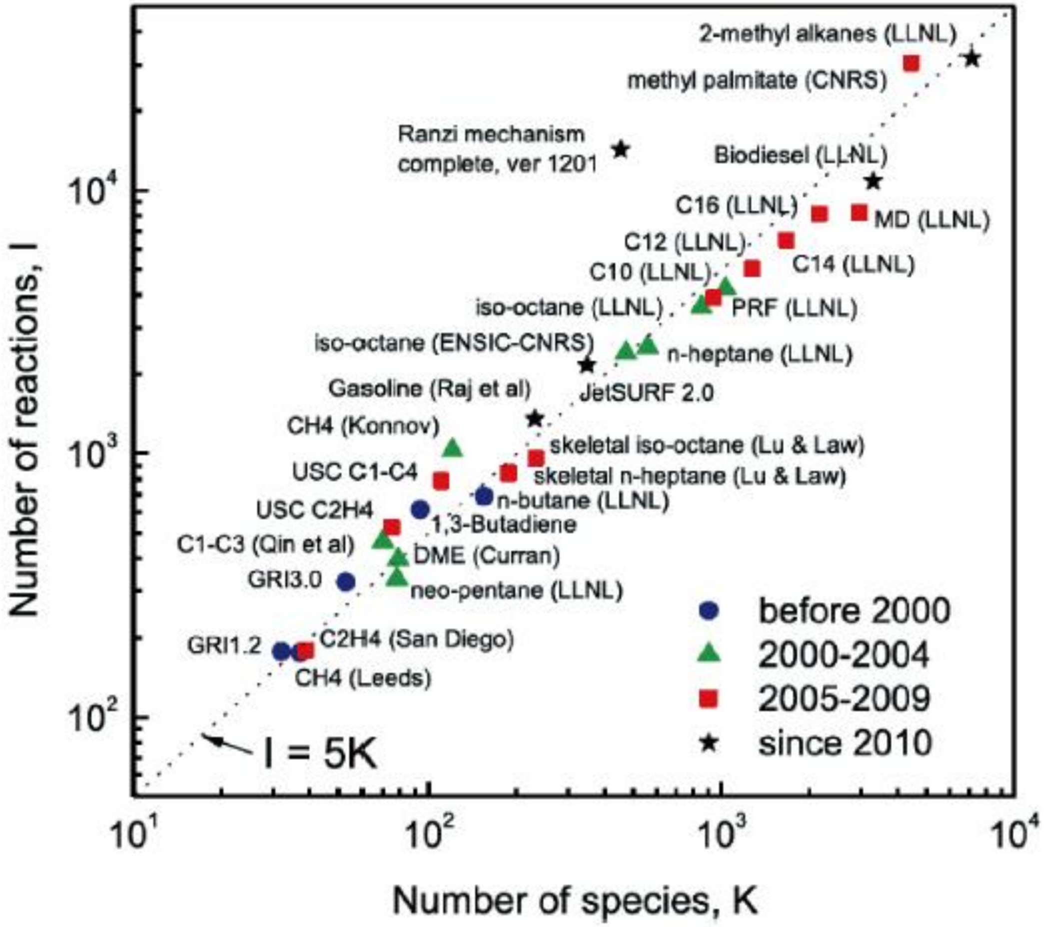

- Larger mechanisms require thousands of rate constants.
- Can't measure them all – calculation essential

Synopsis

- Look at potential energy surfaces (PES) for stable molecules and for reactions
- Theoretical methods for PES determination
- Examine the basis of transition state theory (TST)
- Treatment of reactions with no (or small) energy barrier – variational transition state theory (VTST)
- Reactions with two transition states
- Pressure dependent reactions and reactions involving multiple wells – master equation (ME) methods)

Statistical mechanics – a reminder

- The equilibrium constant for a generalised reaction

$$\sum_i \nu_i X_i = 0$$

where X_i is a chemical species and ν_i is the stoichiometric coefficient (positive products, negative reactants) is given by:

$$K_c = \prod (q_{X_i}/V)^{\nu_i} \exp\left(-\frac{\Delta\varepsilon_0}{kT}\right)$$

- Dividing the total partition function by V removes the volume term from the translational partition function. q/V is given the symbol Q
- $\Delta\varepsilon_0$ is the difference in zero point energies of the products and reactants.
- This equation is used in the formulation of the Transition State Theory expression for the rate constant.

Transition State Theory

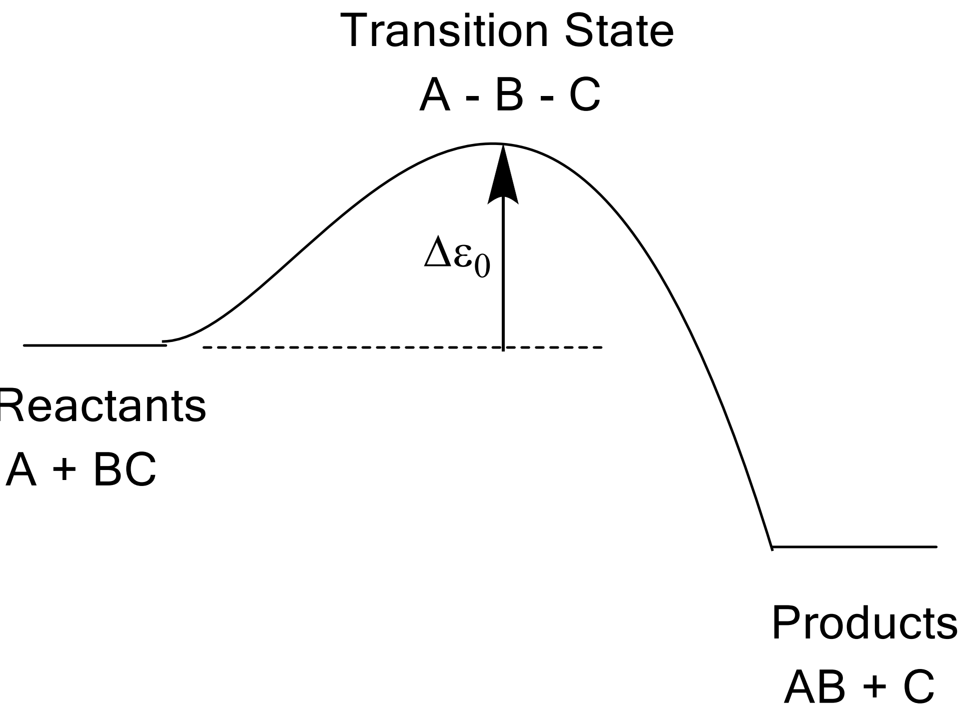

- Transition State Theory provides a method for calculating the rate constant, *k*(*T*), using statistical mechanics.
- *Q* is the molecular partition function, *q*, divided by the volume, *V*.
- The ‡ sign indicates that one vibrational mode has been removed from the partition function for TS (see later)
- Don't confuse the *k* terms – rate constant and Boltzmann constant

$$\boxed{k(T) = \alpha \frac{kT}{h} \frac{Q^{\ddagger}_{TS}}{Q_A Q_{BC}} \exp\left(\frac{-\Delta\varepsilon_0}{kT}\right)}$$

- α is a correction factor; its most common source is from the incorporation of tunnelling through the barrier in H atom transfer reactions.

Thermodynamic formulation of TST

$$K(T) = \prod_i Q_i^{\nu_i} \exp\left(-\frac{\Delta\varepsilon_0}{kT}\right) = \exp\left(-\frac{\Delta G^\theta}{RT}\right)$$

where *K* is the equilibrium constant and $\Delta\varepsilon_0$ is the difference in zero point energies of the reactants and products. ΔG is the (molar) Gibbs energy change for the reaction. Note the change from molecular to molar units and that $R = kN_A$, whereN_A is the Avogadro number. Applying this equation to TST:

$$k(T) = \alpha \frac{kT}{h} \frac{Q_{TS}^{\ddagger}}{Q_A Q_{BC}} \exp\left(\frac{-\Delta\varepsilon_0}{kT}\right) \qquad = \alpha \frac{kT}{h} \exp\left(-\frac{\Delta G^{\ddagger}}{RT}\right)$$

$\Delta G^{\ddagger}$ is the Gibbs energy of activation. We will discuss later when we talk about variational transition state theory

Born-Oppenheimer Approximation

- Electrons are light and have high kinetic energies, so they move very fast compared to the nuclei. So expect nuclei to feel time-averaged force exerted by swarm of electrons.
- Electrons are very quantum mechanical (wave-like), described by the Schroedinger Wave Equation.
- Atoms/Nuclei are much heavier, move more slowly.
- So solve the electron-motion problem first, assuming the nuclei are stationary at different geometries R, yielding a potential field V(R) that the nuclei are moving in.
- Having determined V(R), we need to understand and quantify the motion of the nuclei, again using the Schroedinger equation.

Molecular degrees of freedom

- A molecule composed of N atoms has 3N nuclear degrees of freedom:
  - 3 translation
  - 2 rotation (linear molecule), 3 rotation (non-linear)
  - 3N-5 vibration (linear), 3N-6 vibration (non-linear)
- The interaction between the electrons and the nuclei provides a potential energy surface that defines the equilibrium geometry of the molecule and the response to the relative motion of the atoms – the vibrations and internal rotations
- The molecule is described by an overall wavefunction, ψ; the Born-Oppenheimer principle states that this can be separated into nuclear and electronic components, because of the difference in masses (last slide)

$$\psi = \Psi_{\text{electronic}} \Psi_{\text{nuclear}}$$

Potential energy surfaces. 1. diatomic molecule

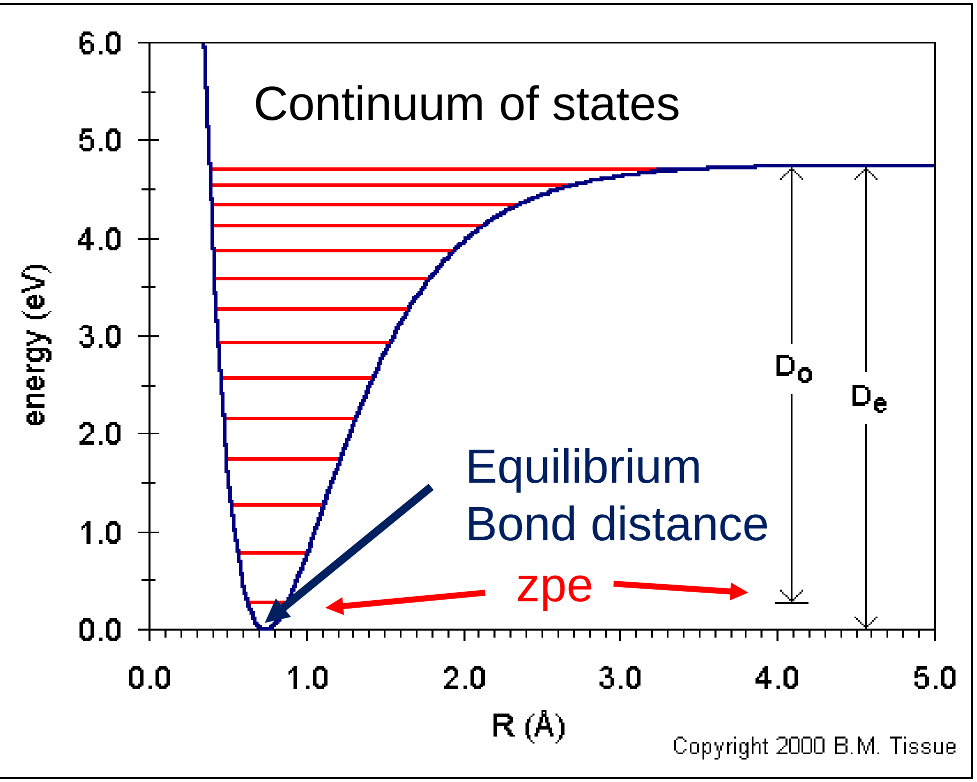

Copyright 2000 B.M. Tissue

- The potential energy surface in a diatomic depends on one variable – the internuclear distance: V(R).
- The vibration is anharmonic because the molecule dissociates if sufficient energy is incorporated. As a result, the energy levels are not evenly spaced, but converge.
- Note the zero-point energy (zpe) = $h\nu/2$. The dissociation energy from this state is D_0. Electronic structure calculations of the potential energy return an energy without zpe, which must be added once the frequencies have been determined. The dissociation energy from the minimum in V(R) is D_e. Note that many calculations use a rigid rotor harmonic oscillator model for the rotations and vibrations.

Vibrational energy levels and wavefunctions

Model for vibrational motion in a molecule – harmonic oscillator:

- Potential energy, E_{PE}=V:

$$V = \frac{1}{2}k(r - r_0)^2$$

- Note the quantized energy levels, spacing = *hv; zpe= hv /2*
- *Wavefunctions are Gaussian functions – they are not simple sine functions because (E-V) depends on r.*
- Note the penetration of the wavefunction into the *non-classical* region where $V > E$: the kinetic energy is negative – *quantum mechanical tunnelling*
- In this region, the wavefunction is no longer oscillatory but decreases to zero at $(r - r_0) = \infty$

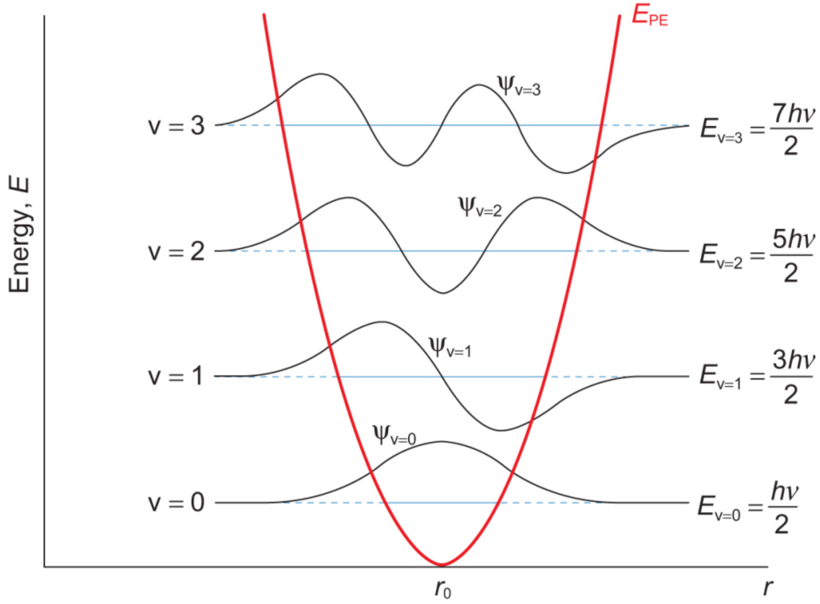

Rotation - rotational motion is slower than vibrational. The energy levels depend on the moment of inertia and hence on the <u>average</u> bond distance.

Translation - just depends on the mass. Energy level spacing small. Treat classically.

Normal modes of vibration - triatomic molecule

3N-6 vibrations (non-linear)
3N-5 vibrations (linear)

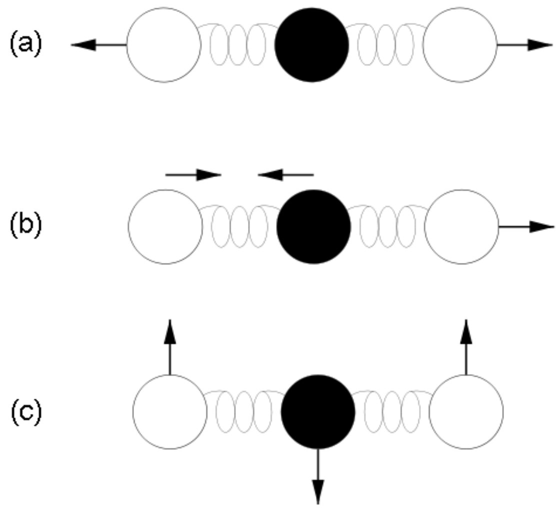

- Carbon dioxide (4 vibrations)
- Symmetric stretch
- Asymmetric stretch
- Bend (doubly degenerate)

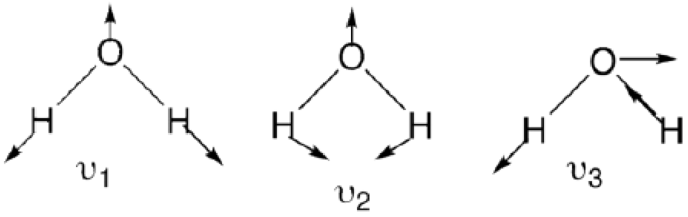

- Water (3 vibrations)
- Symmetric stretch
- Bend (non- degenerate)
- Asymmetric stretch

Potential energy surface. 2. triatomic molecule

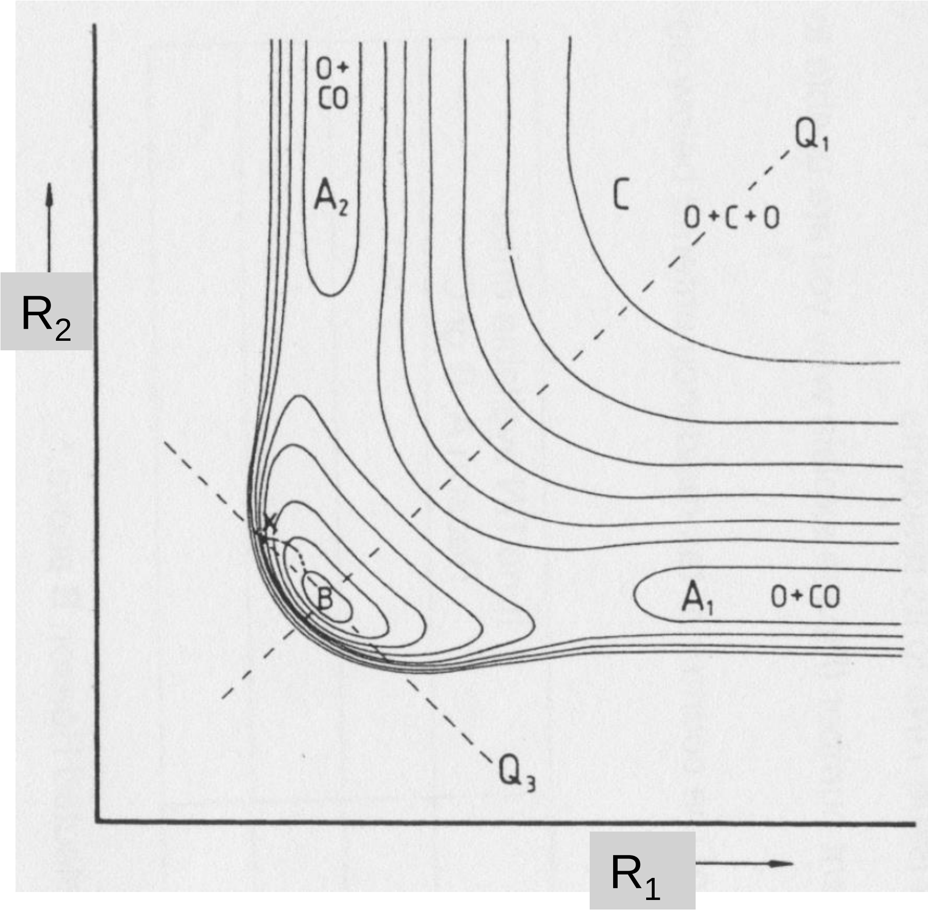

- There are 3 internal coordinates for a triatomic – the bond distances, R_1 and R_2 and the bond angle θ. This 2D figure is for constant θ.
- Two normal modes of vibration are shown – the symmetric stretch (Q_1) – both R_1 and R_2 increase (and decrease) together and the asymmetric stretch (Q_3) where R_1 decreases as R_2 increases
- The other vibration(s) – bending – involve changes in θ.

Potential energy surface 3. reaction: A + BC

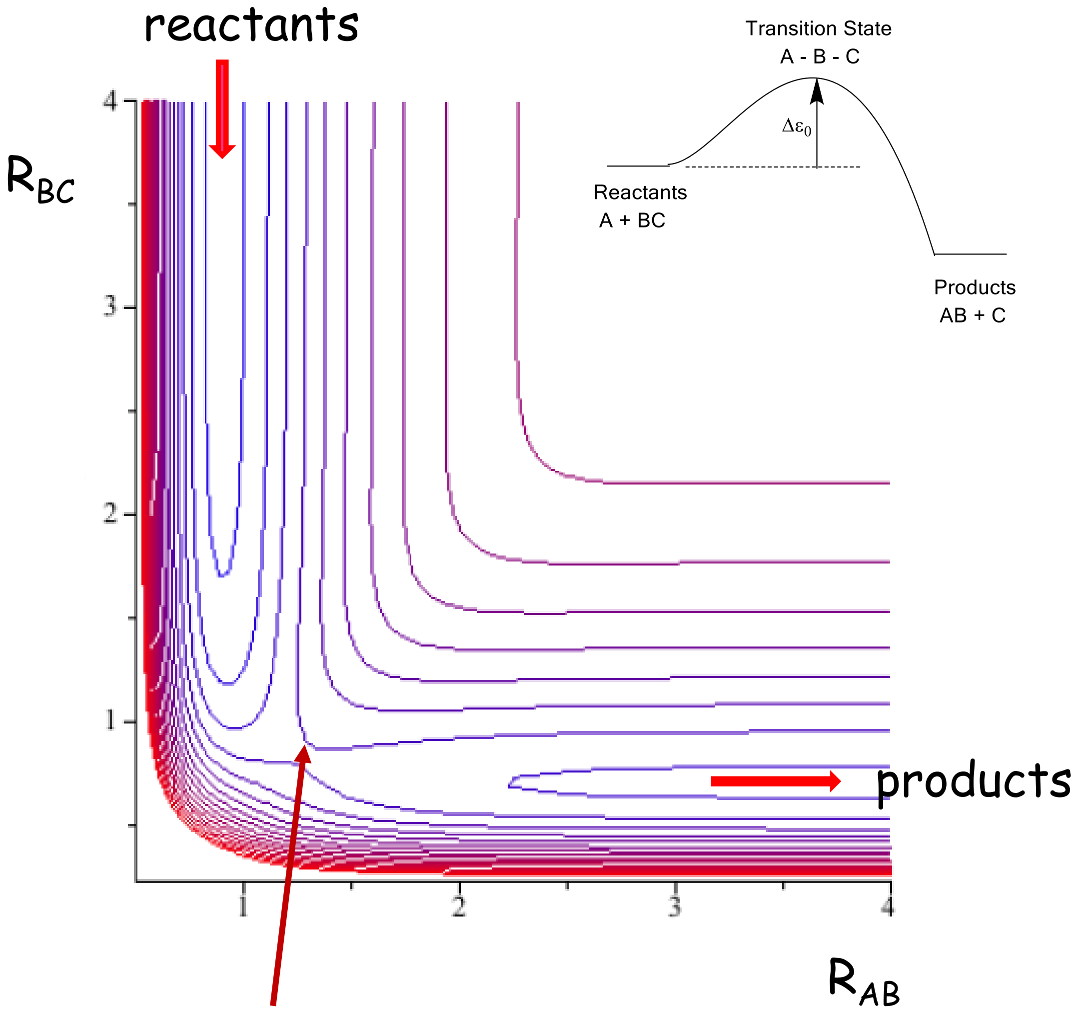

- Reactants approach as R_{AB} decreases. Products separate as R_{BC} increases.

  The figure relates to a fixed angle of approach.

  The symmetric stretch (R_{AB} and R_{BC} both increase (or decrease) is at a potential minimum – this is a true vibration.

  The asymmetric stretch (R_{BC} decreases as R_{AB} increases is at a potential maximum – this is the reaction coordinate and is not included in $Q^{\ddagger}_{TS}$. It is the source of the $\frac{kT}{h}$ term

$$k(T) = \alpha \frac{kT}{h} \frac{Q^{\ddagger}_{TS}}{Q_A Q_{BC}} \exp\left(\frac{-\Delta\varepsilon_0}{kT}\right)$$

Electronic structure calculations

- We need to calculate the potential energy surface for the reaction system, in order to determine the energy of the transition state, its geometry (to determine the moments of inertia) and its vibrational frequencies. We also need these quantities for the reactants.
- For many kinetic problems, this reduces to determining these properties at the maximum (TS) and minimum (reactants) of the surface – the whole surface itself is not needed. More information is needed for variational transition state theory.
- This requires us to solve the Schroedinger equation – a difficult task. We have to make approximations about the nature of the wavefunctions of the electrons and of their interactions.

Approaches to accurate electronic structure calculations 1.

- A basis set is composed of atomic orbitals , yielding linear combination of atomic orbitals approach (LCAO). The CBS limit is an extrapolated estimate of a result obtained using an infinitely large (complete) basis set
- Electron correlation is the interaction between electrons. The correlation energy is a measure of how much the movement of one electron is influenced by the presence of all other electrons.
- The Hartree Fock method has minimal electron correlation. **Full configuration interaction** (or **full CI**) is a linear variational approach which provides numerically exact solutions (within the infinitely flexible complete basis set) to the electronic Schroedinger equation.

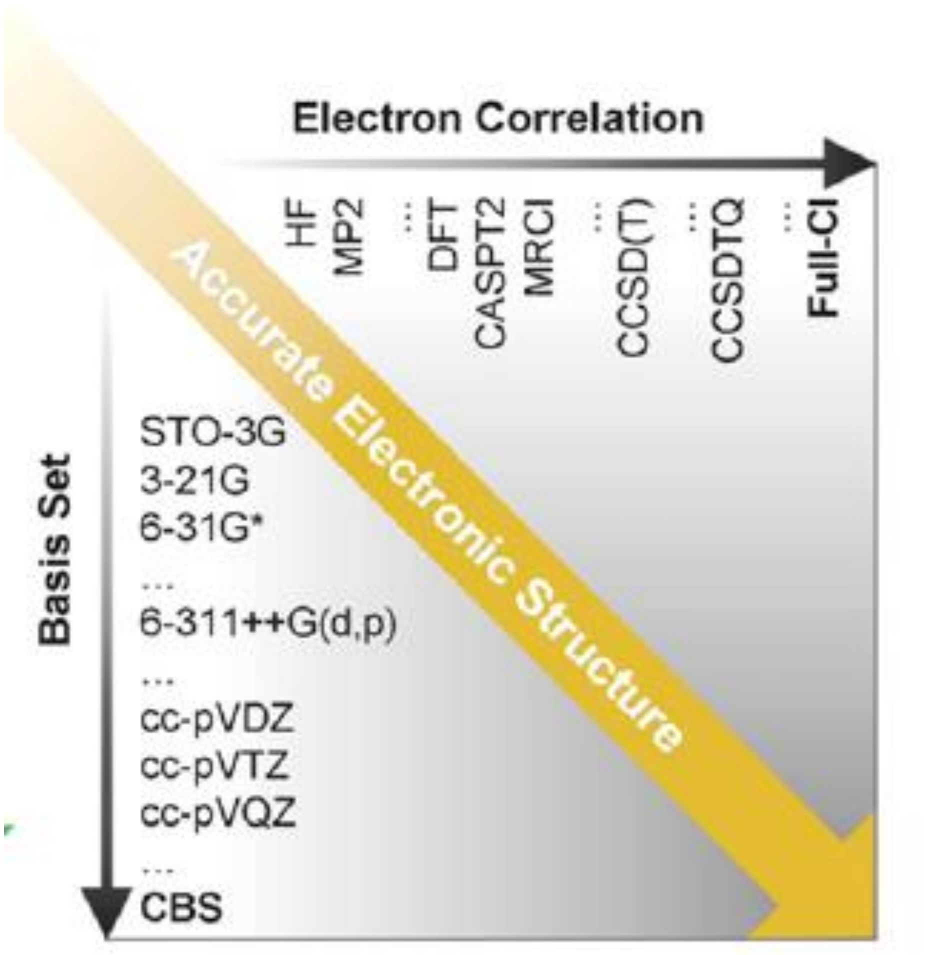

Zador et al Prog Energy Comb Sci 2011, 37, 371

Approaches to accurate electronic structure calculations 2.

- CCSD(T) (coupled cluster with singles, doubles and perturbative triples) is a widely used, high level method.
- Even with such methods, the 2x standard deviation errors are of the order of 1 kcal mol^{-1}
- For some reactions involving certain radicals, multireference techniques are needed. In such cases multiple wavefunction descriptions are needed to describe a single transition state.
- Examples include CASSCF (complete active space, self consistent field)and CASPT2 (second order perturbation theory. The treatment of electron correlation is greater in the latter
- Several software packages are available and Molpro is widely used in kinetics calculations (Werner et al. J Chem Phys, 2020, 152, 144107 and https://www.molpro.net

Density functional theory (DFT)

- Density functional theory (DFT) is widely used in combustion applications. DFT uses functionals operating on electron density to generate molecular energies. The B3LYP functional, which has been tuned to experimental reaction energies and molecular enthalpies of formation, is widely used. More recent functionals include M06-2X and M08.
- DFT is widely used to explore the PES and determine the energy maxima and minima and associated geometries and frequencies. Higher level *ab initio* methods are then used to refine the energies of these turning points on the surface.

Approach to calculating rate coefficients using TST

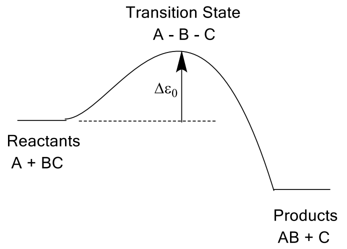

- The approach is most simple for a constrained transition state – one where there is a significant maximum on the reaction coordinate.
- The potential energy surface (PES) is calculated using electronic structure methods and the TS located.
- The energy of the TS relative to the reactants is determined along with the structure of the TS (which allows the moments of inertia to be calculated) and the vibrational frequencies. *k* (T) can then be calculated using Transition State Theory, and assuming rigid rotor – harmonic oscillator (RRHO) behaviour
- Problems arise with hindered internal rotors and more complex calculations are needed.
- Quantum mechanical tunnelling through the energy barrier can be important, especially for H transfer reactions.

A-B + C

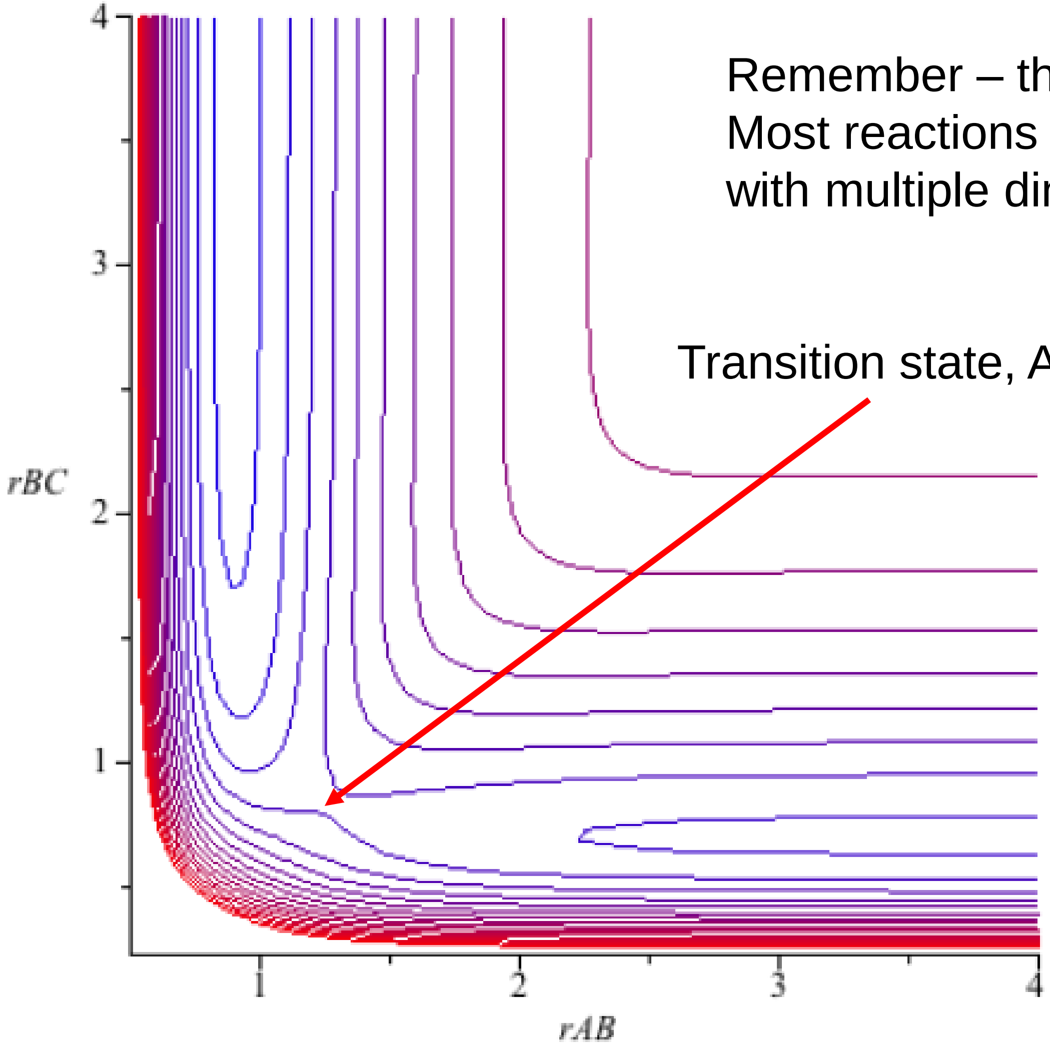

Transition state, A-B-C

A + BC

Remember – this diagram is for A +BC. Most reactions are much more complex with multiple dimensions

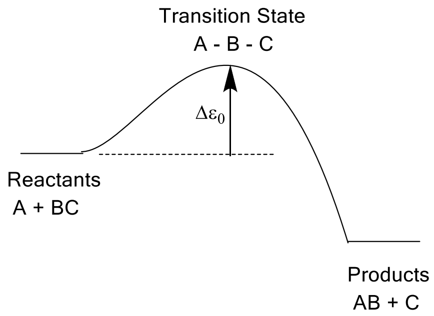

$$k(T) = \alpha \frac{kT}{h} \frac{Q^{\ddagger}_{TS}}{Q_A Q_{BC}} \exp\left(\frac{-\Delta\varepsilon_0}{kT}\right)$$

Molecular partition functions: rigid rotor harmonic oscillator (RRHO) - a reminder

$$q_{total} = q_{trans} q_{rot} q_{vib} q_{elect}$$

$$q_{trans} = \left[\frac{2\pi mkT}{h^2}\right]^{3/2} V$$

$$Q = q/V$$

$$q_{rot} = \frac{kT}{\sigma hBc}$$

$$q_{rot} = \frac{\sqrt{\pi}}{\sigma}\left\{\frac{(\frac{kT}{hc})^3}{ABC}\right\}^{1/2}$$

$$q_{vib} = (1 - e^{-\frac{hc\omega}{kT}})^{-1}$$

$$q_{vib} = \prod_{i=1}^{\alpha}(1 - e^{-\frac{hc\omega_i}{kT}})^{-1}$$

$$q_{elect} = \sum_{levels,i} g_i\, e^{-\beta\epsilon_i}$$

m is the molecular mass
A,*B*,*C* are the rotational constants (units cm^{-1})
ω is ν/c where ν is the vibrational frequency
ω has units cm^{-1}
σ is the symmetry number, *g* is degeneracy

Transition state theory applied to OH + RH → H···O···H···R → H_2O + R

Write TS (H···O···H···R) as X

$$k(T) = \alpha \frac{kT}{h} \frac{Q_X^{\ddagger}}{Q_{OH} Q_{RH}} \exp\left(\frac{-\Delta\varepsilon_0}{kT}\right)$$

Translational
Partition function

$$Q_t = \left[\frac{2\pi mkT}{h^2}\right]^{3/2} = \frac{q_t}{V}$$

$$\frac{(Q_X)_t}{(Q_{OH})_t (Q_{RH})_t} = \left[\frac{h^2}{2\pi kT}\right]^{3/2} \left[\frac{m_X}{m_{OH} m_{RH}}\right]^{3/2}$$

This is the translation contribution to the partition function quotient in the TS expression for the rate constants – depends on the molecular masses

2. Rotational contribution

Rotational partition function, OH (heteronuclear diatomic)

$$(q_{\mathrm{OH}})_r = \frac{kT}{\sigma h B_{\mathrm{OH}} c} = \frac{8\pi^2 kT I_{\mathrm{OH}}}{h^2} \quad (B = \frac{h}{8\pi^2 c I})$$

Rotational partition functions, RH, X (non-linear polyatomics)

$$q_r = \frac{\sqrt{\pi}}{\sigma}\left\{\frac{(\frac{kT}{hc})^3}{ABC}\right\}^{1/2} \qquad (A \propto \frac{1}{I})$$

$$\frac{(q_{\mathrm{X}})_r}{(q_{\mathrm{RH}})_r} = \frac{\sigma_{\mathrm{RH}}}{\sigma_{\mathrm{X}}}\left\{\frac{(ABC)_{\mathrm{RH}}}{(ABC)_{\mathrm{X}}}\right\}^{1/2} = \frac{\sigma_{\mathrm{RH}}}{\sigma_{\mathrm{X}}}\left\{\frac{(I_A I_B I_C)_{\mathrm{X}}}{(I_A I_B I_C)_{\mathrm{RH}}}\right\}^{1/2}$$

Need geometries to obtain moments of inertia. Obtain from spectroscopy for stable molecules, from electronic structure calcs for X

Vibrational and electronic contributions

Vibrational partition function for OH, $\omega = \nu / c$

$$(q_{\mathrm{OH}})_v = (1 - e^{-\frac{hc\omega}{kT}})^{-1}$$

Vibrational partition functions for RH and X

$$q_v = \prod_{i=1}^{n} (1 - e^{-\frac{hc\omega_i}{kT}})^{-1}$$

Where *n* = 3N-6 for RH and 3(N+2)-7 for X. (one vibrational mode is along the reaction coordinate has been removed.

Electronic partition function for OH$^2\Pi$ = (2+2exp(-$\Delta\varepsilon$/kT)

Electronic partition function for RH = 1

Electronic partition function for X = 2 (unpaired electron)

Temperature and ω dependence of a vibrational partition function

T/K					
200	3.31	1.95	1.13	1.00	1.00
300	4.69	2.62	1.31	1.01	1.00
500	7.46	4.00	1.73	1.06	1.00
1000	14.41	7.46	2.85	1.31	1.01
1500	21.35	10.93	4.00	1.62	1.06
2000	28.30	14.41	5.15	1.95	1.13
3000	42.20	21.35	7.46	2.62	1.31

$$q_{vib} = (1 - e^{-\frac{hc\omega}{kT}})^{-1}$$

The table shows partition functions at different *T* for ω values of 50, 100, 300, 1000 and 3000 cm^{-1}

Note: *k*/*hc* = 0.695 $cm^{-1}K^{-1}$

kT/*hc* = 695 cm^{-1} at 1000 K

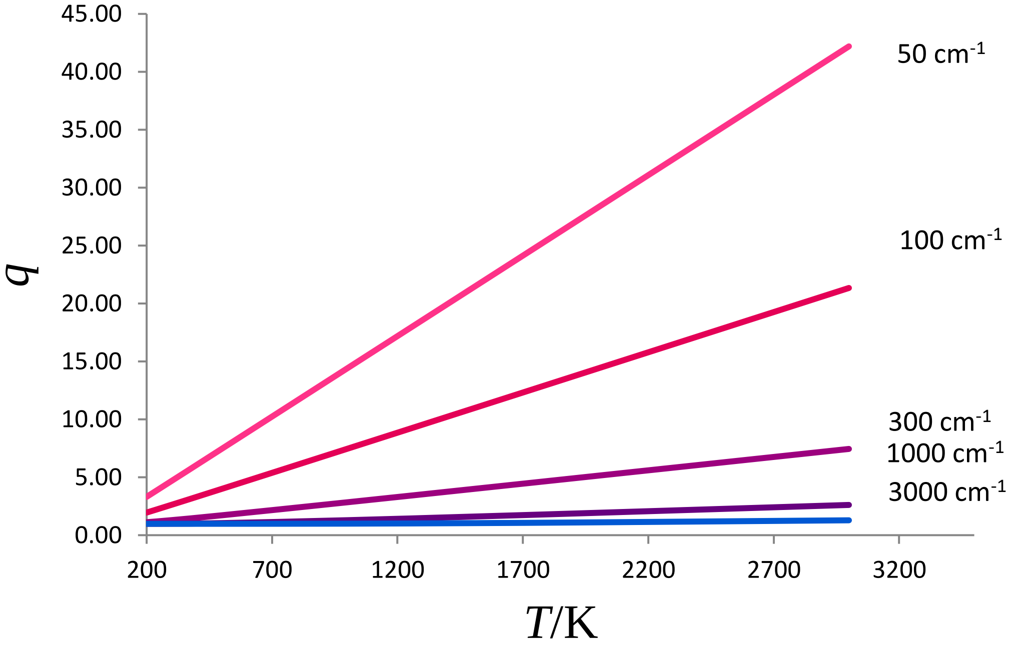

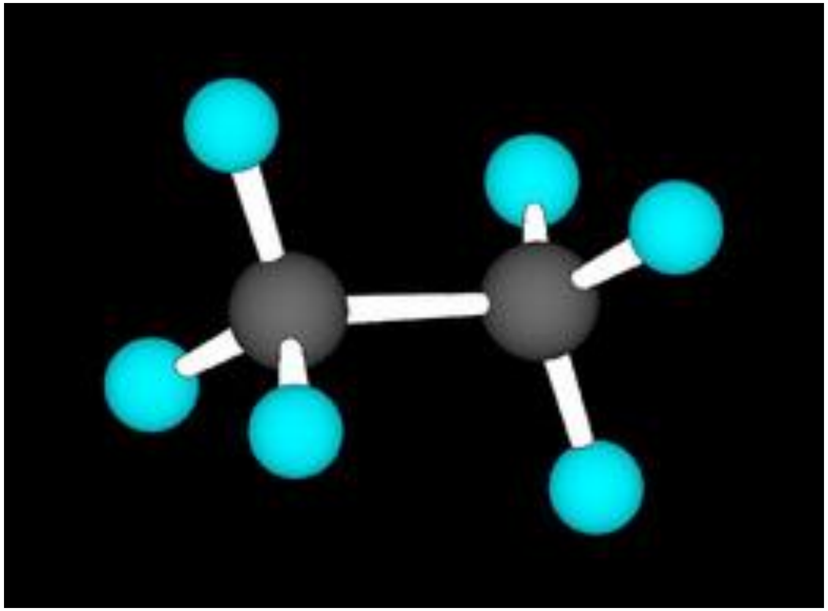

Internal rotation; hindered internal rotation and torsional vibrations; e.g. ethane

- Energy levels in torsional wells and effect of temperature on freedom of motion

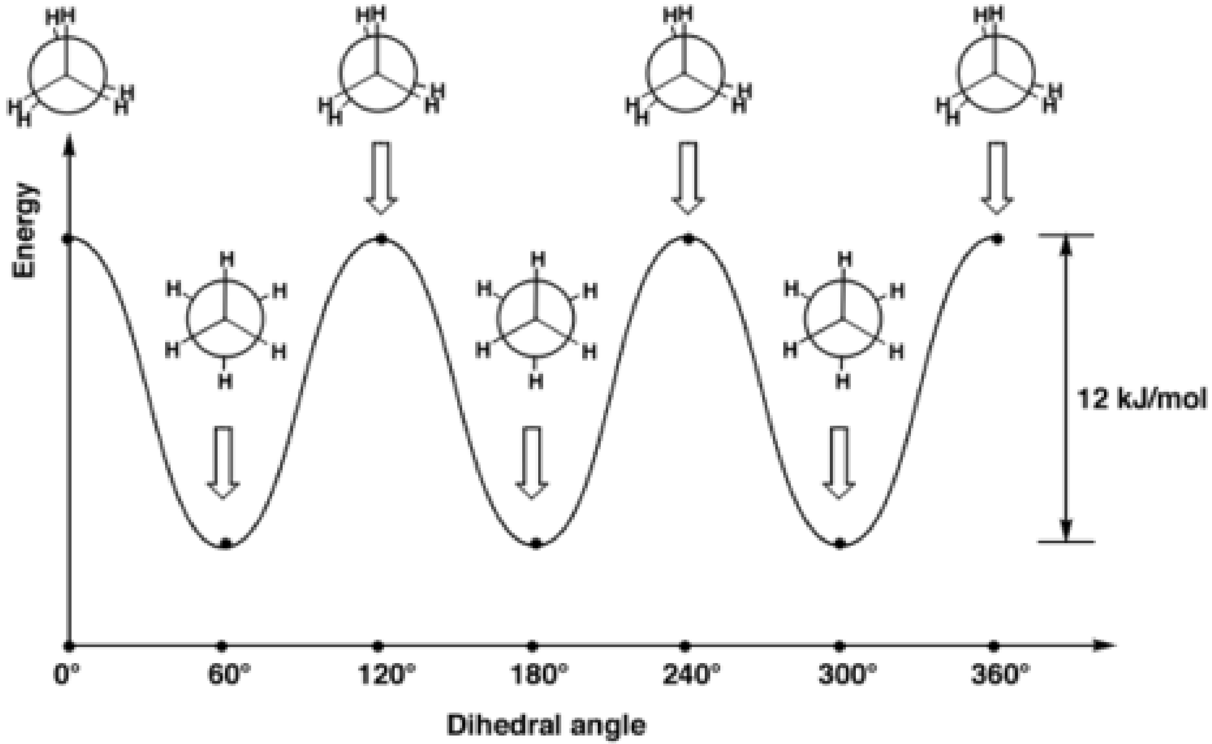

Quantum mechanical tunnelling – a reminder from Topic 1.

$$-\frac{\mathrm{d}^2\psi}{\mathrm{d}x^2} = \frac{8\pi^2 m}{h^2}(E - V)\psi$$

For *E*-*V* = constant a solution of the Schroedinger equation is

$$\psi = A exp(ikx)$$

$$k = \sqrt{\frac{8\pi^2 m(E - V)}{h^2}}$$

For *E* > *V* the solution is oscillatory, as discussed for the particle in a box

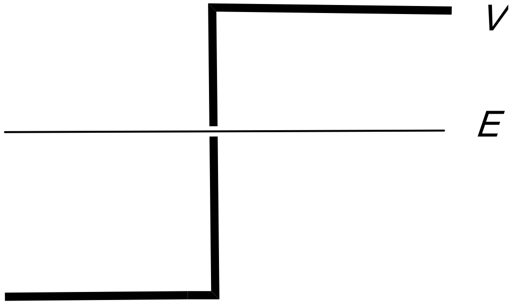

For *V* > *E*, *k* = *i*κ, where

$$\kappa = \sqrt{\frac{8\pi^2 m(V - E)}{h^2}}$$

$$\psi = B exp(-\kappa x)$$

i.e. the wavefuction penetrates into the non-classical region where V > E (and the kinetics energy is negative) and decays exponentially in this region

NB the dependence on mass

Tunnelling in chemical reactions

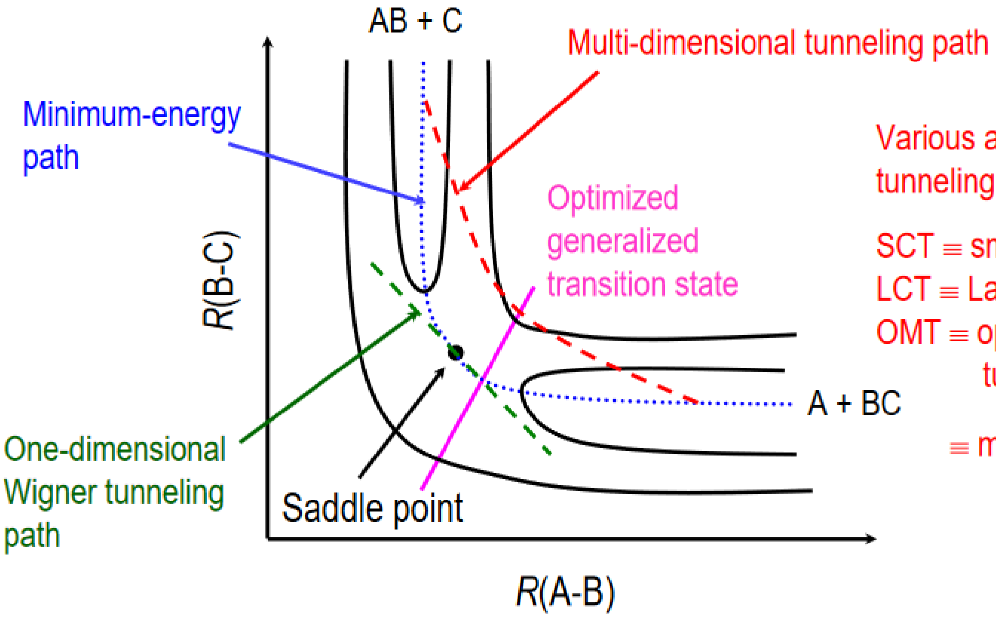

Various approximations for the tunneling paths may be considered:

SCT ≡ small-curvature tunneling
LCT ≡ Large-curvature tunneling
OMT ≡ optimized multidimensional tunneling

$\equiv \max \begin{cases} \text{SCT} \\ \text{LCT} \end{cases}$

- Simplest calculations use a barrier shape based on the imaginary frequency
- Eckart model is widely used.
- Leads to curvature in Arrhenius plot.
- For more discussion and details, see reviews:
  - Truhlar, Garrett, and Klippenstein J. Phys. Chem. 1996, 100, 12771.
  - Fernandez-Ramos, Ellingson, Garrett, and Truhlar, Rev. Comp. Chem. 2007, 23, 125
  - Truhlar et al https://comp.chem.umn.edu/polyrate/ - polyrate code

Heavy atom tunnelling in $\cdot CH_2(CH_3)_2COOH$

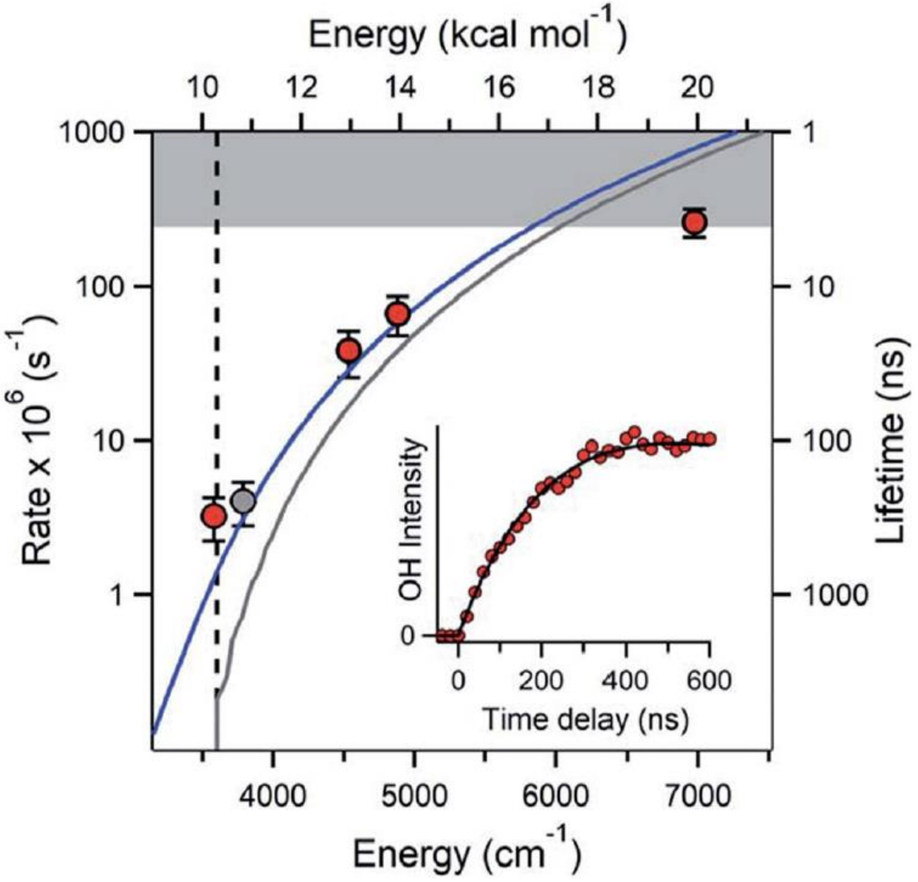

The solid lines denote ab initio RRKM predictions with (blue) and without (gray) tunneling corrections. The vertical dashed line denotes the saddle point barrier of 10.3 kcal mol^{-1}

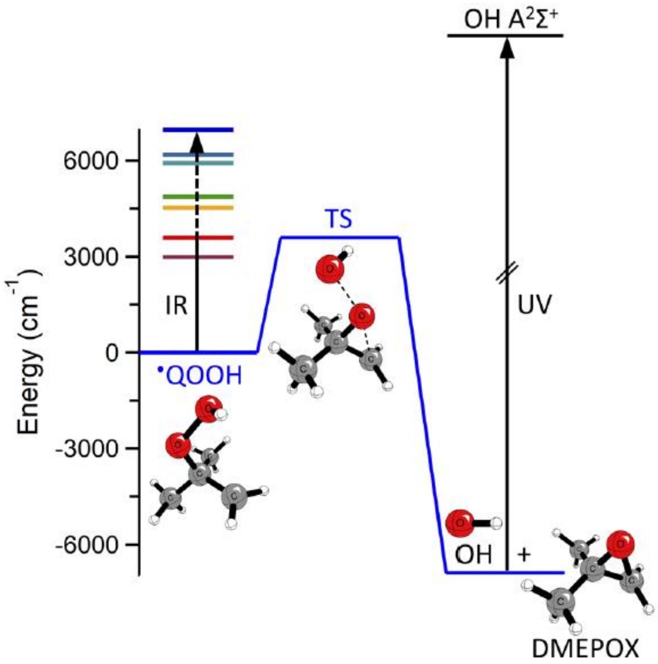

- The transition state involves the breaking of the O-OH bond and the making of the C-O bond.
- Substituting D for H changes the rate constant very little, showing that H motion is not important.
- Hansen et al *J. Chem. Phys.* 156, 014301 (2022)

Microcanonical rate theory

Microcanonical rate theory examines the rate at a specific energy; it gives:

$$k(E) = \frac{hW^{\ddagger}(E)}{N(E)}$$

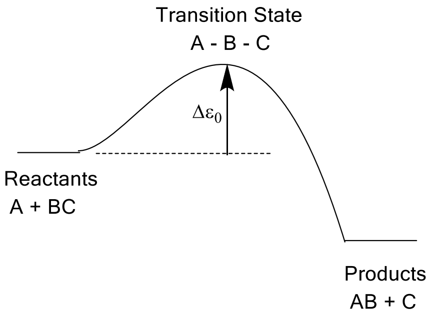

where $W^{\ddagger}(E)$ is the sum of states at the transition state, from energy zero at the TS to E and $N(E)$ is the density of states at energy E for the reactant(s). We will use this approach when dealing with master equation calculations.

Integrating this expression over a Boltzmann distribution of reactants gives the TST result for $k(T)$.

Sums and densities of vibrational states for CH_4 at low energies

n_1	n_2	n_3	n_4	E/cm^{-1}	degeneracy	W(E)	N(E)/cm
0	0	0	0	0	1	1	
1	0	0	0	1306	3	4	0.00230
0	1	0	0	1534	2	6	0.00877
2	0	0	0	2612	6	12	0.00557
1	1	0	0	2840	6	18	0.0263
0	0	1	0	2917	1	19	0.01299
0	0	0	1	3020	3	22	0.02913
0	2	0	0	3068	3	25	0.0625
3	0	0	0	3918	10	35	0.01177

Methane is treated as a harmonic oscillator. The wavenumbers of the four vibrational modes in cm^{-1} are:

1306(3), 1534(2), 2917(1) and 3020(3)

Where the numbers in parentheses are the degeneracies of the vibrations

Accuracy of TST calculations

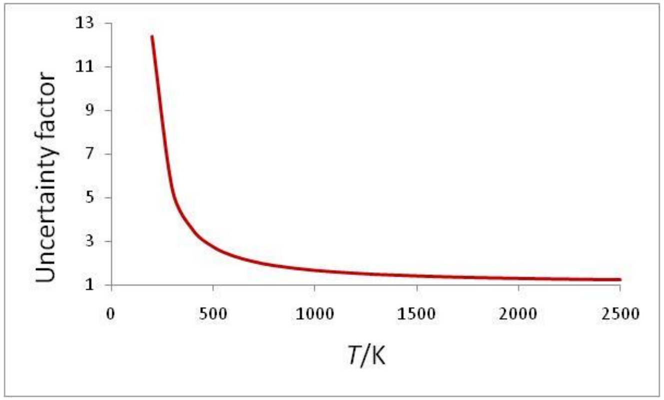

- Kinetic accuracy
  - Uncertainty of barrier height is typically ~ 4 kJ mol^{-1} (1 kcal mol^{-1}). Graph shows a plot of exp(E/RT) vs T with E = 4 kJ mol-1, which represents the uncertainty factor in *k* deriving from the uncertainty in the activation energy.
  - Deficiencies in the TS model
  - Rigid rotor harmonic oscillator model
  - Tunnelling model – generally use Eckart.
- Improvements – higher level ab initio calculations, variational effects, anharmonicities, multidimensional tunnelling …
- Often tune the barrier height obtained from lower level calculations to experimental data, allowing improved extrapolation of the latter. But see Klippenstein's discussion of purely ab initio calculations (PCI 2017, 36, 77)

Effects of incorporating higher level methods into TST

- Barker et al.: Chem Phys Letters, 2010, 499, 9-15. OH + H_2. High level ab intio calculation (CFOUR) + anharmonicity and coupling between different modes + multidimensional tunnelling.

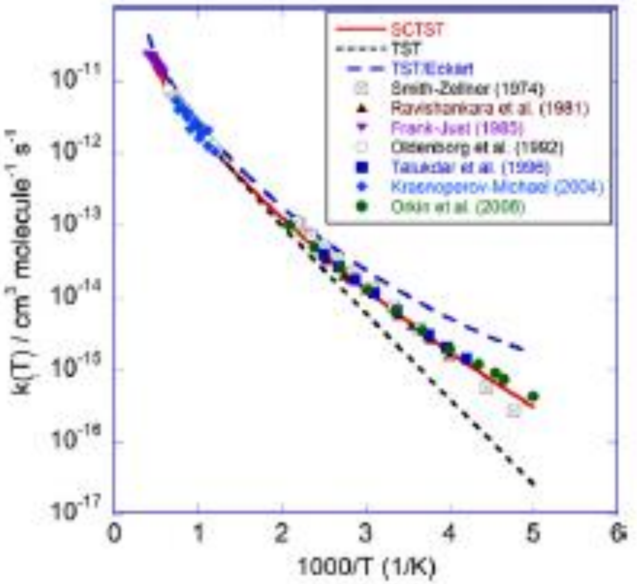

- Klippenstein: OH + OH → O + H_2O
  - Green: calculation from moderate level ab initio. (Barrier = 2.8 kcal mol^{-1})
  - Barrier constrained to experimental data (1.2 kcal mol^{-1})
  - Black: High level ab initio (0.7 kcal mol^{-1})
  - Red: High level constrained to experimental data (1.0 kcal mol^{-1})

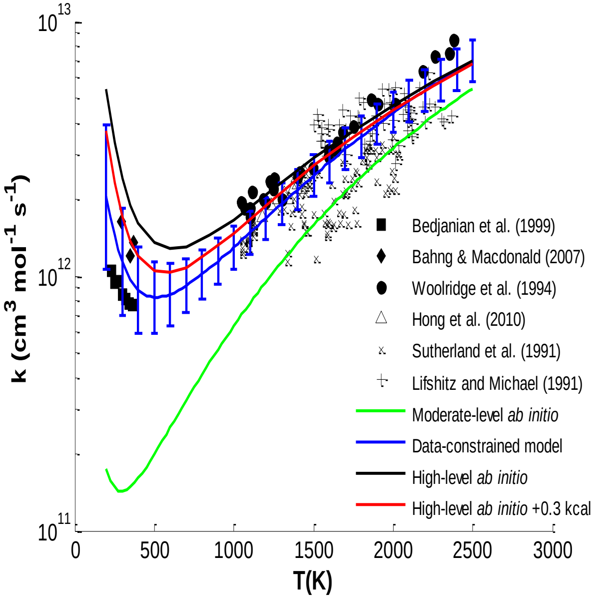

$OH + NH_3 \rightarrow H_2O + NH_2$

Nguyen and Stanton, J Chem Phys, 2017, 147, 152704

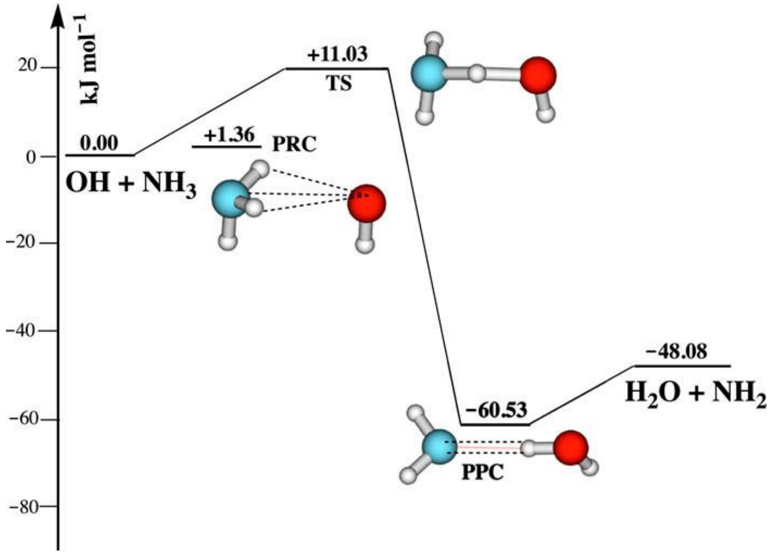

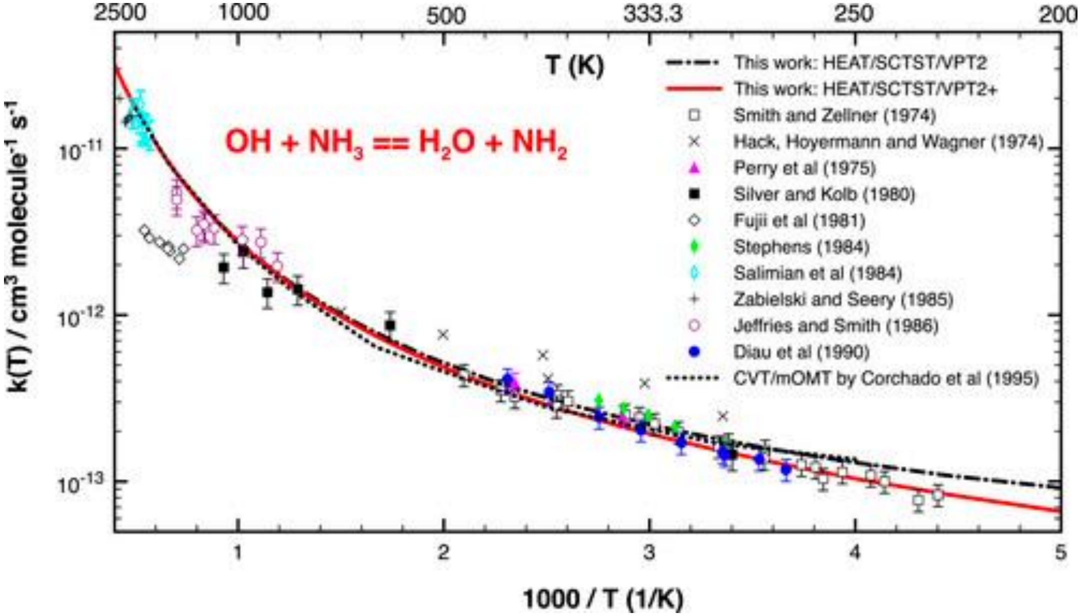

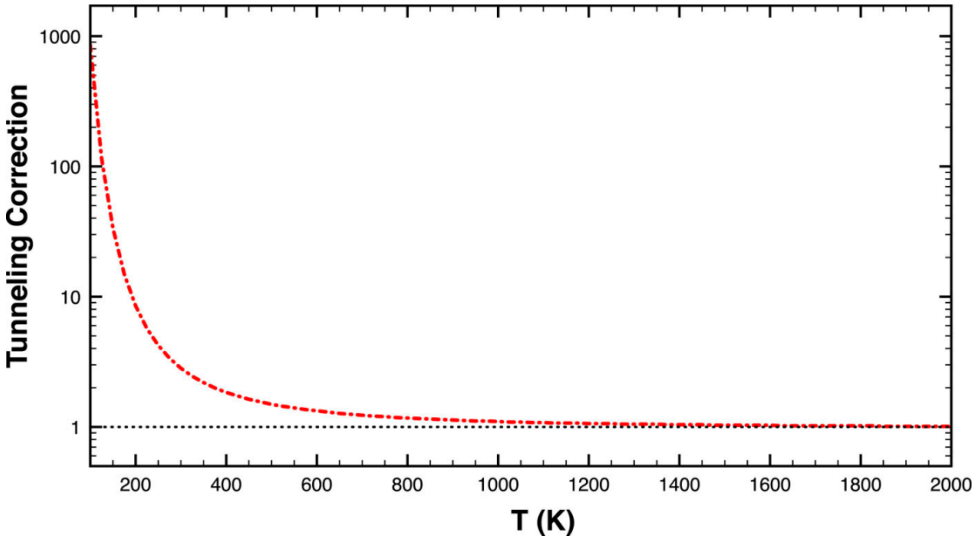

Uses the HEAT (High-accuracy Extrapolated Thermochemistry) ab intio Protocol – accurate to ± 1 kJ mol^{-1}.

Includes new treatment of tunnelling.

See paper for a clear discussion of the methods involved

Recent assessment of approaches to accurate models Klippenstein, Faraday Disc, 2022, 238,11

- Recent thermodynamics calculation for the Active Thermochemical Tables (Topic 4) have uncertainties of ~0.2 kcal mol^{-1}. Difficult to achieve this level of accuracy for transition states.
- Accurate geometries and zero-point energies essential. Vibrational anharmonicities can significantly affect the zero-point energy.
- For densities of states calculations (N(E) – see earlier), torsional modes are not well represented as harmonic oscillators; umbrella/inversion modes (e.g. the motion of the 3H atoms in planar CH3) also highly anharmonic and coupled to torsional modes. Accurate representations of these modes is challenging.
- Recent use of Monte Carlo phase space integration to calculate fully anharmonic partition functions – see Jasper et al. J Phys ChemA, 2018, 122, 1727; 2019, 123, 6210)

Radical + radical reactions

e.g. CH_3 + H, CH_3 + CH_3

No barrier on surface. Transition states determined <u>variationally</u>

Variational TST (VTST)

- Some reactions have only a small or no energy barrier. In these circumstances, the exact location of the TS is problematic.
- In canonical variational TST (CVTST), the Gibbs energy of the system is determined along the reaction coordinate and the transition state is given by the maximum in the Gibbs energy. Recall that $G = H - TS$ so that maximising G involves a combination of maximising energy and minimising entropy.
- The next slides examine microcanonical TST (μTST) and its variational form (μVTST), which focuses on a specific energy rather than temperature as in canonical approaches.

Where is the Transition State?

Calculate Q(T,R) or W(E,R) as a function of R

Transition State is at position of minimum in Q or W

Radical - Molecule

Saddle Point

Exp (-βE) dominates

Radical - Radical

No Saddle Point

With Decreasing R

- Entropy Decreases
- Exp $(-\beta V_{min})$ Increases

$CH_3 + H$

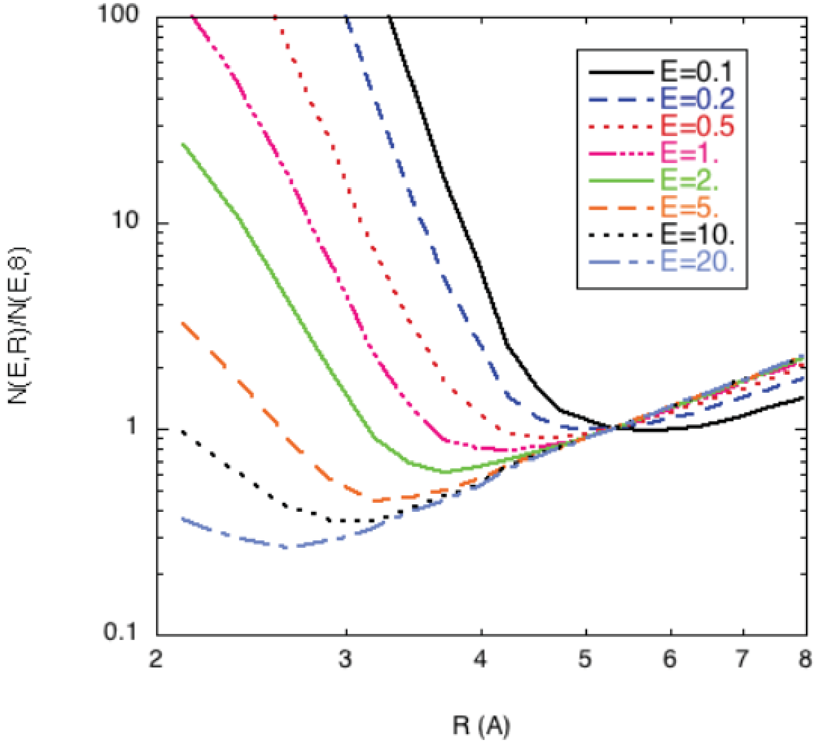

Where is the transition state?

- In a canonical treatment at temperature *T*, calculate *Q(T,R)*. Transition state is at minimum *Q*.
- In microcanonical treatment calculate the density of states vs *R*. TS at energy E is at minimum *N(E,R)*
- Radical + molecule: TS lies at saddle point, because the exp(-*E/kT*) term dominates.
- Radical + radical: no saddle point, potential energy *V* decreases as radicals approach: exp(-*V/kT*) increases, but frequencies of some vibrational modes increase.

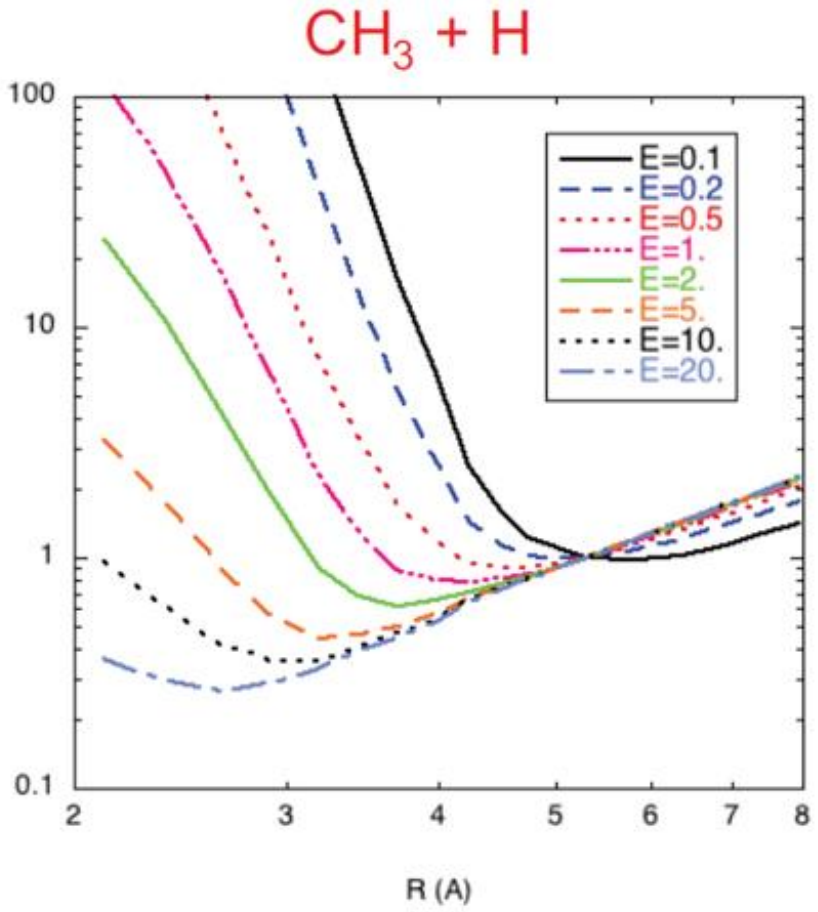

Decreasing R gives a lower potential energy and more energy available to distribute among modes. As spacings of mode energy levels increase, N(E,R) begins to increase. The TS is at the minimum and moves to smaller R as E increases.

Correlation of reactant and product modes for CH_3+H

- Conserved Modes – Vibrations of Fragments
- Transitional Modes – Fragment Rotations, Orbital Motion, and Reaction Coordinate

Vibrational frequencies / cm^{-1}

CH_3

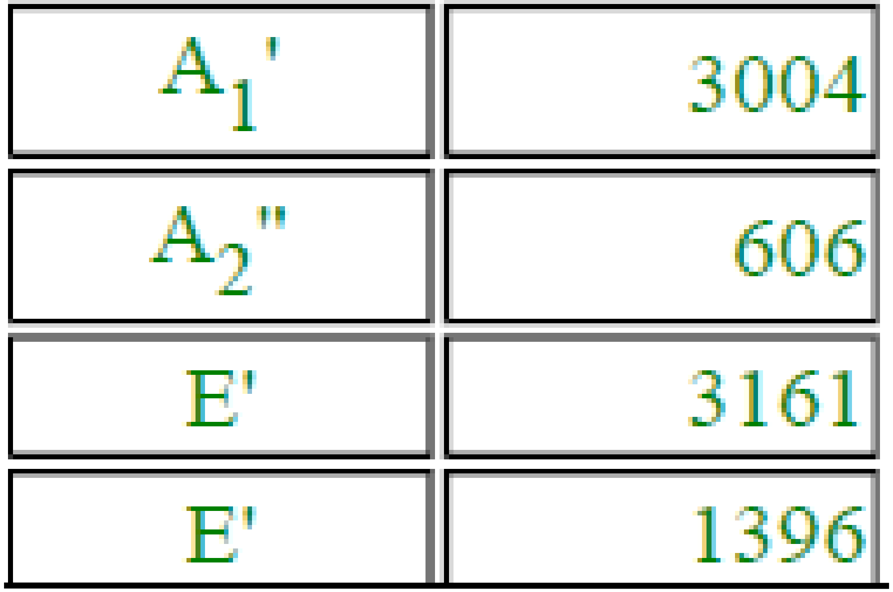

A_1'	3004
A_2''	606
E'	3161
E'	1396

CH_4

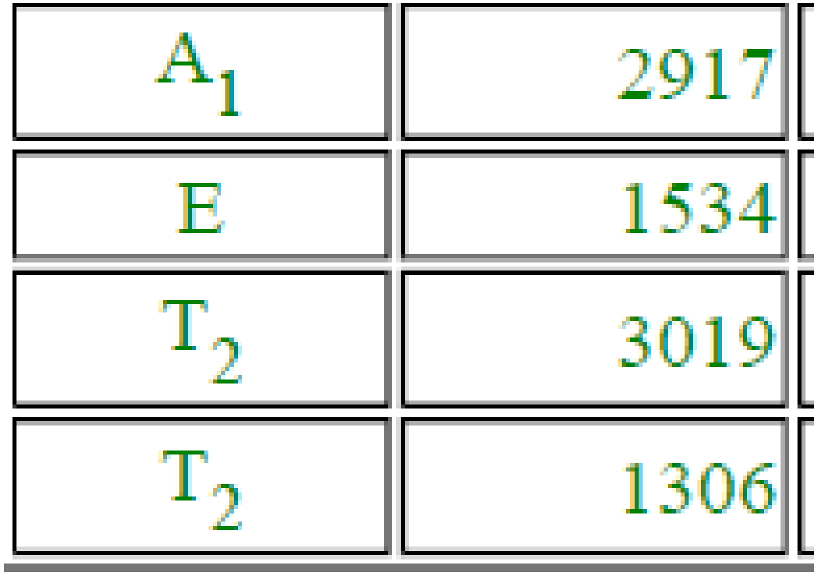

A_1	2917
E	1534
T_2	3019
T_2	1306

Correlation of reactant and transition state modes of motion

- A molecule has 3N degrees of freedom where N is the number of atoms.
- An atom has 3 degrees of translational freedom
- A linear molecule has 3 translational, 2 rotational and 3N-5 vibrational degrees of freedom
- A non-linear molecule has 3 translational, 3 rotational and 3N-6 vibrational degrees of freedom.

	CH_3	+	H	→	$CH_4^{\ddagger}$
T	3		3		3
R	3		0		3
V	6		0		8(+reaction coord)

3T → 3T

1R → 1R

2T → 2R ***

1T → Reaction coordinate

2R → 2V(deformation) ***

1V(umbrella) + 2V(deformation) → 3V(deformation) ***

3V(C-H stretch) → 3V(C-H stretch)

Methyl and Ethane frequencies

CH_3

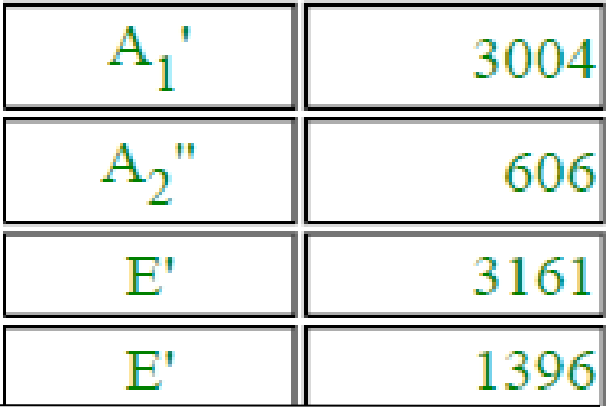

A_1'	3004
A_2''	606
E'	3161
E'	1396

C_2H_6

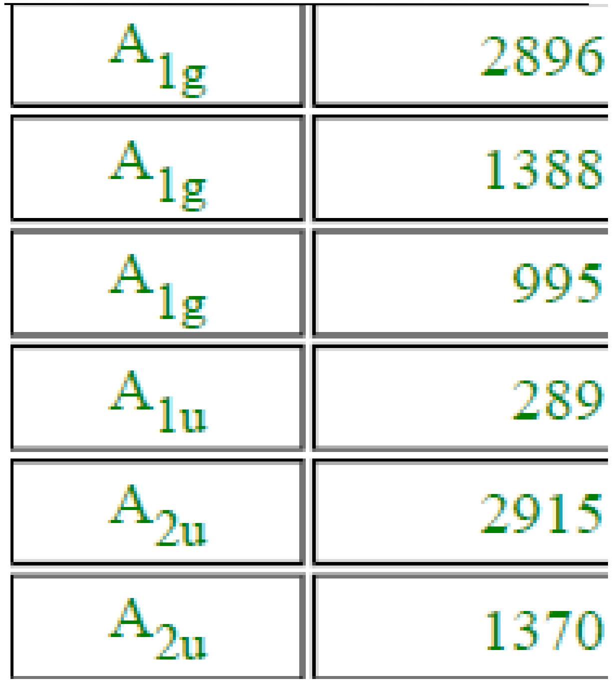

A_{1g}	2896
A_{1g}	1388
A_{1g}	995
A_{1u}	289
A_{2u}	2915
A_{2u}	1370

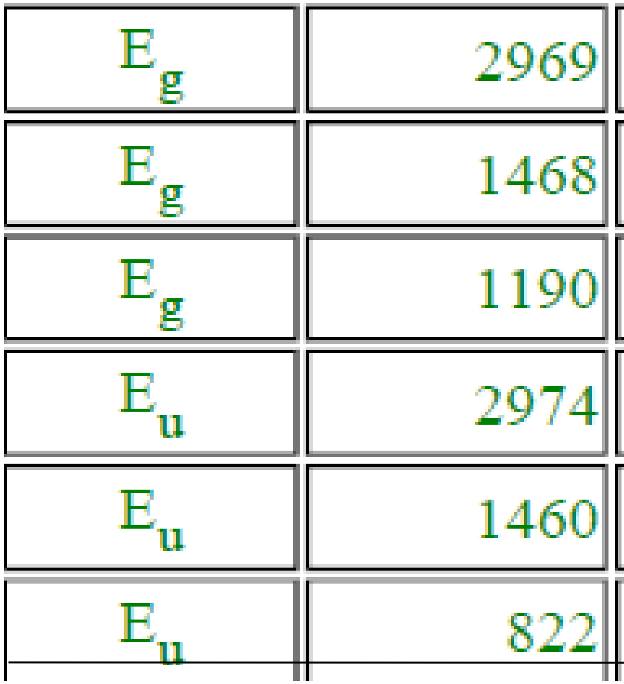

E_g	2969
E_g	1468
E_g	1190
E_u	2974
E_u	1460
E_u	822

Calculations, based on ab intio surfaces CH_3 +CH_3

Harding et al Phys. Chem. Chem. Phys., *2007*, 9,4055

- k_∞ depends sensitively on potential energy, V, as radicals approach.
- V_{calc} depends on the level of theory used.
- The color key is as follows: gray, CASPT2; green, CASSCF; purple,

  B3LYP; blue, MPW1K; orange, MP2.
- $k_\infty(T)_{calc}$ may be more accurate than $k_\infty(T)_{expt}$, because the latter depends on extrapolation (but see discussion in the section on the master equation)

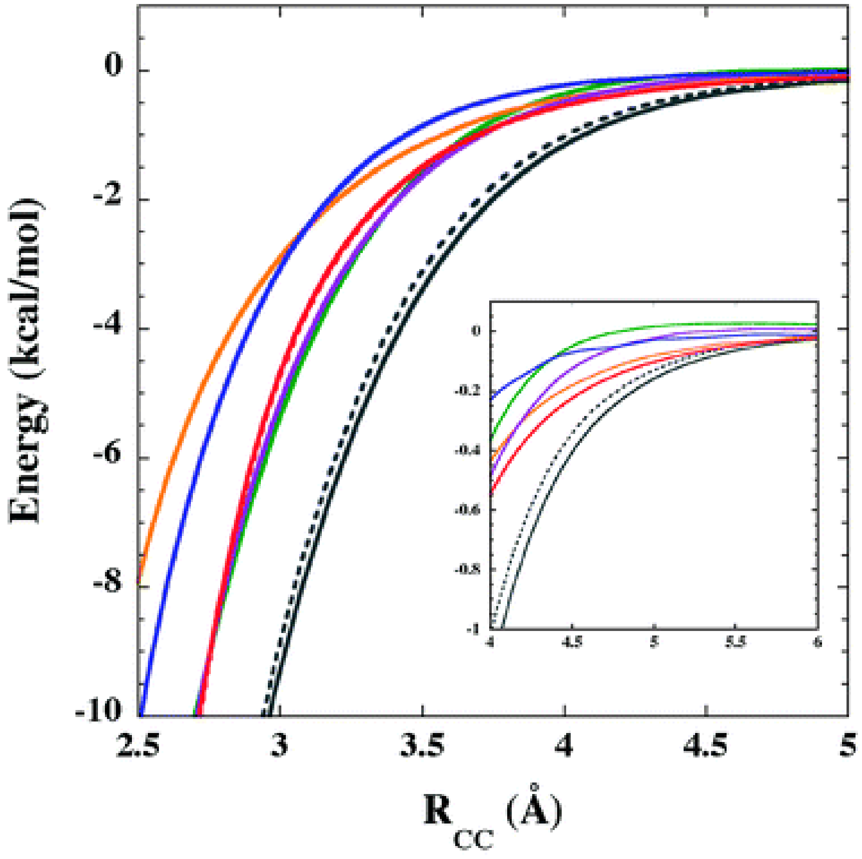

- High pressure limit rate coefficients for $CH_3+CH_3 \rightarrow C_2H_6$.
- Calculated values: the color key is as follows: gray, CASPT2; green, CASSCF; purple, B3LYP; blue, MPW1K; orange, MP2.
- The black symbols represent experimental results – see the refinement of these values in the section on the master equation

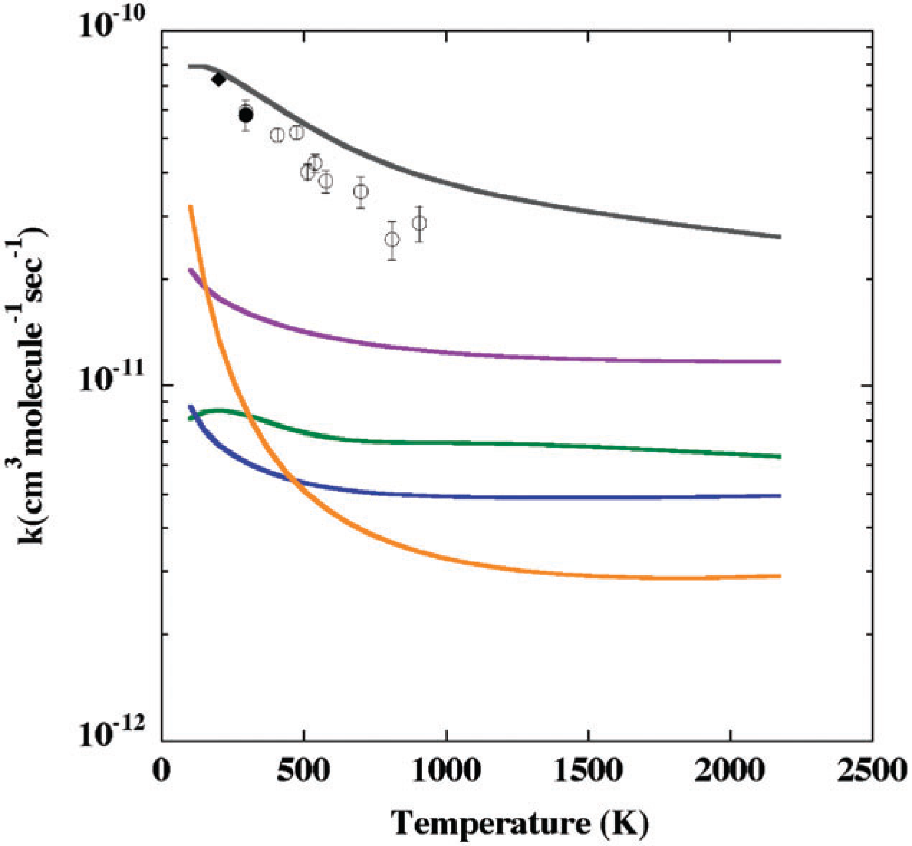

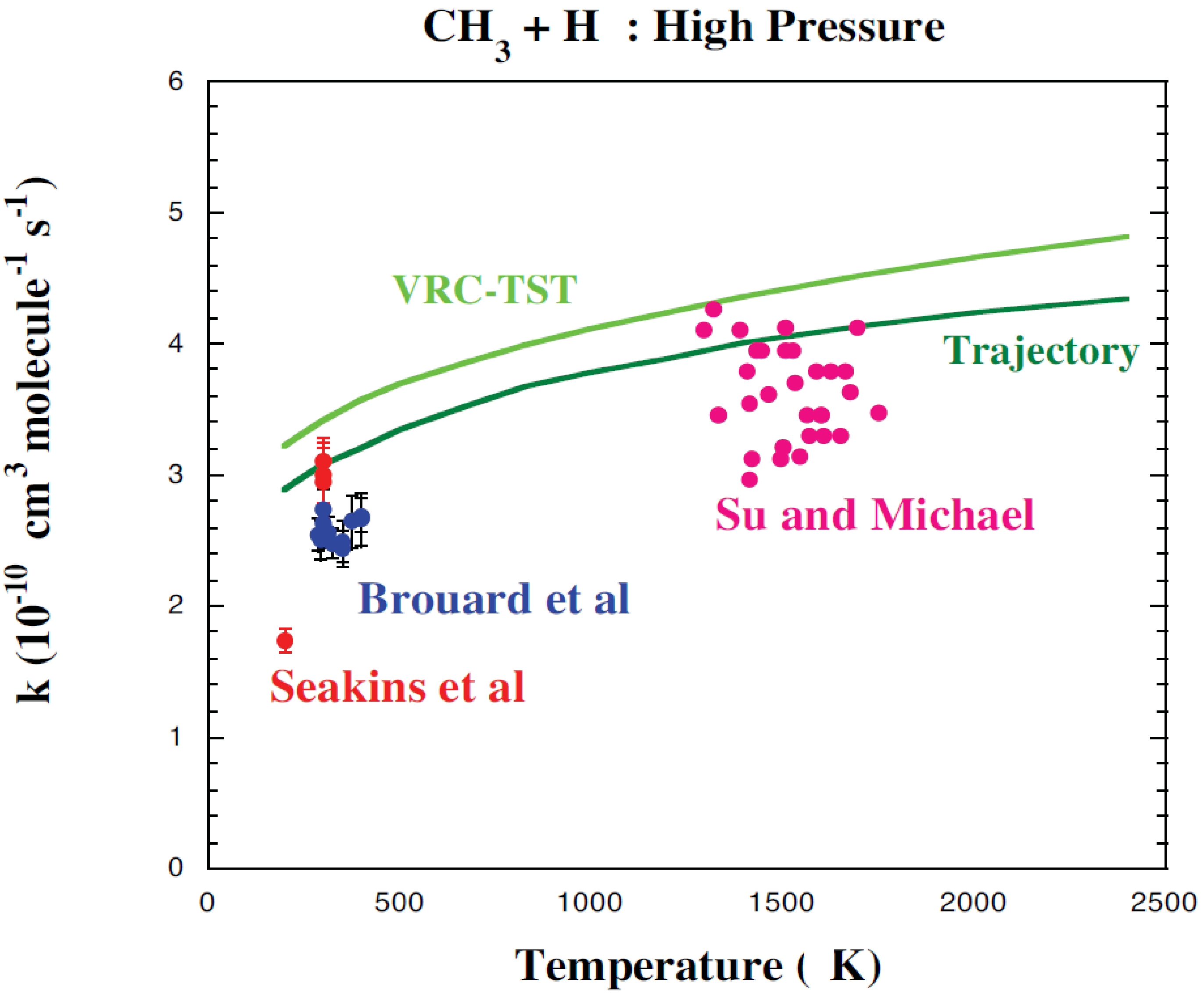

Recall experimental measurements from Topic 2

Positive T dependence for k_∞ : contrast –ve dependence for CH_3+CH_3.

H + Alkyl Radical

Potential Energy Surface

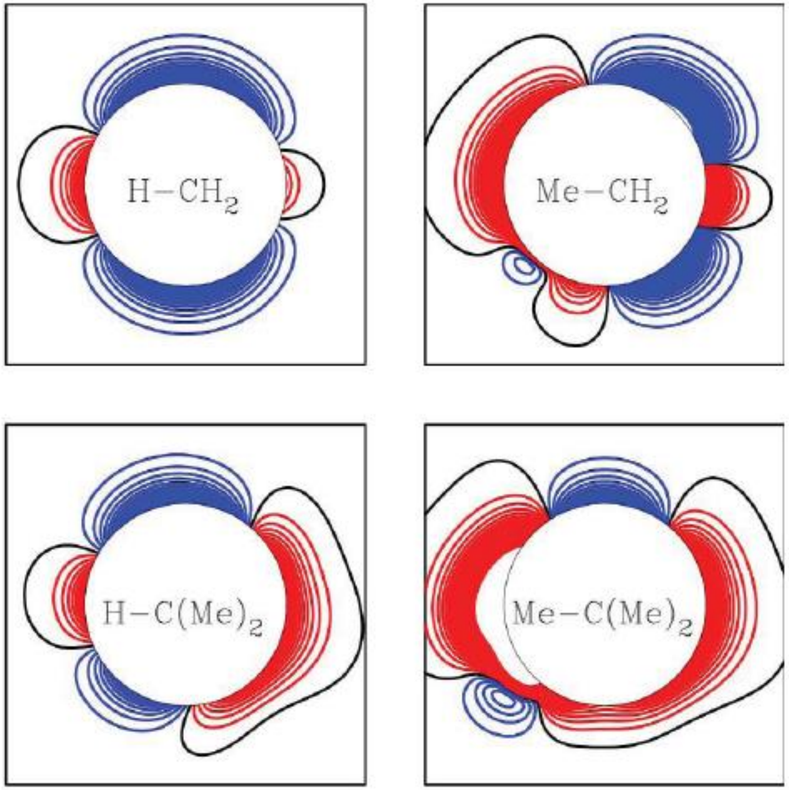

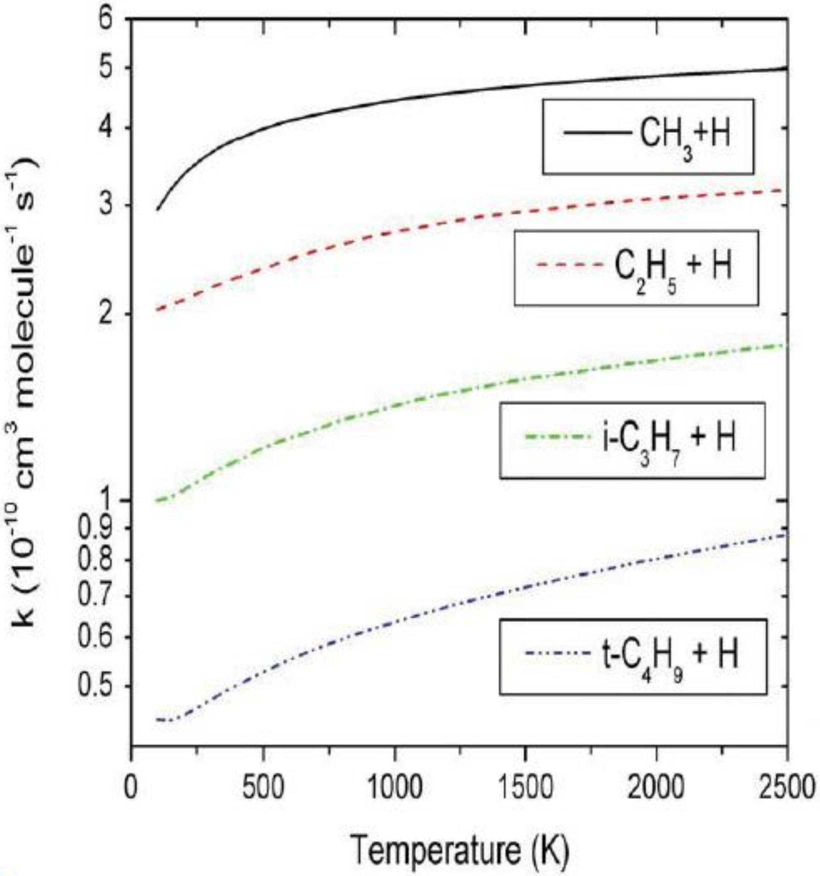

Blue = attractive contours

Red = repulsive contours

Gorin model (D M Golden)

Excluded angles of approach

Two Transition States

Schematic Potential Energy Surface for Radical Molecule Addition

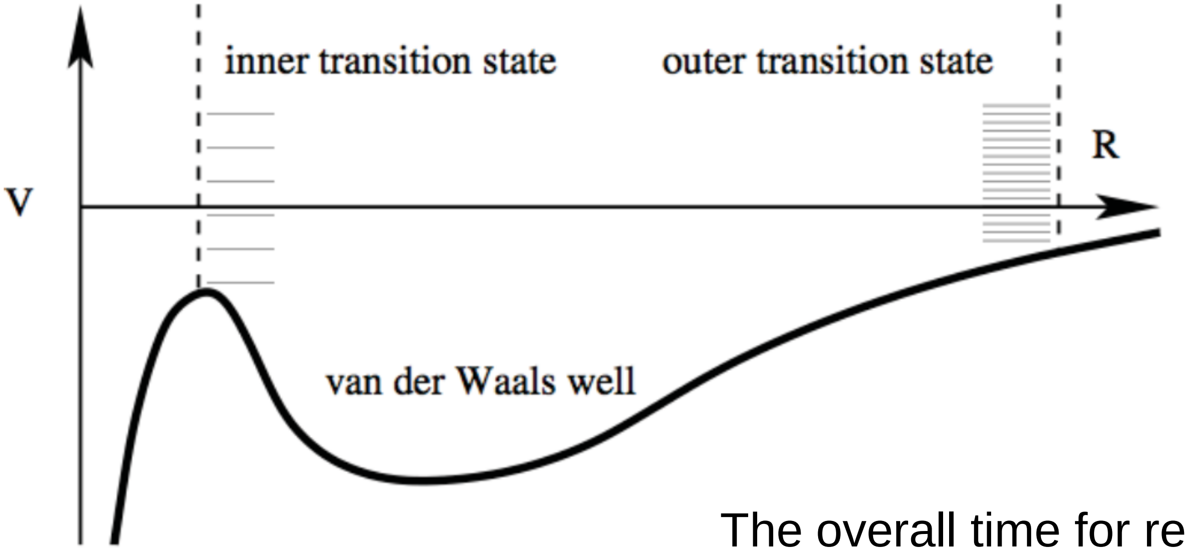

$$k_{inner} = \frac{hW^{\ddagger}_{inner}(E)}{N(E)}$$

$$k_{outer} = \frac{hW^{\ddagger}_{outer}(E)}{N(E)}$$

The overall time for reaction, τ, is the reciprocal of *k*

$$\tau = \frac{1}{k_{inner}} + \frac{1}{k_{outer}} = \frac{N(E)}{h}\left\{\frac{1}{W^{\ddagger}_{inner}(E)} + \frac{1}{W^{\ddagger}_{outer}(E)}\right\}$$

The smaller of the sums of states at energy *E* dominates the rate constant. This transition state acts as the reaction bottleneck

$OH + C_2H_4$

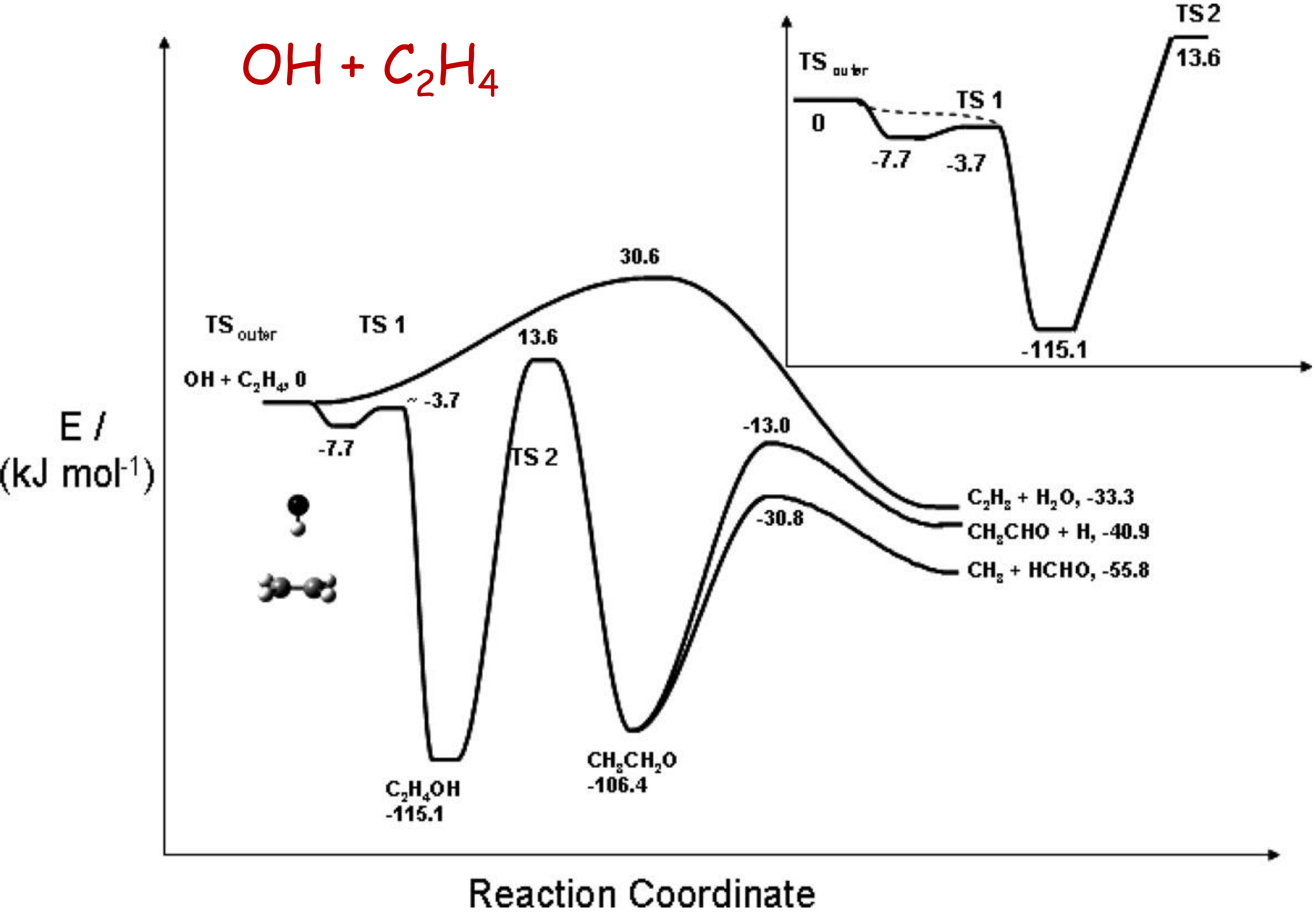
TS outer
TS 1
OH + C_2H_4, 0
30.6
13.6
~ -3.7
-7.7
TS 2
-13.0
-30.8
C_2H_2 + H_2O, -33.3
CH_3CHO + H, -40.9
CH_3 + HCHO, -55.8
C_2H_4OH
-115.1
CH_3CH_2O
-106.4
E / (kJ mol^{-1})
Reaction Coordinate
TS outer
0
TS 1
-7.7
-3.7
TS 2
13.6
-115.1

C_2H_4 + OH High P Limit

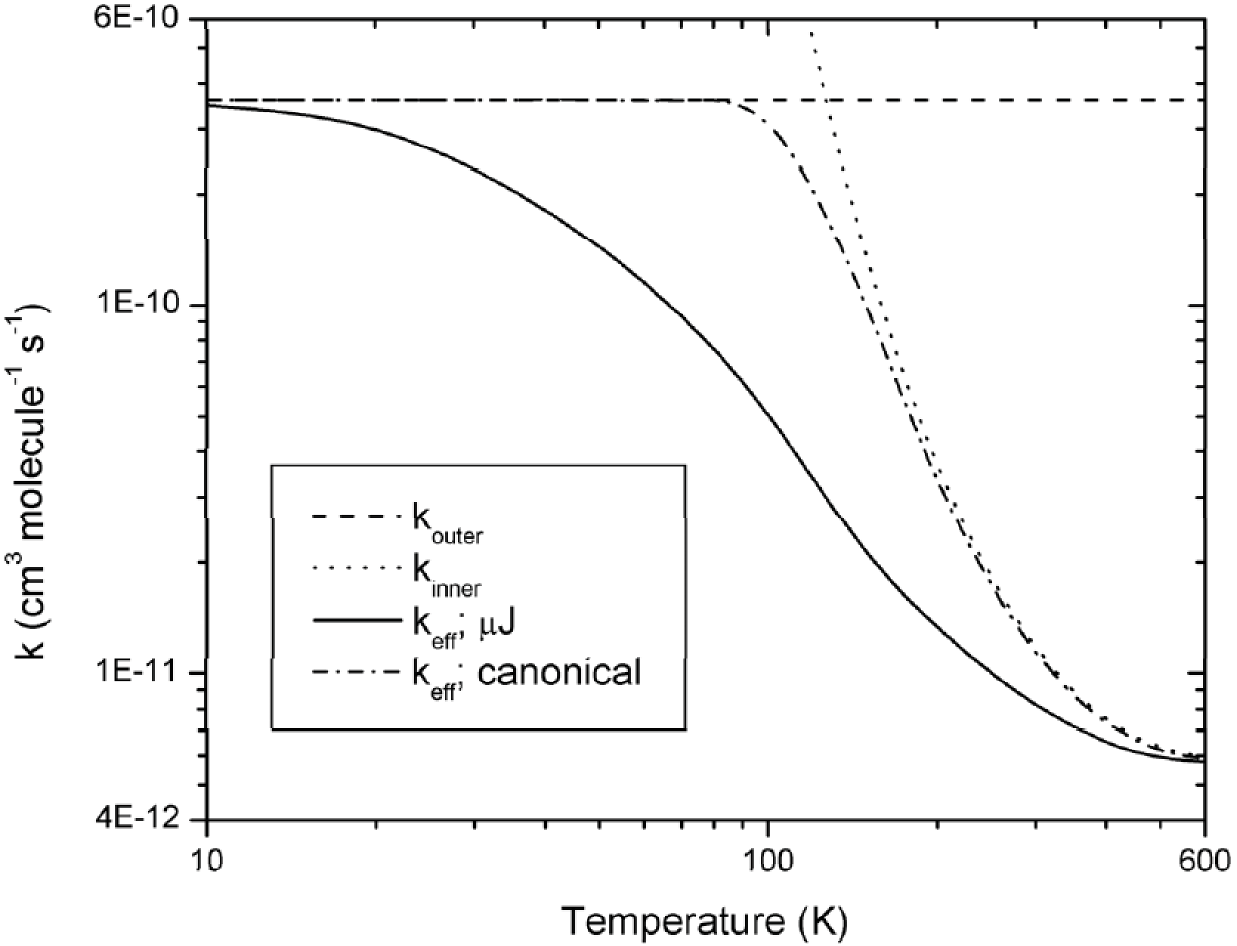

E. E. Greenwald, S. W. North, Y. Georgievskii and S. J. Klippenstein, J. Phys. Chem. A, 2005, 109, 6031–6044.

Fits to available data
slight adjustment of inner TS energy

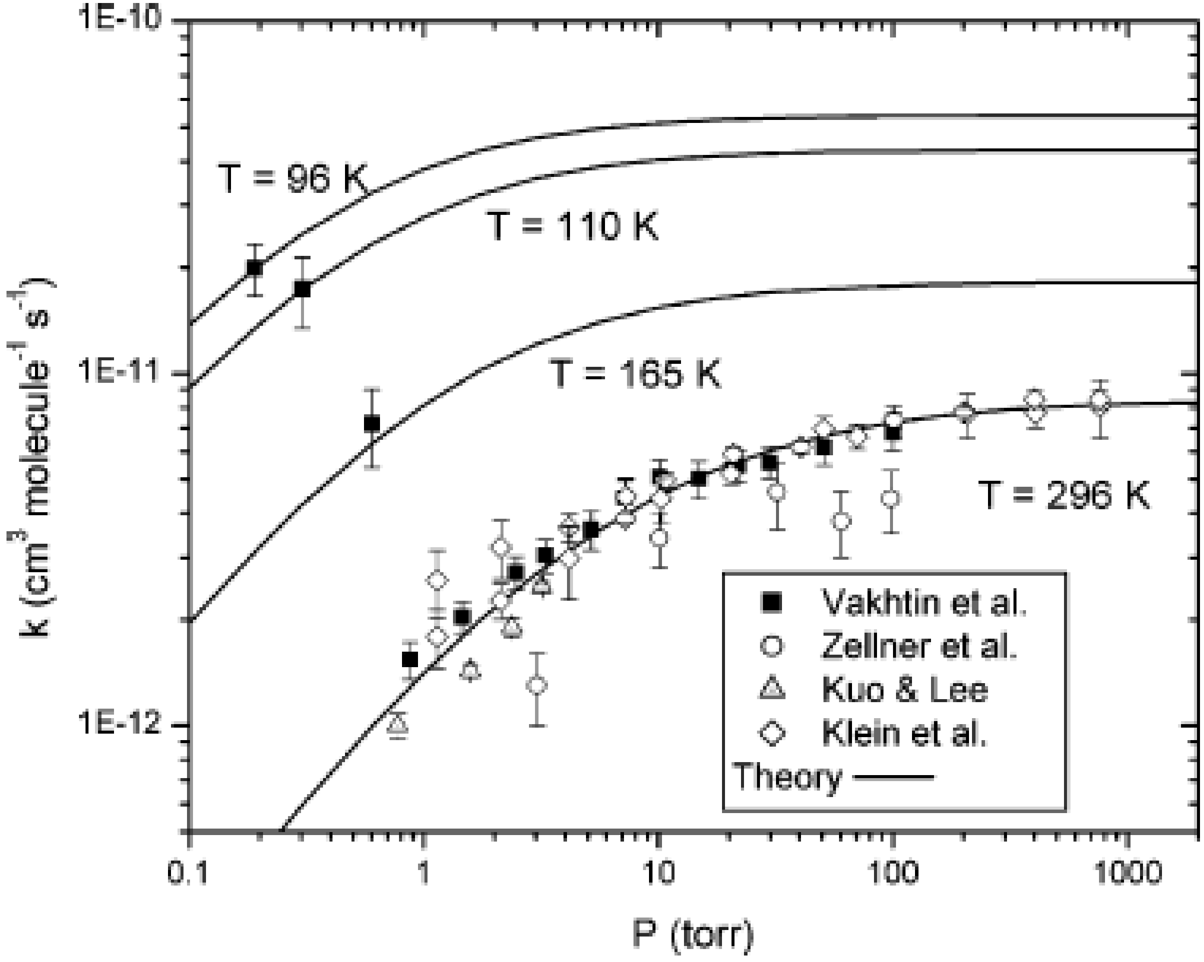

OH + CH_3OCH_3

- PES shown on right – deep van der Waals well and two transition states.
- Lower Fig shows experimental data and detailed TST calculations (see Klippenstein, Proc Comb Inst 2017, 36, 77)
- Excellent agreement – no tuning demonstrating predictive power of theory.
- Note lower T behaviour where the outer transition state becomes important – the reaction behaves like an association to form the outer complex, with tunnelling through the barrier to form the products.

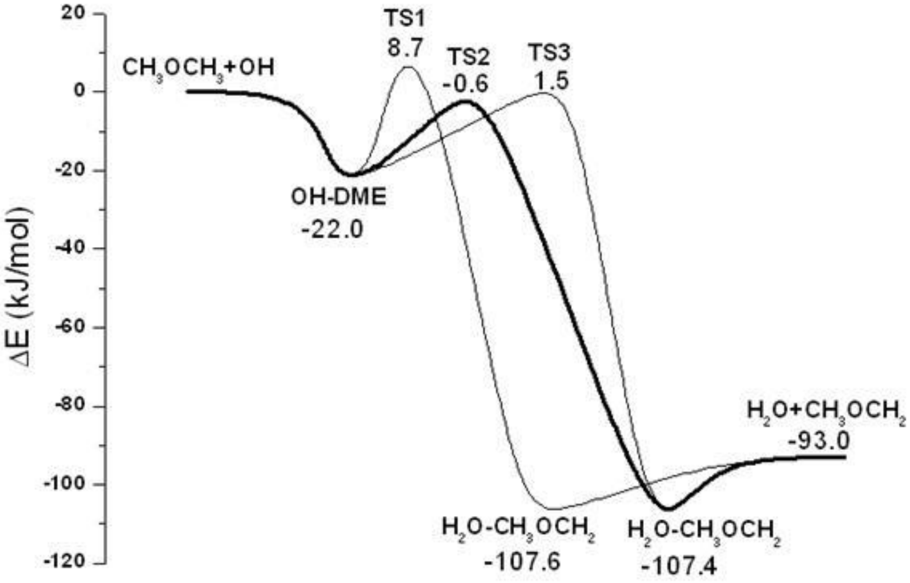

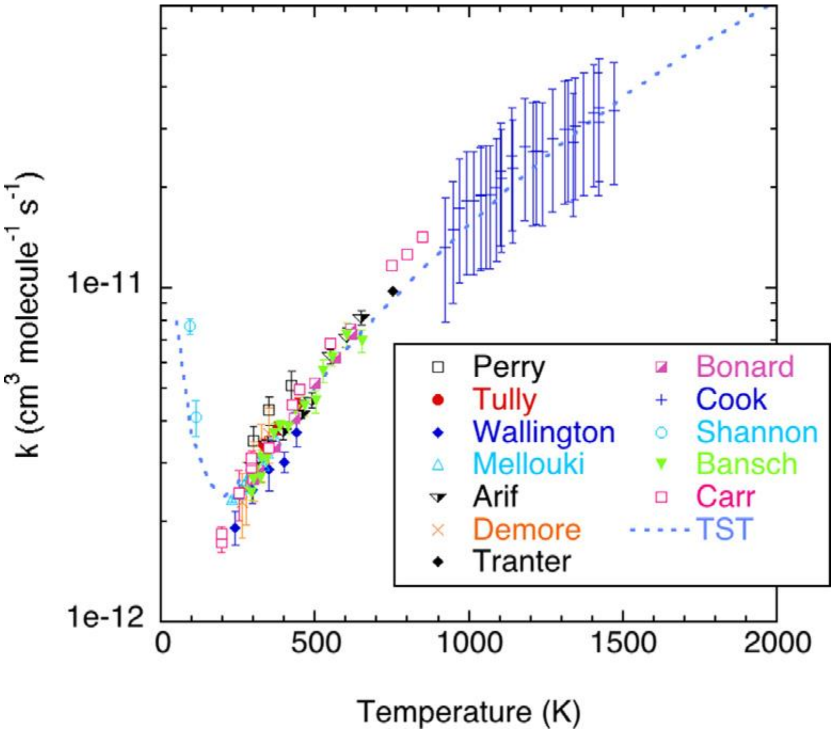

Reminder from Topic 2

$HO_2 + HO_2 \rightarrow H_2O_2 + O_2$

- < 800 K. Flash photolysis, absorption spectroscopy
- Open circles: shock tube, absorption spectroscopy (Kappel et al, Phys Chem Chem Phys, 2002, 4, 4392)
- Reference 5: Hippler et al. J Chem Phys 1990, 93, 1755
- Significant disagreement > 1000 K
- Burke etal. 'Difficult to discern which, if any, (of the high T) determinations is reliable.' More measurements needed under combustion conditions.

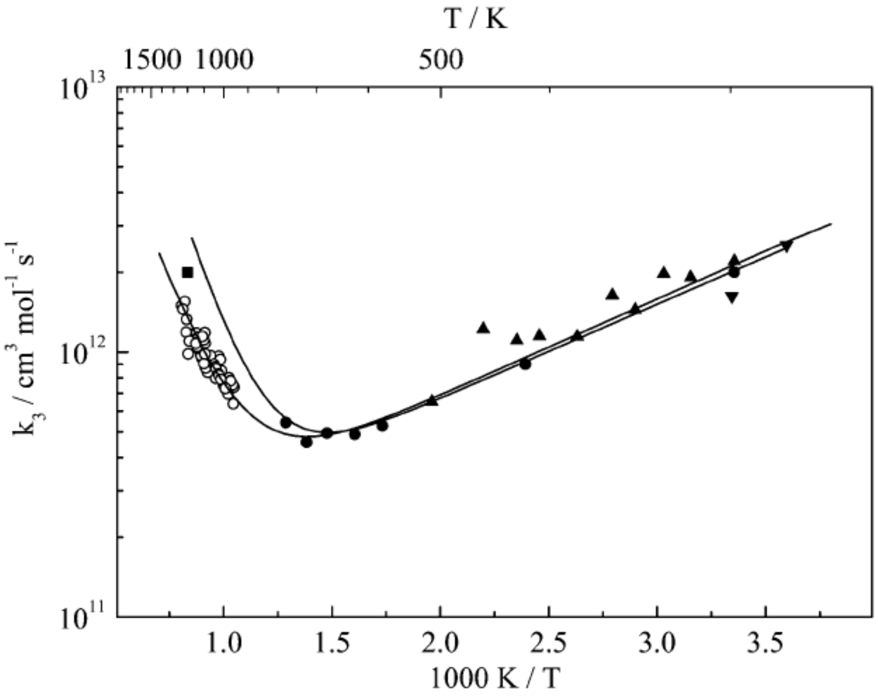

Fig. 10 Rate constants k_3 (■: ref. 2, ▲: ref. 35, ▼: ref. 36, ●: ref. 37, ○ and lower line: this work, upper line: ref. 5).

Theoretical Determination of the Rate Coefficient for the HO_2+ HO_2 → H_2O_2+O_2 Reaction: Adiabatic Treatment of Anharmonic Torsional Effects (Zhou et al J Phys ChemA, 2012, 116, 2089)

- High level calcs (CASPT2/CBS/aug-cc-PVTZ)
- TS2 has two transition states corresponding to different torsional conformations.
- New treatment needed to allow reaction at any torsional angle.
- Also needed to include tunnelling in new approach
- Good agreement with low T data, but calculated rate constants are lower than expt at higher T (recall discussion in Topic 2)
- Will return to this reaction again in Topic 5

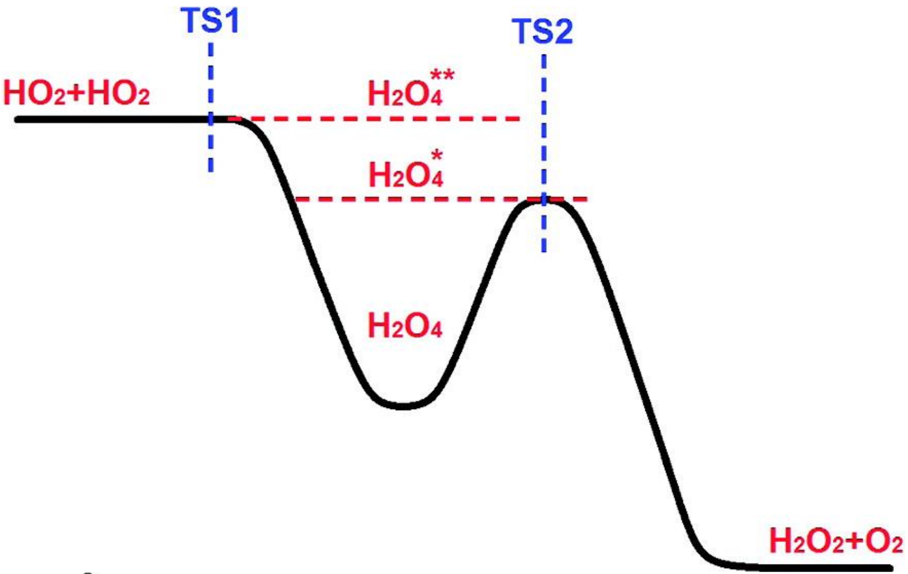

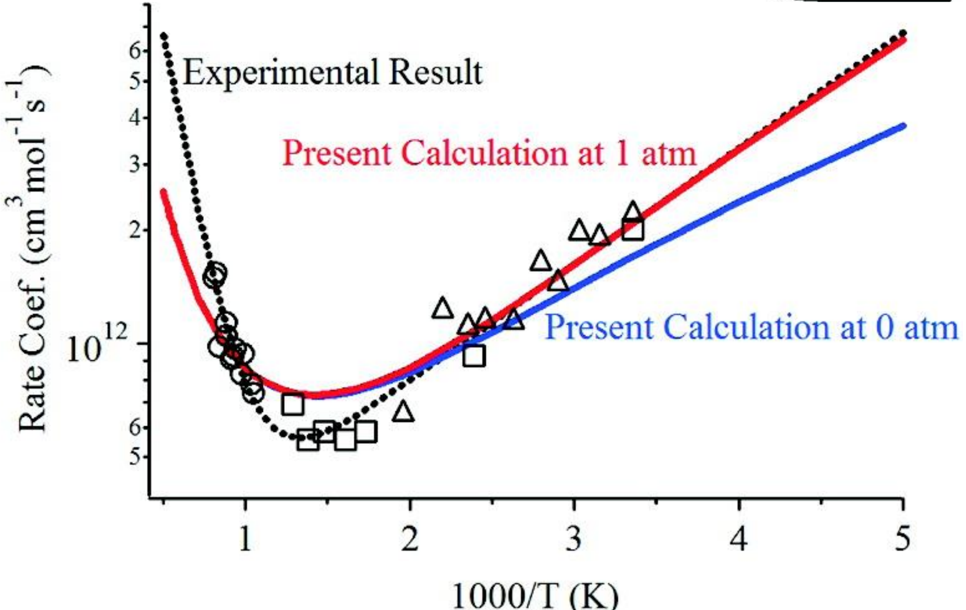

Structures and energies of torsional conformers that form TS2 and TS2'

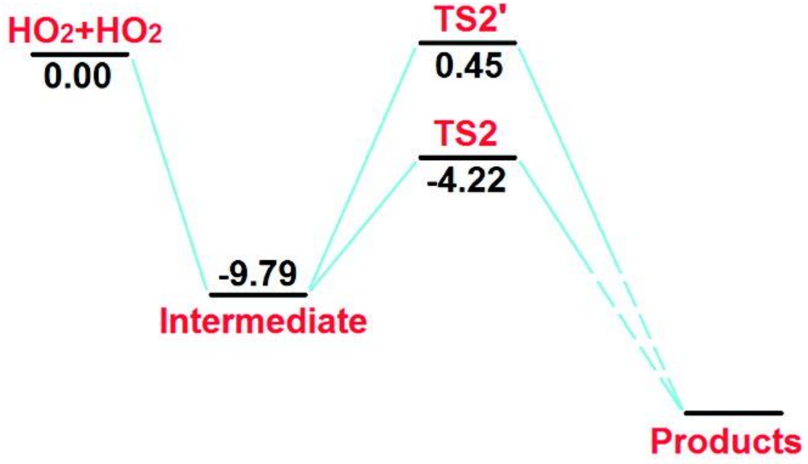

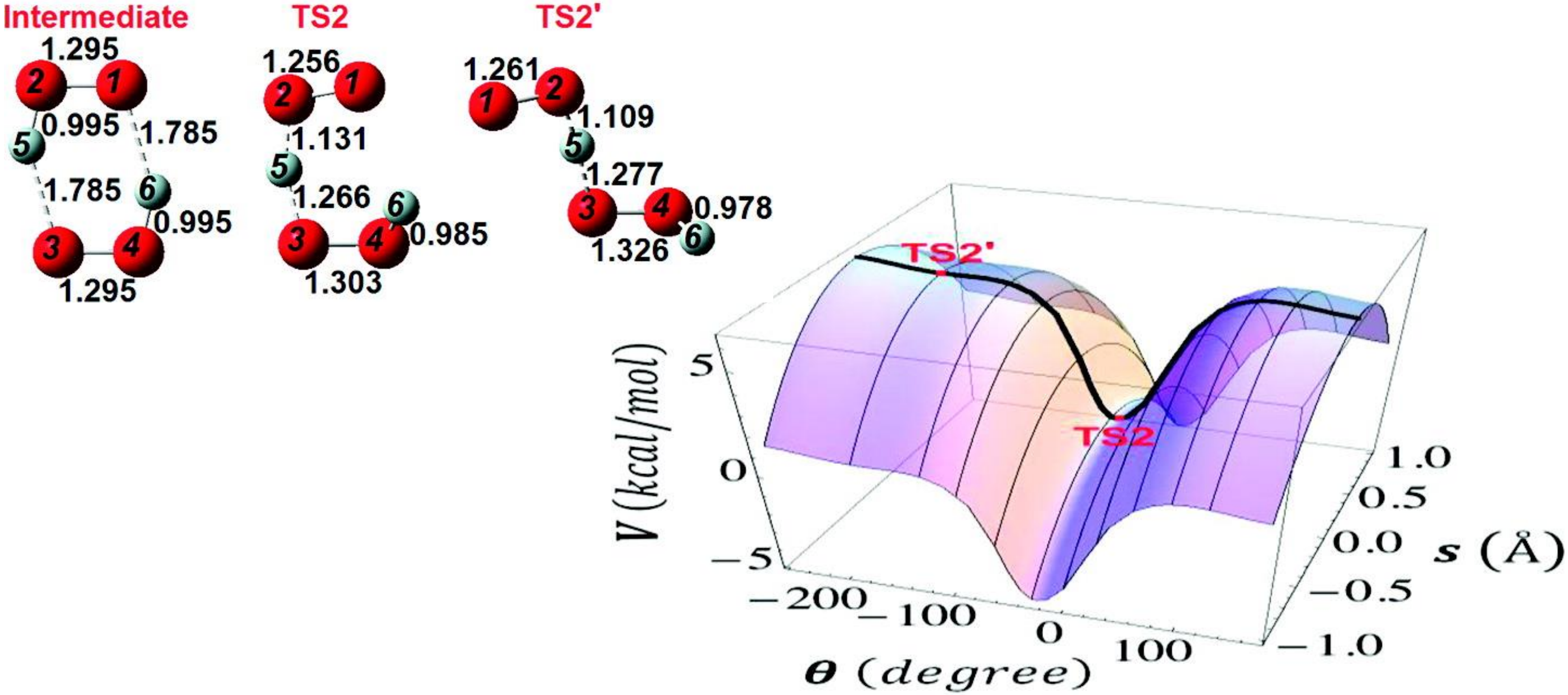

Master equation model for pressure dependent reactions

Pressure dependent association reactions (see Topic 1)

An association reaction involves collisional stabilisation of the adduct:

$$A + B \underset{k_{-a}}{\overset{k_a}{\rightleftharpoons}} AB^* \xrightarrow{k_s[M]} AB.$$

We applied the QSSA to AB *, obtaining the expression shown on the right.

$$k = \frac{k_0[M]k^{\infty}}{k^{\infty} + k_0[M]}$$

There are two problems with this model:

1. It assumes that AB* dissociates to form A + B with a constant rate constant regardless of the amount of energy in AB. Should really replace with a model in which k_{-a} is energy dependent ($k_{-a}(E)$)

2. It assumes that all stabilising collisions lead to complete stabilisation of AB*. In reality, stabilisation is likely to take place in a series of steps.

Development of models of unimolecular reactions

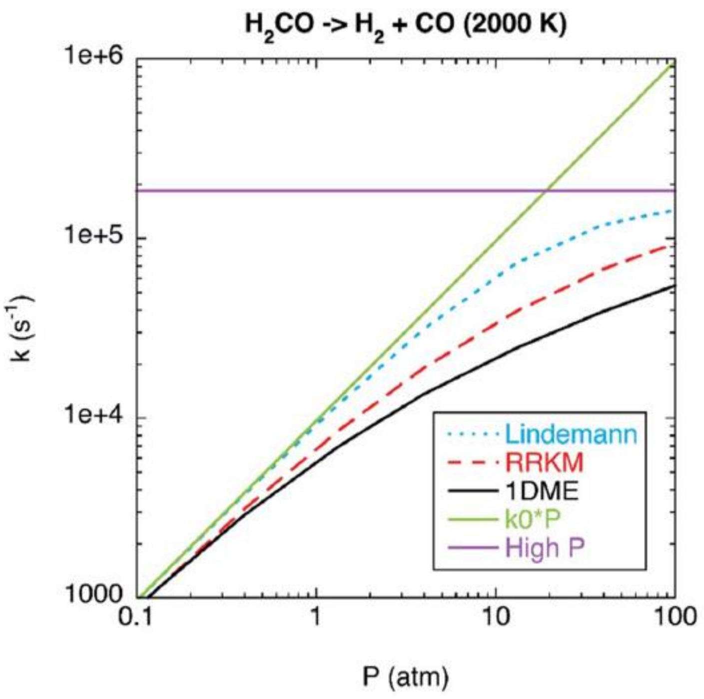

Klippenstein, Faraday Discuss., 2022, 238, 11

$$k = \frac{k_0[\mathrm{M}]k^\infty}{k^\infty + k_0[\mathrm{M}]}$$

- Association, dissociation and isomerization reactions can all be modelled using the theory of unimolecular reactions.
- The original theory was developed by Lindemann in 1922. It suffered from the deficiencies given in the last slide.
- RRKM theory was developed to overcome these problems.
- It was superseded by a master equation approach, that recognizes explicitly the energies of the reacting molecules.
- For a recent discussion of unimolecular reactions see Klippenstein, Faraday Discuss., 2022, 238, 11, the plenary lecture at a meeting to celebrate the 100th anniversary of Lindemann's paper.

Modelling dissociation and association reactions – master equation analysis

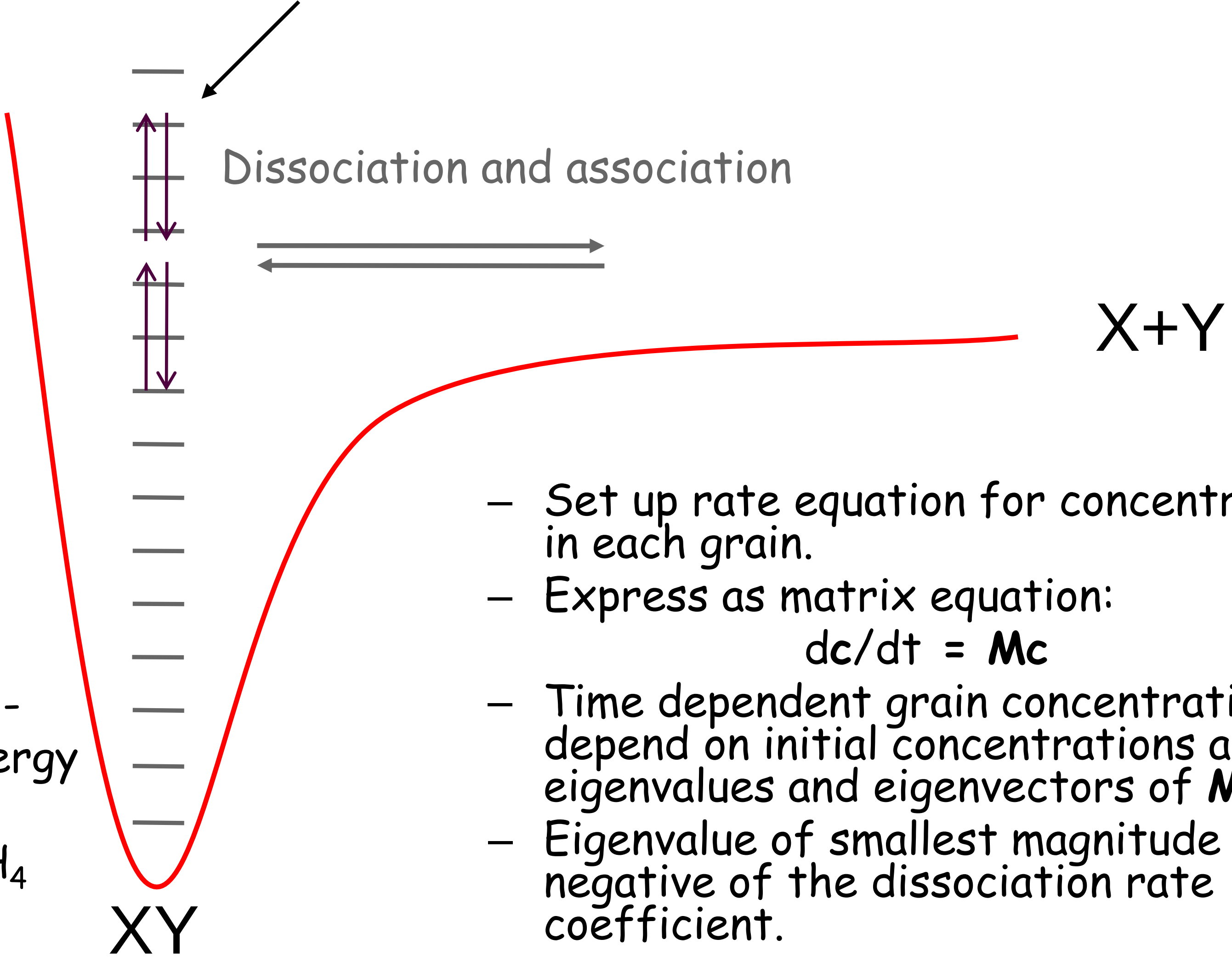

Collisional energy transfer between grains

Dissociation and association

Energy grains - Bundles of energy levels (remember CH_4 discussion)

- Set up rate equation for concentration in each grain.
- Express as matrix equation:

$$dc/dt = \mathbf{Mc}$$

- Time dependent grain concentrations depend on initial concentrations and on eigenvalues and eigenvectors of **M**
- Eigenvalue of smallest magnitude is the negative of the dissociation rate coefficient.

Master equation for dissociation, A → products

p(E) is the concentration density at energy E, k(E) is the dissociation rate constant

$$\frac{dp(E)}{dt} = \omega\int_0^\infty P(E|E')p(E')dE' - \omega p(E) - k(E)p(E)$$

reaction

Collisional energy transfer from other states

energy transfer from states at E

Downward energy transfer – exponential down model, ω is collision frequency

$$P(E|E') = A(E)\exp(-\alpha(E'-E)) \qquad E' \geq E,$$

α is a constant = see later. Upward energy transfer by detailed balance

$$P(E|E') = A(E')\exp\left(-\alpha(E-E')\right)\left(\frac{f(E')}{f(E)}\right) \qquad E > E'$$

Divide the energy states of the A into small grains and set up a matrix equation. Solution is in terms of eigenvalues U and eigenvectors Λ (recall topic 1)

$$\frac{d\mathbf{p}}{dt} = \mathbf{Mp} \qquad \text{Solution:} \qquad \mathbf{p} = \mathbf{U}e^{\Lambda t}\mathbf{U}^{-1}\mathbf{p}(0)$$

p is a vector of grain concentration densities, **M** is a square matrix of transition probabilities between grains and of dissociation rates. The dimension of M is equal to the number of grains. The eigenvalues are all negative

Rate constant for dissociation

Dissociation of A first order kinetics:
$$\frac{d[A]}{dt} = -k_u [A],$$

Solution of the master equation gives:
$$[A](t) = [A](t=0)\sum_E p(E,t)$$

At long times, when collisional relaxation is complete, the time dependence is governed by the eigenvalue of smallest magnitude

$$[A](t) = [A](t=0)\exp(\lambda_1 t)$$

The dissociation rate constant is the modulus of the smallest magnitude eigenvalue.

$$\boxed{k_u = -\lambda_1}$$

Requirements for ME calculation

- Microcanonical rate constants (*k*(*E*)). Use electronic structure + TST
- Collision frequency, ω. = $k_c[\mathrm{M}]$, where k_c is the rate constant for collisions and $[\mathrm{M}]$ is the concentration of the collider (the "third body") – see next slide.
- Energy transfer model: $P(E|E')$. Generally use exponential down model calculating upward transitions using detailed balance (see previous slide)

Rate constants for collisions

- The collision frequency, ω, is the number of collisions per second and is equal to Z[M], where Z is the collision “rate “ constant. For molecules that behave as hard spheres, Z is given by

$$Z_{ij}^{HS} = \sqrt{\frac{8kT}{\pi\mu_{ij}}}\,\pi\sigma_{ij}^2$$

for collisions between species i and j. μ is the reduced mass and σ the collision diameter.

For a Lennard-Jones interaction potential

$$\overline{V}(r) = 4\varepsilon_{ij}\left[\left(\frac{\sigma_{ij}}{r}\right)^{12} - \left(\frac{\sigma_{ij}}{r}\right)^{6}\right]$$

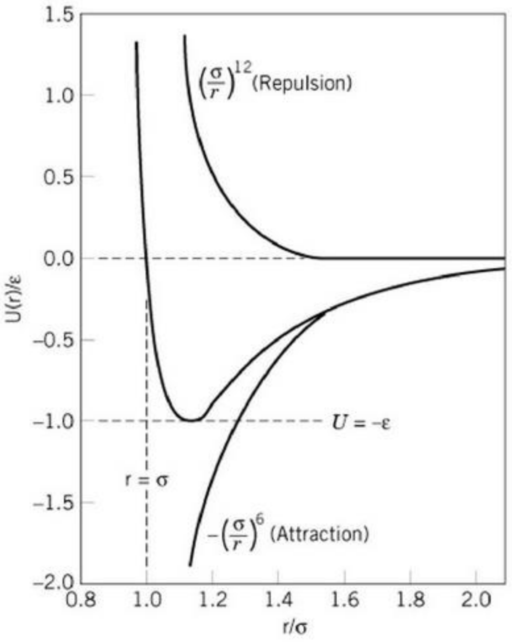

where σ is the separation of the molecules V = 0
ε is the well depth, Z is given by

$$Z_{ij}^{LJ} = Z_{ij}^{HS}\,\Omega_{2.2}^{*}$$

where $\Omega_{2.2}^{*}$ is the collision integral that depends on T/ε

Ab intio calculations of energy transfer parameters

- See Jasper and Miller, J. Phys. Chem. A 2011, 115, 6438–6455
  - Use dynamical calculations with high level ab intio potential energy surfaces for the interaction of the excited molecule and the collision partner, M. Also develop more efficient approximate methods.
  - Assume that the exponential down model applies, that the energy transfer function depends on the amount of energy transferred but is independent of the initial and final energies individually.
  - Determine the size of α ($=\langle \Delta E \rangle_{down}$) and its T dependence.

- Lennard Jones parameters are widely used to calculate the collision frequency, ω. These parameters have been calculated and tabulated for a wide range of species by Jasper and Miller, Combustion and Flame 161 (2014) 101–110.

Results from J. Phys. Chem. A 2011, 115, 6438-6455 and Combustion and Flame 2014, 161, 101-110

Lennard-Jones parameters, CH_4 + M

M	σ, Å	ε, cm^{-1}
CH_4	3.746	98.28
He	2.576	7.089
Ne	2.749	24.74
Ar	3.330	94.87
Kr	3.679	122.3
H_2	2.920	26.41
N_2	3.681	67.89
CO	3.705	71.49

Energy transfer parameters for CH_4+M (eq (1))

M	α_{300}, cm^{-1}	n
He	117	0.95
Ne	104	0.86
Ar	115	0.75
Kr	123	0.67
H_2	162	0.83
N_2	130	0.76
CO	130	0.76
CH_4	390	0.60

Lennard-Jones parameters, from calculated potentials. They compare well with values tabulated in CHEMKIN

Note dependence of a on *T* and on atomic mass, molecular size.

$$\alpha(T) = \alpha_{300}(T/300\ \mathrm{K})^n \quad (1)$$

Calculation of low-pressure-limit rate constants

Jasper, Faraday Discuss., 2022, 238, 68–86

- Calculate ko, using parameterized ab initio intermolecular potentials and classical trajectories

$$k_0(E,J) = ZF(E,J) \qquad F(E,J) = \sum_{J'=0}^{\infty} \int_{E_{J'}}^{\infty} \mathrm{d}E' \; P(E',J';\; E,J)$$

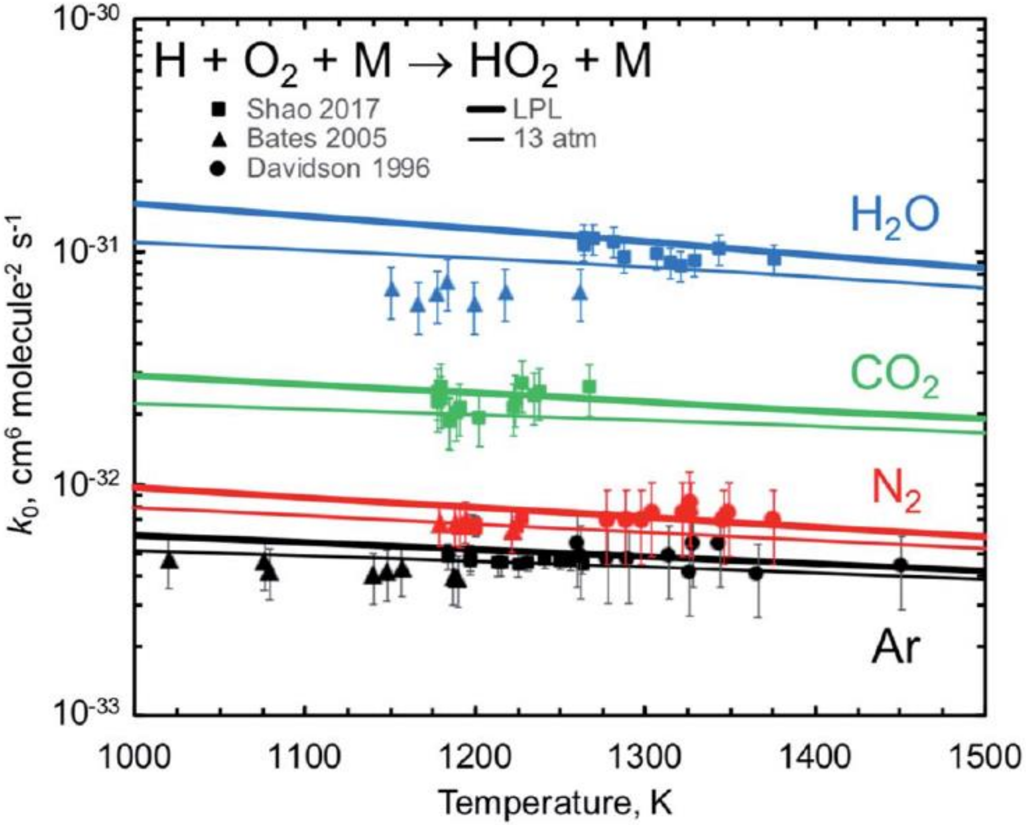

Comparison with experiment

Predicted and experimental(bracketed) thermal collision efficiencies relative to Ar (Jasper)

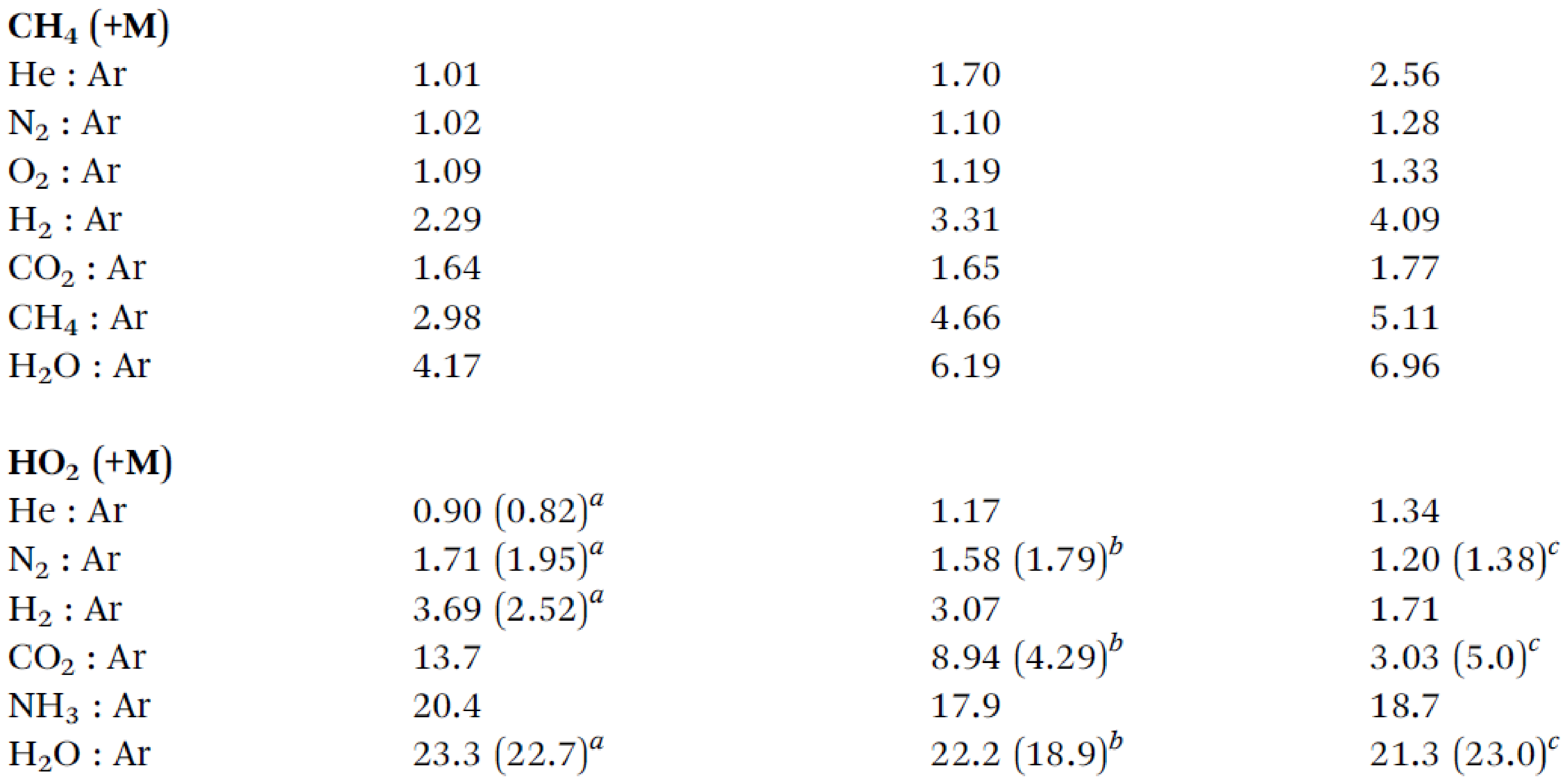

CH_4 (+M)			
He : Ar	1.01	1.70	2.56
N_2 : Ar	1.02	1.10	1.28
O_2 : Ar	1.09	1.19	1.33
H_2 : Ar	2.29	3.31	4.09
CO_2 : Ar	1.64	1.65	1.77
CH_4 : Ar	2.98	4.66	5.11
H_2O : Ar	4.17	6.19	6.96
HO_2 (+M)			
He : Ar	0.90 (0.82)^a	1.17	1.34
N_2 : Ar	1.71 (1.95)^a	1.58 (1.79)^b	1.20 (1.38)^c
H_2 : Ar	3.69 (2.52)^a	3.07	1.71
CO_2 : Ar	13.7	8.94 (4.29)^b	3.03 (5.0)^c
NH_3 : Ar	20.4	17.9	18.7
H_2O : Ar	23.3 (22.7)^a	22.2 (18.9)^b	21.3 (23.0)^c

- Note the high values for CO_2, H_2O, NH_3 and H_2O – important for chemical mechanisms for combustion, especially at high pressures (see Topic 6)

Association reaction

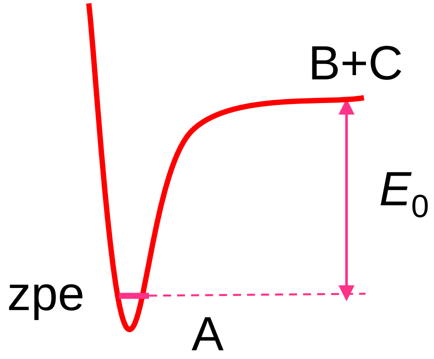

$$B + C \rightleftharpoons A.$$

k_a, k_u, [C] >> [B], so [C] is constant

$$\frac{dp(E)}{dt} = \omega \int_0^\infty P(E|E')p(E')dE' - \omega p(E) - k(E)p(E) + g(E,t)$$

$$g(E,t) = R(t)\phi(E) = k_{a,\infty}[B](t)[C](t)\phi(E),$$

$$\phi(E) = \frac{k(E)f(E)}{\int k(E)f(E)dE}$$

Boltzmann distribution

Microcanonical rate constant for dissociation of *A*

k(E) is only non-zero above the dissociation threshold, E_0

As zero pressure is Approached, and there is no Stabilisation, the distribution of *A* <u>above the threshold</u> is Boltzmann – the microcanonical association and dissociation steps are balanced

$$k_a = \frac{-\lambda_2}{[C] + 1/K_{eq}}$$

$$k_u = \frac{-\lambda_2}{1 + K_{eq}[C]}.$$

Conservative problem : λ_1 is zero. At low *T*, when k_u is small, $\lambda_1 = -k_a[C]$

Structure of the matrix **M** for association reactions

$$\begin{pmatrix} M_{11}^A & \cdots & M_{1n}^A & k_1 f_1 K_{eq}[C] \\ \vdots & \ddots & \vdots & \vdots \\ M_{n1}^A & \cdots & M_{nn}^A & k_n f_n K_{eq}[C] \\ k_1 & \cdots & k_n & -k_{a,\infty}[C] \end{pmatrix} \cdot \begin{pmatrix} A_1 \\ \cdot \\ \cdot \\ \cdot \\ A_n \\ B \end{pmatrix}$$

$k_i = 0$ for $E_i < E_0$

- The diagonal elements, $M_{11}^A \dots M_{nn}^A$, contain the rate constants for collisional loss from the grain; for those grains above the dissociation threshold, the elements also include the energy dependent rate constant for dissociation. They are all negative.
- The off-diagonal elements M_{ij}^A and are the collisional rate constants for collisional transfer between grains i and j.
- The first n elements in the n+1 column are the first order rate constants for formation of the grains of A from B+C. k_n is the dissociation rate constant for the grain at energy E_i. These elements are zero for grains below the threshold energy ($k_i = 0$ for $E_i < E_0$)
- The (n+1)th diagonal element is the total first order rate constant for transfer of B (+C) to A (negative). $k_{a,\infty}$ is the high-pressure limit for the association rate constant.

More complex reactions.

$$C+D \rightleftharpoons A \rightleftharpoons B \longrightarrow E+F$$

Competition
between relaxation
and reaction

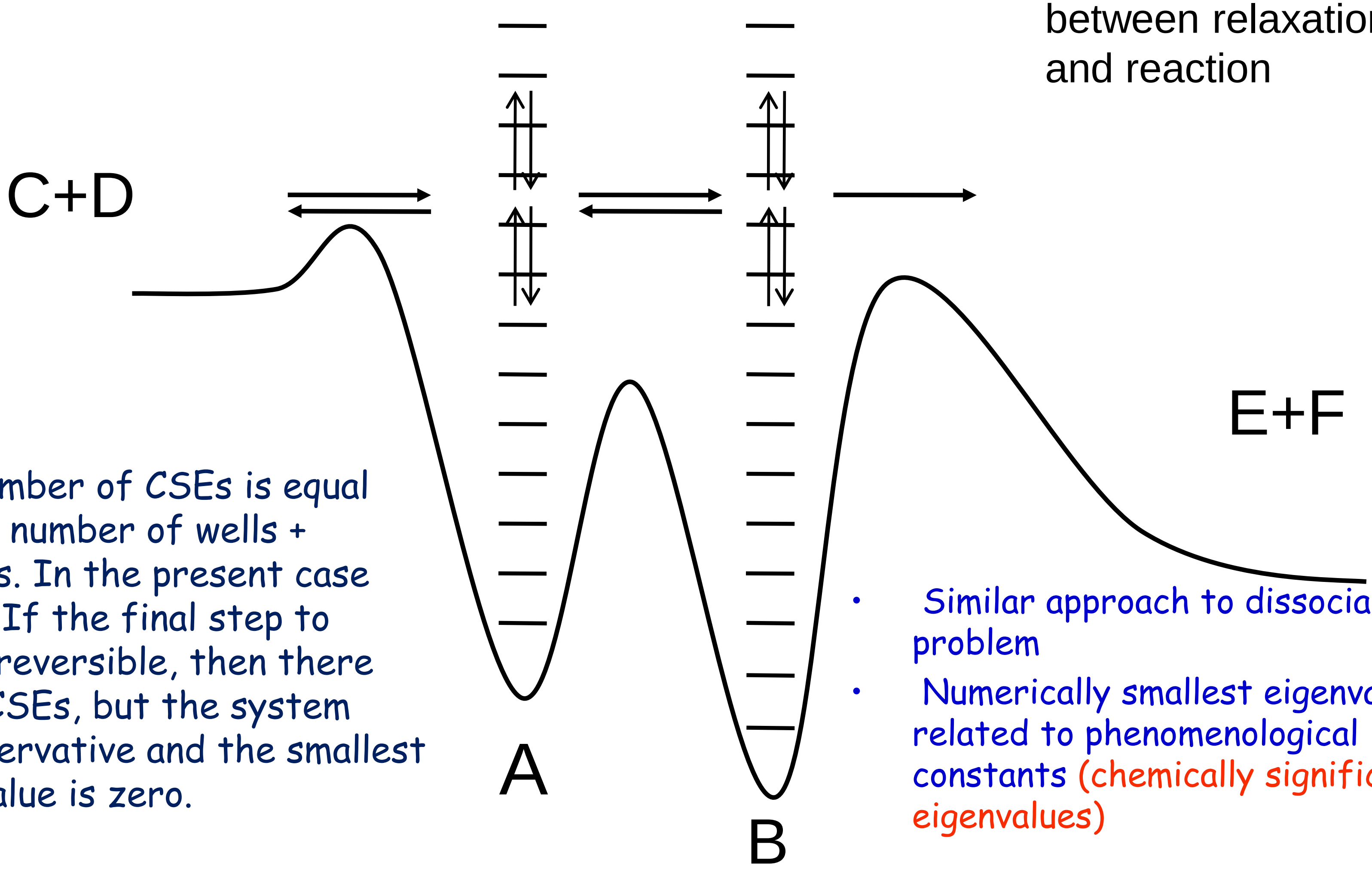

The number of CSEs is equal to the number of wells + sources. In the present case it is 3. If the final step to E+F is reversible, then there are 4 CSEs, but the system is conservative and the smallest eigenvalue is zero.

- Similar approach to dissociation problem
- Numerically smallest eigenvalues related to phenomenological rate constants (chemically significant eigenvalues)

Structure of **M** for an isomerisation reaction – a subset of the above problem

$$\boxed{\mathrm{A} \rightleftharpoons \mathrm{B}.}$$

$$\frac{\partial}{\partial t}\rho^A(E,t) = \omega \sum_{E'} P(E|E')\rho^A(E',t) - \omega\rho^A(E,t) - k^A(E)\rho^A(E,t) + k^B(E)\rho^B(E,t),$$

Rate equation for the concentration density of isomer A at energy E. There is a similar set of equations for isomer B

$$\begin{pmatrix}
M^{\mathrm{A}}_{11} & \omega P^{\mathrm{A}}_{12} & \dots & \omega P^{\mathrm{A}}_{1n} & 0 & \dots & 0 & 0 \\
\omega P^{\mathrm{A}}_{21} & M^{\mathrm{A}}_{22} & \dots & \omega P^{\mathrm{A}}_{2n} & \vdots & \ddots & \vdots & \vdots \\
\vdots & \vdots & \ddots & \vdots & 0 & \dots & k^{\mathrm{B}}_{l-1} & 0 \\
\omega P^{\mathrm{A}}_{n1} & \omega P^{\mathrm{A}}_{n2} & \dots & M^{\mathrm{A}}_{nn} & 0 & \dots & 0 & k^{\mathrm{B}}_{l} \\
0 & \dots & 0 & 0 & M^{\mathrm{B}}_{11} & \omega P^{\mathrm{B}}_{12} & \dots & \omega P^{\mathrm{B}}_{1l} \\
\vdots & \ddots & \vdots & \vdots & \omega P^{\mathrm{B}}_{21} & M^{\mathrm{B}}_{22} & \dots & \omega P^{\mathrm{B}}_{2l} \\
0 & \dots & k^{\mathrm{A}}_{n-1} & 0 & \vdots & \vdots & \ddots & \vdots \\
0 & \dots & 0 & k^{\mathrm{A}}_{n} & \omega P^{\mathrm{B}}_{l1} & \omega P^{\mathrm{B}}_{l2} & \dots & M^{\mathrm{B}}_{ll}
\end{pmatrix}$$

M is structured in blocks. The diagonal blocks relate to energy transfer within each isomer and reaction from that isomer. The off-diagonal blocks relate to reaction into that isomer from the other isomer.

Chemically significant eigenvalues for isomerisation

$$\mathrm{A} \rightleftharpoons \mathrm{B}.$$

Two species, two CSEs

System is conservative, so $\lambda_1 = 0$

Reaction system relaxes to equilibrium state . Relaxation rate constant $= |\lambda_2| = k_f + k_r$

Relaxation time = τ

$\tau \quad = \quad (k_f + k_r)^{-1}$

$$\frac{d[A]}{dt} = -k_f[A] + k_r[B]$$

$$\frac{d[B]}{dt} = k_f[A] - k_r[B],$$

$$\mathbf{c} = \begin{pmatrix} [A] \\ [B] \end{pmatrix}.$$

$$\frac{d\mathbf{c}}{dt} = \mathbf{M}_c\mathbf{c},$$

The eigenvalues of this matrix are the same as those for the CSEs from a full energy resolved ME

$$\mathbf{M}_c = \begin{pmatrix} -k_f & k_r \\ k_f & -k_r \end{pmatrix}.$$

$$-\lambda_2 = k_f + k_r.$$

$$k_f/k_r = K_{eq}, \qquad k_f = \frac{-\lambda_2}{1 + 1/K_{eq}}$$

$$k_r = \frac{-\lambda_2}{1 + K_{eq}}.$$

Detailed balance, $A \rightleftharpoons B$.

- In an isomerisation, the microcanonical forward and reverse rate constants obey detailed balance $k_f(E)N_A(E) = k_r(E)N_B(E)$. Similar arguments also apply to association and reverse dissociation steps.
- Does detailed balance apply at the canonical level?
- At the high pressure limit, Boltzmann distributions apply in A and B, so that $k_f(T)/k_b(T) = K_{eq}$.
- At lower pressures, the distributions in A and B are non-Boltzmann. Does detailed balance apply?
- It has not been possible to prove that detailed balance applies strictly, but there is strong evidence that it applies approximately, but to a good degree of precision (see Miller et al Phys. Chem. Chem. Phys., 2009, 11, 1128-1137 and references therein.)
- So thermodynamics can be confidently applied to calculate the reverse rate constant from the forward rate constant, whatever the pressure, provided the IEREs and CSEs are well separated. If not, neither rate constant is defined.

Types of eigenvalue: CSEs and IEREs
H.O. Pritchard, The quantum theory of unimolecular reactions (Cambridge University Press 1982)

Plot of log(- λ_i) vs log(pressure for a dissociation reaction

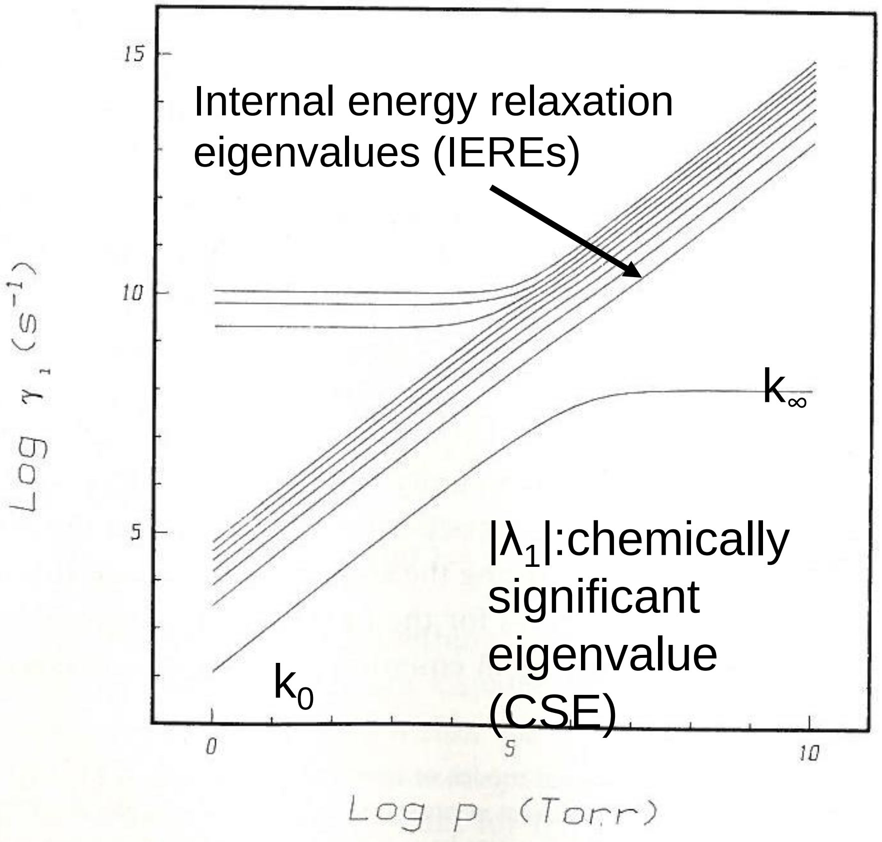

Internal energy relaxation eigenvalues (IEREs)

k_∞

$|\lambda_1|$:chemically significant eigenvalue (CSE)

k_0

- Log(-λ_i) for dissociation vs pressure at fixed *T*. The number of eigenvalues = number of grains
- Numerically smallest eigenvalue gives the rate coefficient – fig shows limits k_∞ at high *p* and k_0[M] at low p.
- Relaxation eigenvalues (IEREs)are well separated from the single chemically significant eigenvalue(CSE) and the system is well behaved – a rate coefficient can be assigned.
- Collisional relaxation occurs on a shorter timescale than reaction. During these timescales a steady state distribution of the reactant is established and this determines the rate constant. The steady state distribution depends on pressure and approaches the Boltzmann distribution at high p – that distribution is established at the high pressure limit.

High energy states with dissociation rate constants larger than the IEREs. Not usually important, but see later discussion on corannulene

Chemically significant eigenvalues - summary

- The eigenvalues of M exhibit a separation in magnitude: all are negative and the majority are large in magnitude and govern the time evolution of the energy transfer process (IERE), while a smaller group of eigenvalues (CSE) govern the chemical evolution of the system.
- At low temperatures the number of CSE corresponds to the number of distinct chemical species being modelled and is usually the sum of the number of wells and source terms in the model.
- The separation in time scales allows a matrix rate equation to be set up relating purely to the CSEs that is identical to the rate equation for the chemical system. The rate constants can be determined from an eigenpair analysis of the whole master equation.
- This is only possible provided the IEREs and CSEs are well separated in time
- References: J. Chem. Phys., 1974, 60, 3474; J. Phys. Chem. A, 2002, 106, 9267; J. Phys. Chem. A, 2006, 110, 10528; Phys. Chem. Chem. Phys., 2007, 9, 4085–4097.

Code for solving reaction systems with many wells

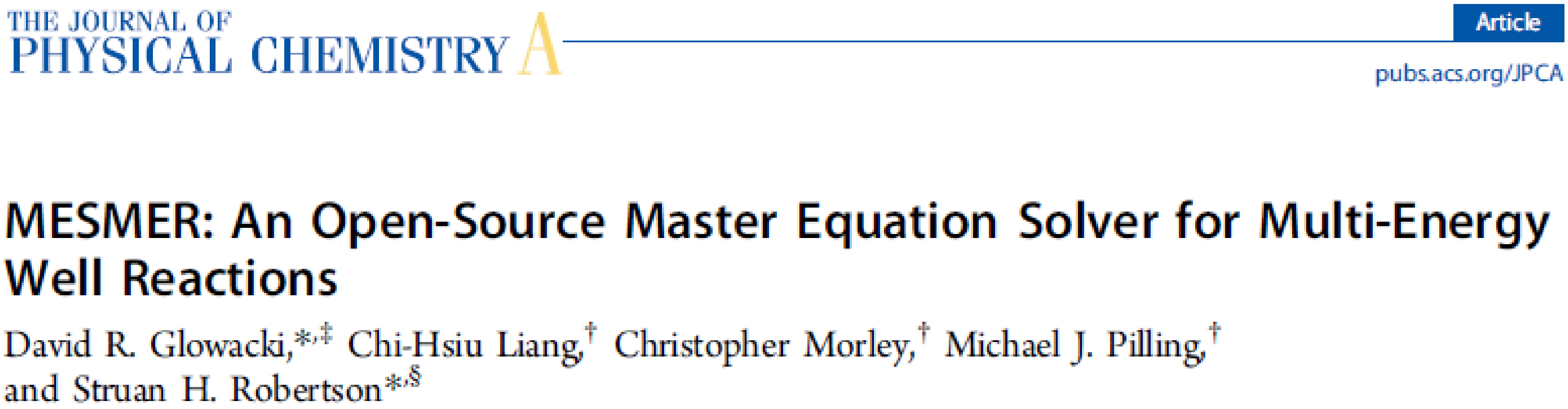

THE JOURNAL OF PHYSICAL CHEMISTRY A

Article

pubs.acs.org/JPCA

MESMER: An Open-Source Master Equation Solver for Multi-Energy Well Reactions

David R. Glowacki,*,‡ Chi-Hsiu Liang,† Christopher Morley,† Michael J. Pilling,†
and Struan H. Robertson*,§

J. Phys. Chem. A 2012, 116, 9545–9560

Abstract

"…….Master Equation Solver for Multi-Energy Well Reactions (MESMER), a user-friendly, object-oriented, open-source code designed to facilitate kinetic simulations over multi-well molecular energy topologies where energy transfer with an external bath impacts phenomenological kinetics. MESMER offers users a range of user options specified via keywords ……."

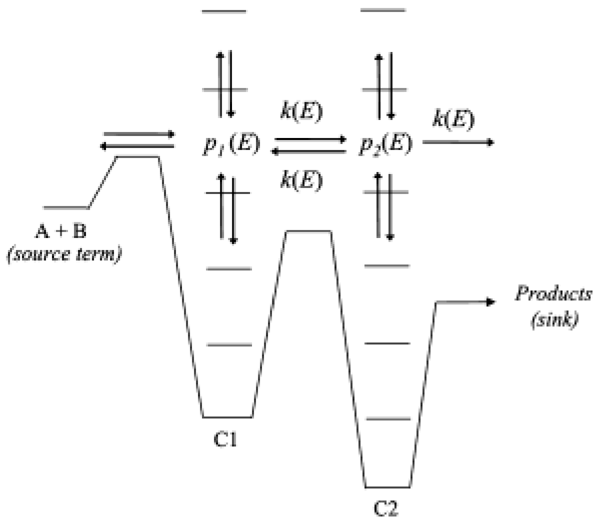

Master Equation Solver for Multi-Energy well Reactions (MESMER)

- Open source, object oriented code (C++)
- http://sourceforge.net/projects/mesmer/
- facilitates kinetic simulations of multi-well systems where energy transfer with a bath gas impacts phenomenological kinetics
- Provides interface with results of electronic structure calculations to allow set up of multi-well system
- Output choices include chemically significant (and other) eigenvalues, species concentrations vs time, phenomenological rate constants.
- Allows fitting to experimental data using χ^2 minimisation
- Includes MPI parallelization
- Allows fitting to experimental decay traces
- Latest version, 7.0, March 2023. For manual see:
- https://master.dl.sourceforge.net/project/mesmer/mesmer/7.0/MESMER%207.0.pdf?viasf=1

Other master equation codes

1. Multiwell. Uses a stochastic approach rather than the matrix methodology used in MESMER. Developed by John Barker. See:

   http://clasp-research.engin.umich.edu/multiwell/. and Int J Chem Kinet. 33, 232-45 (2001), 41, 748-763 (2009)
2. MESS. A matrix method, developed at Argonne National Labs by Georgevskii et al. Incorporates 2DME. See: http://tcg.cse.anl.gov/papr/codes/mess.html

   J. Phys. Chem. A 2013, 117, 12146–12154
3. TUMME. Tsinghua University Minnesota Master Equation. Matrix method. https://comp.chem.umn.edu/tumme/

Two-dimensional master equation (2DME). Application to CH_3 + H

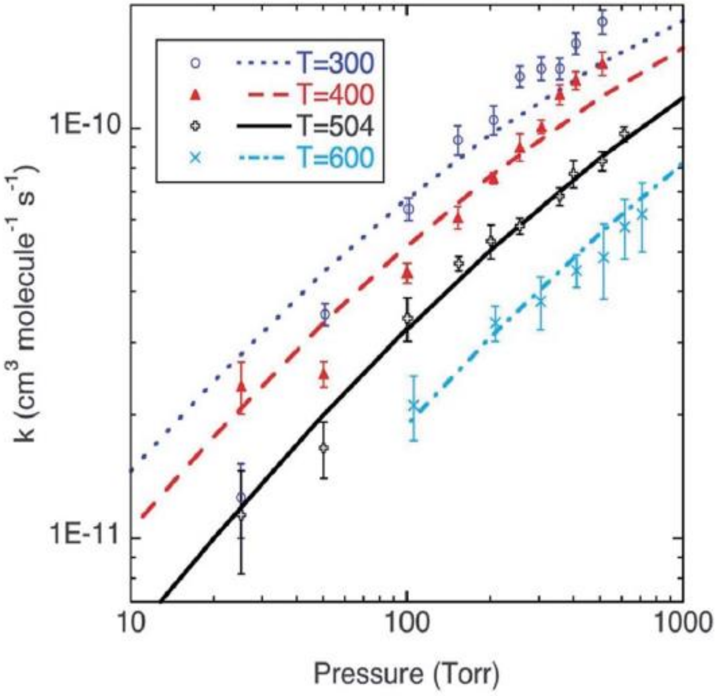

- 1DME approach neglects the dependence of the kinetics on the total angular momentum, *J*.
- This dependence can be important, especially in reactions with small barriers and variational transition states
- It is necessary to describe collisional relaxation of both the energy *E* and the angular momentum, *J* – hence the 2 dimensional master equation.
- The code MESS incorporates a 2DME. The plot shows an a priori calculation; a 1DME approach significantly overestimated the rate constants
- Experimental: Brouard et al J Phys Chem 1989, 93, 4047
- 2DME calculations, Jasper et al, Science, 2014, 346, 1212

Master equation
Some examples

Effect of sulfur oxides on fuel oxidation

Peter Glarborg Hidden interactions—Trace species governing combustion and emissions. 31st Symposium

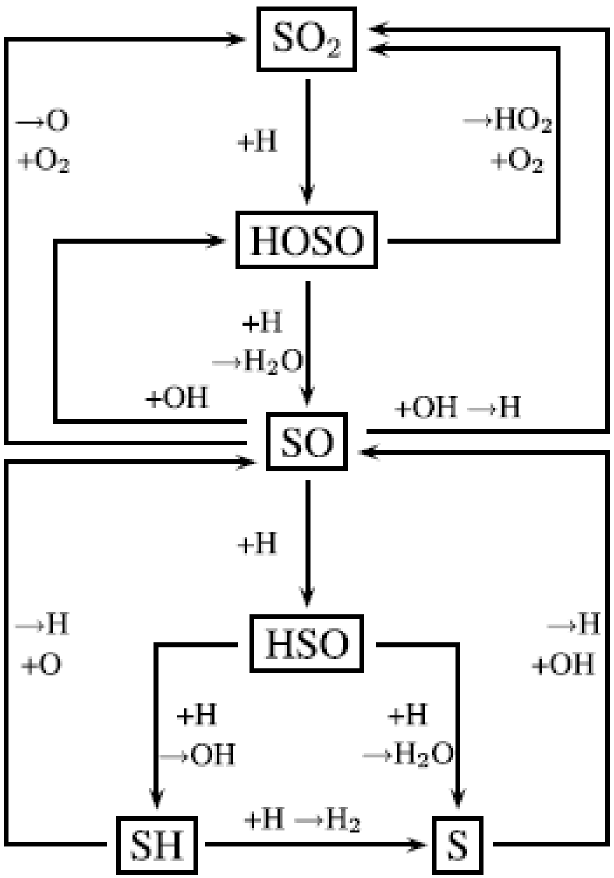

Component reactions:

- $SO_2 + H\ (+M) \leftrightarrows HOSO\ (+M)$ (R1)
- $HOSO + H \leftrightarrows SO + H_2O$ (R2)
- $SO + O_2 \leftrightarrows SO_2 + O$ (R3)

- How do we provide rate data for reactions of this sort?

- Are there hidden complexities in a simple association reaction like (R1)?

$H + SO_2$ experiment + theory

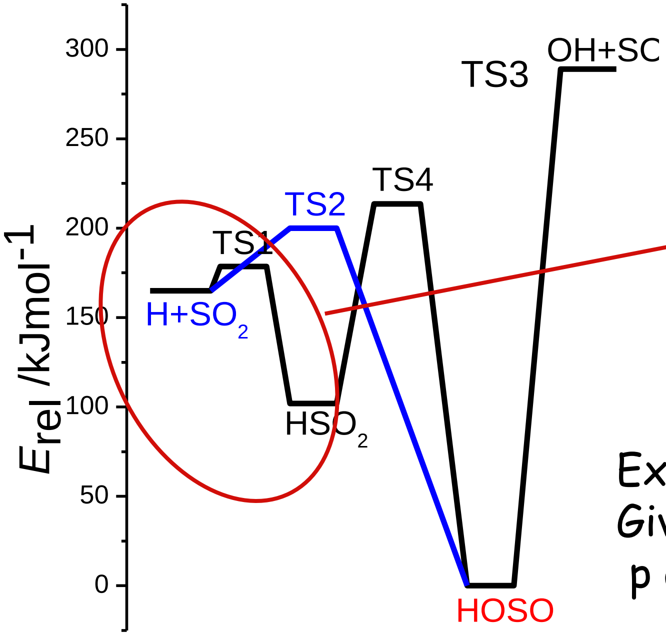

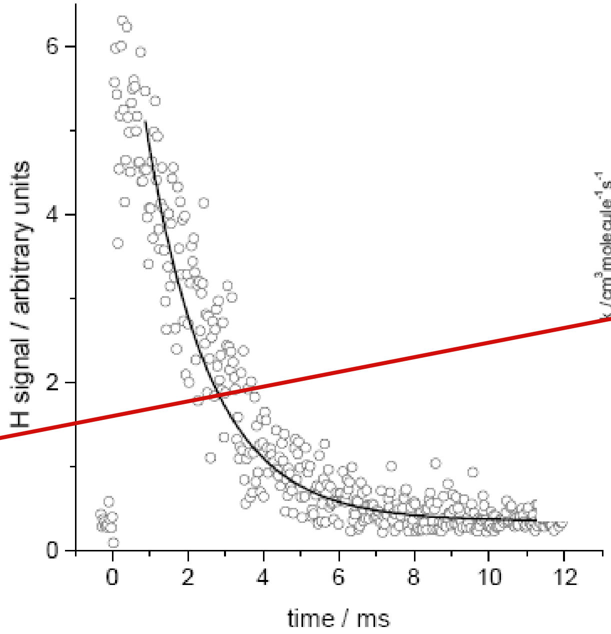

Experimental decay trace for $H + SO_2$
Gives eigenvalue and hence k at selectec
p and T.

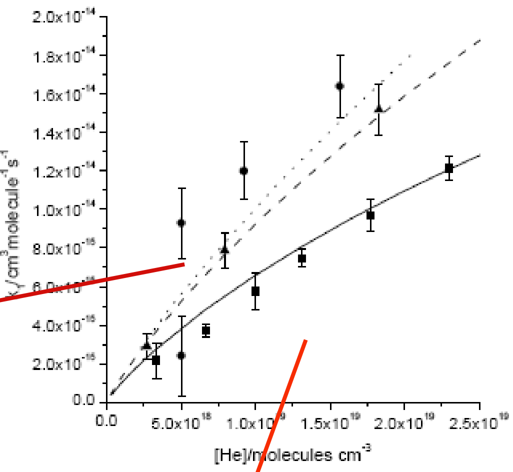

k vs p at T = 295, 363 and 423 K

Smallest IERE

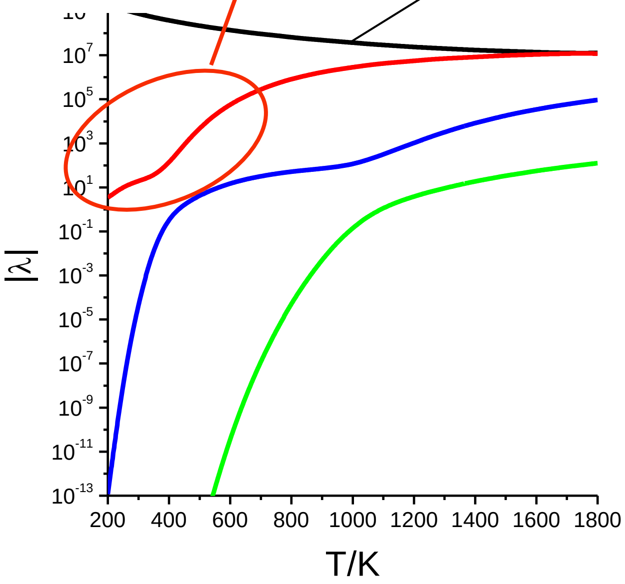

- Potential energy surface for $H + SO_2$, from electronic structure calcs
- Approach: Experimental investigation using vuv LIF for H
- Master equation analysis, constrained to experimental data

Eigenvalues from ME analysis.
Red – TS1
Blue TS2
Green TS3

Blitz et al, J. Phys. Chem. A **2006,** 110, 2996-3009

Determination of individual phenomenological rate constants from eigenvalues / eigenvectors

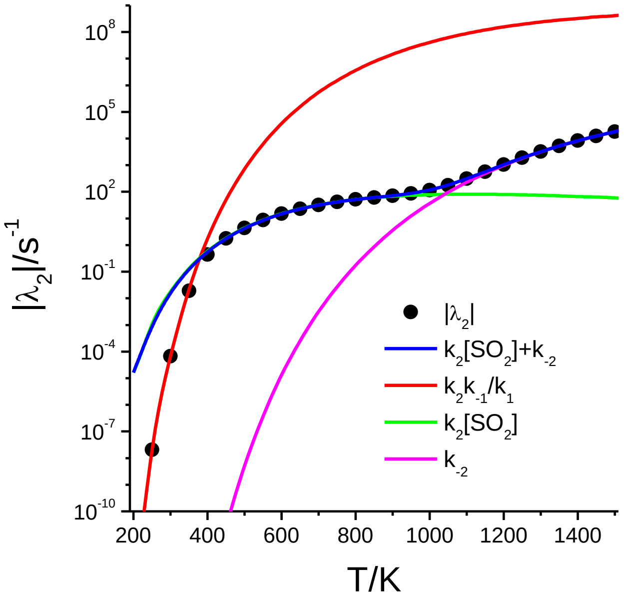

Total number of eigenvalues is equal to the total number of grains.

The 3 eigenvalues of smallest magnitude relate to the phenomenological rate coefficients of the macroscopic chemical system (*chemically significant eigenvalues*)

$H + SO_2 \leftrightarrows HSO_2$ (1)
$H + SO_2 \leftrightarrows HOSO$ (2)
$H + SO_2 \rightarrow OH + SO$ (3)
$H\ SO_2 \leftrightarrows HOSO$ (4)
$HSO_2 \rightarrow OH + SO$ (5)
$HOSO \rightarrow OH + SO$ (6)

$$\mathrm{d}c/dt = \begin{pmatrix} -k_{-1} - k_4 - k_5 & k_{-4} & k_1 \\ k_4 & -k_{-4} - k_{-2} - k_6 & k_2 \\ k_{-1} & k_{-2} & -k_1 - k_2 - k_3 \end{pmatrix} \begin{pmatrix} [HSO_2] \\ [HOSO] \\ [H] \end{pmatrix}$$

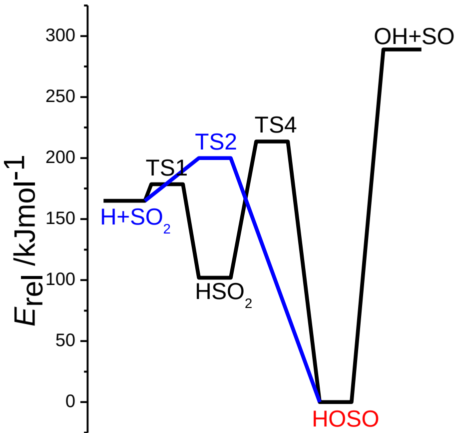

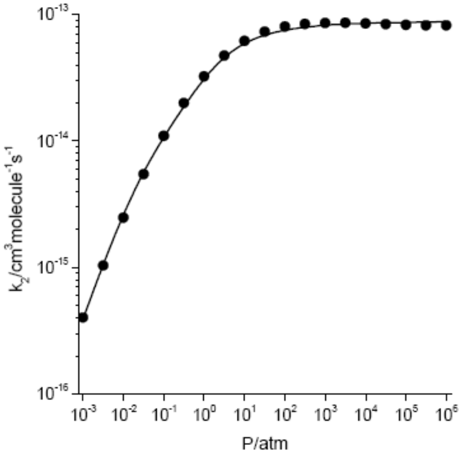

Experimental characterisation of the TS2 and TS3 regions of the surface

- TS2 is significant in the 400 – 800 K region.
- Too slow to study experimentally using LFP.
- ?Characterise using flow reactor methods?

- TS3 is even more difficult to investigate. Use the reverse reaction, OH + SO, via detailed balance

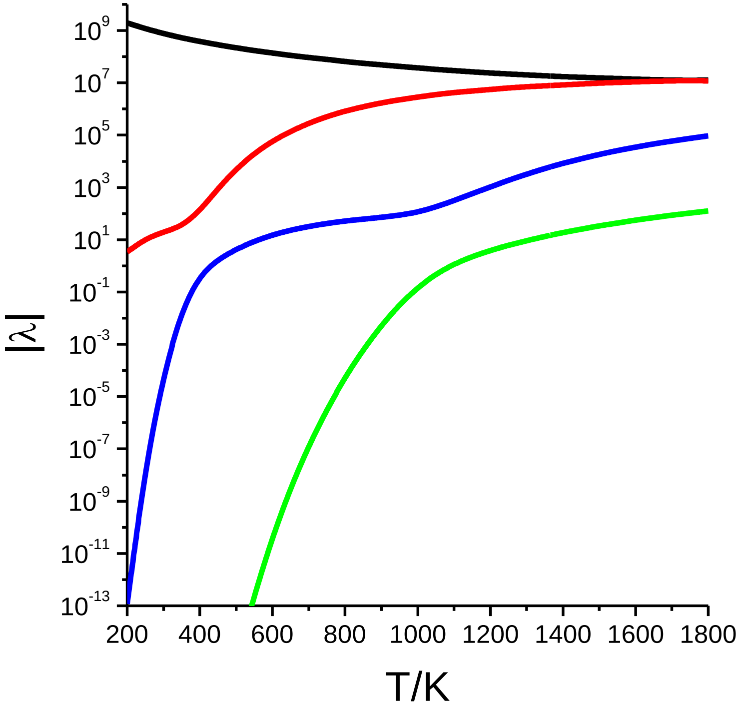

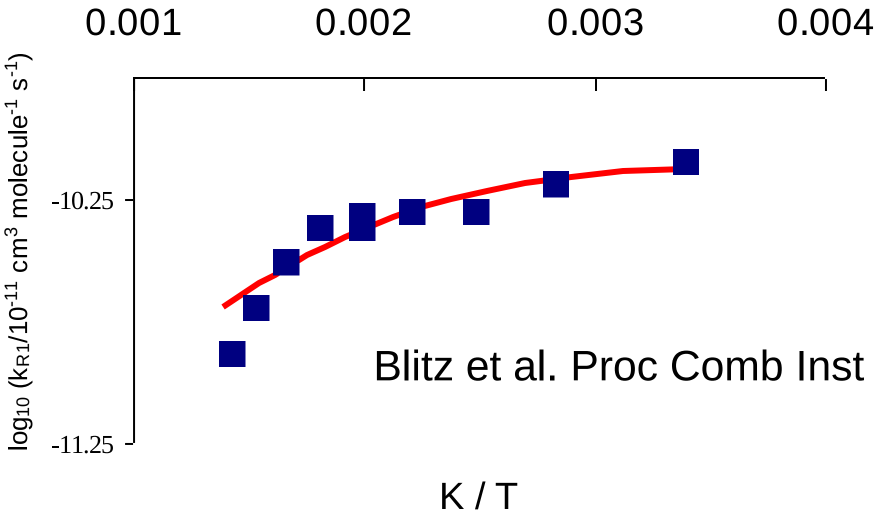

Blitz et al. Proc Comb Inst

Issues

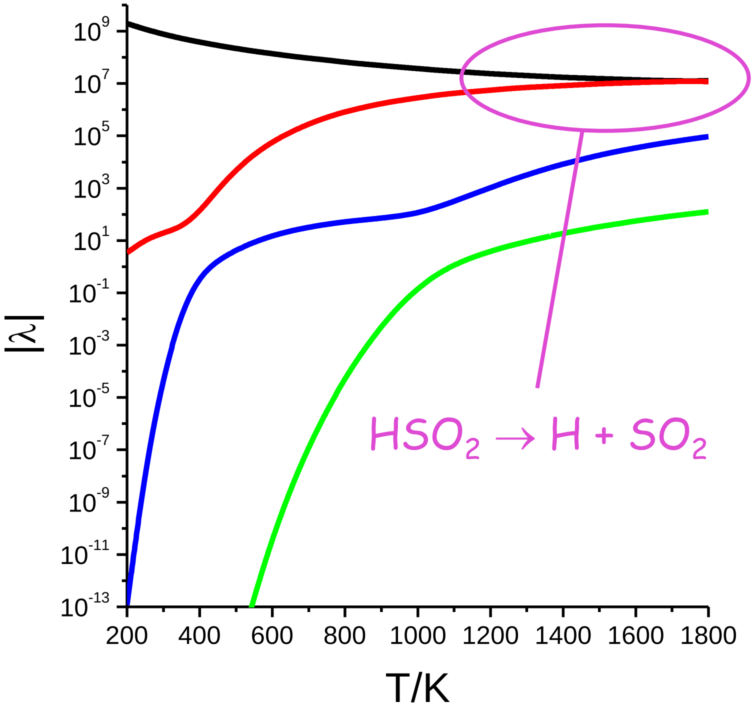

- Overlap of chemically significant eigenvalues with energy relaxation eigenvalues: can lead to problems in defining rate constants (see subsequent slides)
- Use of OH + SO to calculate forward ks using detailed balance. Does detailed balance always apply – are the forward and reverse rate constants always related through the equilibrium constant? (See earlier discussion - Miller and Klippenstein, Miller et al.)
- Important issue in combustion – e.g. CHEMKIN generally introduces forward and reverse reactions, linked via thermodynamics.

1,2-Pentyl isomerisation and dissociation

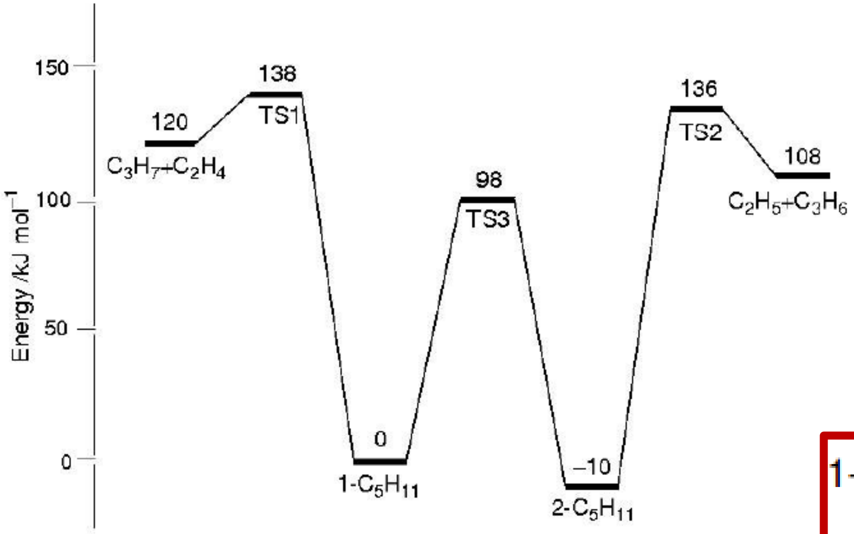

$$1\text{-}C_5H_{11} \rightleftharpoons 2\text{-}C_5H_{11} \quad \text{(R7)}$$

$$1\text{-}C_5H_{11} \rightarrow C_2H_4 + C_3H_7 \quad \text{(R8)}$$

$$2\text{-}C_5H_{11} \rightarrow C_2H_5 + C_3H_6 \quad \text{(R9)}$$

Well-skipping reactions

$$1\text{-}C_5H_{11} \rightarrow C_2H_5 + C_3H_6 \quad \text{(R10)}$$

$$2\text{-}C_5H_{11} \rightarrow C_2H_4 + C_3H_7 \quad \text{(R11)}$$

Two well, two CSEs

$$\lambda_{1,2} = \frac{-(k_C + k_D) \pm \sqrt{(k_C + k_D)^2 - 4(k_C k_D - k_7 k_{-7})}}{2}$$

where $k_C = k_7 + k_8 + k_{10}$ and $k_D = k_{-7} + k_9 + k_{11}$.

1,2 pentyl isomerisation and dissociation Rate coefficients extracted from eigenpairs with Bartis Widom analysis (Robertson et al, Phys Chem Chem Phys, 2007, 9, 4085)

$1\text{-}C_5H_{11} \rightleftharpoons 2\text{-}C_5H_{11}$ (R7)

$1\text{-}C_5H_{11} \rightarrow C_2H_4 + C_3H_7$ (R8)

$2\text{-}C_5H_{11} \rightarrow C_2H_5 + C_3H_6$ (R9)

$1\text{-}C_5H_{11} \rightarrow C_2H_5 + C_3H_6$ (R10)

$2\text{-}C_5H_{11} \rightarrow C_2H_4 + C_3H_7$ (R11)

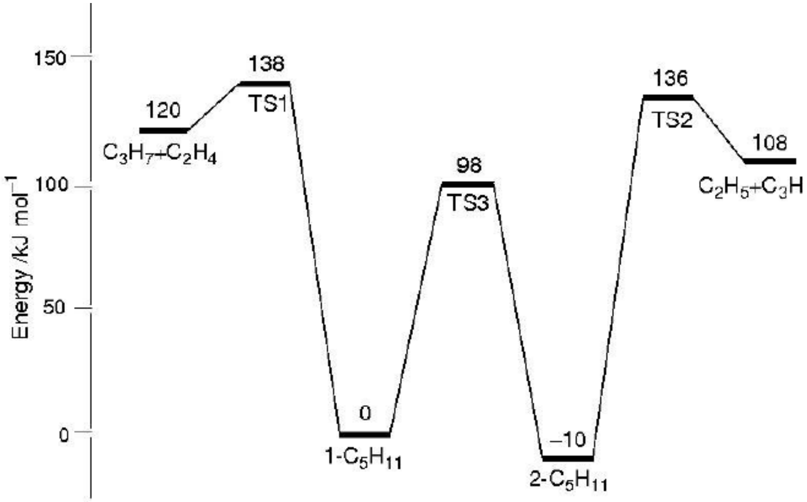

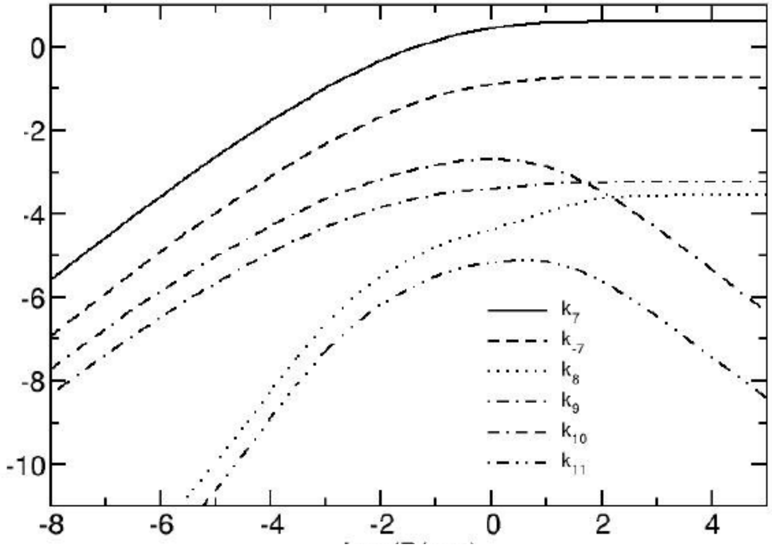

400 K

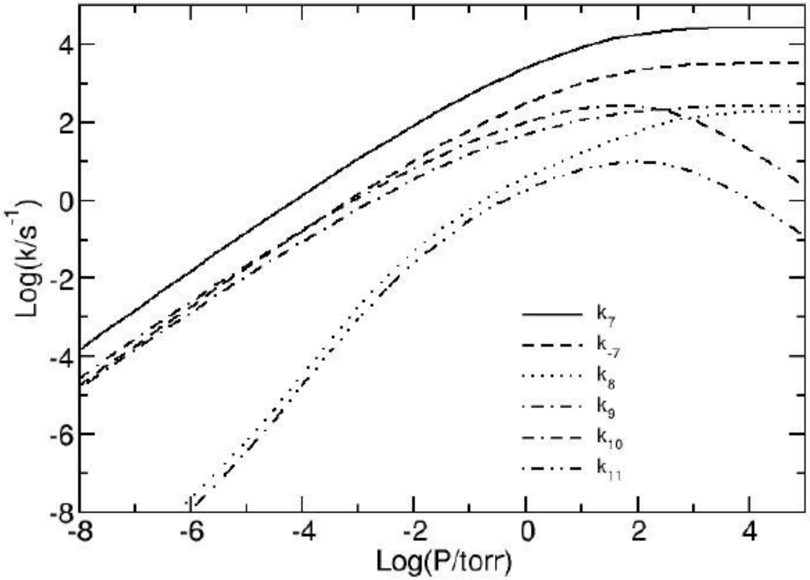

600 K

Behaviour at high temperatures: overlap of CS and internal energy relaxation eigenvalues

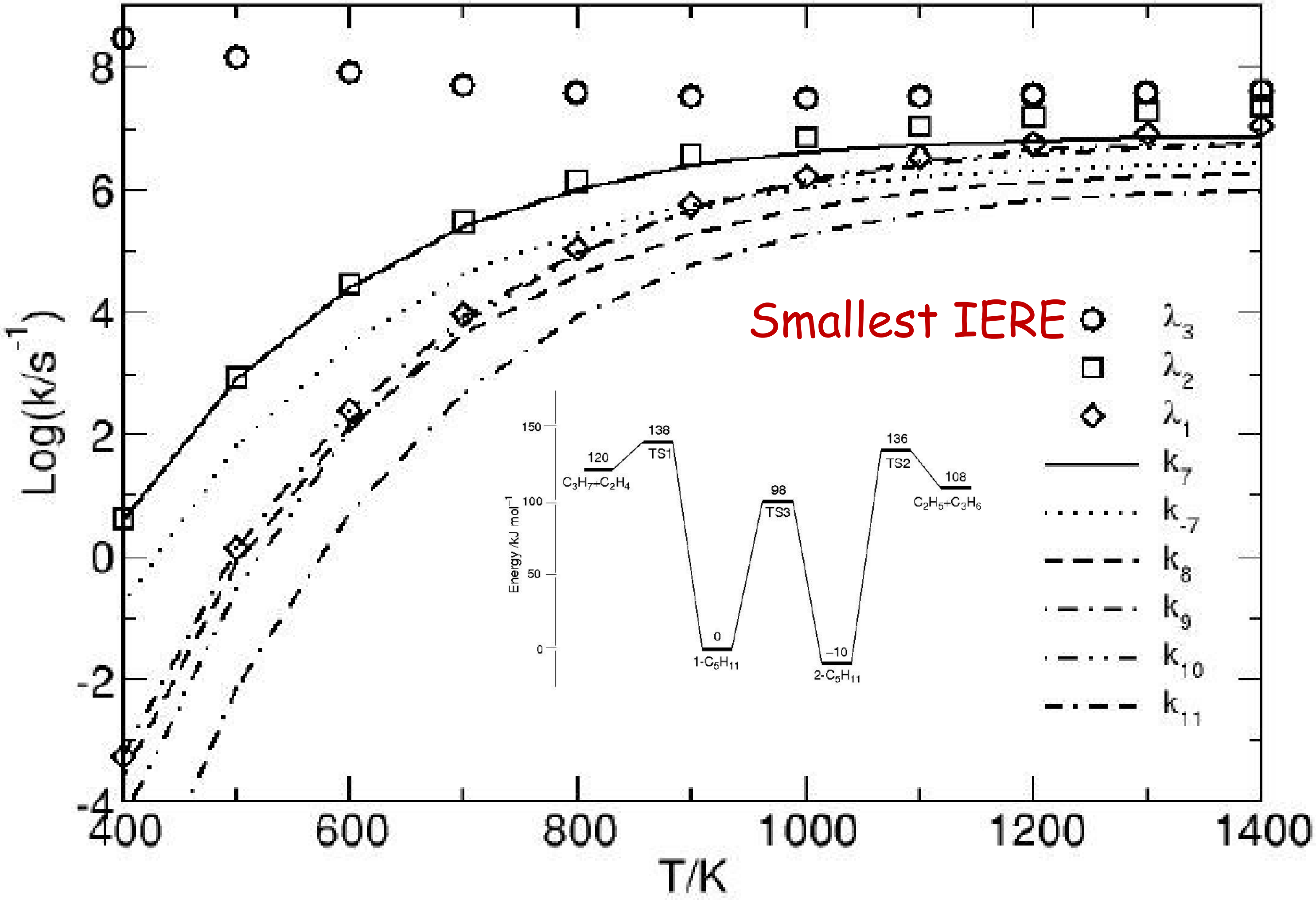
Smallest IERE

Binomial expansion of quadratic solution for λ_2

$$-\lambda_2 \approx k_7 + k_{-7} + k_8 + k_9 + k_{10} + k_{11} \approx \boxed{k_7 + k_{-7}}$$

Low T

- full diamonds: ratio of λ_2 from full quadratic solution to λ_2 from the ME.
- Open triangles: ratio of λ_2 from Eq. full quadratic solution to λ_2 from equatioı above (full expression.)
- Open squares: ratio of $-\lambda_2$ from full quadratic expression to $(k_7 + k_{-7})$.

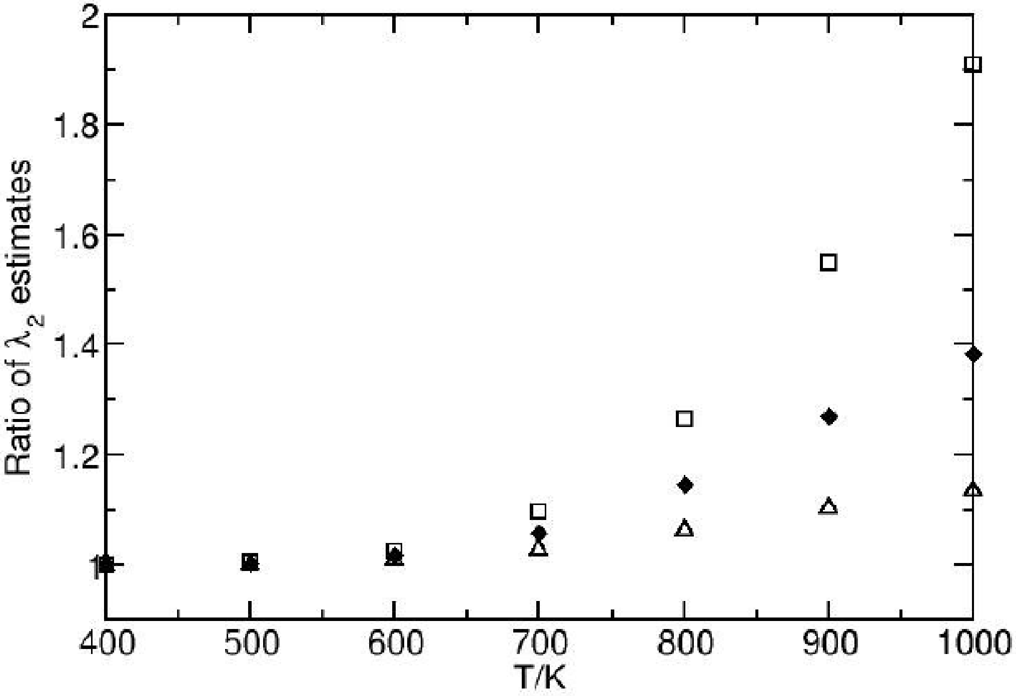

Binomial expansion of quadratic solution for λ_1

$$-\lambda_1 \approx \frac{\boxed{k_8 + k_{10}}}{1 + K_7} + \frac{\boxed{k_9 + k_{11}}}{1 + K_7^{-1}}$$ where $\boxed{K_7 = k_7/k_{-7}.}$

1-C_5H_{11} $\rightleftharpoons$ 2-C_5H_{11} (R7)

1-C_5H_{11} → $C_2H_4 + C_3H_7$ (R8)

2-C_5H_{11} → $C_2H_5 + C_3H_6$ (R9)

1-C_5H_{11} → $C_2H_5 + C_3H_6$ (R10)

2-C_5H_{11} → $C_2H_4 + C_3H_7$ (R11)

Full triangles: ratio of λ_1 from the full quadratic solution to λ_1 from the ME.

Open squares: ratio of λ_1 from the full quadratic solution to λ_1 from above approximation

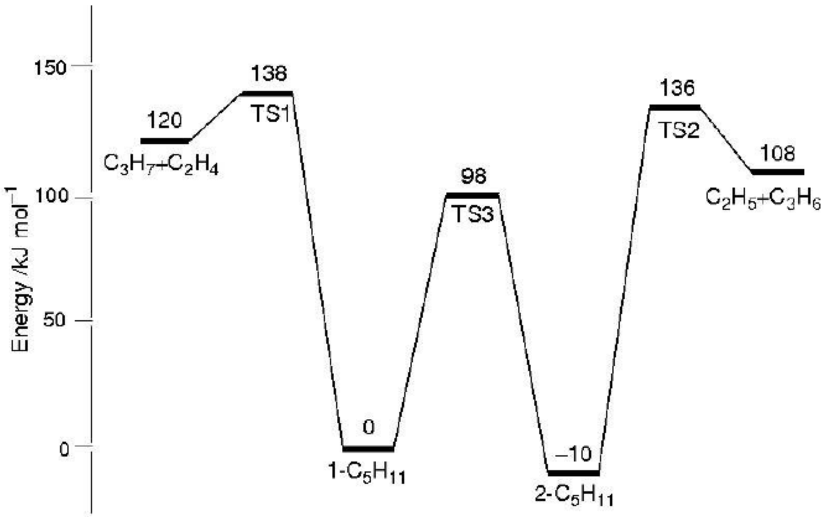

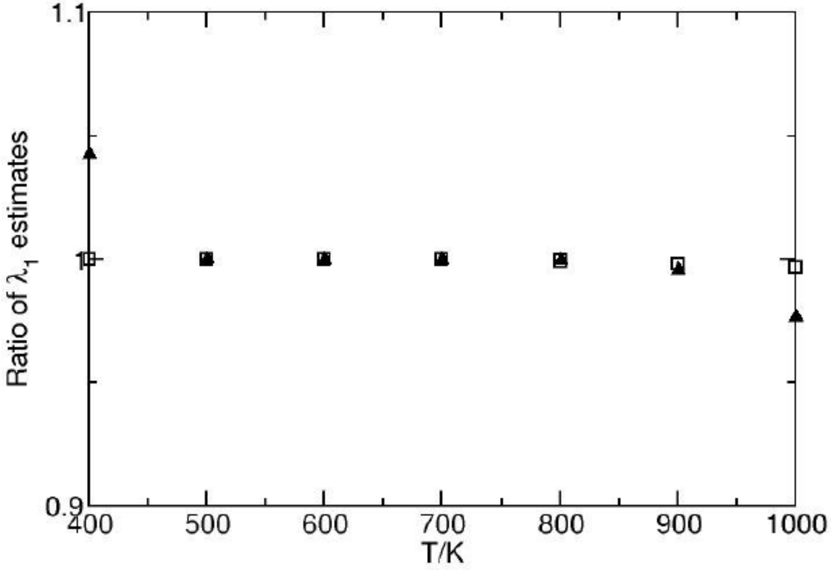

Comparison of the time dependence of the mole fraction of the 1- and 2-pentyl isomers using the summed grain populations from the ME and using the phenomenological rate coefficients from the ME in a biexponential representation: (a) 600 K; (b) 1000 K.

At 1000 K, the biexponential representation is inadequate. This is because of overlap of IEREs and CSEs. Normal phenomenological rate constants cannot be defined, because of this overlap.

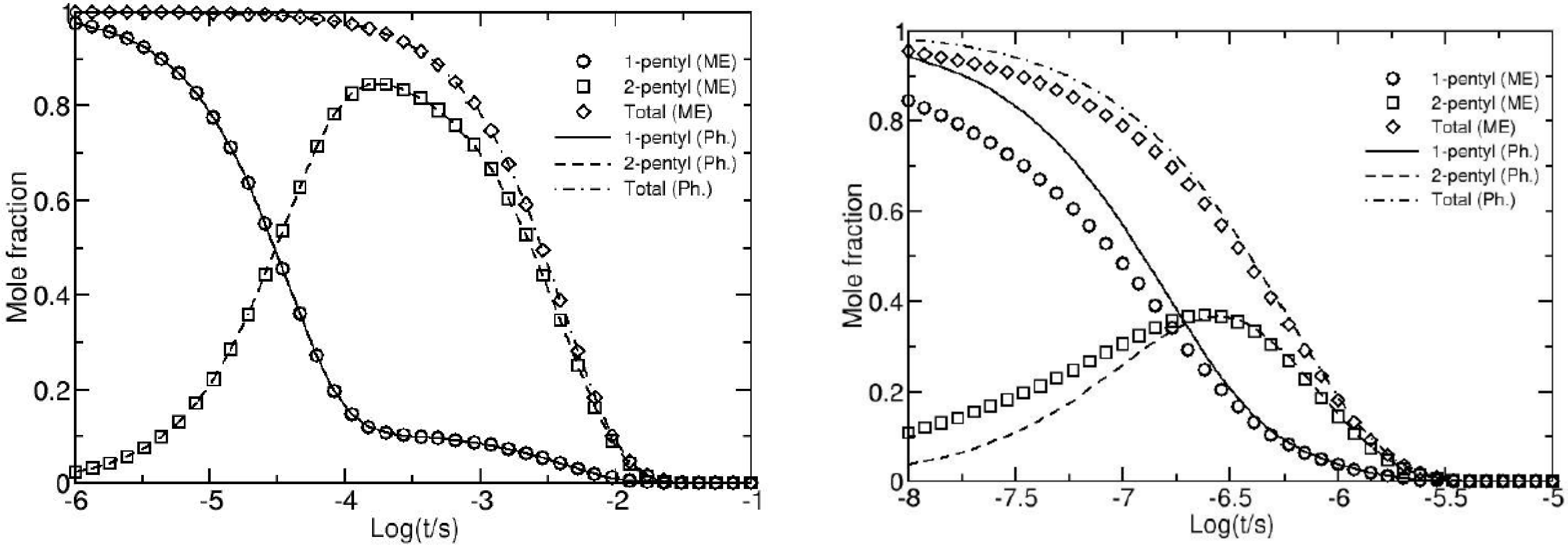

a

b

Conclusions

- All wells can contribute to all sink channels irrespective of whether they are directly connected to the transition state that leads to a given set of products.
- 'Well-skipping' is significant and is characterized by non-standard fall-off curves which exhibit a decline in rate coefficient with increasing pressure, indicative of the competition between collisional relaxation and reaction.
- Product yields are very sensitive to the difference in dissociation energies for 1- and 2-pentyl. The calculations give a difference of only 4 kJ mol$^{-1,}$ and ancillary experiments are essential to define the system more accurately. Because of the complexity of the system, the experiments must be interpreted with a master equation analysis.
- At high temperatures, there is overlap between the CSEs and the IEREs, so that time independent phenomenological rate constants cannot be determined.
- Miller and Klippenstein (Phys.Chem. Chem. Phys., 2013, 15, 4744) have developed a species reduction approach that overcomes the overlap problem in some cases. It cannot be applied to the pentyl problem

A second example of CSE / IERE overlap

Wang et al Physical Chemistry Chemical Physics, 2017, 19, 11064 - 11074

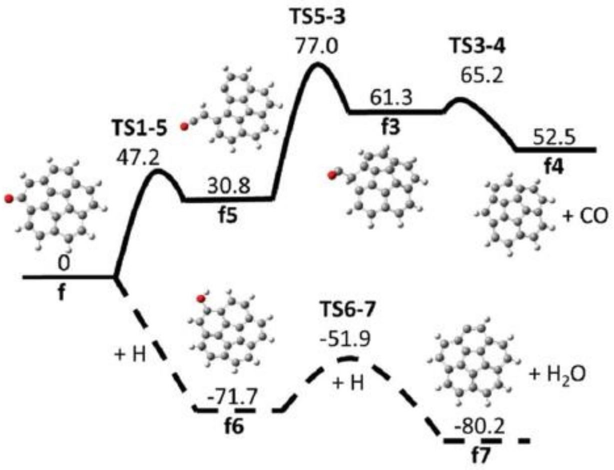

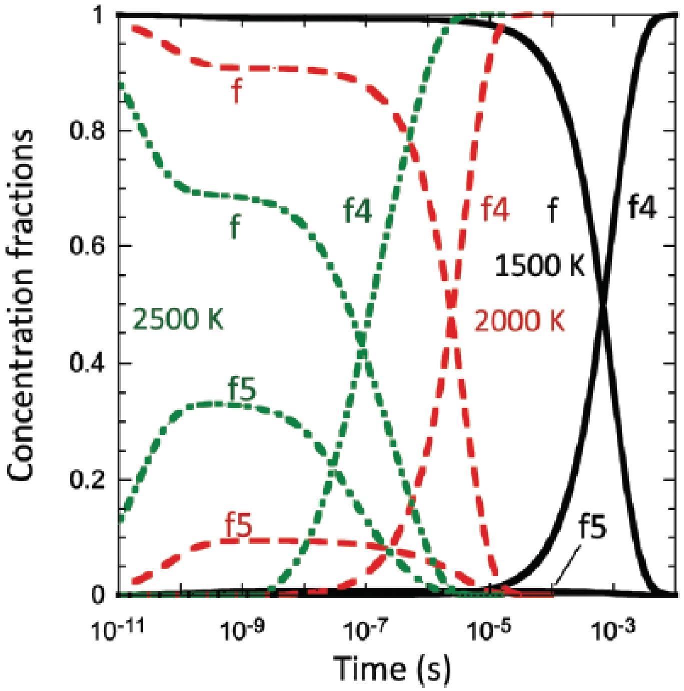

- The full curve in the PES diagram shows the dissociation of the corannulene oxyradical, f, via the intermediate isomer f5.
- The right hand figure shows the time dependence of f, f5 and the product f4 calculated using MESMER. The isomerisation occurs on very short timescales

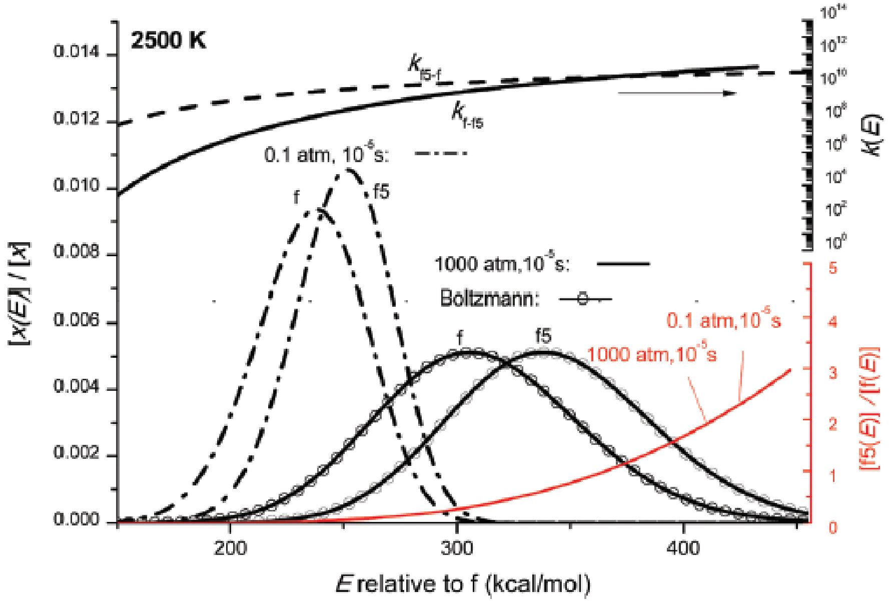

Fig. 4 Boltzmann distribution of f and f5 at 2500 K; microcanonical rate coefficients of f and f5 isomerization; concentration distributions of f5, f, and their ratios over energy from the master equation modelling of corannulene oxyradical f decomposition at 10^{-5} s, 2500 K and at 0.1 and 1000 atm.

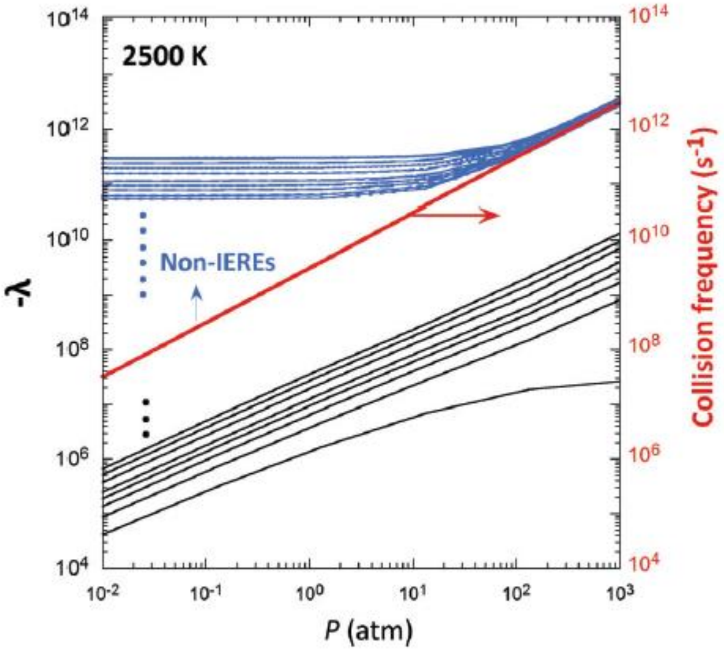

The left hand figure shows the Boltzmann distributions for f and f5 at 2500 K. The threshold for the isomerisation is 47 kcal mol-1. The rate constants are consequently very high and exceed the collision frequency – reaction occurs before collision. Each energy grain reacts independently of the others and there is a wide range of reactive eigenvalues, most of which are larger than the IEREs.

Behaviour of dissociation step

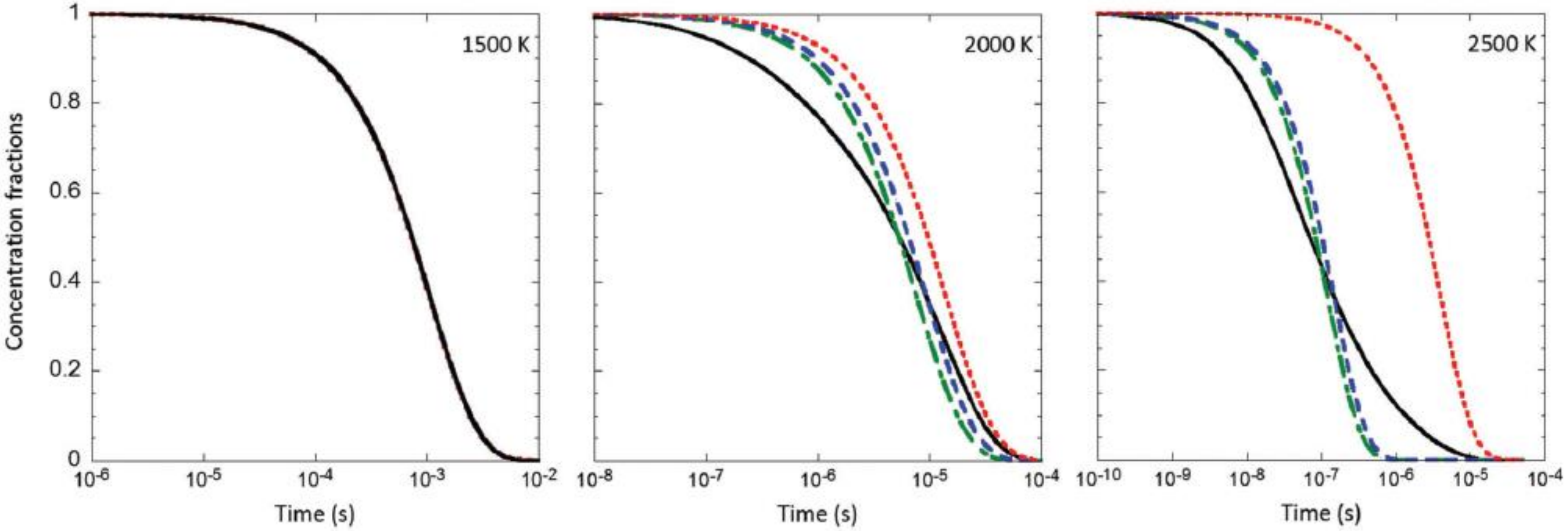

- Dissociation occurs on a longer timescale, but there is still considerable overlap of IEREs and the single remaining CSE at higher T.
- The above figures show the loss of f+f5 (black) and compares it with the smallest eigenvalue (in red) and two ways of fitting the decay to an exponential (in green and blue). At 1500 K, all curves are identical. The CSE provides a good description of the decay.
- At higher Ts, this is no longer the case. A steady state distribution in f+f5 is not fully established before dissociation occurs, so that the reaction shows a non-exponential time profile. A phenomenological rate constant that fully describes the reaction cannot be determined. The green and blue curves allow approximate rate constants to be determined, but their shortcomings must be recognised.

A further example of IERE / CSE overlap

- Klippenstein, Proc Comb Inst 2017, 36, 77
- Xylyl decomposition – 20 wells
- Black lines - lowest 20 eigenvalues, which correspond to the CSEs at low temperature.
- At higher temperatures these eigenvalues merge with the sea of IEREs, the lowest 10 of which are depicted with blue dotted lines.
- Red line - constant pressure collision rate, effective upper bound for the IEREs.

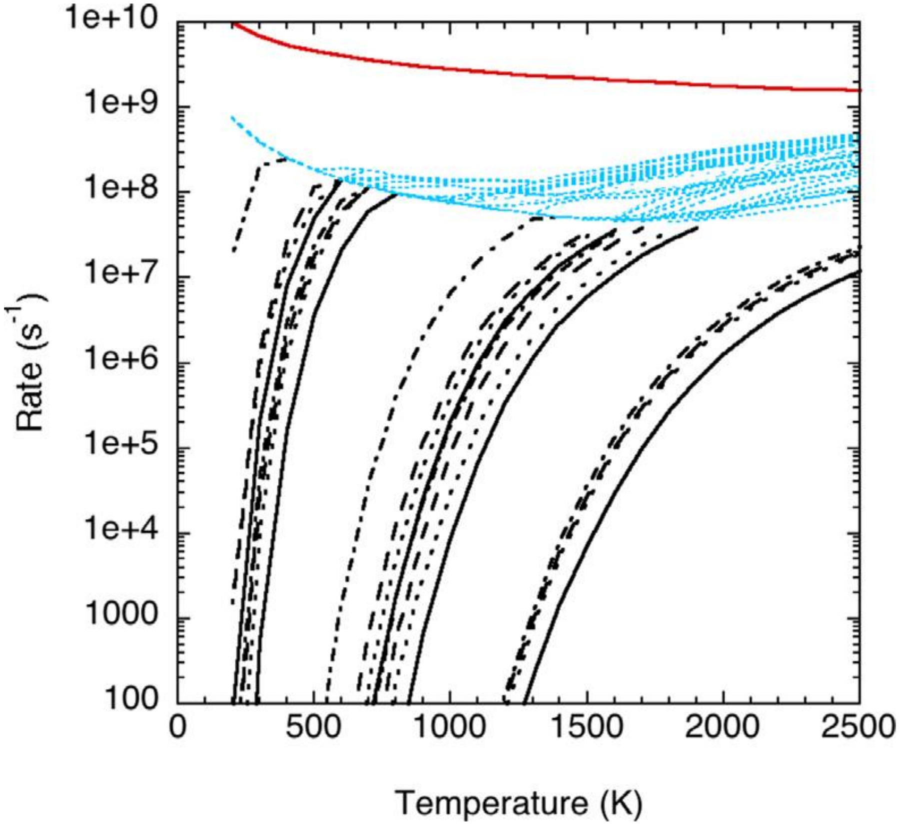

Use of MESMER to fit experimental data

- MESMER has a fitting facility that uses the Marquardt algorithm to fit to extensive sets of experimental data by minimising χ^2.
- The method is often linked to electronic structure calculations of the PES, with sensitive parameters (e.g. a transition state energy) allowed to float in the fitting process. Other parameters that are often fitted include those for energy transfer. MESMER can cope with different experiments using different bath gases.
- It is difficult to calculate association rate constants accurately (see earlier), but MESMER allows them to be fitted to experimental data using inverse Laplace transformation (ILT).

Inverse Laplace transform and association rate coefficients

$$\mathcal{L}^{-1}\{F(s)\} = f(t) = \frac{1}{2\pi i}\lim_{T\to\infty}\int_{\gamma-iT}^{\gamma+iT} e^{st}F(s)\,ds,$$

$$k_\infty(T) = \frac{\int_0^\infty k(E_R)\,N(E_R)\exp(-\beta E_R)\,dE_R}{\int_0^\infty N(E_R)\exp(-\beta E_R)\,dE}$$

$$= \int_0^\infty k(E_R)\,N(E_R)\exp(-\beta E_R)\,dE\,/Q_R$$

- Inverting this relationship allows k(E) to be determined from the high pressure limiting rate constant. Most effectively performed using the association rate constant.
- Davies et al. Chem Phys Letters, 1986, 126, 373-379.

Microcanonical dissociation rate constants from inverse Laplace transform of canonical association rate constant

β = 1/kT Q(β) is the rovibronic partition function, K(β) is the equilibrium constant and N(E) is the rovibronic density of states of the association complex. N_p is the convoluted densities of states of the reactant species

A + B → C

$$k_\infty(\beta) = A'_\infty \left(\frac{1}{\beta}\right)^{n_\infty} \exp\left(-\beta E_\infty\right)$$

$$k(E) = \frac{\mathcal{L}^{-1}[Q\,(\beta)K(\beta)k_\infty(\beta)]}{N(E)}, \quad E > 0$$

$$k(E) = \frac{A'_\infty C'}{N(E)\Gamma(n_\infty + 1.5)} \int_0^{E-E_\infty} N_\mathrm{P}(x) \times [E - E_\infty - \Delta H_0^0 - x]^{n_\infty + 0.5}$$

$$C' = \left(\frac{2\pi(M_A M_B}{M_A + M_B}\right)^{3/2}$$

An example: $CH_3 + CH_3$

Slagle et al. (J. Phys. Chem. 1988, 92, 2455–2462)

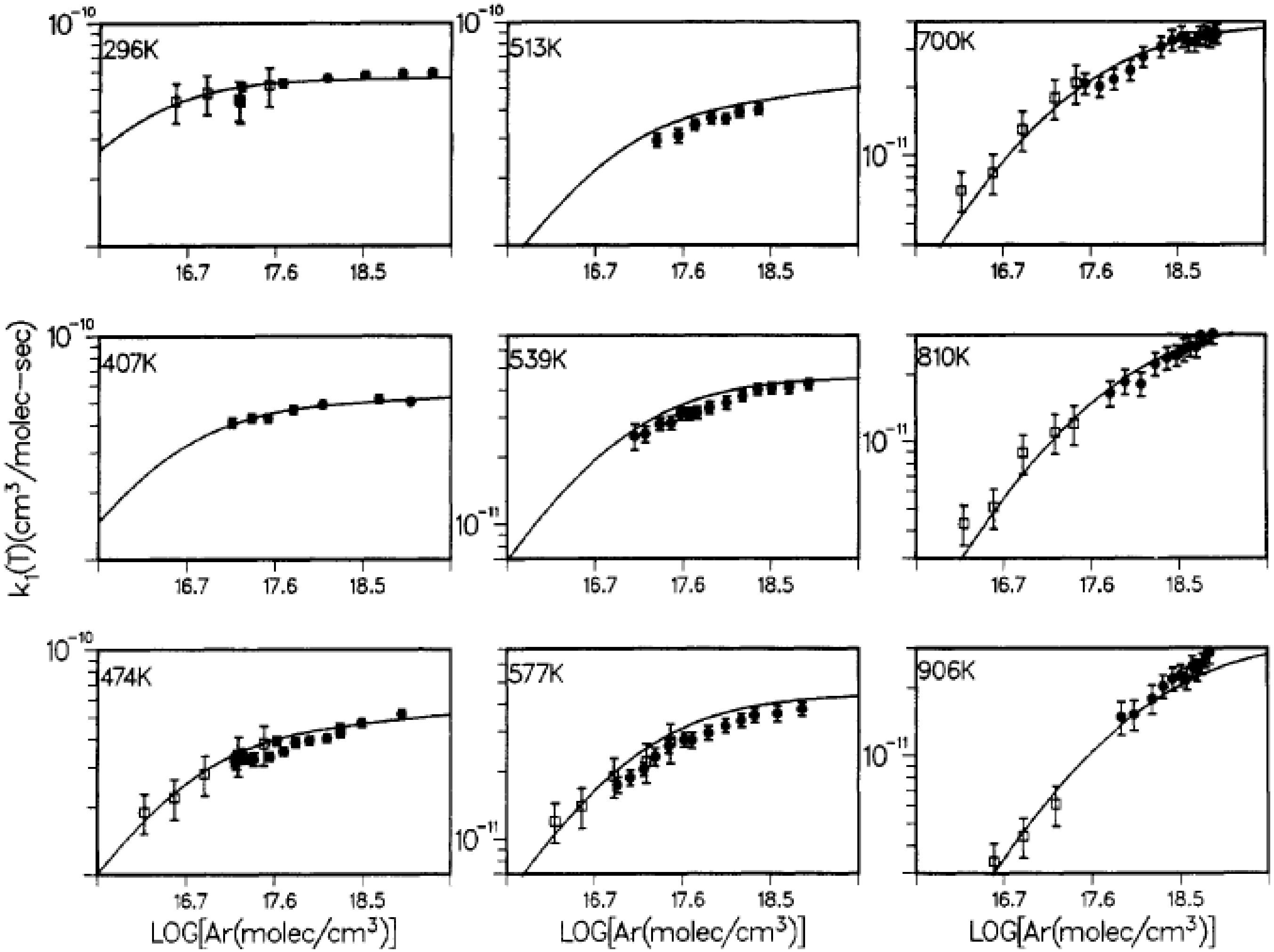

All experiments used pulsed laser photolysis in Ar. Low pressure data (open squares) by photoionization mass spectrometry, high pressure data (filled circles) by absorption spectroscopy/ Curves show non-master equation fit

An example: CH_3 + CH_3

- The absorption cross sections used in the determination of k(CH_3+CH_3) by Slagle et al. were recently redetermined, necessitating a reanalysis of the pressure and temperature dependent experimental data.* This was achieved using MESMER, using a global fit to all the absorption data
- The variable parameters in the fit were the high pressure limit ($k_\infty = AT^n$) and the energy transfer parameters for Ar as bath gas.
- The plot shows the experimental vs the best fit calculated data. The total number of datapoints (k at a specific T and P) is 102.

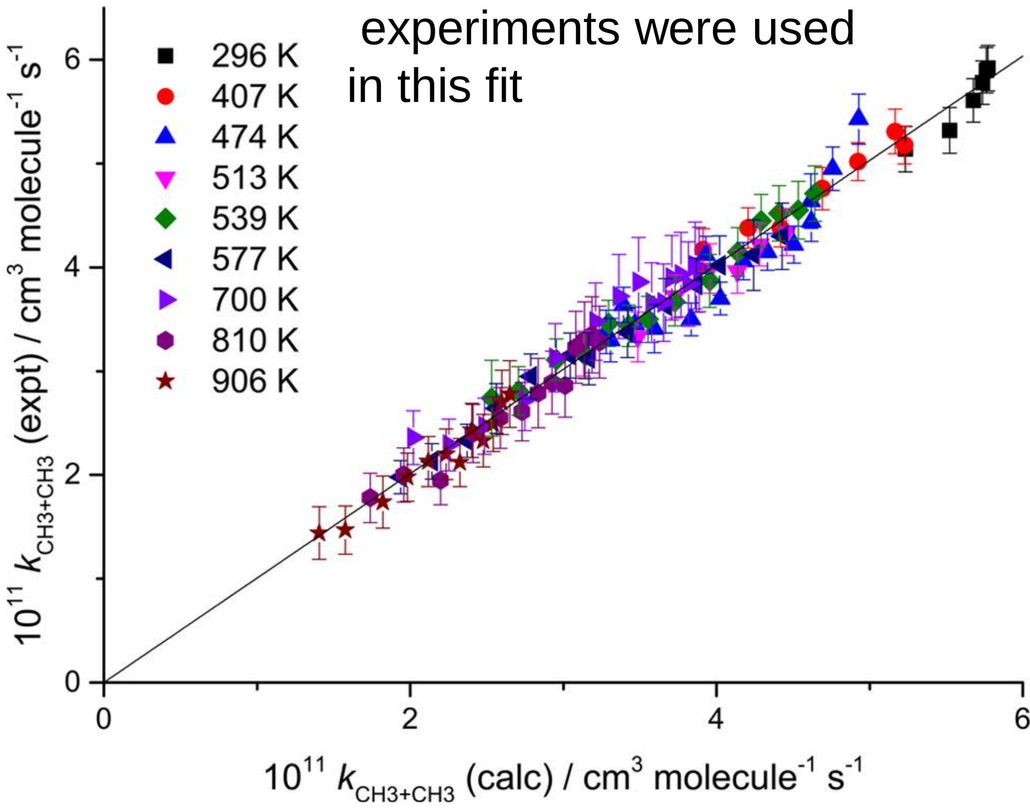

Only the data from absorption experiments were used in this fit

*This reaction is second order in radical, so the concentration of the radical is needed. In effect, the experiment determines k/σ, where σ is the absorption cross-section.

Extended fit to all available data

- The data cover the temperature range 296 – 1924 K.
- Techniques used include pulsed photolysis with absorption spectroscopy and mass spectrometric detection and shock tubes with absorption spectroscopy. He and Ar were used as bath gases
- k_∞ is most sensitive to the lower T data, especially that using absorption spectroscopy, and the energy transfer parameters to the higher T data.

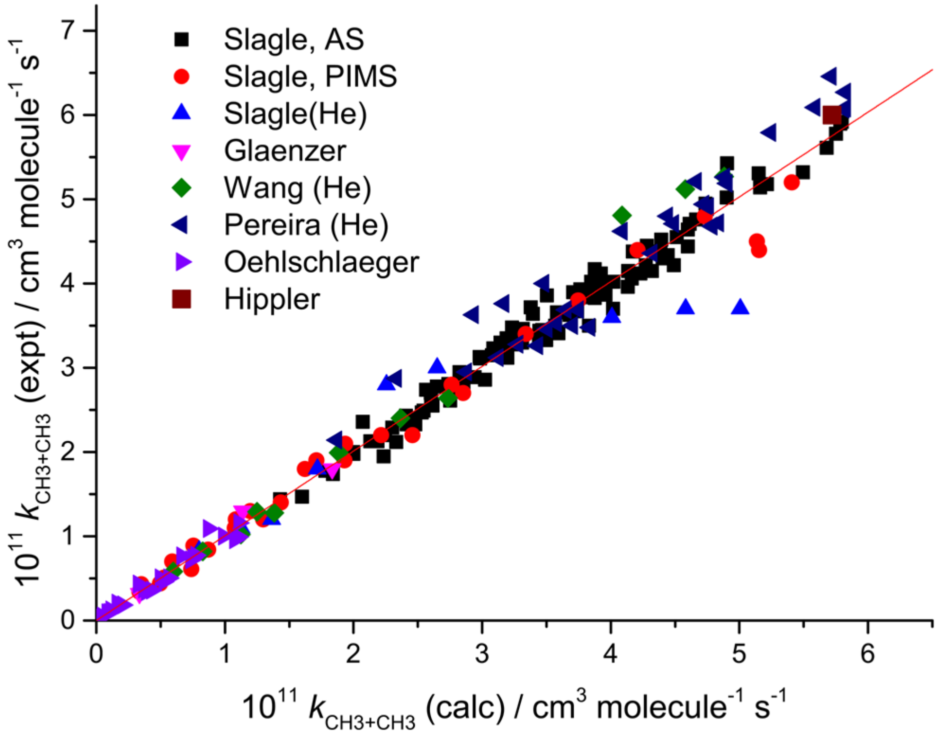

Note that the reaction is second order in radical; a modified "local linearization" of the second order decay was used to allow the use of standard matrix diagonalization methods

Comparison with theory for the high pressure limit

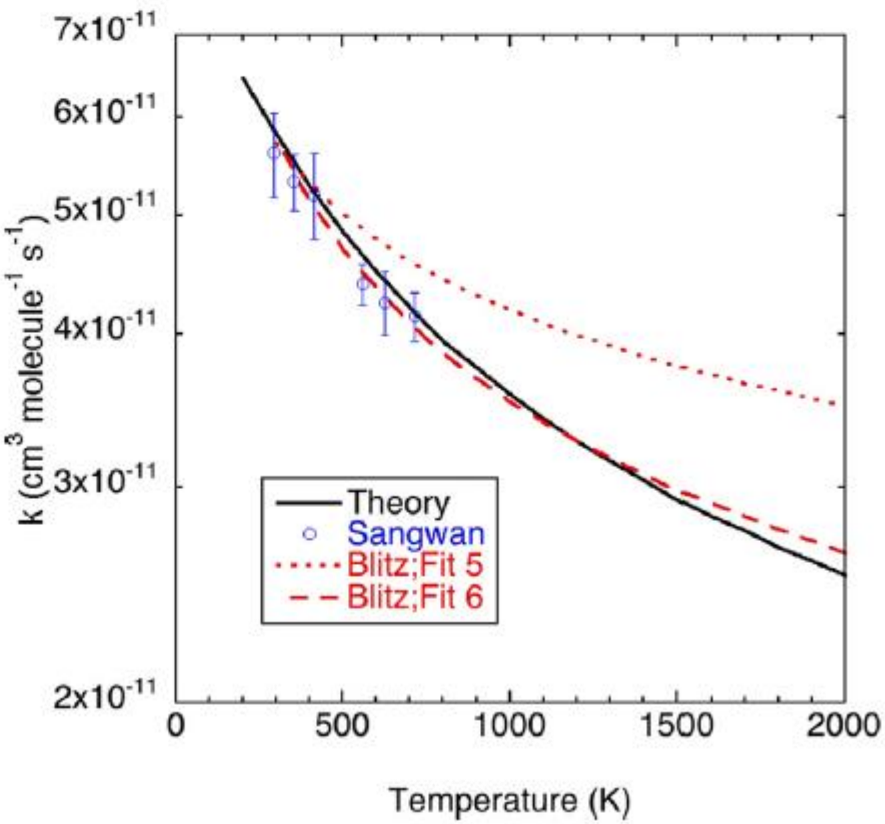

Blitz et al
J Phys Chem, 2015, 119, 7668
Sangwan et al.
J Phys Chem, 2015, 119, 7847
Theory discussed in Klippenstein
Proc Comb Inst 2017, 36, 77

- The theory curve is the CASPT2 + dynamical correction (see earlier). The Sangwan data are recent high pressure pulsed photolysis data, not used in the fit. The two Blitz fits refer to different models for the absorption cross section. Note that theory and experiment are totally independent.

Fitting directly to experimental decay curves
OH + C_2H_4

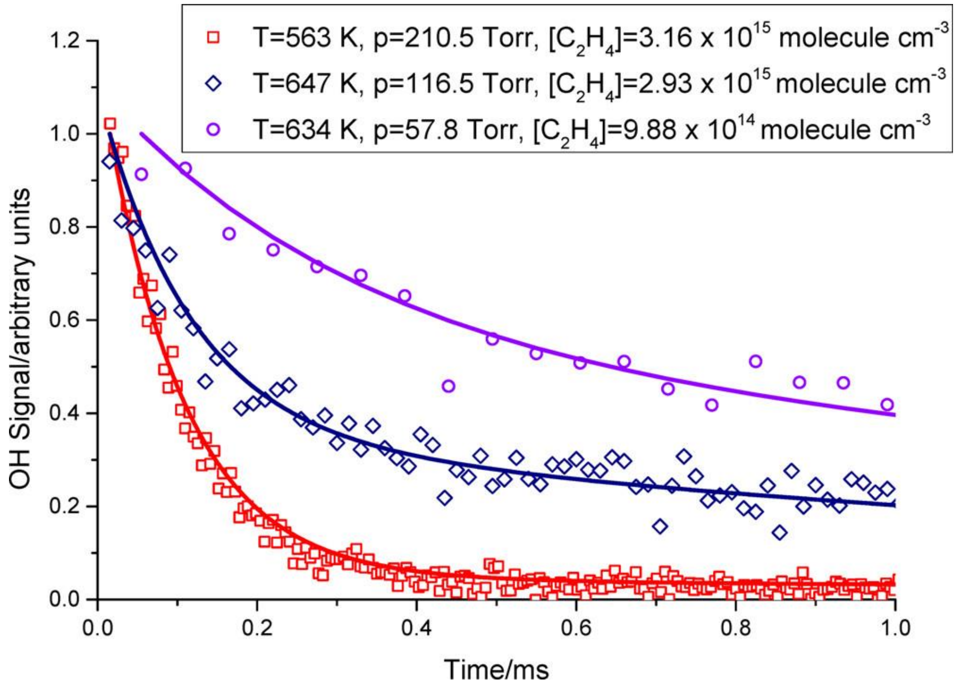

- 96 traces analysed globally, over the 563–723 K and at bath gas (N_2) pressures of from 58 to 250 Torr
- *Ab initio* calculations used to determine PES, refined in global fits.
- Analysis gave:
  - Pressure dependent rate constants including high pressure limit.
  - Rate constants for competing abstraction reaction(→ $H_2O+C_2H_3$)
  - ΔrH_0^0 = 111.8 kJ mol^{-1} (cf high level theory = 111.4 kJ mol^{-1})

$$OH + C_2H_4 \rightleftharpoons HO\text{-}C_2H_4$$

KinBot: Automated stationary point search on potential energy surfaces (Computer Physics Communications 2020, 248, 106947)

- Automatically characterizes kinetically important stationary points (TS, intermediates, products) on reactive potential energy surfaces. Sets up for master equation calculations
- C, H, O, N and S atom containing species; isomerization and dissociation reactions
- Iteratively changes the geometry of the reactant to obtain initial guesses for reactive saddle points defined by KinBot's reaction types. Then optimized by a quantum chemistry.
- For a given reactant, looks for structural features compatible with range of reaction types, e.g. HO2 elimination, bond dissociation.
- The transition state geometries are guessed and then refined using density functional theory.
- New calculations can be automatically generated from the products to obtain complete potential energy surfaces.
- KinBot includes conformer searches, projected frequency and hindered rotor calculations, and the automatic determination of the rotational symmetry numbers.
- https://github.com/zadorlab/KinBot/wiki

An example: OH addition to propene at the central C atom

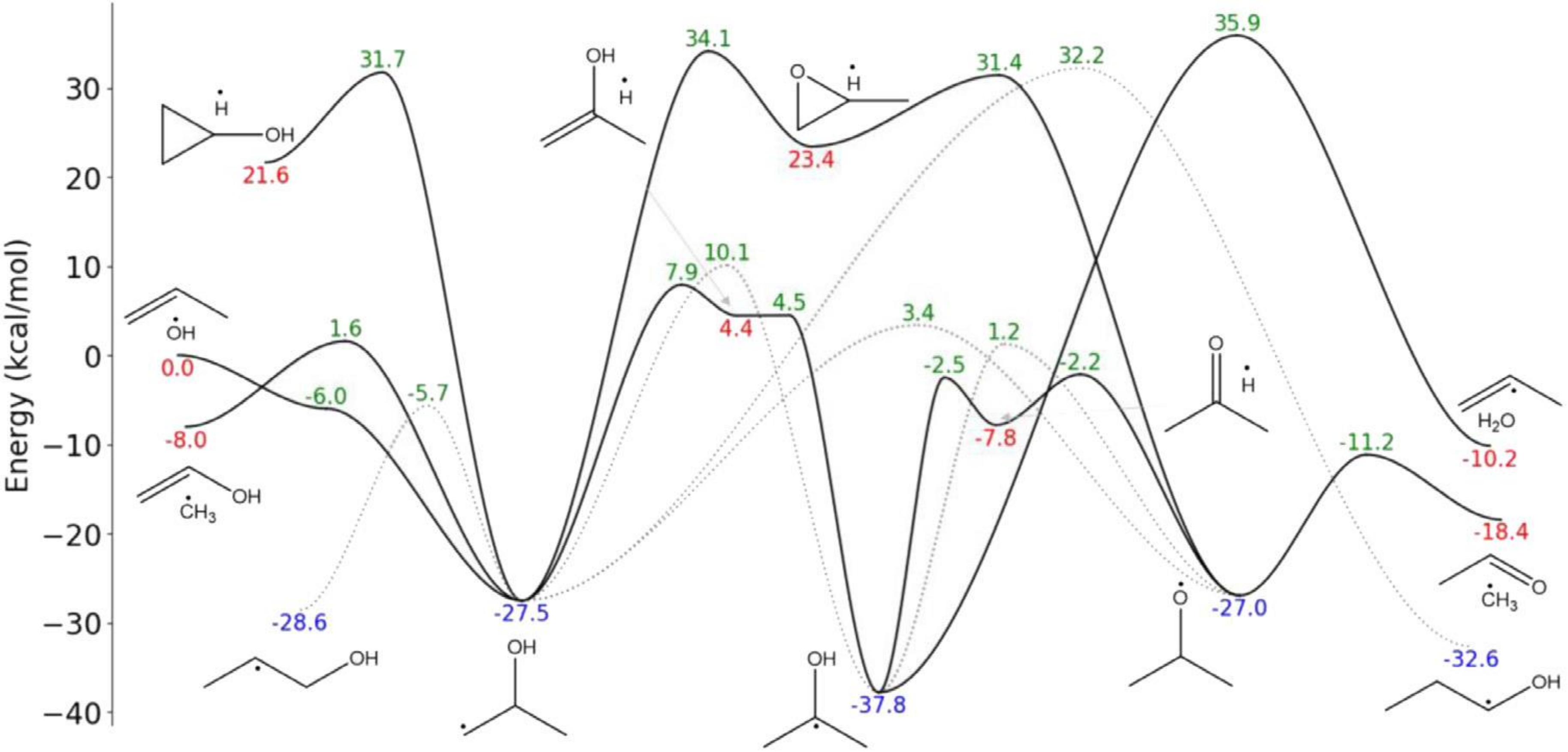

Calculated at the B3LYP/6-311++G(d,p) level of theory. Dashed gray lines correspond to isomerization reactions, solid black lines to bimolecular product formations. Blue values are the well energies, red values are the bimolecular product energies and green values are the transition state energies.

EStokTP: Electronic Structure to Temperature- and Pressure-Dependent Rate ConstantsA Code for Automatically Predicting the Thermal Kinetics of Reactions

Cavallotti et al, J. Chem. Theory Comput. 2019, 15, 1122–1145; https://github.com/PACChem/EStokTP

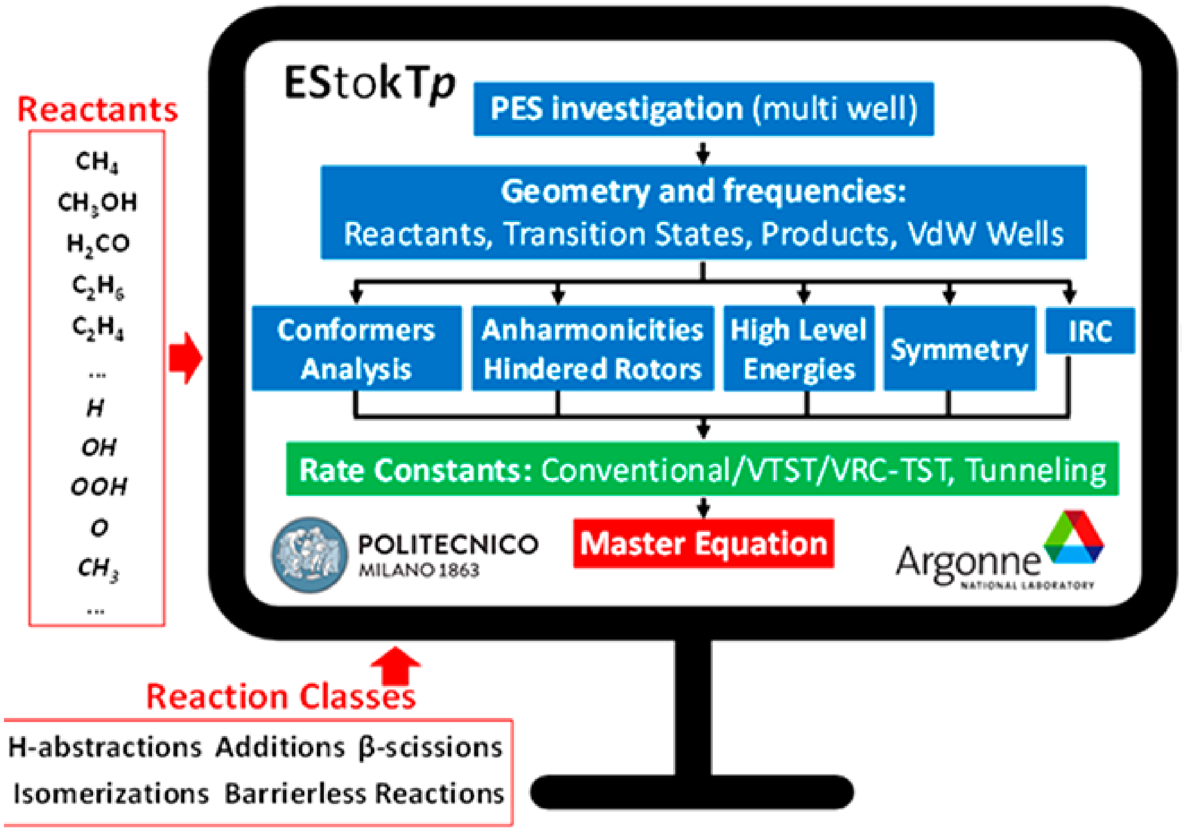

Reactants

CH_4
CH_3OH
H_2CO
C_2H_6
C_2H_4
...
H
OH
OOH
O
CH_3
...

EStokTp

PES investigation (multi well)

Geometry and frequencies:
Reactants, Transition States, Products, VdW Wells

Conformers Analysis
Anharmonicities Hindered Rotors
High Level Energies
Symmetry
IRC

Rate Constants: Conventional/VTST/VRC-TST, Tunneling

Master Equation

POLITECNICO MILANO 1863

Argonne NATIONAL LABORATORY

Reaction Classes

H-abstractions Additions β-scissions
Isomerizations Barrierless Reactions

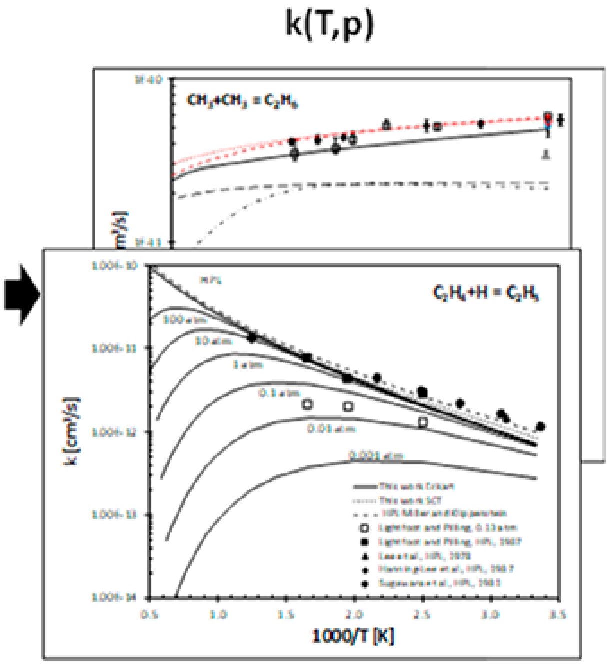

- 2 steps: (a) electronic structure calculations (b) kinetic solver, such as a transition state theory (TST)-based master equation solver

Conclusions

- We've examined theoretical approaches to determining rate constants for reactions, from quite simple single step reactions to multiwell multiproduct processes.
- High level theory can increasingly play an important predictive role.
- Theory also allows us to understand and interpret experimental studies. This interaction is key to understanding the validity of the more accessible theoretical methods.
- Theory provides a more flexible approach than experiment to determining rate data over a wide range of conditions – it is essential we understand both its strengths and its weaknesses.

Topic 4
Thermodynamics

Thermodynamics

- We need thermodynamic data to:
  - Determine the heat release in a combustion process (need enthalpies and heat capacities)
  - Calculate the equilibrium constant for a reaction – this allows us to relate the rate coefficients for forward and reverse reactions (need enthalpies, entropies (and hence Gibbs energies), and heat capacities.
- This lecture considers:
  - Classical thermodynamics and statistical mechanics – relationships for thermodynamic quantities
  - Sources of thermodynamic data
  - Measurement of enthalpies of formation for radicals
  - Active Thermochemical Tables
  - Representation of thermodynamic data for combustion models

Various thermodynamic relations are needed to determine heat release and the relations between forward and reverse rate coefficients

$$\text{at constant } p, \Delta H = \Delta U + p\Delta V$$

$$\Delta_r H = \sum_{\text{products}} \nu_{\mathrm{i}} \Delta_f H_i - \sum_{\text{reactants}} \nu_{\mathrm{i}} \Delta_f H_i$$

A statement of Hess's Law

ν_i is the stoichiometric coefficient

$$\Delta_r H(T_2) = \Delta_r H(T_1) + \int_{T_1}^{T_2} \sum_i \nu_{\mathrm{i}} C_{\mathrm{p,i}} \mathrm{d}t$$

Hess's Law:
The standard enthalpy of an overall reaction is the sum of the standard enthalpies of the individual reactions into which the reaction may be divided

$$\text{at constant } T, \Delta G = \Delta H - T\Delta S$$

$$RT\ln K = -\Delta G$$

$$K = \frac{\prod_{products}(a_i^{\nu_i})}{\prod_{reactants}(a_i^{\nu_i})}$$

Tabulated thermodynamic quantities.
1. Standard enthalpy of formation

Standard enthalpy change of formation, $\Delta_f H^\ominus$

The standard enthalpy change when 1 mol of a substance is formed from its elements in their reference states, at a stated temperature (usually 298 K). The reference state is the most stable state at that temperature, and at a pressure of 1 bar.

e.g. $C(s) + 2H_2(g) \rightarrow CH_4(g) \quad \Delta_f H^\ominus = -74.8$ kJ mol^{-1}

The standard enthalpies of formation of $C(s)$ and $H_2(g)$ are both zero

The reference state for carbon is graphite.

Standard entropy

Standard entropy

Based on the 3rd law of Thermodynamics:

The entropy of any perfectly crystalline material at $T = 0$ is zero

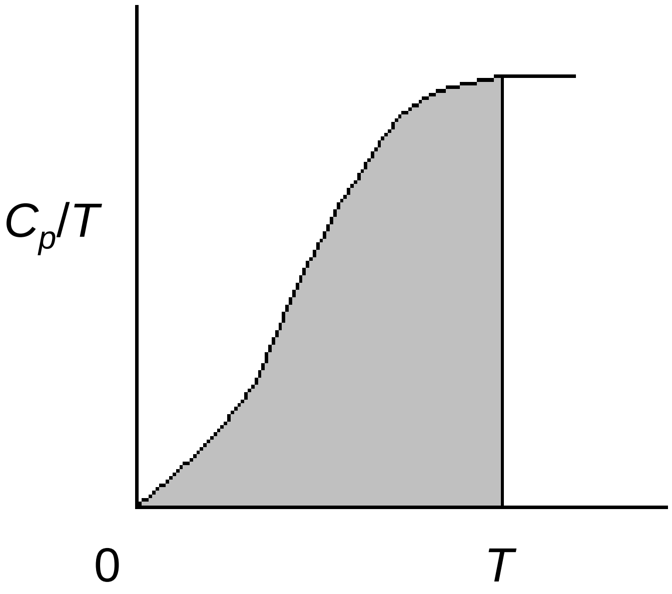

NB – calculation using statistical mechanics – next slide

Standard molar entropy, $S^\ominus_m$

The entropy of 1 mol of a substance in its standard state based on the 3rd law

Sometimes entropies of formation are used, but this makes no difference to entropies of reaction provided consistency is maintained

Molecular partition functions: rigid rotor harmonic oscillator (RRHO) – a reminder

$$q_{total} = q_{trans} q_{rot} q_{vib} q_{elect}$$

$$q_{trans} = \left[\frac{2\pi mkT}{h^2}\right]^{3/2} V$$

$$Q = q/V$$

$$q_{rot} = \frac{kT}{\sigma hBc}$$

$$q_{rot} = \frac{\sqrt{\pi}}{\sigma}\left\{\frac{(\frac{kT}{hc})^3}{ABC}\right\}^{1/2}$$

$$q_{vib} = (1 - e^{-\frac{hc\omega}{kT}})^{-1}$$

$$q_{vib} = \prod_{i=1}^{\alpha}(1 - e^{-\frac{hc\omega_i}{kT}})^{-1}$$

$$q_{elect} = \sum_{levels,i} g_i\, e^{-\beta\epsilon_i}$$

These expressions allow thermodynamic data to be calculated from spectroscopic data and from electronic structure calculations

Thermodynamic quantities from partition functions

$$U = U(0) - N\left(\frac{\partial \ln q}{\partial \beta}\right)_V = U(0) + NkT^2\left(\frac{\partial \ln q}{\partial T}\right)_V$$

$$\beta = \frac{1}{kT} \qquad U(0) = N_A\,\varepsilon_0$$

$$S = \frac{U - U(0)}{T} + R\ln q - R\ln N_A + R$$

$$C_V = \left(\frac{\partial U}{\partial T}\right)_V \;;\; C_p = \left(\frac{\partial H}{\partial T}\right)_p \; C_p$$

$$= C_V + R \;\; (\text{ideal gas})$$

Thermodynamic and spectroscopic data from NIST

- http://webbook.nist.gov/chemistry/
- E.g. Methane, gas phase. Selected thermodynamic data, infra-red spectra, vibrational and electronic energy levels

Quantity	**Value**	**Units**	**Method**	**Reference**
$\Delta_f H^\ominus$	-74.87	kJ mol^{-1}	Review	Chase 1998
$\Delta_f H^\ominus$	-74.6±0.3	kJ mol^{-1}	Review	Manion
$S^\ominus$	188.66±0.42	J mol^{-1} K^{-1}	N/A	Colwell 1963

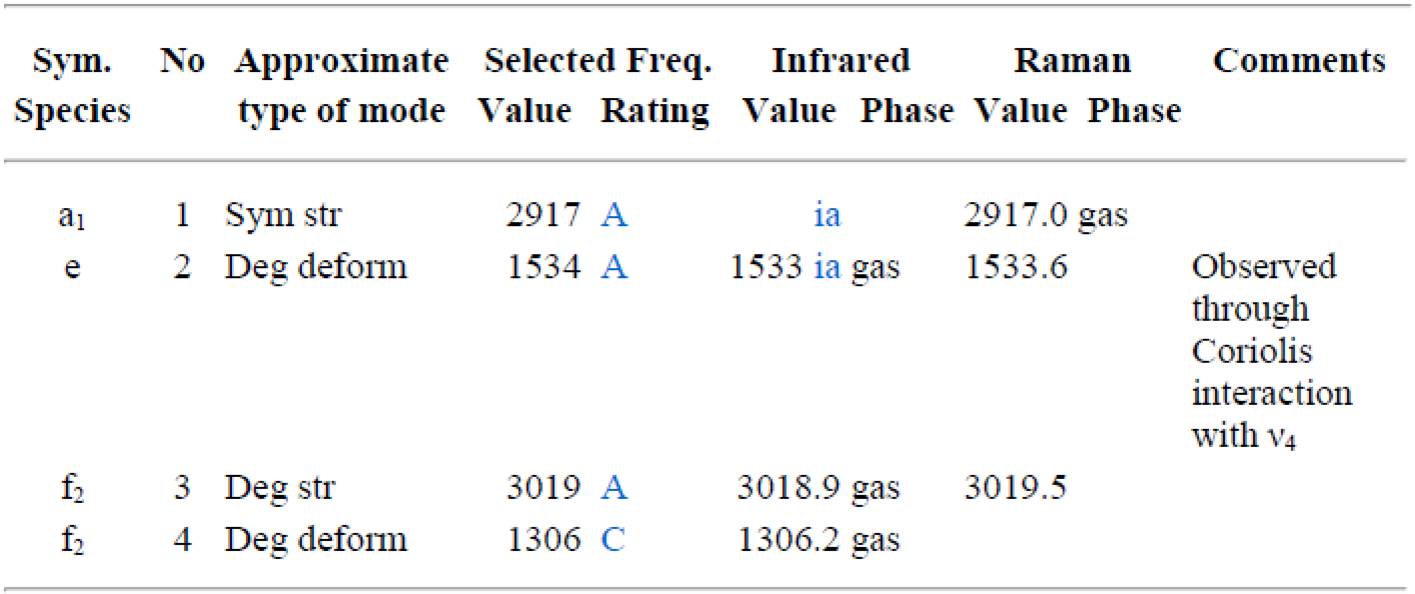

Sym. Species	No	Approximate type of mode	Selected Freq.		Infrared		Raman		Comments
			Value	Rating	Value	Phase	Value	Phase	
a_1	1	Sym str	2917	A	ia		2917.0	gas	
e	2	Deg deform	1534	A	1533 ia	gas	1533.6		Observed through Coriolis interaction with ν_4
f_2	3	Deg str	3019	A	3018.9	gas	3019.5		
f_2	4	Deg deform	1306	C	1306.2	gas			

Computational Chemistry Comparison and Benchmark DataBase - http://cccbdb.nist.gov/

- The CCCBDB contains links to experimental and computational thermochemical data for a large selected set of **gas-phase** atoms and molecules. Tools for comparing experimental and computational ideal-gas thermochemical properties
- **Species in the CCCBDB**
  - Mostly compounds with atoms with atomic number less than 18 (Argon). A few have Se or Br.
  - Six or fewer heavy atoms and twenty or fewer total atoms. *Exception:* Versions 8 and higher have a few substituted benzenes with more than six heavy atoms. Versions 12 and higher have bromine-containing molecules.
- Specific experimental properties 1. Atomization energies 2. Vibrational frequencies 3. Bond lengths 4. Bond angles 5. Rotational constants 6. Experimental barriers to internal rotation

Computed data

- Geometries, vibrational frequencies, entropies, energies, means for comparing data

CH_3

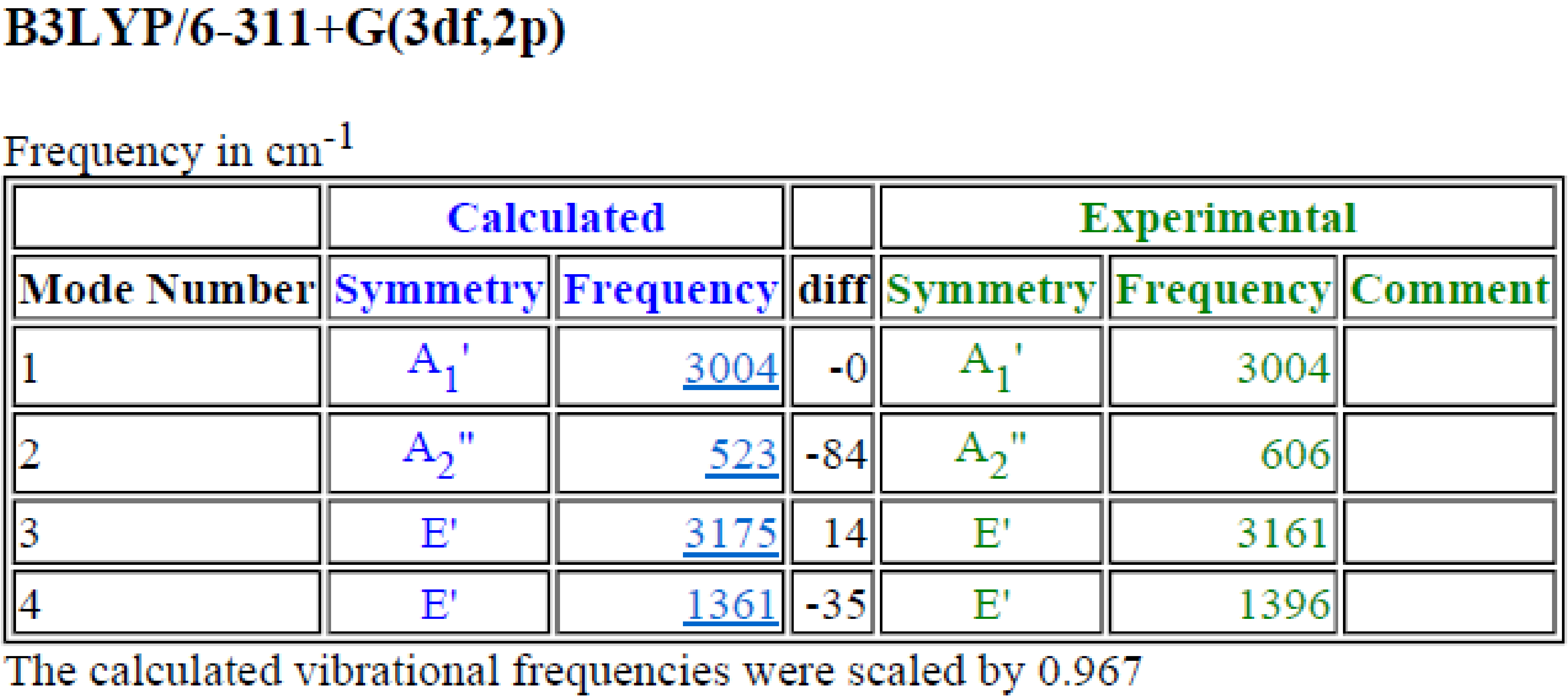

B3LYP/6-311+G(3df,2p)

Frequency in cm^{-1}

	Calculated			Experimental		
Mode Number	**Symmetry**	**Frequency**	**diff**	**Symmetry**	**Frequency**	**Comment**
1	A_1'	3004	-0	A_1'	3004	
2	A_2''	523	-84	A_2''	606	
3	E'	3175	14	E'	3161	
4	E'	1361	-35	E'	1396	

The calculated vibrational frequencies were scaled by 0.967

Methane

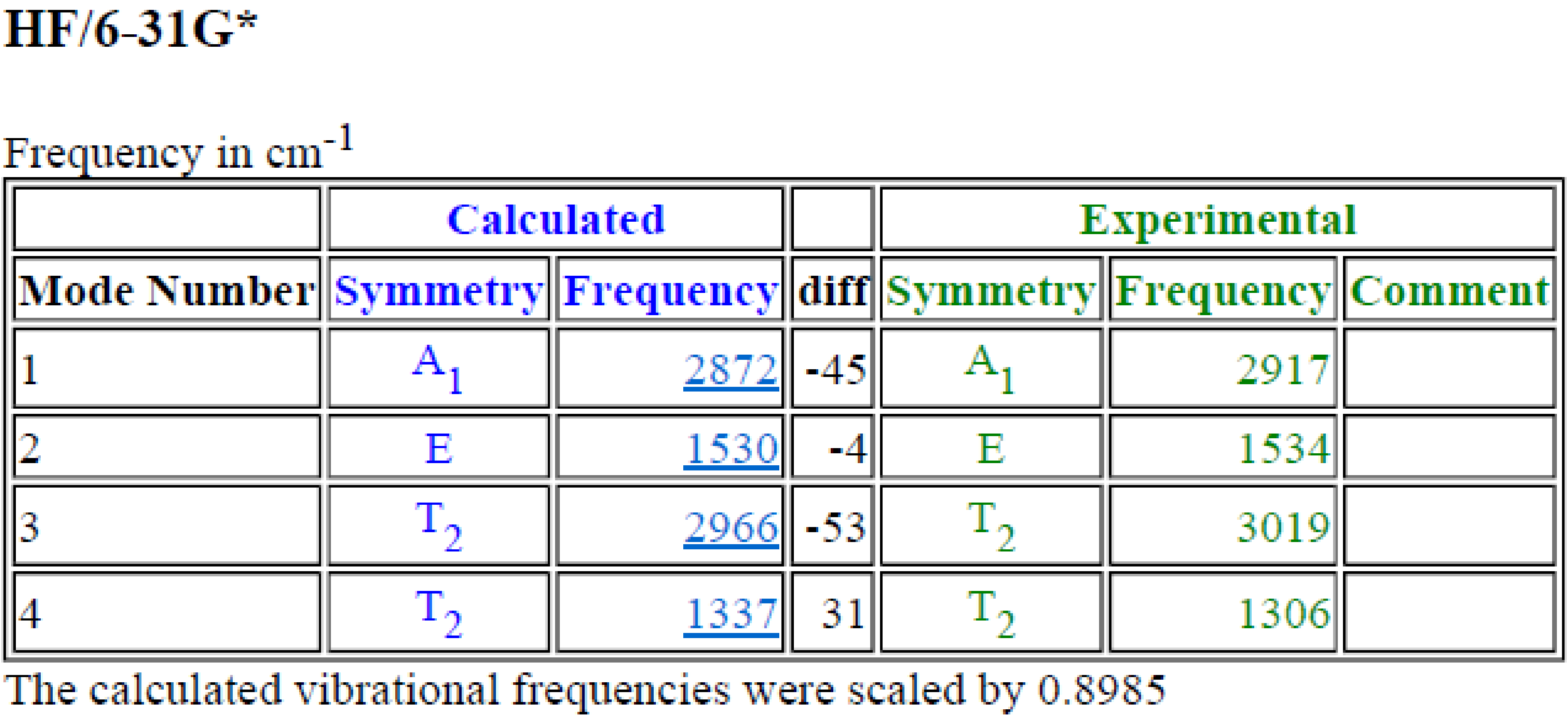

HF/6-31G*

Frequency in cm^{-1}

	Calculated			Experimental		
Mode Number	**Symmetry**	**Frequency**	**diff**	**Symmetry**	**Frequency**	**Comment**
1	A_1	2872	-45	A_1	2917	
2	E	1530	-4	E	1534	
3	T_2	2966	-53	T_2	3019	
4	T_2	1337	31	T_2	1306	

The calculated vibrational frequencies were scaled by 0.8985

Enthalpies of formation of radicals

- Enthalpies of formation of stable compounds, such as hydrocarbons, are determined from measurements of enthalpies of combustion, using Hess's Law.
- This approach is not feasible for radicals. An IUPAC evaluation of thermodynamic data for radicals can be found in Ruscic et al

  J Phys Chem Ref Data, 2005, 34, 573.
- Example: CH_3. Determined by:
  - Kinetics, e.g. J Am Chem Soc, 1990, 112, 1347
  - Photionization spectroscopy, e.g. J Chem Phys, 1997, 107, 9852
  - Electronic structure calculations, e.g. J Chem Phys, 2001, 114, 6014
- Recommended value by IUPAC: $\Delta_f H^{\ominus}(298.15\ \mathrm{K}) = 146.7 \pm 0.3\ \mathrm{kJ\ mol^{-1}}$

Kinetics and thermodynamics of alkyl radicals

Seetula et al. J Am Chem Soc, 1990, 112, 1347

- Measured *k*(*T*) for R + HI, using laser flash photolysis / photoionization mass spectrometry, and combined with existing data for reverse reaction (I + RH) to determine equilibrium constant. Enthalpy of reaction determined by second and third law methods

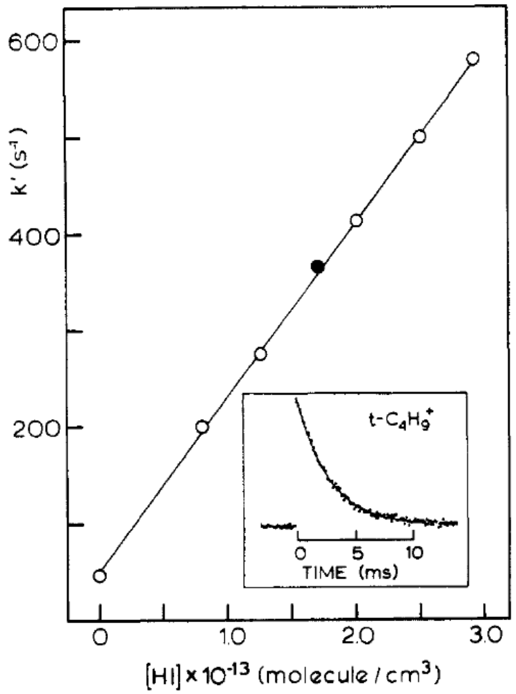

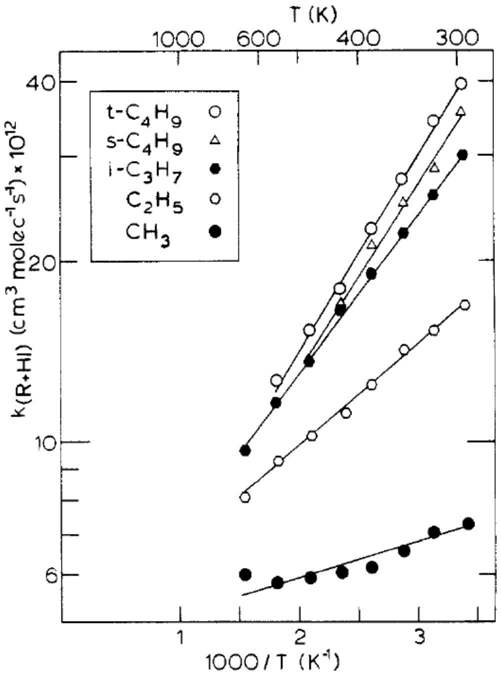

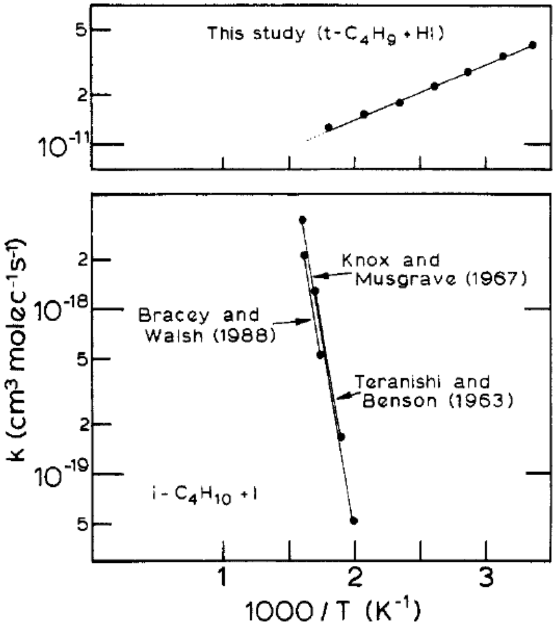

Direct measurement of equilibrium constant for reactions involving radicals: $H + C_2H_4 \rightleftharpoons C_2H_5$

- Brouard et al. J. Phys. Chem. 1986, 90,445-450
- Laser flash photolysis, H atom resonance fluorescence.
- Reactions involved:

$H + C_2H_4 \rightarrow C_2H_5$ k_1

$C_2H_5 \rightarrow H + C_2H_4$ k_{-1}

$H \rightarrow$ diffusive loss k_d

- Solve rate equations – gives bi-exponential decay of H, k_1 and k_{-1} and hence K_1 from analysis. Vary T, enthalpy of reaction from second or third law.

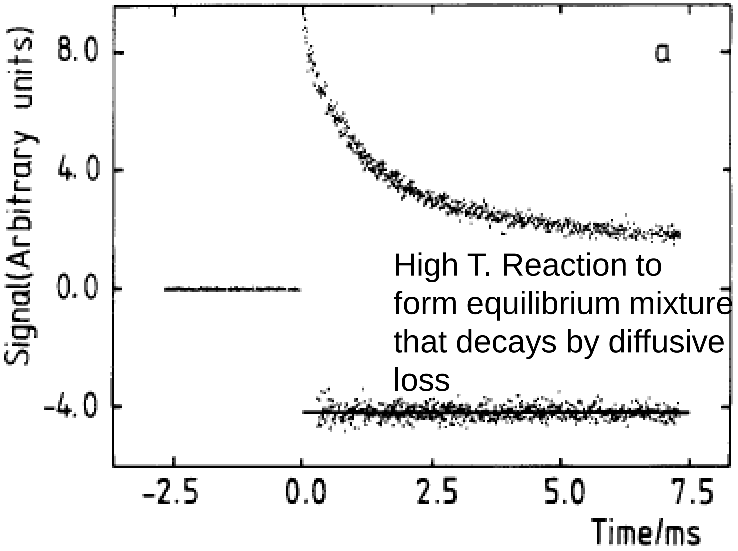

High T. Reaction to form equilibrium mixture that decays by diffusive loss

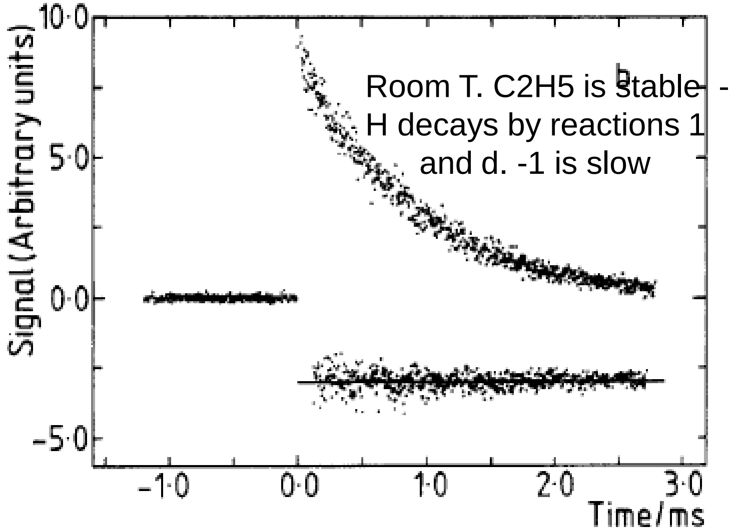

Room T. C2H5 is stable - H decays by reactions 1 and d. -1 is slow

Photoionization spectrum of CH_3
Litorja and Ruscic, J Chem Phys, 1997, 107, 9852

- Mesaure the photionization threshold for CH_3 and the appearance potential of CH_{3+} from CH_4 photexcitation. Obtain the dissociation energy of CH_3-H:

$$CH_3 \rightarrow CH_3^+ + e \qquad R1$$

$$CH_4 \rightarrow CH_3^+ + H + e \qquad R2$$

R2-R1: $$CH_4 \rightarrow CH_3 + H$$

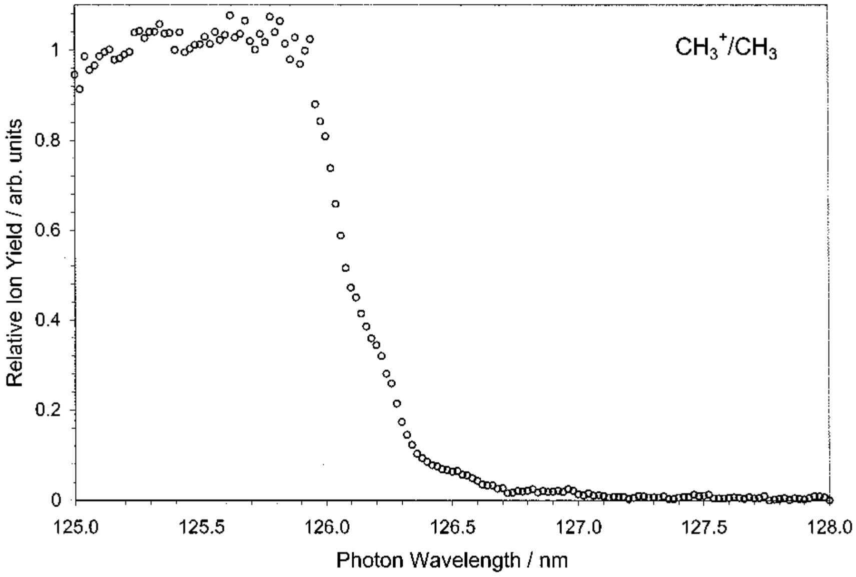

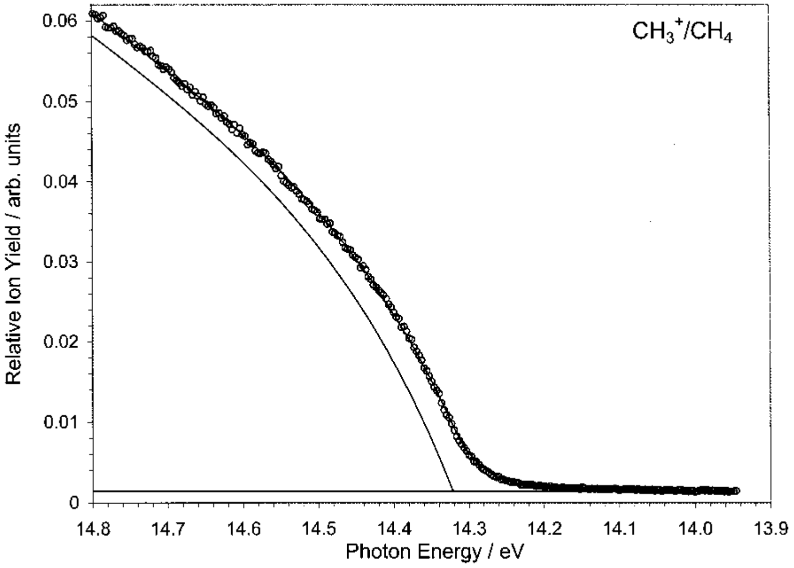

R-H bond energies: Extensive tabulation and review Berkowitz et al. 1994, **98**, 2744

- The bond enthalpy change at 298 K is the enthalpy change for the reaction R-H → R + H:

$$DH_{298}(\mathrm{R-H}) = \Delta_f H_{298}(\mathrm{R}) + \Delta_f H_{298}(\mathrm{H}) - \Delta_f H_{298}(\mathrm{RH})$$

- The bond energy (change) or dissociation energy at zero K is:

$$D_0(\mathrm{R-H}) = E_0(\mathrm{R}) + E_0(\mathrm{H}) - E_0(\mathrm{RH})$$

- Bond energies can be converted to bond enthalpy changes using the relation $U = H + pV = H + RT$, so that, for R-H → R + H,

  $\Delta U = \Delta H + RT$. At zero K, the dissociation energy is equal to the bond enthalpy change.

- Berkowitz et al provide an extensive dataset for R-H bond energies using radical kinetics, gas-phase acidity cycles, and photoionization mass spectrometry

Thermodynamic databases

- Active, internally consistent thermodynamic databases:
  - ATcT Active thermochemical tables. Uses and network approach. Ruscic et al. J. Phys. Chem. A 2004, 108, 9979-9997.
  - NEAT . Network of atom based thermochemistry. Csaszar and Furtenbacher: Chemistry – A european journal, 2010,16, 4826

Active Thermochemical Tables

https://atct.anl.gov/

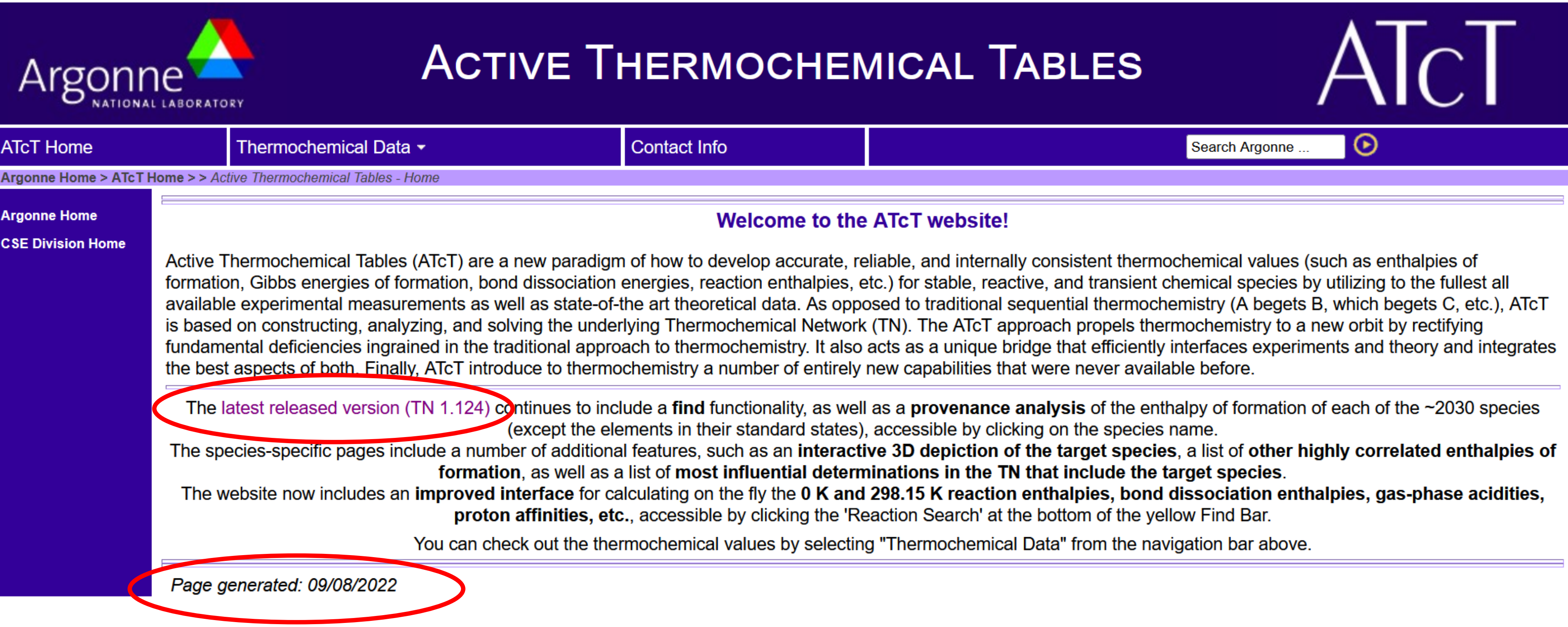

Welcome to the ATcT website!

Active Thermochemical Tables (ATcT) are a new paradigm of how to develop accurate, reliable, and internally consistent thermochemical values (such as enthalpies of formation, Gibbs energies of formation, bond dissociation energies, reaction enthalpies, etc.) for stable, reactive, and transient chemical species by utilizing to the fullest all available experimental measurements as well as state-of-the art theoretical data. As opposed to traditional sequential thermochemistry (A begets B, which begets C, etc.), ATcT is based on constructing, analyzing, and solving the underlying Thermochemical Network (TN). The ATcT approach propels thermochemistry to a new orbit by rectifying fundamental deficiencies ingrained in the traditional approach to thermochemistry. It also acts as a unique bridge that efficiently interfaces experiments and theory and integrates the best aspects of both. Finally, ATcT introduce to thermochemistry a number of entirely new capabilities that were never available before.

The latest released version (TN 1.124) continues to include a **find** functionality, as well as a **provenance analysis** of the enthalpy of formation of each of the ~2030 species (except the elements in their standard states), accessible by clicking on the species name.

The species-specific pages include a number of additional features, such as an **interactive 3D depiction of the target species**, a list of **other highly correlated enthalpies of formation**, as well as a list of **most influential determinations in the TN that include the target species**.

The website now includes an **improved interface** for calculating on the fly the **0 K and 298.15 K reaction enthalpies, bond dissociation enthalpies, gas-phase acidities, proton affinities, etc.**, accessible by clicking the 'Reaction Search' at the bottom of the yellow Find Bar.

You can check out the thermochemical values by selecting "Thermochemical Data" from the navigation bar above.

Page generated: 09/08/2022

A Grid Service-Based Active Thermochemical Table Framework von Laszewski et al.

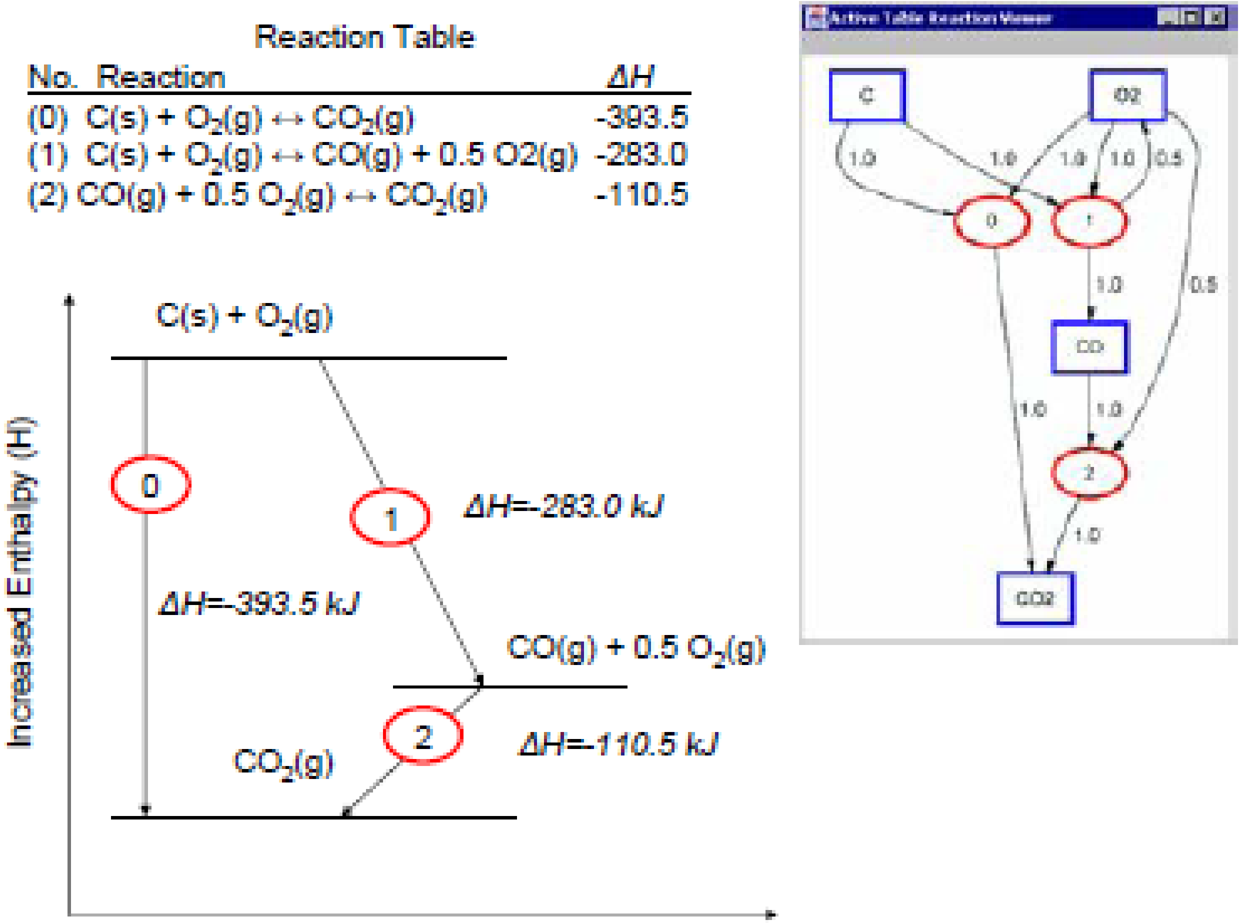

Reaction Table

No.	Reaction	ΔH
(0)	$C(s) + O_2(g) \leftrightarrow CO_2(g)$	-393.5
(1)	$C(s) + O_2(g) \leftrightarrow CO(g) + 0.5\ O2(g)$	-283.0
(2)	$CO(g) + 0.5\ O_2(g) \leftrightarrow CO_2(g)$	-110.5

Fig. 1. Enthalpy diagrams and thermochemical reaction tables.

An Part of a thermochemical network showing the basic ideas

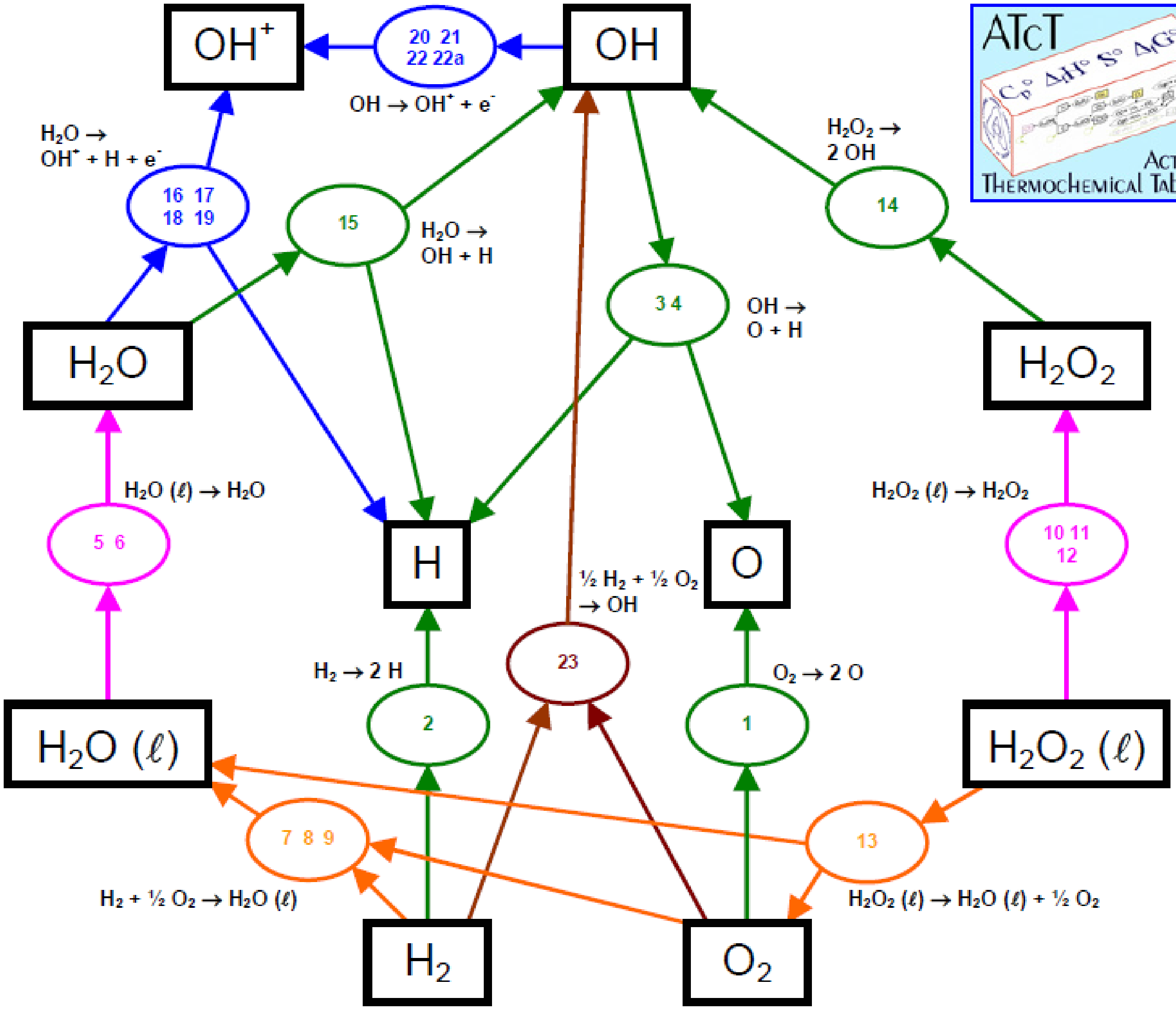

Figure 1. A small subsection of the current Core (Argonne) Thermochemical Network. The full network currently contains >600 primary vertices and >3200 secondary vertices. See text for further details

ATcT C_p° ΔH° S° ΔG° Active Thermochemical Tables

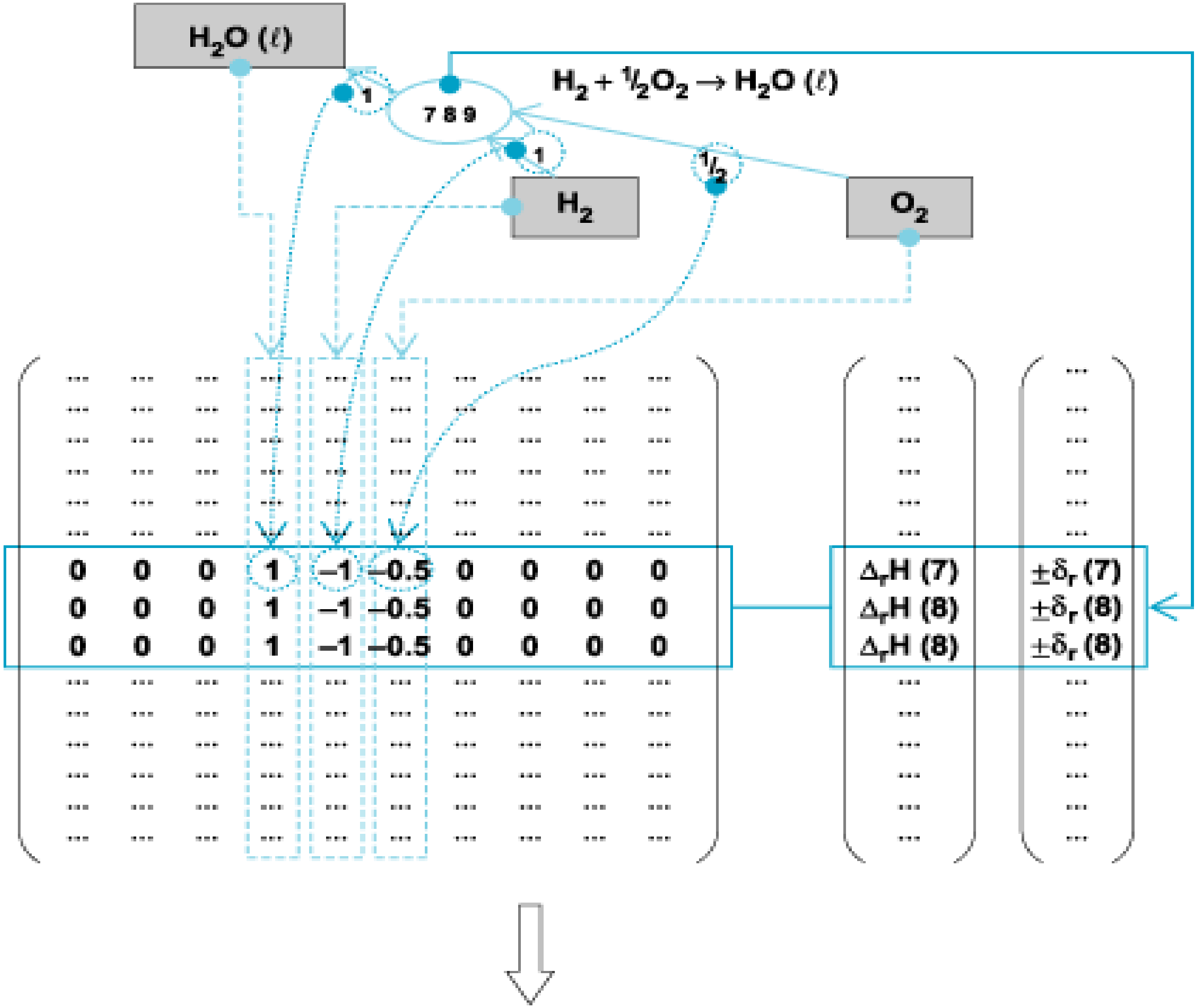

...

Eq. (7): $\Delta_f H(\mathrm{H_2O} <\ell>) - \Delta_f H(\mathrm{H_2}) - 0.5\ \Delta_f H(\mathrm{O_2}) = \Delta_r H\ (7) \pm \delta_r\ (7)$

Eq. (8): $\Delta_f H(\mathrm{H_2O} <\ell>) - \Delta_f H(\mathrm{H_2}) - 0.5\ \Delta_f H(\mathrm{O_2}) = \Delta_r H\ (8) \pm \delta_r\ (8)$

Eq. (9): $\Delta_f H(\mathrm{H_2O} <\ell>) - \Delta_f H(\mathrm{H_2}) - 0.5\ \Delta_f H(\mathrm{O_2}) = \Delta_r H\ (9) \pm \delta_r\ (9)$

...

Evidence for a Lower Enthalpy of Formation of Hydroxyl Radical

Ruscic et al. J Phys Chem, 2001, 105, 1

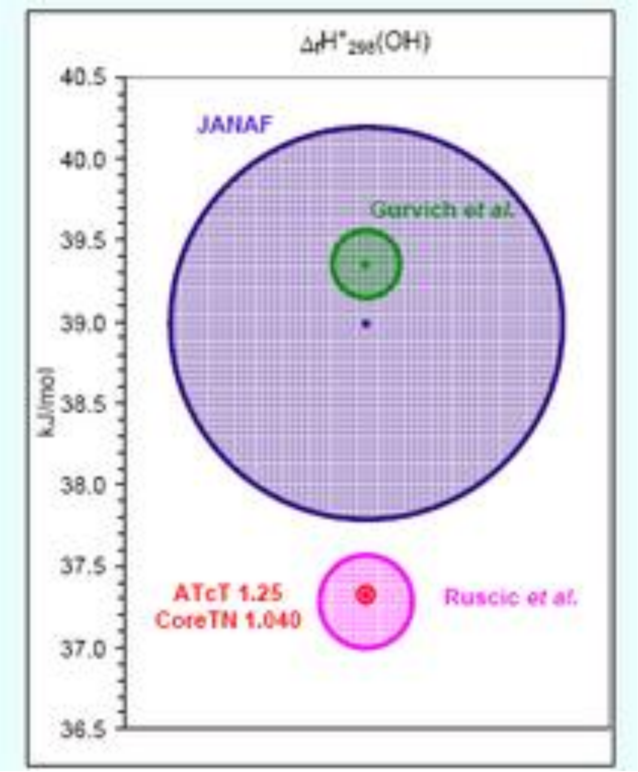

Note that these are values at 0 K
Current ATcT value is
8.904 ± 0.006 kcal mol^{-1}

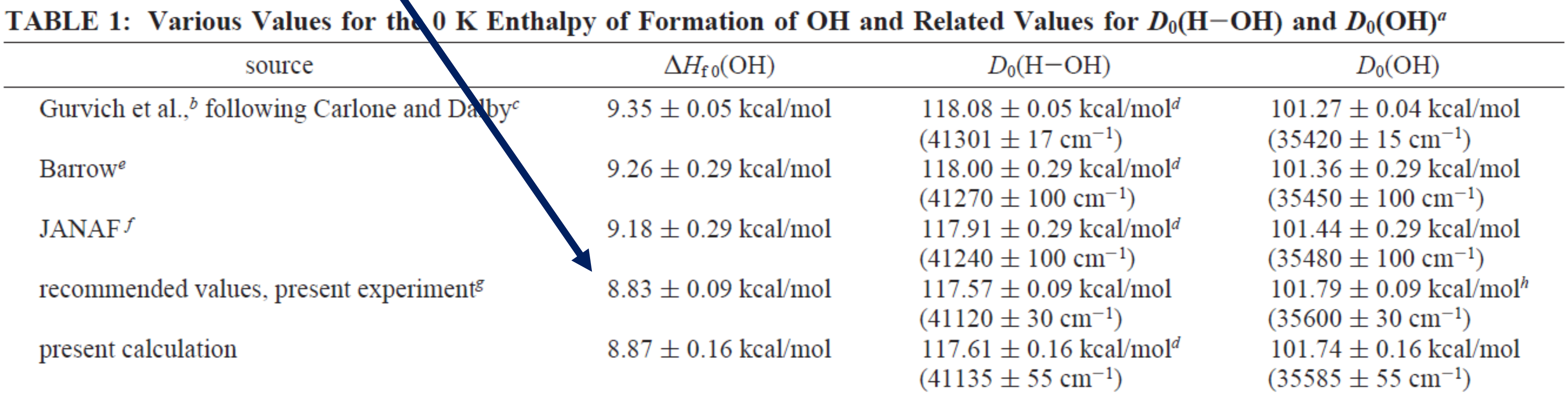

TABLE 1: Various Values for the 0 K Enthalpy of Formation of OH and Related Values for D_0(H−OH) and D_0(OH)[a]

source	$\Delta H_{f\,0}$(OH)	D_0(H−OH)	D_0(OH)
Gurvich et al.,[b] following Carlone and Dalby[c]	9.35 ± 0.05 kcal/mol	118.08 ± 0.05 kcal/mol[d] (41301 ± 17 cm^{-1})	101.27 ± 0.04 kcal/mol (35420 ± 15 cm^{-1})
Barrow[e]	9.26 ± 0.29 kcal/mol	118.00 ± 0.29 kcal/mol[d] (41270 ± 100 cm^{-1})	101.36 ± 0.29 kcal/mol (35450 ± 100 cm^{-1})
JANAF[f]	9.18 ± 0.29 kcal/mol	117.91 ± 0.29 kcal/mol[d] (41240 ± 100 cm^{-1})	101.44 ± 0.29 kcal/mol (35480 ± 100 cm^{-1})
recommended values, present experiment[g]	8.83 ± 0.09 kcal/mol	117.57 ± 0.09 kcal/mol (41120 ± 30 cm^{-1})	101.79 ± 0.09 kcal/mol[h] (35600 ± 30 cm^{-1})
present calculation	8.87 ± 0.16 kcal/mol	117.61 ± 0.16 kcal/mol[d] (41135 ± 55 cm^{-1})	101.74 ± 0.16 kcal/mol (35585 ± 55 cm^{-1})

Example 1: CH_3

Formula	$\Delta_f H^\circ$(0 K)	$\Delta_f H^\circ$(298K)	Uncertainty	Units
CH_3(g)	149.788	146.374	± 0.08	kJ mol^{-1}

95% uncertainty limits

- **Top contributors to the provenance of $\Delta_f H^\circ$ of CH_3 (g):** The top **20** contributors account only for **72.5%** of the provenance of $\Delta_f H^\circ$ of CH_3 (g). A total of **99** contributors would be needed to account for **90%** of the provenance.
- Link to latest version of ATcT: https://atct.anl.gov/Thermochemical%20Data/version%201.122/index.php

Provenance of ATcT determination of the enthalpy of formation of ethyl

Formula	$\Delta_f H^\ominus$(0 K)	$\Delta_f H^\ominus$(298K)	Uncertainty	Units
C_2H_5(g)	131.38	120.63	± 0.22	kJ mol^{-1}

Top 5 contributors to the provenance – contribution from these 5 =27.5%

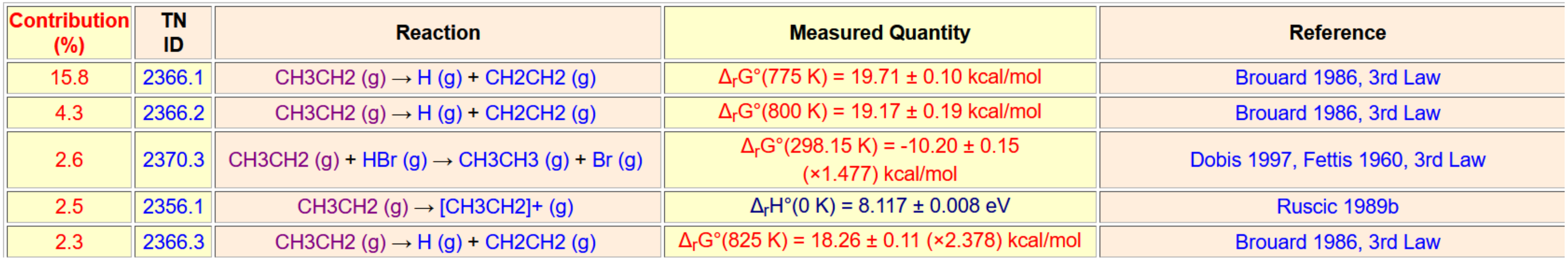

Contribution (%)	TN ID	Reaction	Measured Quantity	Reference
15.8	2366.1	CH3CH2 (g) → H (g) + CH2CH2 (g)	$\Delta_r G°$(775 K) = 19.71 ± 0.10 kcal/mol	Brouard 1986, 3rd Law
4.3	2366.2	CH3CH2 (g) → H (g) + CH2CH2 (g)	$\Delta_r G°$(800 K) = 19.17 ± 0.19 kcal/mol	Brouard 1986, 3rd Law
2.6	2370.3	CH3CH2 (g) + HBr (g) → CH3CH3 (g) + Br (g)	$\Delta_r G°$(298.15 K) = -10.20 ± 0.15 (×1.477) kcal/mol	Dobis 1997, Fettis 1960, 3rd Law
2.5	2356.1	CH3CH2 (g) → [CH3CH2]+ (g)	$\Delta_r H°$(0 K) = 8.117 ± 0.008 eV	Ruscic 1989b
2.3	2366.3	CH3CH2 (g) → H (g) + CH2CH2 (g)	$\Delta_r G°$(825 K) = 18.26 ± 0.11 (×2.378) kcal/mol	Brouard 1986, 3rd Law

The Brouard measurements determined the forward and reverse rate constants and hence *K*. ATcT used high level entropy calculations to determine $\Delta_r S$ and hence $\Delta_r H$ from $\Delta_r G$. These 3 single temperature determinations contribute over 20% Of the total provenance

Enthalpy of formation for ethyl from analysis of forward and reverse kinetic data for $H + C_2H_4 \rightleftarrows C_2H_5$

- The Brouard measurements were made under equilibrating conditions, which can only be done over a very narrow temperature range.
- Many forward and reverse rate constant measurements have been made under irreversible conditions, over a very wide range of *T*. However, the reaction is pressure dependent and the forward and reverse rate constants cannot be directly used to calculate *K*.
- Problem can be overcome using a master equation method to analyse the experimental data globally. Data available:
- 16 independent experimental studies.
- 7 sets of measurements of the addition rate constant, covering the temperature range 198 – 604 K, mainly in a He diluent, but also studies in other bath gases. Range of diluent concentrations, [M] = 0.1 – 200x10^{17} molecule cm^{-3}.
- 6 sets of measurements of the dissociation rate constant, covering the temperature range 670 – 1094 K, in He and C_2H_6 [M] = 0.7 – 100x10^{17} molecule cm^{-3}.
- Three sets of measurements under equilibration conditions, giving forward and reverse rate constants. Temperatures 775 – 828 K in He ([He] = 12 – 72 x10^{17} molecule cm^{-3}.

Approach

- Use density functional and ab initio calculations to locate and refine energies of transition state and of reaction.
- Determine vibrational frequencies and rotational constants for transition state and for C_2H_5 – needed for $k(E), \Delta_r S_T^{\ominus}$ and ΔC_p
- Key issue – internal rotation and inversion modes in C_2H_5.
- Include tunnelling via Eckart model with imaginary frequency, ν_i
- Calculate microcanonical rate constants for dissociation

$$k(E) = \frac{hW^{\ddagger}(E)}{N(E)}$$

where $W^{\ddagger}(E)$ is the sum of states at the transition state, from energy zero at the TS to E and $N(E)$ is the density of states at energy E for C_2H_5

- Parameterise energy transfer via $\langle \Delta E \rangle_d = \langle \Delta E \rangle_{d,298} (T/298)^n$
- Fit experimental data by minimising χ^2, with $\Delta_r H_0^{\ominus}$, ΔE_a, ν_i, $\langle \Delta E \rangle_{d,298}$ and n as variable parameters, using Levenberg – Marquardt algorithm. $\chi^2 = \sum_1^N (k_{i,expt} - k_{i,model})^2 / \sigma_i^2$. Theoretical values used as input for $\Delta_r H_0^{\ominus}$, ΔE_a, ν_i
- Use the MESMER master equation code (J. Phys. Chem. A 2012, 116, 9545–9560)

Enthalpy of formation for ethyl

The fitting gives: $\Delta_r H_0^\ominus$ = -145.34 ± 0.56 kJ mol^{-1}

The enthalpy of reaction can then be used to calculate the enthalpy of formation of ethyl.

$$\Delta_r H_0^\ominus = \sum \nu_m \Delta_f H_{m,0}^\ominus = \Delta_f H_0^\ominus(C_2H_5) - \Delta_f H_0^\ominus(H) - \Delta_f H_0^\ominus(C_2H_4)$$

From ATcT,

$\Delta_f H_0^\ominus$(H) = 216.034 ±0.000 kJ mol^{-1};

$\Delta_f H_0^\ominus(C_2H_4)$ = 60.87 ±0.12 kJ mol^{-1};

Giving $\Delta_f H_0^\ominus(C_2H_5)$ = 131.57 ± 0.57 kJ mol-1

Compare with ATcT $\Delta_f H_0^\ominus(C_2H_5)$ = 131.38 ± 0.22 kJ mol-1

Uncertainties are 2σ

Blitz et al, *J. Phys. Chem. A* 2021, 125, 9548–9565

Ab Initio Computations and Active Thermochemical Tables Hand in Hand: Heats of Formation of Core Combustion Species

Klippenstein, Harding, Ruscic, J. Phys. Chem. A 2017, 121, 6580–6602

- High level ab initio electronic structure based predictions of $\Delta_f H^o(0\ K)$ for 348 C, N, O, and H containing species - essentially all core combustion species with 34 or fewer electrons.

- The accuracy of the theoretical predictions is explored through (i) examination of the magnitudes of the various corrections,
  (ii) comparisons with other high level calculations, and
  (iii)through comparison with the ATcT values.

- Inclusion of these theoretical results into the ATcT thermochemical network is expected to significantly improve the thermochemical knowledge base for less-well studied species

RESPECTH

Reaction Kinetics, Spectroscopy, Thermodynamics database

- http://respecth.chem.elte.hu/respecth/

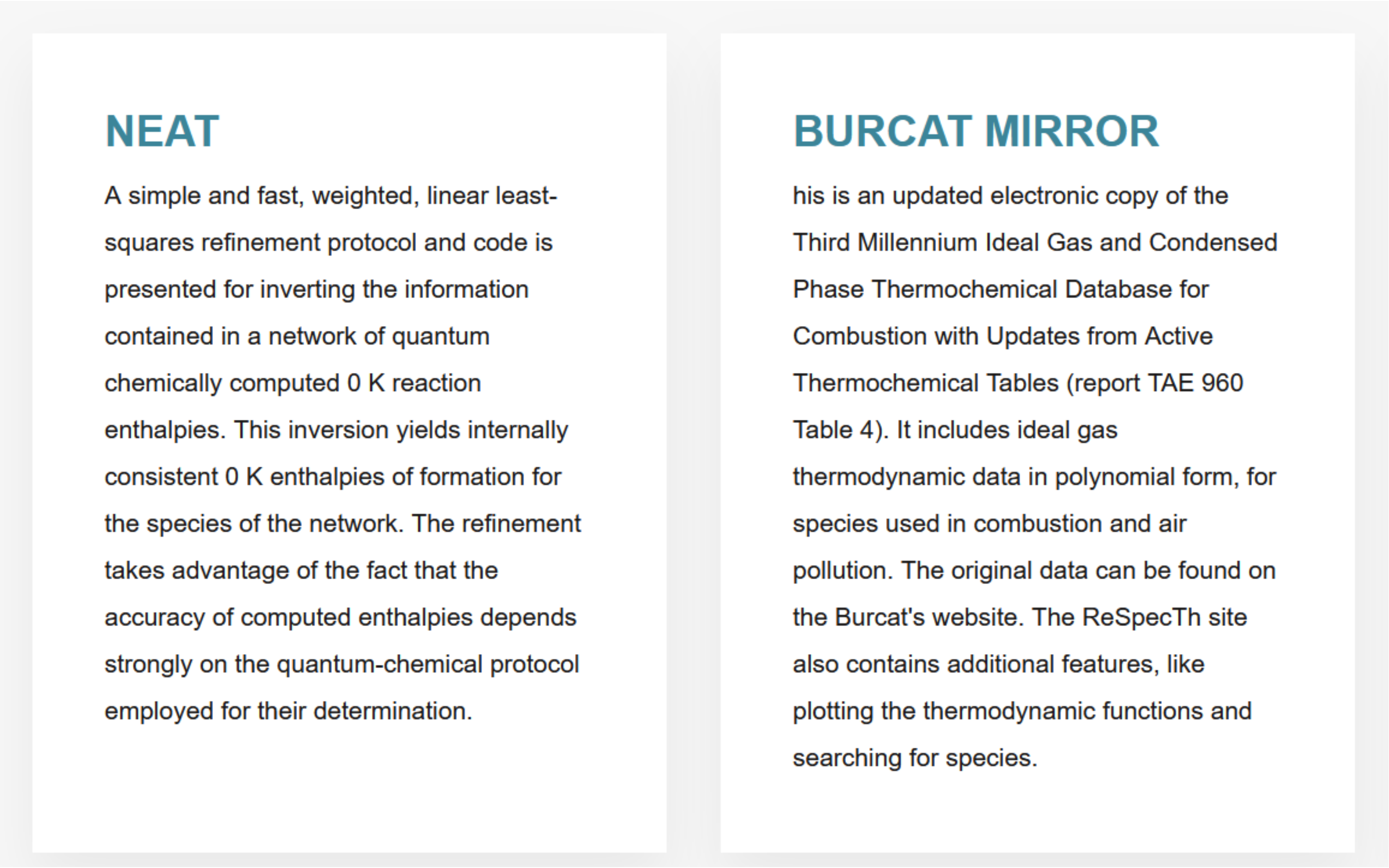

NEAT

A simple and fast, weighted, linear least-squares refinement protocol and code is presented for inverting the information contained in a network of quantum chemically computed 0 K reaction enthalpies. This inversion yields internally consistent 0 K enthalpies of formation for the species of the network. The refinement takes advantage of the fact that the accuracy of computed enthalpies depends strongly on the quantum-chemical protocol employed for their determination.

BURCAT MIRROR

his is an updated electronic copy of the Third Millennium Ideal Gas and Condensed Phase Thermochemical Database for Combustion with Updates from Active Thermochemical Tables (report TAE 960 Table 4). It includes ideal gas thermodynamic data in polynomial form, for species used in combustion and air pollution. The original data can be found on the Burcat's website. The ReSpecTh site also contains additional features, like plotting the thermodynamic functions and searching for species.

From a Network of Computed Reaction Enthalpies to Atom-Based Thermochemistry (NEAT)

A. G. Csaszar and T. Furtenbacher,

Chemistry – A european journal, 2010,16, 4826

Abstract: A simple and fast, weighted, linear least-squares refinement protocol and code is presented for inverting the information contained in a network of quantum chemically computed 0 K reaction enthalpies. This inversion yields internally consistent 0 K enthalpies of formation for the species of the network.

Incorporation of thermodynamics data into rate calculations:
Burcat: see RESPECTH website, also http://garfield.chem.elte.hu/Burcat/burcat.html

- Provides data in NASA polynomial form, with 7 parameters that are related to necessary thermodynamic functions of state via:

Cp/R = a1 + a2 T + a3 T^2 + a4 T^3 + a5 T^4

H/RT = a1 + a2 T /2 + a3 T^2 /3 + a4 T^3 /4 +
a5 T^4 /5 + a6/T

S/R = a1 lnT + a2 T + a3 T^2 /2 + a4 T^3 /3 +
a5 T^4 /4 + a7

Where H(T) = $\Delta H_f(298)$ + [H(T) - H(298)]

- Linked to ATcT and used in Chemkin.

Burcat database. Entry for CH_3

- CH3 METHYL-RAD STATWT=1. SIGMA=6. IA=IB=.2923 IC=.5846 NU=3004,606.4,3161(2), 1396(2) HF298=146.7 +/-0.3 KJ HF0=150.0+/-0.3 kJ REF= Ruscic et al JPCRD 2003. {HF298=146.5+/-0.08 kJ REF=ATcT C} Max Lst Sq Error Cp @ 6000 K 0.44%. METHYL RADICAL IU0702C 1.H 3. 0. 0.G 200.000 6000.000 B 15.03452
  1
- 0.29781206E+01 0.57978520E-02 -0.19755800E-05 0.30729790E-09 -0.17917416E-13
  2
- 0.16509513E+05 0.47224799E+01 0.36571797E+01 0.21265979E-02 0.54583883E-05
  3
- -0.66181003E-08 0.24657074E-11 0.16422716E+05 0.16735354E+01 0.17643935E+05
  4
- First 7 entries are a1-7 for 1000 – 6000 K. 2nd set are a1-a7 for 200 – 1000 K. Temp ranges specified in line 1

A big data framework to validate thermodynamic data for chemical species

Buerger et al. Combustion and Flame 176 (2017) 584-591

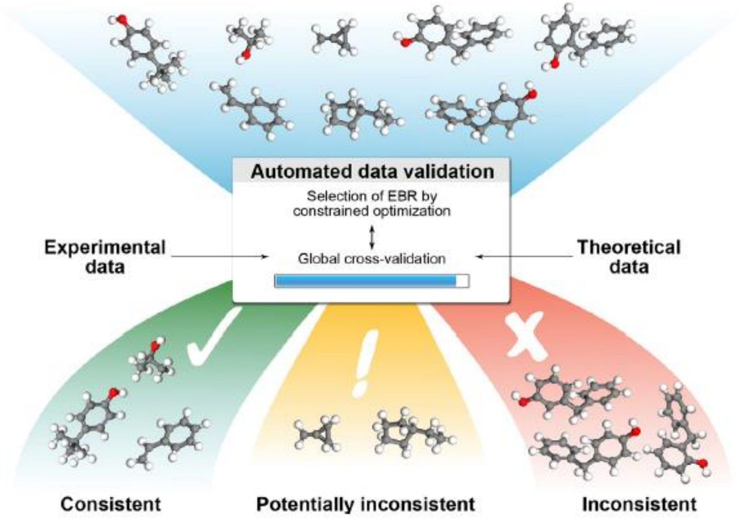

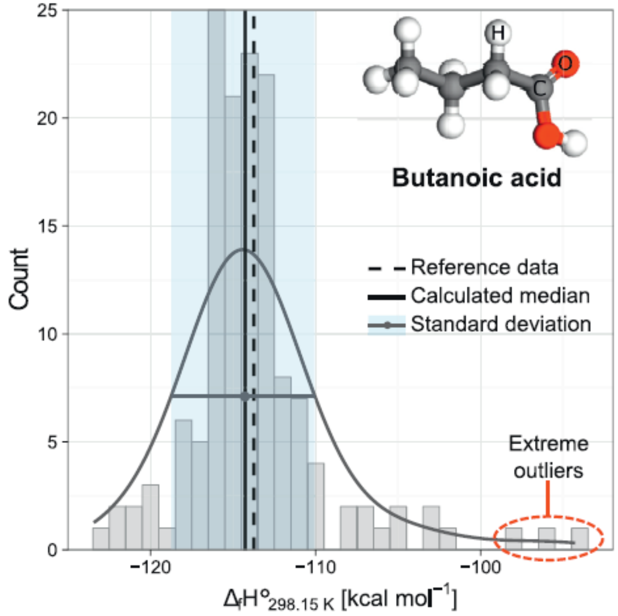

- validate data for the standard enthalpy of formation for 920 gas-phase species containing carbon, oxygen and hydrogen retrieved from the NIST Chemistry WebBook.
- Use error cancelling balanced reactions (specifically isodesmic reactions) to calculate a distribution of possible values for the standard enthalpy of formation of each species.
- method automates the identification and exclusion of inconsistent data
- exploits knowledge of the structural similarities between species and the consistency of the data to identify which species introduce the most error and recommend what future experiments and calculations should be considered

High-Accuracy Heats of Formation for Alkane Oxidation: From Small to Large via the Automated CBH-ANL Method

Elliot et al, J. Phys. Chem. A 2023, 127, 1512–1531

- 94 alkane oxidation species, it can be used to produce ΔHf(0 K) values with 2σ uncertainties of 0.2–0.5 kcal mol−1. This set includes the alkanes, hydroperoxides, and alkyl, peroxy, and hydroperoxyalkyl radicalsfor 17 representative hydrocarbon fuels containing up to 10 heavy atoms with various degrees of branching in the alkane backbone.
- connectivity-based hierarchy (CBH)
- error cancellation in ΔHf(0 K)

Exercise 3

The NASA polynomial coefficients, a1-a5, between 1000 K and 3000 K for N_2 are:

2.952257637E+00 1.39690040E-03 -4.92631603E-07

7.86010195E-11 -4.60755204E-15

Cp/R = a1 + a2 T + a3 T^2 + a4 T^3 + a5 T^4

Calculate the heat capacity over the temperature range 1000 – 3000 K. Calculate the vibrational contribution to the heat capacity given that the translational and rotational contributions are 3R/2 and R respectively. (Remember $C_p=C_v+R$)

Compare these results from those calculated from statistical mechanics. The vibrational heat capacity is given by:

$C_v = R\Omega^2 e^{\Omega}/(e^{\Omega}-1)^2$ where $\Omega = \frac{hc\omega}{kT}$

hc/k = 0.659 cm K; ω (N_2) = 2359 cm^{-1}

Comment on the differences

Reminder

- Look back at slides on Statistical Mechanics:
- Translational partition function $q_{trans} = \left[\frac{2\pi mkT}{h^2}\right]^{3/2} V$
- Rotational partition function $q_{rot} = \frac{kT}{\sigma hBc}$
- Energy $U = U(0) - N\left(\frac{\partial \ln q}{\partial \beta}\right)_V = U(0) - NkT^2\left(\frac{\partial \ln q}{\partial T}\right)_V$
- Heat Capacity $C_V = \left(\frac{\partial U}{\partial T}\right)_V ; C_p = \left(\frac{\partial H}{\partial T}\right)_p$

Topic 5
Sources of rate data

Examination of available rate data from the literature and recommendation of rate parameters over specified temperature range, together with uncertainties.

Compatibility with experimental global observables

1. Evaluation

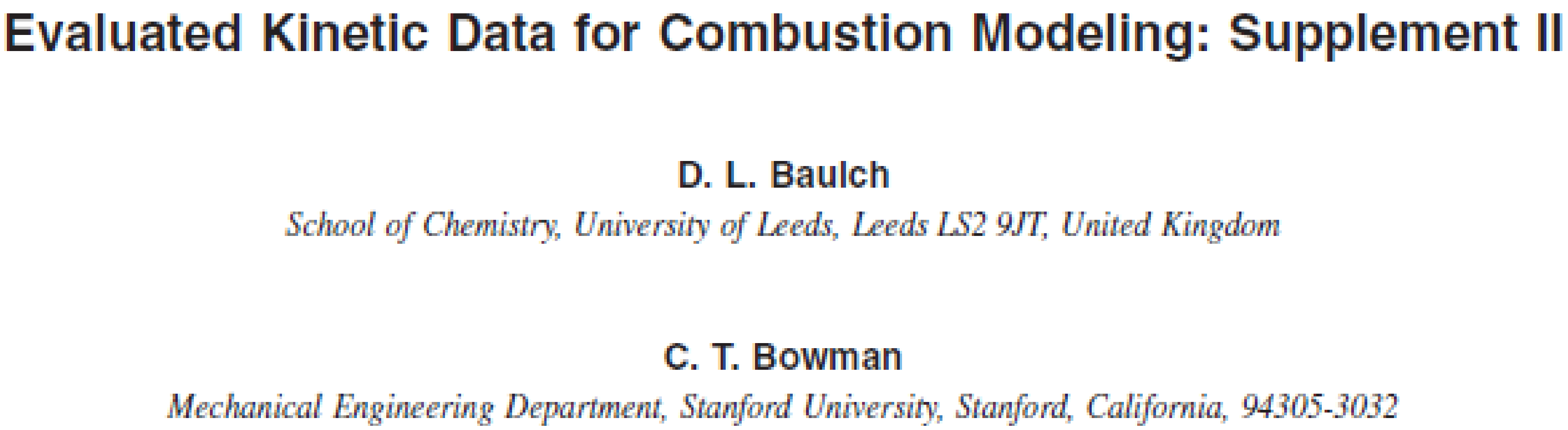

Evaluated Kinetic Data for Combustion Modeling: Supplement II

D. L. Baulch

School of Chemistry, University of Leeds, Leeds LS2 9JT, United Kingdom

C. T. Bowman

Mechanical Engineering Department, Stanford University, Stanford, California, 94305-3032

And ten co-authors

J Phys Chem Ref Data 2005, **34**, No 3.

The next few slides show the structure of a typical data sheet

Example $O + OH \rightarrow O_2 + H$

1. Thermodynamic Data

$\Delta H^\circ_{298} = -68.29 \text{ kJ mol}^{-1}$

$\Delta S^\circ_{298} = -25.04 \text{ J K}^{-1} \text{ mol}^{-1}$

$K_c = 3.48 \cdot 10^{-3}\, T^{\,0.367} \exp(+8390/T)$

$(300 \leq T/\text{K} \leq 5000)$

2. Rate coefficient data

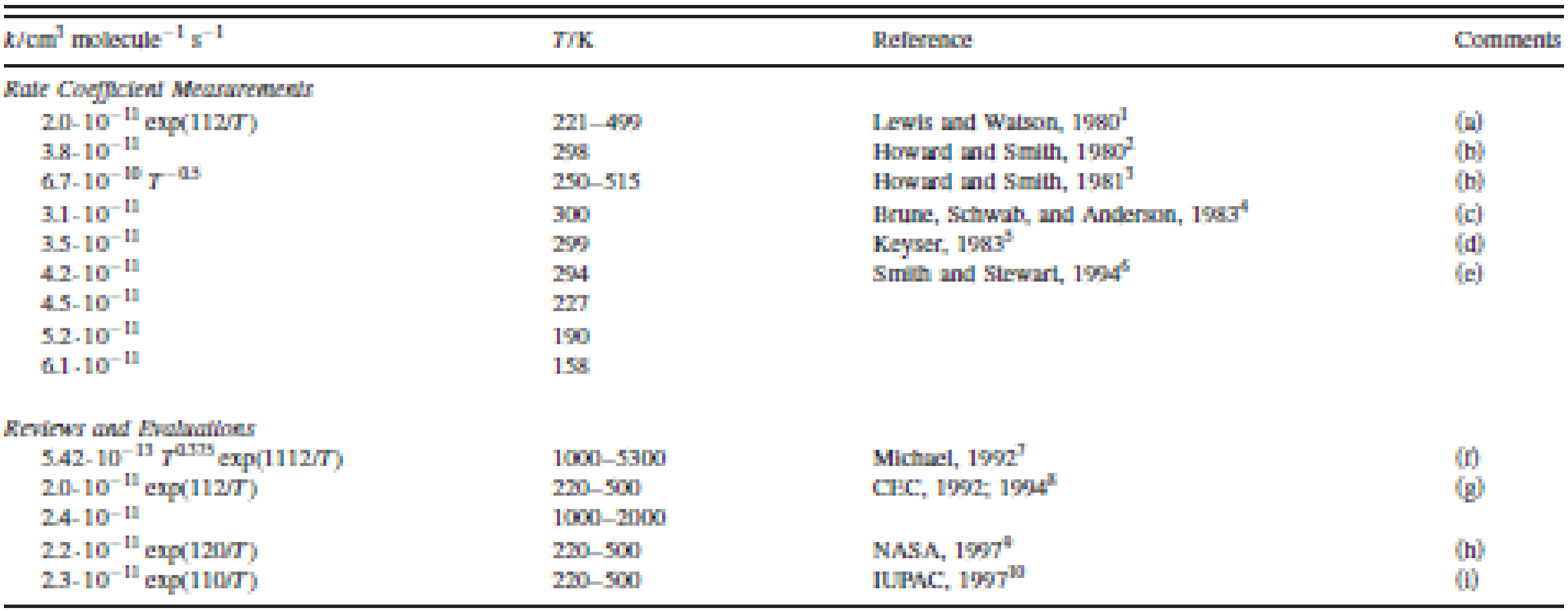

k/cm^3 molecule^{-1} s^{-1}	T/K	Reference	Comments
Rate Coefficient Measurements			
$2.0 \cdot 10^{-11} \exp(112/T)$	221–499	Lewis and Watson, 1980[1]	(a)
$3.8 \cdot 10^{-11}$	298	Howard and Smith, 1980[2]	(b)
$6.7 \cdot 10^{-10}\, T^{-0.5}$	250–515	Howard and Smith, 1981[3]	(b)
$3.1 \cdot 10^{-11}$	300	Brune, Schwab, and Anderson, 1983[4]	(c)
$3.5 \cdot 10^{-11}$	299	Keyser, 1983[5]	(d)
$4.2 \cdot 10^{-11}$	294	Smith and Stewart, 1994[6]	(e)
$4.5 \cdot 10^{-11}$	227		
$5.2 \cdot 10^{-11}$	190		
$6.1 \cdot 10^{-11}$	158		
Reviews and Evaluations			
$5.42 \cdot 10^{-13}\, T^{0.335} \exp(1112/T)$	1000–5300	Michael, 1992[7]	(f)
$2.0 \cdot 10^{-11} \exp(112/T)$	220–500	CEC, 1992; 1994[8]	(g)
$2.4 \cdot 10^{-11}$	1000–2000		
$2.2 \cdot 10^{-11} \exp(120/T)$	220–500	NASA, 1997[9]	(h)
$2.3 \cdot 10^{-11} \exp(110/T)$	220–500	IUPAC, 1997[10]	(i)

Provides data on recent measurements and evaluations, including
Rate coefficient
T/K
Reference
Link to comments

Comments (examples)

(e) Fast flow system in which OH radicals were created by pulsed laser photolysis at 266 nm of HNO_3 in the presence of a much higher concentration of O atoms previously produced upstream of the HNO_3 injection point by the N+NO reaction. [OH] was monitored by LIF, pumping at ~ 282.5 nm and observing at ~ 310 nm. The time delay between the pulse generating OH and the LIF probe pulse was varied. Results were also obtained at 103 K, 50 K, and 10 K but with large uncertainties.

(f) Calculated from thermodynamic data and $k(H+O_2)$.

(g) Expression of Lewis and Watson[1] adopted for low temperature range and high temperature expression derived from thermodynamic data and $k(H+O_2)$.

Preferred values

- $k = 2.00 \cdot 10^{-10}\ T^{-0.352} \exp(113/T)$ cm^3 molecule^{-1} s^{-1} over the range 250-3000 K.

- ***Reliability***
- $\Delta \log k = \pm 0.2$ over the range 250-3000 K.

Comments on preferred values

- The only direct studies on this reaction have been carried out at low temperatures where there is excellent agreement among the more recent of them.

- Although there have been no direct measurements of *k* above 515 K the reverse reaction has been extensively investigated at temperatures in the range 800-3400 K. The preferred expression for *k* has been derived, therefore, by a fit to the data obtained by combining the expression for $k(\mathrm{H+O_2})$ from the present evaluation with the thermodynamic data at temperatures above 800 K together with the directly obtained experimental data at temperatures below 500 K. The reaction has been the subject of a number of theoretical studies; see Miller,[19-21] Troe,[22] Harding *et al.*[23] and Troe and Ushakov.[24]

Arrhenius Plot

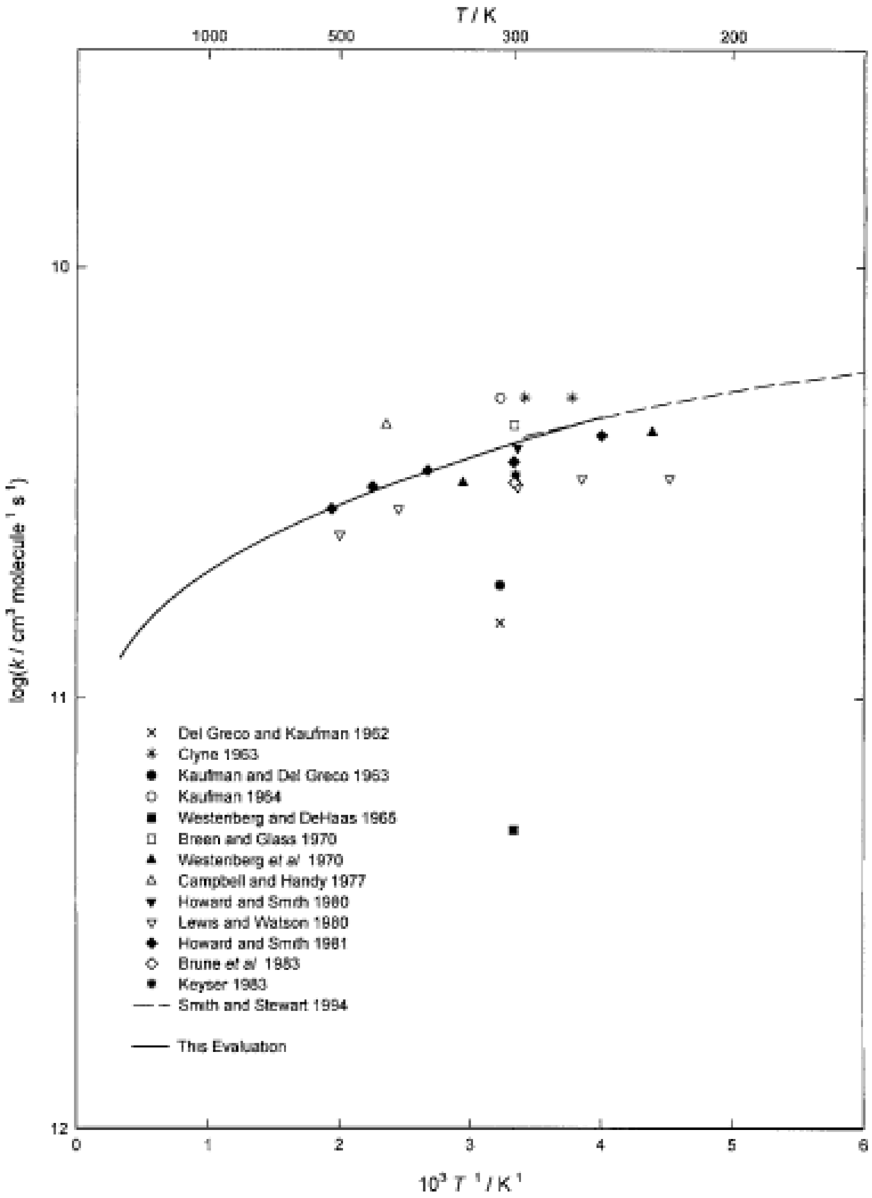

Reverse reaction: $H + O_2 \rightarrow O + OH$

- $k = 3.43 \cdot 10^{-10}\, T^{-0.097} \exp(-7560/T)$ cm^3 molecule^{-1} s^{-1} over the range 800-3500 K.
- $\Delta \log k = \pm 0.1$ at 800 K, rising to ± 0.2 at 3500 K.
- There are no direct measurements of *k* below 500 K and the recommended values are based on data obtained at temperatures above 800 K. The majority of the determinations of *k* have been made using shock tube techniques and, generally, are in good agreement.[1-10,15-25] There is a trend in the more recent studies[1-10] to give slightly lower values of *E/R* than most of the older determinations.[11,5-25] Our preferred expression for *k* is based on the more recent studies, which are cited in the Table. The expression derived gives values very similar to the expression used by Smith *et al.*[26] in modelling studies using the GRI mechanism.

$H + O_2 \rightarrow O + OH$

Figure is too small to read but it shows the large number of Investigations and demonstrates how the results mainly cluster around the best fit line.
Illustrates the ideas of upper and lower bounds and of a probability distribution function (pdf)

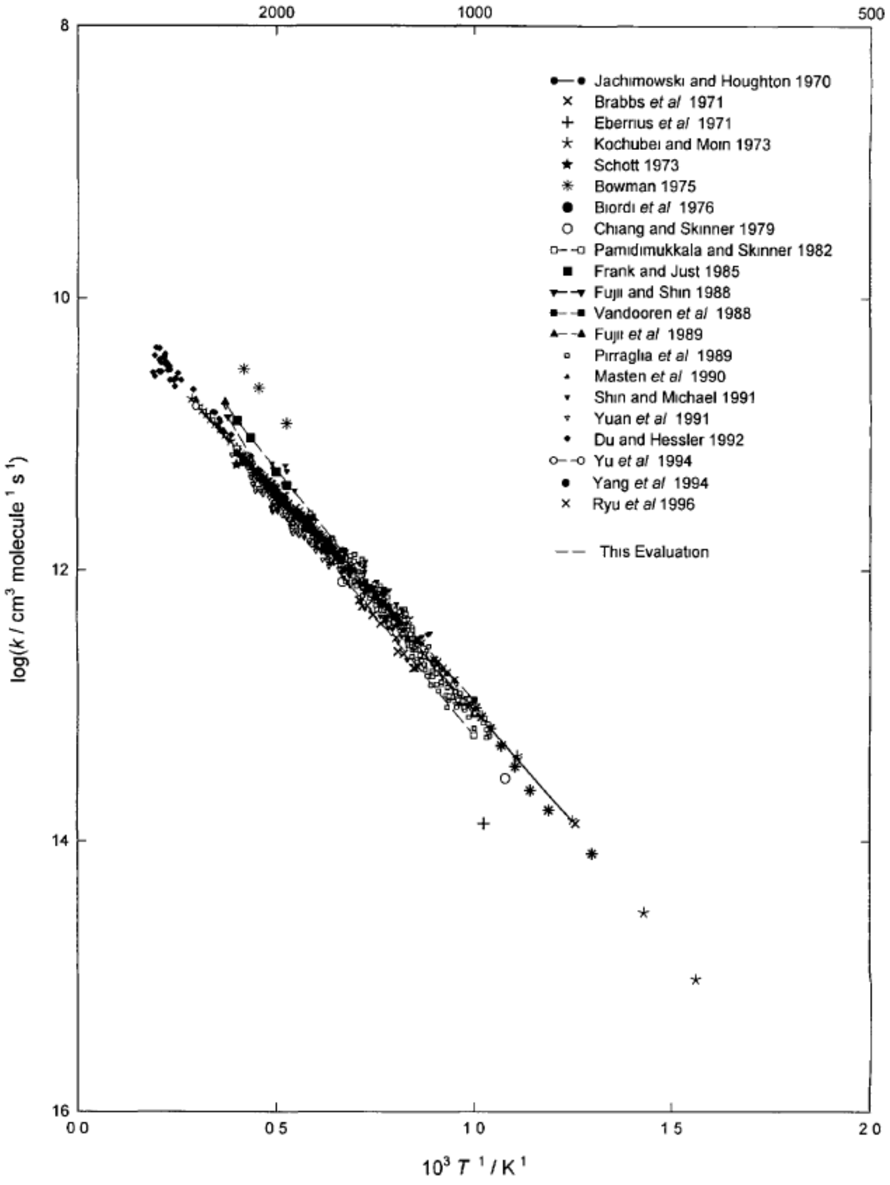

REMINDER: earlier slide on H + $O_2 \rightarrow$ OH + O

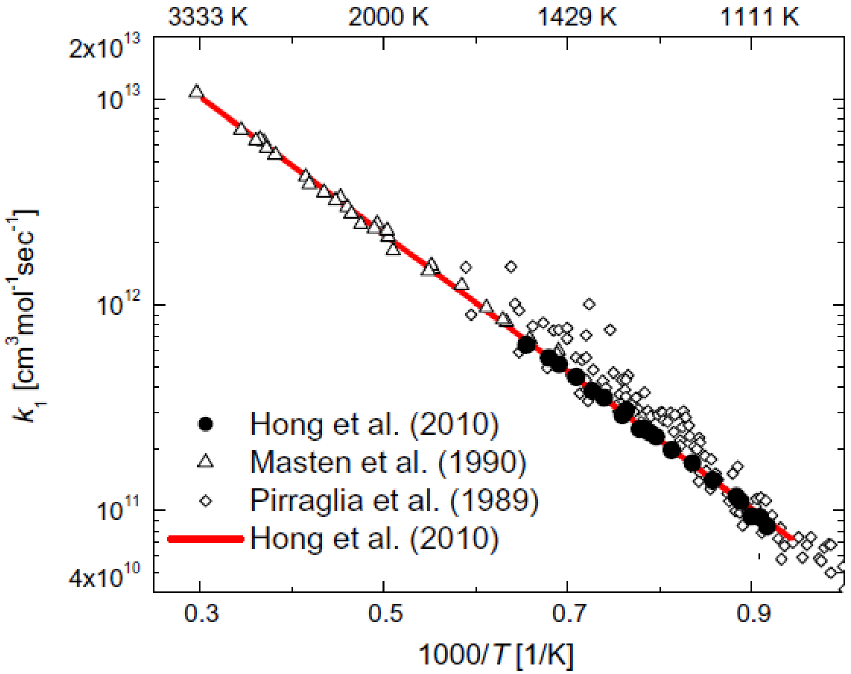

- From Hong et al., shock tube measurements. Comb Flame 2011, 158,633, $k = 1.7\times 10^{-10} \exp(-7670/T)$ (1100 – 3370 K). Uncertainty ± 10%.
- See Burke et al. Int J Chem Kinet, 2012, 44, 444, who support the rate coefficient

Pressure dependent reactions - reminder

Troe Fitting

Need to represent k(T,P) for Global Models

Standard is Troe Fitting

$$k(T,p) = \frac{k_0[M]k^{\infty}}{k^{\infty} + k_0[M]} F \qquad \log_{10} F = \frac{\log_{10} F_{cent}}{1 + \left[\frac{\log_{10}(p^*) + c}{N - d\left(\log_{10}(p^*) + c\right)} \right]^2}$$

$$p^* = k_0[M] / k^{\infty} \qquad d = 0.14$$

$$c = -0.4 - 0.67 \log_{10} F_{cent} \qquad N = 0.75 - 1.27 \log_{10} F_{cent}$$

Fit k_0 & k^{∞} to modified Arrhenius $k_0 = A_0 T^{n_0} \exp(-E_0 / T)$

Fit F_{cent} to:

$$F_{cent} = (1-a)\exp\left(-T/T^{***}\right) + a\exp\left(-T/T^{*}\right) + \exp\left(-T^{**}/T\right)$$

Pressure dependent reaction: $H + C_2H_4$

- $k_0 = 1.3 \cdot 10^{-29} \exp(-380/T)$ cm^6 molecule^{-2} s^{-1} for M = He over the range 300-800 K.
- $k_0 = 1.3 \cdot 10^{-29} \exp(-380/T)$ cm^6 molecule^{-2} s^{-1} for M = N_2 over the range 300-800 K.
- $k_\infty = 6.6 \cdot 10^{-15}\ T^{1.28} \exp(-650/T)$ cm^3 molecule^{-1} s^{-1} over the range 200-1100 K.
- $F_c = 0.24 \exp(-T/40) + 0.76 \exp(-T/1025)$ for M = He and N_2 over the range 300-800 K.

Reliability

- $\Delta \log k_0 = \pm 0.3$ for M = He, N_2 over the range 300-800 K.
- $\Delta \log k_\infty = \pm 0.3$ over the range 200-1100 K.
- $\Delta F_c = \pm 0.1$ for M = He, N_2 over the range 300-800 K.

$H + C_2H_4 (+M) \rightarrow$ (a) $C_2H_5 + M$; (b) $C_2H_3 + H_2$

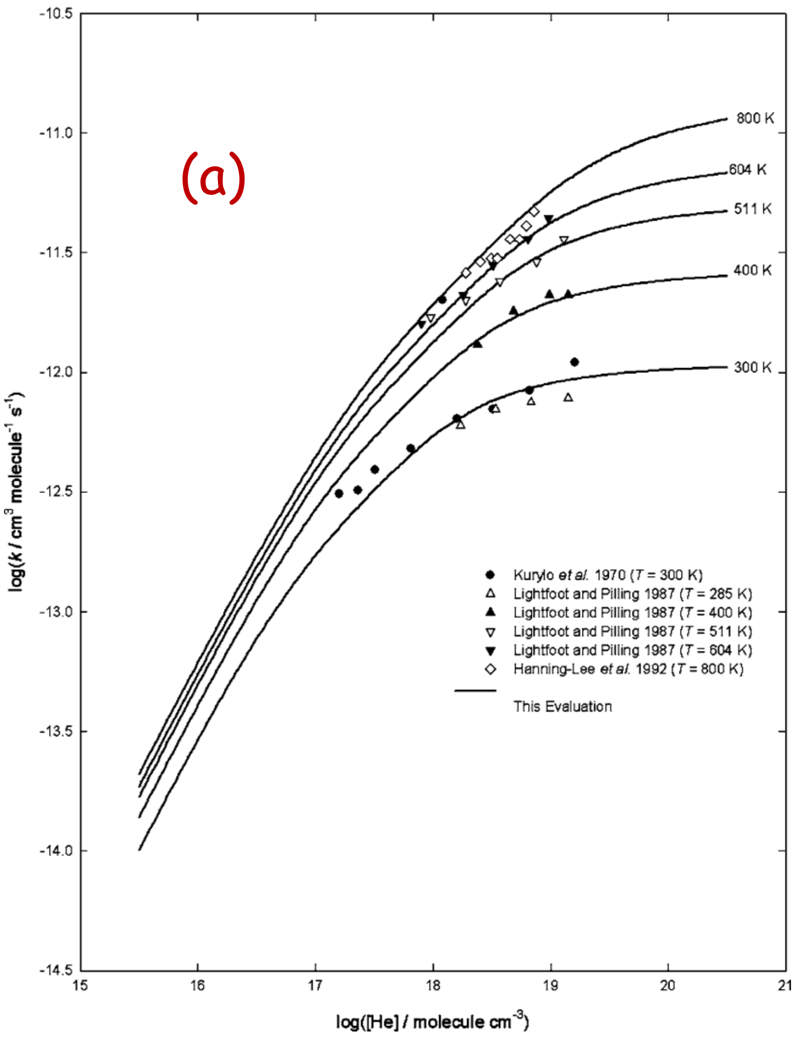

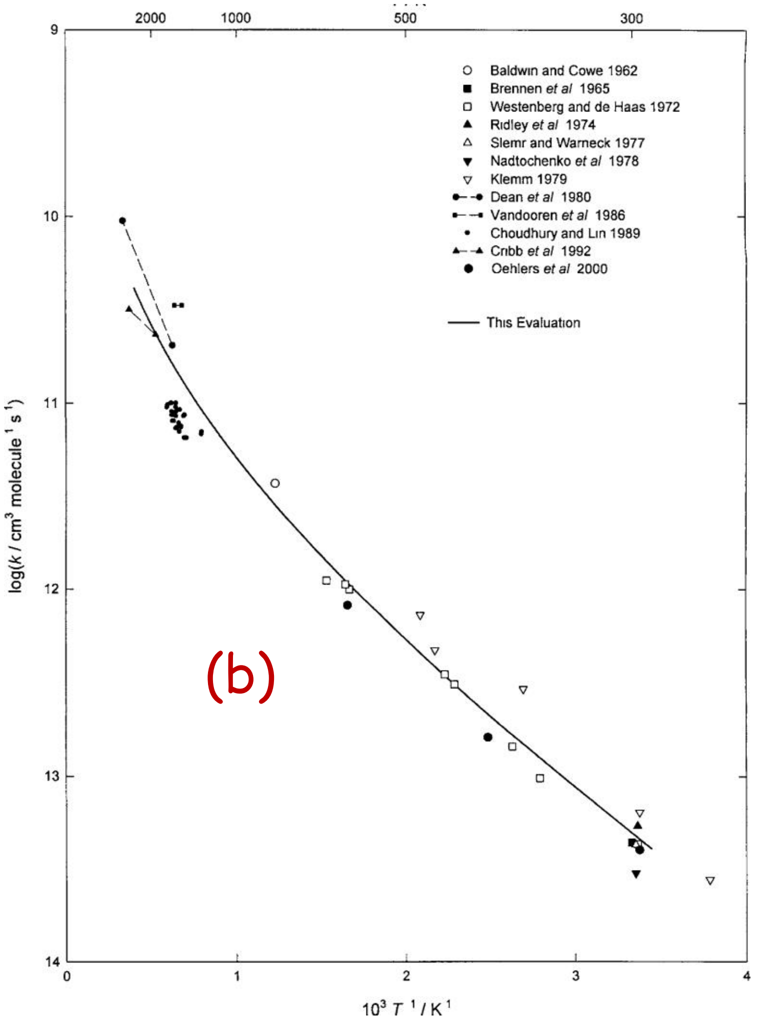

Access to rate data

- These evaluations provided a major service for combustion through the provision of recommended rate constants, with associated errors. They are becoming out of date. Alternative data sources must be used but they do not contain recommended rate constants. See following slides.
- Turanyi and Nagy have provided a more statistically correct way of assessing errors (see later)
- Turanyi and coworkers have developed a method for evaluating rate data from direct measurements / calculations and indirect measurements of combustion processes that depend on reaction kinetics, e.g. ignition delay times. See Topic 6 on Chemical Mechanisms

RESPECTH website
https://respecth.elte.hu/

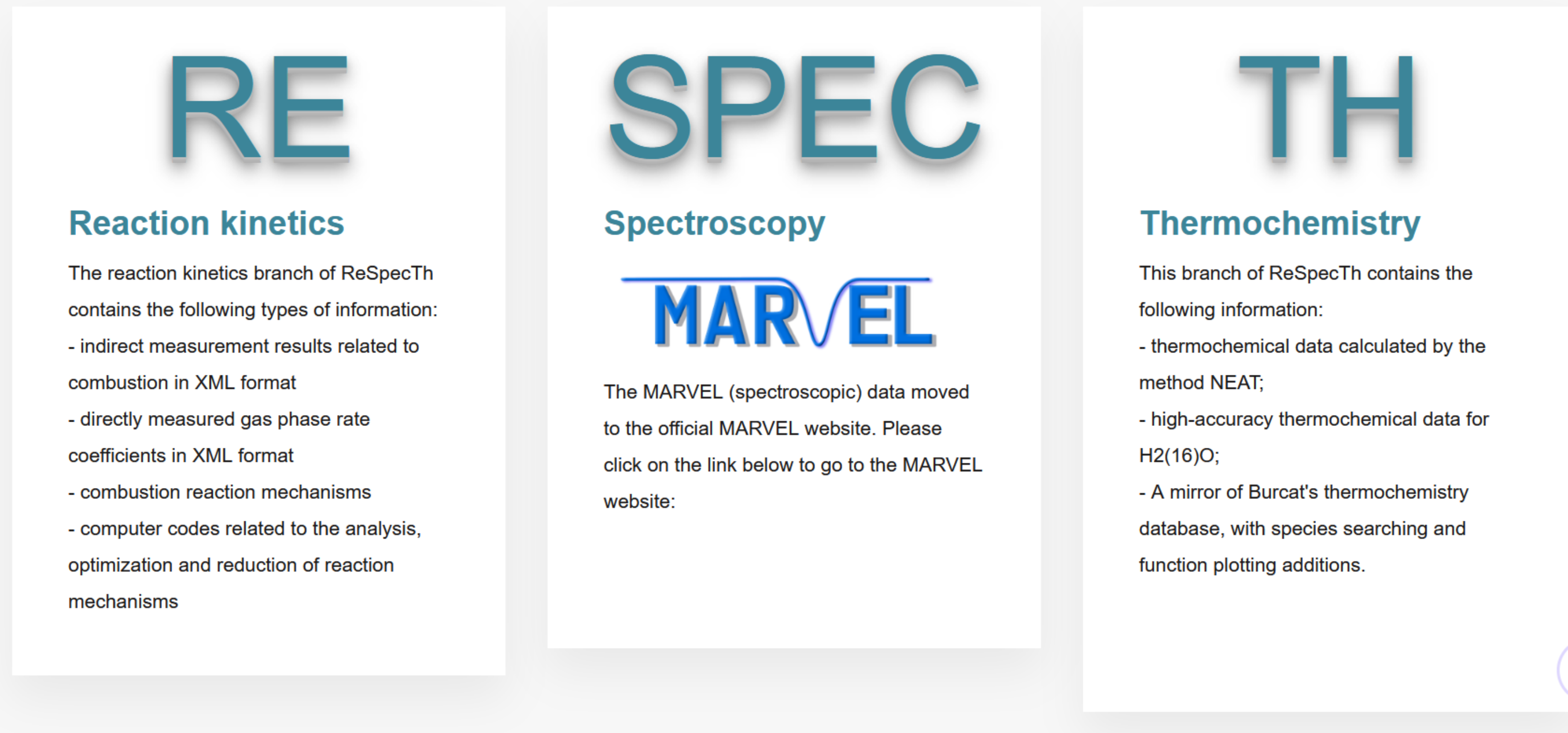

RE

Reaction kinetics

The reaction kinetics branch of ReSpecTh contains the following types of information:

- indirect measurement results related to combustion in XML format
- directly measured gas phase rate coefficients in XML format
- combustion reaction mechanisms
- computer codes related to the analysis, optimization and reduction of reaction mechanisms

SPEC

Spectroscopy

The MARVEL (spectroscopic) data moved to the official MARVEL website. Please click on the link below to go to the MARVEL website:

TH

Thermochemistry

This branch of ReSpecTh contains the following information:

- thermochemical data calculated by the method NEAT;
- high-accuracy thermochemical data for H2(16)O;
- A mirror of Burcat's thermochemistry database, with species searching and function plotting additions.

Content of the reaction kinetics site

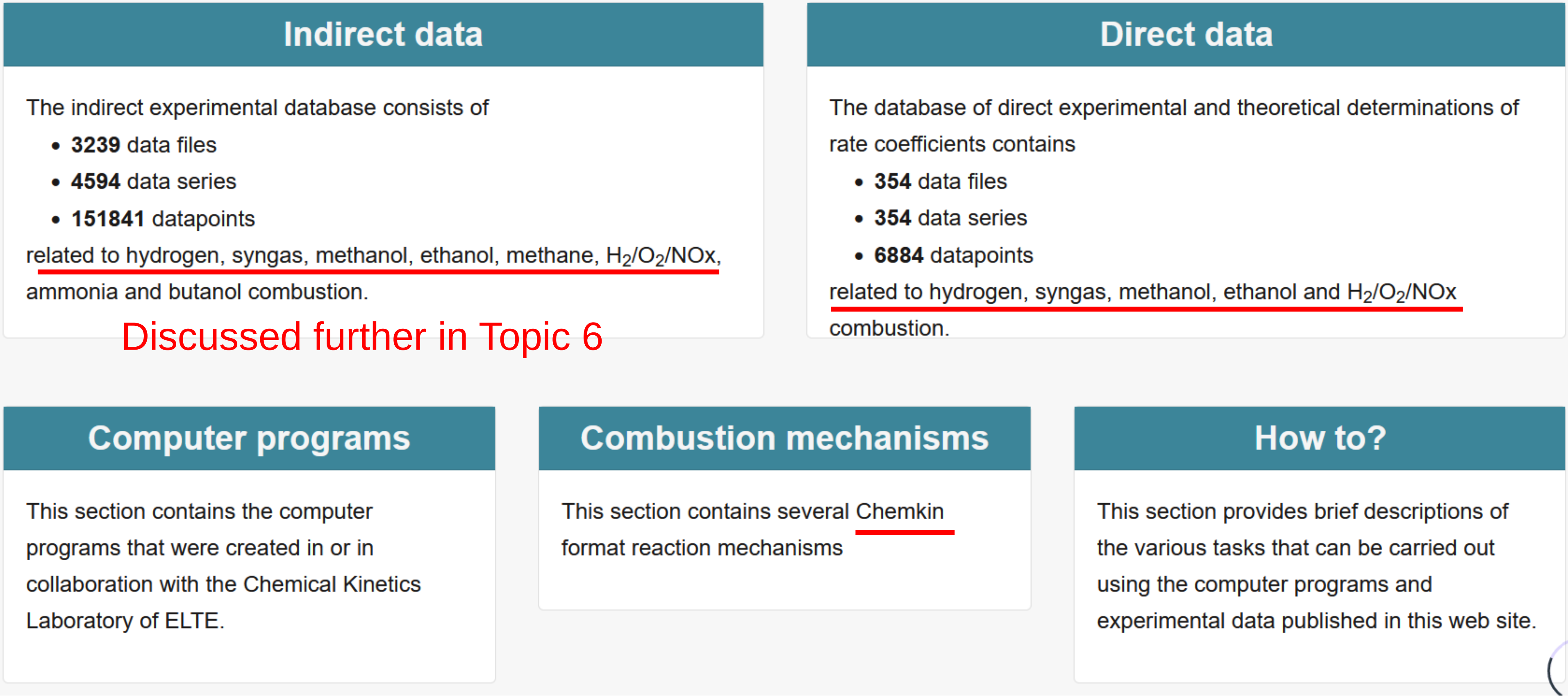

Indirect data

The indirect experimental database consists of

- **3239** data files
- **4594** data series
- **151841** datapoints

related to hydrogen, syngas, methanol, ethanol, methane, $H_2/O_2/NOx$, ammonia and butanol combustion.

Discussed further in Topic 6

Direct data

The database of direct experimental and theoretical determinations of rate coefficients contains

- **354** data files
- **354** data series
- **6884** datapoints

related to hydrogen, syngas, methanol, ethanol and $H_2/O_2/NOx$ combustion.

Computer programs

This section contains the computer programs that were created in or in collaboration with the Chemical Kinetics Laboratory of ELTE.

Combustion mechanisms

This section contains several Chemkin format reaction mechanisms

How to?

This section provides brief descriptions of the various tasks that can be carried out using the computer programs and experimental data published in this web site.

Some of the data links and references for O + H_2

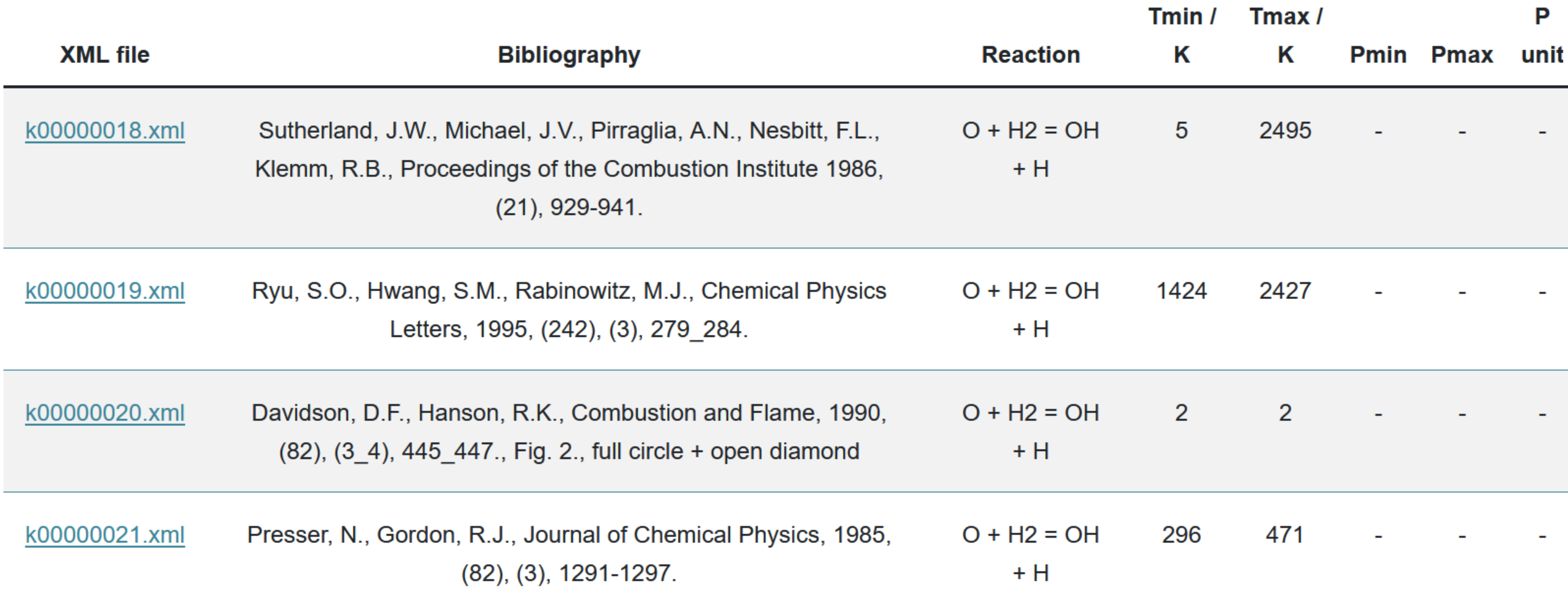

XML file	Bibliography	Reaction	Tmin / K	Tmax / K	Pmin	Pmax	P unit
k00000018.xml	Sutherland, J.W., Michael, J.V., Pirraglia, A.N., Nesbitt, F.L., Klemm, R.B., Proceedings of the Combustion Institute 1986, (21), 929-941.	O + H2 = OH + H	5	2495	-	-	-
k00000019.xml	Ryu, S.O., Hwang, S.M., Rabinowitz, M.J., Chemical Physics Letters, 1995, (242), (3), 279_284.	O + H2 = OH + H	1424	2427	-	-	-
k00000020.xml	Davidson, D.F., Hanson, R.K., Combustion and Flame, 1990, (82), (3_4), 445_447., Fig. 2., full circle + open diamond	O + H2 = OH + H	2	2	-	-	-
k00000021.xml	Presser, N., Gordon, R.J., Journal of Chemical Physics, 1985, (82), (3), 1291-1297.	O + H2 = OH + H	296	471	-	-	-

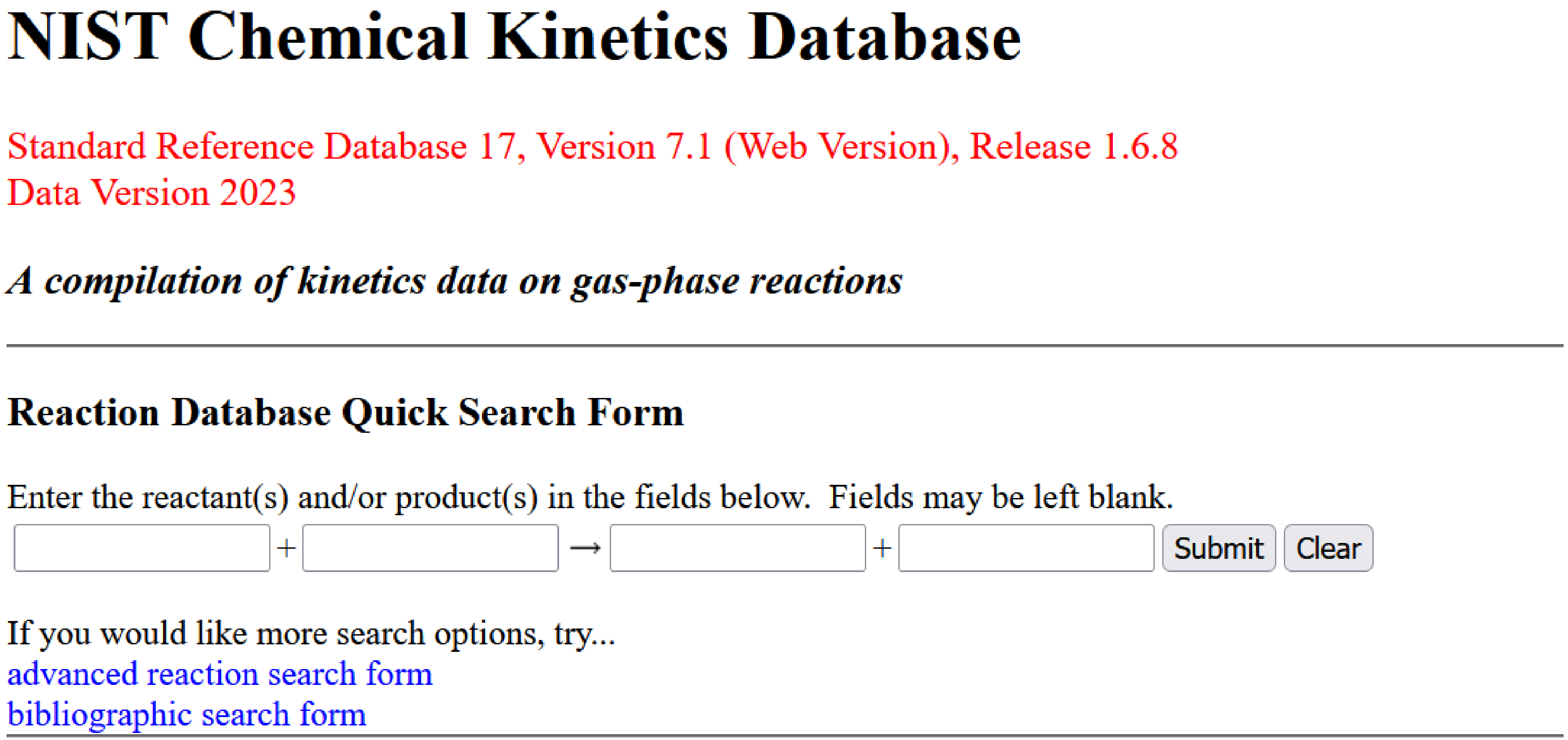

NIST Chemical Kinetics Database

Standard Reference Database 17, Version 7.1 (Web Version), Release 1.6.8
Data Version 2023

A compilation of kinetics data on gas-phase reactions

Reaction Database Quick Search Form

Enter the reactant(s) and/or product(s) in the fields below. Fields may be left blank.

If you would like more search options, try...
advanced reaction search form
bibliographic search form

https://kinetics.nist.gov/kinetics

Experimental data for $OH + CO \rightarrow H + CO_2$.
Also provides references to Reviews and theoretical data

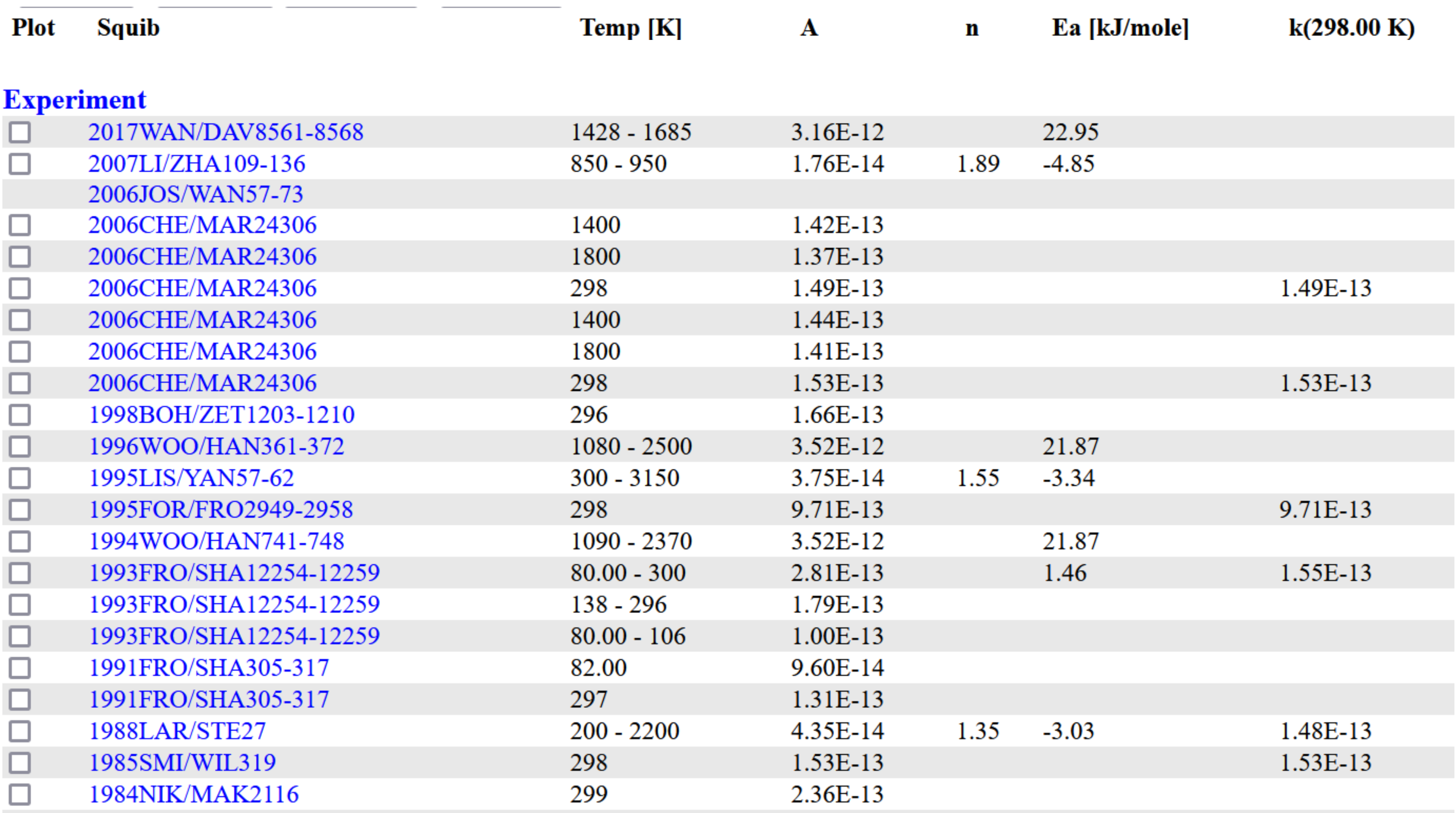

Plot	Squib	Temp [K]	A	n	Ea [kJ/mole]	k(298.00 K)
Experiment						
☐	2017WAN/DAV8561-8568	1428 - 1685	3.16E-12		22.95	
☐	2007LI/ZHA109-136	850 - 950	1.76E-14	1.89	-4.85	
	2006JOS/WAN57-73					
☐	2006CHE/MAR24306	1400	1.42E-13			
☐	2006CHE/MAR24306	1800	1.37E-13			
☐	2006CHE/MAR24306	298	1.49E-13			1.49E-13
☐	2006CHE/MAR24306	1400	1.44E-13			
☐	2006CHE/MAR24306	1800	1.41E-13			
☐	2006CHE/MAR24306	298	1.53E-13			1.53E-13
☐	1998BOH/ZET1203-1210	296	1.66E-13			
☐	1996WOO/HAN361-372	1080 - 2500	3.52E-12		21.87	
☐	1995LIS/YAN57-62	300 - 3150	3.75E-14	1.55	-3.34	
☐	1995FOR/FRO2949-2958	298	9.71E-13			9.71E-13
☐	1994WOO/HAN741-748	1090 - 2370	3.52E-12		21.87	
☐	1993FRO/SHA12254-12259	80.00 - 300	2.81E-13		1.46	1.55E-13
☐	1993FRO/SHA12254-12259	138 - 296	1.79E-13			
☐	1993FRO/SHA12254-12259	80.00 - 106	1.00E-13			
☐	1991FRO/SHA305-317	82.00	9.60E-14			
☐	1991FRO/SHA305-317	297	1.31E-13			
☐	1988LAR/STE27	200 - 2200	4.35E-14	1.35	-3.03	1.48E-13
☐	1985SMI/WIL319	298	1.53E-13			1.53E-13
☐	1984NIK/MAK2116	299	2.36E-13			

+ Many more

Example of a report on a dataset

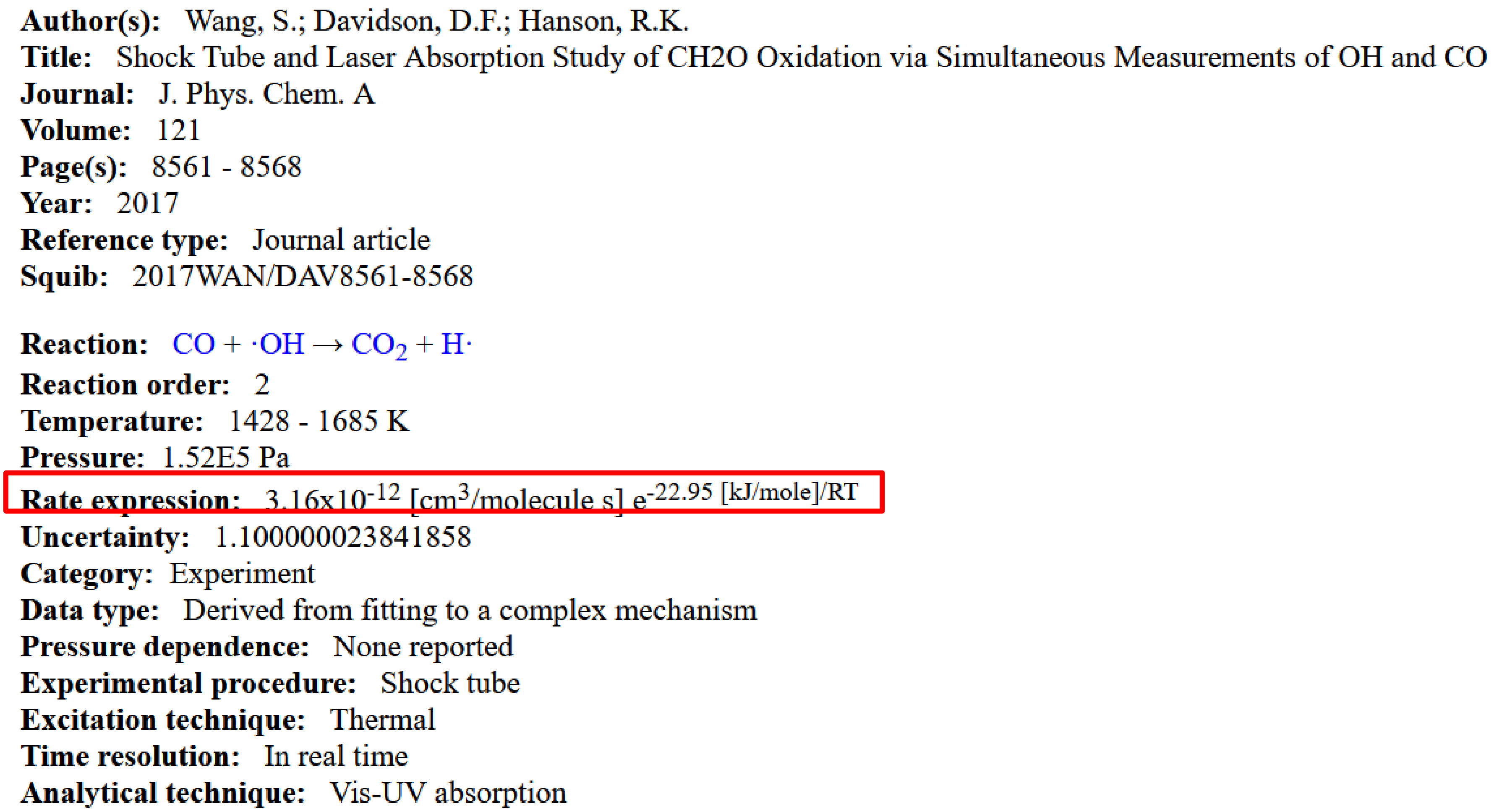

Author(s): Wang, S.; Davidson, D.F.; Hanson, R.K.
Title: Shock Tube and Laser Absorption Study of CH2O Oxidation via Simultaneous Measurements of OH and CO
Journal: J. Phys. Chem. A
Volume: 121
Page(s): 8561 - 8568
Year: 2017
Reference type: Journal article
Squib: 2017WAN/DAV8561-8568

Reaction: $CO + \cdot OH \rightarrow CO_2 + H\cdot$
Reaction order: 2
Temperature: 1428 - 1685 K
Pressure: 1.52E5 Pa
Rate expression: $3.16\text{x}10^{-12}$ [cm^3/molecule s] $e^{-22.95\ [\text{kJ/mole}]/RT}$
Uncertainty: 1.100000023841858
Category: Experiment
Data type: Derived from fitting to a complex mechanism
Pressure dependence: None reported
Experimental procedure: Shock tube
Excitation technique: Thermal
Time resolution: In real time
Analytical technique: Vis-UV absorption

Plot facility

Rate Constant Plot

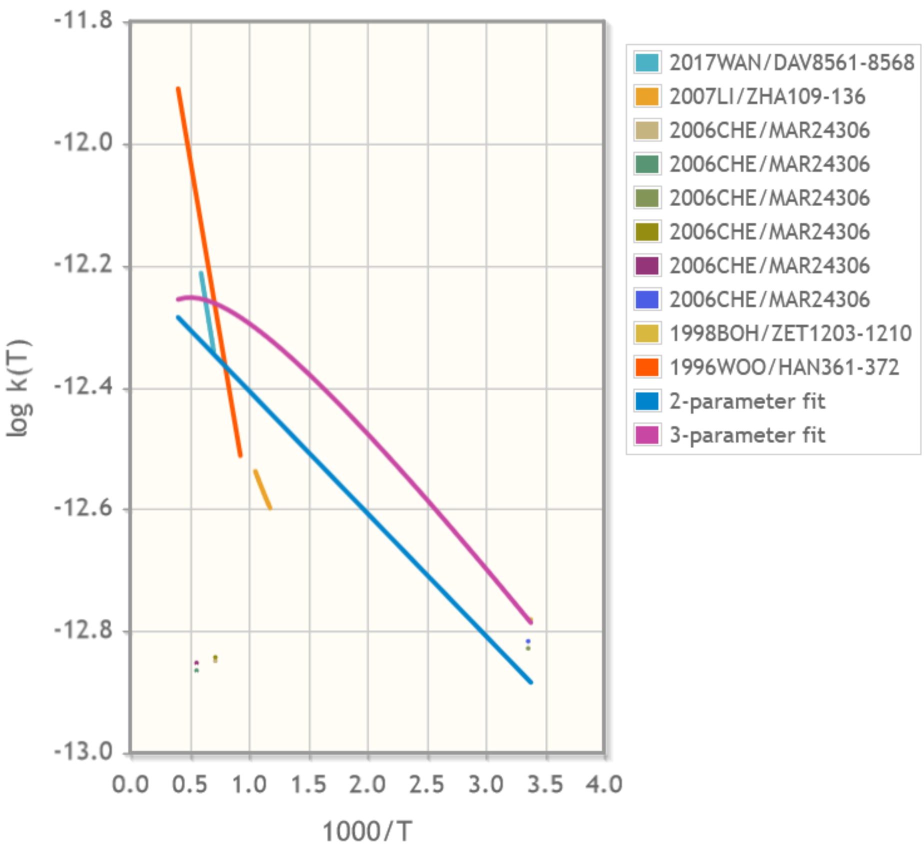

Fit of Arrhenius parameters to set:

Temperature range: 296 - 2500 K

Two-parameter fit:

$$k(T) = A exp(-E_a/RT)$$

A = 6.24E-13 [cm^3/molecule s]
E_a = 3.8 [kJ]
RMSD = 0.9

Three-parameter fit:

$$k(T) = A(T/T_{ref})^n exp(-E_a/RT)$$

A = 1.41E-12 [cm^3/molecule s]
n = -0.3
T_{ref} = 298 [K]
E_a = 5.3 [kJ]
RMSD = 1.1

Nagy and Turanyi, Uncertainty of Arrhenius Parameters Int J Chem Kinet 43: 359-378, 2011

- Analytical expression is derived that describes the temperature dependence of the uncertainty of *k* as a function of the elements of the covariance matrix of the Arrhenius parameters.
- Recommendations are given for an improved representation of the uncertainty information in future chemical kinetics databases using the covariance matrix of the Arrhenius parameters
- method suggested for determination of covariance matrix and joint probability density function of Arrhenius parameters from the present uncertainty information given in the kinetics databases.

Representations of uncertainty

- The evaluations contain subjective estimates of the “reliability” of a rate constant, determined by agreement between different measurements and data availability. The values given need to be converted into statistical quantities, e.g. standard deviation, that are continuous, in order to be used in models

  - If evaluation available then *f* value may be given.

$$f = \log_{10}\left(\frac{k^{0}}{k^{\min}}\right) = \log_{10}\left(\frac{k^{\max}}{k^{0}}\right) \qquad \frac{k^{\max}}{k^{0}} = 10^{f}$$

  - k_0 recommended value of rate coefficient. k_{min}, k_{max} extreme values.

$$\sigma^2(\ln\{k\}) = ((f\ \ln 10)/m)^2$$

where m is the level of uncertainty suggested.
m = 2, 2σ deviation or 95 %ile,
m= 3, 3σ deviation or 99.7 %ile

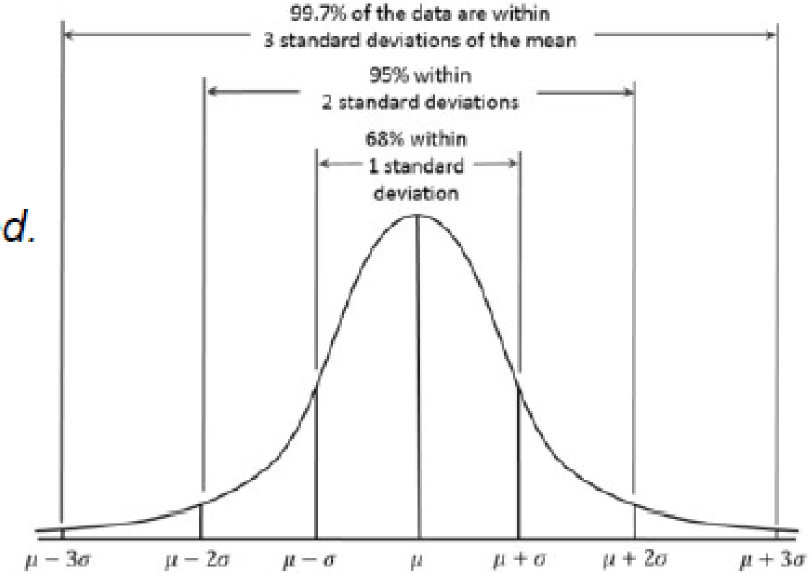

$O + C_2H_4$: evaluation

- $k = 2.25 \cdot 10^{-17}\ T^{1.88} \exp(-92/T)\ \mathrm{cm}^3\ \mathrm{molecule}^{-1}\ \mathrm{s}^{-1}$ over the range 220-2000 K.
- Reliability

  $\Delta \log k = \pm 0.1$ over the range 300-1000 K, rising to ± 0.3 at 220 K and 2000 K

$O + C_2H_4 \rightarrow CH_2CHO + H$ (1)

$\rightarrow HCO + CH_3$ (2)

$\rightarrow HCHO + CH_2$ (3)

$\rightarrow CH_2CO + H_2$ (4)

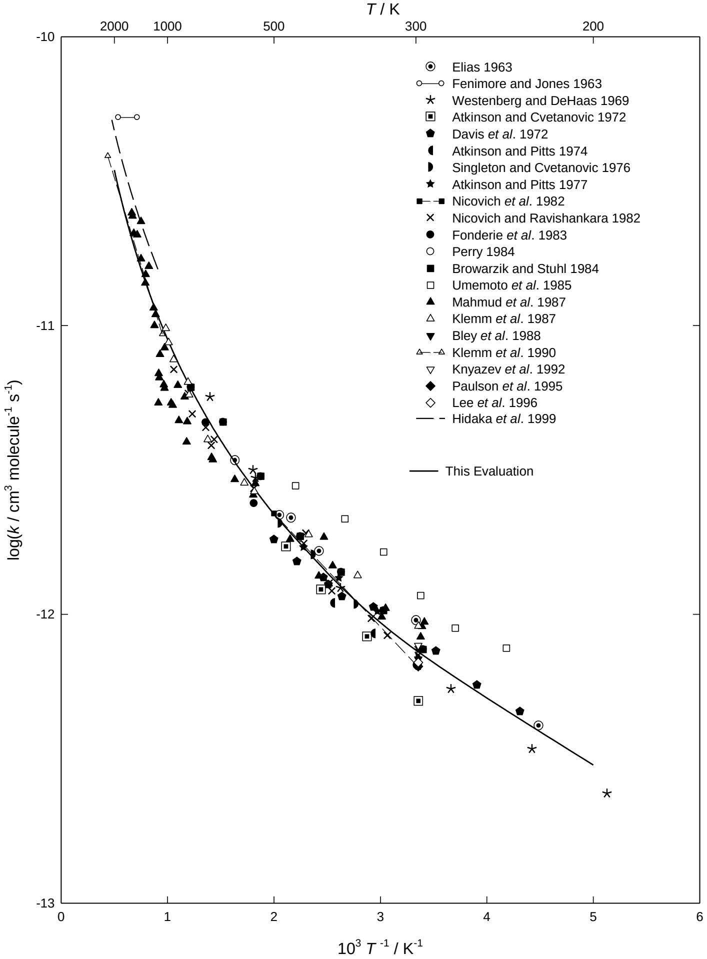

O + C_2H_4 → products (Nagy and Turanyi)

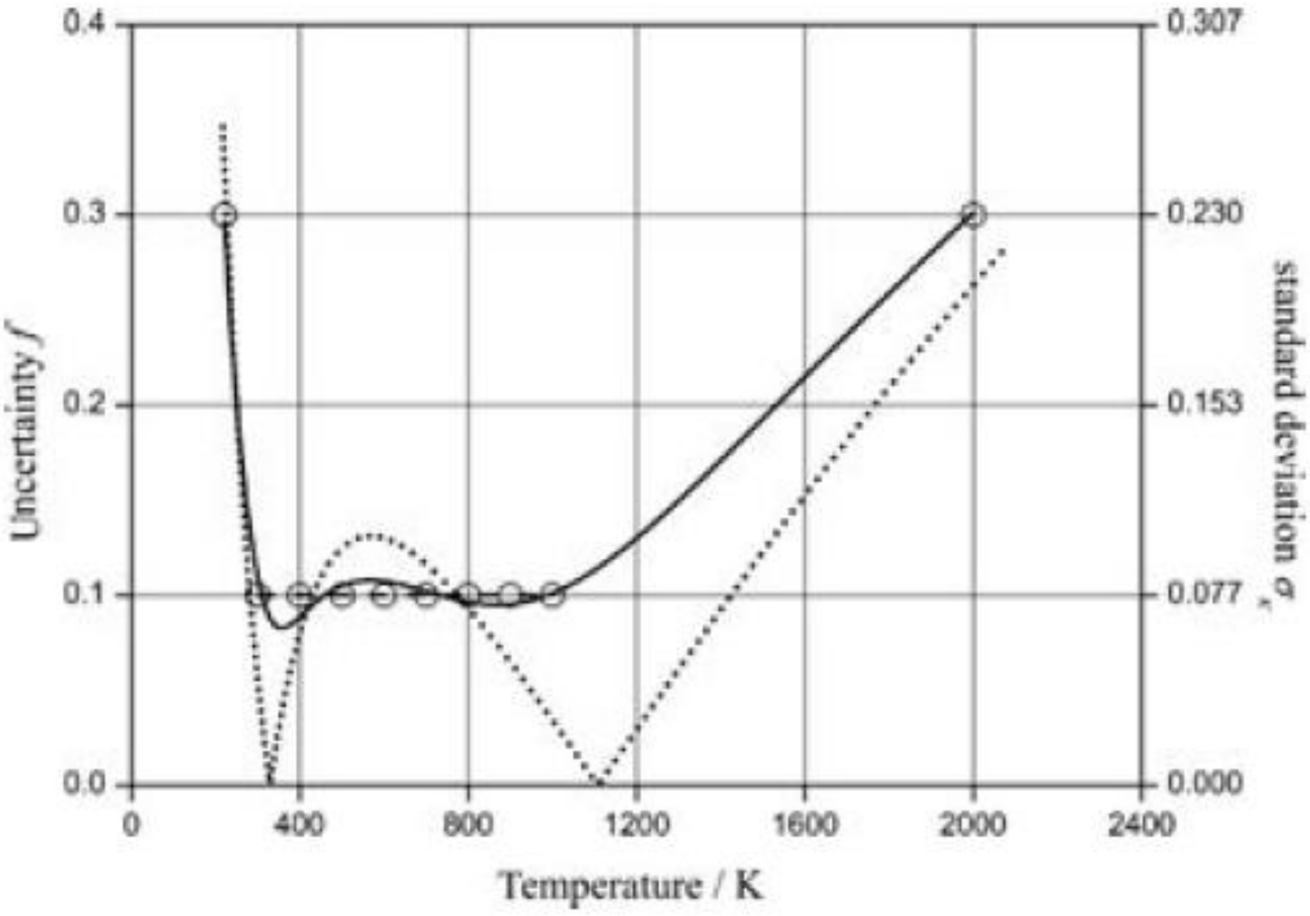

$CH_3 + H \rightarrow {}^1CH_2 + H_2$

- $k = 2.1 \cdot 10^{-8}\, T^{-0.56} \exp(-8000/T)$ cm^3 $molecule^{-1}$ s^{-1} over the range 300-2500 K.
- Reliability

  $\Delta \log k = \pm 0.15$ over the range 300-1000 K, ± 0.3 over the range 1000-1700 K, and ± 0.2 over the range 1700-2500 K.
- Comments on Preferred Values

  The values of *k* obtained in the shock tube studies of Bhaskaran *et al.*[1] and Davidson *et al.*[3] are in reasonable agreement and also agree to within a factor of ~ 3 with the rate constants predicted by combining the thermodynamic data with the low temperature data on the reverse reaction, whereas the value of *k* obtained in the flame study of Langley and Burgess[2] seems unacceptably high.

T dependent uncertainty parameter, $k = AT^{n}\exp(-E/RT)$

- Covariance matrix:

$$\mathbf{\Sigma_p} = \overline{(\mathbf{p}-\bar{\mathbf{p}})\,(\mathbf{p}-\bar{\mathbf{p}})^{\mathrm{T}}}$$

$$= \begin{bmatrix} \sigma_\alpha^2 & r_{\alpha n}\,\sigma_\alpha\,\sigma_n & r_{\alpha\varepsilon}\,\sigma_\alpha\,\sigma_\varepsilon \\ r_{\alpha n}\,\sigma_\alpha\,\sigma_n & \sigma_n^2 & r_{n\varepsilon}\,\sigma_n\,\sigma_\varepsilon \\ r_{\alpha\varepsilon}\,\sigma_\alpha\,\sigma_\varepsilon & r_{n\varepsilon}\,\sigma_n\,\sigma_\varepsilon & \sigma_\varepsilon^2 \end{bmatrix}$$

- Uncertainty parameter ($M = 3/\ln 10$ or $2/\ln 10$) depending on definition of reliability in evaluation

$$F(T) = M\sqrt{\sigma_\alpha^2 + \sigma_n^2 \ln^2 T + \sigma_\varepsilon^2 T^{-2} + 2r_{\alpha n}\sigma_\alpha\sigma_n \ln T - 2r_{\alpha\varepsilon}\sigma_\alpha\sigma_\varepsilon T^{-1} - 2r_{n\varepsilon}\sigma_n\sigma_\varepsilon T^{-1}\ln T}$$

$CH_3 + H \rightarrow {}^1CH_2 + H_2$ (Nagy and Turanyi)

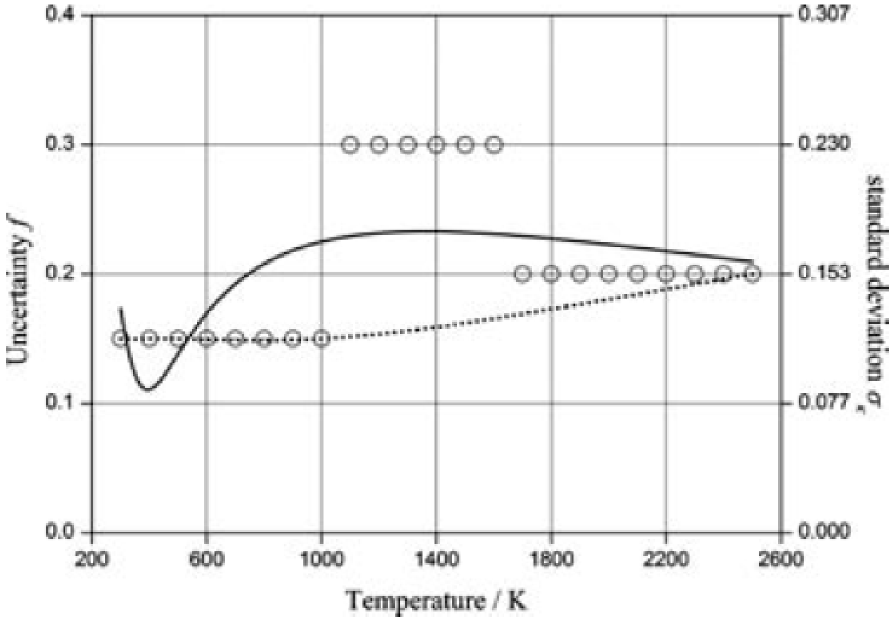

Figure 7 Uncertainties of reaction R5 are defined [14] in three temperature intervals and the uncertainty–temperature function was fitted to the values represented by the circles. The best least squares fit (solid line; see row **R5** in Table IV) does not approach these points well, because the recommended uncertainties were not consistent. The alternatively proposed $f(T)$ curve (dotted line) remains below all uncertainty points and has the highest average value of $\sigma_\kappa^2(T)$ in the inverse temperature interval of $[1/T_2, 1/T_1]$ (see text and row **R5m** in Table IV).

Uncertainty of the rate parameters of several important elementary reactions of the H_2 and syngas combustion systems (Nagy et al. Comb and Flame, 2015, 162, 2059)

- Re-evaluation of uncertainty parameters for 22 reactions using all available experimental and theoretical data.
- Based on lnA, n and E, uncertainty function, $f(T)$ stored as covariance matrix. $f(T)$ is the uncertainty range placed symmetrically about the mean rate constant.
- Discuss uncertainty in backward rate constant using forward rate constant and thermodynamics.
- A set of software tools is provided to allow the approach to be applied to any set of measured + calculated rate constants.

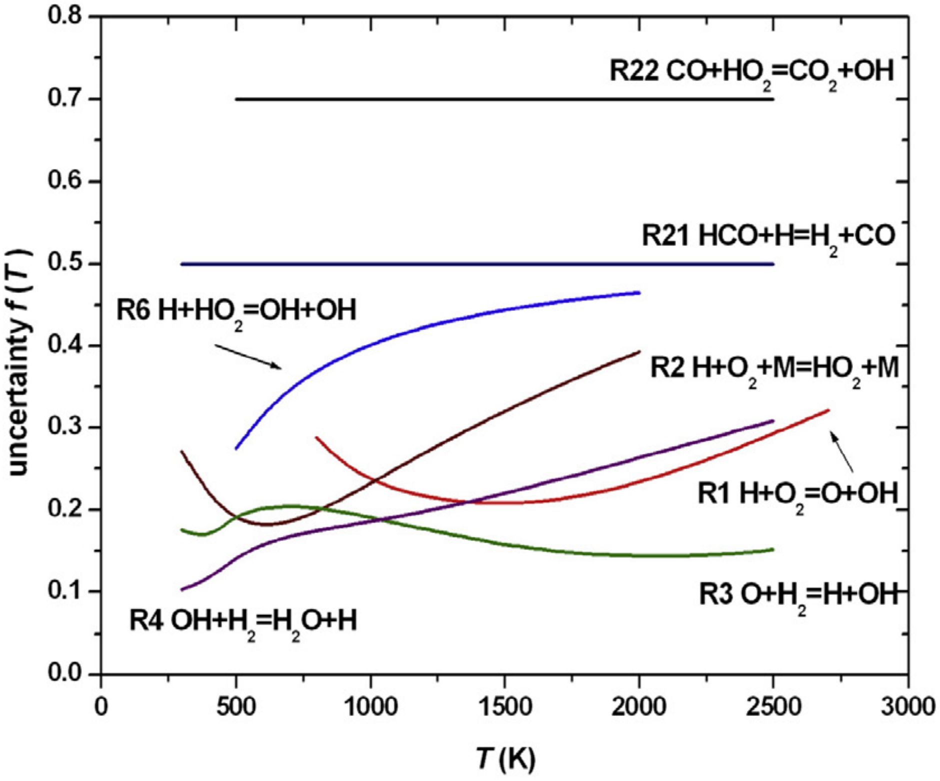

Examples of uncertainties for 7 of the 22 reactions studied. All taken from H_2 and syngas combustion mechanisms

Topic 6
Chemical mechanisms

Examine ways in which mechanisms are constructed, their dependence on rate and thermodynamic data, their evaluation using experimental targets and the optimization of component rate constants using direct and indirect data

Approaches to mechanism development

- Manual construction. Assemble mechanism by including all relevant reactions.
- Include rate constants, based on evaluations, experimental measurements, calculations, optimized rate constants from model / measurement comparisons. Should be kept updated but legacy mechanisms exist.
- Reverse rate constants from thermodynamic data.
- Mechanisms tested against experimental data, e.g. for ignition delay times.
- Many mechanisms include tuned rate constants. Great care is needed.
- Automatic mechanism generation methods available.

Numbers of species and reactions in mechanisms for combustion of hydrocarbon fuels (Lu and Law, Prog En Comb Sci, 2009, 35, 192, updated Yuan et al, Science China (Chemistry), 2017, 60, 1391)

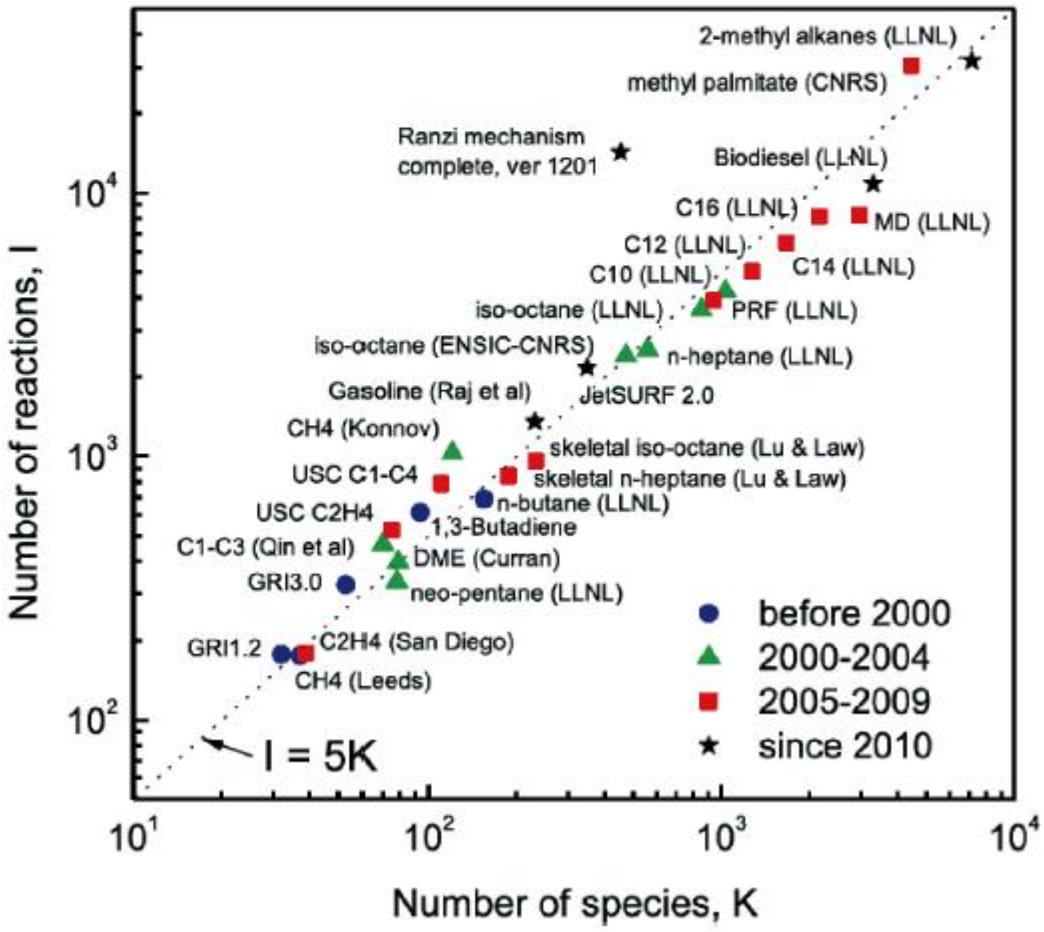

- Larger mechanisms require thousands of rate constants.
- Can't measure them all – calculation essential

Techniques used to evaluate mechanisms

Ignition time delay

A. Shock tube:

time interval between the arrival of the reflected shock and the onset of ignition determined, for example, by extrapolating the maximum slope of OH* signal back to the baseline.

Shao et al, Proc Comb Inst, 2019, 37, 4555

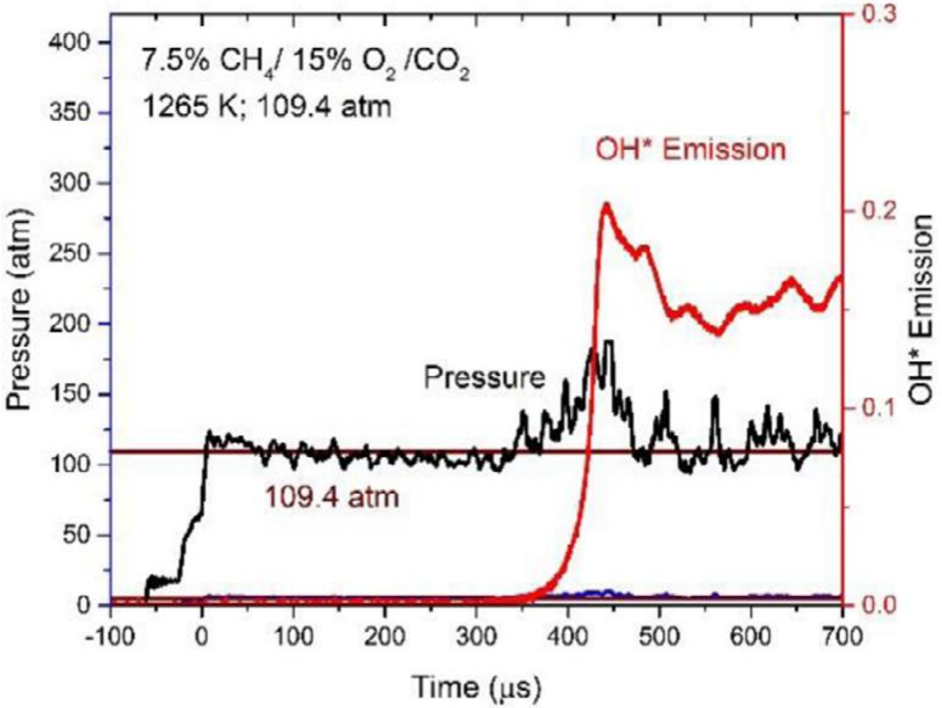

B. Rapid compression machine (RCM)

See discussion by Keromnes et al(Comb Flame, 2013, 160, 995)

Results shown H2/O2, Mittal et al, Int J Chem Kinet 2006, 38, 516 2006

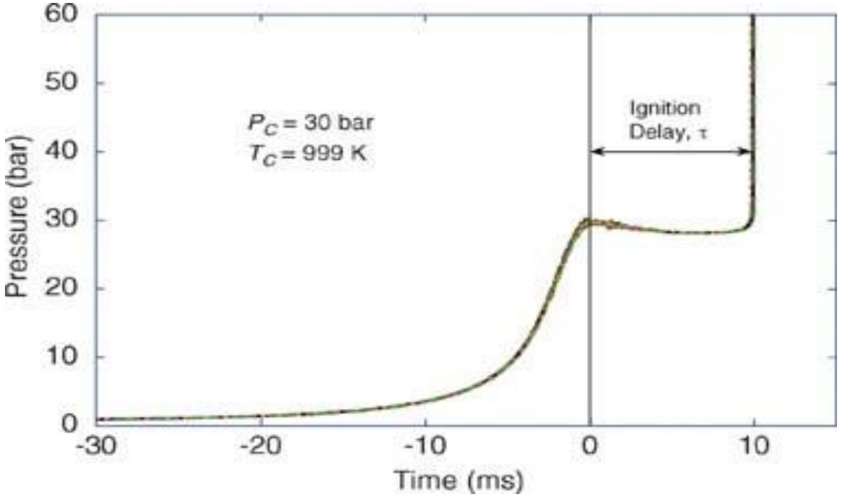

Other methods

- Flame speed
- Measurement of products and of molecular intermediates by spectroscopy, gas chromatography, mass spectroscopy. Techniques used:
  - Shock tubes
  - Flow reactors, especially high pressure
  - Jet stirred reactors
- See for example Comb and Flame, 2014, 161, 2765
- Species (reactants, products and intermediates) widely used for higher hydrocarbons and other fuels. See later slides.

Hierarchical approach to combustion mechanisms

- Westbrook and Dryer, Proc. Comb. Inst. 18 (1981) 749–766, Prog. Energy Combust. Sci. 10 (1981) 1–57. Construction of comprehensive, hierarchical chemical mechanisms.
- Build mechanisms up with increasing complexity – O_2 + (i) H_2 (ii) CO/H_2O (iii) CH_4 …… (Figure below from CRECK)

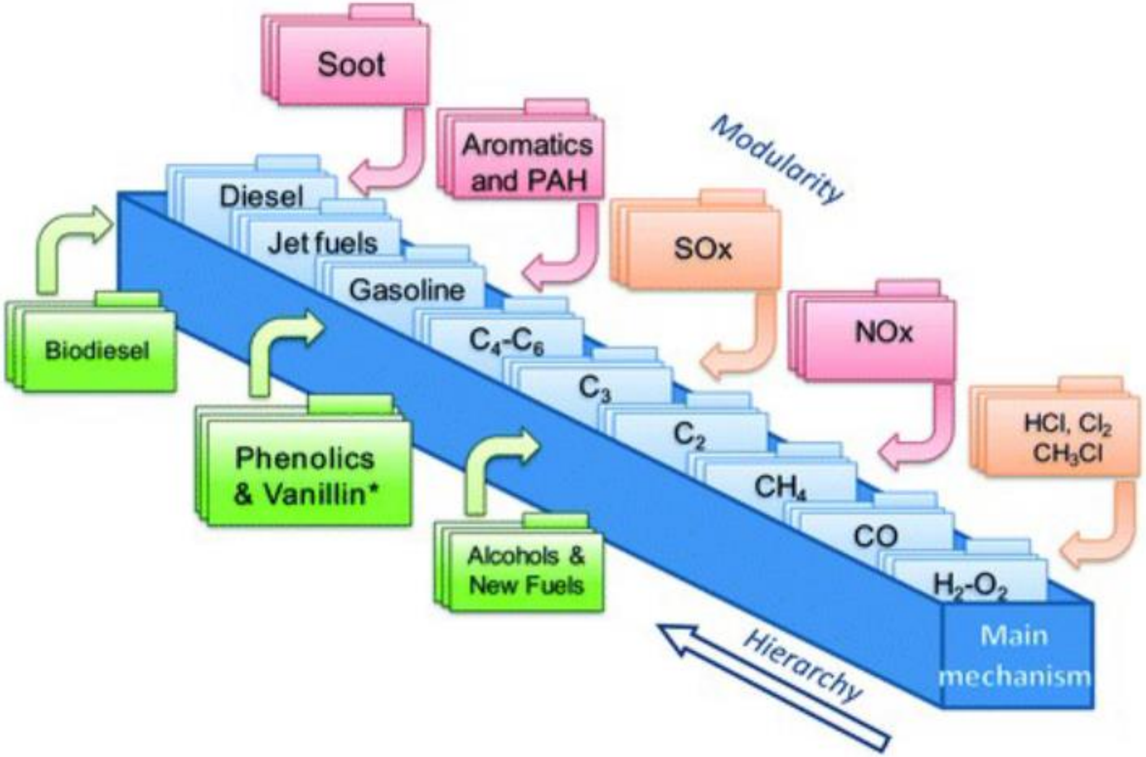

Pelucchi , 2019

Sensitivity analysis in combustion modelling

To which reaction (rate constant) is the model most sensitive?

Local first-order sensitivity coefficient

$$S_{ij} = \frac{\partial Y_i}{\partial x_j}$$

Normalised first-order sensitivity coefficient

$$S'_{ij} = \frac{x_j}{Y_i}\,\frac{\partial Y_i}{\partial x_j}$$

Y is an observable, such as ignition delay time, $[\mathrm{OH}]$ or T; x is an input parameter such as a rate constant

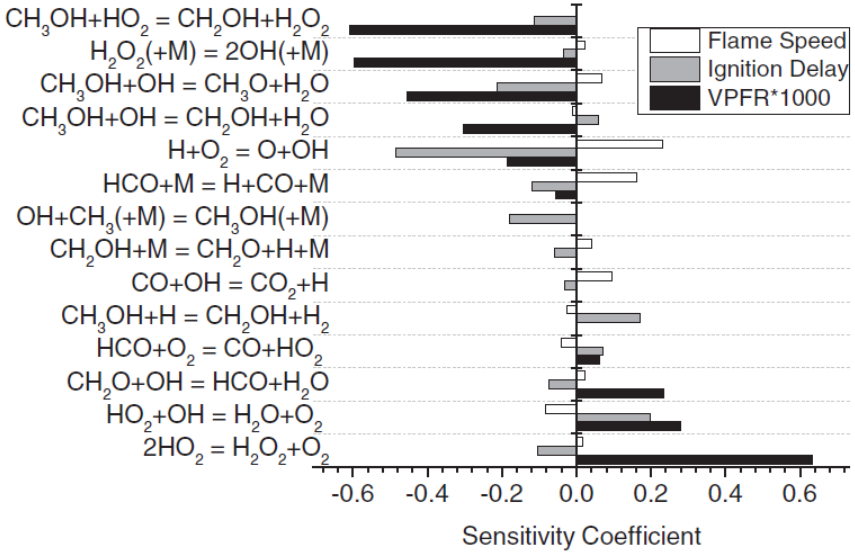

Sensitivity coefficients for flow reactor, shock tube and laminar premixed flame studies of methanol combustion

Uncertainty contributions

- How much does a parameter contribute to model uncertainty?
- Some parameters have high sensitivity but are well quantified
- Other may have lower sensitivity but are have a high uncertainty
- The overall uncertainty is given by

$$\sigma^2(\mathbf{Y}) = \sum_j (\mathbf{S}'_j)^2 \frac{\sigma^2(x_j)}{x^2{}_j}$$

- where $\sigma(x_j)$ is the known, or estimated, uncertainty (standard deviation) for parameter x_j and σ the overall uncertainty.
- The fractional contribution of each parameter to this uncertainty can be estimated
- Allows us to understand better which parameters need further study to reduce the overall modelling uncertainty

The role of sensitivity and uncertainty analysis in combustion modelling (A S Tomlin, Proc Comb Inst 34 (2013) 159-176)

- significant uncertainties in the data used to parameterise combustion models still exist.
- input uncertainties propagate through models of combustion devices leading to uncertainties in the prediction of key combustion properties.
- focus efforts on those parameters which drive predictive uncertainty, which may be identified through sensitivity analysis.
- Paper discusses how sensitivity and uncertainty analysis can be incorporated into strategies for model improvement

Examples of H_2 + O_2 mechanisms

- Li et al. Int J Chem Kinet 36, (2004) 566–575 based on earlier mechanism by Mueller et al. Updated Burke et al, Int J Chem Kinet 44: 444-474, 2012
- Konnov, Combustion and Flame 152 (2008) 507–528. Examination of uncertainties in rate coefficients based on earlier (2004)mechanism
- Hong et al., Comb and Flame, 158, (2011) 633-644
- Keromnes et al Comb and Flame 160 (2013) 995–1011. Also includes syngas (CO + H_2)
  - Test mechanism against ignition delay times and flame velocities
  - Emphasis on high pressures (up to 70 bar)
  - 31 reaction mechanism for H_2 + CO

Reminder from Topic 1

1	$H_2 + O_2 \rightarrow .H + .HO_2$	initiation
2	$.OH + H_2 \rightarrow .H + H_2O$	propagation
3	$.H + O_2 \rightarrow .OH + :O$	branching
4	$:O + H_2 \rightarrow .OH + .H$	branching
5	$.H + O_2 + M \rightarrow .HO_2 + M$	termination*
6	$.H \rightarrow \text{wall}$	termination
7	$:O \rightarrow \text{wall}$	termination
8	$.OH \rightarrow \text{wall}$	termination
9	$.HO_2 + H_2 \rightarrow .H + H_2O_2$	initiation *
10	$2\ .HO_2 \rightarrow H_2O_2 + O_2$	termination
11	$H_2O_2 \rightarrow 2\ .OH$	initiation, branching

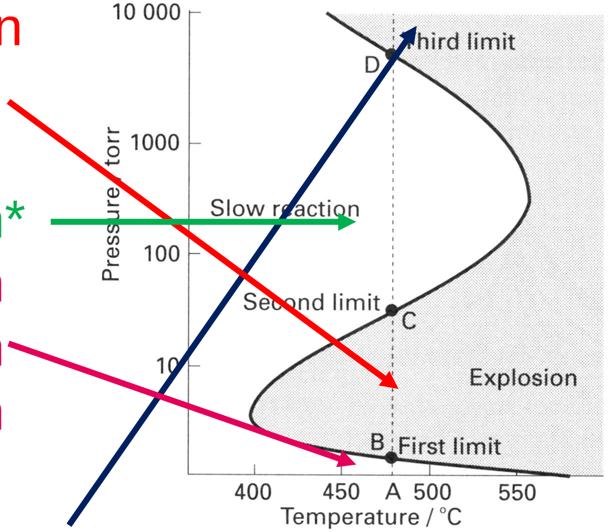

above the 3rd explosion limit

Reactions (9), (10), and (11) become important. While reaction 10 has been classed as a termination, it is a key reaction in this region, because it forms H_2O_2, which leads to branching

Testing mechanisms against global observables: Li et al

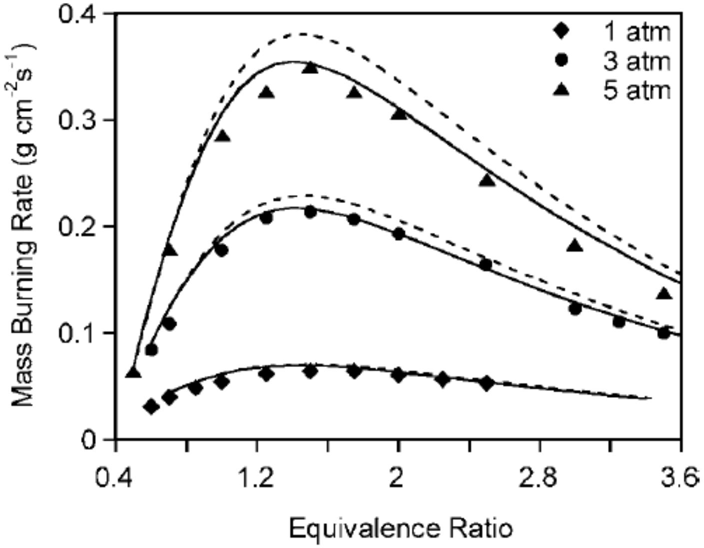

Figure 7 Laminar flame mass burning rate at 1, 3, and 5 atm for $H_2/O_2/He$ mixture (O_2:He = 1:7). Symbols: experimental data [7]; solid lines: the present model; dashed lines: the model of Mueller et al. [1].

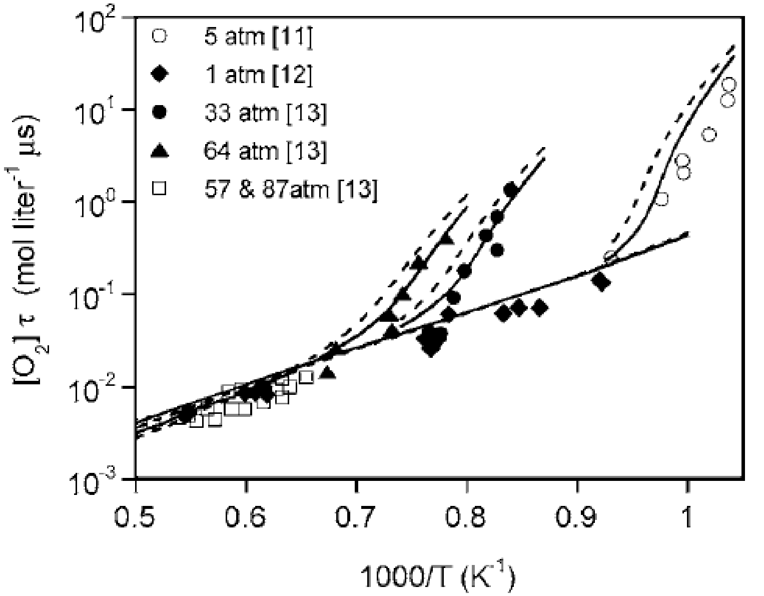

Figure 11 Ignition delay of $H_2/O_2/Ar$ mixtures in shock tubes. Initial conditions: $H_2 = 8.0\%$, $O_2 = 2.0\%$ at 5 atm [11]; $H_2 = 1.0\%$, $O_2 = 2.0\%$ at 1 atm [12]; $H_2 = 2.0\%$, $O_2 = 1.0\%$ at 33, 57, 64, and 87 atm [13]. Symbols: experimental data [11–13]; solid lines: the present model; dashed lines: Mueller et al. [1]. Ignition delay time for the cases of Ref. [11] is defined by the maximum of OH concentration; for Ref. [12], as the time when OH concentration reaches 1×10^{-6} mol/L; and for Ref. [13], by the maximum of $\frac{d[OH]}{dt}$.

Hong et al.
Revised mechanism using own shock tube data on
$H + O_2 \rightarrow OH + O$, $H_2O_2 + M$, $OH + H_2O_2$, $OH + HO_2$

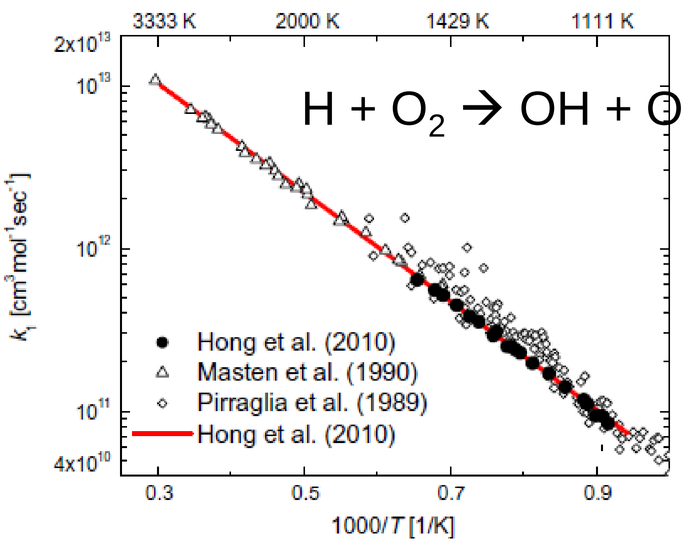

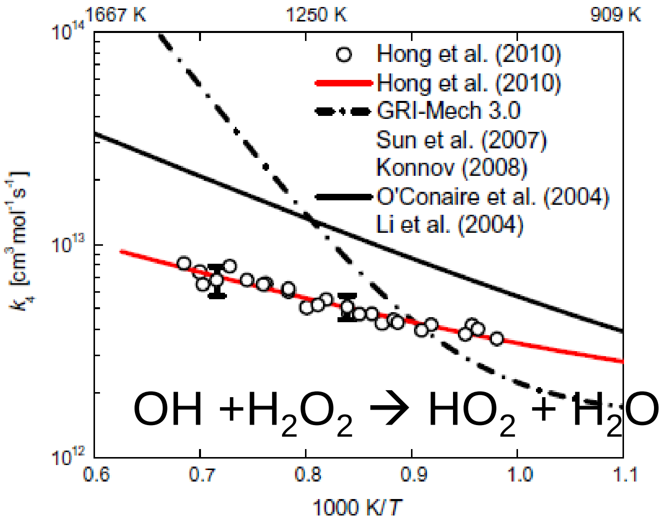

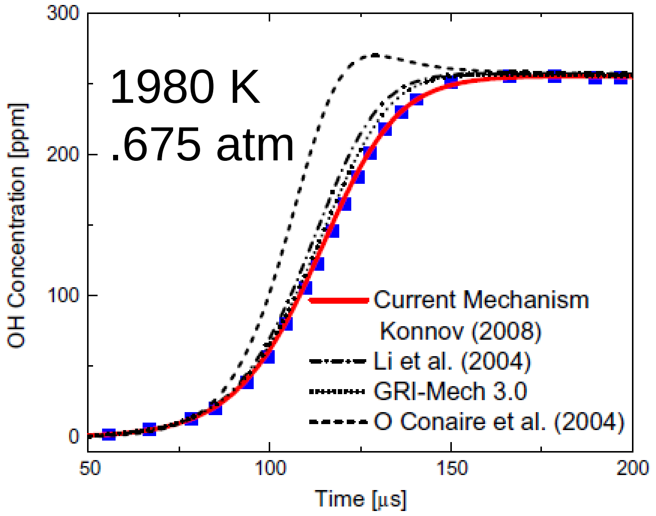

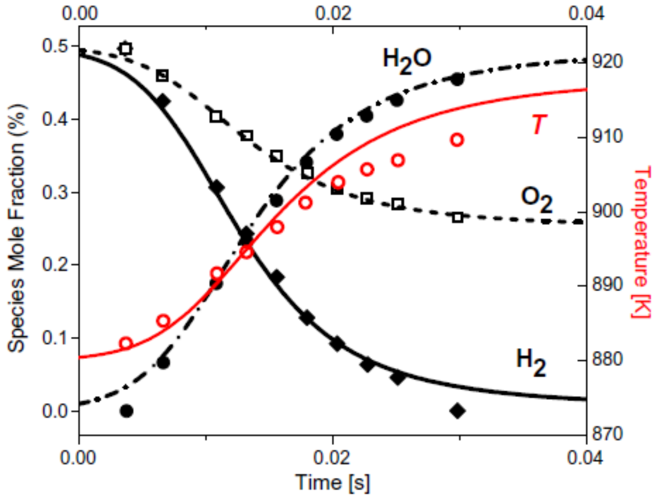

Species profiles, 880 K, 0.3 atm

Burke et al. (see also topic 1)

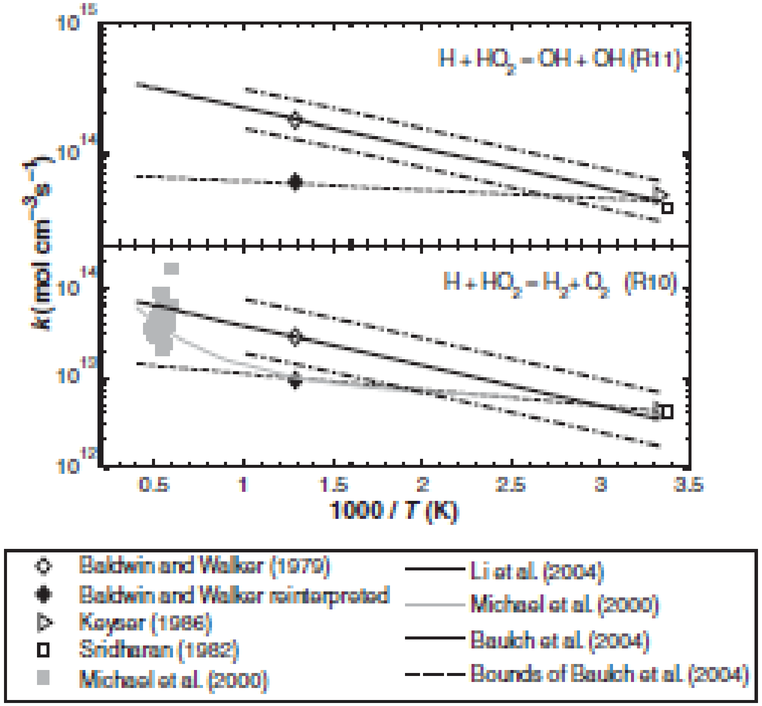

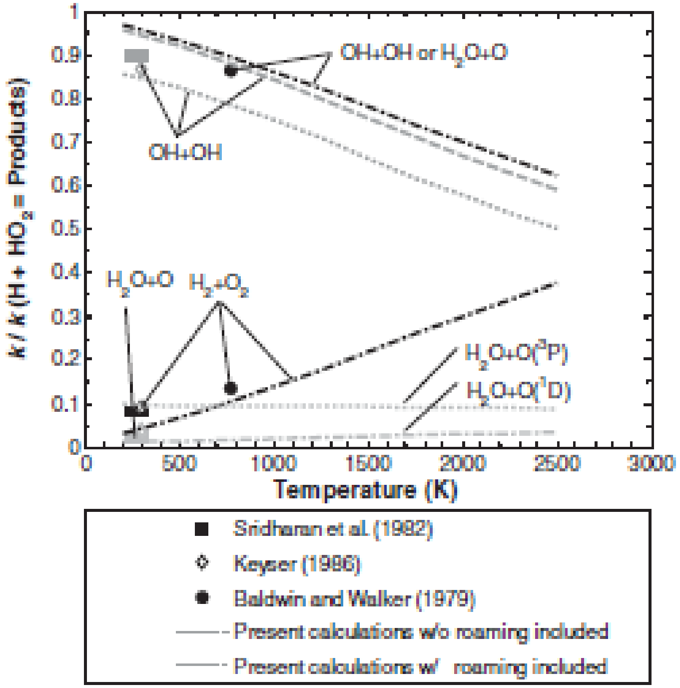

$H + HO_2$

Branching ratios

Sensitivity analysis
(Burke et al)

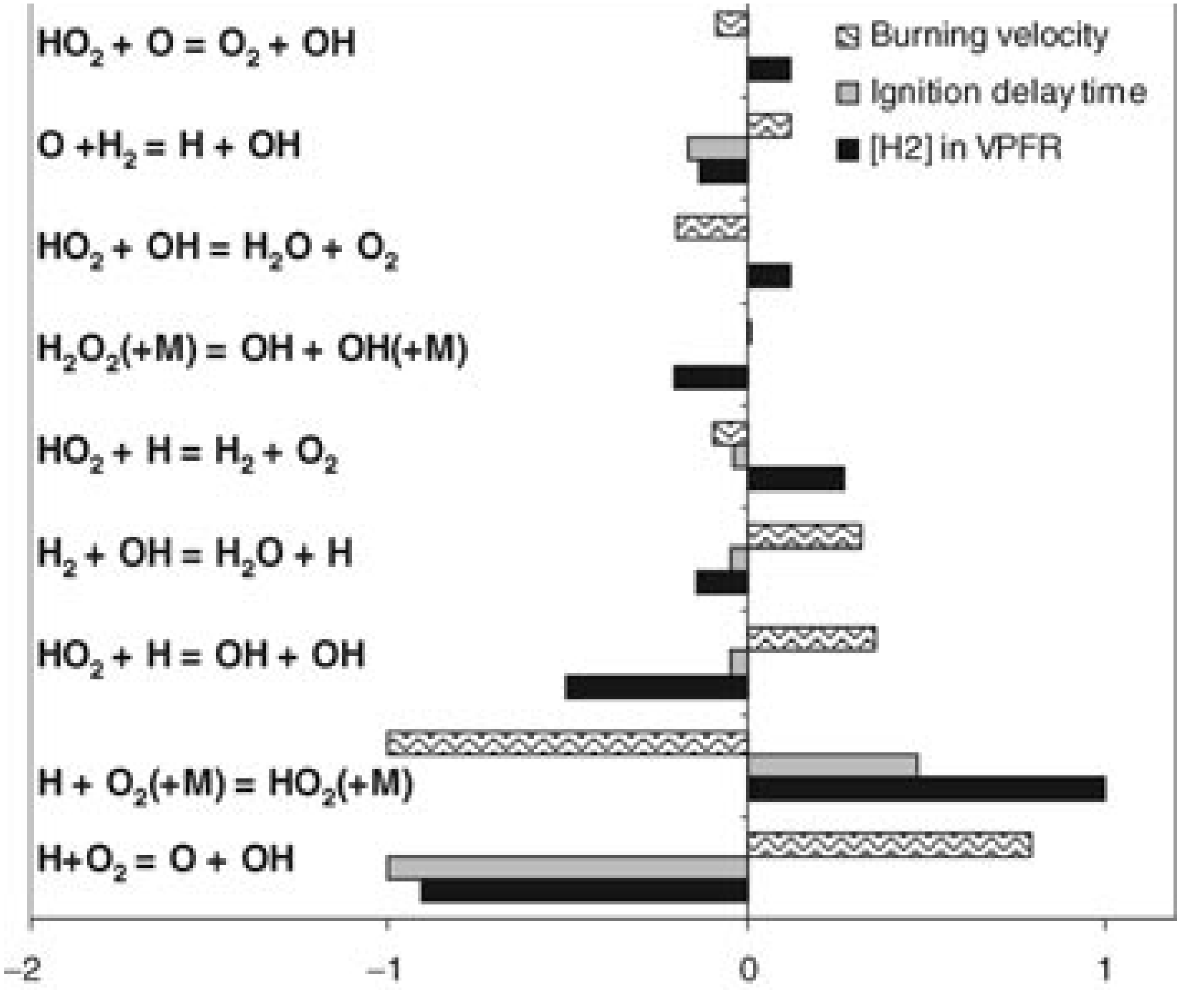

Dependence of H_2+O_2 reaction characteristics on T and p, including high pressures (Keromnes et al. 2013)

Main reactions as a function of p

32 bar

16 bar

8 bar

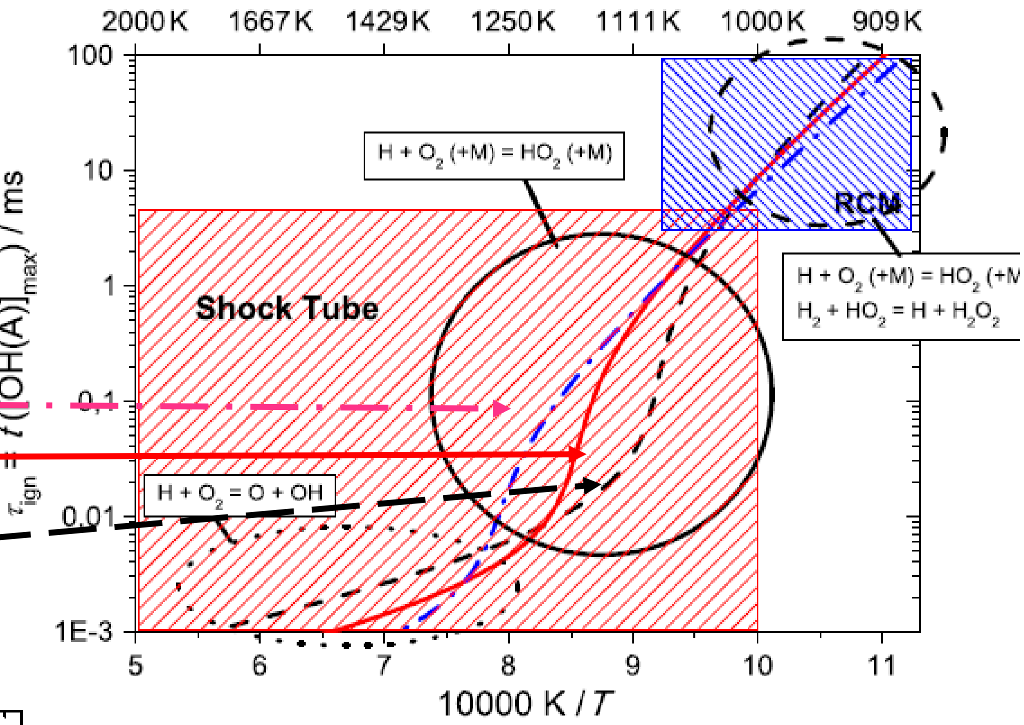

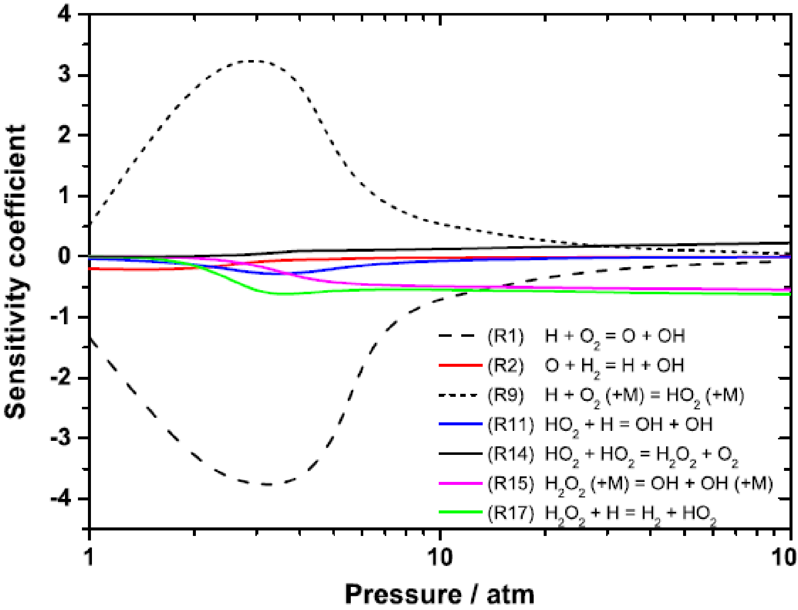

Sensitivity analysis for ignition time delays vs pressure 1000 K, N_2 and Ar diluent.

SYNGAS ($CO + H_2$)

- Comparison of the performance of several recent syngas combustion mechanisms (Olm et al., Combustion and Flame, 2015, 162, 1793
- 16 mechanisms, tested against measurements of (bracketed: numbers of datasets)
  - Ignition delay time: ST (62), RCM (47)
  - Flame velocity (217)
  - Species concentrations: Flow reactors (58), ST (21), JSR (3)
- Five mechanisms performed better than others.
- Sensitivity analysis used to identify key reactions and those requiring further study.

Comparison of rate constants for most sensitive reactions

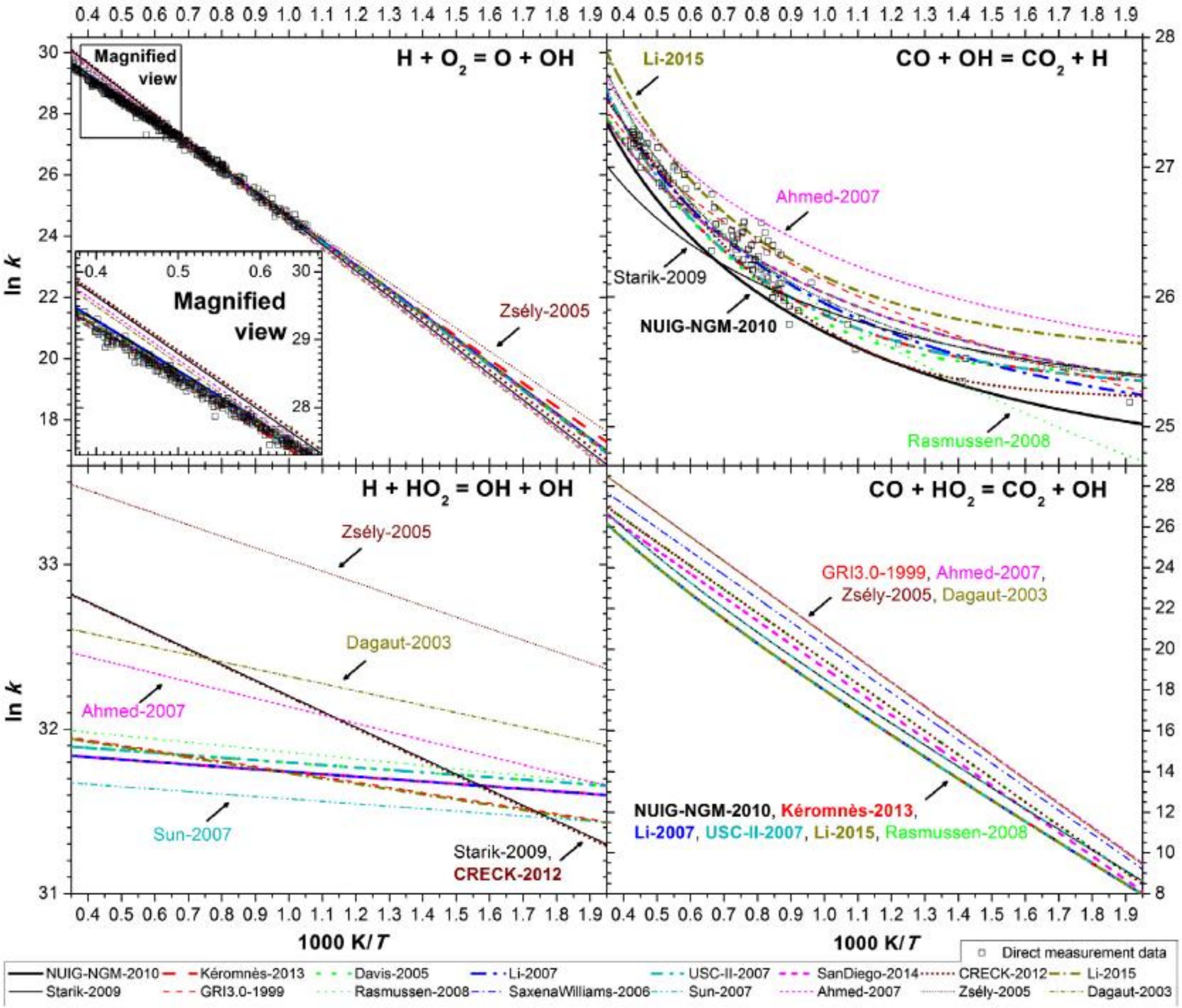

High-pressure oxidation of methane (Hashemi et al, Combustion and Flame 2016, 172, 349–364)

- Combined experiment (laminar flow reactor (LFR), rapid compression machine (RCM)) and high-level theory.
- LFR: 700-900 K, 100 bar, ϕ = 0.06-19.7
- RCM: 800 – 1250 K, 15 – 80 bar, , ϕ = , 0.5, 1.0
- Theory (all high level, comparable to HEAT)
  - thermodynamic properties of CH_3OO and CH_3OOH (2σ uncertainty of 0.2-0.3 kcal mol^{-1};
  - rate constants for the abstraction reactions $CH_3OOH + CH_3 = CH_3OO + CH_4$ and $CH_3OH + CH_3 = CH_3O + CH_4$, included treatment of internal rotors and using variational transition state theory (VTST)

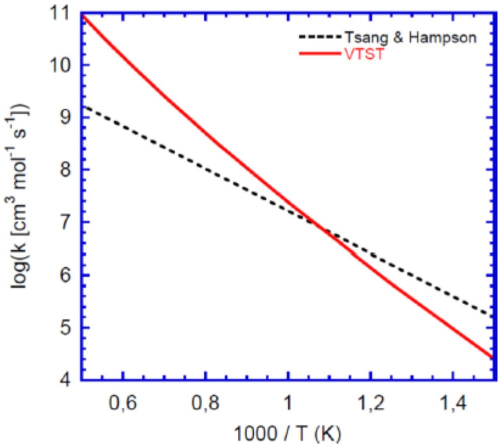

Tsang and Hampson is an evaluation from 1986

Methanol underpredicted in model

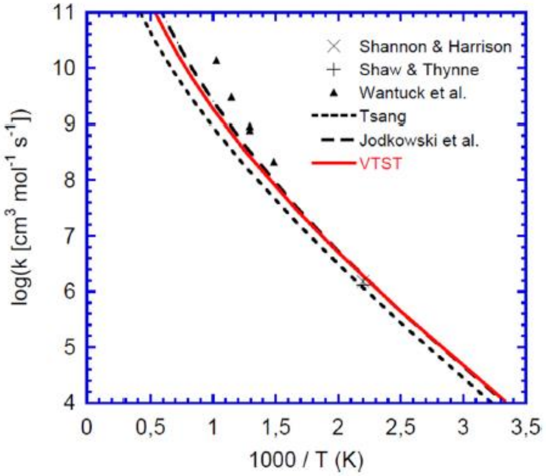

Comparison of METHANE Combustion Mechanisms Using Shock Tube and Rapid Compression Machine Ignition Delay Time Measurements

Zhang et al., Energy Fuels 2021, 35, 12329–12351

- Shock tubes: (4939 data points in 574 datasets) and in RCMs (582 data points in 69 datasets).
- Wide range of temperature, pressure and equivalence ratio
- 13 recent methane combustion mechanisms examined.
- SanDiego-2014, Caltech-2015, Aramco-II-2016, and Glarborg-2018 were found to be the most accurate mechanisms under Shock Tube experimental conditions
- Aramco-II-2016 had the smallest prediction error under RCM conditions.
- Local sensitivity analysis was carried out to identify the critical reaction steps for improving the methane combustion models.

Temperature and pressure ranges of the original methane IDT experimental data originally used in the validation of the mechanisms

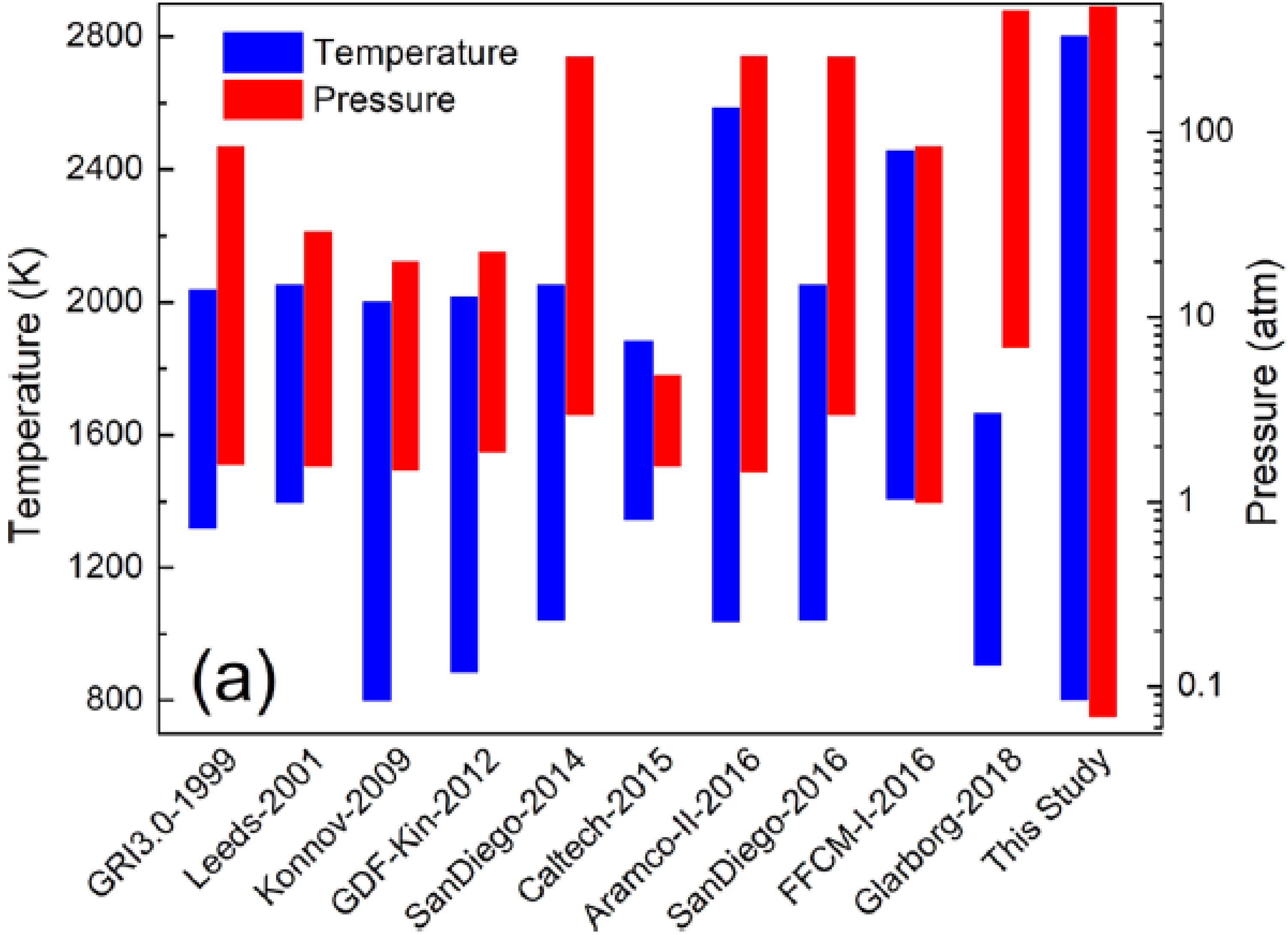

Sensitive reactions

Most sensitive:

$H + O_2 = O + OH$

$CH_4 + H = CH_3 + H_2$

$HO_2 + HO_2 = H_2O_2 + O_2$

$CH_3 + O_2 = CH_2O + OH$

$CH_3 + O_2 = CH_3O + O$

Second most sensitive set:

$CH_4 + OH = CH_3 + H_2O$

$OH + H_2 = H + H_2O$

$CH_4 + O = CH_3 + OH$

$CH_3 + H + M = CH_4 + M$

$H + O_2 + M = HO_2 + M$

$CH_4 + HO_2 = CH_3 + H_2O_2$

$CH_3 + O_2$

- At lower *T* the main route is formation of CH_3OO(A). As *T* increases CH_3OO starts to dissociate
- PE curves (B: Walch) show two higher temperature channels:
- HCHO + OH formation lower barrier but involves curve crossing: small A factor
- CH_3O + O high barrier, but large A factor
- Arrhenius plot (C: Srinivasan et al; large uncertainties)

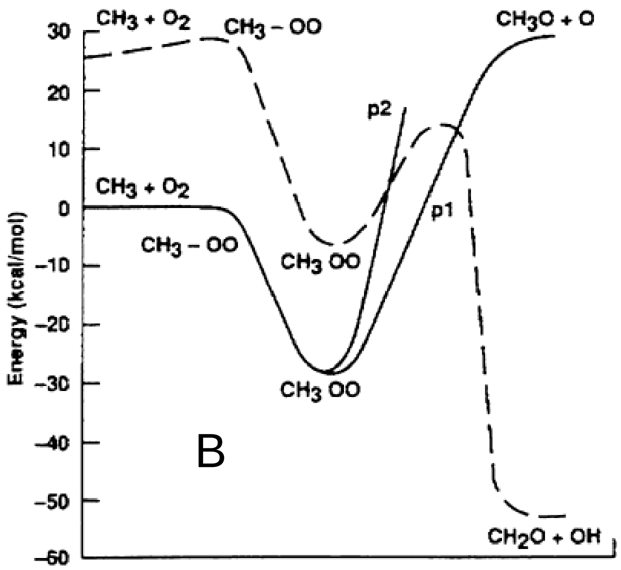

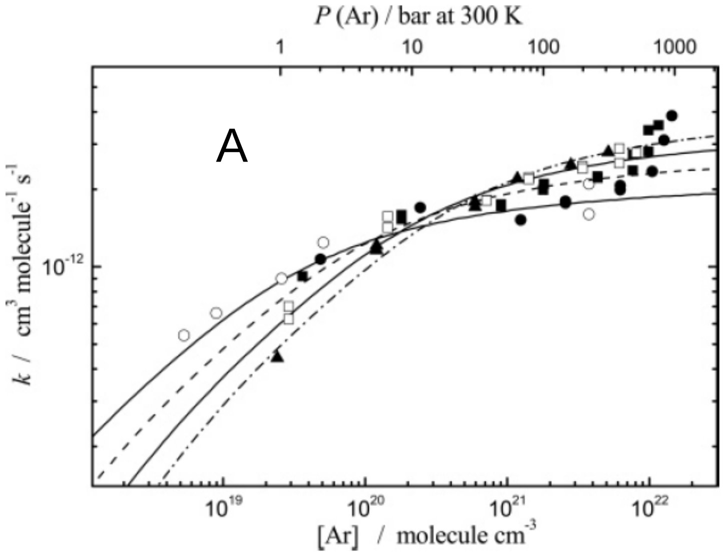

Figure 4. Rate constants *k* for the reaction $CH_3 + O_2\ (+ M) \rightarrow CH_3O_2\ (+ M)$ with M = Ar. Lines from top to bottom at 10^{19} molecule cm^{-3} for 300, 400, 500, and 600 K, respectively, constructed with eqs 4.1–4.3. Experimental results: ●, 300; ■, 400; □, 500; ▲, 600 K from this work; ○, 300 K from ref 4.

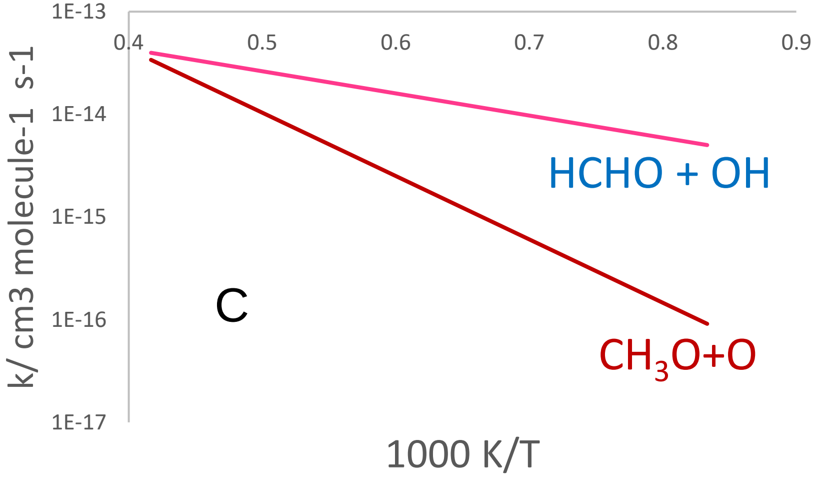

Conclusions from Zhang et al.

- Four mechanisms (SanDiego-2014, Caltech-2015, Aramco-II-2016, and Glarborg-2018) showed the lowest overall errors for STs and Aramco-II for RCMs, but performance varied depending on conditions.
- If an accurate methane combustion mechanism is needed under a specific range of conditions, it can be selected based on graphical data given in the paper.
- For high-temperature ignitions, the rate coefficients of the most sensitive reactions of all the four mechanisms were close to each other, except for $CH_3+O_2 = CH_2O + OH$: highly sensitive in all mechanisms but very different rate parameters used. Reaction needs further study.
- Rate parameters of reactions involving peroxides, HO_2, and H_2O_2 must be known more accurately in order to improve the performance of the mechanisms at low temperatures.

Comparison of methane combustion mechanisms using laminar burning velocity measurements
(Zhang et al, 2022, 111,11867)

- 5500 data points in 646 datasets for methane + H_2 + CO in a range of diluents.
- 12 mechanisms studied, Aramco-II-2016, Konnov-2009, Caltech-2015 and Glarborg-2018 have the lowest average errors.
- 29 important elementary reactions, - not present in all the 12 mechanisms.
- Also assembled data from measured and theoretically calculated rate constants.
- Adding missing sensitive rate constants significantly improved performance of mechanisms
- Key missing reactions: $CH_3 + O \rightarrow CO + H + H_2$ and $HCHO + H \rightarrow H_2 + CO + H$; both reactions involve prompt dissociation of the initially formed HCO. Rapid HCO dissociation also discussed by Hashemi et al (see earlier for reference)

Chemical regimes in methane-air ignition
Valko et al, Proceedings of the Combustion Institute 2022

- Ignition simulations + local sensitivity calculations of CH_4 – air mixtures with Aramco-II-2016 mechanism: 14,417 combinations of initial temperature (500 - 3000 K), initial pressure (0.05 –500 atm) and ϕ (0.05 –8.0).
- Five well-defined kinetic regions, well defined borders, different sets of important reactions and linked kinetic schemes.

#	*T*/K	*p*/atm	ϕ	Number points
1	800-1100	6.4-500	0.15-8	214
2	1000-2000	0.05-500	0.05-8	328
3	2000-3000	0.05-117	0.05-3.5	3
4	1500-3000	0.05-308	1.5-8	0
5	1400-3000	0.05-500	0.1-7.5	237

- Regions well-defined but intervals overlap – see 3d figure to understand
- Some regions very poorly characterized with IDT measurements – need experiments

Region 1 CH_3O_2/CH_3O_2H

800-1100 K, 6.4-500 atm, ϕ=0.15-8

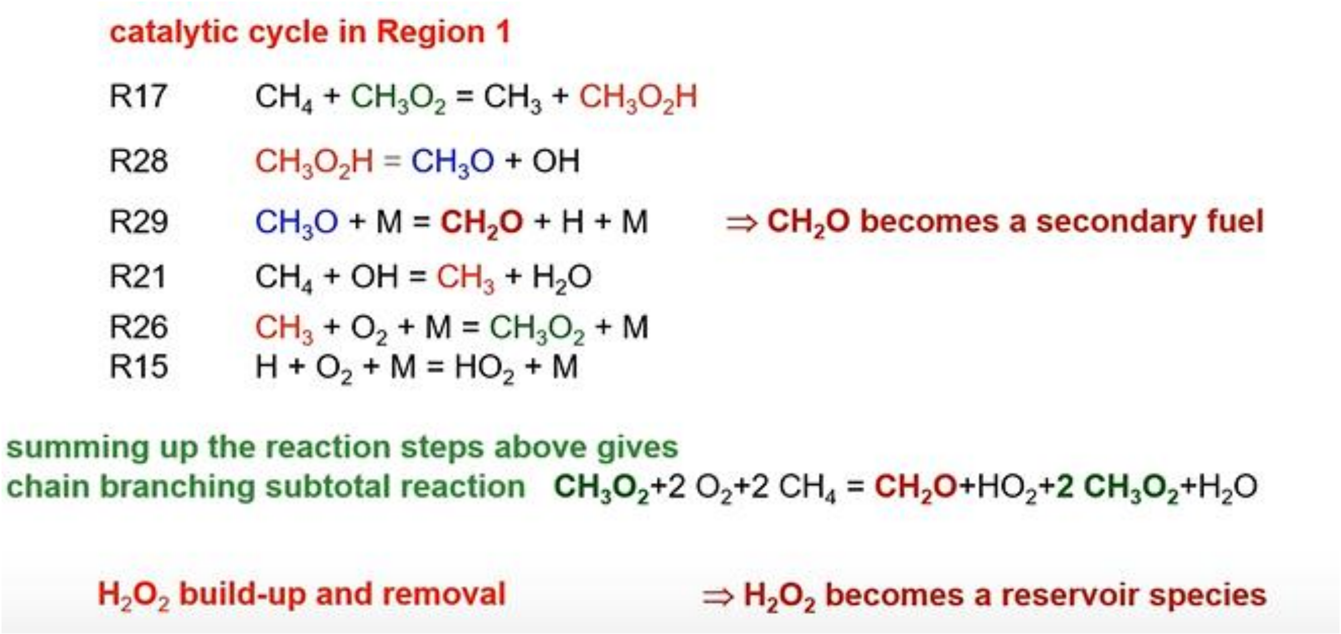

catalytic cycle in Region 1

R17 $CH_4 + CH_3O_2 = CH_3 + CH_3O_2H$

R28 $CH_3O_2H = CH_3O + OH$

R29 $CH_3O + M = \mathbf{CH_2O} + H + M$ ⇒ **CH_2O becomes a secondary fuel**

R21 $CH_4 + OH = CH_3 + H_2O$

R26 $CH_3 + O_2 + M = CH_3O_2 + M$

R15 $H + O_2 + M = HO_2 + M$

summing up the reaction steps above gives
chain branching subtotal reaction $\mathbf{CH_3O_2}+2\ O_2+2\ CH_4 = \mathbf{CH_2O}+HO_2+\mathbf{2\ CH_3O_2}+H_2O$

H_2O_2 build-up and removal ⇒ **H_2O_2 becomes a reservoir species**

R8 $CH_4 + HO_2= CH_3 + \mathbf{H_2O_2}$

R14 $2HO_2 = \mathbf{H_2O_2} + O_2$

R9 $H_2O_2 + M = 2\ OH + M$

Region 2 HO_2/ H_2O_2/CH_3O

1000-2000 K, 0.05-500 atm, ϕ=0.05-8

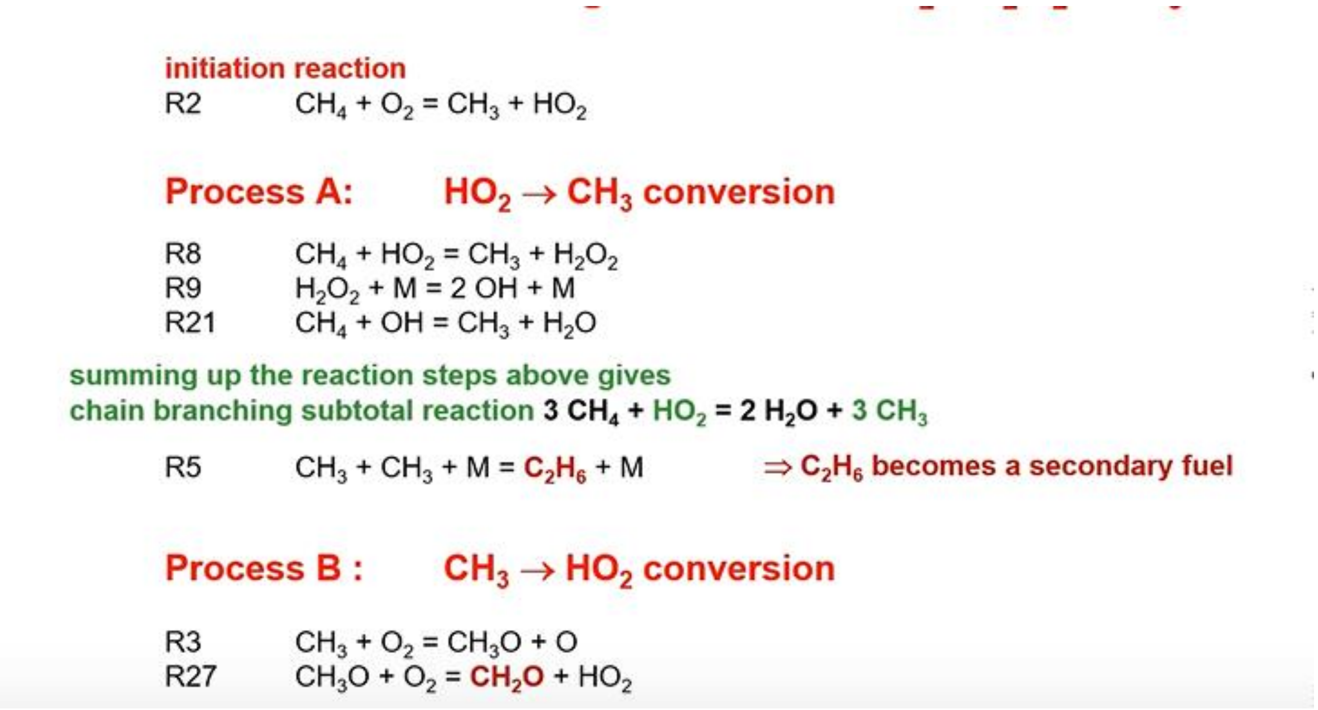

initiation reaction

R2 $CH_4 + O_2 = CH_3 + HO_2$

Process A: $HO_2 \rightarrow CH_3$ conversion

R8 $CH_4 + HO_2 = CH_3 + H_2O_2$

R9 $H_2O_2 + M = 2\ OH + M$

R21 $CH_4 + OH = CH_3 + H_2O$

summing up the reaction steps above gives

chain branching subtotal reaction $3\ CH_4 + HO_2 = 2\ H_2O + 3\ CH_3$

R5 $CH_3 + CH_3 + M = C_2H_6 + M$ **⇒ C_2H_6 becomes a secondary fuel**

Process B : $CH_3 \rightarrow HO_2$ conversion

R3 $CH_3 + O_2 = CH_3O + O$

R27 $CH_3O + O_2 = CH_2O + HO_2$

Summing up the above reaction steps gives

Chain branching subtotal reaction $CH_3 + 2\ O_2 = HO_2 + O + CH_2O$

CH_2O becomes a secondary fuel

Region 3 H/O/OH + CH_3O/HCO
2000-3000 K, 0.05-117 atm, ϕ=0.05-3.5

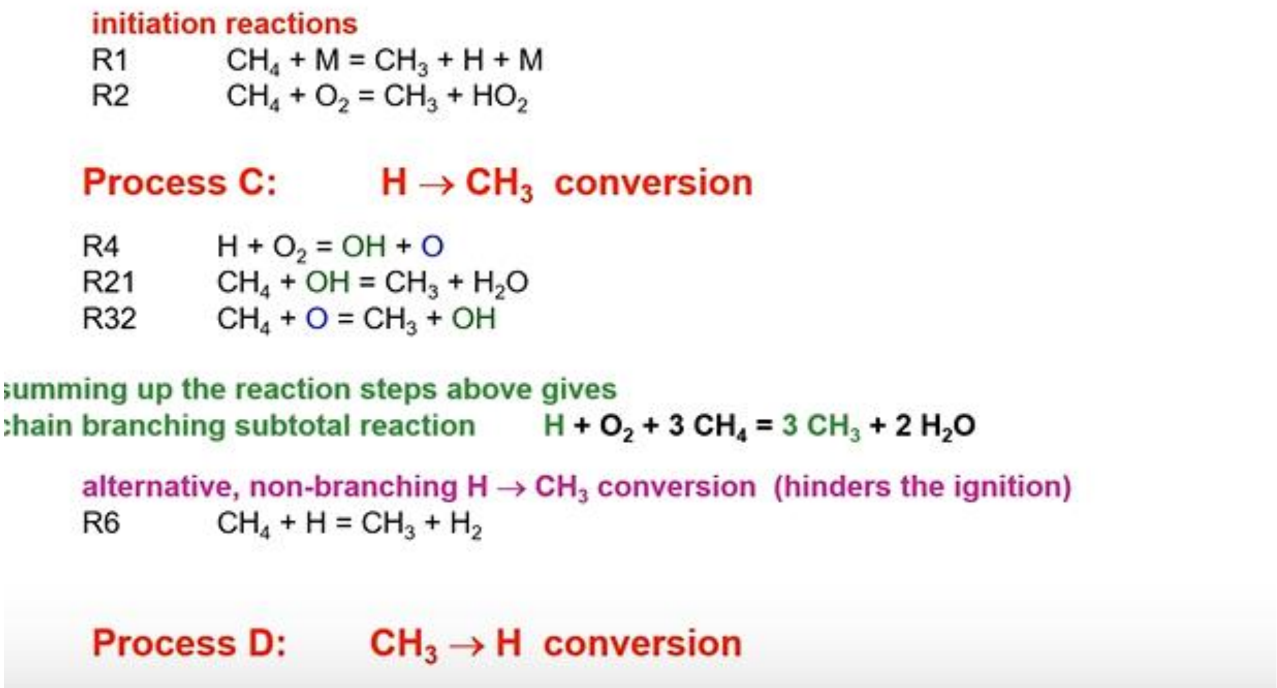

initiation reactions

R1 $CH_4 + M = CH_3 + H + M$

R2 $CH_4 + O_2 = CH_3 + HO_2$

Process C: $H \rightarrow CH_3$ conversion

R4 $H + O_2 = OH + O$

R21 $CH_4 + OH = CH_3 + H_2O$

R32 $CH_4 + O = CH_3 + OH$

umming up the reaction steps above gives

hain branching subtotal reaction $\mathbf{H + O_2 + 3\,CH_4 = 3\,CH_3 + 2\,H_2O}$

alternative, non-branching $H \rightarrow CH_3$ conversion (hinders the ignition)

R6 $CH_4 + H = CH_3 + H_2$

Process D: $CH_3 \rightarrow H$ conversion

R33 $CH_3 + O = CH_2O + H$

R11 $CH_3 + O_2 = CH_2O = OH$

R10 $CH_2O + O_2 = HCO + HO_2$

R23 $HCO + M = H + CO$

Region 4 H/O/OH + C_2H_5
1500-3000 K, 0.05-308 atm, ϕ=1.5-8

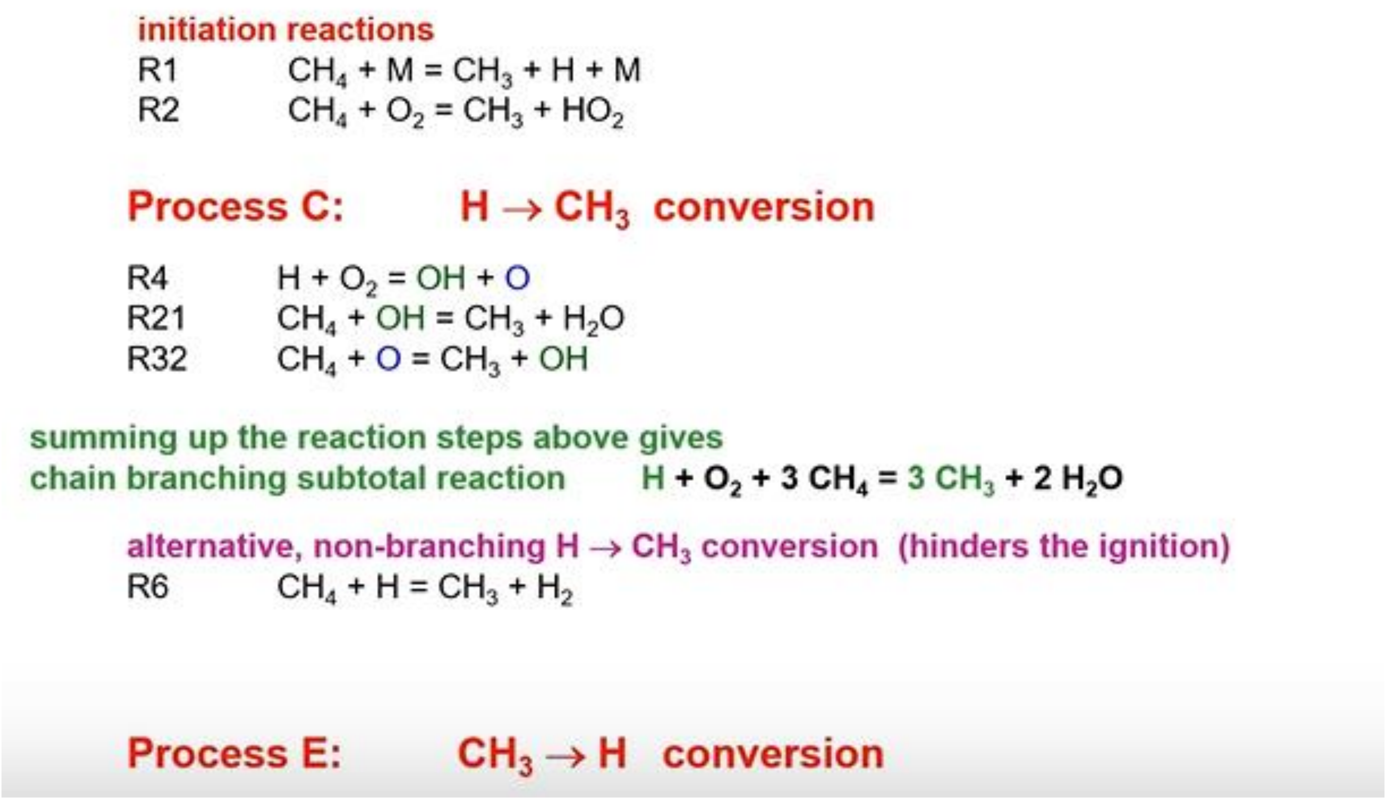

initiation reactions

R1 $CH_4 + M = CH_3 + H + M$

R2 $CH_4 + O_2 = CH_3 + HO_2$

Process C: **$H \rightarrow CH_3$ conversion**

R4 $H + O_2 = OH + O$

R21 $CH_4 + OH = CH_3 + H_2O$

R32 $CH_4 + O = CH_3 + OH$

summing up the reaction steps above gives
chain branching subtotal reaction **$H + O_2 + 3\ CH_4 = 3\ CH_3 + 2\ H_2O$**

alternative, non-branching $H \rightarrow CH_3$ conversion (hinders the ignition)

R6 $CH_4 + H = CH_3 + H_2$

Process E: **$CH_3 \rightarrow H$ conversion**

R7 $CH_3 + CH_3 = C_2H_5 + H$

R36 $C_2H_5 + M = C_2H_4 + H$ **C_2H_4 becomes a secondary fuel**

Region 5 H/O/OH + C_2H_5/OH
1400-3000 K, 0.05-500 atm, ϕ=0.1-7.5

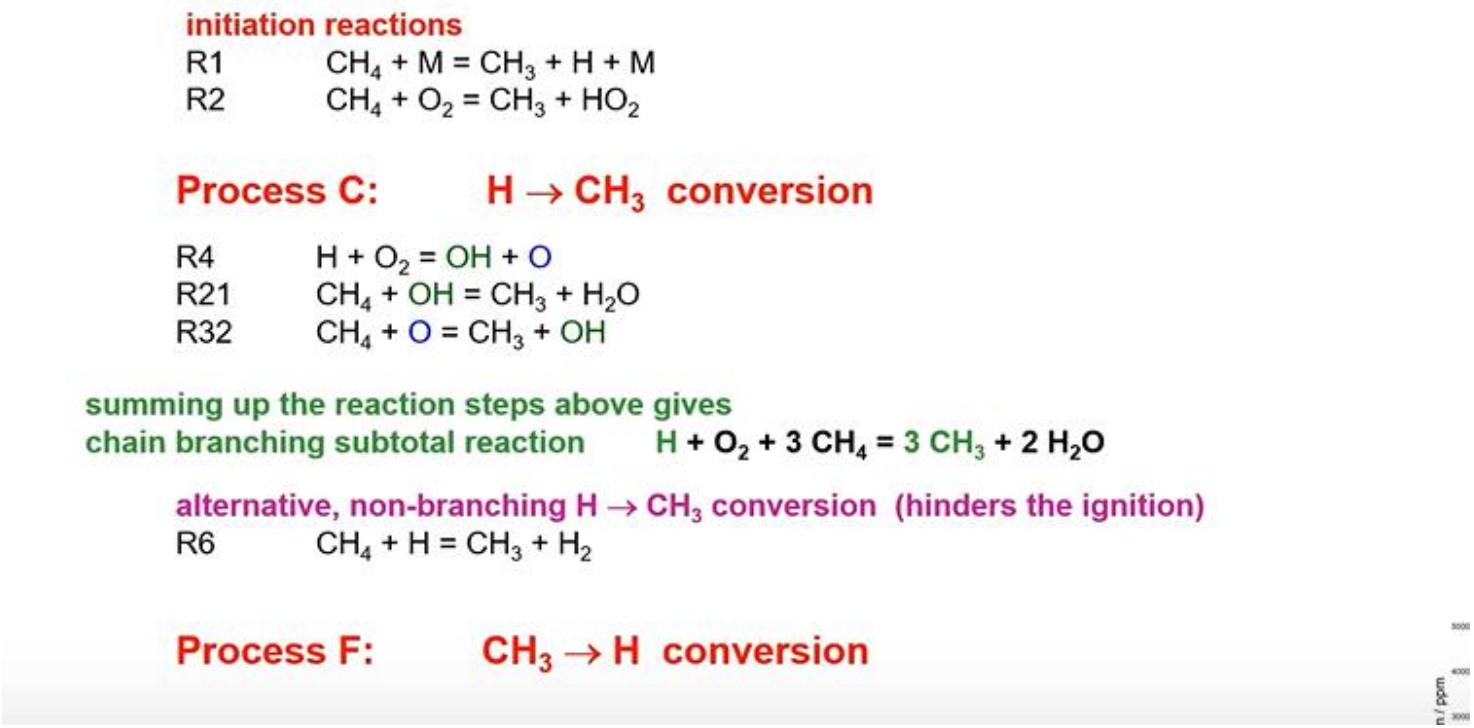

initiation reactions

R1 $CH_4 + M = CH_3 + H + M$

R2 $CH_4 + O_2 = CH_3 + HO_2$

Process C: $H \rightarrow CH_3$ conversion

R4 $H + O_2 = OH + O$

R21 $CH_4 + OH = CH_3 + H_2O$

R32 $CH_4 + O = CH_3 + OH$

summing up the reaction steps above gives
chain branching subtotal reaction **$H + O_2 + 3\ CH_4 = 3\ CH_3 + 2\ H_2O$**

alternative, non-branching $H \rightarrow CH_3$ conversion (hinders the ignition)

R6 $CH_4 + H = CH_3 + H_2$

Process F: $CH_3 \rightarrow H$ conversion

R7 $CH_3 + CH_3 = C_2H_5 + H$

R36 $C_2H_5 + M = C_2H_4 + H$

R33 $CH_3 + O = CH_2O + H$ **CH_2O becomes a secondary fuel**

R11 $CH_3 + O_2 =$ **CH_2O** $+ OH$

R24 $CH_3 + OH = CH_2OH + H$

3d visualization of 5 regions

- Because there are overlaps between the *T*, *p* and / or ϕ intervals, the well-defined regions are best understood from 3d plots
- See video https://youtu.be/CGliv6JbzWc

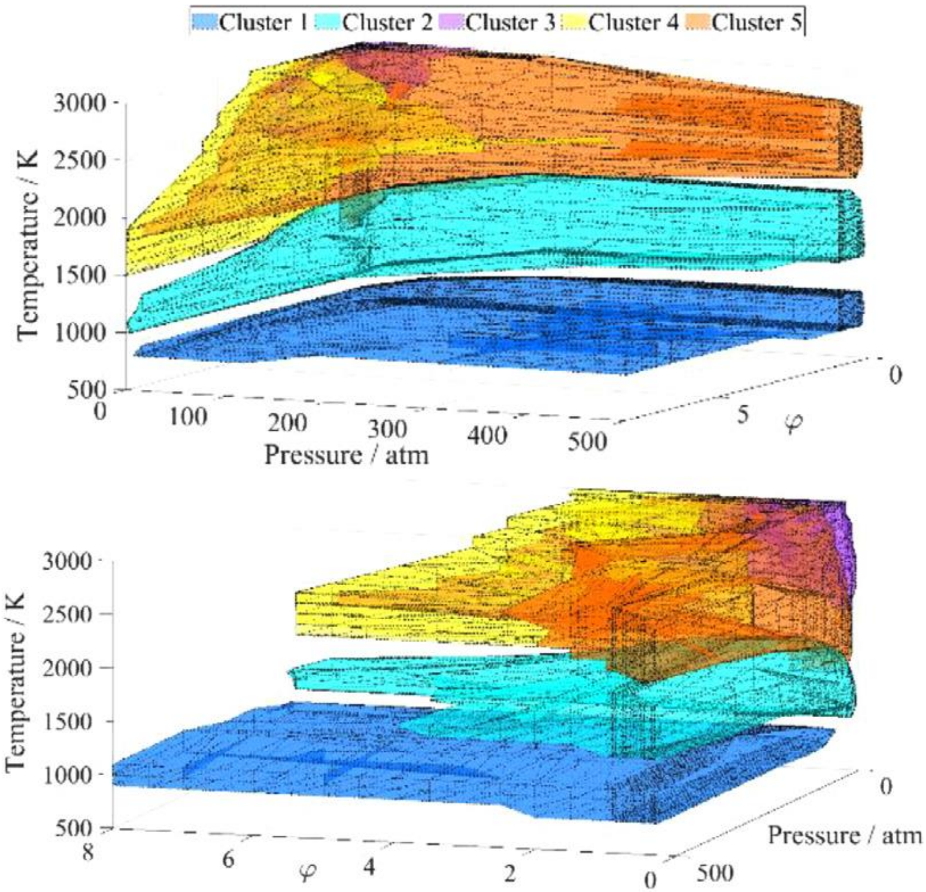

#	*T*/K	*p*/atm	ϕ	Number points
1	800-1100	6.4-500	0.15-8	214
2	1000-2000	0.05-500	0.05-8	328
3	2000-3000	0.05-117	0.05-3.5	3
4	1500-3000	0.05-308	1.5-8	0
5	1400-3000	0.05-500	0.1-7.5	237

More complex fuels: oxygenates and higher hydrocarbons

1. A Hierarchical and Comparative Kinetic Modeling Study of C1–C2 Hydrocarbon and Oxygenated Fuels

Metcalfe et al, Int J Chem Kinet, 45, 638 (2013)

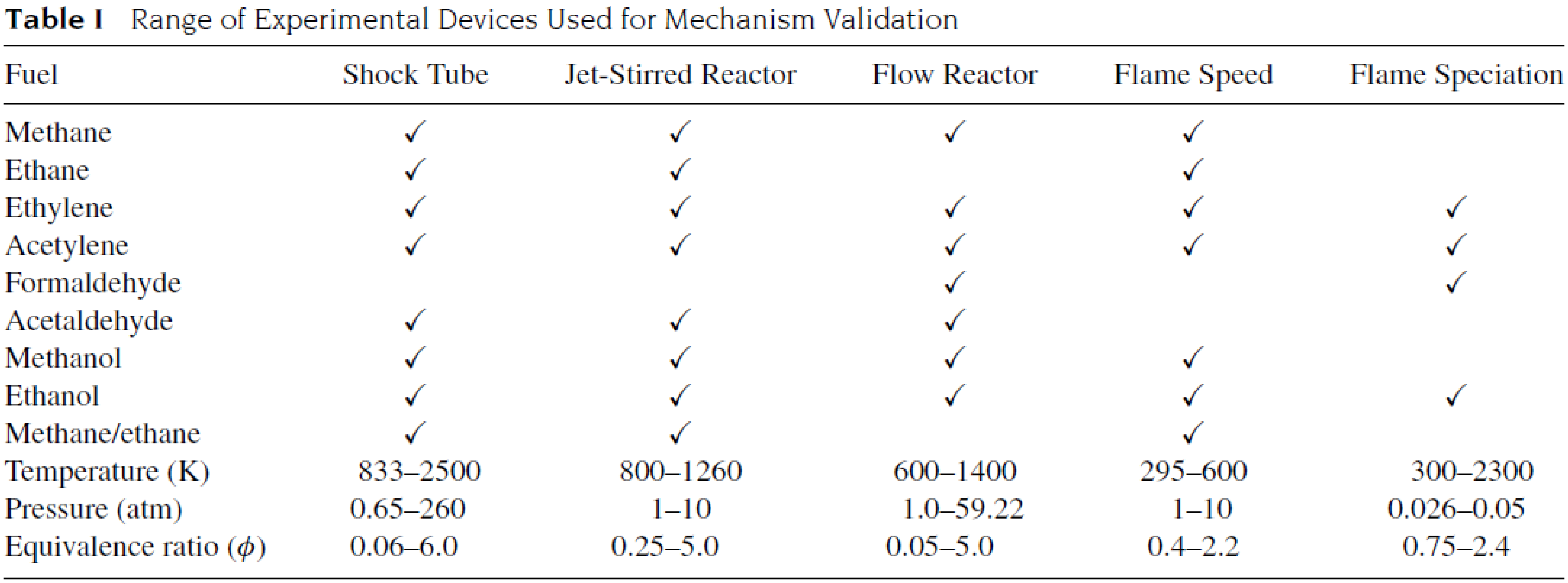

Table I Range of Experimental Devices Used for Mechanism Validation

Fuel	Shock Tube	Jet-Stirred Reactor	Flow Reactor	Flame Speed	Flame Speciation
Methane	✓	✓	✓	✓	
Ethane	✓	✓		✓	
Ethylene	✓	✓	✓	✓	✓
Acetylene	✓	✓	✓	✓	✓
Formaldehyde			✓		✓
Acetaldehyde	✓	✓	✓		
Methanol	✓	✓	✓	✓	
Ethanol	✓	✓	✓	✓	✓
Methane/ethane	✓	✓		✓	
Temperature (K)	833–2500	800–1260	600–1400	295–600	300–2300
Pressure (atm)	0.65–260	1–10	1.0–59.22	1–10	0.026–0.05
Equivalence ratio (ϕ)	0.06–6.0	0.25–5.0	0.05–5.0	0.4–2.2	0.75–2.4

- Mechanisms evaluated using ignition delays, laminar burning velocities and flame speeds,

Examples of sensitivity analyses and and optimised rate data

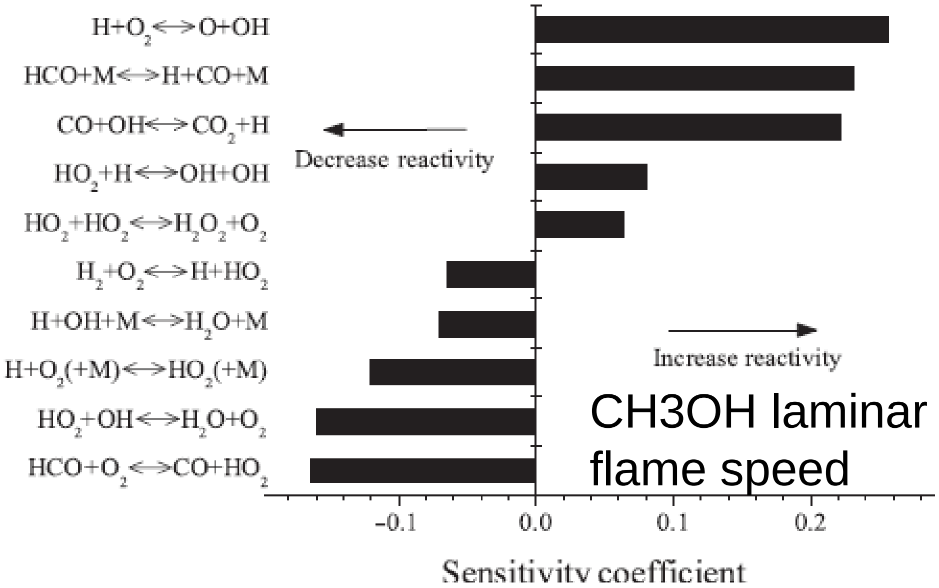

CH3OH laminar flame speed

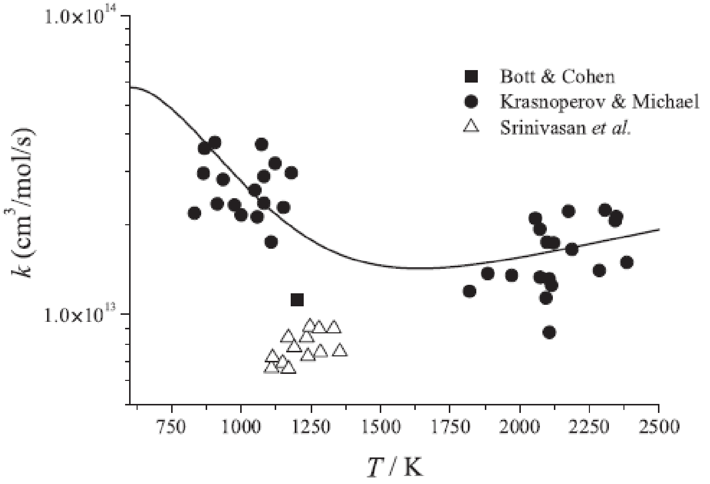

Recommended k(CH_3 + OH)

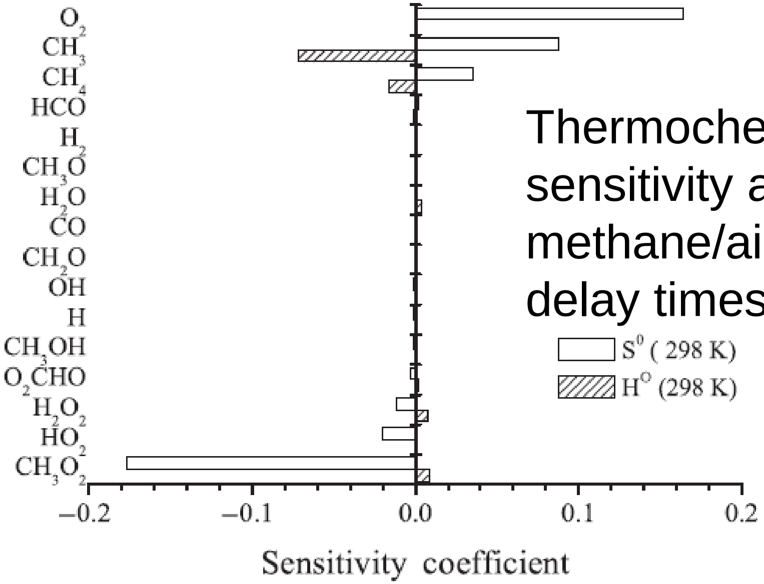

Thermochemistry sensitivity analysis methane/air ignition delay times

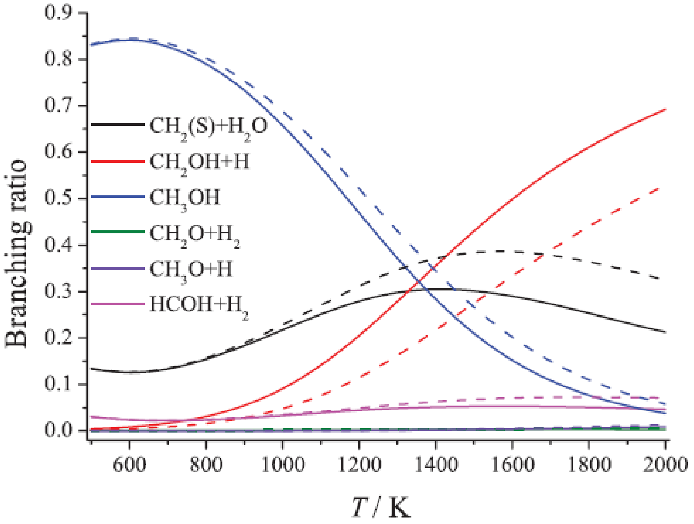

Reaction channels in CH_3+OH vs the

More complex mechanisms 2.
Oxidation of C1-C5 Alkane Quinternary Natural Gas Mixtures at High Pressures Energy Fuels 2010, 24, 1521-1528

- Rapid compression machine and shock tube
- detailed chemical kinetic mechanism
- . Mixtures of$CH_4/C_2H_6/C_3H_8/n\text{-}C_4H_{10}/n\text{-}C_5H_{12}$ studied in the temperature range 630-1550 K, in the pressure range 8-30 bar, and at equivalence ratios of 0.5, 1.0, and 2.0 in air
- Mechanism: NUIG Combustion Chemistry Centre, Natural Gas III mechanism, 2011. (See more recent developments later in lecture)

Characterizing combustion of larger Molecules

1. Cyclohexane pyrolysis

Wang et al, Comb and Flame 159 (2012) 2243-2253

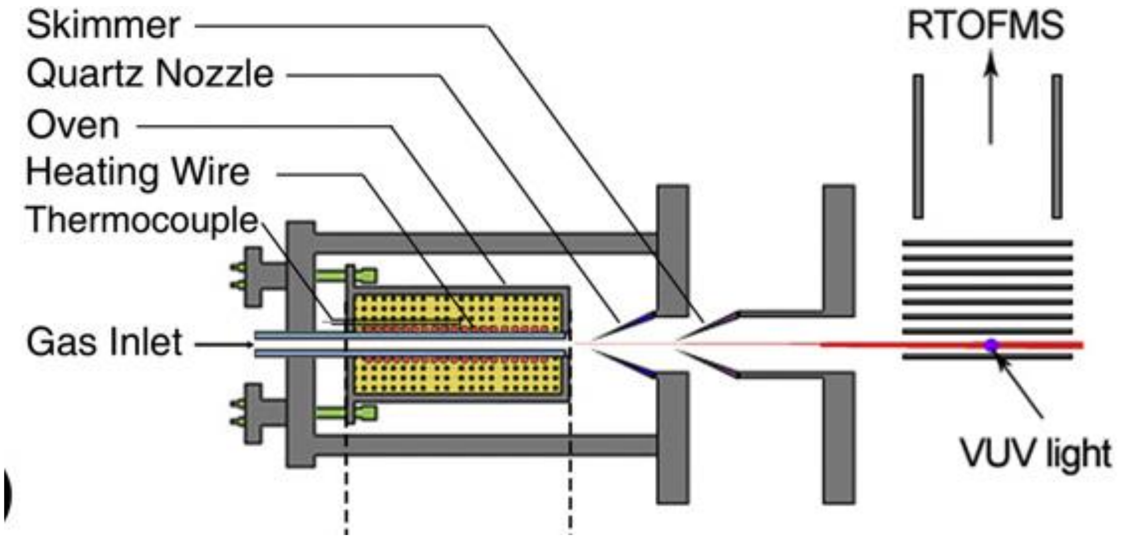

- Heated flow reactor, 950 to 1520 K, synchrotron VUV photoionization mass spectrometry.
- 30 species identified by photoionization efficiency (PIE) spectra, including some radicals like methyl, propargyl, allyl and cyclopentadienyl radicals, and stable products (e.g., 1-hexene, benzene and some aromatics).

Observed products vs temperature

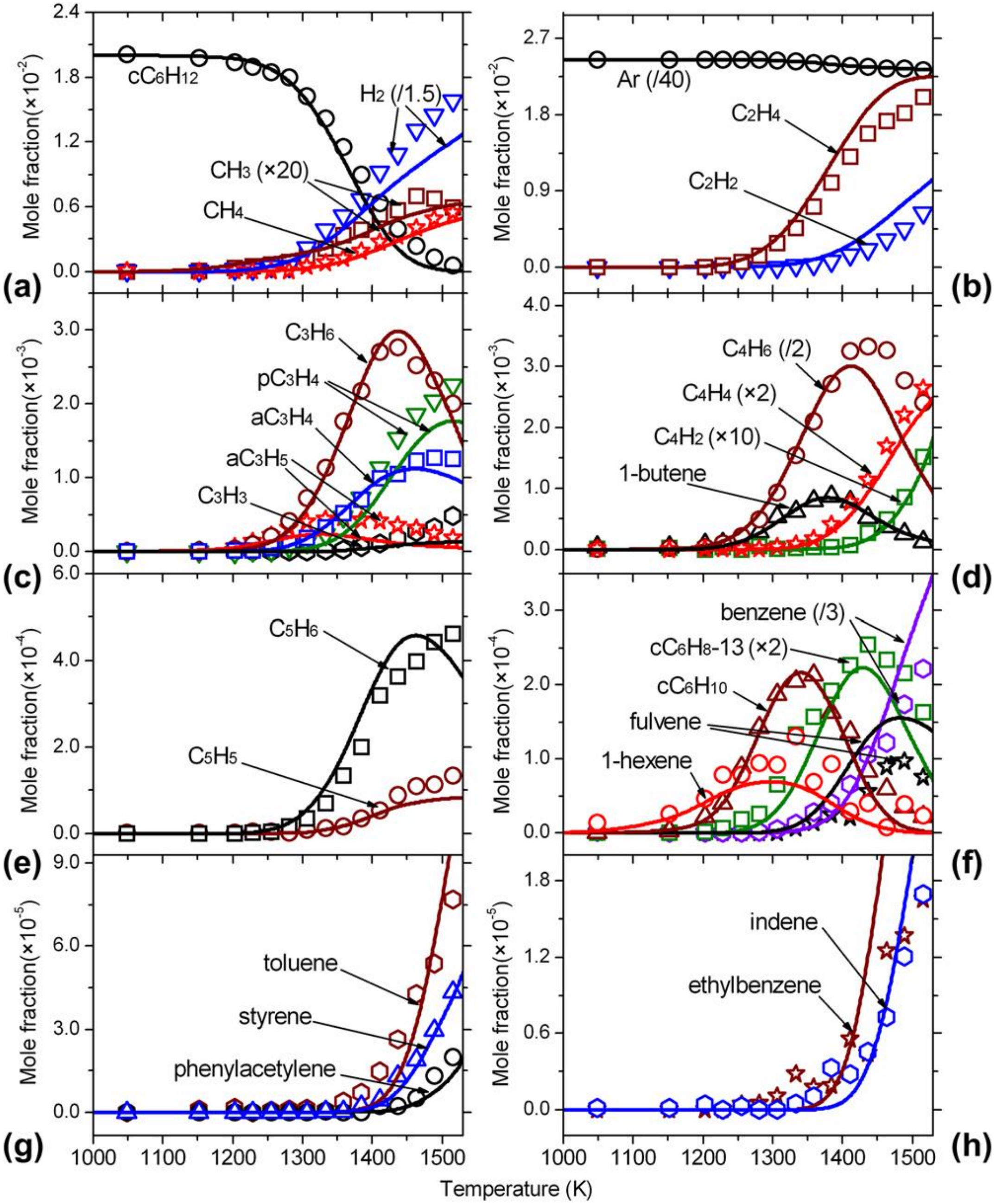

- Open symbols – experiment; full lines simulations
- Mechanism based on earlier work at Hefei and on A High-temperature Chemical Kinetic Model of n-alkane (up to n-dodecane), Cyclohexane, and Methyl-, ethyl-, n-propyl and n-butyl-cyclohexane Oxidation at High Temperatures, JetSurF Version 2.0, September 19, 2010. <http://melchior.usc.edu/JetSurF/ JetSurF2.0>.

Rate of production analysis of cyclohexane pyrolysis at 1360 K

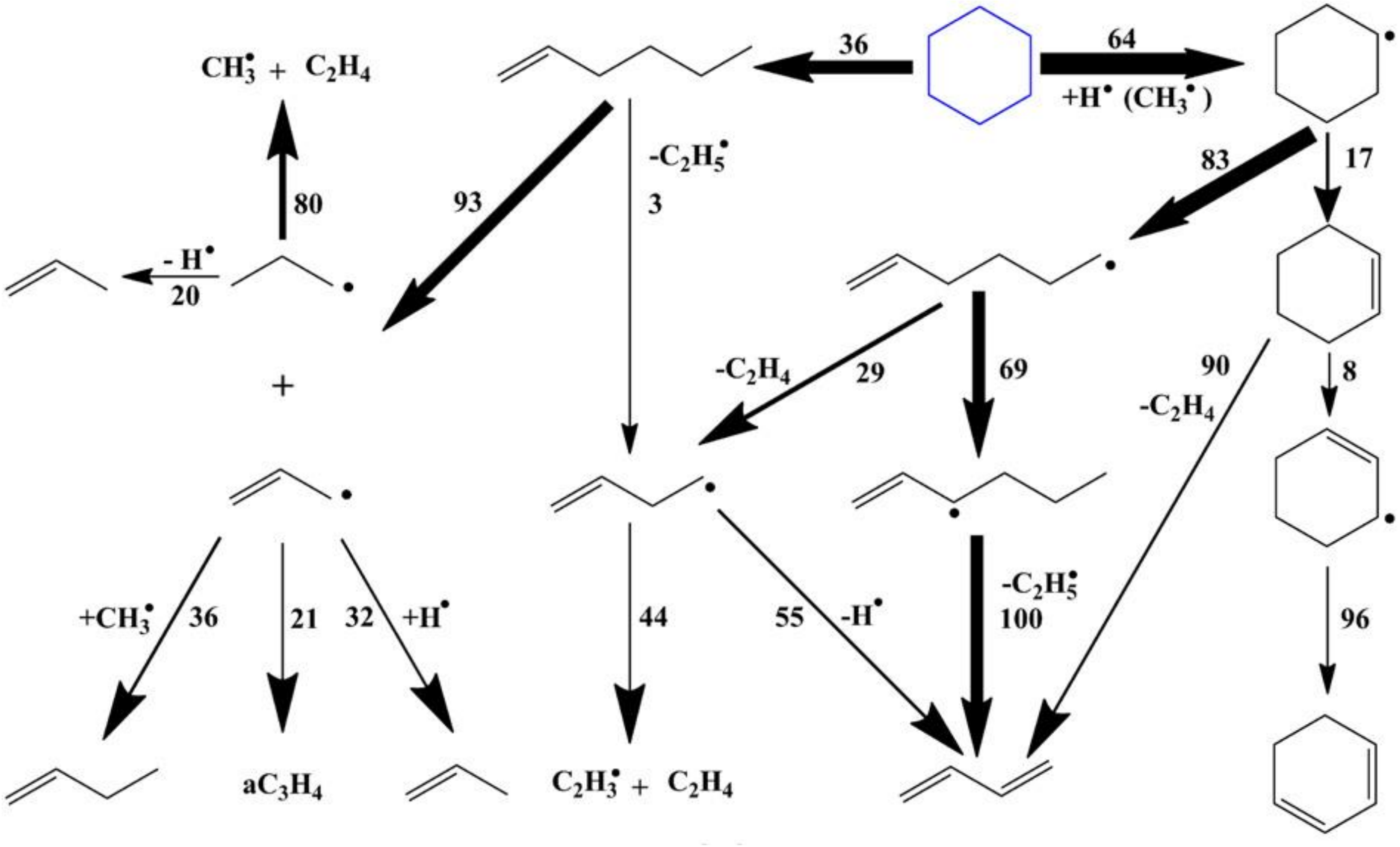

- Thickness of arrows denotes relative rate, numbers show percentage conversion

Larger molecules 2

Experimental and kinetic modeling study on methylcyclohexane pyrolysis and combustion, Wang et al, Comb and Flame, 161 (2014) 84–100

- synchrotron vacuum ultraviolet photoionization mass spectrometry combined with molecular-beam sampling was used to investigate the species formed during the pyrolysis of methylcyclohexane and in premixed flame of methylcyclohexane.

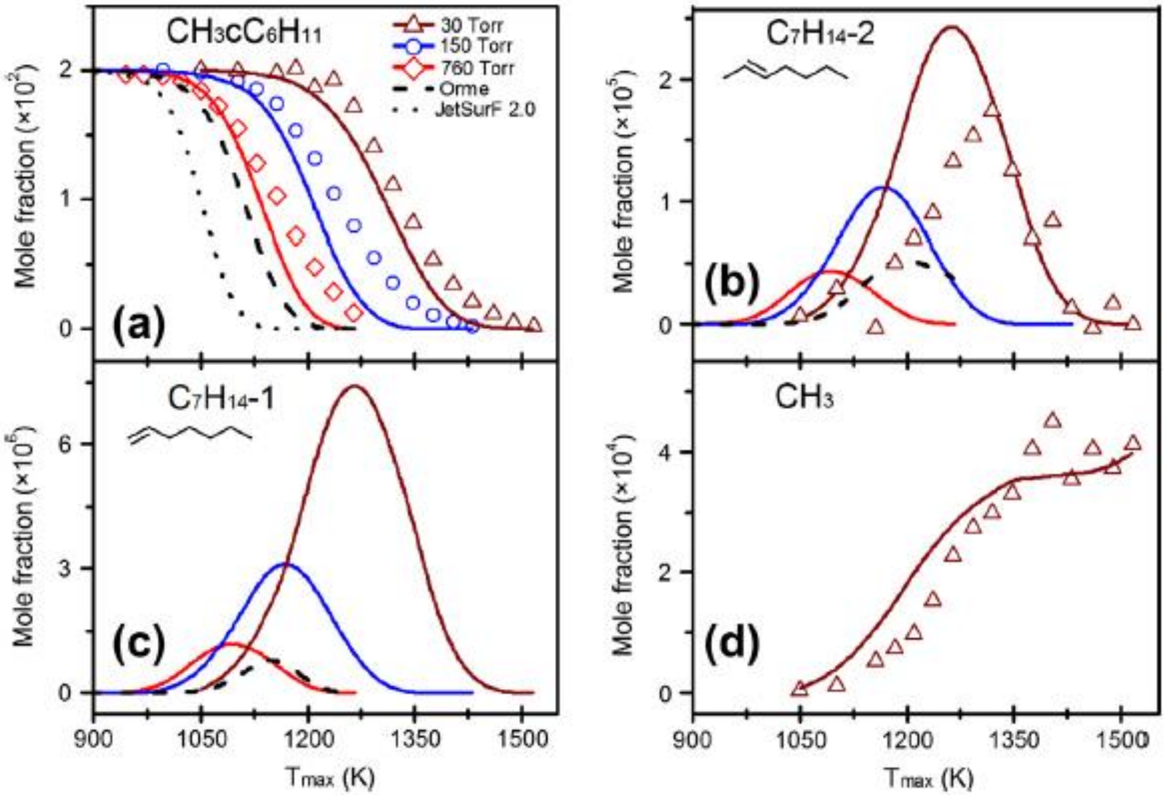

Solid lines: Wang et al mechanisms
Other mechanisms at 760 Torr

Mechanism based on cyclohexane mechanism; development also included
Theoretical calculations of abstraction by H

Comprehensive mechanisms:
1. NUIGMech1.1, AramcoMech3.0

- Kinetic and thermochemical properties of a large number of C_1–C_4 based hydrocarbon and oxygenated fuels over a wide range of experimental conditions. Developed by Curran et al., at NUI Galway.
- Developed in a hierarchical way 'from the bottom up', starting with a H_2/O_2 sub-mechanism, followed by a C1 sub-mechanism and has grown to include larger carbon species such as ethane, ethylene, acetylene, allene, propyne, propene, n-butane, isobutane, isobutene, 1-butene and 2-butene, and oxygenated species including formaldehyde, acetaldehyde, methanol, ethanol, and dimethyl ether.
- Validated against a large array of experimental measurements including data from shock tubes, rapid compression machines, flames, jet-stirred and plug-flow reactors.
- Website for NUIGMech1.1 (2020) and AramcoMech 3.0 (2018) see https://www.universityofgalway.ie/combustionchemistrycentre/mechanismdownloads/

References

- **M.K. Ghosh,et al.** The influence of thermochemistry on the reactivity of propane, the pentane isomers and *n*-heptane in the low temperature regime Proceedings of the Combustion Institute 39 (2023) 653–662.
- **Y. Li, et al.** The Oxidation of 2-Butene: A High Pressure Ignition Delay, Kinetic Modeling Study and Reactivity Comparison with Isobutene and 1-Butene Proceedings of the Combustion Institute **(2017)** *36(1)* 403–411.
- **C-W. Zhou et al.** " A Comprehensive experimental and modeling study of isobutene oxidation", Combust. Flame (2016) 167 353–379.
- **U. Burke, et al.**, " A Detailed Chemical Kinetic Modeling, Ignition Delay time and Jet-Stirred Reactor Study of Methanol Oxidation", Combust. Flame (2016) 165 125–136.
- **S.M. Burke, et al.** ," An experimental and modeling study of propene oxidation. Part 2: Ignition delay time and flame speed measurements", Combust. Flame (2015) 162(2) 296–314.
- **S.M. Burke et al.** ," An experimental and modeling study of propene oxidation. Part 1: Speciation measurements in jet-stirred and flow reactors", Combust. Flame (2014) 161(11) 2765–2784.
- **W.K. Metcalfe et al.**, " A hierarchical and comparative kinetic modeling study of C_1–C_2 hydrocarbon and oxygenated fuels", Int. J. Chem. Kinet. (2013) 45(10) 638–675.
- **A. Kéromnès, et al.** " An Experimental and Detailed Chemical Kinetic Modelling Study of Hydrogen and Syngas Mixtures at Elevated Pressures" *Combustion and Flame* (2013) *160* 995–1011.

Development of a tuned mechanism
GRI-Mech

- G.P. Smith, D.M. Golden, M. Frenklach, N.W.Moriarty, B. Eiteneer, M. Goldenberg, C.T. Bowman,R. Hanson, S. Song, W.C. Gardiner, Jr., V.Lissianski, Z. Qin, Available at: https://combustion.berkeley.edu/gri-mech
- Sensitivity tests against target experimental data allow selection of rate parameters for tuning
- process of automatic simultaneous parameter optimization, to get the parameter set for each successive release of GRI-Mech. Strict constraints keep the rate parameters within predetermined bounds based on
  - evaluations of the uncertainties in measurements of the rates of elementary reactions
  - applications of conventional reaction rate theory

GRI-Mech contd

- GRI-Mech is optimized as a whole, substitutions, further selective tuning should not be done.
- All reactions treated as reversible; thermodynamic data (based on NASA, Burcat) provided.
- to use the input files directly you need the Chemkin-II programs
- GRI-Mech 3.0 has 53 species, 325 reactions, with associated rate and thermodynamic data.
- Optimized for methane as a fuel. Includes C2 and propane chemistry.
- Optimized against chosen targets in ranges: $T = 1000$ to 2500 K, $p = 10$ Torr to 10 atm, $\phi = 0.1$ to 5 for premixed systems
- For information on Chemkin see:
- http://akrmys.com/public/chemkin/CKm_inp.html.en

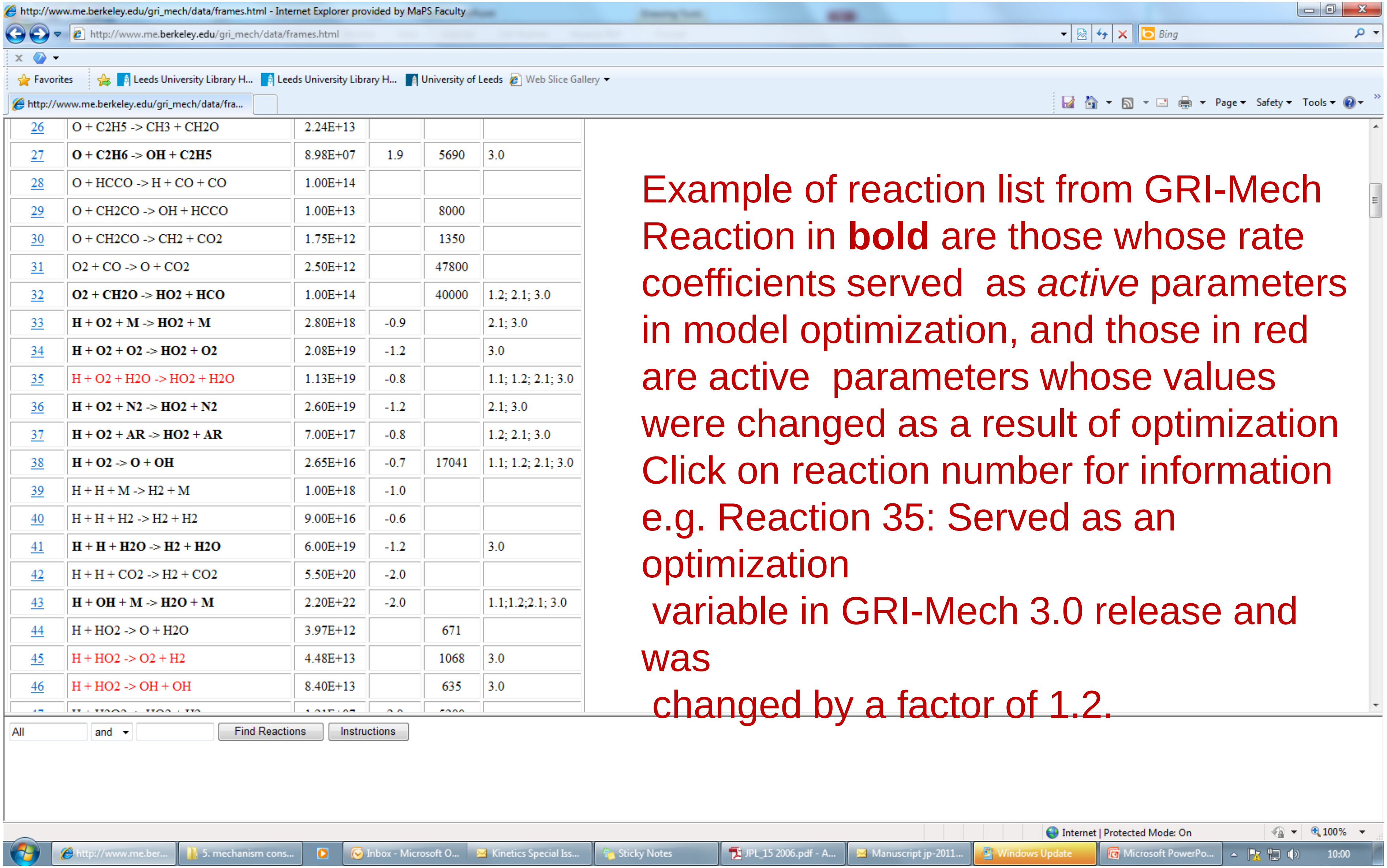

26	O + C2H5 -> CH3 + CH2O	2.24E+13			
27	**O + C2H6 -> OH + C2H5**	8.98E+07	1.9	5690	3.0
28	O + HCCO -> H + CO + CO	1.00E+14			
29	O + CH2CO -> OH + HCCO	1.00E+13		8000	
30	O + CH2CO -> CH2 + CO2	1.75E+12		1350	
31	O2 + CO -> O + CO2	2.50E+12		47800	
32	**O2 + CH2O -> HO2 + HCO**	1.00E+14		40000	1.2; 2.1; 3.0
33	**H + O2 + M -> HO2 + M**	2.80E+18	-0.9		2.1; 3.0
34	**H + O2 + O2 -> HO2 + O2**	2.08E+19	-1.2		3.0
35	H + O2 + H2O -> HO2 + H2O	1.13E+19	-0.8		1.1; 1.2; 2.1; 3.0
36	**H + O2 + N2 -> HO2 + N2**	2.60E+19	-1.2		2.1; 3.0
37	**H + O2 + AR -> HO2 + AR**	7.00E+17	-0.8		1.2; 2.1; 3.0
38	**H + O2 -> O + OH**	2.65E+16	-0.7	17041	1.1; 1.2; 2.1; 3.0
39	H + H + M -> H2 + M	1.00E+18	-1.0		
40	H + H + H2 -> H2 + H2	9.00E+16	-0.6		
41	**H + H + H2O -> H2 + H2O**	6.00E+19	-1.2		3.0
42	H + H + CO2 -> H2 + CO2	5.50E+20	-2.0		
43	**H + OH + M -> H2O + M**	2.20E+22	-2.0		1.1;1.2;2.1; 3.0
44	H + HO2 -> O + H2O	3.97E+12		671	
45	H + HO2 -> O2 + H2	4.48E+13		1068	3.0
46	H + HO2 -> OH + OH	8.40E+13		635	3.0

Example of reaction list from GRI-Mech
Reaction in **bold** are those whose rate coefficients served as *active* parameters in model optimization, and those in red are active parameters whose values were changed as a result of optimization
Click on reaction number for information
e.g. Reaction 35: Served as an optimization
variable in GRI-Mech 3.0 release and was
changed by a factor of 1.2.

Optimisation against a wide list of targets

- Shock tube ignition delay and species profiles, reactors, laminar flame speed, prompt NO, HCN oxidation, reburning. Examples:

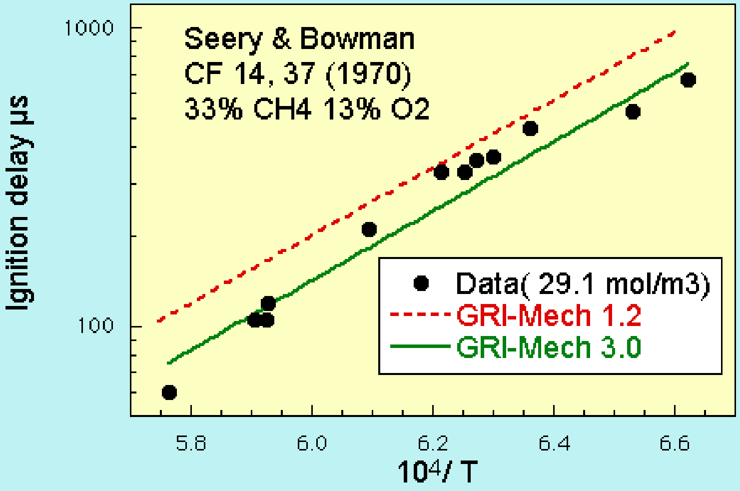

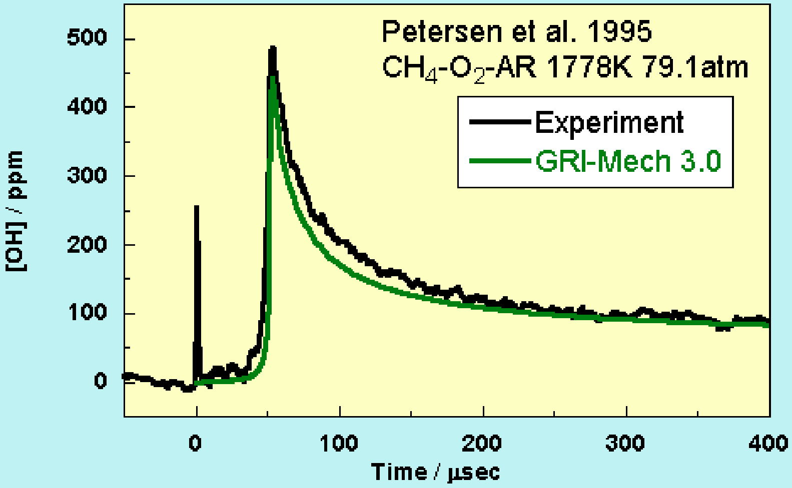

FFFC (Foundational Fuel Chemistry Model)

https://web.stanford.edu/group/haiwanglab/FFCM1/pages/FFCM1.html

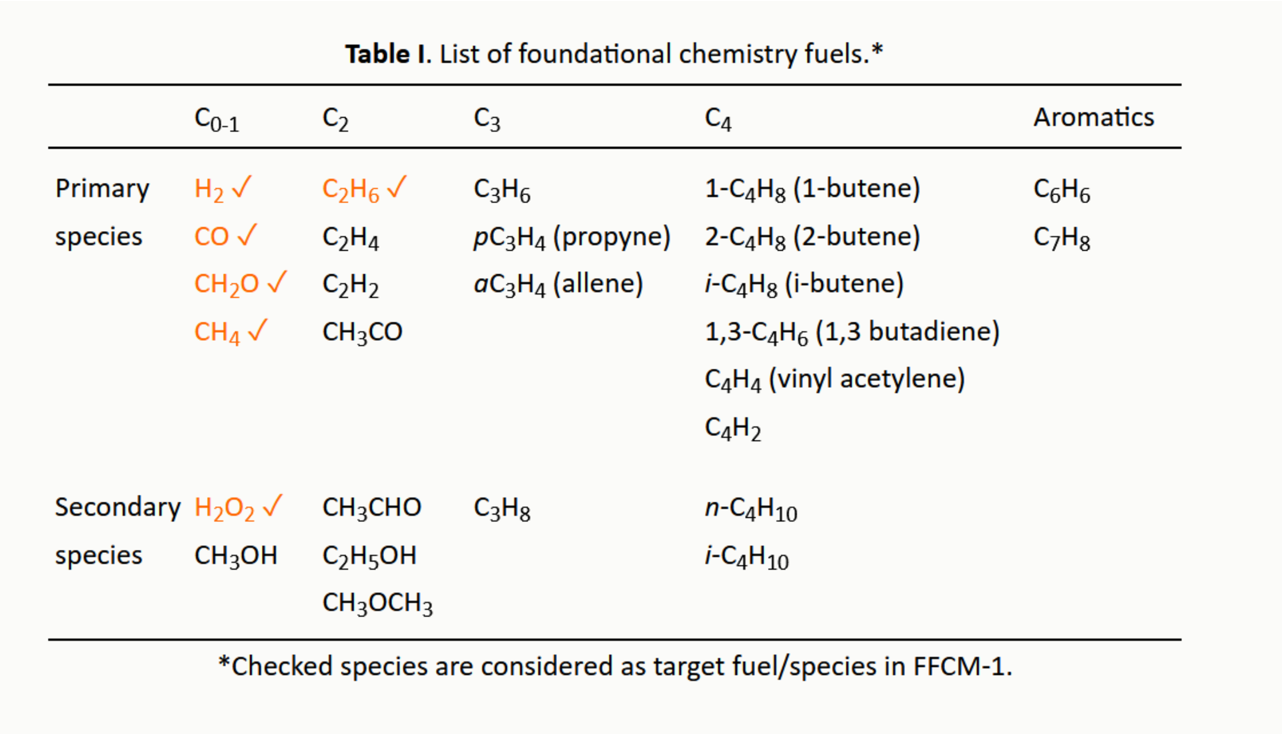

Table I. List of foundational chemistry fuels.*

	$C_{0\text{-}1}$	C_2	C_3	C_4	Aromatics
Primary species	H_2 ✓	C_2H_6 ✓	C_3H_6	1-C_4H_8 (1-butene)	C_6H_6
	CO ✓	C_2H_4	*p*C_3H_4 (propyne)	2-C_4H_8 (2-butene)	C_7H_8
	CH_2O ✓	C_2H_2	*a*C_3H_4 (allene)	*i*-C_4H_8 (i-butene)	
	CH_4 ✓	CH_3CO		1,3-C_4H_6 (1,3 butadiene)	
				C_4H_4 (vinyl acetylene)	
				C_4H_2	
Secondary species	H_2O_2 ✓	CH_3CHO	C_3H_8	*n*-C_4H_{10}	
	CH_3OH	C_2H_5OH		*i*-C_4H_{10}	
		CH_3OCH_3			

*Checked species are considered as target fuel/species in FFCM-1.

- Approach derives from GRI, with following developments:
- Collaboration with experimentalists and theoreticians on key, under-characterised reactions.
- Use optimization (cf GRI) but against a target set of fundamental combustion data over a wide range of conditions
- Explore the remaining uncertainty and unresolved issues in the reaction rate coefficients and the fundamental combustion data
- See also Combustion and Flame 2018, 195 18–29

Systematic provision of targets

- E.g. Davidson et al. Combustion and Flame 157 (2010) 1899–1905: Multi-species time-history measurements during n-heptane oxidation behind reflected shock waves
- 1300–1600 K, 2 atm (Ar) 300 ppm n-heptane, 3300 ppm oxygen ($\phi = 1$)
- Monitoring:
  - n-Heptane and ethylene, IR gas laser absorption, 3.39 and 10.53 μm, resp.
  - OH UV laser absorption at 306.5 nm
  - CO_2 and H_2O tunable IR diode laser absorption at 2.7 and 2.5 μm, resp.

Example of experimental measurements and comparison with existing mechanism

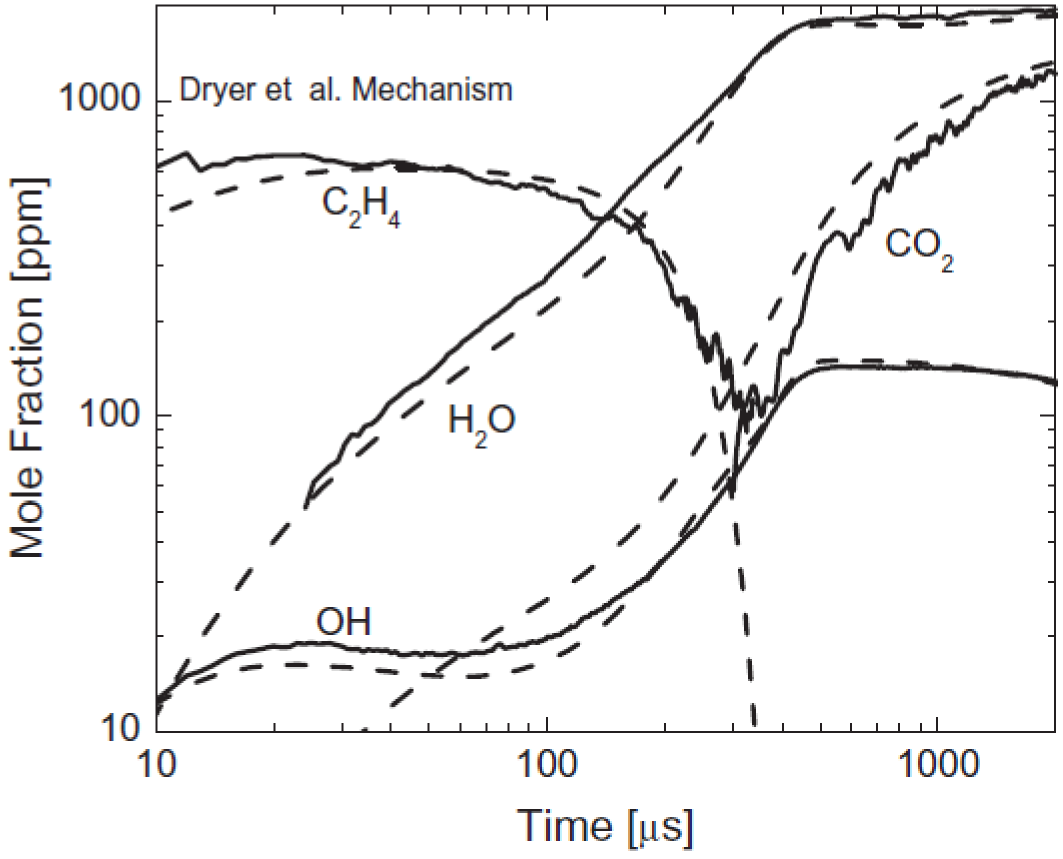

Fig. 7. Comparison of laser-absorption measurements with the Dryer et al. model [4]. Reflected shock wave conditions: 1494 K, 2.15 atm, 300 ppm *n*-heptane/O_2/argon, $\phi = 1$.

Use of target data from Davidson et al. Sheen and Wang, Combustion and Flame 158 (2011) 645-656 (quotes from abstract)

<u>Combustion kinetic modeling using multispecies time histories in shock-tube oxidation of heptane</u>

- Precise nature of measurements of Davidson et al. impose critical constraints on chemical kinetic models of hydrocarbon combustion.
- while an as-compiled, prior reaction model of n-alkane combustion can be <u>accurate</u> in its prediction of the detailed species profiles, the kinetic parameter uncertainty in the model remains too large to obtain a <u>precise</u> prediction of the data.
- Constraining the prior model against the species time histories within the measurement uncertainties led to notable improvements in the <u>precision</u> of model predictions against the species data as well as the global combustion properties considered.
- accurate data of <u>global</u> combustion properties are still necessary to predict fuel combustion.

Model measurement comparisons

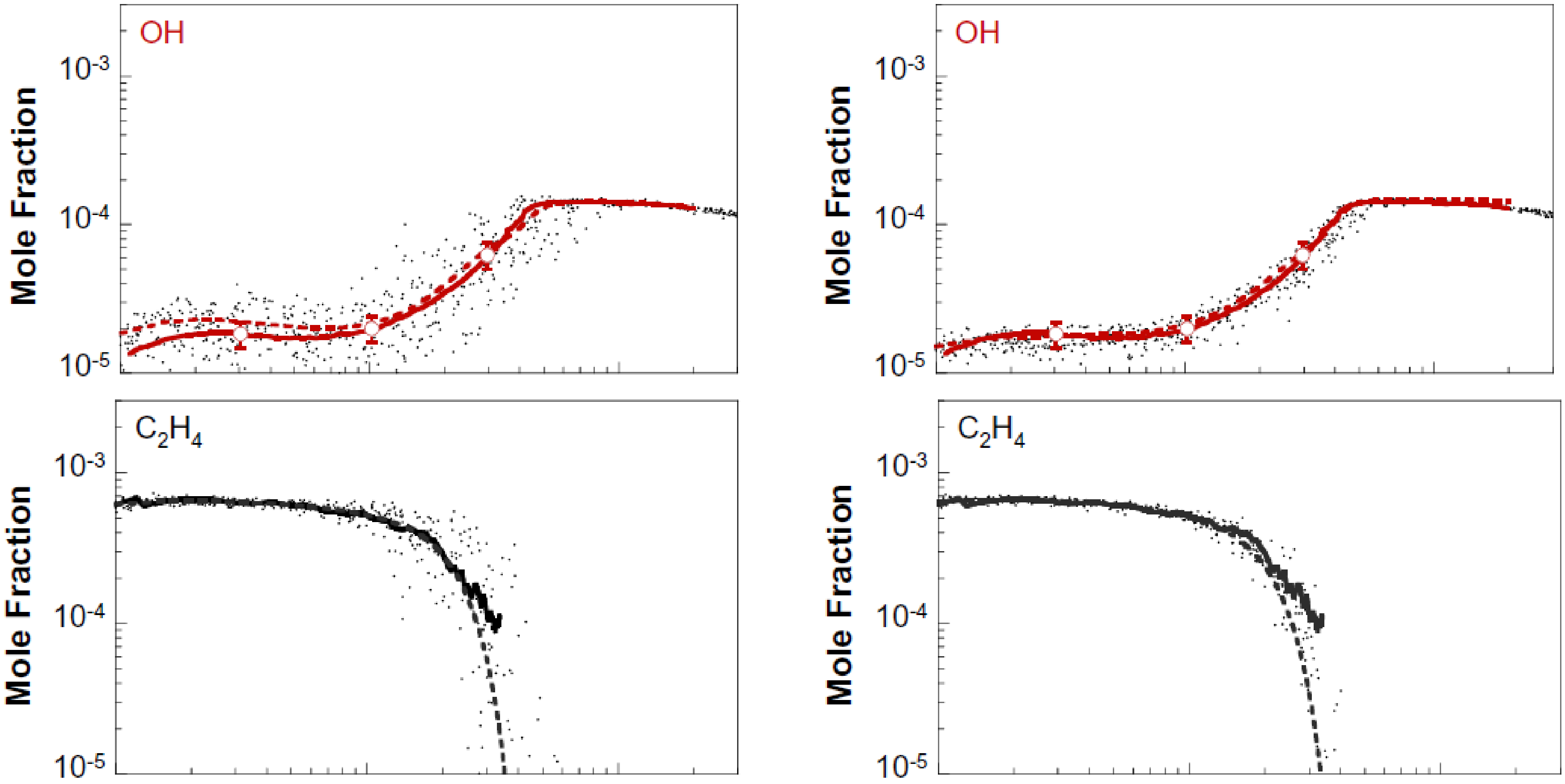

- Experimental (solid lines) and computed (dashed lines: nominal prediction; dots: uncertainty scatter). The open circles and the corresponding error bars designate data used as Series 1 targets and 2σ standard deviations, respectively. Left panel: prior model (Model I). Right panel: posterior model (Model II).

Turanyi et al. Determination of Rate Parameters Based on Both Direct and Indirect Measurements

International Journal of Chemical Kinetics 2012 DOI 10.1002/kin.20717

(R1): $H + O_2 = OH + O$

(R2): $H + O_2 + M = HO_2 + M$ (low-pressure limit, $M = N_2$ or Ar)

- new approach that takes into account both direct and indirect measurements and optimizes all influential rate parameters
- First, the domain of feasibility of the Arrhenius parameters is determined from all of the available direct measurements (see topic 5).
- the optimal Arrhenius parameters are then sought within this domain to reproduce the selected direct and indirect measurements
- 9 direct measurements for reaction (R1) (745 data points)
- 10 direct measurements for reaction (R2) (258 data points)
- 11 ignition time measurements (79 data points) were taken into account.
- A new fitting algorithm and a new method for error calculation were developed to determine the optimal mean values and the covariance matrix of all parameters

Arrhenius plots and uncertainties

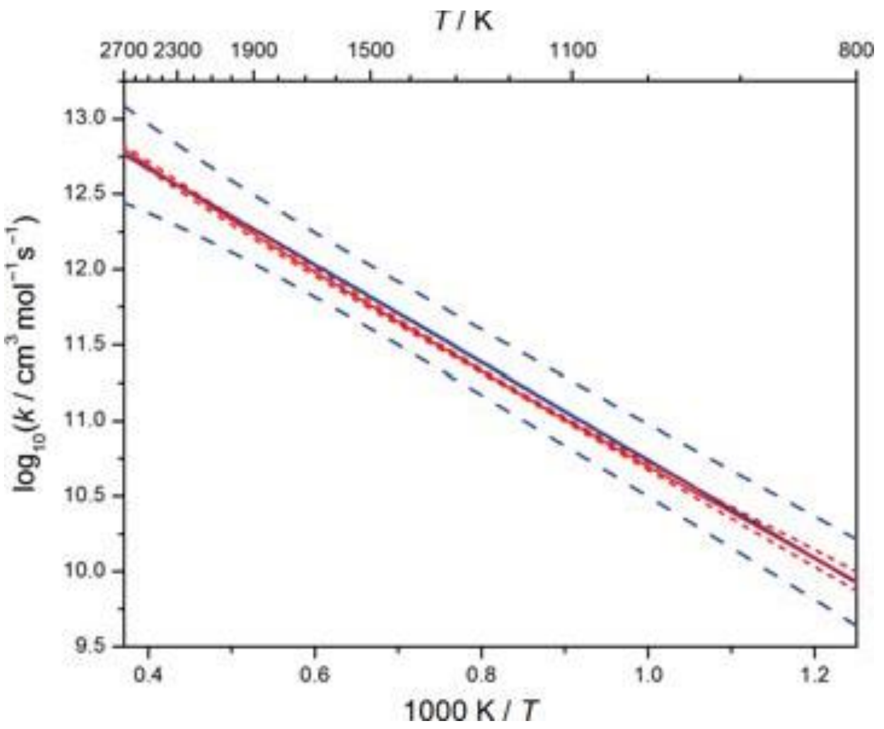

Arrhenius plots of the initial and optimized main values and uncertainty limits for reaction (R1): H + O_2 = OH + O. Thin solid blue line: initial value, recommended by Baulch et al.; blue dashed lines: initial uncertainty limits; red line: optimized rate coefficient; red dashed lines: optimized uncertainty limits.

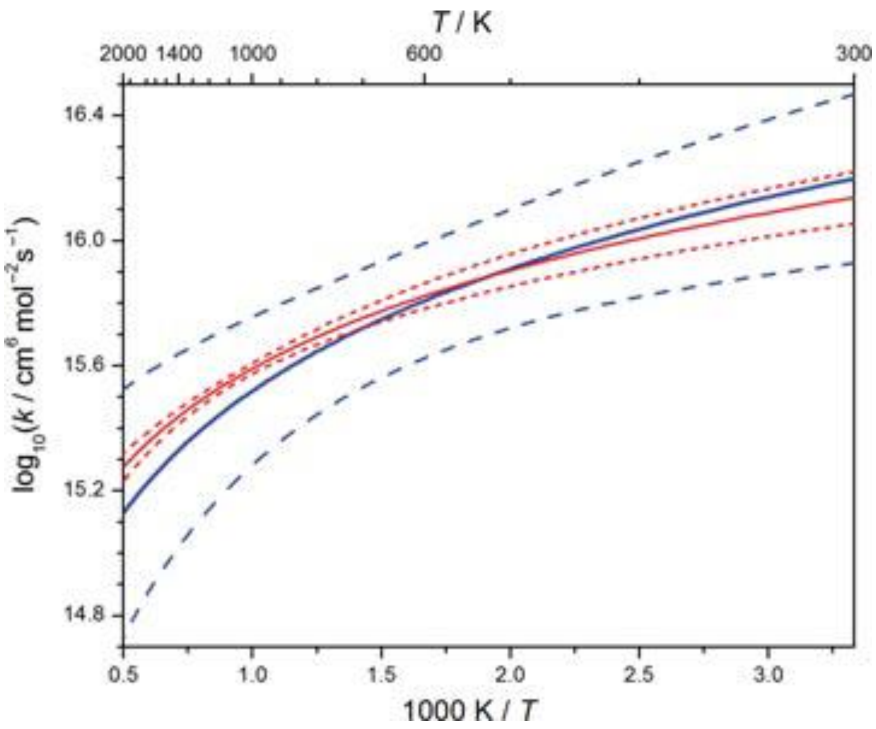

Arrhenius plots of the initial and optimized main values and uncertainty limits for reaction (R2): H + O_2 + N_2 = HO_2 + N_2 (low-pressure limit). Thin solid blue line: initial value, recommended by Baulch et al.; blue dashed lines: initial uncertainty limits; red line: optimized rate coefficient; red dashed lines: optimized uncertainty limits.

Uncertainty parameters for reactions R1 and R2.

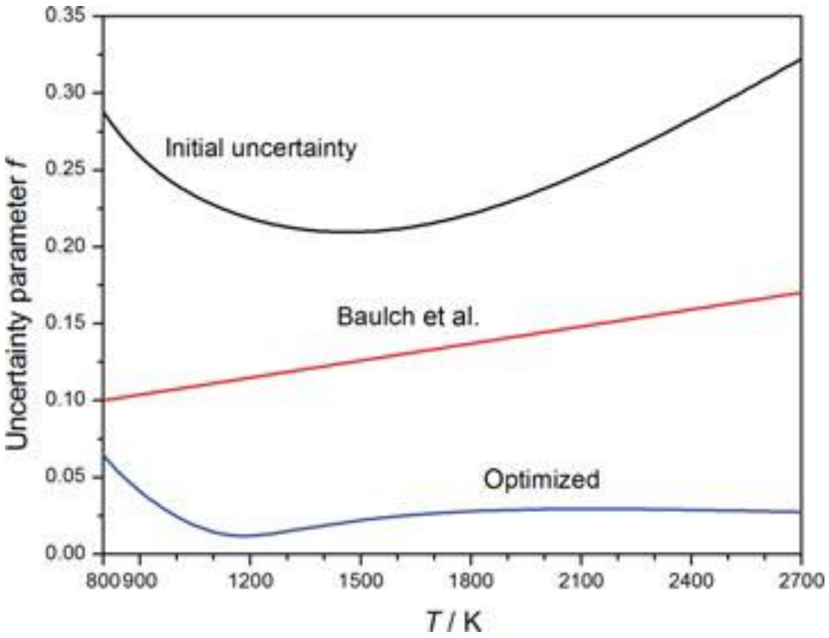

Uncertainty parameter (*f*) *as a function of temperature* for reaction (R1): H + O2 = OH + O, according to the evaluation of Baulch et al. [3] (red line), and *f calculated*from the covariance matrix of the Arrhenius parameters in two different ways: The "initial uncertainty" belongs to the *kmin(T) and kmax(T) functions* (black *line), and the "optimized"* belongs to the optimized rate parameters (blue line).

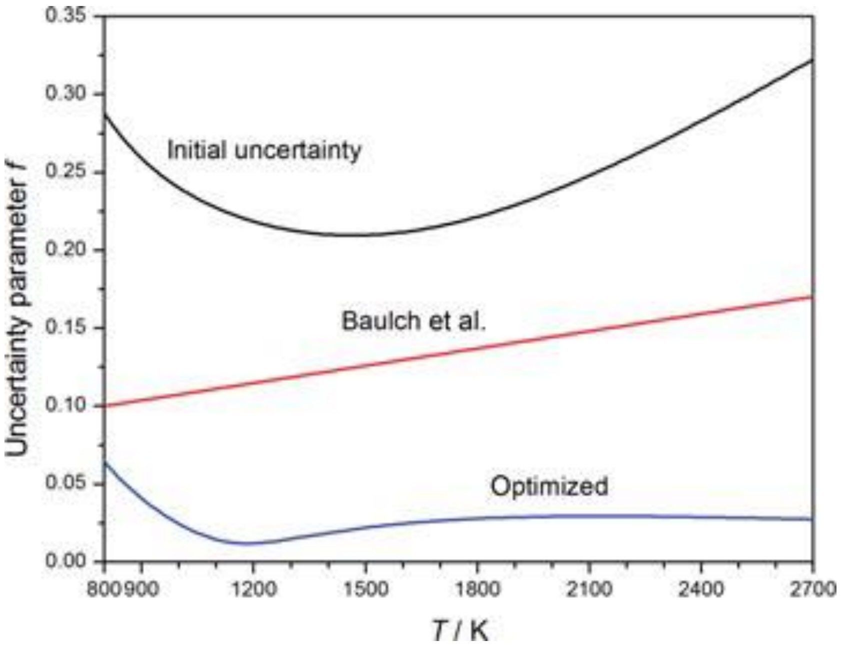

Uncertainty parameter (*f*) *as a function of temperature* for reaction (R2): H + O2 + N2 = HO2 + N2 (low-pressure limit) according to the evaluation of Baulch et al. (red line), and *f calculated from the covariance* matrix of the Arrhenius parameters in two different ways: The "initial uncertainty" belongs to the *kmin(T) and kmax(T)* functions (black line), and the "optimized" belongs to the optimized rate parameters (blue line).

Table VII The Determined Covariances of the Rate Parameters

	$\ln A_1$	n_1	E_1/R	$\ln A_2$	n_2	m (Ar)
$\ln A_1$	1.0609×10^0	-1.2149×10^{-1}	2.3661×10^2	-4.4080×10^{-1}	6.3586×10^{-2}	-3.0367×10^{-3}
n_1		1.3924×10^{-2}	-2.6989×10^1	4.9745×10^{-2}	-7.1782×10^{-3}	3.5276×10^{-4}
E_1/R			5.3824×10^4	-1.0438×10^2	1.5020×10^1	-6.0886×10^{-1}
$\ln A_2$				3.3293×10^{-1}	-4.7993×10^{-2}	7.4402×10^{-4}
n_2					6.9222×10^{-3}	-1.1576×10^{-4}
m (Ar)						9.2352×10^{-5}

Table VIII The Determined Correlations of the Rate Parameters

	$\ln A_1$	n_1	E_1/R	$\ln A_2$	n_2	m (Ar)
$\ln A_1$	1	−0.99957	0.99015	−0.74170	0.74199	−0.30679
n_1		1	−0.98586	0.73062	−0.73116	0.31108
E_1/R			1	−0.77976	0.77814	−0.27309
$\ln A_2$				1	−0.99973	0.13418
n_2					1	−0.14478
m (Ar)						1

Table I Evaluated and Optimized Rate Parameters for Reaction $H + O_2 = OH + O$ (R1)

Reference	A (cm^3 mol^{-1} s^{-1})	n	E/R (K)	f	T Range (K)
Baulch et al. [3]	2.07×10^{14}	–0.097	7560	0.1 at 800 K, 0.2 at 3500 K	800–3500
Li et al. [41]	3.55×10^{15}	–0.41	8359	–	–
Ó Conaire et al. [42]	1.91×10^{14}	0	8278	–	–
Konnov [43]	2.06×10^{14}	–0.097	7564	0.176	800–3500
Hong et al. [44]	1.04×10^{14}		7705		1100–3370
This work	3.003×10^{10}	0.965	6158	0.025 at 1000 K, 0.022 at 1500 K, 0.029 at 2000 K	950–3550

Table II Evaluated Rate Parameters for Low-Pressure Limit Reaction $H + O_2 + M = HO_2 + M$ (R2)

Reference	Bath Gas	A (cm^6 mol^{-2} s^{-1})	n	E/R (K)	f	T Range (K)
Baulch et al. [3]	N_2	2.65×10^{19}	–1.3	0	0.1 at 298 K, 0.2 at 2000 K	298–2000
Baulch et al. [3]	Ar	6.9×10^{18}	–1.2	0	0.1 at 298 K, 0.2 at 2000 K	298–2000
Li et al. [41]	N_2	6.37×10^{20}	–1.72	261.8	–	–
Li et al. [41]	Ar	9.04×10^{19}	–1.50	246.7	–	–
Ó Conaire et al. [42]	N_2	3.482×10^{16}	–0.41	–561.5	–	–
Konnov [43]	N_2	5.70×10^{19}	–1.4	0	0.079	300–2000
Konnov [43]	Ar	7.43×10^{18}	–1.2	0	0.079	300–2000
Hong et al. [44]	N_2	2.65×10^{19}	–1.3	0	–	–
Hong et al. [44]	Ar	6.81×10^{18}	–1.2	0	–	–
This work	N_2	7.856×10^{18}	–1.100	0	0.032 at 800 K, 0.018 at 1000 K, 0.045 at 1500 K	300–1850

Optimization of a hydrogen combustion mechanism using both direct and indirect measurements

Varga et al, Proc Comb Inst 35 (2015) 589–596

- Optimisation of Keromnes mechanism using ignition measurements from shock tubes (566 datapoints, 43 datasets) and rapid compression machines (219/19) + flame velocities (364/59)
- Sensitivity analysis showed that parameters for 11 elementary reactions could be optimised. Also utilized 1749 direct k measurements from 56 datasets, with prior uncertainty ranges
- Analysis provides new mechanism including new k(T)s, with covariance matrix and T dependent posterior uncertainty ranges
- Demonstrate much reduced overall error function compared with 13 earlier mechanisms

Examples of results for rate constants

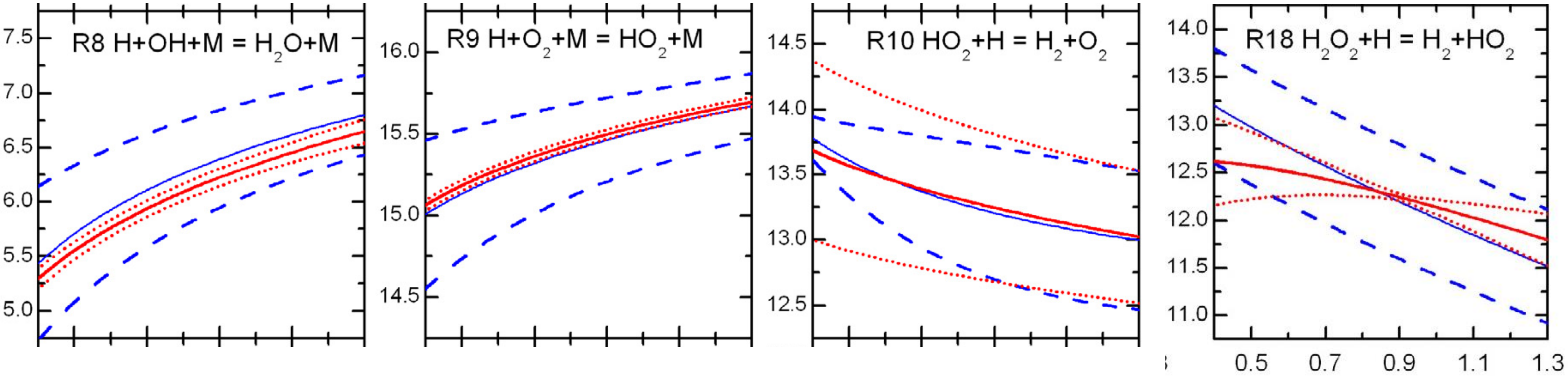

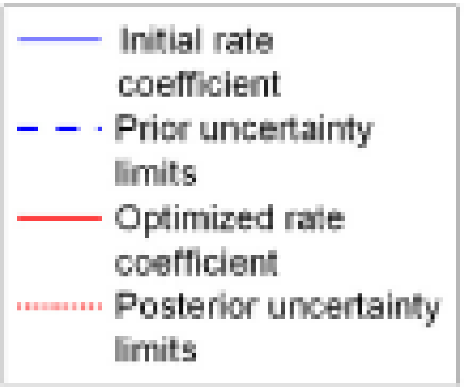

- Global parameter optimization from Int J Chem Kinet, 44 (2012) 284 - 302
- Based on minimization of objective function:

$$E(p) = \frac{1}{N}\sum_{i=1}^{N}\frac{1}{N_i}\sum_{j=1}^{N_i}\left(\frac{Y_{ij}^{mod} - Y_{ij}^{exp}}{\sigma(Y_{ij}^{exp})}\right)^2$$

where *N* is the total number of datasets and N_i is the number of datapoints in the ith dataset. $\sigma(Y_{ij}^{exp})$ is the experimental std deviation in the jth datapoint, ith dataset

Comparison of the performance of several recent syngas combustion mechanisms

Olm et al Comb and Flame 162 (2015) 1793–1812

- Used same objective function approach to compare performance of 16 syngas (wet CO) mechanisms ignition studies in shock tubes and rapid compression machines, flame velocities and species concentration measurements from flow reactors, shock tubes and jet-stirred reactors. 4970 data points in 408 datasets from 52 publications.
- Some observations not well modelled.
- Five mechanisms performed better than others.
- influence of poorly reproduced experiments and weighting on the performance of the mechanisms investigated
- analysis of local sensitivity coefficients showed the influence of selected reactions and helped identify those reactions that require more attention

Uncertainty quantification optimized methanol, formaldehyde combustion mechanism (Olm et al, Comb & Flame 2017, 186, 45)

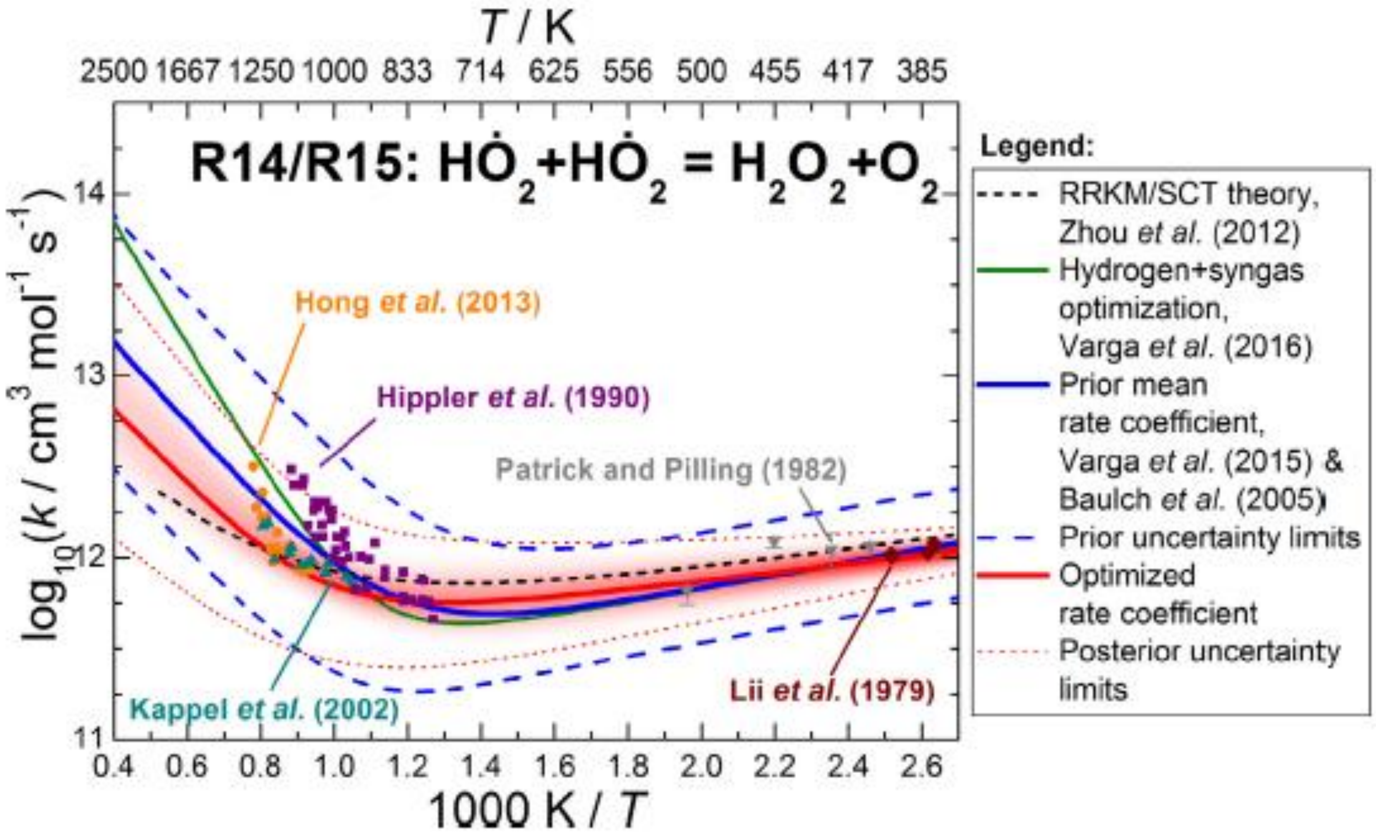

- The prior uncertainty limits are large especially at high T, reflecting substantial disagreements between direct experimental datasets (se Topic 2). Also theory gives lower values .
- The extensive set of indirect measurements (24900 points from 265 datasets) change the optimized k and substantially narrow the uncertainty limits

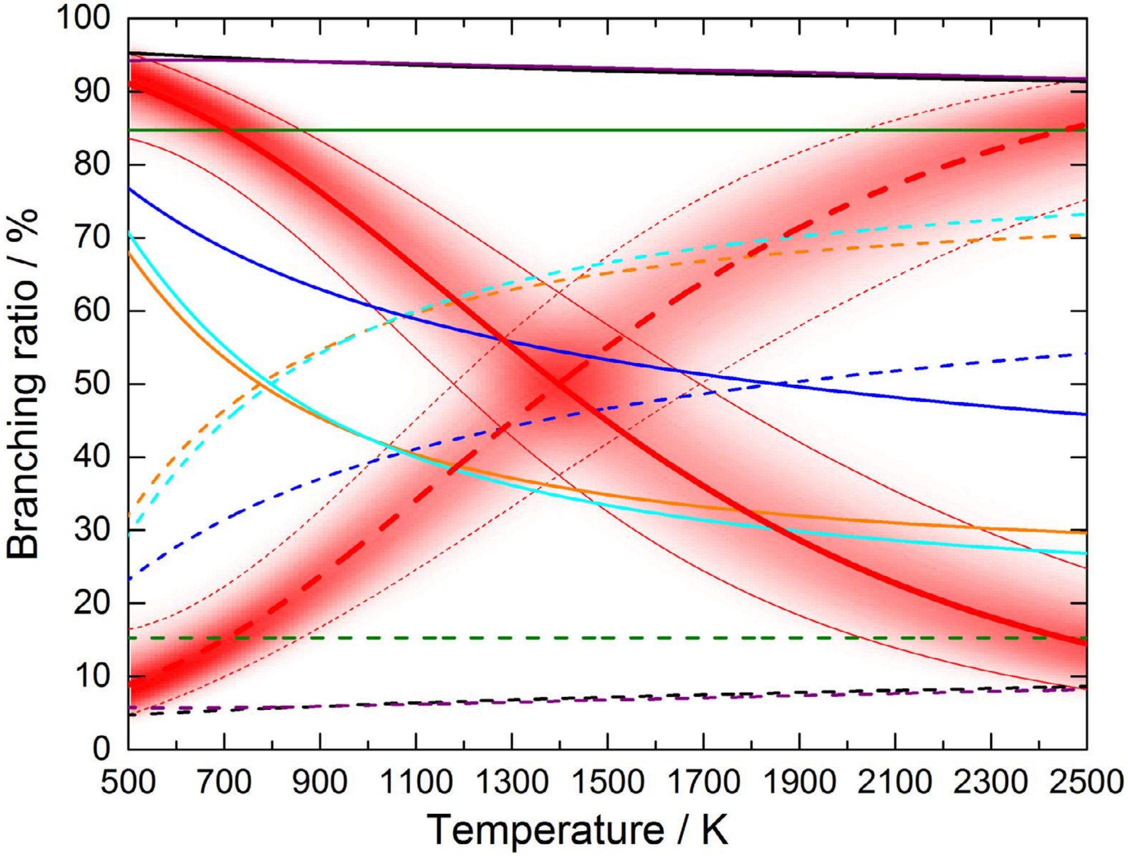

Channel Yields

$CH_3OH + OH \rightarrow$

$CH_2OH + H_2O$ (R84)

$CH_3O + H_2O$ (R83)

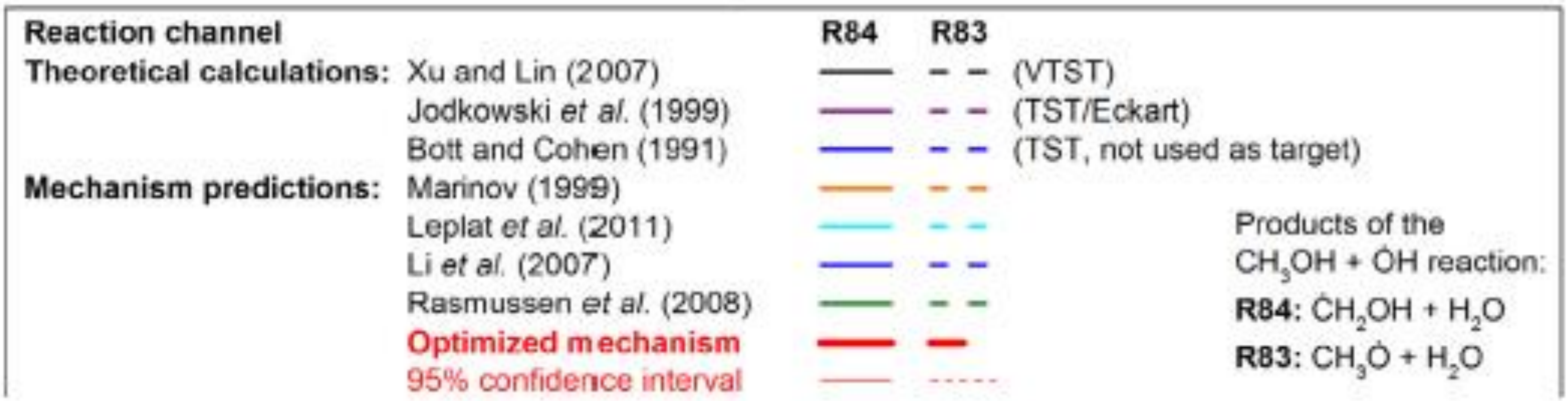

Reaction channel		**R84**	**R83**	
Theoretical calculations:	Xu and Lin (2007)	—	- -	(VTST)
	Jodkowski *et al.* (1999)	—	- -	(TST/Eckart)
	Bott and Cohen (1991)	—	- -	(TST, not used as target)
Mechanism predictions:	Marinov (1999)	—	- -	
	Leplat *et al.* (2011)	—	- -	
	Li *et al.* (2007)	—	- -	
	Rasmussen *et al.* (2008)	—	- -	
	Optimized mechanism	—	- -	
	95% confidence interval	—	- - - -	

Products of the $CH_3OH + \dot{O}H$ reaction:

R84: $\dot{C}H_2OH + H_2O$

R83: $CH_3\dot{O} + H_2O$

Mechanism optimization

- Wang et al Combustion and Flame 2018, 195 18–29. Critical kinetic uncertainties in modelling hydrogen/carbon monoxide, methane, methanol, formaldehyde, and ethylene combustion using FFCM-1. The paper examines ignition and extinction times in a perfectly stirred reactor (PSR)
- Examine both sensitivities and reaction impact factors, $I_{s,r}$

$$I_{s,r} = \sigma_r \sqrt{\frac{1}{N_{\text{fuel}}}\sum_{j=1}^{N_{\text{fuel}}}\left[\frac{1}{n_{s,j}}\sum_{k=1}^{n_j}\left(\frac{\partial \ln \tau_{s,k}}{\partial x_r}\right)^2\right]}.$$

- N_{fuel} is the number of fuels considered, and $n_{s,j}$ is the total number of conditions tested for fuel j. $\tau_{s,k}$ is the ignition or extinction time (label *s*) and the impact factor is for a specific reaction, *r*, with rate constant *k*. *I* can also be calculated for a single fuel
- Compare with earlier discussion on fractional contributions to model uncertainties.

Sensitivities and reaction impact factors

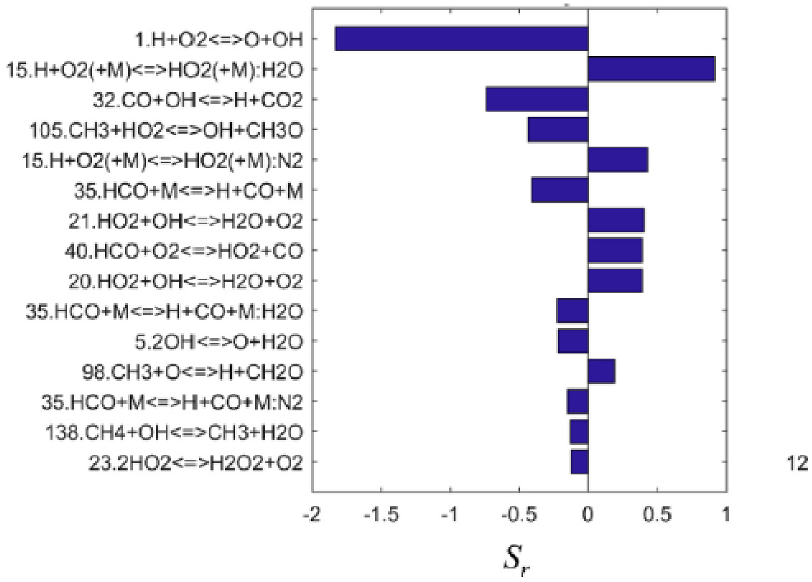

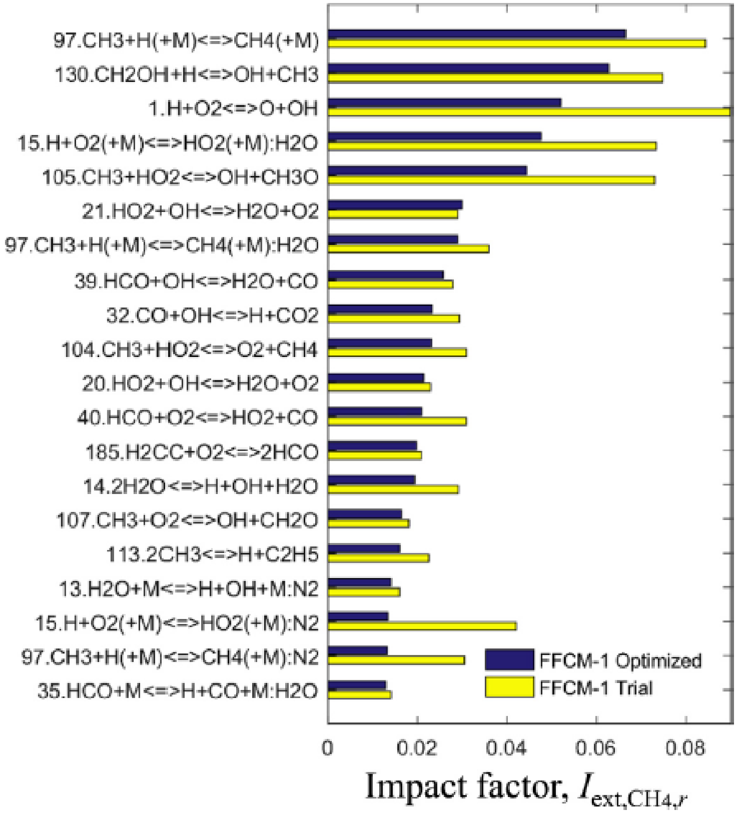

- Ranked sensitivity coefficients for extinction times for CH_4/air, 10 atm, inlet *T* 400 K, equivalence ration 0.5
- Ranked impact factors for extinction times for all methane air test cases.

Harnessing the Combined Power of Theoretical and Experimental Data through Multiscale Informatics

M P Burke, Int J Chem Kinet 2016, 48,

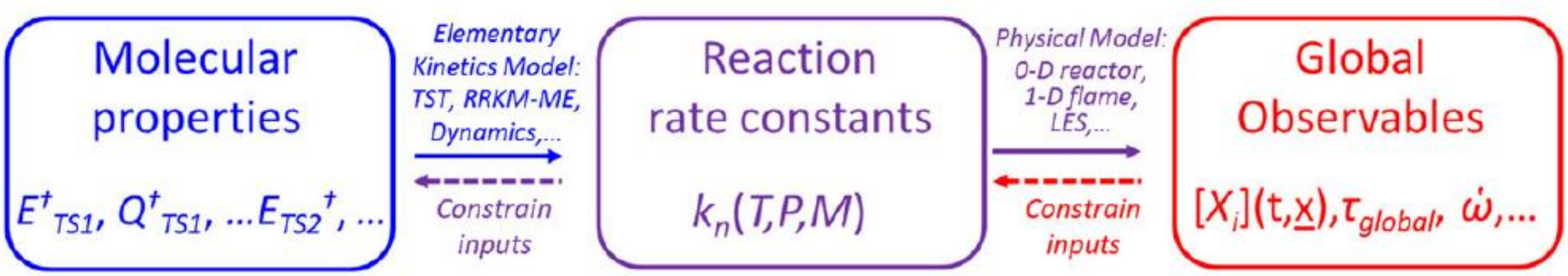

Molecular properties

$E^{\dagger}_{TS1}$, $Q^{\dagger}_{TS1}$, ...$E_{TS2}^{\dagger}$, ...

Elementary Kinetics Model: TST, RRKM-ME, Dynamics,...

Constrain inputs

Reaction rate constants

$k_n(T,P,M)$

Physical Model: 0-D reactor, 1-D flame, LES,...

Constrain inputs

Global Observables

$[X_i](t,\underline{x}),\tau_{global}, \dot{\omega},...$

- Approach integrates information from a wide variety of sources and scales:
  - Theoretical parameters, e.g. TS energies, with constrained uncertainties
  - Through elementary kinetics models to rate constants, with propagated uncertainties
  - Through physical models to global observables, such as ignition delay times, with propagated uncertainties

Multiscale Informatics - an example

- A quantitative explanation for the apparent anomalous temperature dependence of OH + HO_2=H_2O+O_2 through multi-scale modelling, Burke et al, Comb and Flame, 2013, 34, 547
- Used:
  - Ab intio quantum chemistry calculations
  - Direct rate constant measurements
  - Shock tube studies of H2O2,H2O, O_2, Ar with species concentration measurements
- Reactions mechanism studied:

R1	$H_2O_2(+M) = OH + OH(+M)$
R2	$H_2O_2 + OH = HO_2 + H_2O$
R3	$HO_2 + HO_2 = H_2O_2 + O_2$
R4	$HO_2 + OH = H_2O + O_2$
R5	$OH + OH = O + H_2O$

Results

1. *k*(OH + HO_2)
2. 215 m, absorbance, H_2O_2, Ar, 968 – 1218, K, p ~3 atm
3. [OH] in H_2O, O_2, Ar, 1880 K, 1.74 atm

The *a priori* model is that from the quantum chemistry calculations.

The constrained model is after optimization of the *a priori* model with the experimental data

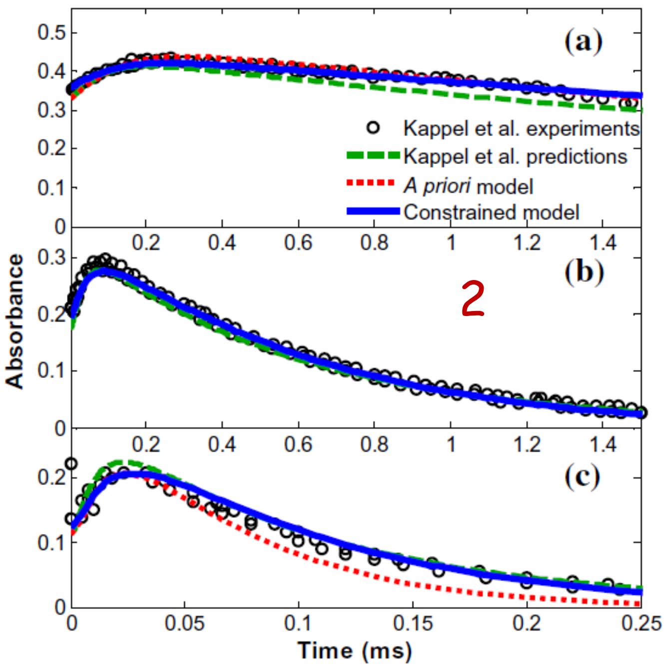

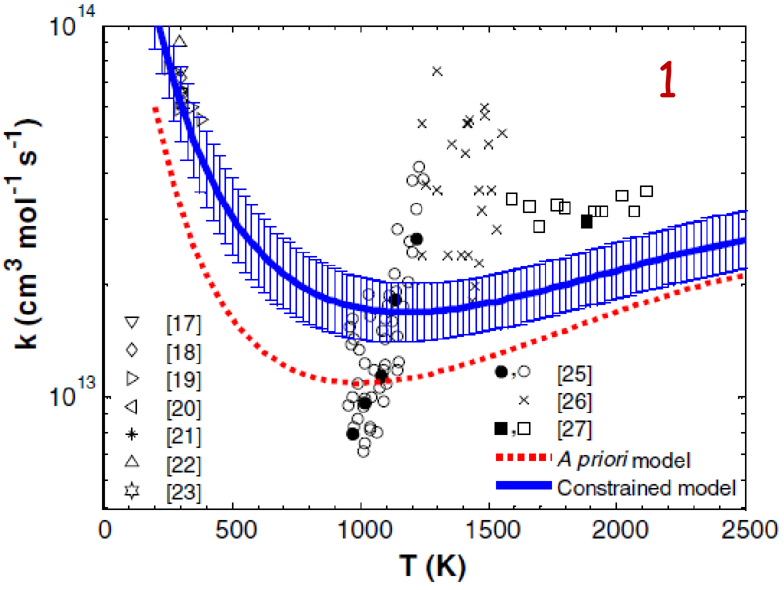

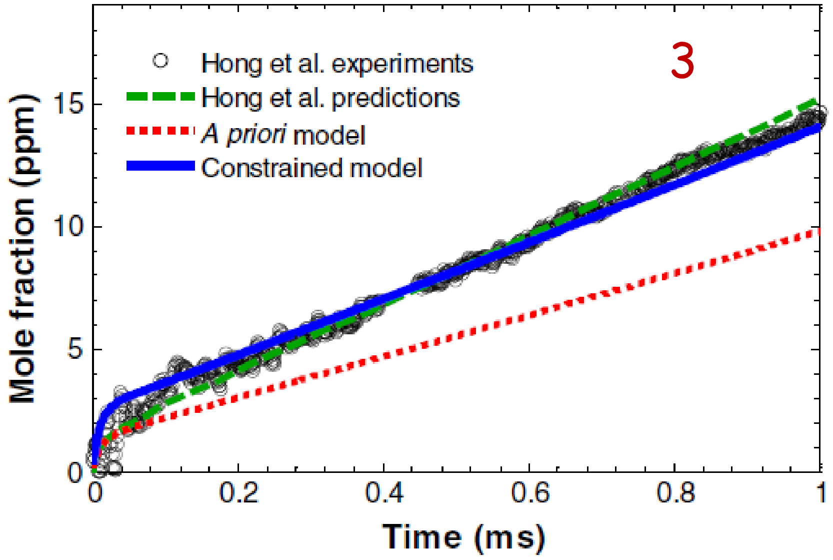

HO_2+ HO_2

LaGrotta et al, J. Phys. Chem. A 2023, 127, 799–816

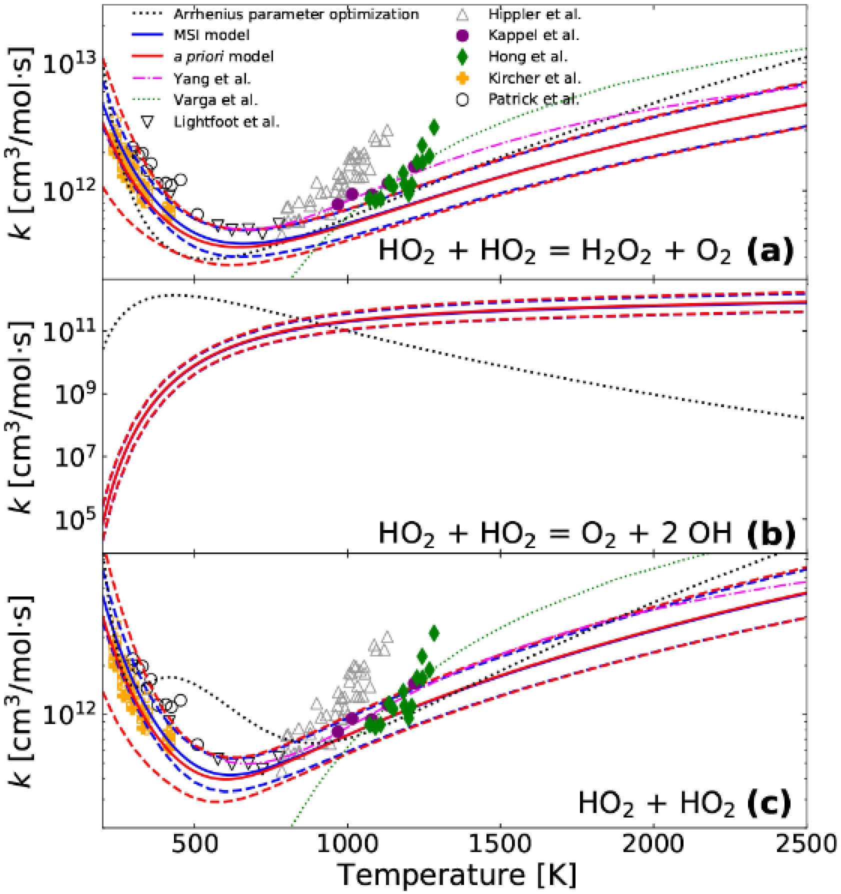

Inconsistencies among theoretical and experimental derived constants can be resolved when constraints imposed by ab initio electronic structure calculations and measured macroscopic observables are considered simultaneously within a multiscale framework

Experimental studies should report raw data (e.g., measured time profiles) and future theoretical studies provide theoretical kinetics input files in addition to derived rate constants to enable rigorous comparisons of theory and experiment in a manner that better reflects the information content and associated uncertainties in each.

Automatic mechanism generation

W H Green (MIT) RH West Northeastern et al https://rmg.mit.edu/

- Open source software, **Reaction Mechanism Generator (RMG)** is an automatic chemical reaction mechanism generator that constructs kinetic models composed of elementary chemical reaction steps using a general understanding of how molecules react.
- Latest version RMG-Py, written in Python
- **Arkane**, developed and distributed as part of RMG-Py, can be used as a stand-alone application for Thermochemistry, Transition State Theory, and Master Equation chemical kinetics calculations
- Website includes a guide to the theory used in RMG
- Flux diagram for the pyrolysis of 1,3-hexadiene, an example model generated with RMG, showing the net carbon flux at an instant near the end of the simulation

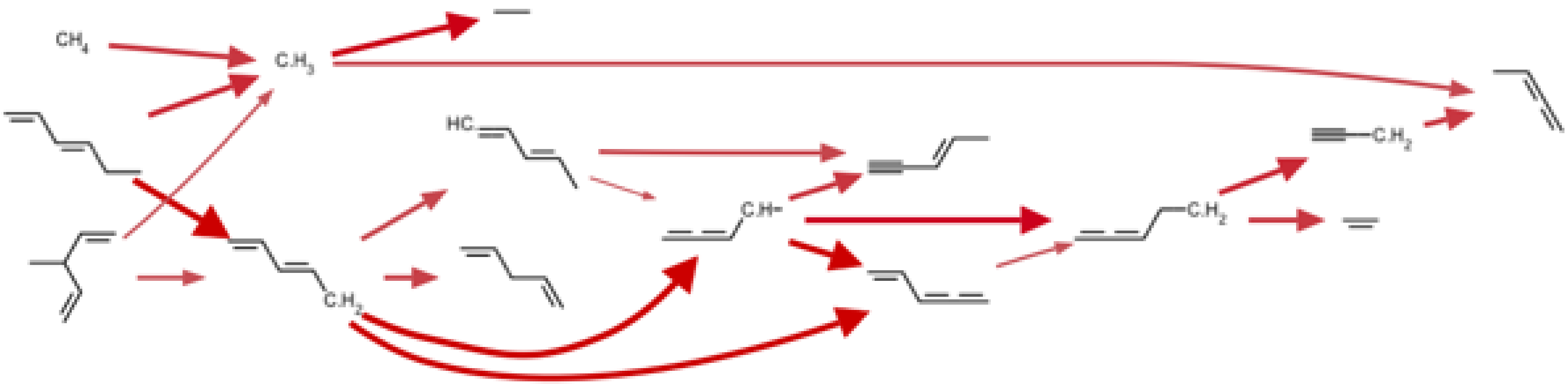

Development of kinetic model

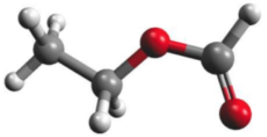

Starting species in “core”

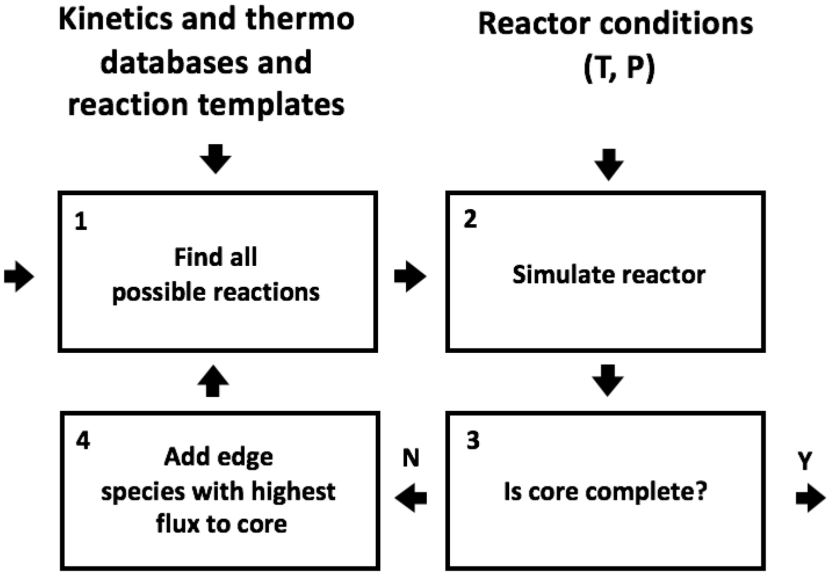

Kinetics and thermo databases and reaction templates

Reactor conditions (T, P)

1 Find all possible reactions

2 Simulate reactor

3 Is core complete?

4 Add edge species with highest flux to core

N

Y

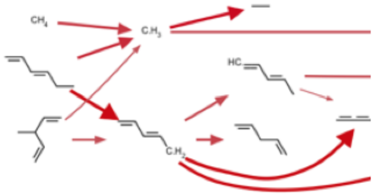

Kinetic model

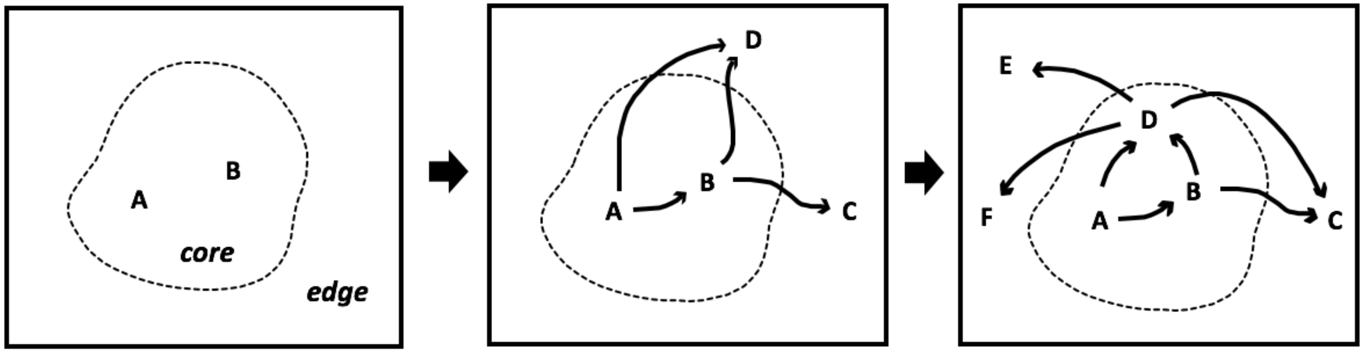

Thermodynamics databases

1. Species thermochemistry libraries
2. Group contribution methods. Uses the Benson's method ("Thermochemical Kinetics 1976). Divides a molecule into functional groups, and the contribution of each functional group to the overall thermochemistry is included. (See RMG website)

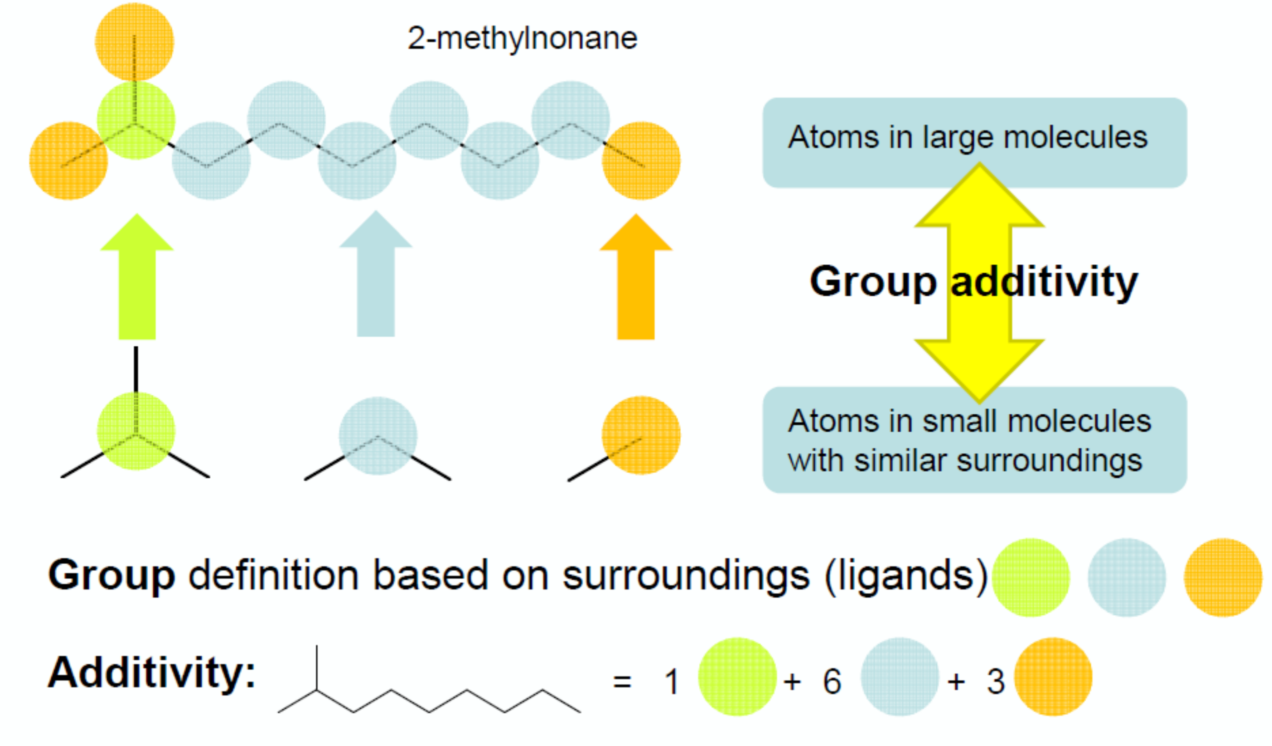

2-methylnonane

Atoms in large molecules

Group additivity

Atoms in small molecules with similar surroundings

Group definition based on surroundings (ligands)

Additivity: = 1 + 6 + 3

3. On-the-fly Quantum-chemical calculation of Thermochemical Properties (QMTP)

Kinetics database

- Series of pre-packaged libraries, e.g. Burke ($H_2/O_{2.}$), FFCM for natural gas. A wide range of libraries are included).

- All other reactions have their kinetic parameters estimated from 74 reaction families, e.g. H_Abstraction:

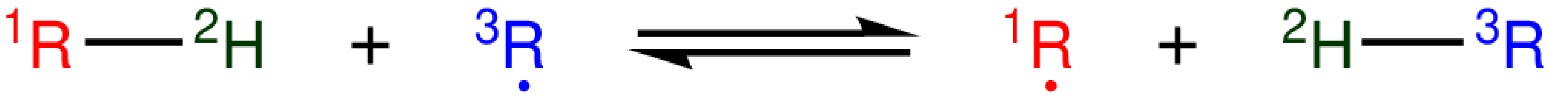

- Algorithms are then used to determine kinetic parameters.

Arkane

- Automated Reaction Kinetics and Network Exploration (Arkane): A Statistical Mechanics, Thermodynamics, Transition State Theory, and Master Equation Software https://chemrxiv.org/engage/chemrxiv/article-details/62d934e1fe12e32facad0d40
- Computations of thermodynamic properties of chemical species, high-pressure limit reaction rate coefficients, and pressure-dependent rate coefficient over multi-well molecular potential energy surfaces.
- Article describes the design of Arkane, how it should be used, and references the theory that it employs.

Example of reaction network: butyl

1-butyl isomerization to 2-butyl (via three- and four-member ring transition states)

the two beta-scission reactions of 1-butyl radical forming H atom + 1-butene and ethane + ethyl radical

the three beta-scission reactions of 2-butyl radical, forming H atom + 1-butene, H atom + 2-butene, and propene + methyl radical.

Example of reaction pathway analysis

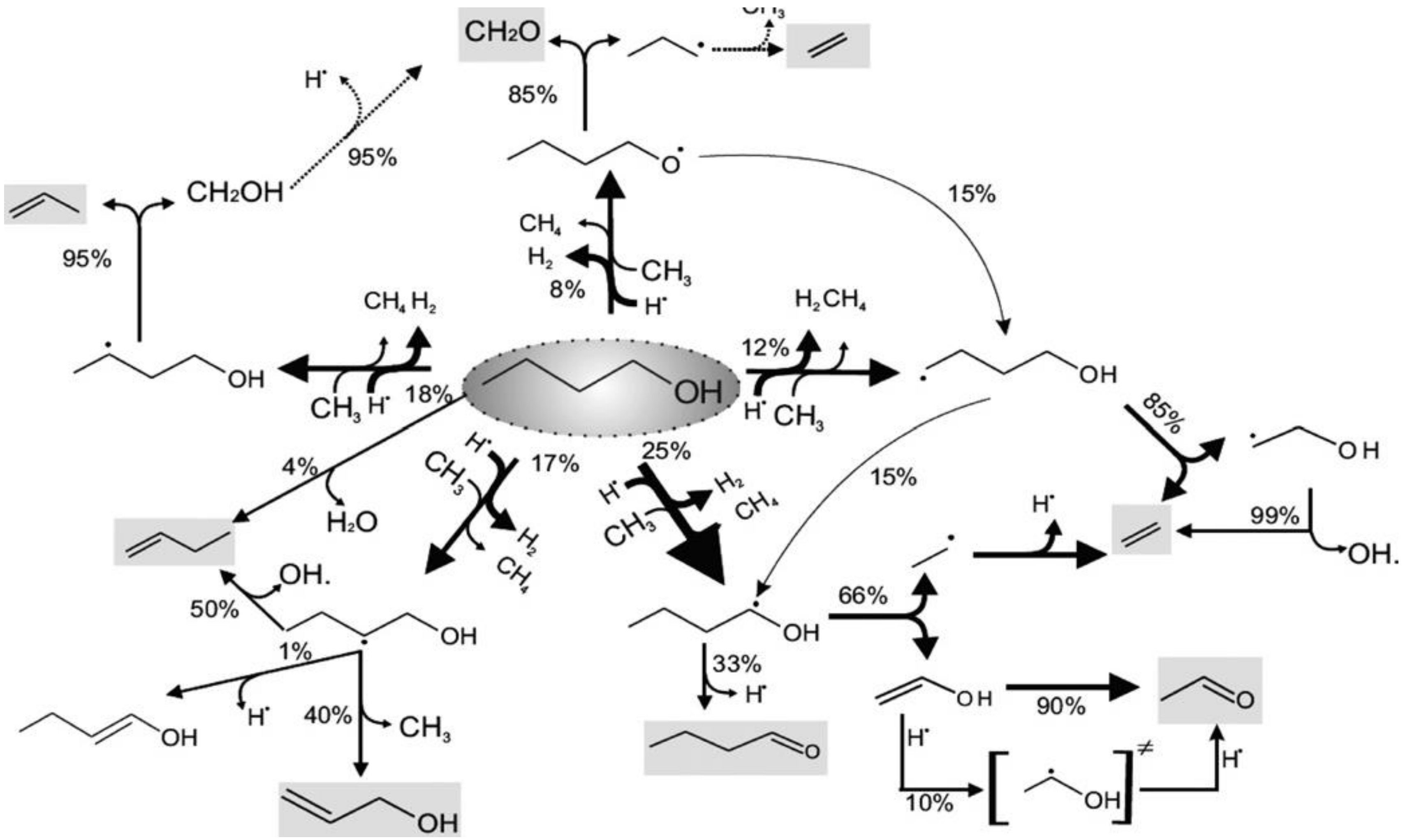

An example of an application of RMG

- Light alkene (up to C_4) combustion, Pio et al, Combustion and Flame 2022, 241, 112080
- Table shows existing mechanisms for alkene combustion
- Substantial discrepancies in prediction of experimental observations, e.g. IDT (Ind. Eng. Chem. Res. 2018, 57, 21, 7130)

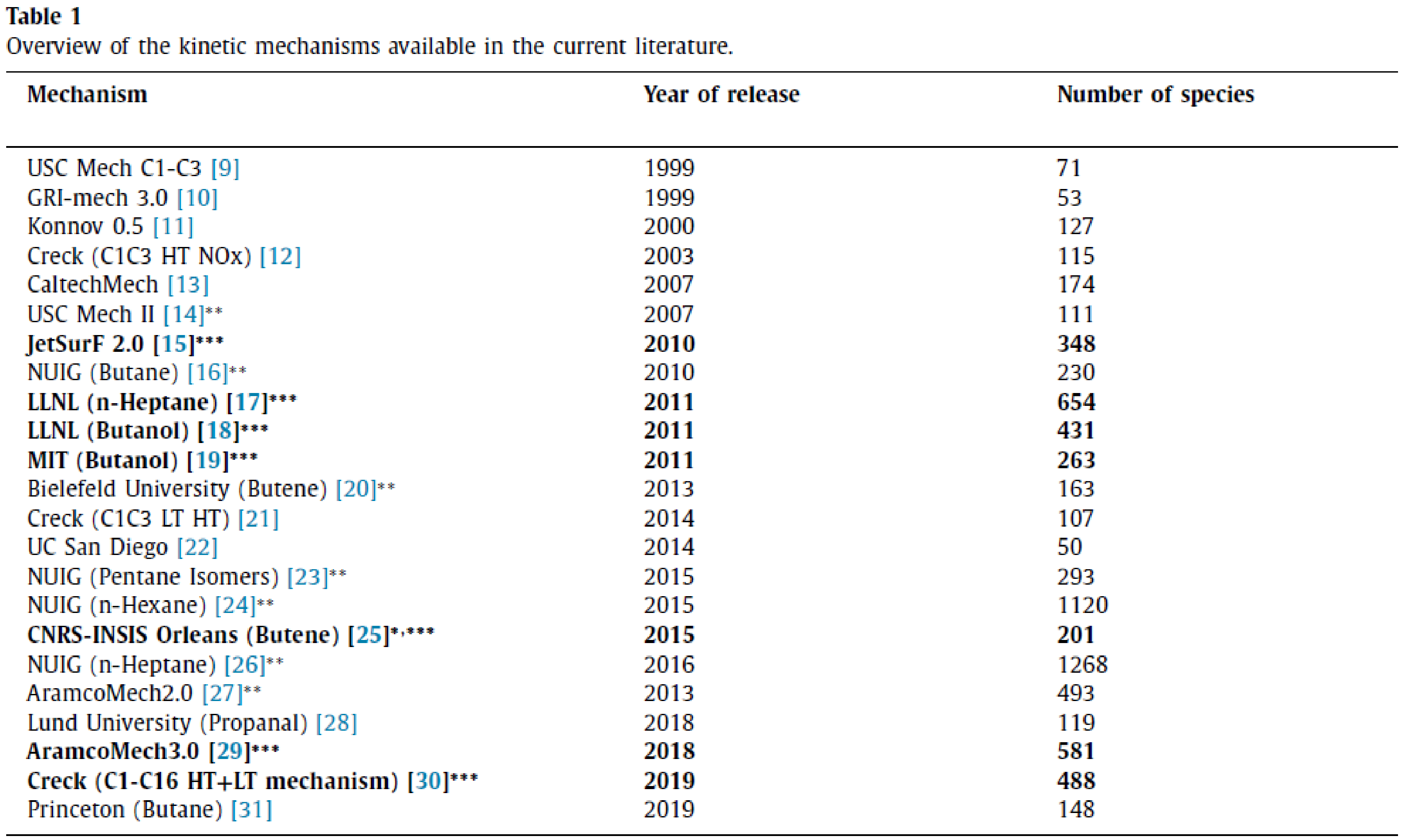

Table 1
Overview of the kinetic mechanisms available in the current literature.

Mechanism	Year of release	Number of species
USC Mech C1-C3 [9]	1999	71
GRI-mech 3.0 [10]	1999	53
Konnov 0.5 [11]	2000	127
Creck (C1C3 HT NOx) [12]	2003	115
CaltechMech [13]	2007	174
USC Mech II [14]**	2007	111
JetSurF 2.0 [15]* **	**2010**	**348**
NUIG (Butane) [16]**	2010	230
LLNL (n-Heptane) [17]* **	**2011**	**654**
LLNL (Butanol) [18]* **	**2011**	**431**
MIT (Butanol) [19]* **	**2011**	**263**
Bielefeld University (Butene) [20]**	2013	163
Creck (C1C3 LT HT) [21]	2014	107
UC San Diego [22]	2014	50
NUIG (Pentane Isomers) [23]**	2015	293
NUIG (n-Hexane) [24]**	2015	1120
CNRS-INSIS Orleans (Butene) [25]*,* **	**2015**	**201**
NUIG (n-Heptane) [26]**	2016	1268
AramcoMech2.0 [27]**	2013	493
Lund University (Propanal) [28]	2018	119
AramcoMech3.0 [29]* **	**2018**	**581**
Creck (C1-C16 HT+LT mechanism) [30]* **	**2019**	**488**
Princeton (Butane) [31]	2019	148

Approach used

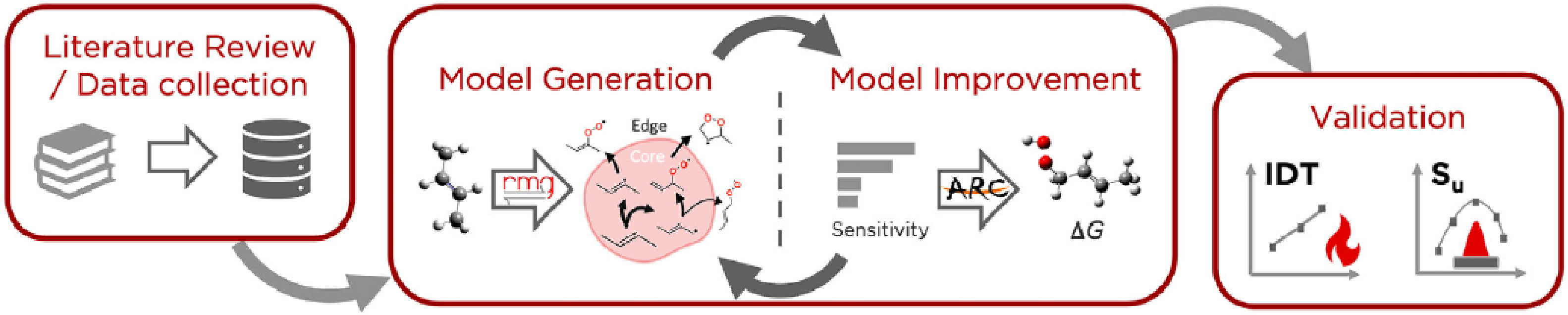

- Model covers 650 – 1500 K and 0.3 – 100 atm, ϕ = 0.3 – 2.0 for equimolar mixtures of ethene, propene and three butene isomers. Model generated using RMG. Use Glarborg C_0 – C_2 mechanism.
- Model improved using sensitivity analysis to identify key parameters. If these had been determined by analogy (e.g. group additivity, then they were redetermined by ab initio quantum mechanics – see original paper for level used and for treatment of internal rotors.
- Final model has 797 species and 37 706 reactions. Ab initio thermochemical parameters determined for 550 species.
- No tuning of parameters to improve fit to experimental data. Model improvement based on Arkane methodology.

Evolution of mechanism

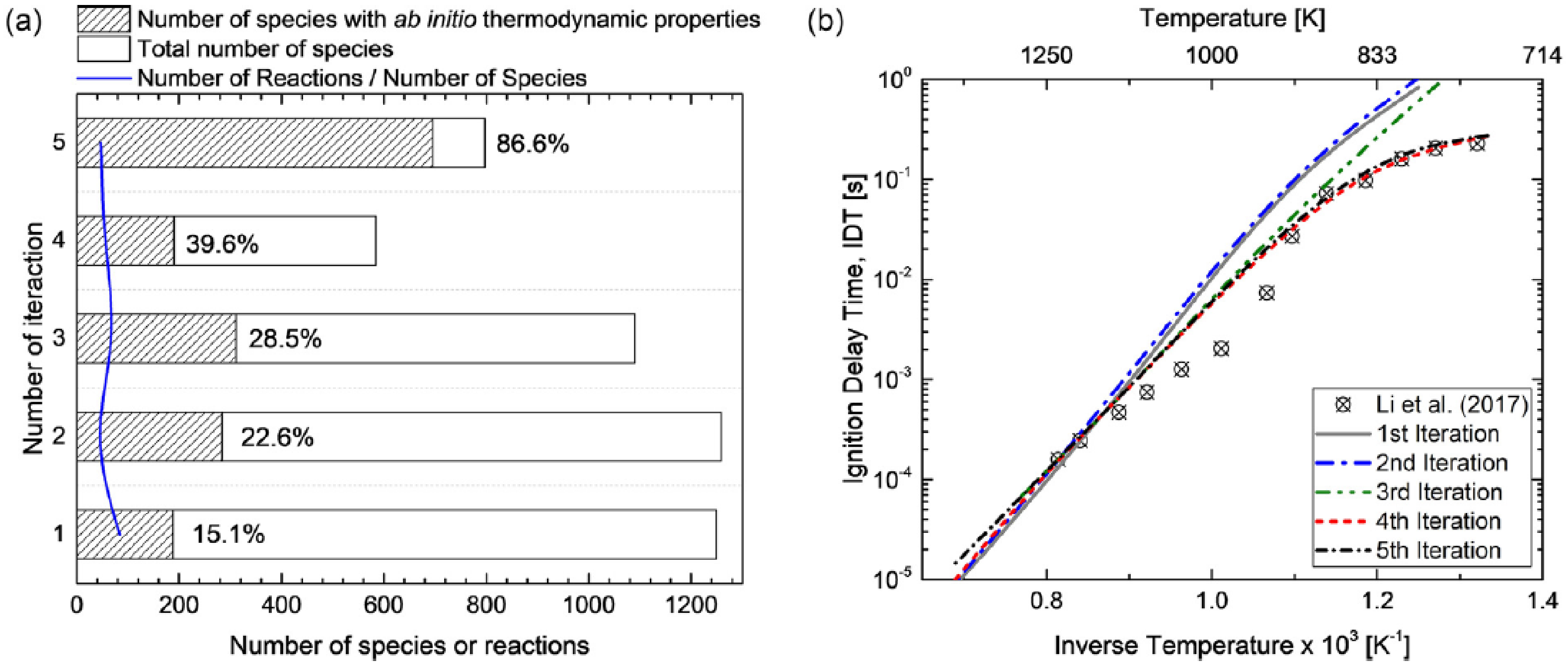

- Stoichiometric 1-butene/air, 10 atm
- Number of species and % with ab initio thermochemistry shown. With higher accuracy thermochemistry in later iterations RMG decides not all species in earlier iterations are kinetically significant

Comparison with experiment

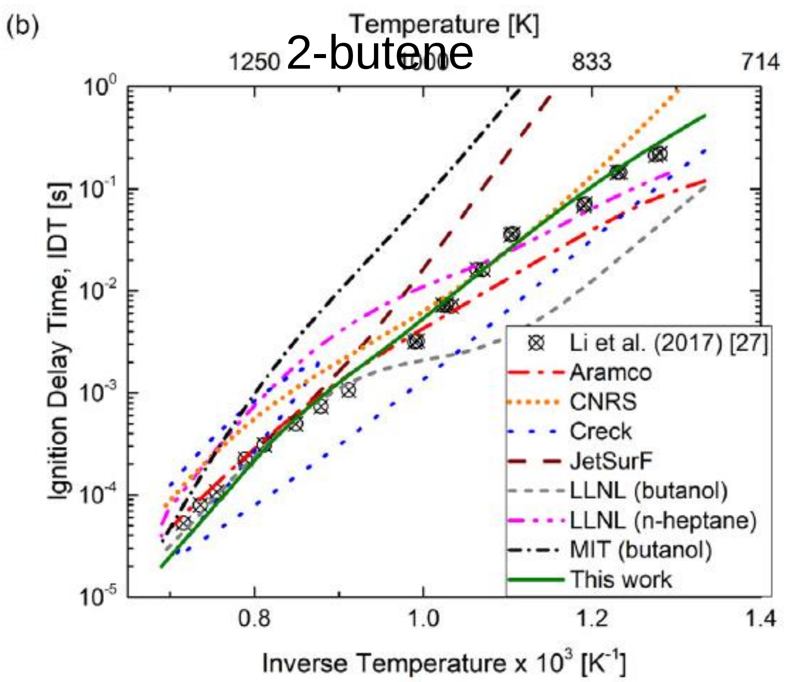

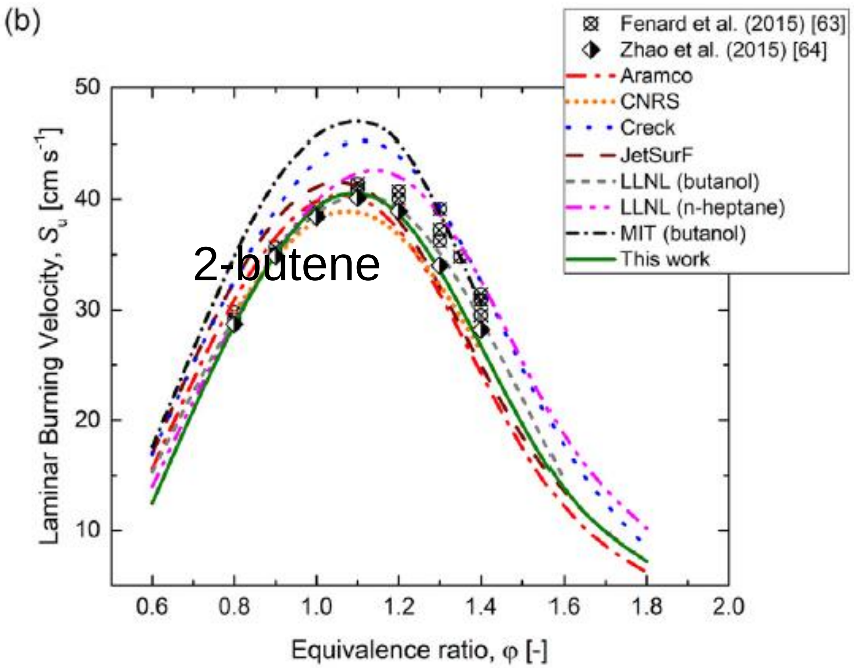

- Comparison with experimental IDT vs T (stoichiometric, 10 atm) and laminar burning velocity vs equivalence ratio (atmospheric conditions)

Sensitivities for OH for 2-butene at 700 K, 10 atm, 10% fuel depletion

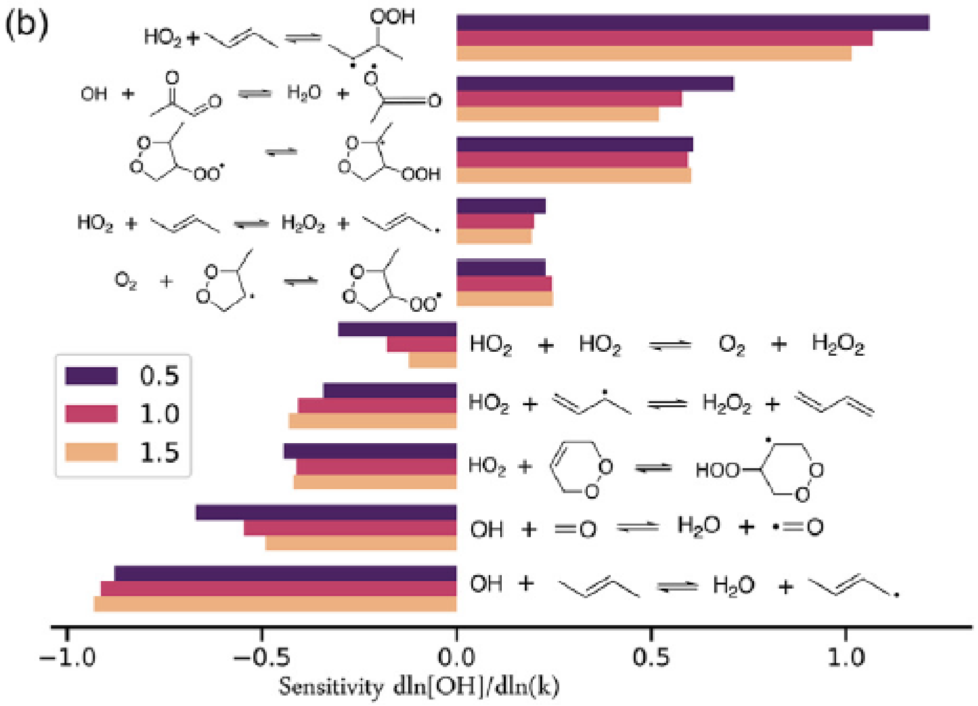

- Some of these reactions are complex, with no experimental data, so that high quality estimates, as provided by RMG, are essential.

Comparison of influential reaction rate

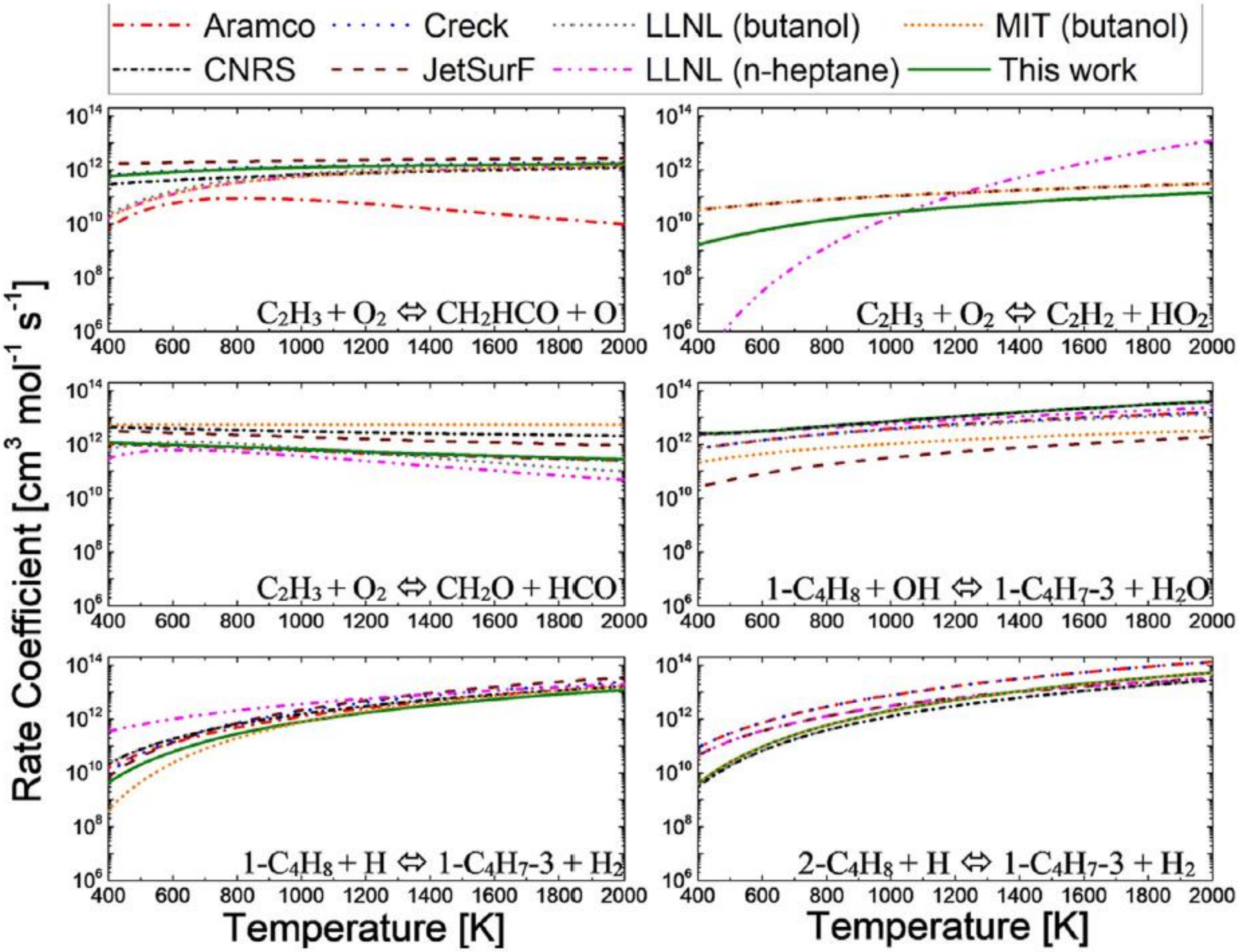

Topic 7
Peroxy radical chemistry and autoignition

Low temperature combustion

- Combustion in the 500 – 1000 K range shows regions of slow reaction and regions of explosion or ignition.
- Cause of 'knock' in gasoline engine and of the desired autoignition in diesel engines
- There is a region of "negative temperature coefficient", where the reaction changes from branching to termination as T increases, in the boundary between low temperature and high temperature combustion
- Peroxy radical chemistry is central to combustion in the low temperature regime

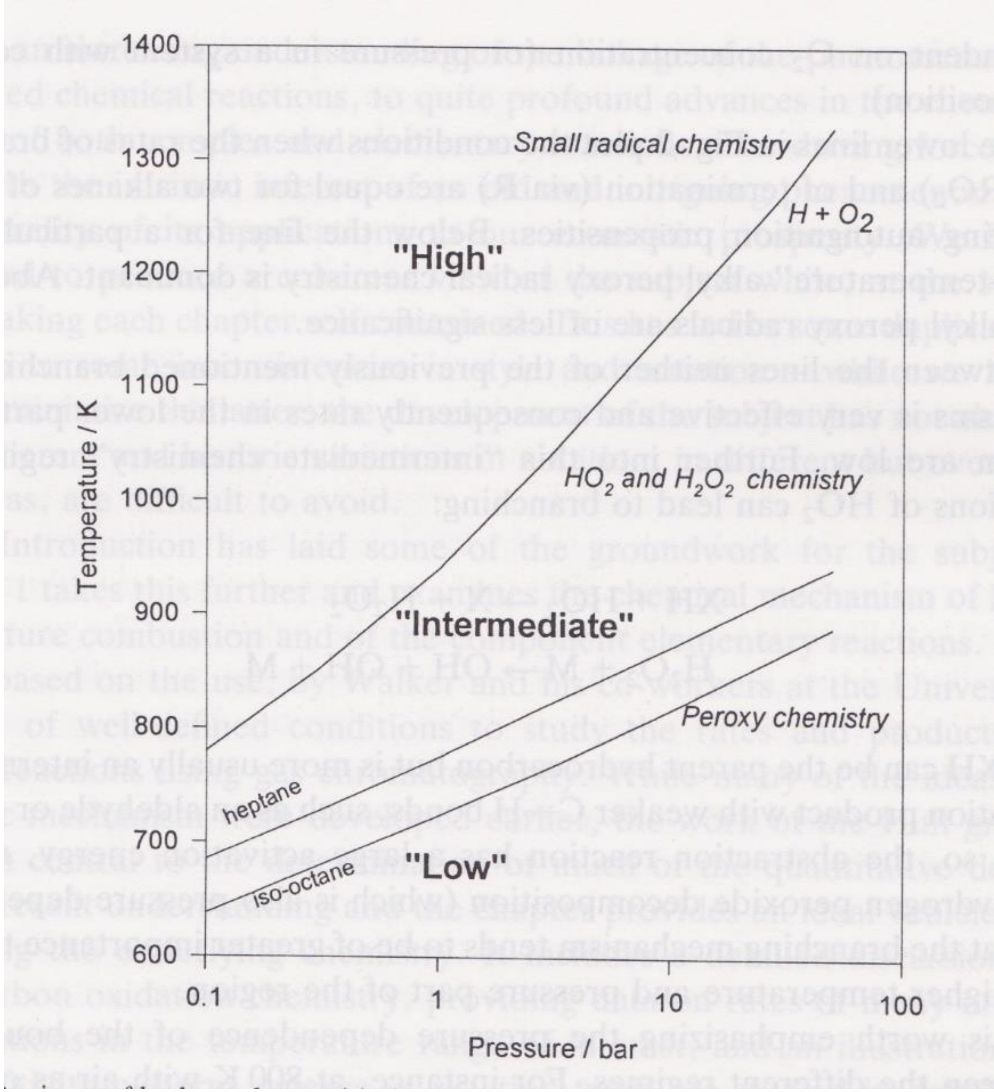

Autoignition chemistry

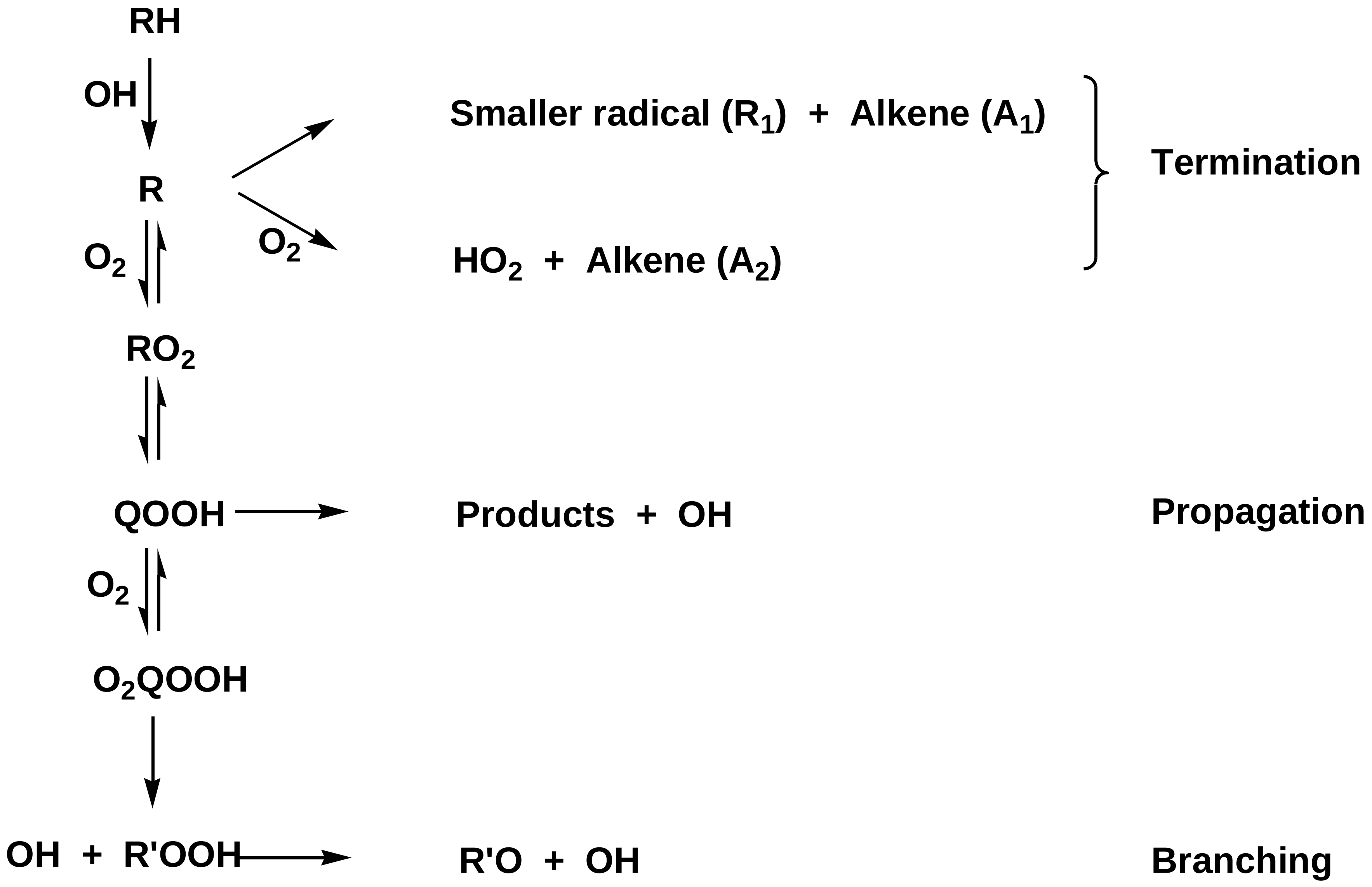

RH

OH

R

O_2

O_2

RO_2

QOOH

O_2

O_2QOOH

OH + R'OOH

Smaller radical (R_1) + Alkene (A_1)

HO_2 + Alkene (A_2)

Termination

Products + OH

Propagation

R'O + OH

Branching

A more detailed view – Curran, Proc Comb Inst, 2019, 37, 57

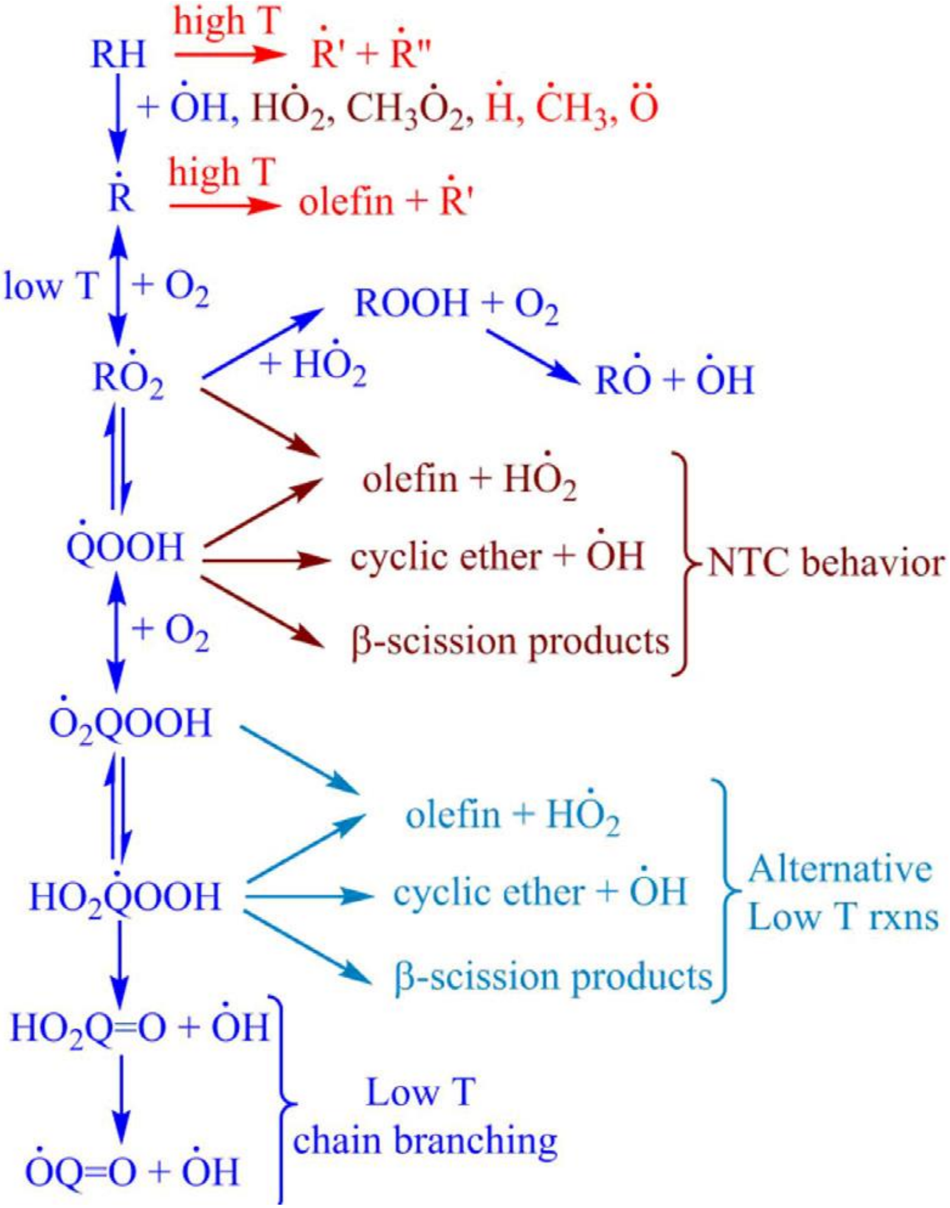

$RH \xrightarrow{\text{high T}} \dot{R}' + \dot{R}''$

$+ \dot{O}H, H\dot{O}_2, CH_3\dot{O}_2, \dot{H}, \dot{C}H_3, \ddot{O}$

$\dot{R} \xrightarrow{\text{high T}} \text{olefin} + \dot{R}'$

low T $+ O_2$

$R\dot{O}_2$

$+ H\dot{O}_2$

$ROOH + O_2$

$R\dot{O} + \dot{O}H$

$\dot{Q}OOH$

olefin $+ H\dot{O}_2$

cyclic ether $+ \dot{O}H$

β-scission products

NTC behavior

$+ O_2$

$\dot{O}_2QOOH$

olefin $+ H\dot{O}_2$

cyclic ether $+ \dot{O}H$

β-scission products

Alternative Low T rxns

$HO_2\dot{Q}OOH$

$HO_2Q{=}O + \dot{O}H$

$\dot{O}Q{=}O + \dot{O}H$

Low T chain branching

Negative temperature coefficient
Westbrook et al, Comb and Flame, 156(2009) 181

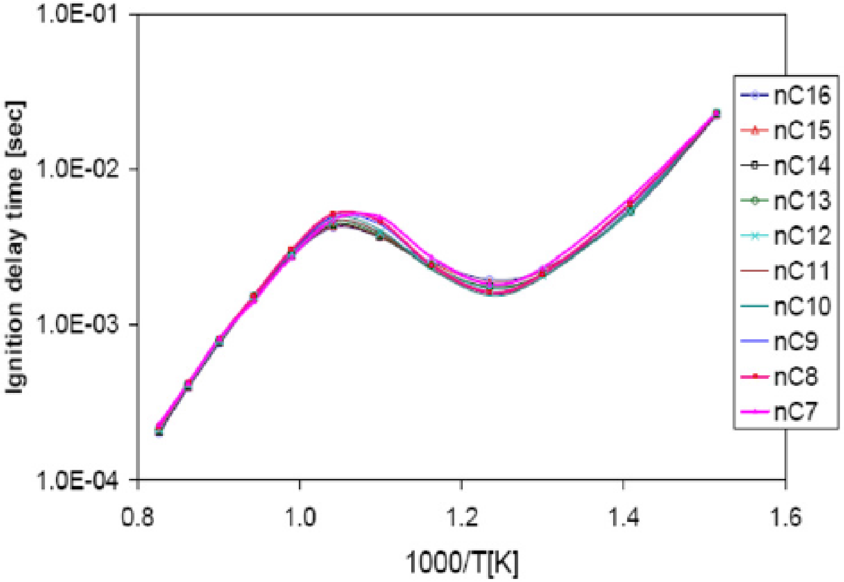

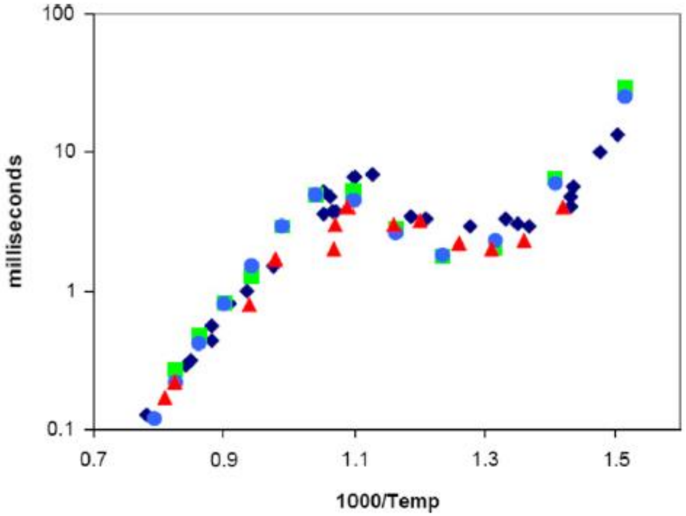

Computed ignition delay times for stoichiometric n-alkanes in air at 13.5 bar.

- Shock tube ignition delay times for n-heptane and n-decane, all at 13.5 bar pressure and stoichiometric fuel/air. Experiments are n-heptane (diamond) and n-decane (Triangle) n-Heptane (square) Computed results n-decane (circle)

Static reactors: Early studies of alkane oxidation kinetics and mechanism by Baldwin, Walker and co-workers

- The techniques rely on end product analysis using gas chromatography. Three techniques were used:
  - Addition of small amounts of alkane, RH, to a slowly reacting $H_2 + O_2$ mixture at ~ 750 K allowed measurements of, e.g. OH, H, HO_2 + RH. $H_2 + O_2$ provides a well-controlled environment containing the radicals. (JCS Faraday Trans 1., 1975, 71, 736)
  - Oxidation of aldehydes (550 – 800 K). Aldehydes act as a source of alkyl radicals, e.g. 2-C_3H_7 from 2-C_3H_7CHO (JCS Faraday Trans 2., 1987, 83, 1509)
  - Decomposition of tetramethylbutane (TMB) in the prsence of O_2. System acts as a source of $HO_{2.}$ (JCS Faraday Trans 1., 1986, 82, 89)

Whole system studies
Provide targets for mechanism evaluation

Flow reactor study of dimethyl ether oxidation at low T

Fischer et al. Int J Chem Kinet (32, 741, 2000)

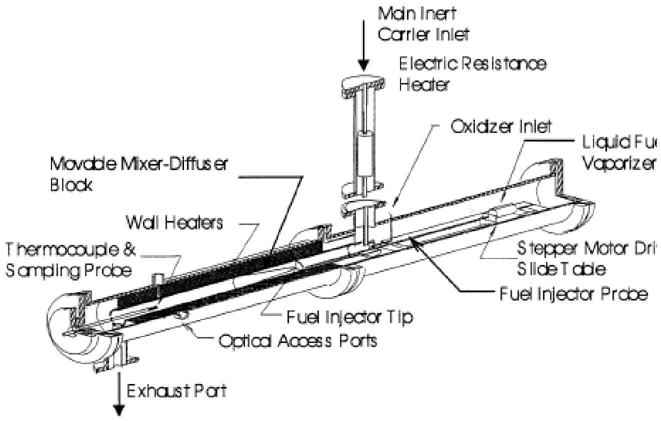

Variable Pressure Flow Reactor

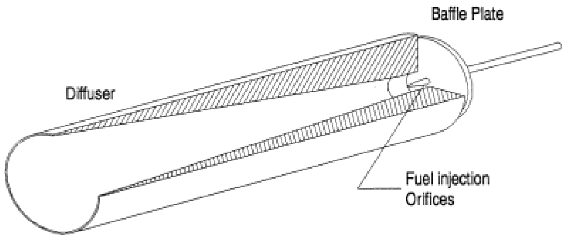

Mixer/Diffuser Block

Figure 1 Princeton variable-pressure flow reactor mixer block assembly.

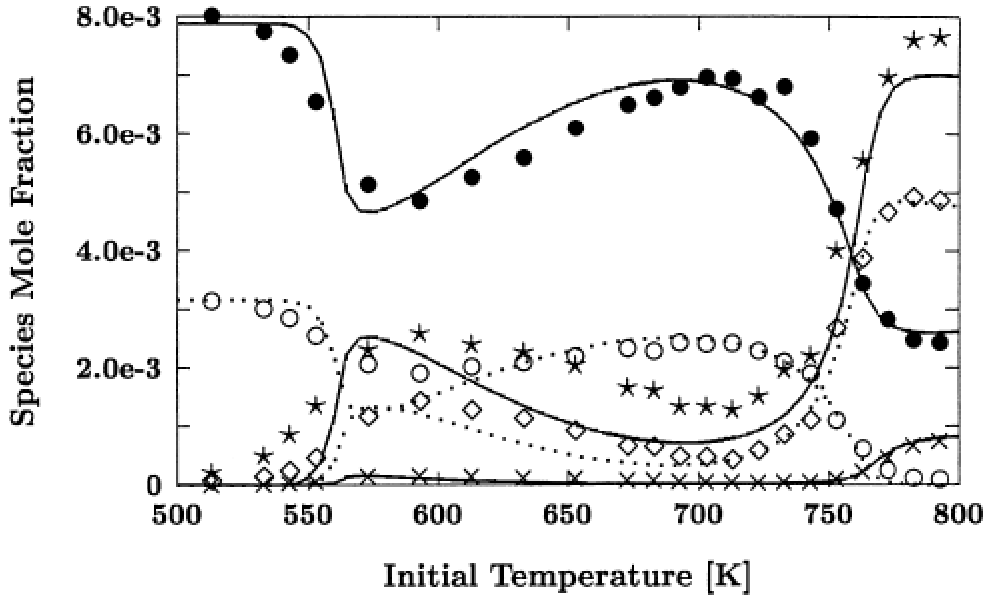

Figure 3 Measured (symbols) and calculated (curves) species concentrations from a flow reactor. 3030 ppm DME, $\phi = 1.19$, $P = 12.5$ atm, $\tau = 1.8$ s. ● O_2, ○ CH_3OCH_3, ★ H_2O, ◇ CO, and × CO_2. Dotted lines correspond to open symbols.

- 550–850 K, 12–18 atm, at equivalence ratios of 0.7 - 4.2
- FTIR, non-dispersive IR (NDIR) (for CO and CO_2), and electrochemical (for O_2)

Mechanism

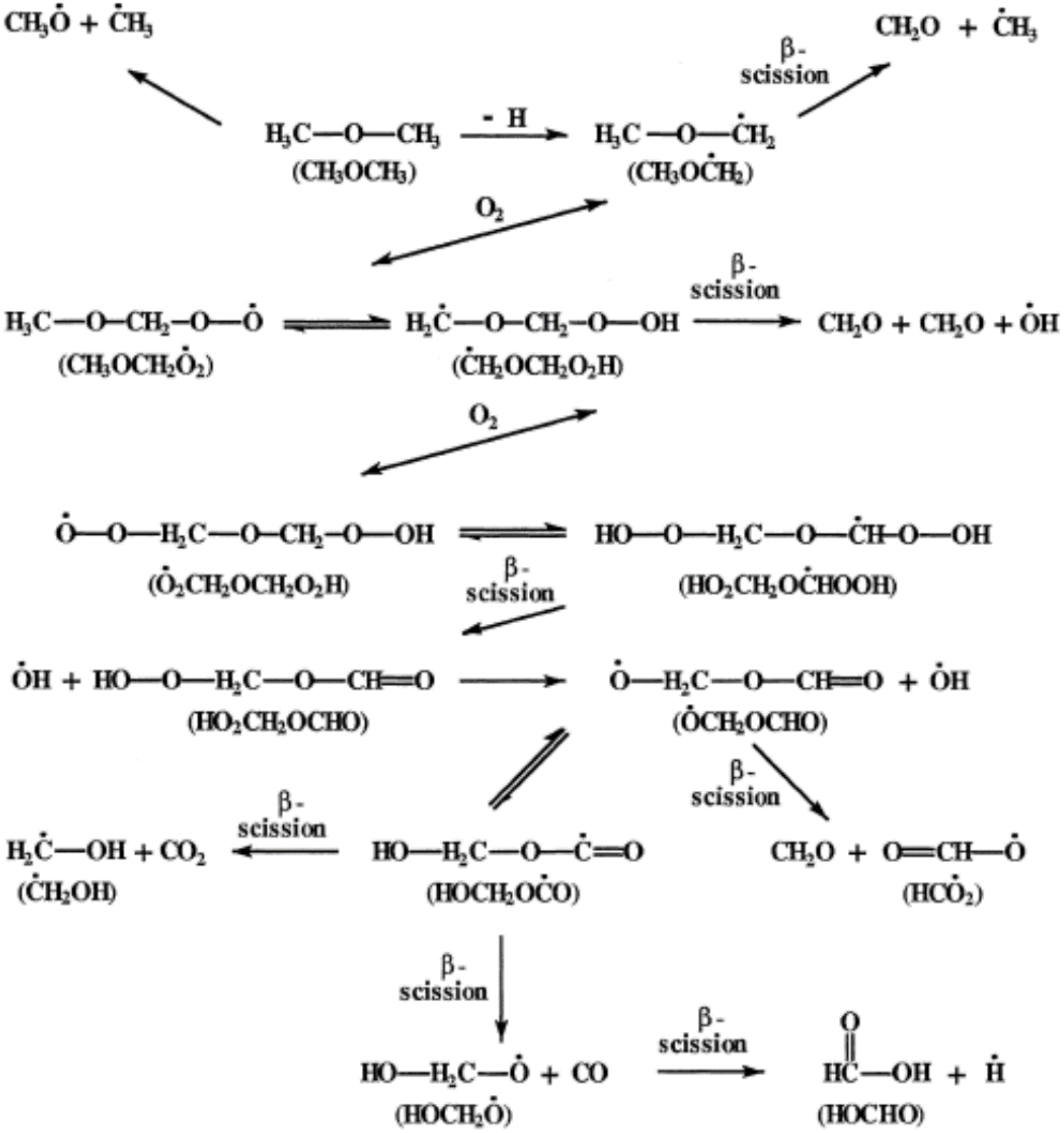
CH3Ȯ + ĊH3
H3C—O—CH3
(CH3OCH3)
- H
H3C—O—ĊH2
(CH3OĊH2)
β-scission
CH2O + ĊH3
O2
H3C—O—CH2—O—Ȯ
(CH3OCH2Ȯ2)
H2Ċ—O—CH2—O—OH
(ĊH2OCH2O2H)
β-scission
CH2O + CH2O + ȮH
O2
Ȯ—O—H2C—O—CH2—O—OH
(Ȯ2CH2OCH2O2H)
HO—O—H2C—O—ĊH—O—OH
(HO2CH2OĊHOOH)
β-scission
ȮH + HO—O—H2C—O—CH═O
(HO2CH2OCHO)
Ȯ—H2C—O—CH═O + ȮH
(ȮCH2OCHO)
β-scission
H2Ċ—OH + CO2
(ĊH2OH)
β-scission
HO—H2C—O—Ċ═O
(HOCH2OĊO)
β-scission
CH2O + O═CH—Ȯ
(HCȮ2)
β-scission
HO—H2C—Ȯ + CO
(HOCH2Ȯ)
β-scission
O
HC—OH + Ḣ
(HOCHO)

Sensitivity analysis

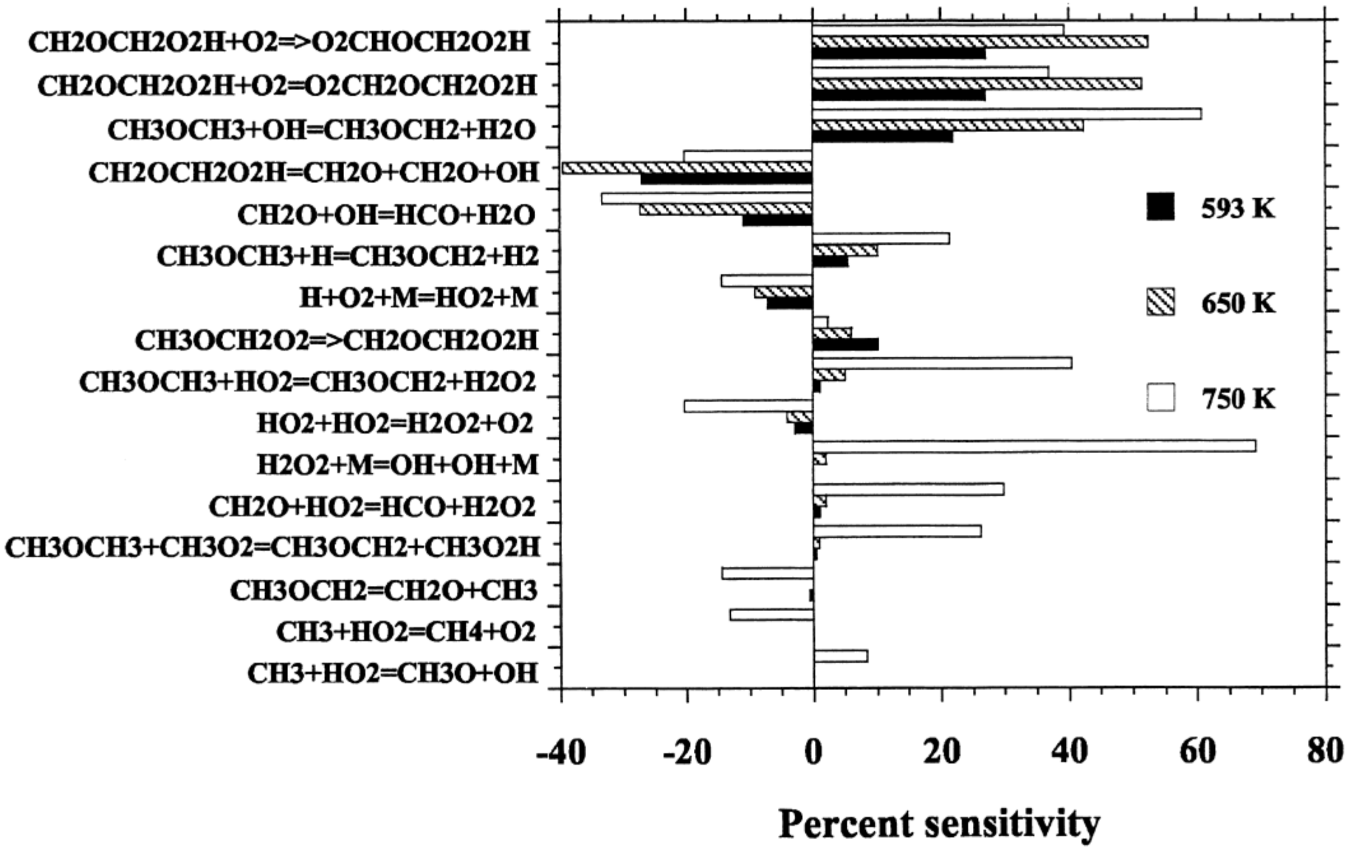

Figure 28 Sensitivity coefficients for dimethyl ether oxidation. 3030 ppm DME, ϕ = 1.19, P = 12.5 atm, τ = 2.1 s.

- See also Fischer et al. Int J Chem Kinet (32, 713, 2000) for a study at higher T (2.5 atm, 1118 K) using the same technique
- Other methods used: Jet Stirred reactor (Proc Comb Inst, 1996, 23, 627).

Jet stirred reactor, coupled with synchrotron vacuum ultraviolet photoionization molecular-beam mass spectrometry

Battin-Leclerc et al, Ang. Chemie (International edition), 49 (2010)3169

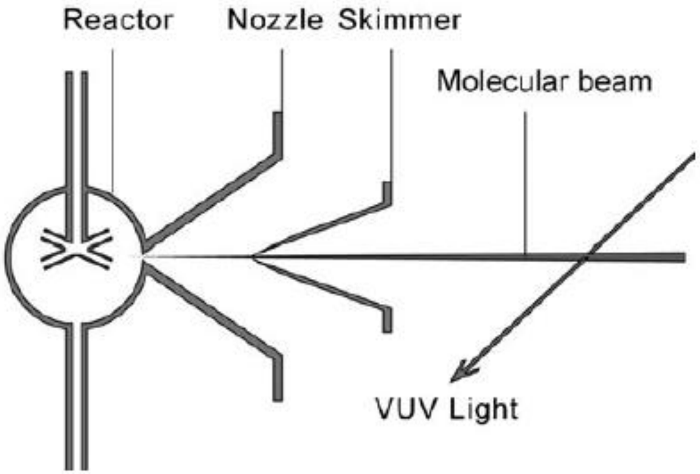

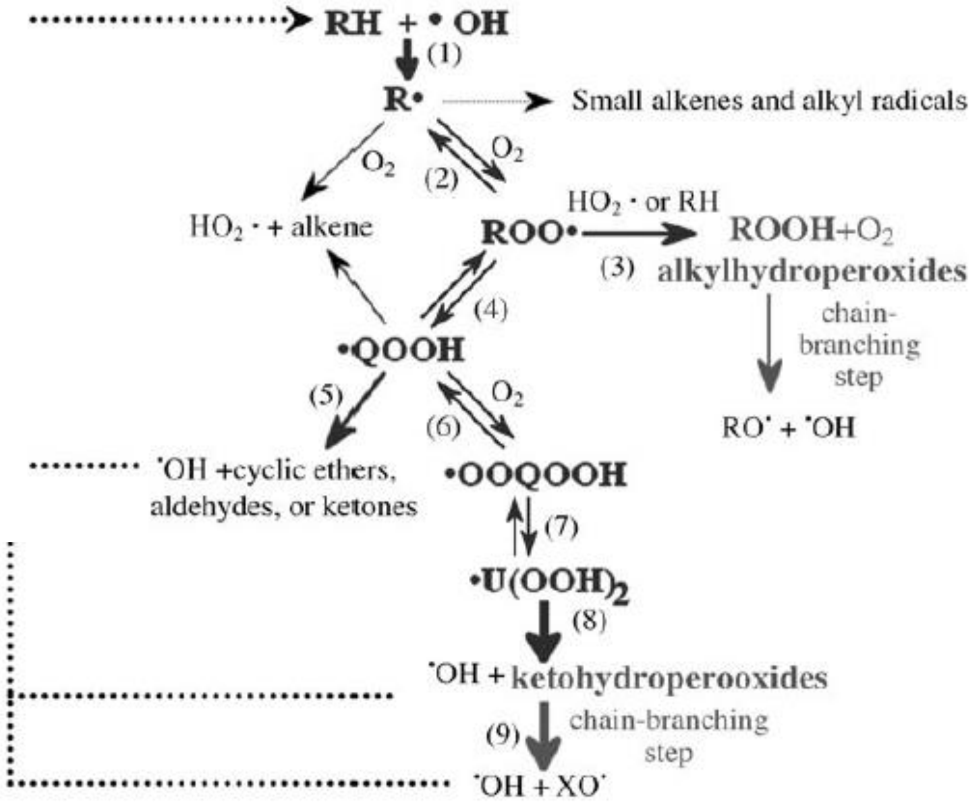

- Provided direct observation of speciated hydroperoxides for the first time

Experimental and modelling observations, oxidation of n-butane

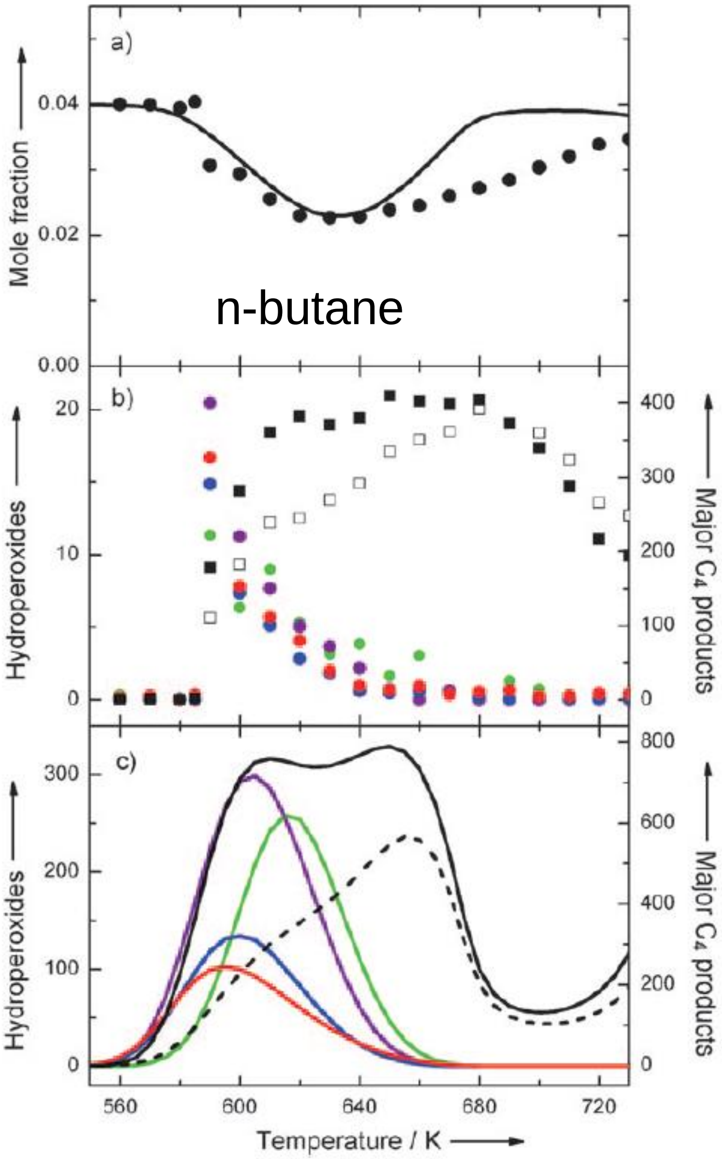

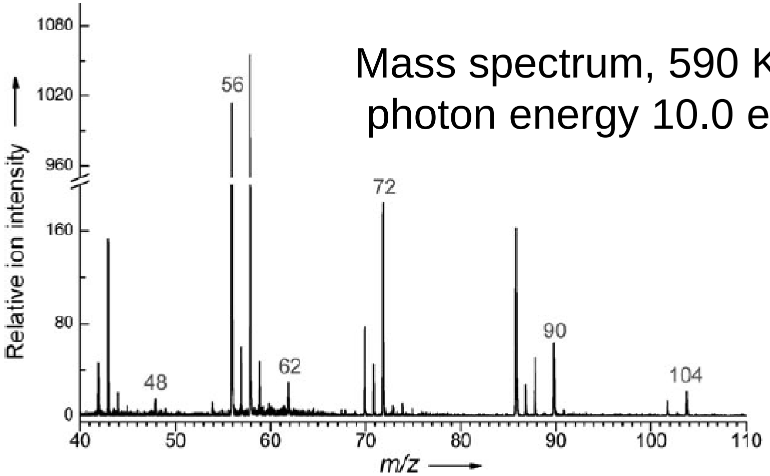

Mass spectrum, 590 K, photon energy 10.0 ev

- **Experiment:** m/z 48 (green circles), 56 (white squares, the signal is divided by 7.5), 62 (purple circles), 72 (black squares), 90 (blue circles, the signal is divided by 4) and 104 (red circles)
- **Calculated:** (ppm) CH3OOH (48) (green line,mole fraction divided by 5), C2H5OOH (62) (purple line), C4H9OOH (90) (blue line), the C4 ketohydroperoxides (104) (red line), butenes(56) (dash line, mole fraction divided by 5), and C4H8O products (72) (black line)

Evidence for a third O_2 addition in 2-methylhexane combustion

Wang et al, Proc Combustion Inst 36 (2017) 373–382

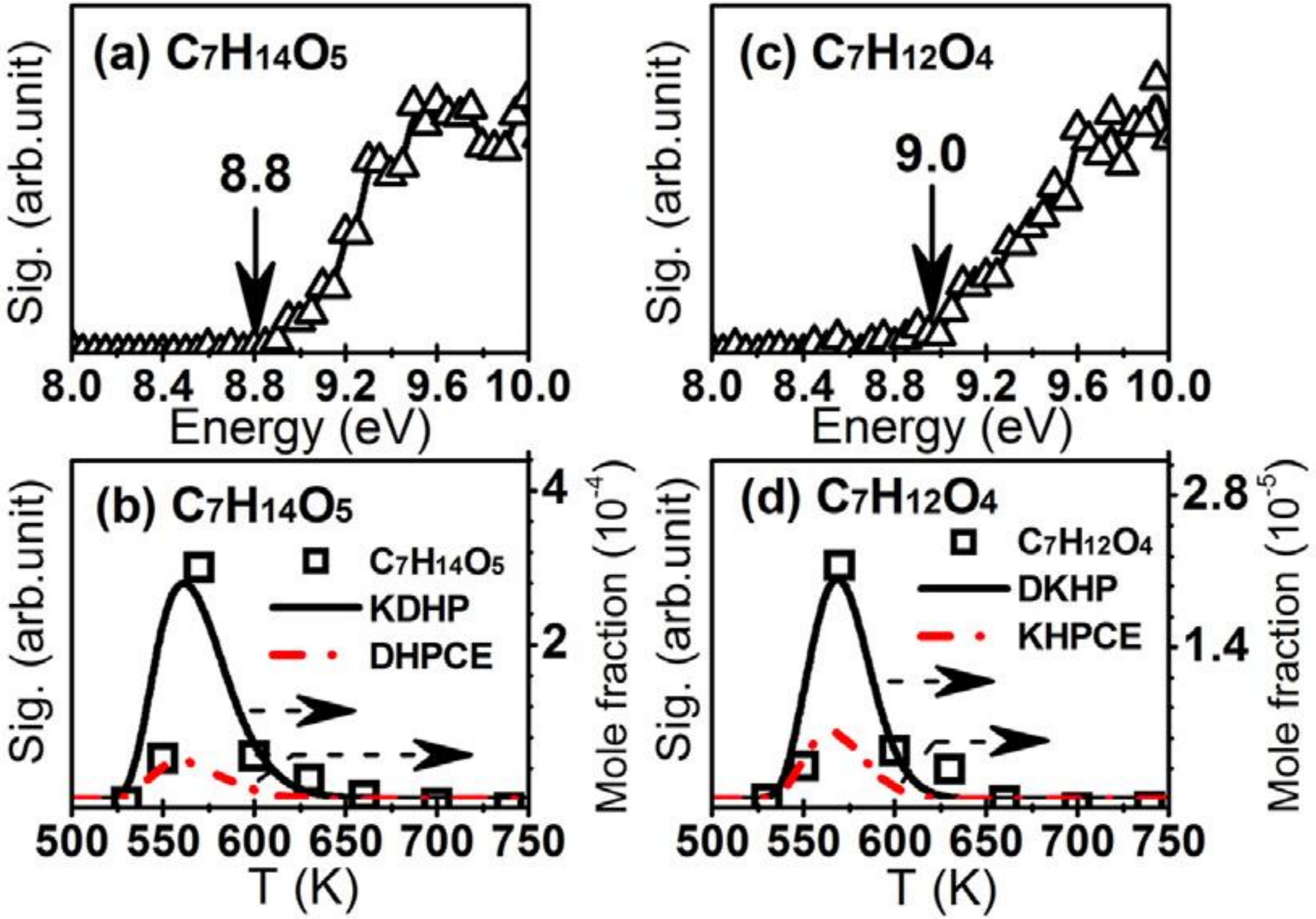

Keto-dihydroperoxide
Dihydroperoxy cyclic ether

Diketo-hydroperoxide
Ketohydroperoxide cycli ether

Mechanism extensions following obeservations

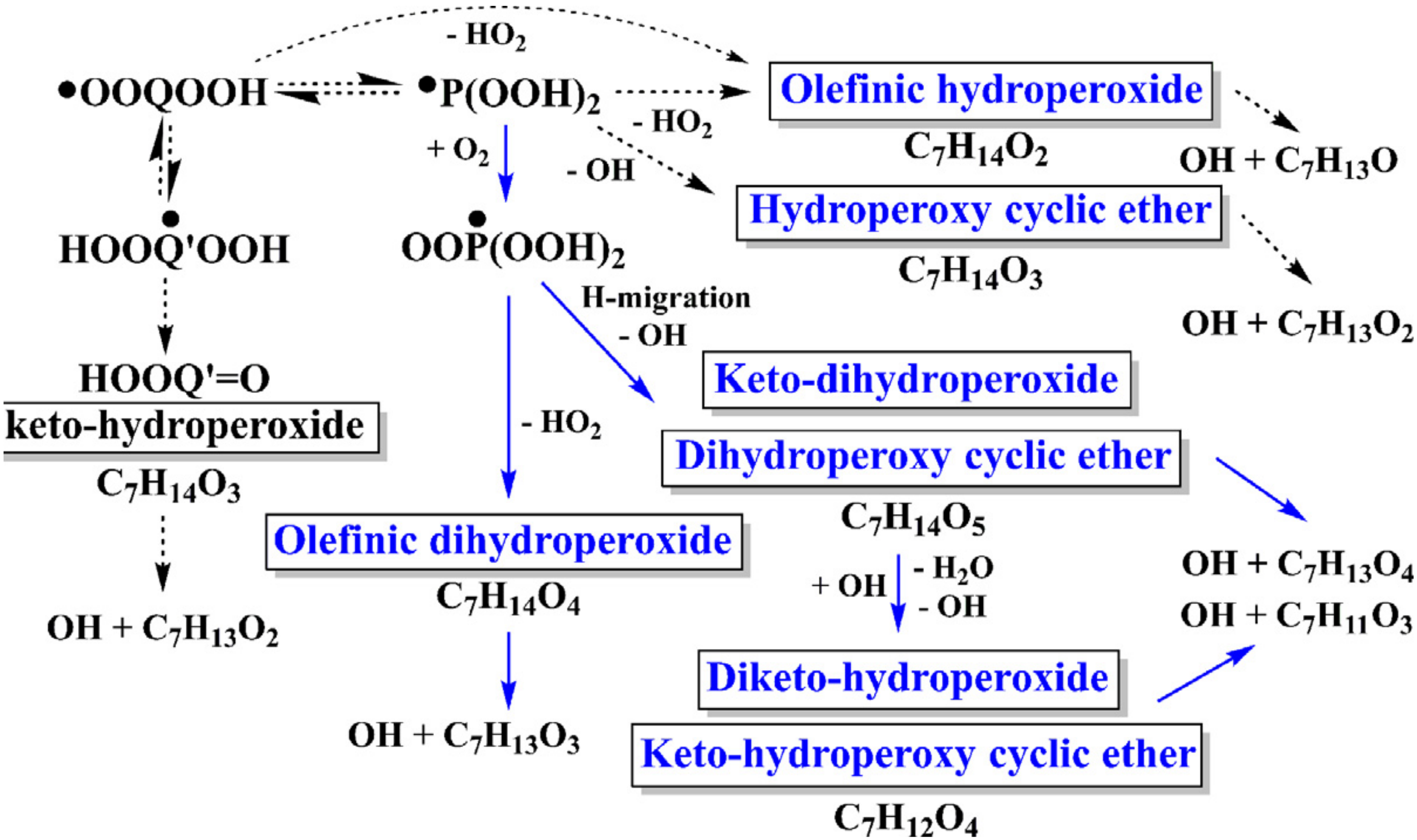

- Blue arrows show extensions to mechanism of Mohamed et al, J Phys Chem, 120 (2010) 3169

Rapid compression machines and ignition delay times: methyl cyclohexane (Proc Comb Inst, 31, 267 (2007))

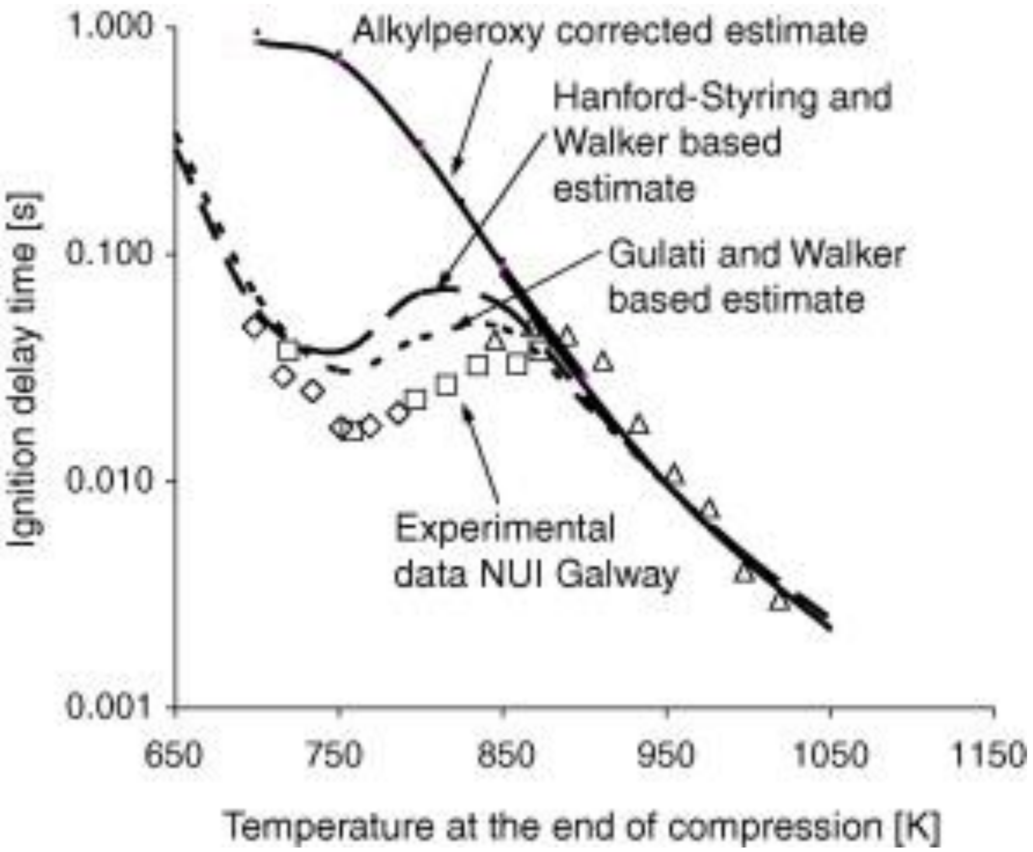

- Measured ignition delay times (symbols) for MCH/O_2/diluent stoichiometric mixtures for 10 atm pressure at the end of compression (◊, 100% N_2; □, 50% N_2/50% Ar; and ▵, 100% Ar). The predicted ignition delays (curves) are for the three estimates of RO_2 isomerization rates for MCH.

Individual reactions or groups of reactions

CH_3 + O_2 (reminder from Topic 6)

- At lower *T* the main route is formation of CH_3OO(A). As *T* increases CH_3OO starts to dissociate
- PE curves (B: Walch) show two higher temperature channels:
- HCHO + OH formation lower barrier but involves curve crossing: small A factor
- CH_3O + O high barrier, but large A factor
- Arrhenius plot (C: Srinivasan et al; large uncertainties)

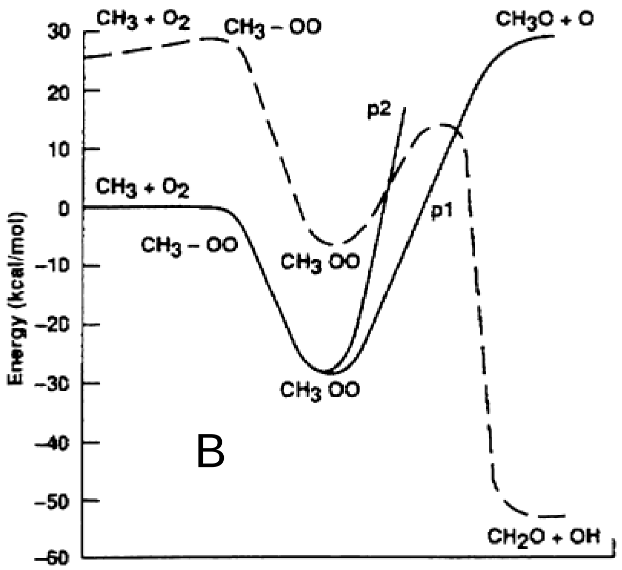

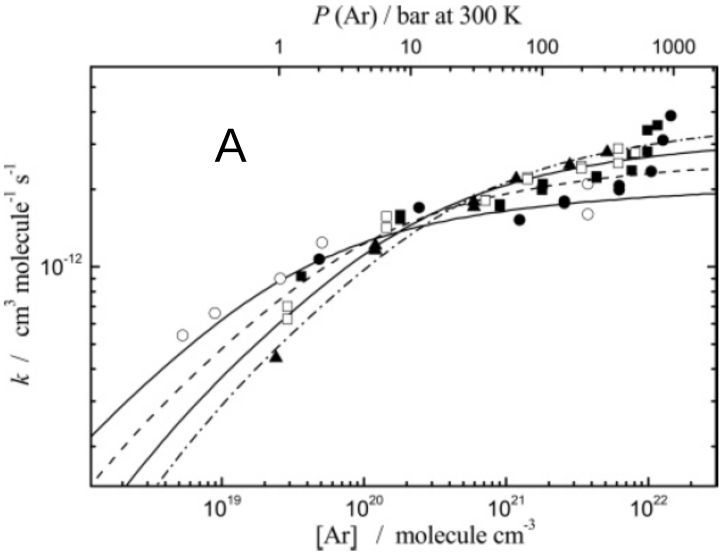

Figure 4. Rate constants *k* for the reaction $CH_3 + O_2 (+ M) \rightarrow CH_3O_2$ (+ M) with M = Ar. Lines from top to bottom at 10^{19} molecule cm^{-3} for 300, 400, 500, and 600 K, respectively, constructed with eqs 4.1–4.3. Experimental results: ●, 300; ■, 400; □, 500; ▲, 600 K from this work; ○, 300 K from ref 4.

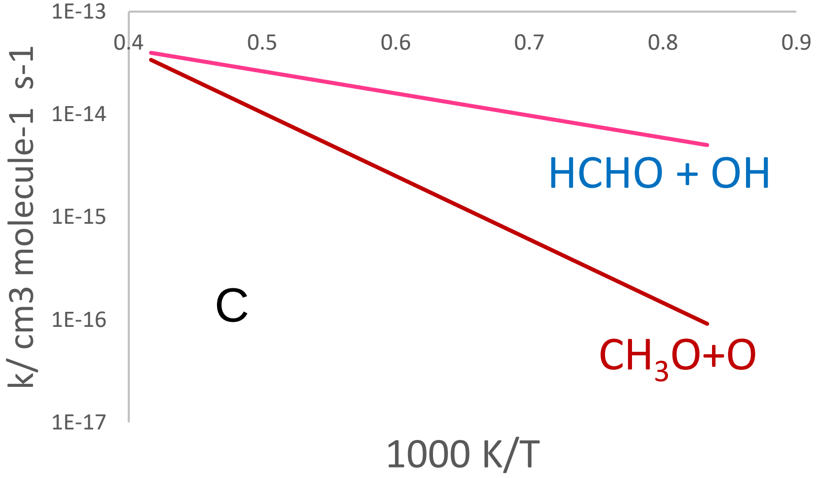

$C_2H_5 + O_2$; Wagner et al J Phys Chem 94 (1990) 1853
Theory + pulsed photolysis, photionization mass spectrometry

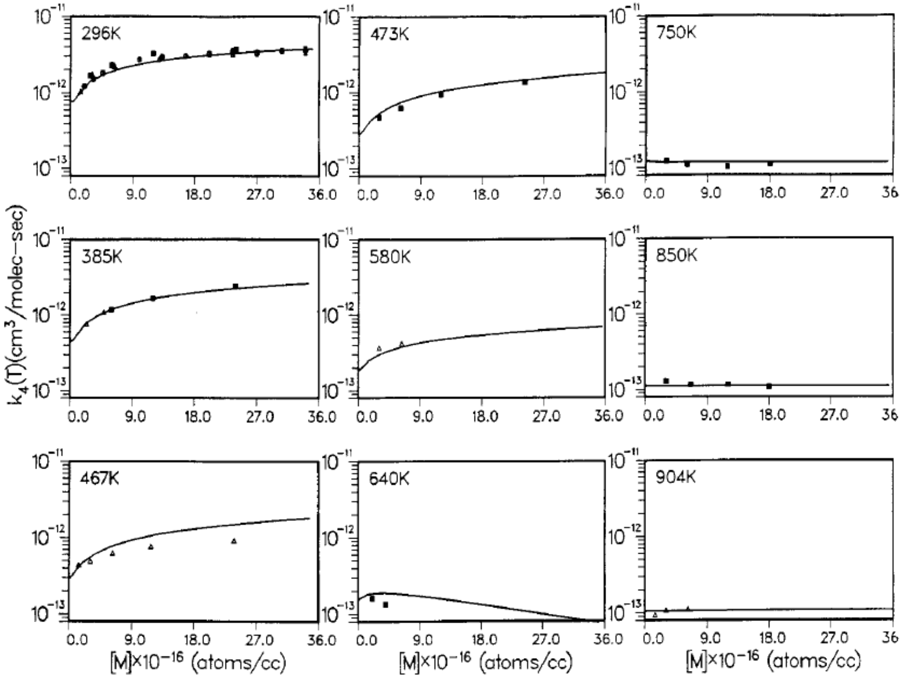

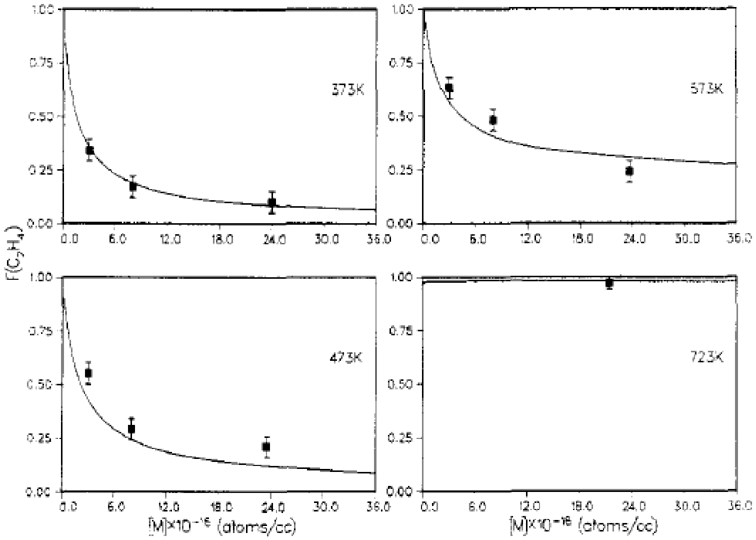

$C_2H_5 + O_2 \rightarrow C_2H_5O_2^*$
$C_2H_5O_2^* + M \rightarrow C2H_5O_2 + M$
$C_2H_5O_2^* \rightarrow C_2H_4 + HO_2$
$C_2H_5O_2 + M \rightarrow C_2H_4 + HO_2$

- The overall rate constant is pressure dependent at low T and beomes pressure independent at high T
- The ethene yield decreases with pressure at low T. It increases with T, and dominates at high T

Determination of product yields in $C_2H_5 + O_2$ pulsed photolysis at higher pressures (see Topic 2)

$$C_2H_5 + O_2 \overset{[M]}{\longleftrightarrow} C_2H_5O_2 \qquad (1a)$$

$$\rightarrow C_2H_4 + HO_2 \qquad (1b)$$

$$\rightarrow c - C_2H_4O(\text{oxirane}) + OH \qquad (1c)$$

- Observed the formation of OH and HO_2, determining the fractional yields.
- Used 100% yield of HO_2 from $CH_2OH + O_2$ to calibrate the system.

$$Cl_2 \xrightarrow{h\nu(355\ \text{nm})} 2Cl\bullet \qquad (2)$$

$$Cl + CH_3OH \xrightarrow{100\%} CH_2OH + HCl \qquad (4)$$

$$CH_2OH + O_2 \xrightarrow{100\%} HO_2 + CH_2O \qquad (5)$$

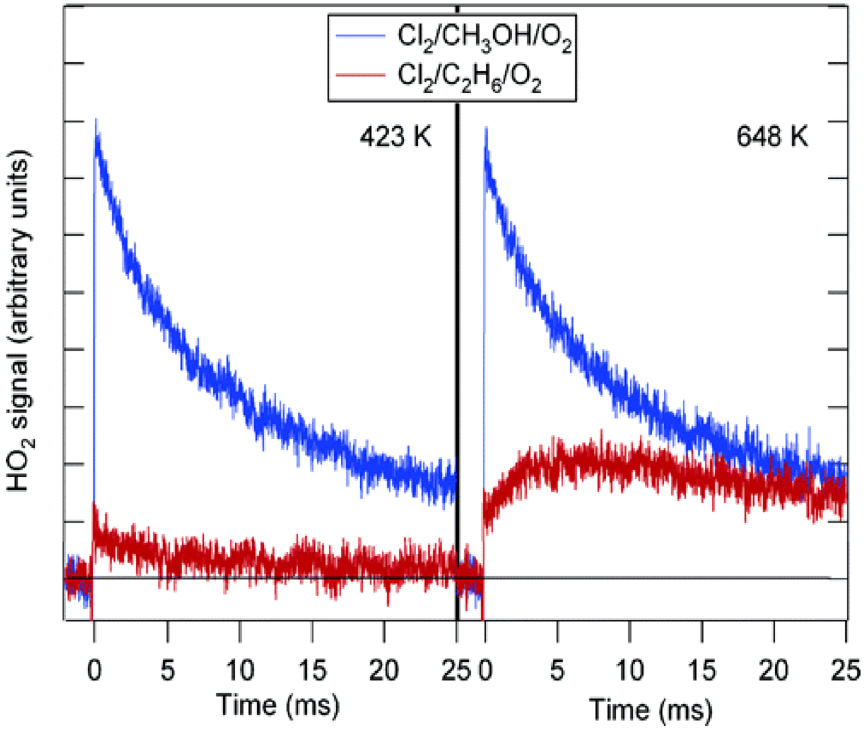

Blue traces, HO_2 from $Cl + CH_3OH$

C_2H_5 produced from $Cl + C_2H_6$

Red trace, HO2 from reaction 1

Growth is formation, decay reaction by HO_2+HO_2

Yield of HO_2 vs T and [M]

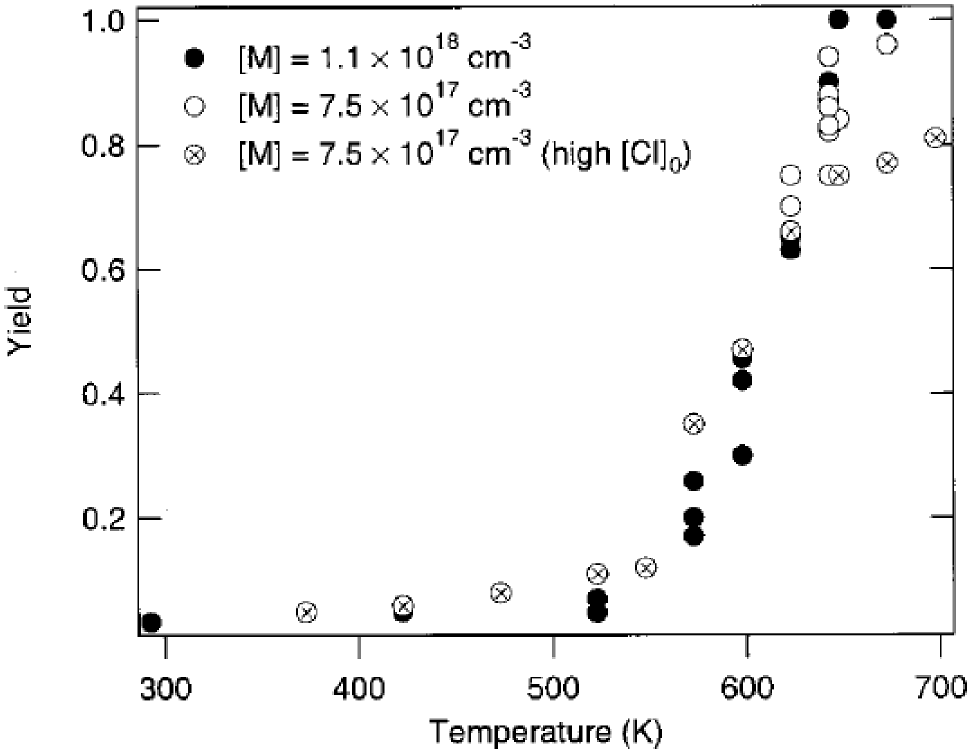

- HO_2 yield↑ as T↑ and p↓
- Two timescales at higher T
- OH yield is small.

C_2H_5, C_3H_7+ O_2

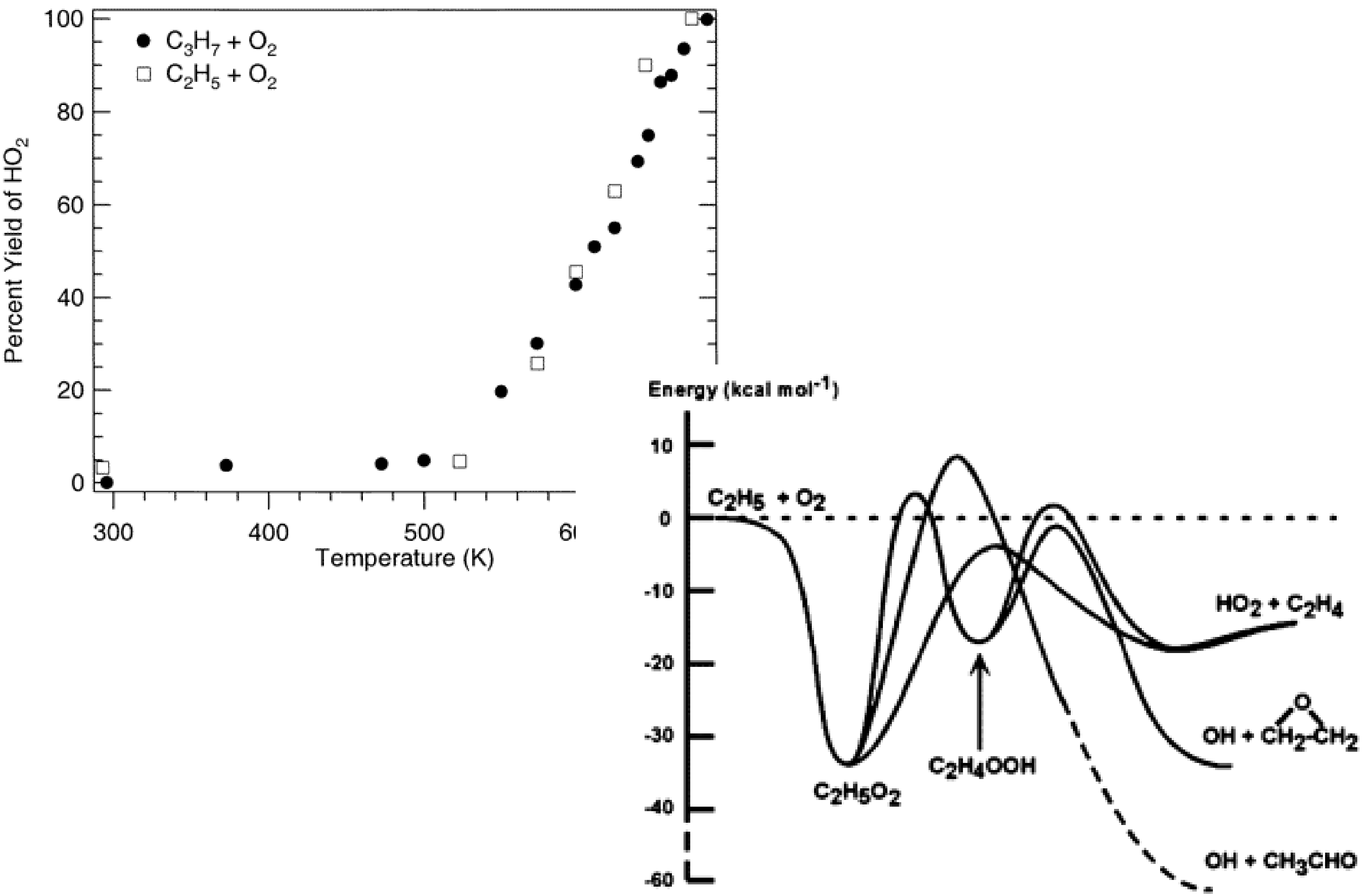
● $C_3H_7 + O_2$
□ $C_2H_5 + O_2$
Percent Yield of HO_2
100
80
60
40
20
0
300
400
500
6
Temperature (K)
Energy (kcal mol^{-1})
10
0
-10
-20
-30
-40
-60
$C_2H_5 + O_2$
$C_2H_5O_2$
C_2H_4OOH
$HO_2 + C_2H_4$
OH + CH_2-CH_2
O
OH + CH_3CHO

Master equation analysis: Miller and Klippenstein, Int J Chem Kinet 33: 654-668, 2001

- Three regimes, low, transition, high T.
- In transition region, thermal rate constant jumps from one eigenvalue to the other – the two eigenvalues are mixed in this region.
- At high T, ethyl peroxy is stabilised and HO_2 is formed from its dissociation. k is, in practical terms, independent of p.
- At low T, reaction involves the pressure dependent formation of RO_2 and direct formation of HO_2

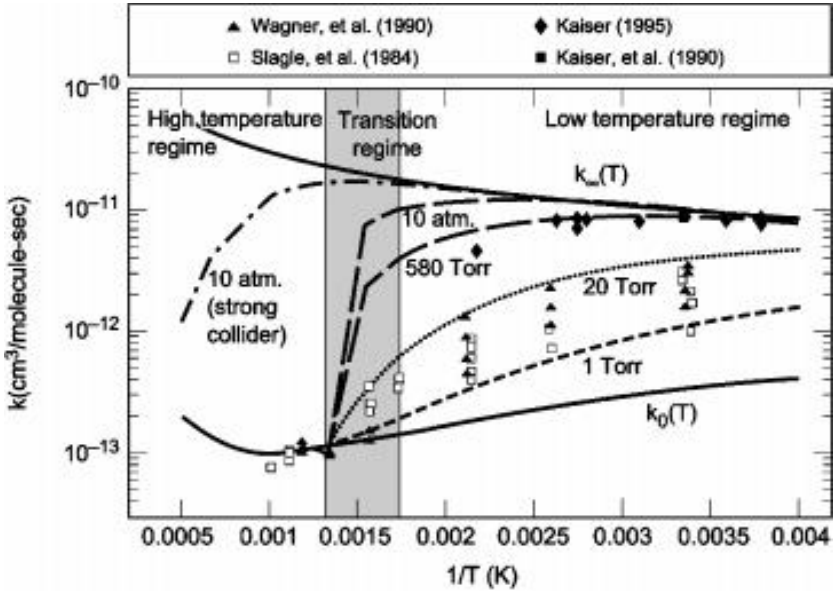

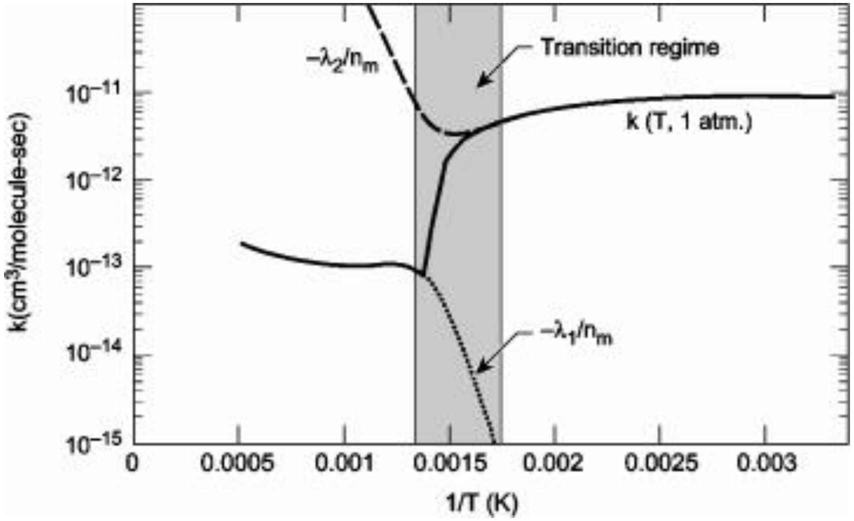

Electronic structure calculations for $C_2H_5 + O_2$

Quelch et al J Am Chem Soc, 116 (1994) 4953 als Sheng et al J Phys Chem A 2002;106:7276

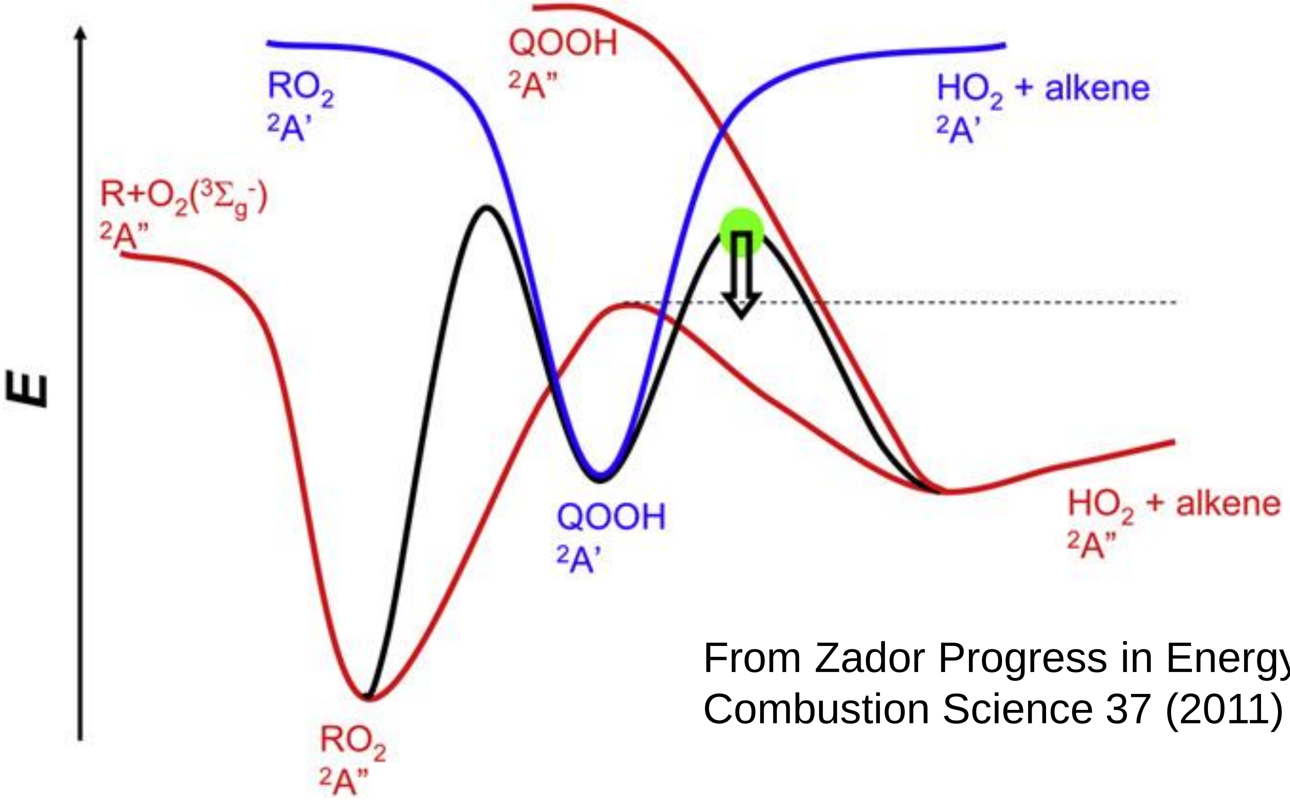

From Zador Progress in Energy and Combustion Science 37 (2011) 371

- Two hydrogen-transfer transition states
  - $^2A''$ electronic state
  - ^2A electronic state derived from a 2A' planar structure
- At the best level of theory used, DZP(double zeta plus polarization) CCSD(T) $^2A''$ transition state lies 4.5 kcal mol-' above the reactants

Importance of level of theory in determining the C_2H_5 + O_2 PES

(Klippenstein, Proc Comb Inst 36 (2017) 77–111)

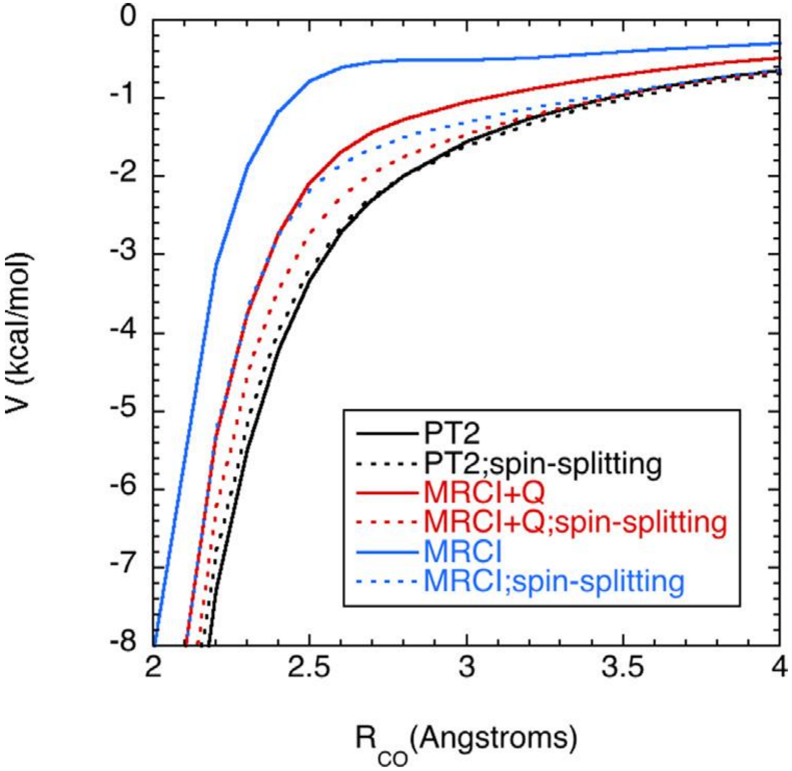

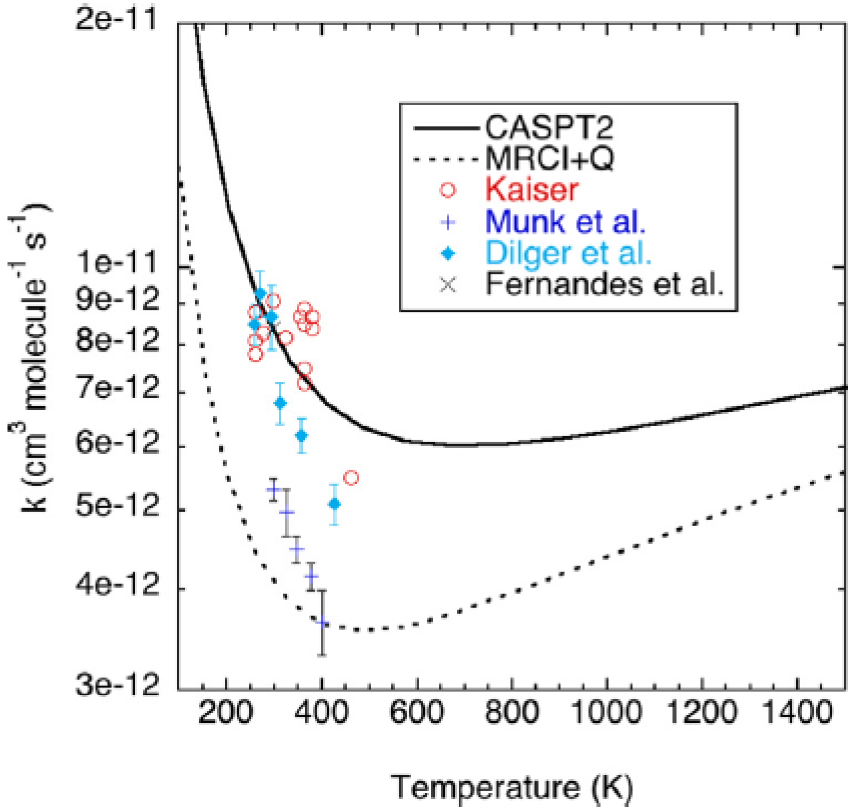

- Plot of the C_2H_5 + O_2 interaction energy along the R (C-O) distinguished coordinate minimum energy path. The black, red, and blue lines correspond to CASPT2, MRCI + Q, and MRCI calculations, respectively. The solid lines denote direct calculations of the interaction energy, while dashed lines denote calculations of the doublet–quartet splitting combined with CCSD(T) calculations of the quartet interaction energy.
- Rate constant: theory, high pressure limit; experiment: 1 atm except Fernandes, 100 atm

$R + O_2 \rightleftharpoons RO_2$ (R = allyl)

Morgan et al JCS Faraday Trans 2 78, 1323-1330 (1982)

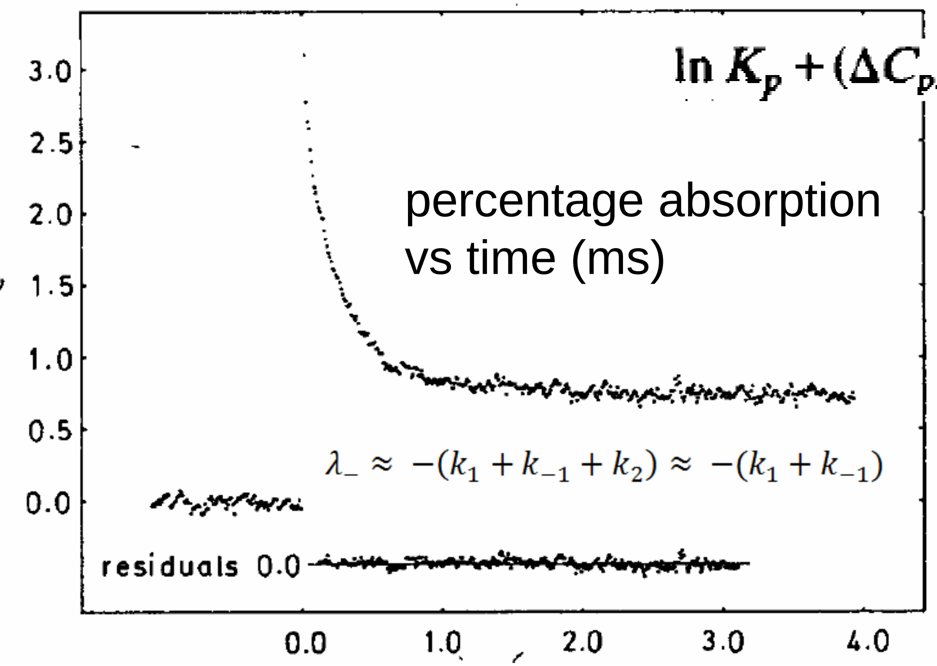

percentage absorption vs time (ms)

$\lambda_- \approx -(k_1 + k_{-1} + k_2) \approx -(k_1 + k_{-1})$

$\ln K_p + (\Delta C_p/R)[\ln(298/T) + (T-298)/T]$ against $1/T$

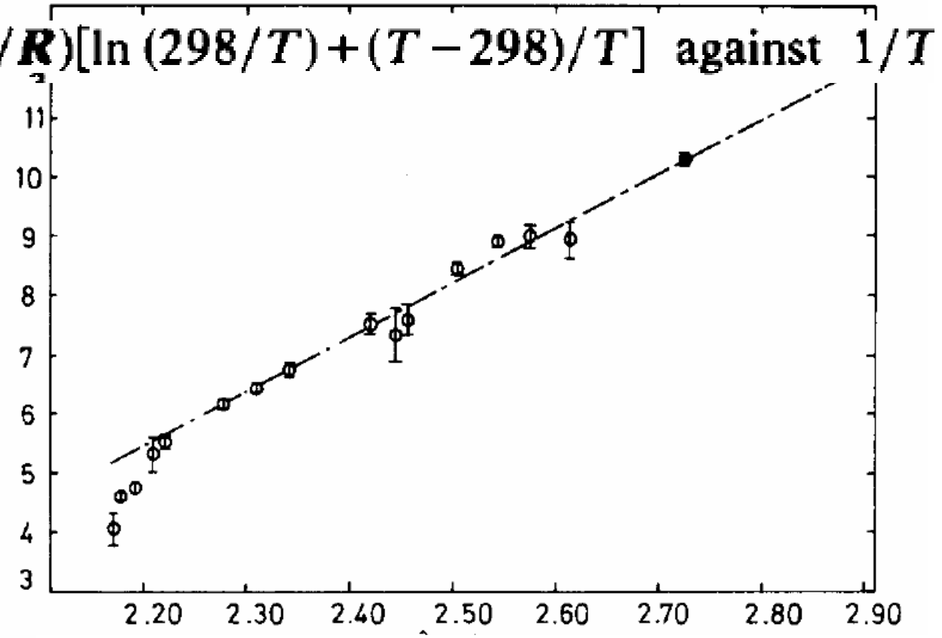

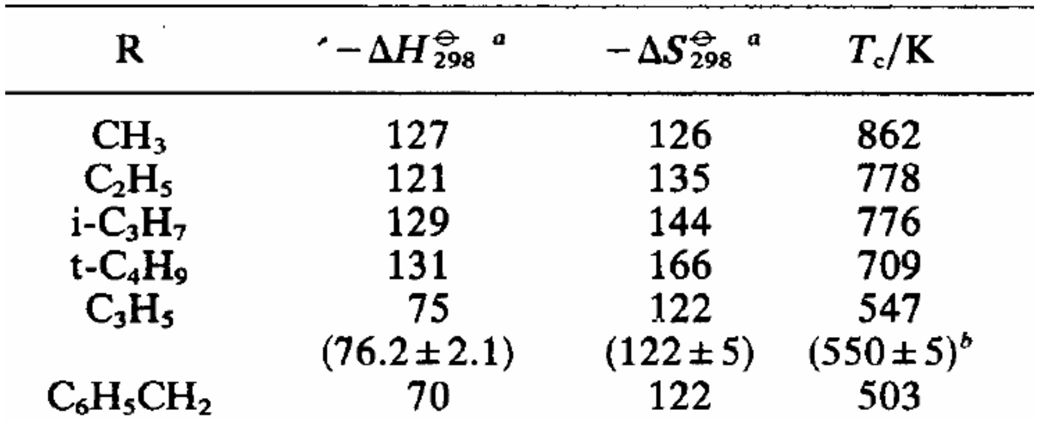

R	$-\Delta H^\ominus_{298}$ [a]	$-\Delta S^\ominus_{298}$ [a]	T_c/K
CH_3	127	126	862
C_2H_5	121	135	778
i-C_3H_7	129	144	776
t-C_4H_9	131	166	709
C_3H_5	75 (76.2 ± 2.1)	122 (122 ± 5)	547 (550 ± 5)[b]
$C_6H_5CH_2$	70	122	503

- Estimated enthalpies and entropies of reaction in kJ mol^{-1}
- (b) experimental values
- Ceiling temperatures/ K (0.1 atm O_2)

Radical dissociation: 1-butyl

Knyazev and Slagle, J. Phys. Chem. 1996, 100, 5318-5328

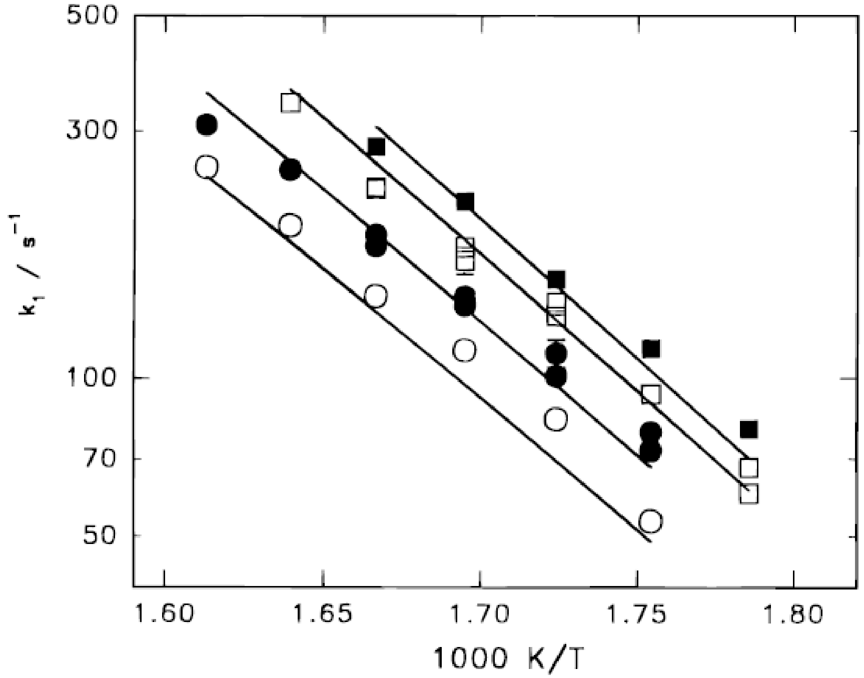

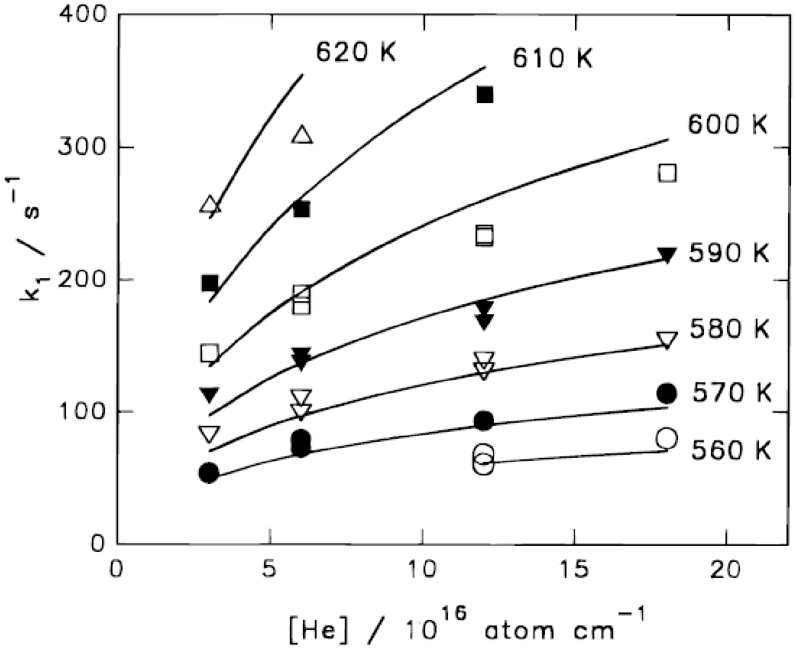

- Pulsed photolysis, photoionization mass spectrometry
- Data fitted with master equation analysis, coupled with TS model based on electronic structure calculations
- Gave limiting high and low pressure rate constants and fall off data based on Troe modification of Lindemann Hinshelwood model

A detailed example: $CH_3OCH_2 + O_2$

1. OH + dimethyl ether (Carr et al. J. Phys. Chem. A 2013, 117, 11142–11154

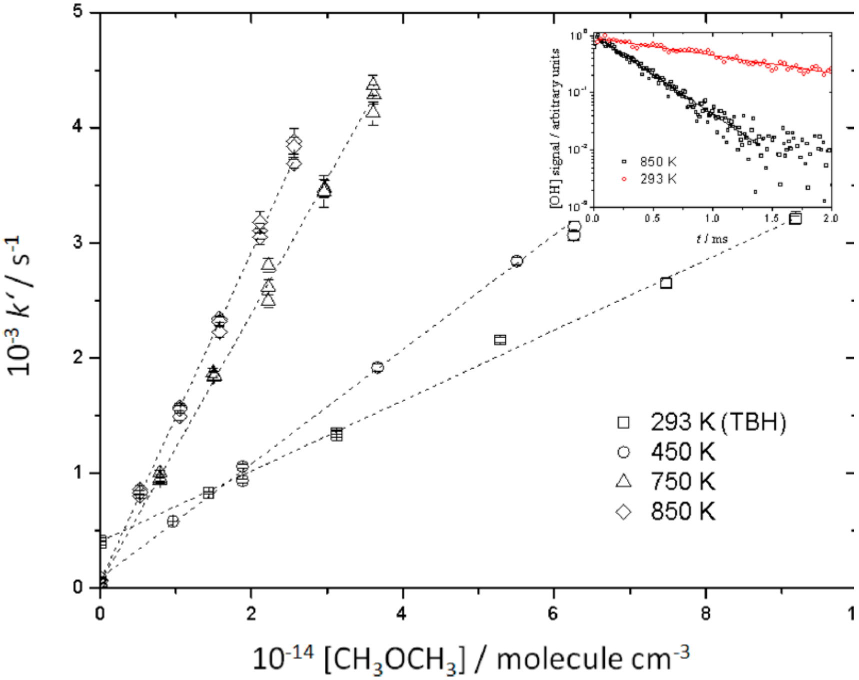

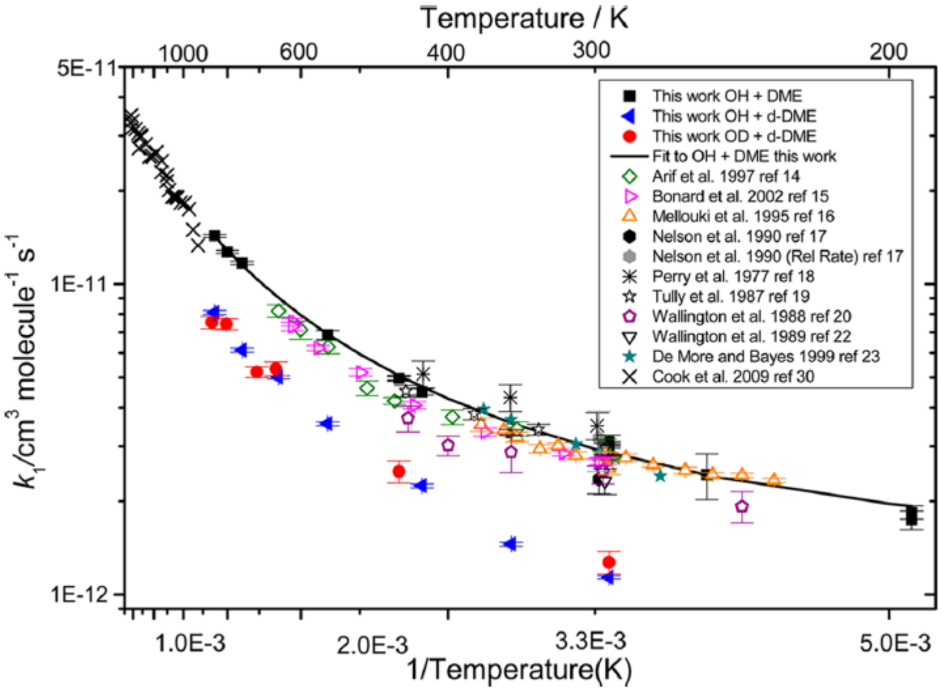

- Left hand plot shows examples of experimental decays using pulsed photolysis / laser induced fluorescence. Main figure shows examples of bimolecular plots (first order decay constant from individual experiments vs [CH_3OCH_3]. Experiments over the range 195 – 850 K
- Right hand plot shows these data and literature data, with fit giving
  $k = (1.54\pm0.48) \times (T/298\ K)^{1.89\pm0.16} \exp(-184\pm112)$ cm3 molecule-1 s-1 (195 – 1423 K)
  Errors are 95% confidence limits)
- Note the results from isotope substitution: blue – OH + d-DME, red OD + d-DME – used in fits to theory

$$k(T) = \alpha \frac{kT}{h} \frac{Q^{\ddagger}_{TS}}{Q_A Q_{BC}} \exp\left(\frac{-\Delta\varepsilon_0}{kT}\right)$$

Fits to theory

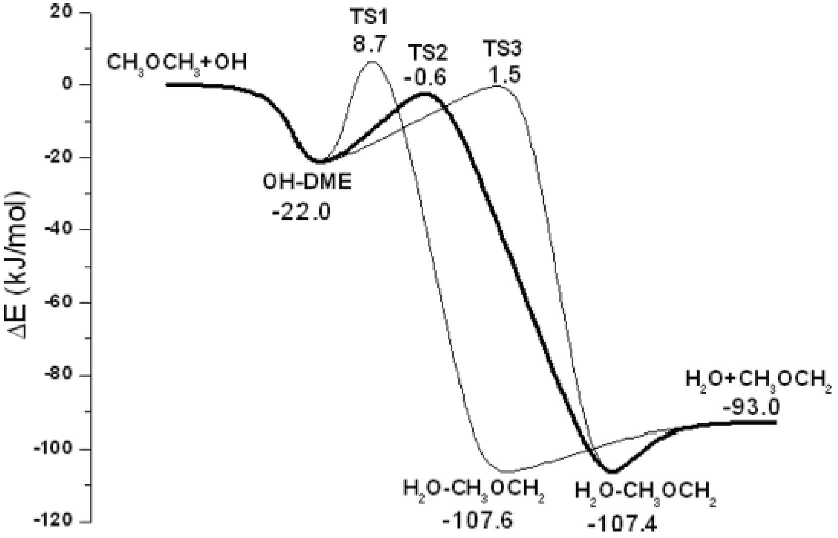

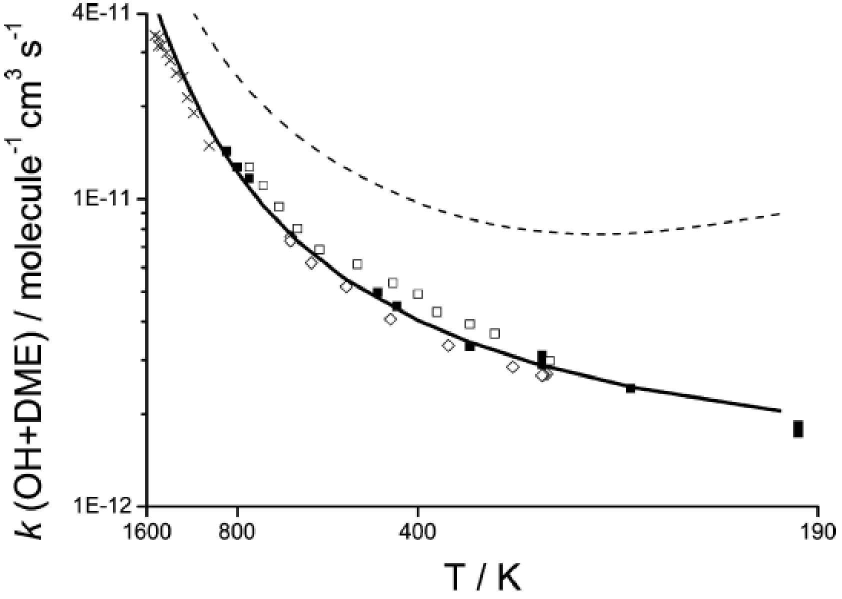

- Left hand plot shows turning points on PES: Geometric parameters were optimized at the CCSD/AVDZ level and the energies were calculated at the FCC/CBS//CCSD/AVDZ level with zero-point energy corrections.
- Right hand plot shows best fit. Dashed line with no adjustments to theory. Full line – best fit barrier energy adjusted to +0.6 kJ mol^{-1}, hindrance parameters scaled by factor of 2.5. Tunnelling using WKB method, reaction path calculated at CCSD(T)/aug-cc-pVDZ level of theory.
- Used two transition state model, using a master equation analysis

3 transition states – not all independent

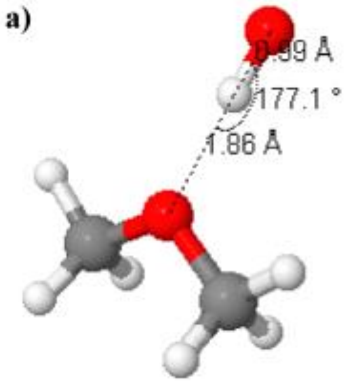

Initial OH/DME complex with C_{2V} or C_s symmetry

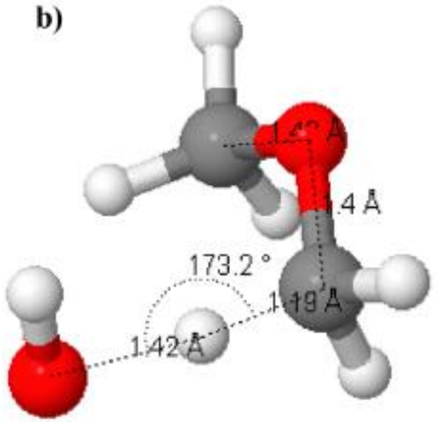

TS2 Out-of-plane transition state with upward pointing OH

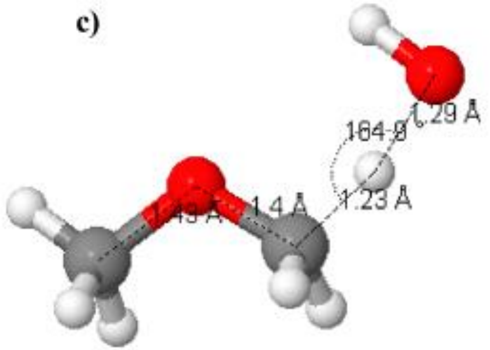

TS1 - In-plane transition state with C_s symmetry

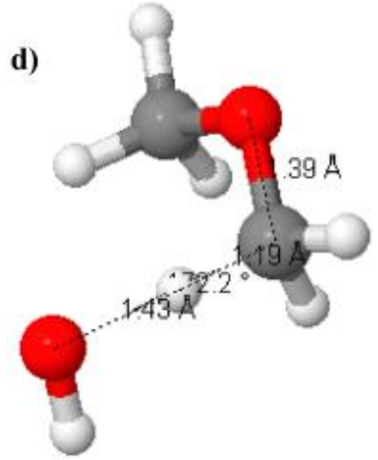

TS3 Out-of-plane transition state with downward pointing OH

$CH_3OCH_2 + O_2$

Eskola et al. J. Phys. Chem. A 2014, 118, 6773–6788

Pulsed laser photolysis, laser induced fluorescence detection of OH
Measured the yield of OH and the rate constants via the formation of OH
Fits to data varying association rate constant (A,n), energy transfer parameters and some TS parameters

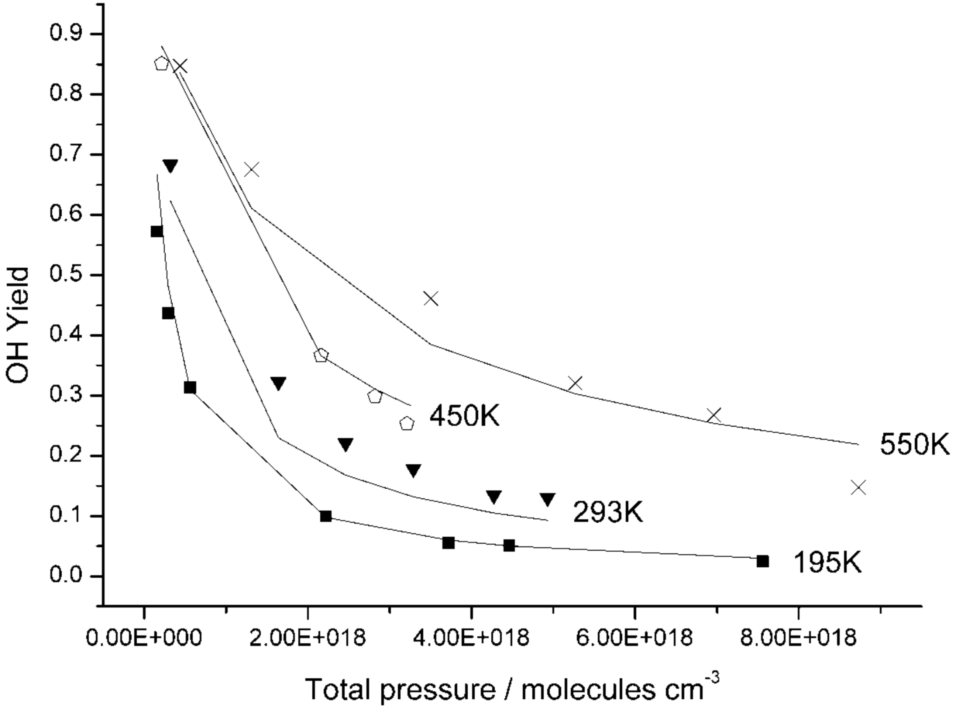

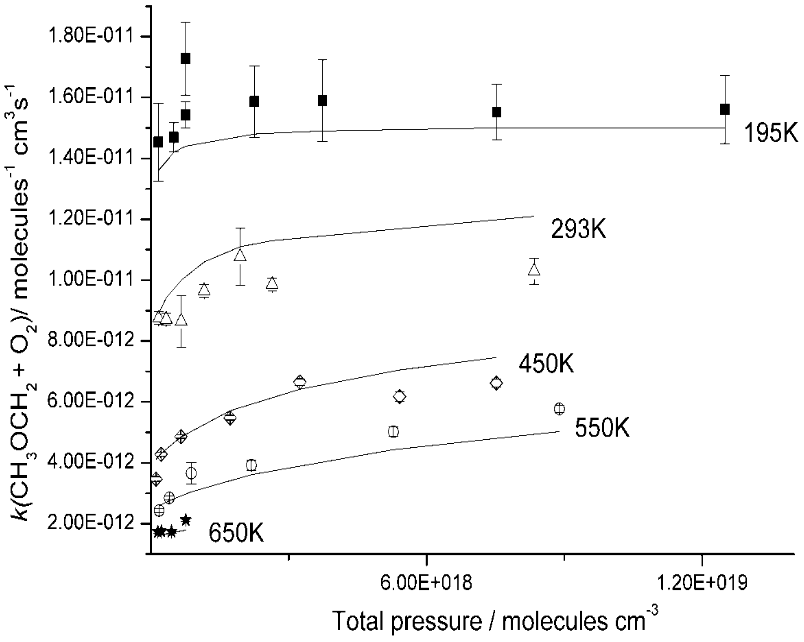

$CH_3OCH_2 + O_2$: major mechanism

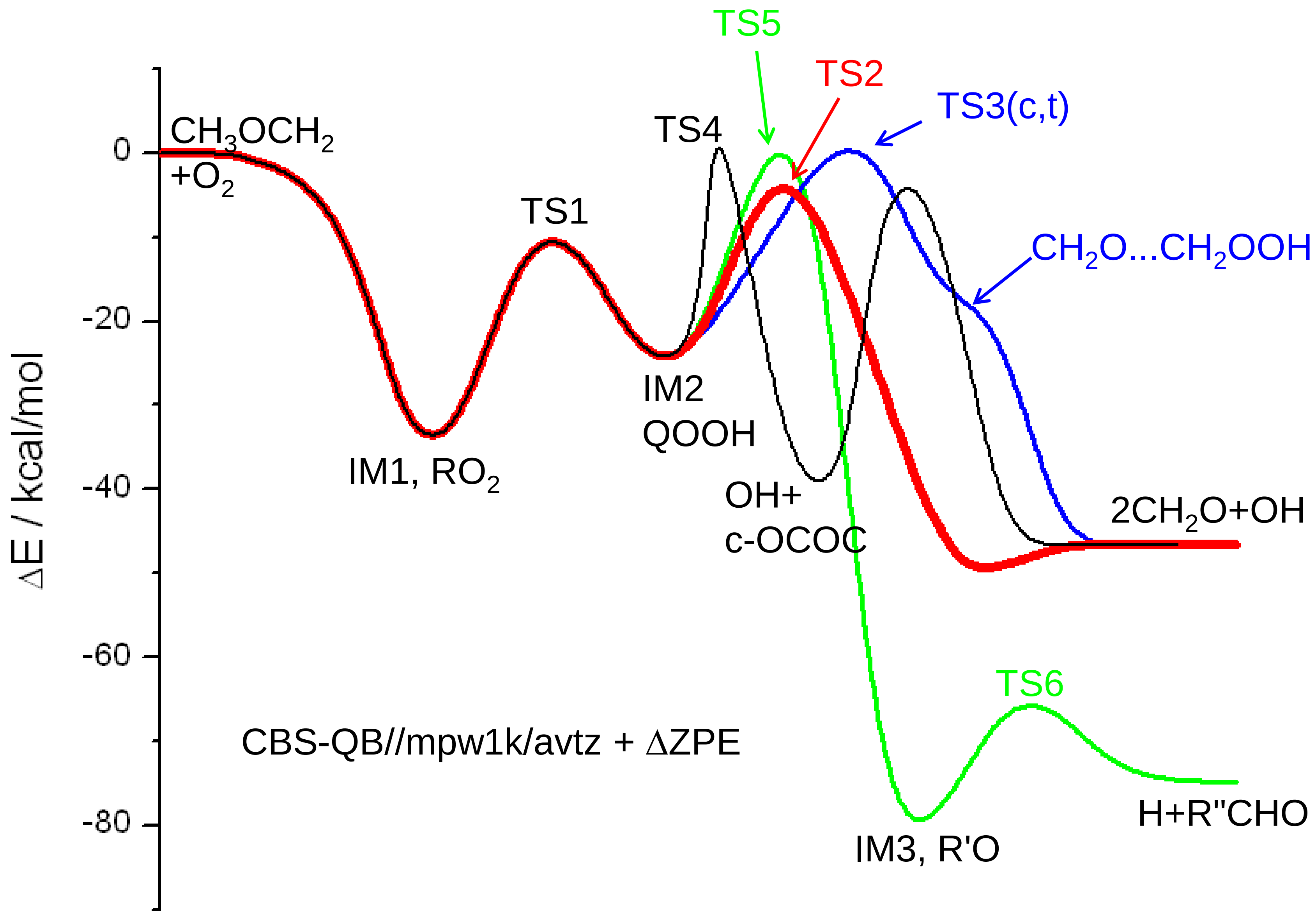

CBS-QB//mpw1k/avtz + ΔZPE

Master equation analysis. Species profiles, 550 K, 1 bar

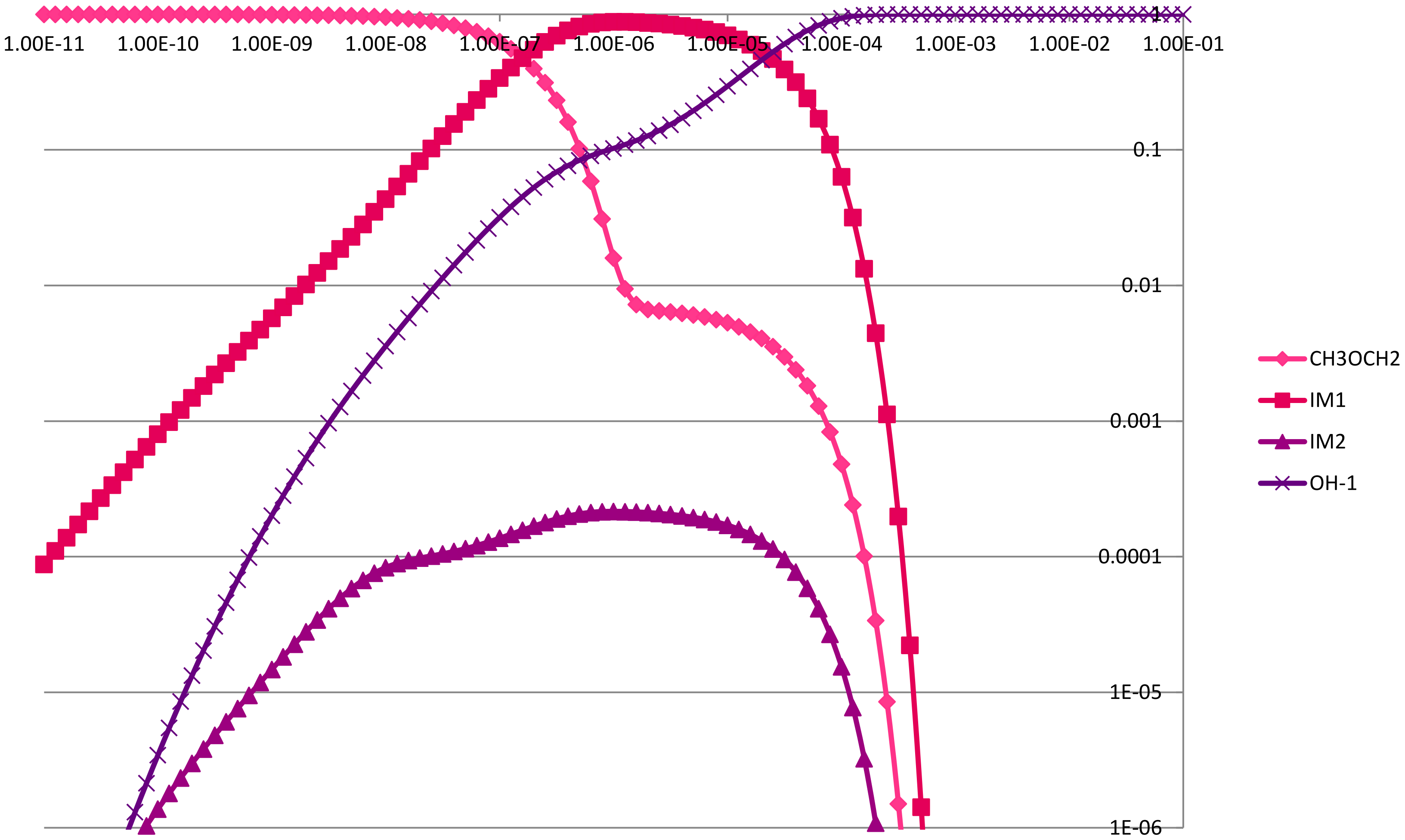

Master equation: rate constant analysis

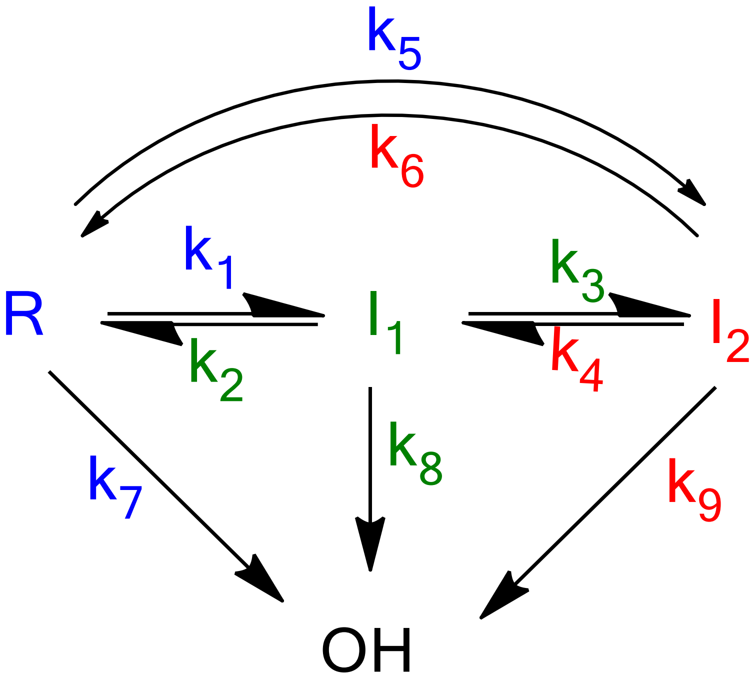

$I_1 = RO_2$

$I_2 = QOOH$

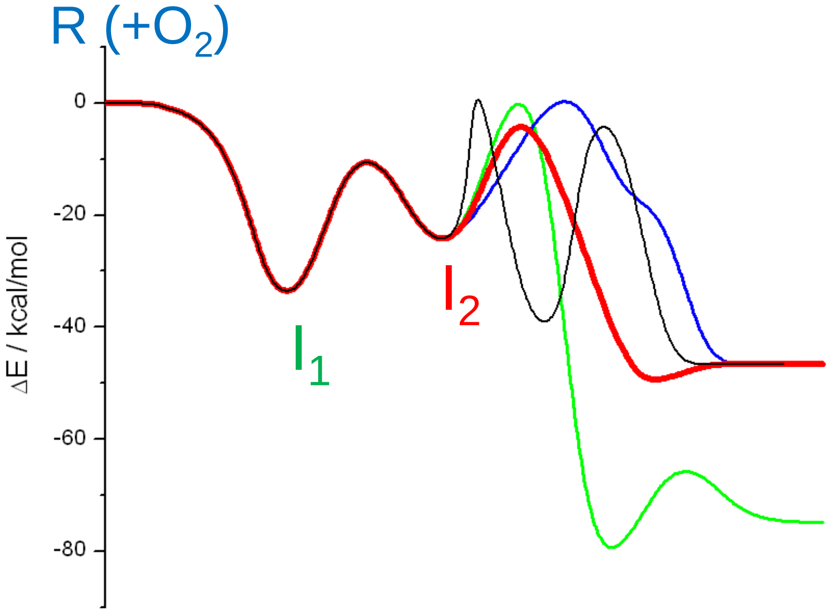

Phenomenological rate coefficients from a Bartis Widom analysis

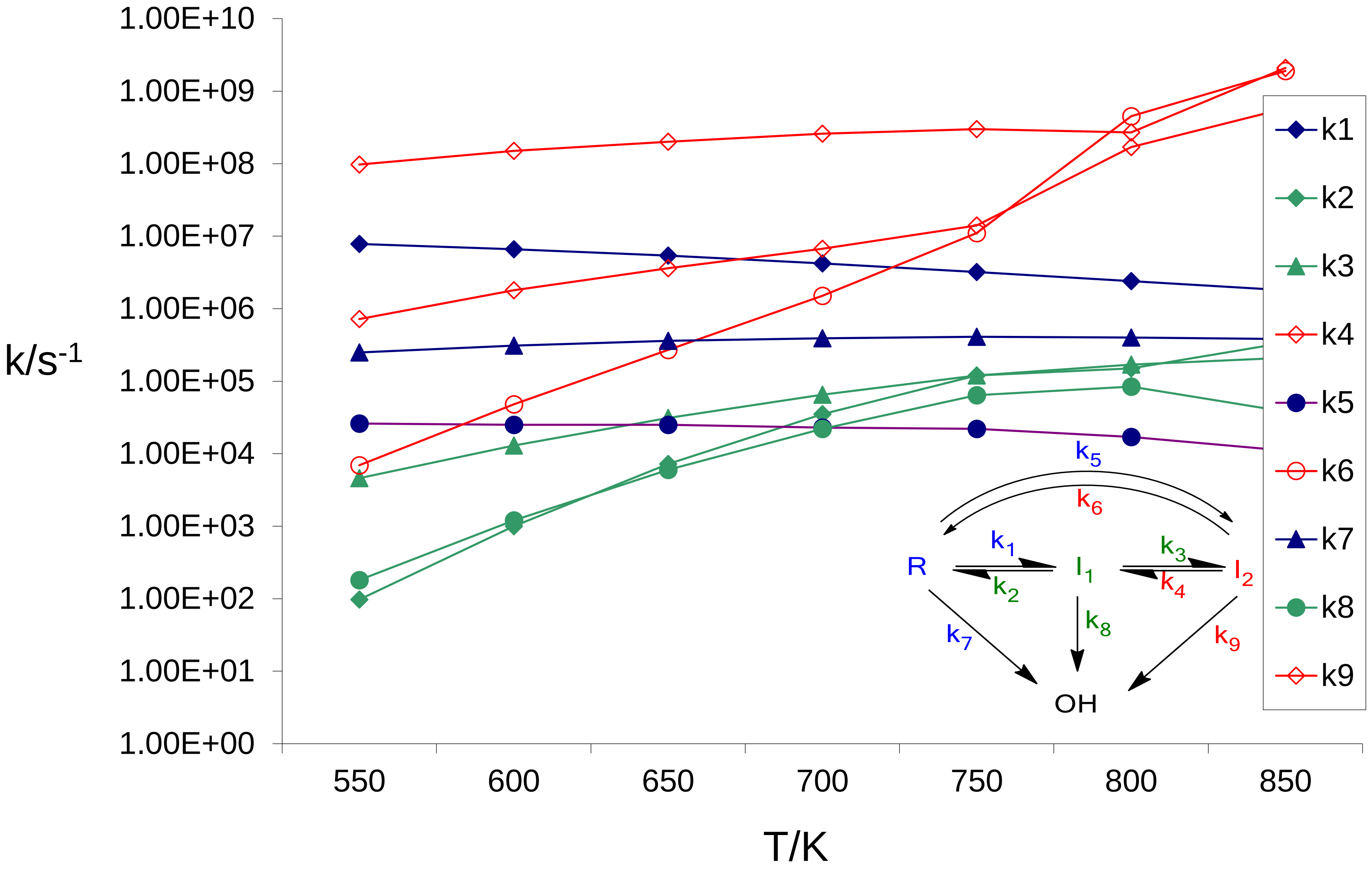

Analytic expressions for the two smallest eigenvalues

- Lifetime of IM2 (=QOOH) is always much less than those for R and RO2
- Let x=R, y=RO2, z = QOOH. Apply QSSA z

$$z = \frac{k_5 x + k_3 y}{k_4 + k_6 + k_9}$$

$$\frac{dc}{dt} = \begin{pmatrix} -(k_1 + k_5\left(1 - \frac{k_6}{k}\right) + k_7) & k_1 + \frac{k_5 k_4}{k} \\ k_2 + \frac{k_3 k_6}{k} & -(k_2 + k_3\left(1 - \frac{k_4}{k}\right) + k_8 \end{pmatrix} \mathbf{c} \quad = \quad \begin{pmatrix} -A & B \\ C & -D \end{pmatrix} \mathbf{c}$$

$$\lambda_{\pm} = \frac{-(A+D) \pm \sqrt{(A+D)^2 - 4(AD - BC)}}{2}$$

$$\mathrm{c} = \begin{pmatrix} x \\ y \end{pmatrix}$$

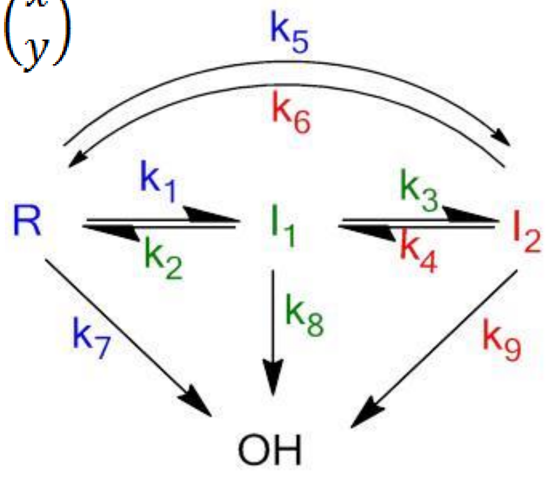

If $(A + D)^2 >> 4(AD\text{-}BC)$, binomial expansion gives

$$\lambda_- = -(A + D)$$

$$\lambda_+ = \frac{-(AD - BC)}{A + D}$$

- CSEs from master equation solution. Two smallest eigenvalues are λ_1, λ_2
- $\lambda_1 = \lambda_+$; $\lambda_2 = \lambda_-$

Time dependence of the OH profiles at 300 K and at 550 K

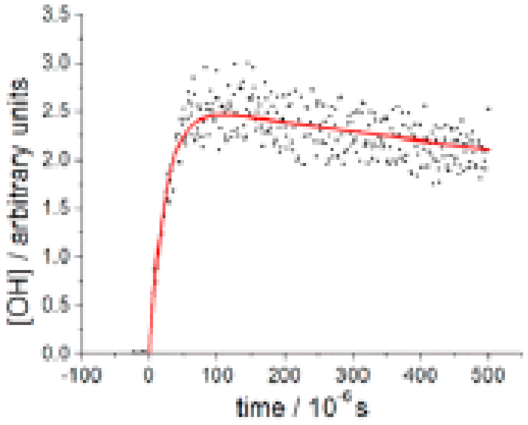

- At low T, the OH signal is biexponential.
- The decay corresponds to loss of OH, e.g. by diffusion from the reaction zone and reaction.
- The increase corresponds to λ_2

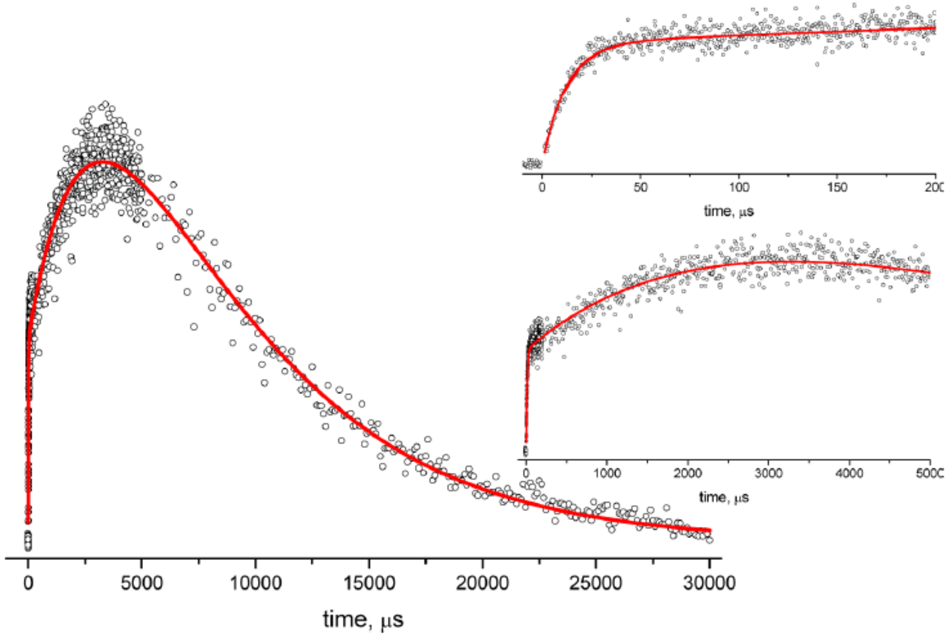

- At higher T, the signal becomes triexponential.
- The fast rise is λ_2 and the slower rise is λ_1; the decay is again loss of OH

Global Uncertainty Propagation and Sensitivity Analysis in the CH3OCH2 + O2 System: Combining Experiment and Theory To Constrain Key Rate Coefficients in DME Combustion

Shannon et al J Phys Chem DOI: 10.1021/acs.jpca.5b00620

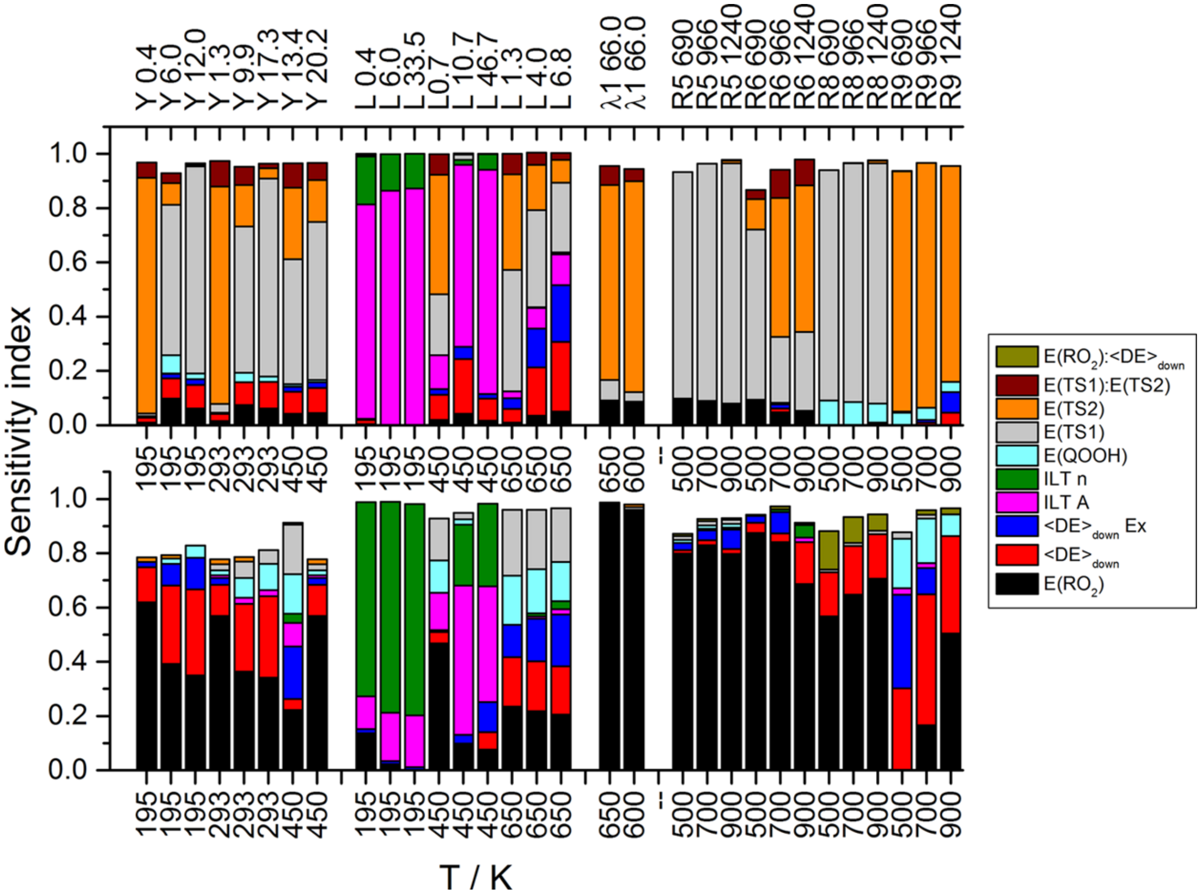

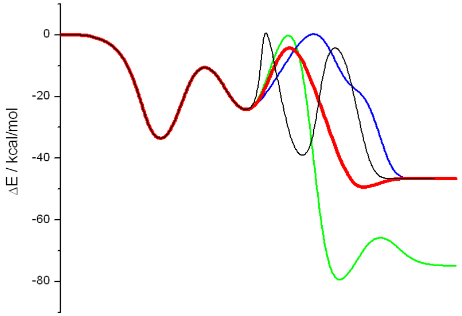

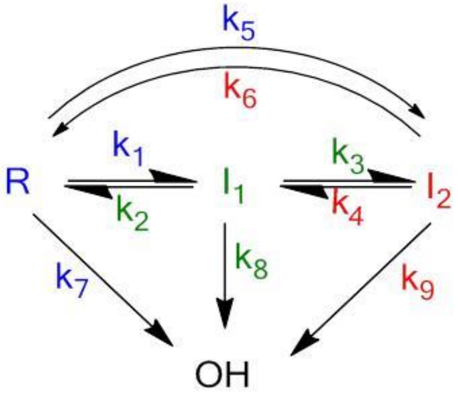

Sensitivity indices for the parameters involved in the master equation modeling with theory-constrained parameter ranges (top) and experimentally constrained parameter ranges (bottom). The labels on the top axis give the pressure at which the calculations were run in kPa and identify the type of observable: Y indicates the OH yield, L indicates the rate coefficient for CH2OCH3 loss, λ1, indicates the time constant corresponding to the longer time formation of OH and R indicates a particular elementary rate coefficient. Where the sensitivities sum to be significantly less than 1, this can be attributed to contributions from the second-order sensitivities that are not included. Where there is a colon between two parameters, this indicates a second-order sensitivity for this pair of inputs.

Harnessing the Combined Power of Theoretical and Experimental Data through Multiscale Informatics

M P Burke, Int J Chem Kinet 48: 212–235, 2016

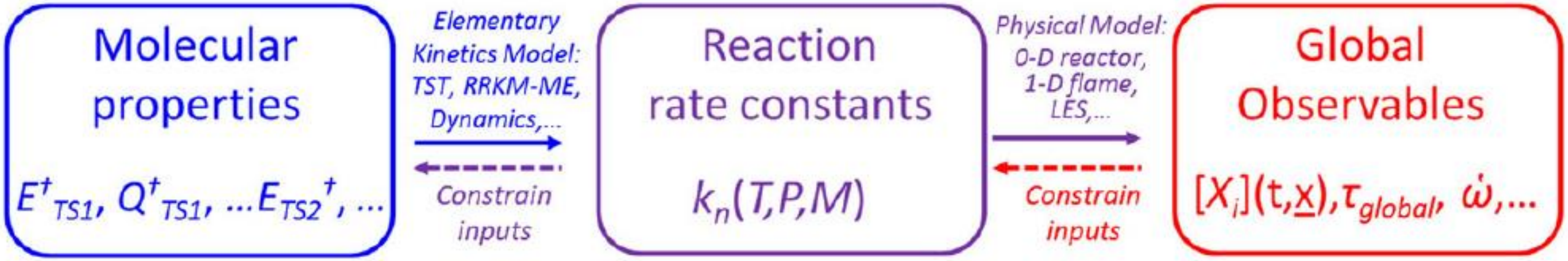

Molecular properties

$E^{\dagger}_{TS1}$, $Q^{\dagger}_{TS1}$, …$E_{TS2}{}^{\dagger}$, …

Elementary Kinetics Model: TST, RRKM-ME, Dynamics,…

Constrain inputs

Reaction rate constants

$k_n(T,P,M)$

Physical Model: 0-D reactor, 1-D flame, LES,…

Constrain inputs

Global Observables

$[X_i](t,\underline{x})$, τ_{global}, $\dot{\omega}$,…

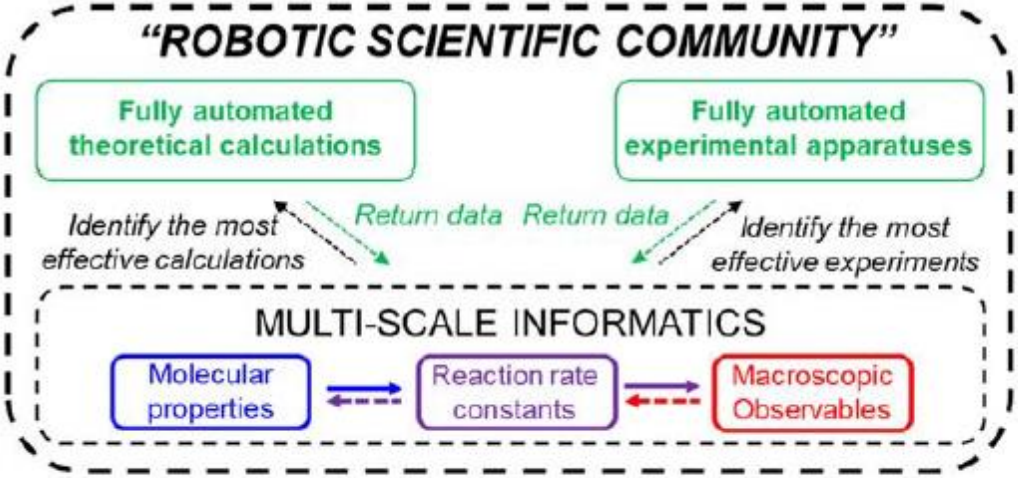

“ROBOTIC SCIENTIFIC COMMUNITY”

Fully automated theoretical calculations

Fully automated experimental apparatuses

Identify the most effective calculations

Return data

Return data

Identify the most effective experiments

MULTI-SCALE INFORMATICS

Molecular properties

Reaction rate constants

Macroscopic Observables

Routes to branching: $CH_3OCH_2 + O_2$ (+ O_2)

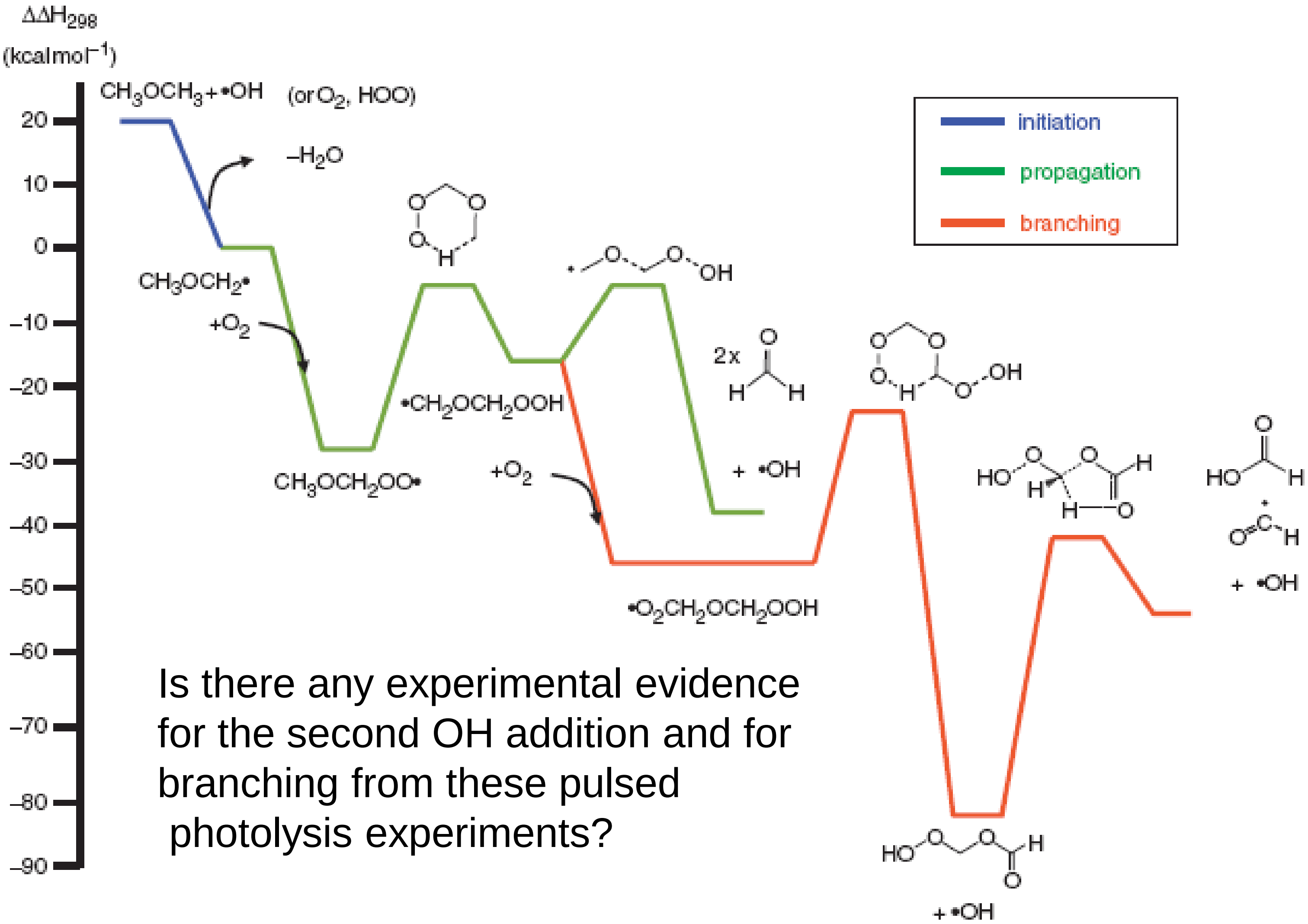

Is there any experimental evidence for the second OH addition and for branching from these pulsed photolysis experiments?

- Anderson and Carter: Molecular Physics 2008, 106, 367-396

Difficulty of observing second O_2 addition with this experimental system

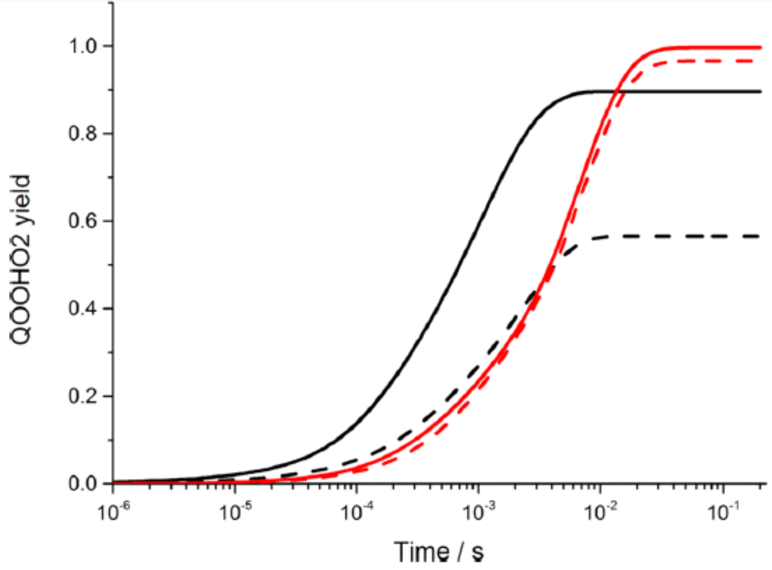

Simulated O_2QOOH formation using a model based upon MESMER rate coefficients from Eskola et al

(black) at 1 bar (solid line) and 10 bar (dashed line) of air (T = 550

K). These are compared with results using rate coefficients from the

Fischer, Dryer, Curran model (red) (Int J Chem Kinet (32, 741, 2000) see slides 7-9).

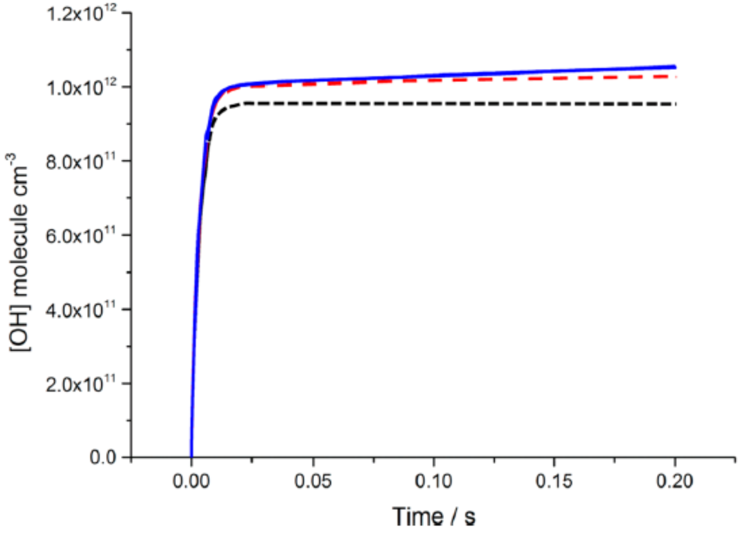

OH simulation at 550 K and 500 Torr with [O2] = 1 × 10^{17} molecule cm^{-3}: QOOH + O_2 rate coefficient of:

0(black short dashed line),

1.16 × 10^{-12} cm^3 $molecule^{-1}$ s^{-1} (red long dashed line),

2.32 × 10^{-12} cm^3 $molecule^{-1}$ s^{-1} (blue solid line)

Effect on OH is small and at long times

Direct observation of QOOH - difficult for dimethyl ether oxidation

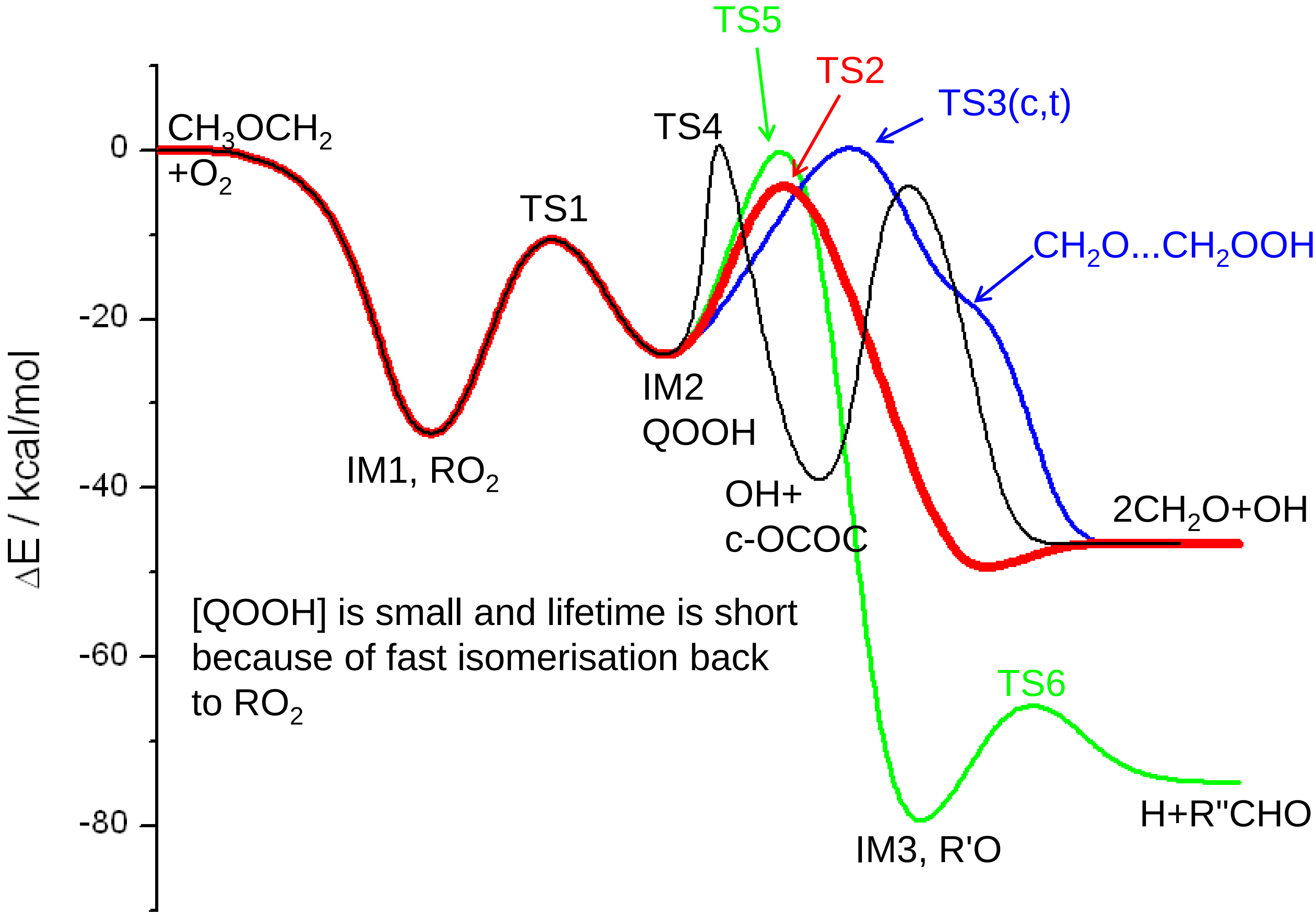

[QOOH] is small and lifetime is short because of fast isomerisation back to RO_2

Reminder: competition between dissociation of QOOH and addition, which leads to branching

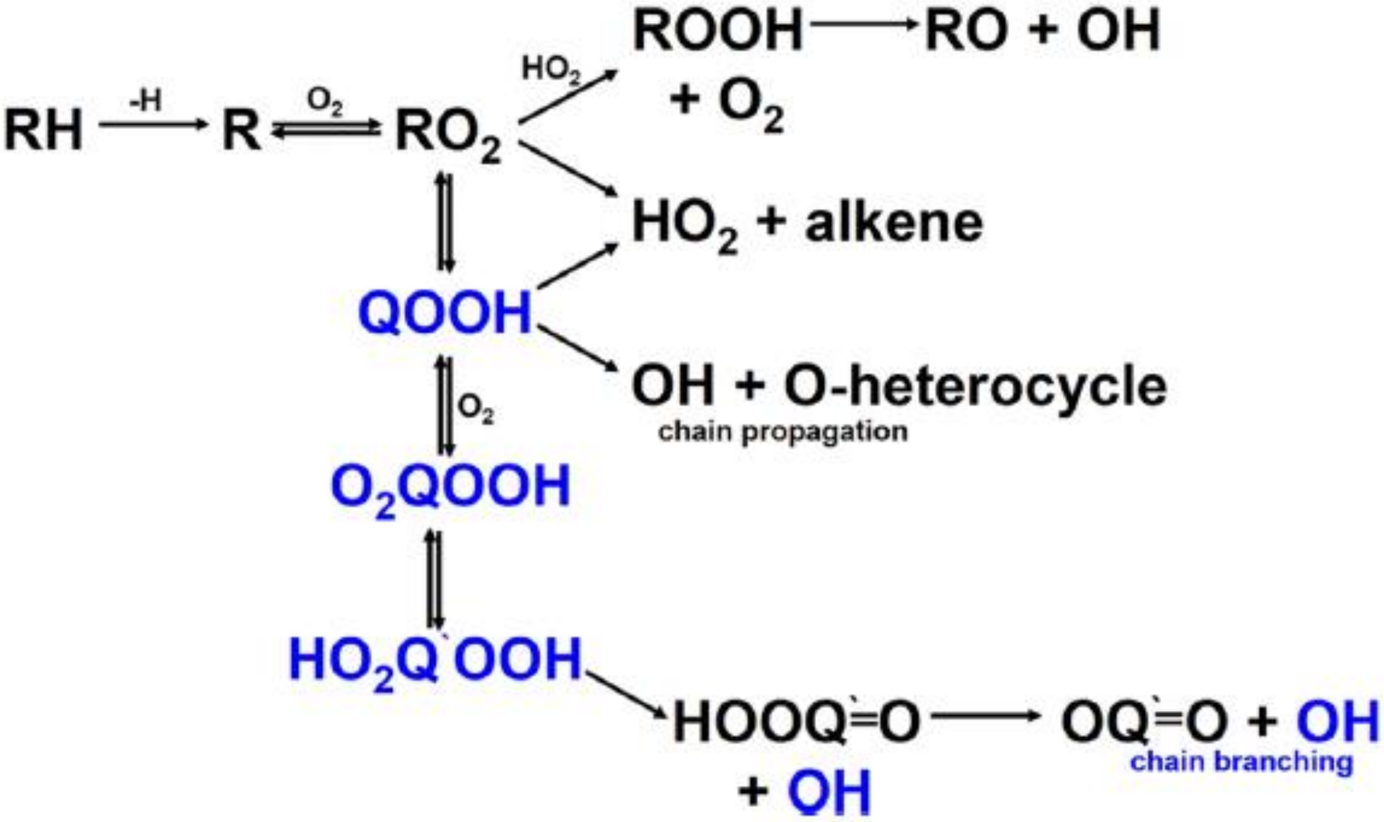

Direct production of QOOH and observation of its kinetics by pulsed laser photolysis and detection of OH product by LIF

$QOOH \rightarrow QO + OH$

$QOOH + O_2 \rightarrow O_2QOOH$

$Cl+(CH)_3COOH \rightarrow CH_2(CH_3)_2COOH+HCl$

$CH_2(CH_3)_2COOH \rightarrow OH+(CH_3)_2C(CH_2)O$ (k_3)

$CH_2(CH_3)_2COOH+O_2 \rightarrow O_2\ CH_2(CH_3)_2COOH$ (k_4)

A shows time profiles of OH for a range of $[O_2]$

k_3 was determined from the trace with $[O_2] = 0$ and was studied at a range of pressure (B)

k_4 was determined from the dependence of the decay of the OH traces on $[O_2]$.

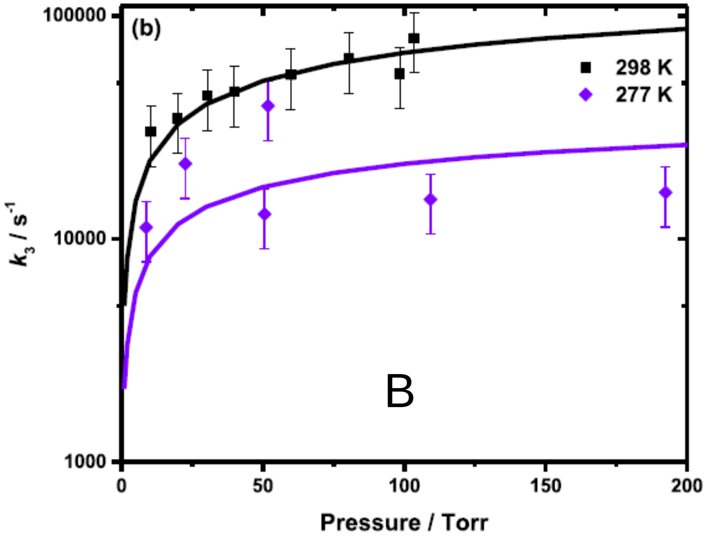

Whelan et al, J Phys Chem A 2019, 123, 10254

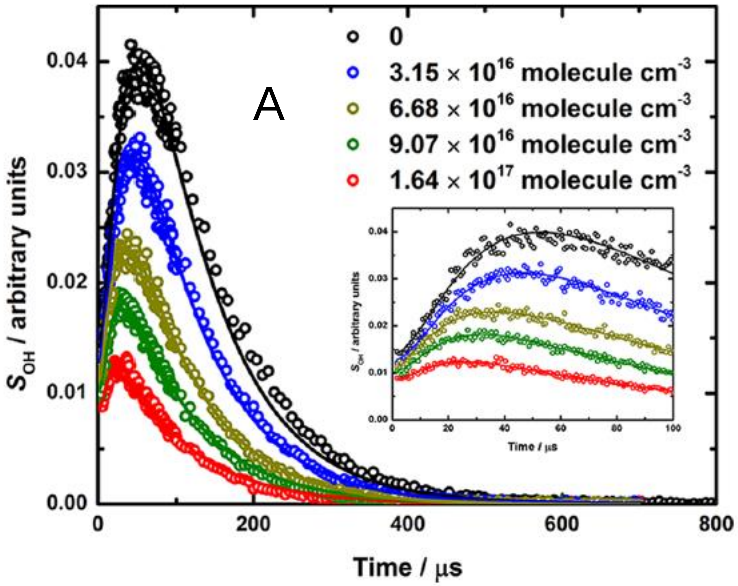

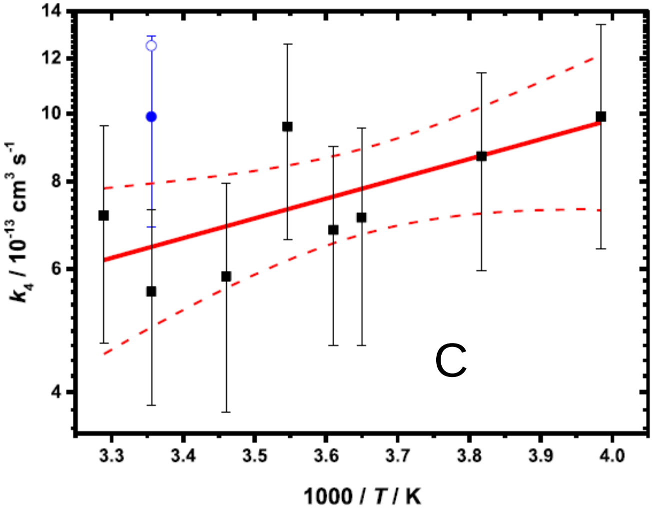

Direct measurements of ·QOOH dissociation

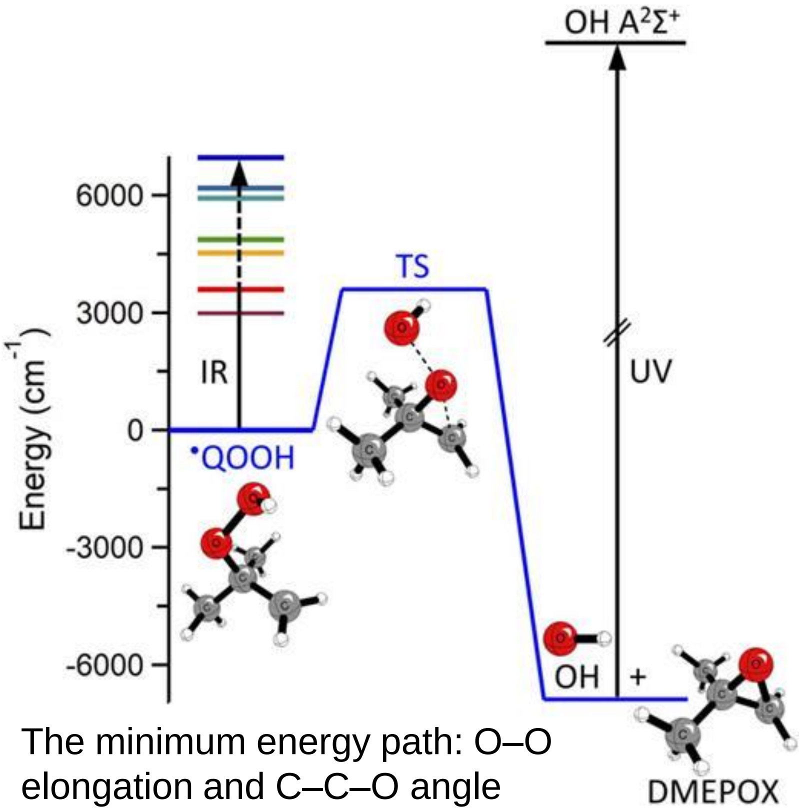

The minimum energy path: O–O elongation and C–C–O angle contraction→O–O bond breakage, ring closure →OH and cyclic ether

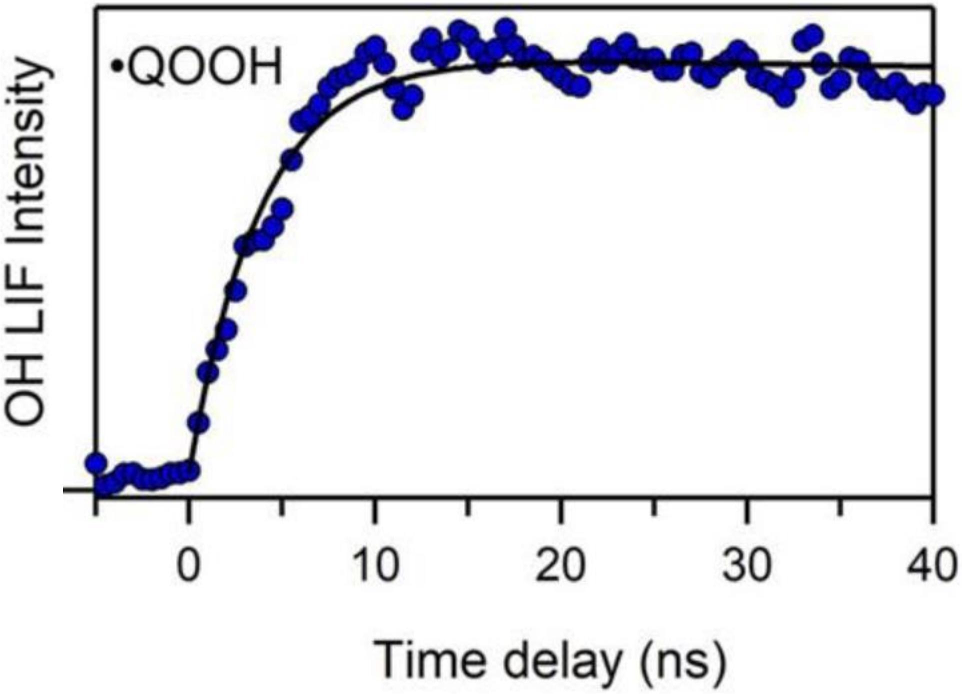

- Experiments on $(CH_3)_3COOH$. Form ·QOOH by reaction with Cl in supersonic jet at 10 K.
- Vibrationally excite radical using range if infra red wavelengths (different colours in Figure)
- Observe OH product by LIF
- Lester et al., Science, 2021, 373, 679; J Chem Phys, 2022, 156, 014301, Faraday Disc, 2022, 238,575

Experimental and theoretical results

A

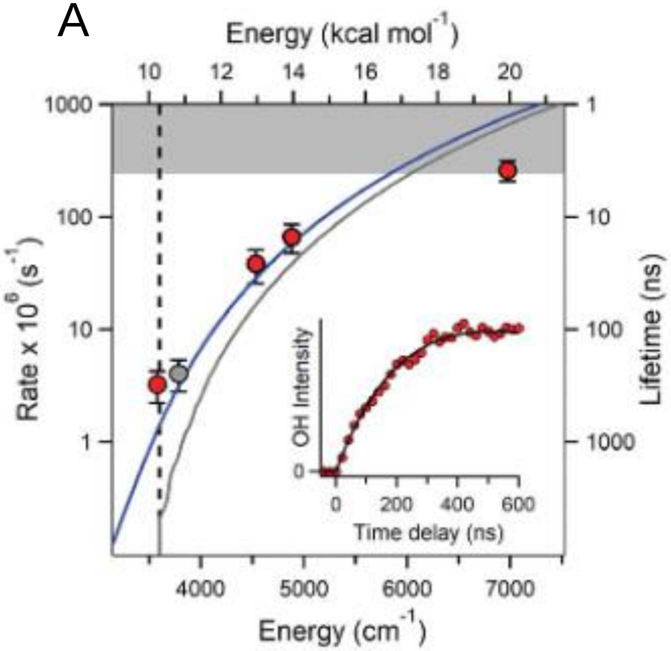

B

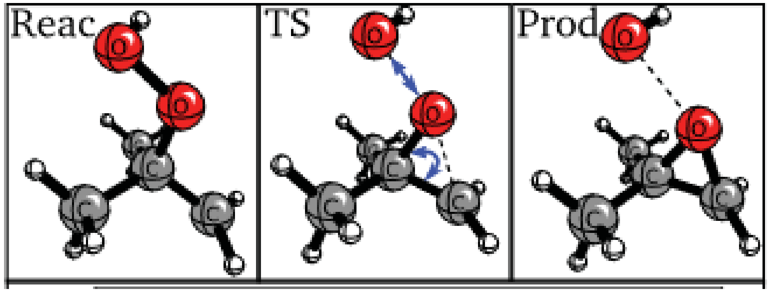

C

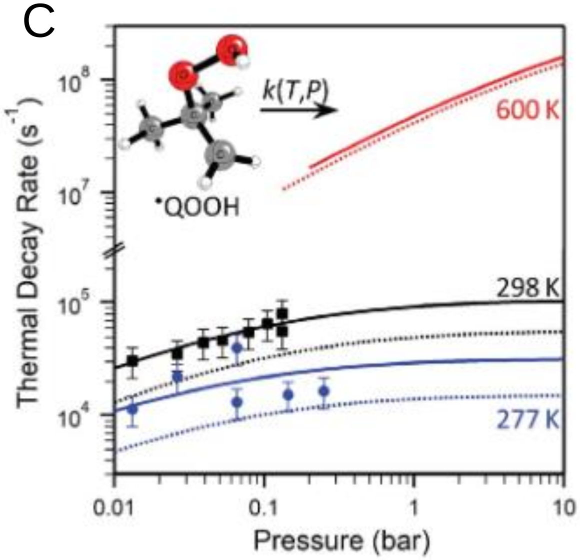

- A shows the dissociation rate constants vs energy of the vibrationally excited QOOH.
- The calculated transition state energy is 10.3 kcal mol-1. The results demonstrate the importance of heavy atom tunnelling. Calculated results: blue with tunnelling, grey without.
- B shows the motion through the transition state
- C shows a comparison with the results of Whelan et al and calculated values at 600 K, close to the autoignition region.

Automatic generation of reaction pathways using KinBot (Faraday Discuss., 2022, 238, 295)

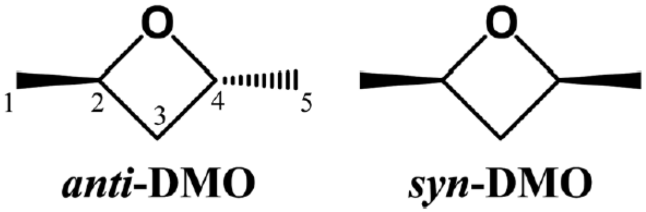

- Oxidation of dimethyloxetane: 2 diastereomers
- Abstraction of H at the five labelled C atoms leads to 5 possible radicals; addition of O_2 then leads to 7 distinct peroxy radicals
- KinBot (see Topic 3) used to explore the transition states, intermediates and products for each of these peroxy radicals
- Master equation calculations then used to determine the kinetics over the ranges 300 – 1000 K, 0.01 – 100 atm. Found that:
  - diastereomeric cyclic ether peroxy radicals show significantly different reactivities
  - the stereochemistry of the peroxy radical determines which QOOH isomerization steps are possible
  - cyclic ether formation and HO2 elimination reactions, compete with ring-opening reactions, which primarily produce OH radicals, the outcome of which is sensitive to stereochemistry.

The stereochemistry of the seven peroxy radicals

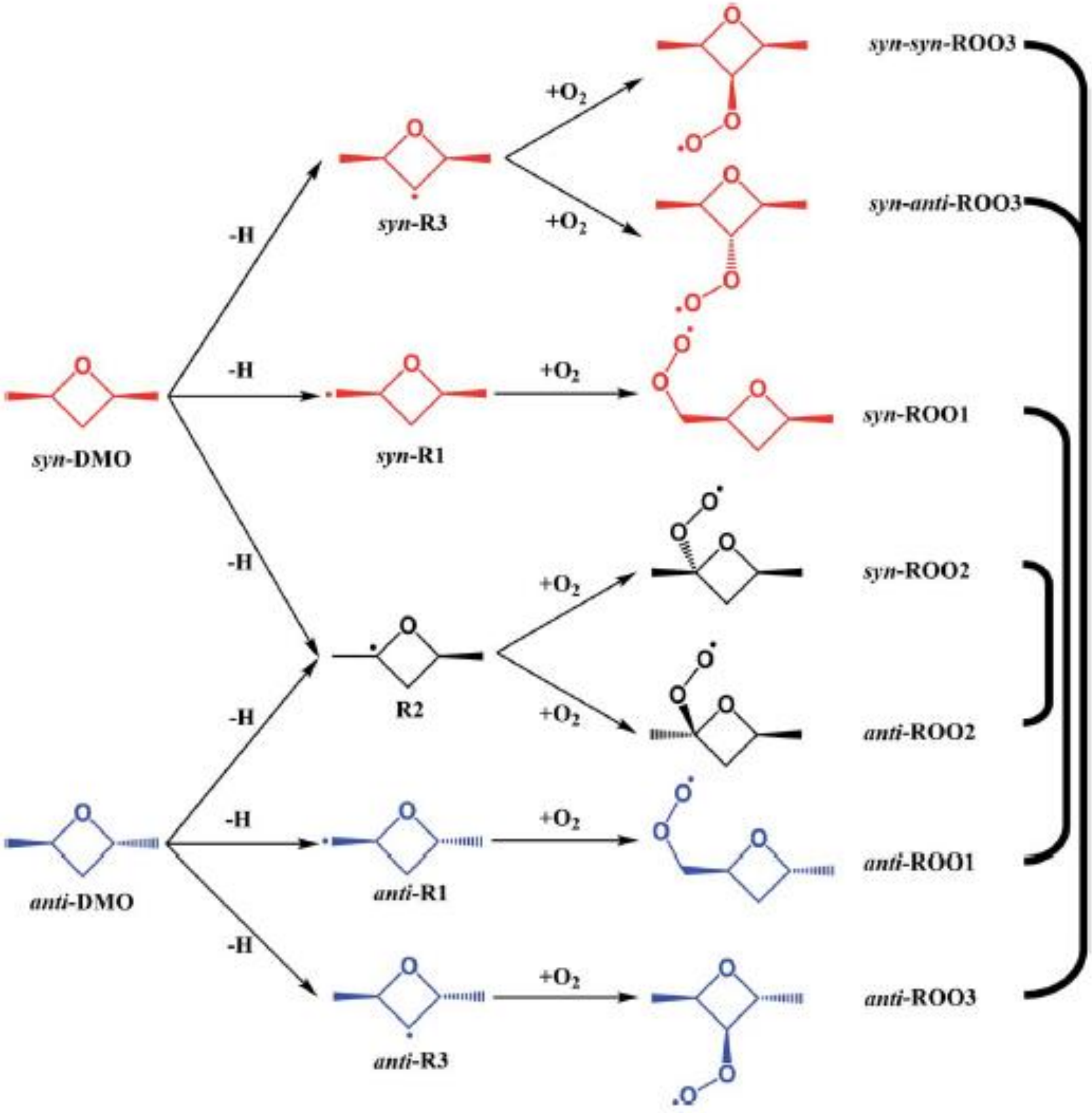

An example of the influence of stereochemistry on the lowest energy pathways: ROO2

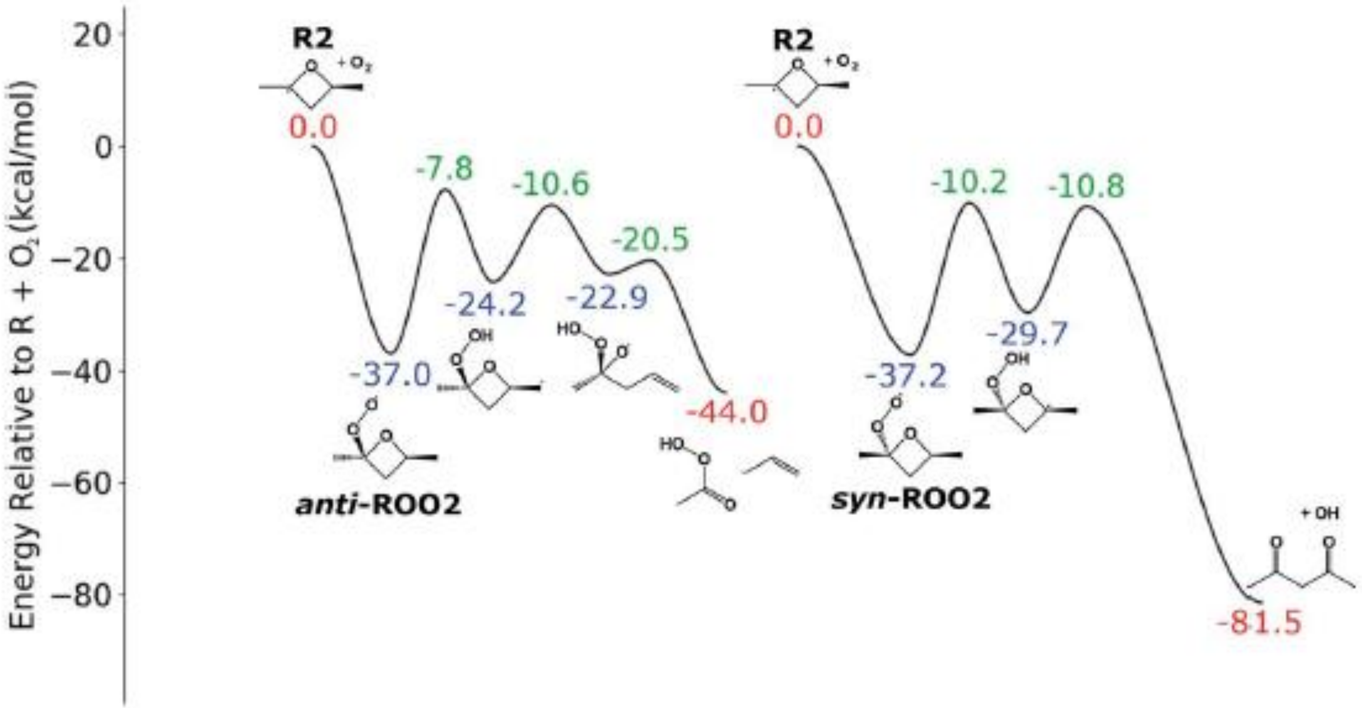

- anti-ROO2 (left): internal H-abstraction from the distal methyl group, followed by ring opening by C–O bond scission to produce a hydroperoxyalkoxy radical, which decomposes to peracetic acid and an allyl radical.
- syn-ROO2 (right): internal H-abstraction from the distal tertiary carbon, followed by simultaneous ring-opening and OH loss, giving acetylacetone

Overall product yields

- There are many more reaction pathways – rate constants for more than 4000 reactions generated.
- Direct reaction and well-skipping both important.
- Well skipping dominates for ROO1 and ROO3 and QOOH becomes unimportant, because it is bypassed.
- Complexity of the system emphasizes the importance of automatic systems like KinBot

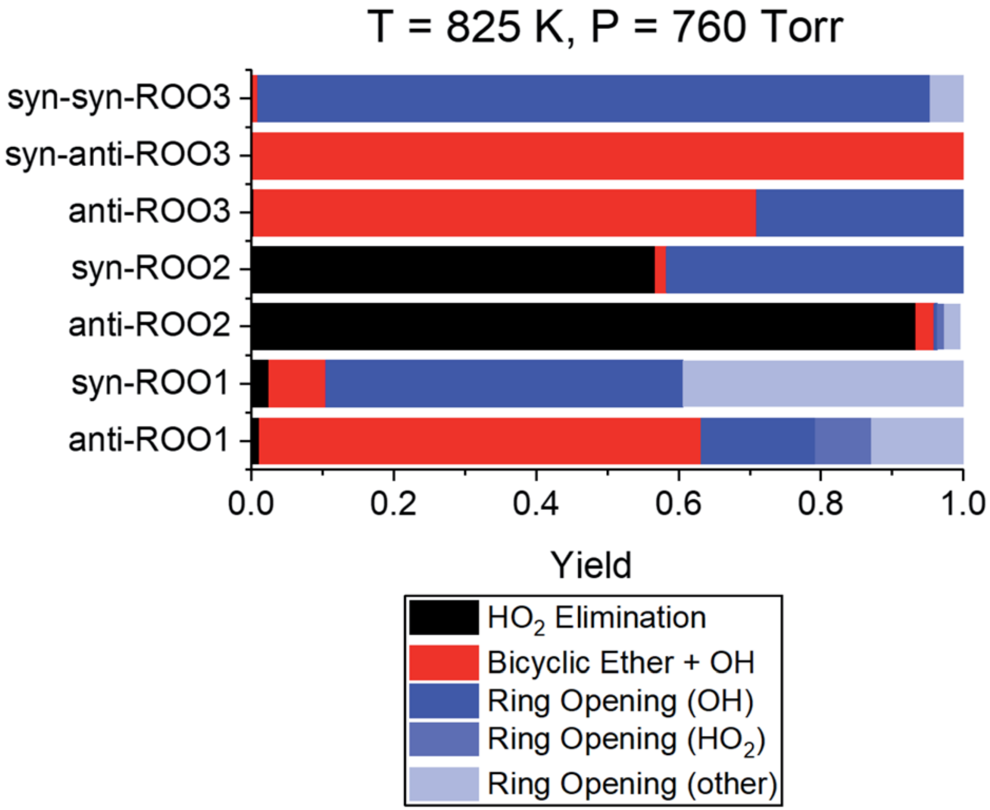

Peroxy radicals in atmospheric chemistry
Oxidation of volatile organic compounds (VOCs)

General oxidation scheme for VOCs

$O_3 + h\nu \rightarrow O^1D + O_2$

$O^1D + H_2O \rightarrow 2OH$

$OH + RH\ (+O_2) \rightarrow RO_2 + H_2O$

$RO_2 + NO \rightarrow NO_2 + RO$

$RO \rightarrow\rightarrow HO_2\ (+R'CHO)$

$HO_2 + NO \rightarrow OH + NO_2$

$NO_2 + h\nu \rightarrow NO + O;\ O + O_2 \rightarrow \boxed{O_3}$

Secondary chemistry from R'CHO photolysis

Termination: $OH + NO_2 \rightarrow HNO_3$, $HO_2/RO_2 + HO_2/RO_2 \rightarrow$ Products. The termination route depends on the NO_x: VOC ratio

OVERALL

$NO_x + VOC + \text{sunlight} \rightarrow \text{ozone}$

The same reactions can also lead to formation of secondary organic aerosol (SOA)

Free radical propagated oxidation cycle

Chain reaction:
- Radical initiation, e.g OH production from O_3
-propagation
-termination: $OH + NO_2$
$HO_2/RO_2 + HO_2/RO_2$

Dependence on:
NO_x
VOC
light

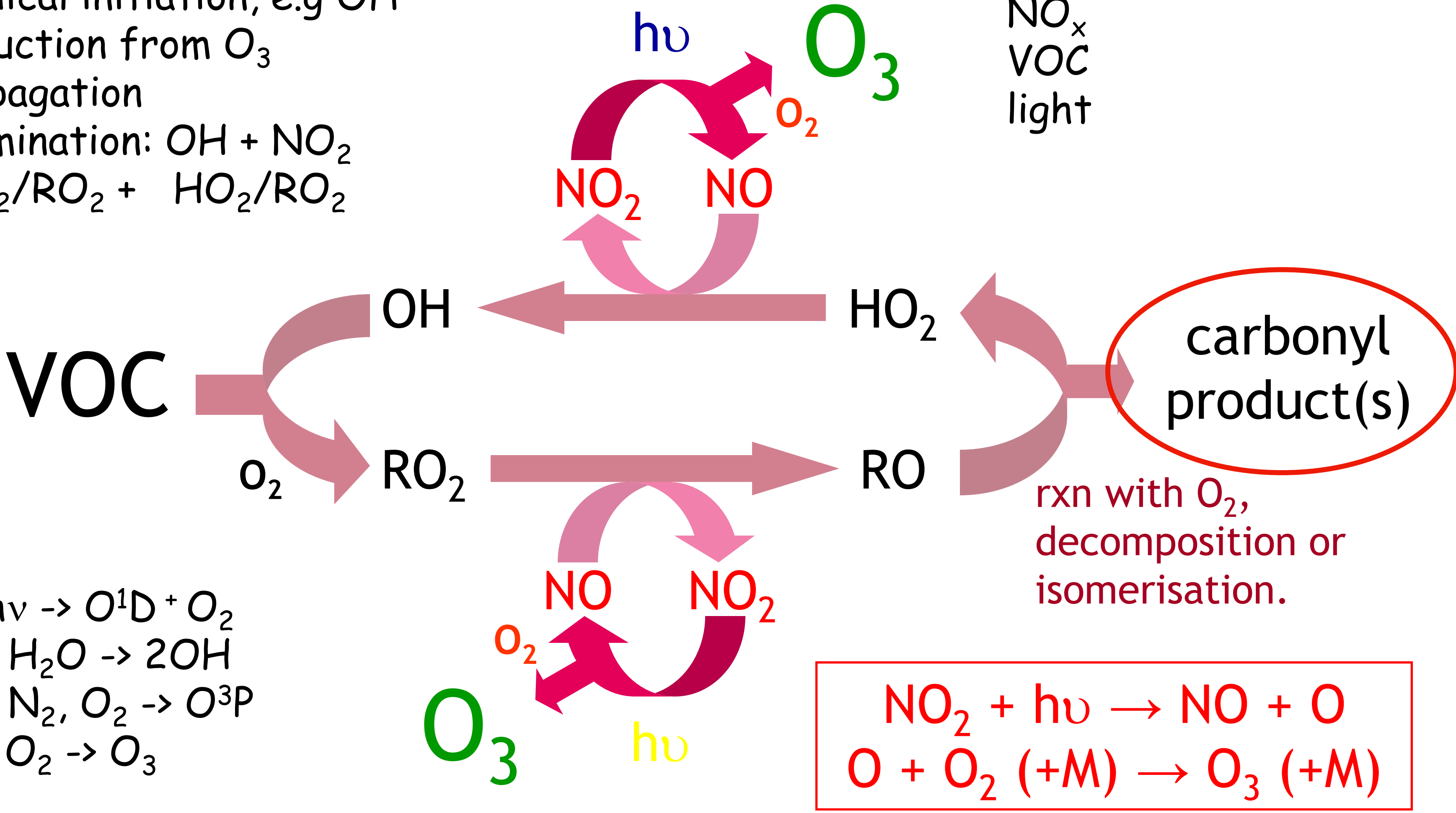

rxn with O_2, decomposition or isomerisation.

$O_3 + h\nu \rightarrow O^1D + O_2$
$O^1D + H_2O \rightarrow 2OH$
$O^1D + N_2, O_2 \rightarrow O^3P$
$O^3P + O_2 \rightarrow O_3$

$NO_2 + h\upsilon \rightarrow NO + O$
$O + O_2\ (+M) \rightarrow O_3\ (+M)$

Ozone formation from conversion of NO to NO_2

Observations incompatible with conventional mechanism

- Field measurements in the Amazon, Pearl River Delta and Borneo found much higher concentrations of OH than conventional mechanisms predict.
- Measurements were made in regions with moderate to low concentrations of NOx high concentrations of the biogenic compound isoprene, C_5H_8.

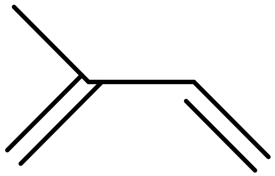

- This led to a focus on the chemistry of the peroxy radicals formed by reaction with O_2 and the radicals formed by OH addition to isoprene

Oxidation of isoprene in the atmosphere
Peeters et al

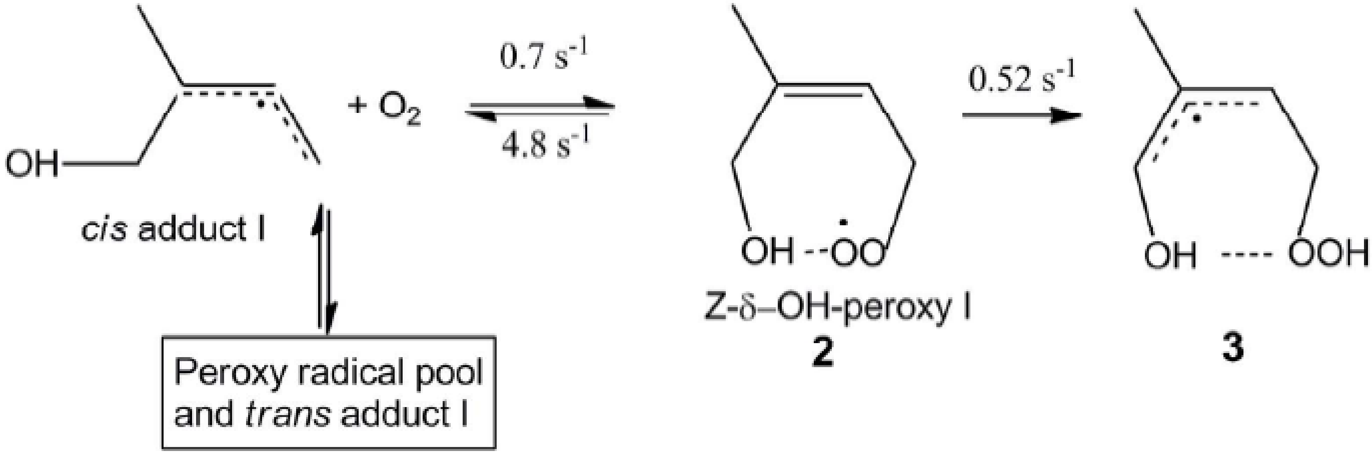

- OH adduct is an allylic radical, which is resonance stabilised. The peroxy radical formed from it is less stable than alkyl peroxy radicals (see earlier slide)
- As a result, the allylic QOOH is formed quite quickly.
- QOOH eliminates HO_2 to form $O{=}CHC(CH_3){=}CHCH_2OOH$, which is photolysed to form OH and an oxy radical

- Now let's look at the links of this type of peroxy radical chemistry to aerosol formation

Composition of aerosol around the world – large contribution from organic compounds

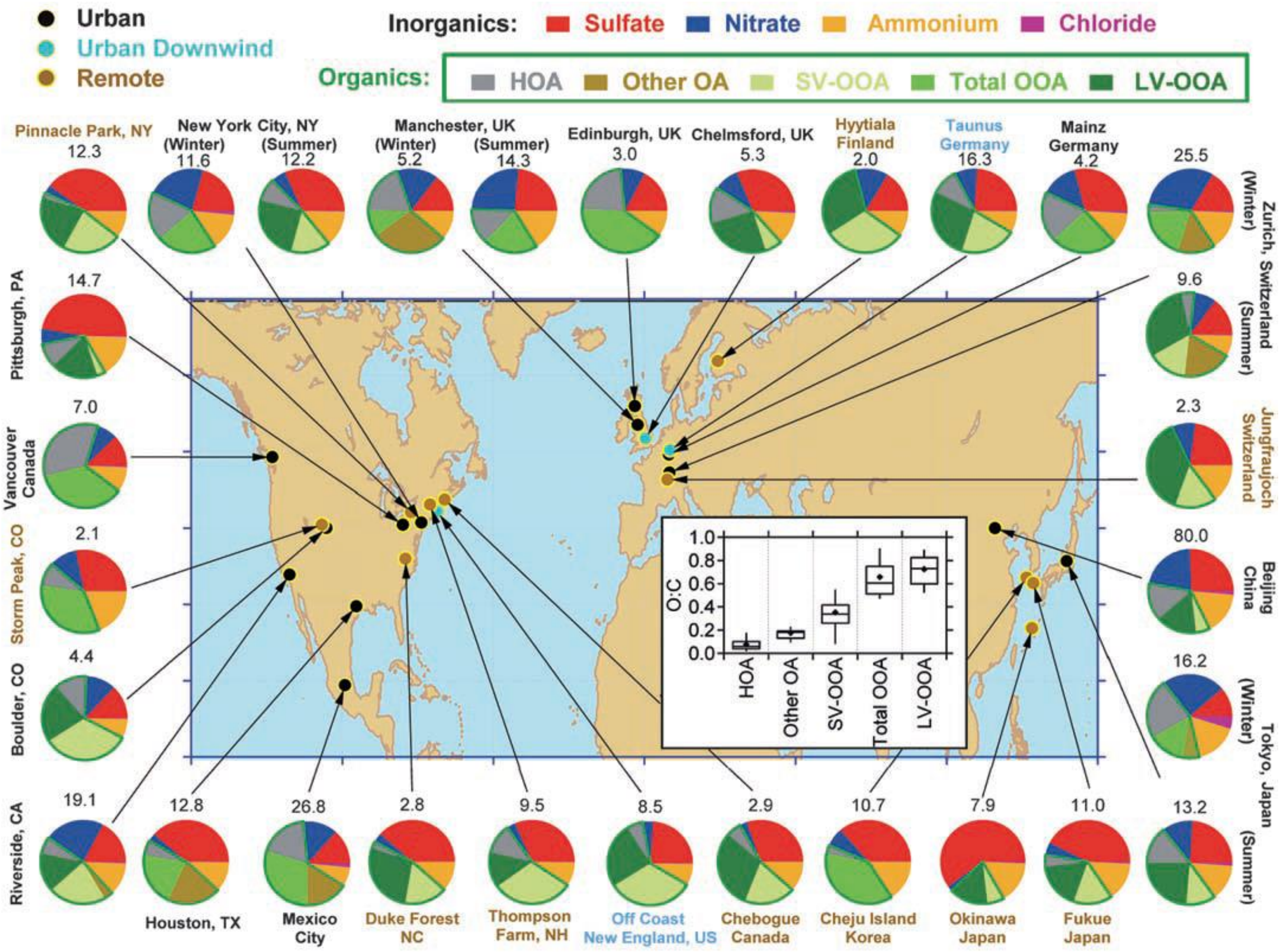

Evolution of Organic Aerosols in the Atmosphere
Route to organic aerosols

Jimenez et al, Science, 2009, 326, 1525

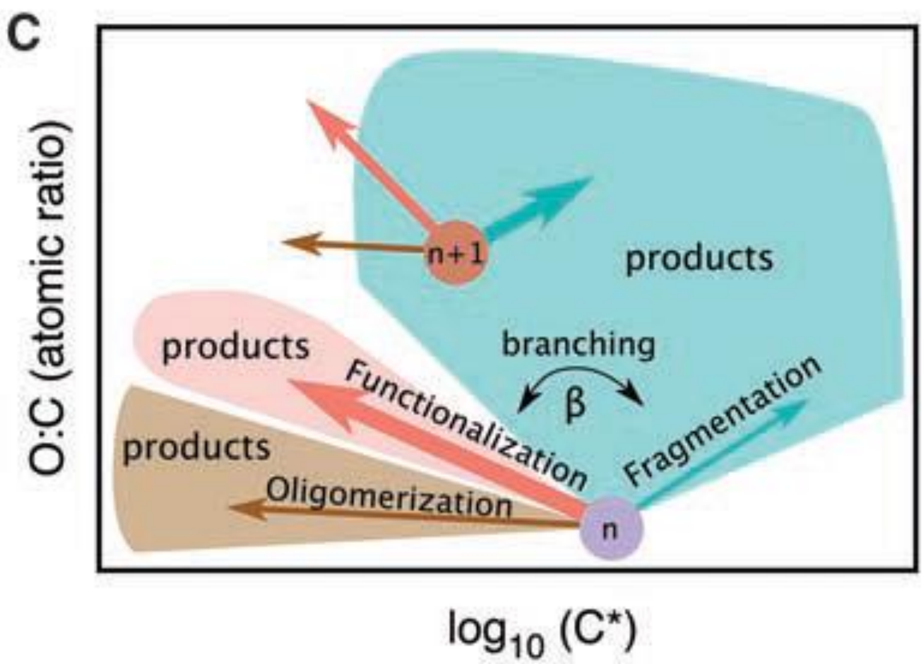

Reactions form three categories: fragmentation, functionalization, or oligomerization, based on whether the carbon number decreases, stays the same, or increases. The figure shows the first two pathways. The branching ratio (β) between these pathways is critical. Functionalization will reduce volatility considerably, whereas fragmentation can generate more-volatile species, which are less likely to partition to the OA.

Riccobono et al. Science 2014, 344, 717

- Experimental evidence that highly oxidized compounds derived from biogenic emissions play an important role, in conjunction with sulphuric acid, in the formation of new particles in the boundary layer, requiring a mechanism in which the increased functionality occurs rapidly.

Autoxidation of aromatic compounds in the atmosphere

Crounse et al, J Phys Chem Lett 2013, 4, 3513

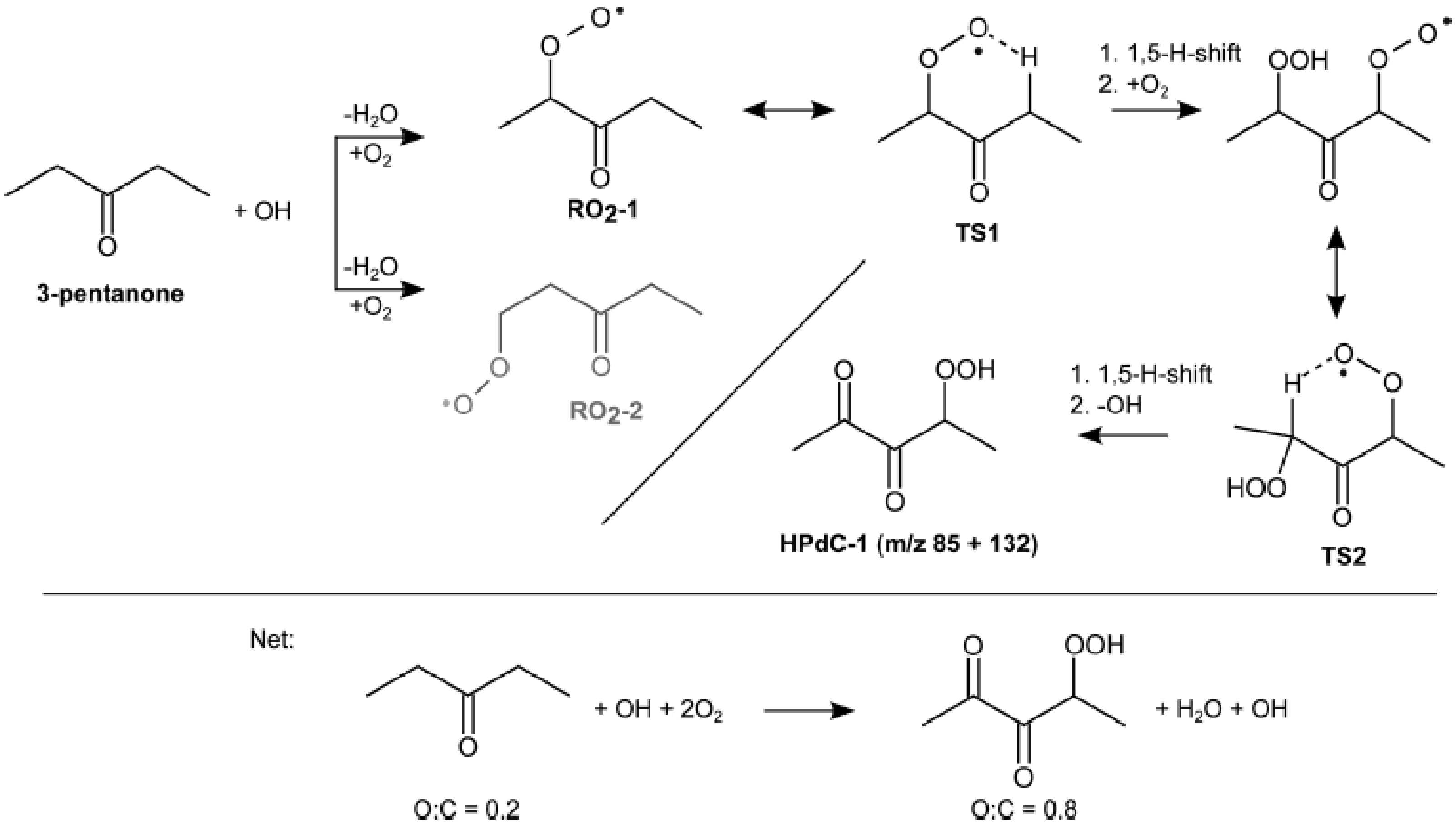

- A single cycle in the oxidation of 3-pentanone leads to a 4-fold increase in the O:C ratio
- There is strong evidence that peroxy-hydroperoxyl radical chemistry plays a key role in secondary organic aerosol production.

Topic 8

Kinetics and thermodynamics in future sustainable energy generation

Combustion in a Sustainable World: From Molecules to Processes

Klippenstein and Kohse-Höinghaus, J Phys Chem 2023, 127, 3737-3924

- Is there a role for fundamental studies of kinetics and thermodynamics in design of sustainable energy generation?
- "Increasing use of advanced experimental and theoretical methods are leading to higher accuracy descriptions of the fundamental thermodynamics and elementary reaction rate data.
- Large-scale implementations of these experimental and theoretical tools, in combination with advanced mathematical and informatics methods, are being used to efficiently obtain ever-higher-fidelity physicochemical combustion models.
- These models are proving useful in the design and investigation of appropriate testbeds for unconventional combustion and combustion-related reactive systems, which will be an important component of decisive progress toward sustainability."

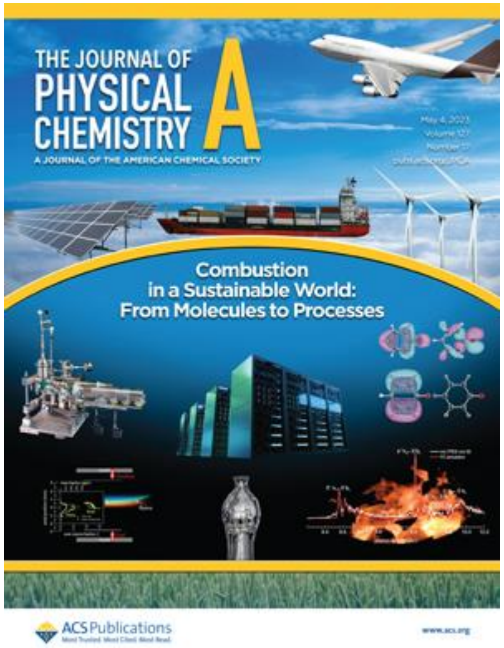

The role of chemical kinetics in future combustion strategies.

- What is the role of chemical kinetics in “Combustion in a sustainable world”, in reducing
  - Carbon dioxide emissions by using new fuels
  - Atmospheric pollutants, such as NOx, in future use of both carbon and non-carbon-based fuels
- Conditions, especially pressure, often different from traditional studies.
- Look at:
  - Sources of NO_x and mechanistic uncertainties
  - Hydrogen
  - NH_3
  - Dimethyl ether as an example of a biofuel
  - Combustion in supercritical CO_2

Formation and destruction of nitrogen oxides (NO_x) in combustion

See Glarborg et al. Progress in Energy and Combustion Science 2018, 67, 3168

NO and NO_2 are involved in the formation of ozone in the troposphere and in acid rain and particle formation. NO_2 is a pollutant with major health risks. N_2O is a greenhouse gas.

Thermal NO formation

$O + N_2 \rightarrow NO + N$

$N + OH \rightarrow NO + H$

$N + O_2 \rightarrow NO + O$

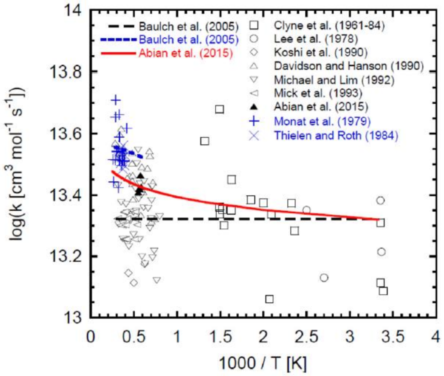

Figure shows data for N + NO, the reverse of the first reaction, which is the main source of kinetic data – require thermodynamic data to obtain k($O + N_2$)

Prompt NO formation

(CH$_n$

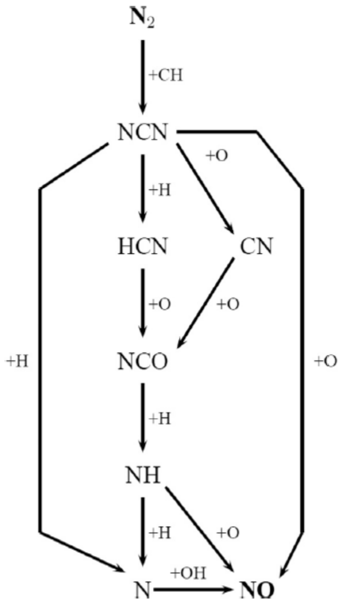

$CH + N_2 \rightarrow NCN + H$ Experiment

- Vasudevan et al. J Phys Chem, 2007, 111, 11818
- Shock tube, 1943 – 3542 K by narrow line laser absorption.
- *k* = $6.03 \times 10^{12} \exp(-11150\ K/T)\ cm^3\ mol^{-1}\ s^{-1}$, uncertainty ±25% at ~3350 K - ±35% at ~2250 K
- Demonstrated yield of NCN is close to 1 (yield of HCN + N products close to zero.
- Good agreement with earlier shock tube results by Dean et al. (Proc Comb Inst, 1990, 23, 259)

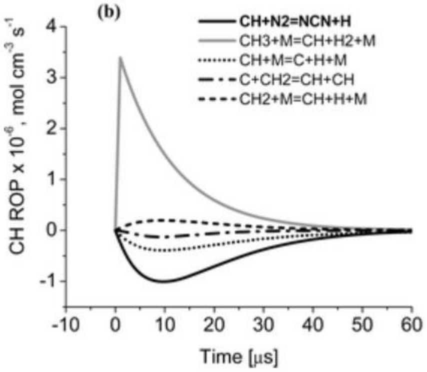

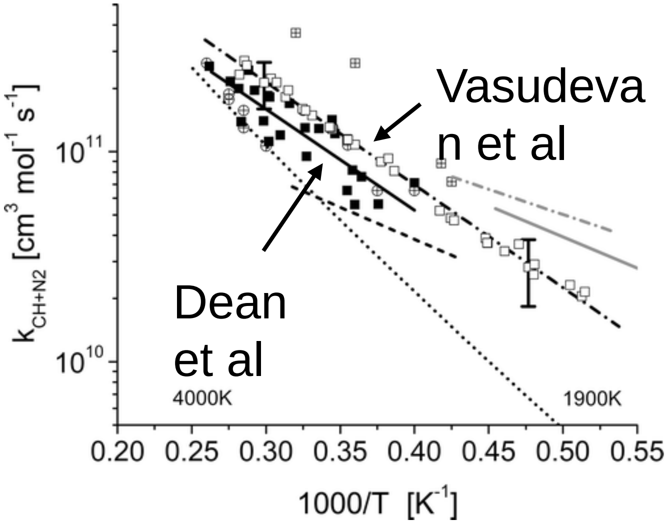

Vasudevan et al

Dean et al

CH + N_2, Theory

Klippenstein et al, Combustion and Flame 2018, 195, 3–17

- High level quantum chemistry calculations coupled with master equation.
- Thermodynamic parameters for NCN
- Kinetics – good agreement with Vasudevan et al and with earlier calculations (Harding et al,J Phys Chem A, 112, 522)
- HNCN stabilized at high pressure and should be included in high pressure combustion models.
- H + NCN – rate constant calculated. Main product CH + N2 but HCN/HNC + N becomes important at high *T*.
- Also determined rate constants and product yields for OH + NCN as a function of pressure. At high *T* the main products are HCN + NO and NCO + NH.
- Combustion modelling shows that NO formation is reduced at high pressures, partly because of stabilisation of HNCN but mainly because of reductions in the radical pool because of, e.g. methyl recombination, reducing the formation of CH

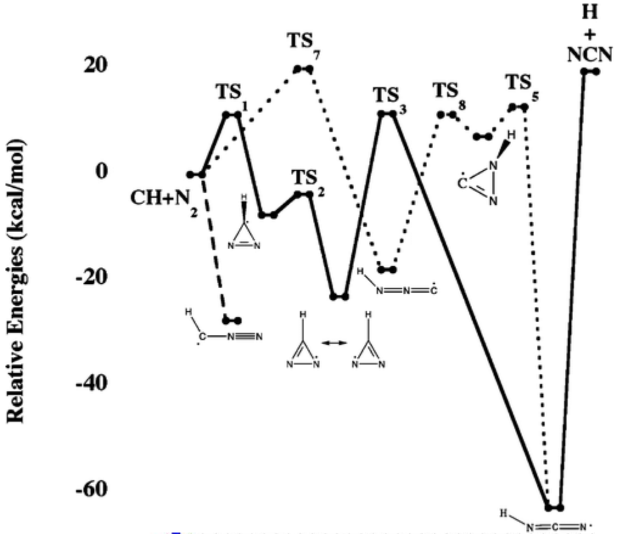

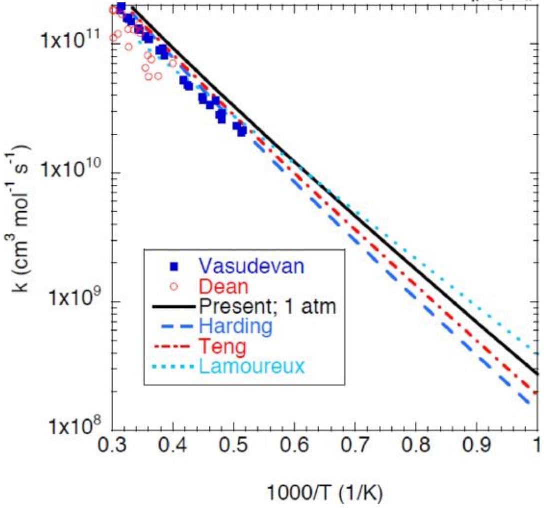

NCN + H: channel yields vs p and T

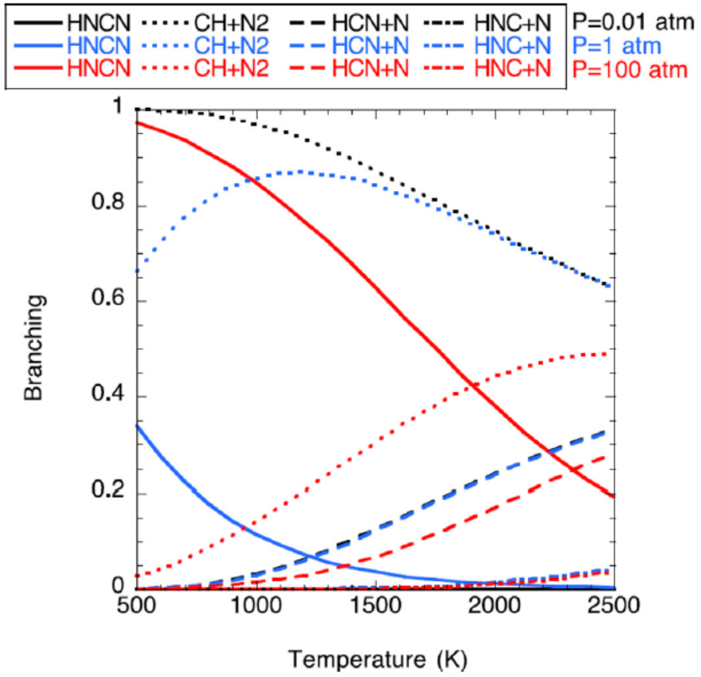

OH + NCN: PES and channel rate constants vs p and T.

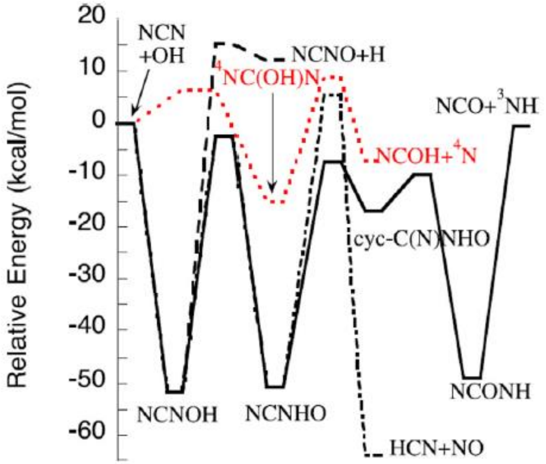

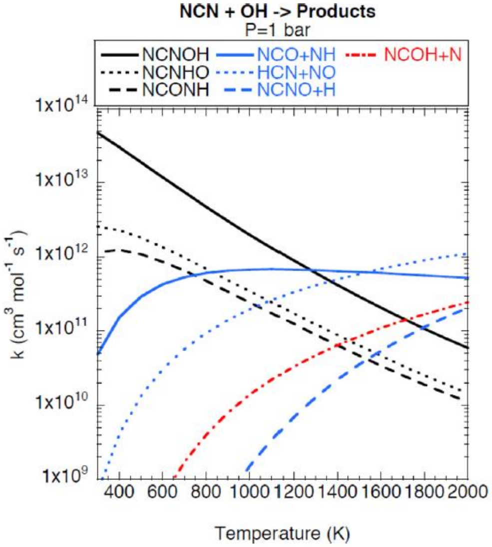

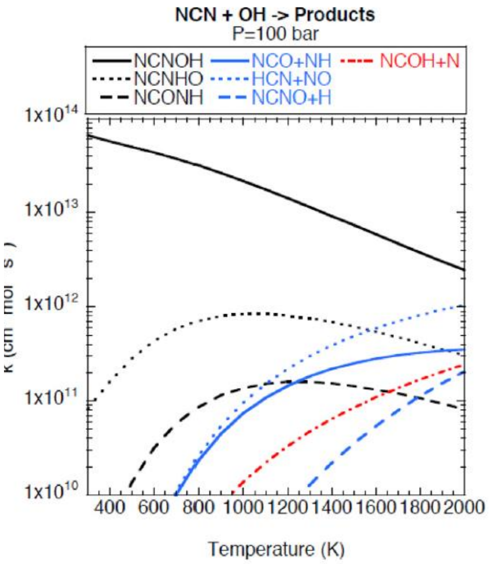

Hydrogen as a fuel

- Green Hydrogen produced from water through electrolysis. High demand for electricity from renewable sources.
- Blue Hydrogen produced from natural gas by steam-reforming but this produces CO_2 and needs carbon capture and storage
  - Pros: Novel storage methods include using hydrides and salt caverns,

  gas networks are existing infrastructure that could be used for heat provision,
  - no CO2/CO/soot emissions, low NOx strategies required.
  - Cons: Storage is a challenge, system energy density is significantly smaller than liquid and solid fuels.
- Mechanisms need to be applicable outside normal ranges. Need to minimize model uncertainty contributions from key reactions (cf Wang et al. Fuel 2022, 319 123705)
- Look at key reactions

Wang et al: A comprehensive kinetic modeling study of hydrogen combustion with uncertainty quantification (See Topic 6)

https://doi.org/10.1016/j.fuel.2022.123705

See earlier discussions of H + O_2 + M, H + O_2 and H_2O_2 + M

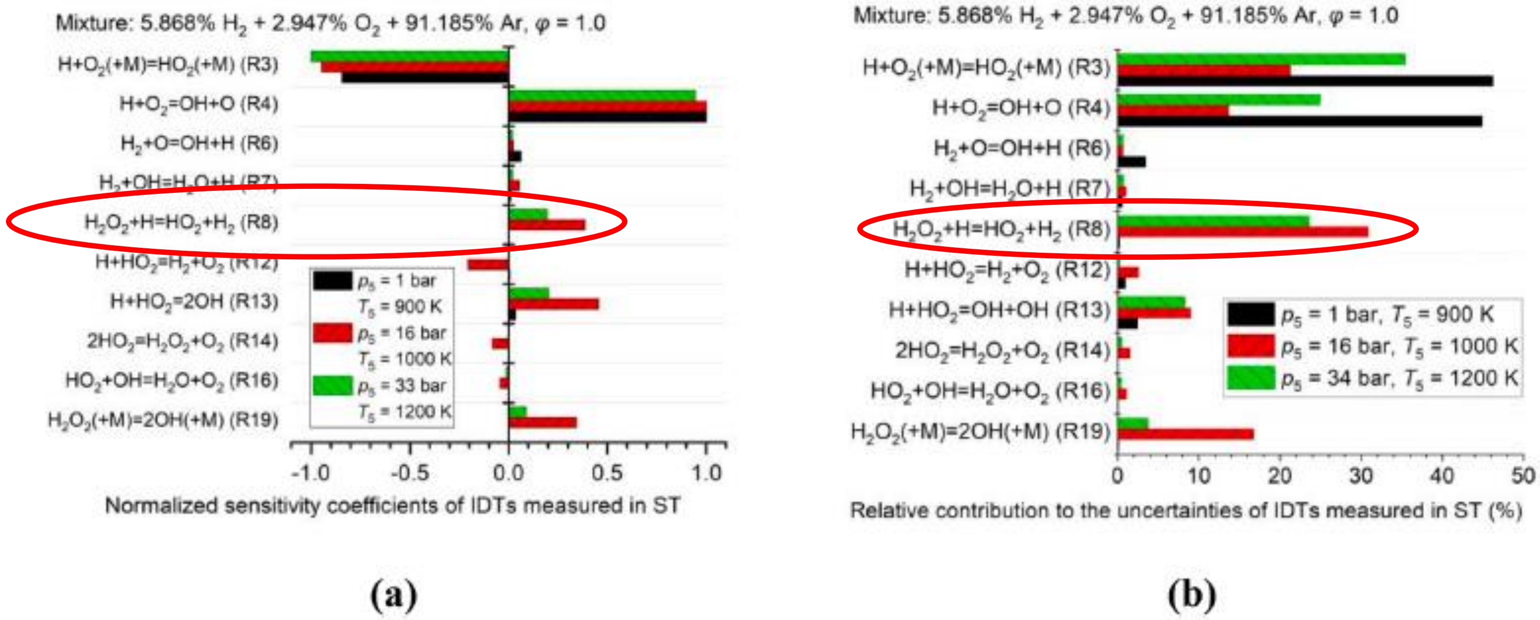

(a)Normalized sensitivity coefficients of IDTs for H2/O2/Ar mixtures;

(b) Comparison of the relative uncertainty contributions of different channels to the IDTs in shock tubes H + H_2O_2 → HO_2 + H_2 has a large contribution to the uncertainty because of a high sensitivity, but especially because the rate constant has been poorly characterized.

What reaction rate data are available for this reaction?

Evaluation of experimental rate data for $H+H_2O_2$, Baulch et al., J Phys Chem Ref Data, 2005, 34, 757

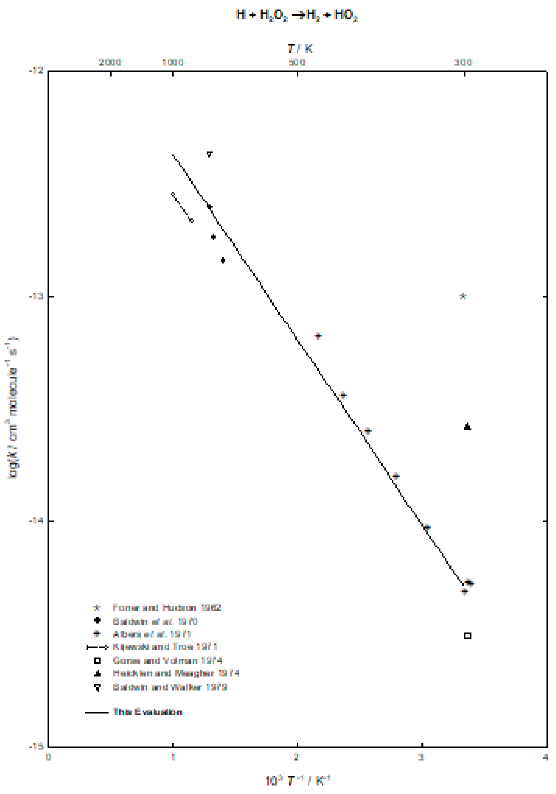

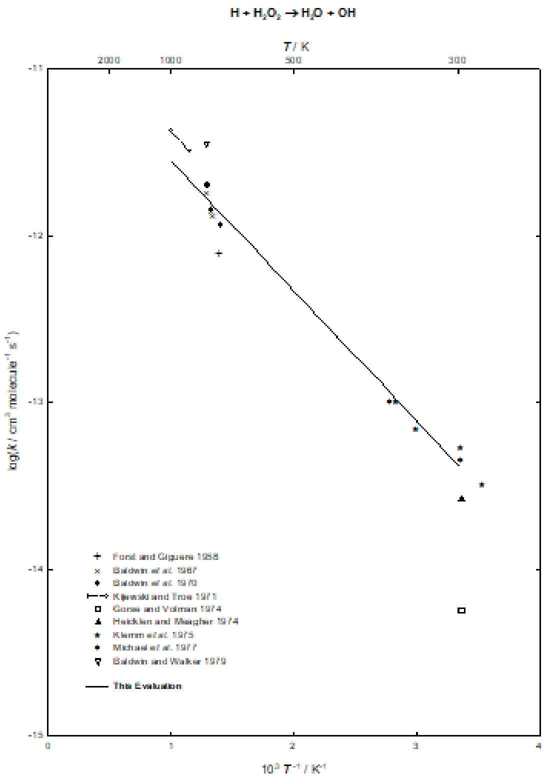

- Experimental data: 1958 – 1979. No direct measurements since then.

Evaluation gives rate constants over the range 300 - 1000 K.

Uncertainties – factor of 2 for OH channel, factor of 3 for HO_2 channel.

Turanyi et al (Combustion and Flame 162 (2015) 2059-2076) increased these uncertainties to factors of 2.5 and 4.

Recent theoretical study:
(a)$H+H_2O_2 \rightarrow H_2O+OH$; Lu et al. J Phys Chem, 2019, 123, 3969
(b)$H+H_2O_2 \rightarrow H_2+HO_2$ Lu et al. J Chem Phys, 2018, 149, 174303
No rate constant recommendations given

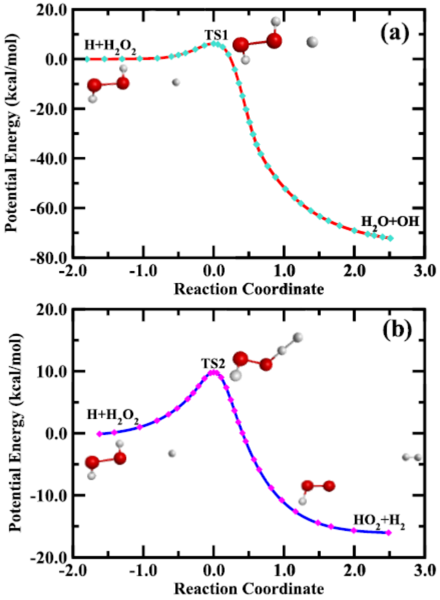

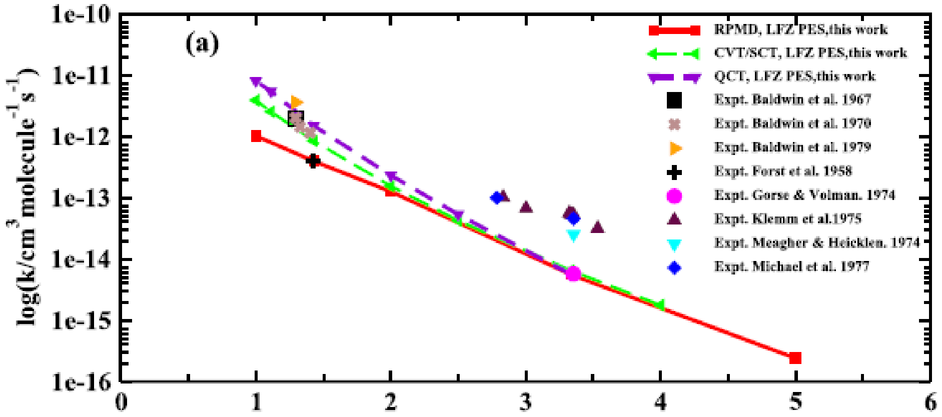

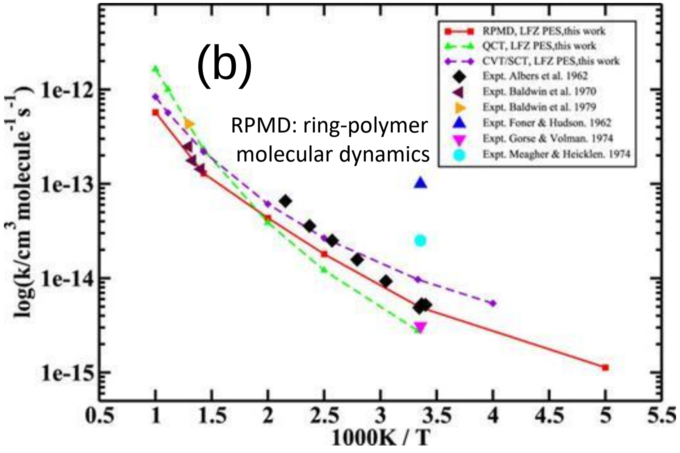

RPMD: ring-polymer molecular dynamics

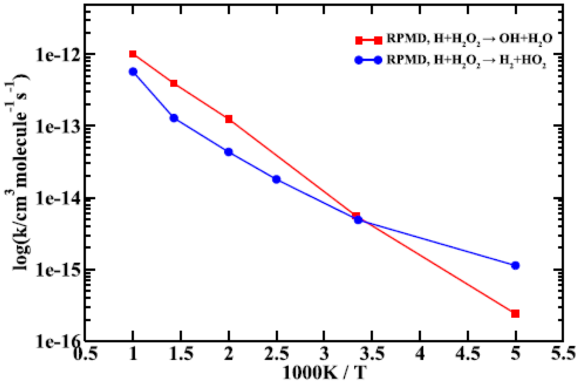

Optimization of a hydrogen combustion mechanism using both direct and indirect measurements, Varga et al, Proc Comb Inst 2015,35,589–596 (see Topic 6)

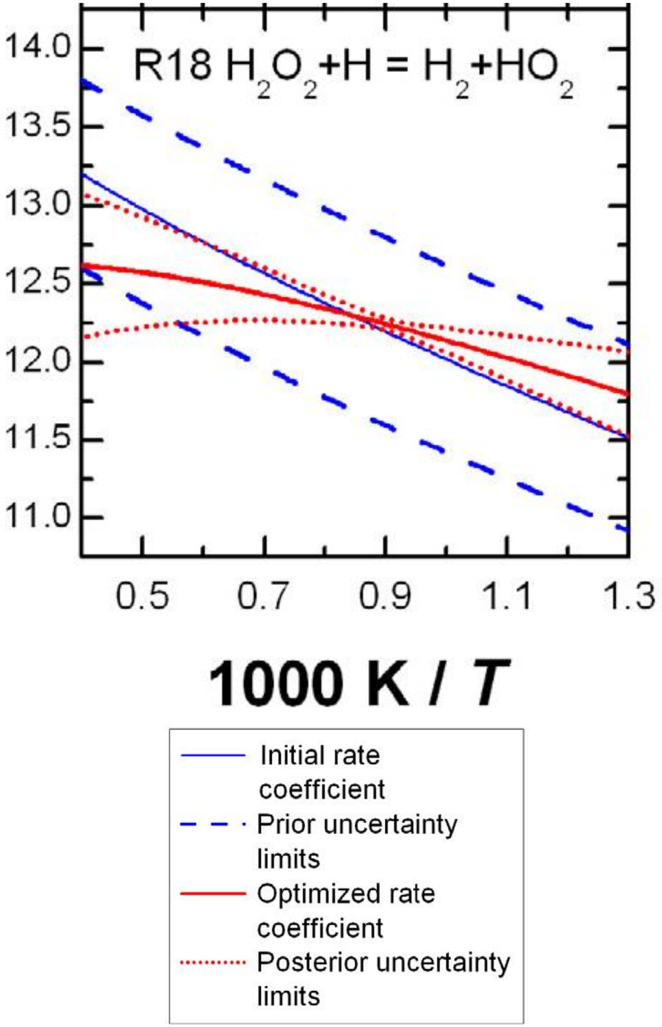

- Based on the optimization of the Keromnes mechanism against a wide range of measurements (ignition delays in shock tubes and RCM and flame velocity measurements. Wide range of temperature (800 K–2300 K), pressure (0.1 bar–65 bar)
- Results emphasise the significant decrease in uncertainty around 1000 K, where this reaction has high sensitivity, and the utility of indirect measurements in refining rate data.
- The limited availability of direct experimental and theoretical data for this reaction, and its large contribution to uncertainty, emphasise the importance of new studies on this reaction.

Ammonia

- Advantages: Economic storage and transport of H_2 remain challenging especially in countries and regions currently lacking natural gas pipelines infrastructure.
- Ammonia in liquid form at room temperature (25°C) when pressurized to 9.90 atm or temperature of −33.4°C at atmospheric pressure.
- Easier to transport and higher energy density than H_2.
- Could be used as a direct fuel or a hydrogen carrier – equipment designed for the storage and transport of propane is likely applicable also for ammonia.
- Good candidate for energy storage
- Existing industrial-scale production processes (Haber-Bosch)
- Challenges: high ignition temperature and low maximum burning velocity. Emissions. Energy costs of production.

Review on Ammonia as a Potential Fuel: From Synthesis to Economics

Valera-Medina et al Energy Fuels 2021, 35, 6964–7029

- Synthesis via Haber-Bosch process:

$$N_2 + 3H_2 \rightarrow 2NH_3 \qquad \Delta_r H^0 = -92 \text{ kJ mol}^{-1}$$

- High T (670 K) for kinetics reasons but yield decreases as T rises for thermodynamic reasons. High pressure (10-30 MPa). Catalyst, e.g. Fe_3O_4 needed.
- Hydrogen is currently produced by steam reforming

$$CH_4 + H_2O \rightarrow CO + 3H_2 \qquad \Delta_r H^0 = 206\text{kJ mol}^{-1}$$

followed by the water gas shift reaction

$$CO + H_2O \rightarrow CO_2 + H_2 \qquad \Delta_r H^0 = -41\text{kJ mol}^{-1}$$

- So the overall process is highly endothermic and requires high T (~1100 K) and pressure (2-3 MPa). Also, CO_2 is formed requiring, in the future, CCS.
- An alternative is to use H_2 from the electrolysis of water using electricity from renewable sources; the electricity demand is high.

Combustion properties of NH_3

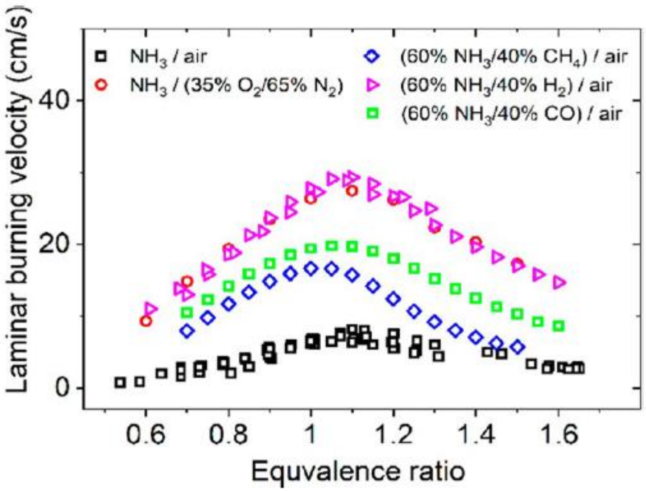

- Long ignition delay time and low laminar burning velocity compared with CH_4 and H_2, but the performance is improved by ac such fuels to NH_3.
- Several mechanisms available,
  e.g. Glarborg at al (Prog. Energy Combust. Sci. 2018, 67, 31–68,)
- The thermodynamic properties of selected key species, such as NHx, NOx, and CHx, were re-evaluated via the active thermochemical tables approach.
- Validated against a wide range of experimental data obtained in shock tubes, premixed flames, and jet-stirred reactors
- Validation should be extended to higher pressures for use in models for engines and gas turbines.

Kinetics of oxidation

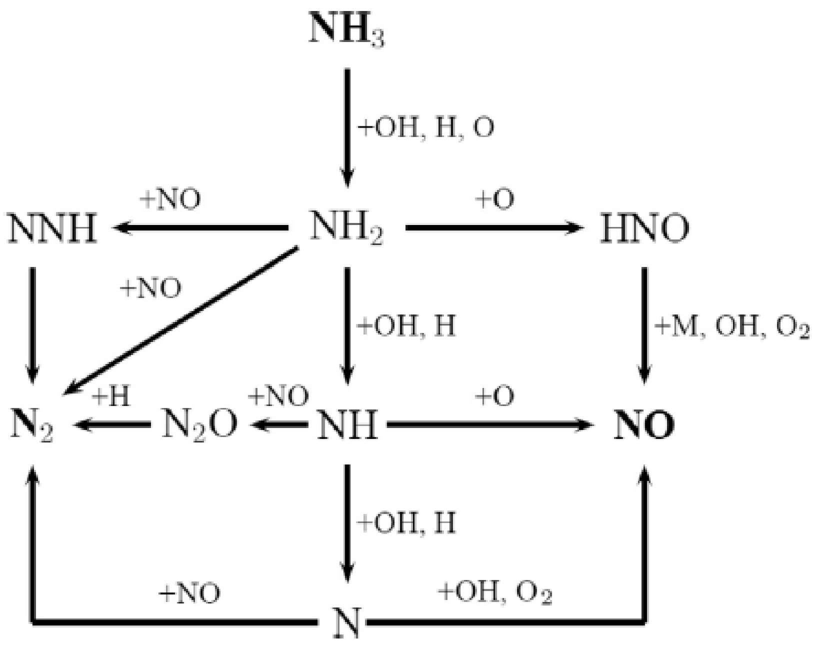

- Ammonia largely consumed by H-abstraction reactions with the radical pool (OH, H, O) – well characterised over range of conditions.
- NH_2 reacts slowly with O_2. Key reaction with NO.
- NNH + OH channel is branching, N_2 + H_2O is terminating – relative yields crucial.
- NNH is weakly bound and has a lifetime of ~1 ns; it dissociates to give N_2 + H.
- Production of NO from NNH depends on NNH + O → NO + NH competing with fast dissociation
- The same chemistry applies in the use of NH_3 in selective non-catalytic reduction (SNCR) of NO to N_2. Restricted T range: above 1100 K or too slow, below 1400 K or NO formed rather than N_2.

NH_2 + NO: Rate constant and channel yields (Glarborg et al, 2018)

$NH_2 + NO \rightarrow NNH + OH$ (a)

$\rightarrow N_2 + H_2O$ (b)

$k = k_a + k_b$

Branching ratio = $k_a/(k_a + k_b) = k_a/k$

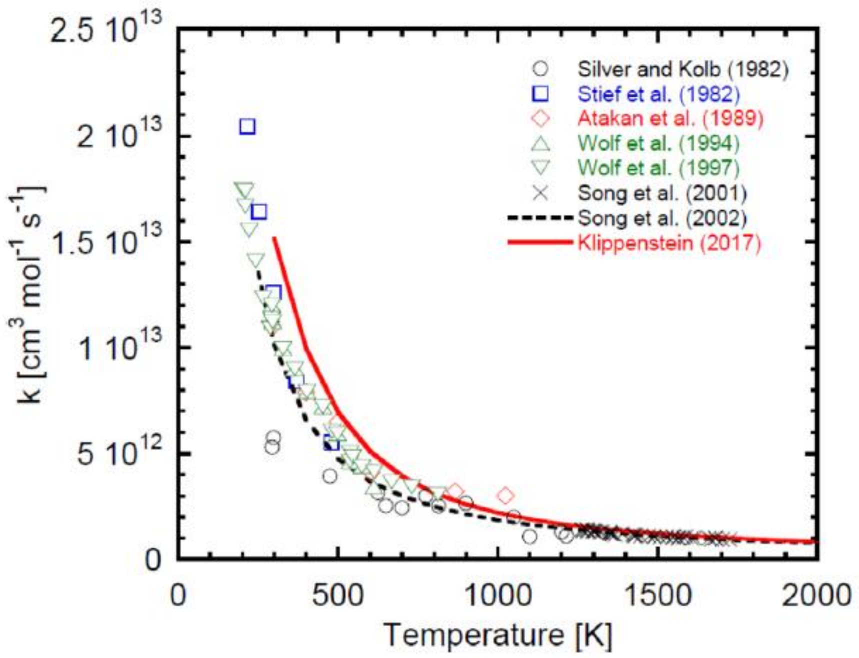

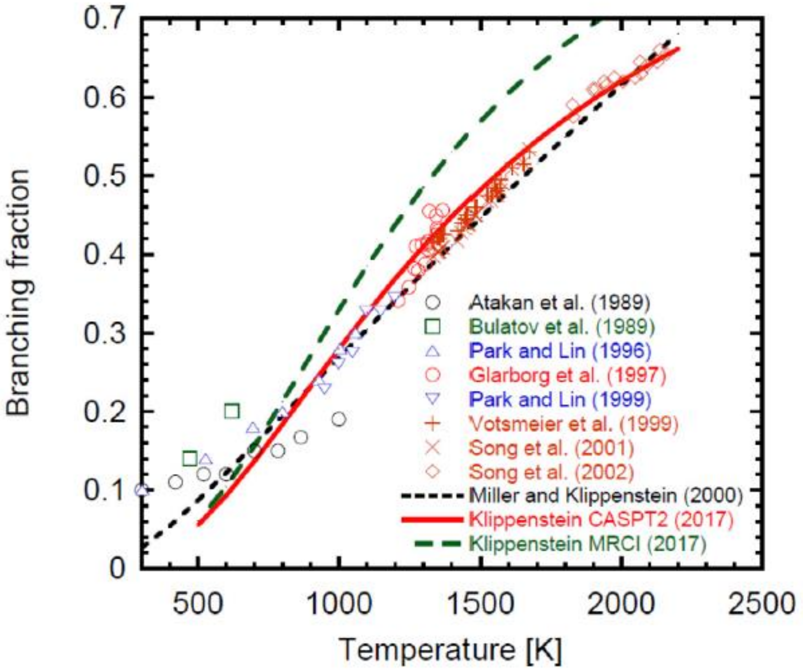

Determination of rate parameters of key N/H/O elementary reactions based on H2/O2/NOx combustion experiments

Turanyi et al Fuel 2020, 264, 116720

- Literature experimental data were collected about hydrogen-oxygen combustion systems + NO, NO_2, N_2O
- No C compounds so doesn't look at prompt NO formation.
- The data included ignition delay times, laminar burning velocities, and concentrations measured in flow reactors, JSRs and burner stabilized flames. In total, 4949 data points in 207 datasets
- 16 NOx mechanisms used; Nakamura-2017, Glarborg-2018 and Zhang-2017 mechanisms were the best
- 9 elementary reactions selected from Glarborg-2018 based on sensitivity analysis and the Arrhenius parameters (A, n, E) of these reactions were fitted the indirect experimental data and to direct experimental and theoretical determinations of the rate coefficients.
- Glarborg-2018 mechanism, modified with the optimized rate parameters, described the experimental data better than any other investigated reaction mechanism

Rate coefficient optimization

Indirect measurements coupled with modelling, sensitivity analysis and fitting gave more accurate rate parameters with lower uncertainty

New rate parameter values give a more accurate detailed mechanism (next slide)

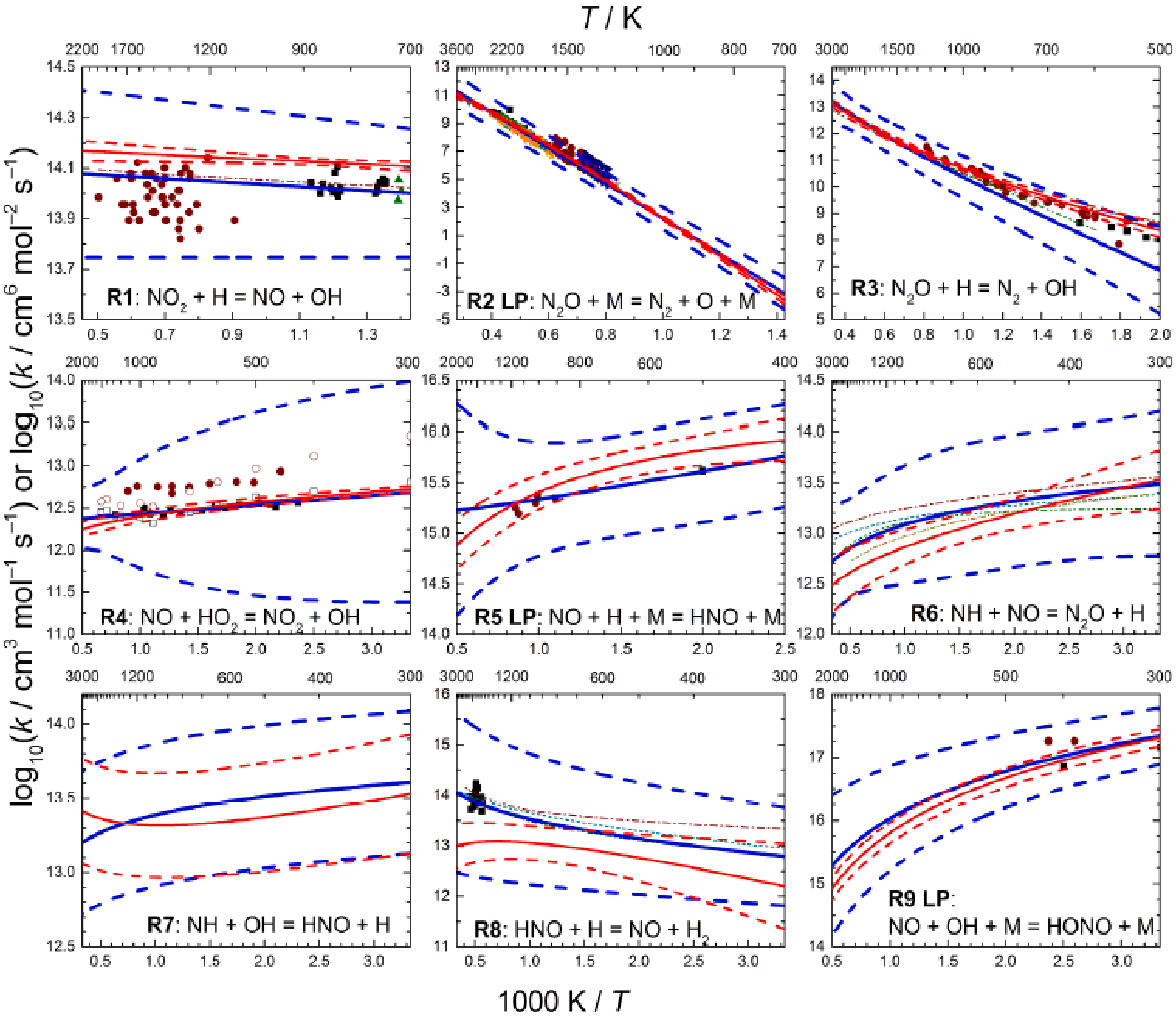

▬ Initial rate coefficient
▬ ▪ Prior uncertainty limits
▬ Optimized rate coefficient
▬ ▬ Posterior uncertainty limits

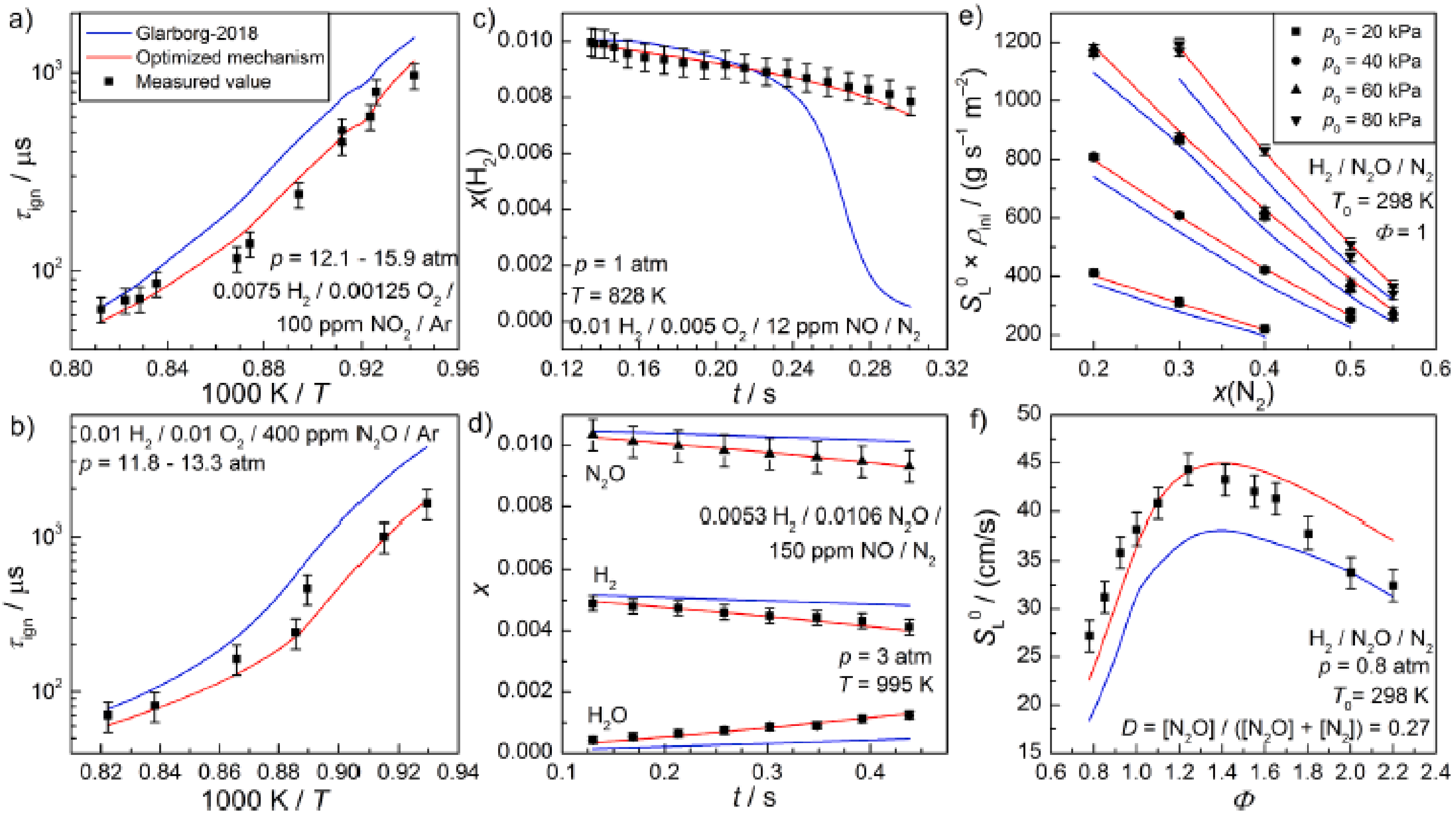

Comparison of the Glarborg-2018 mechanism and the optimized mechanism using the newly determined rate parameters. a) and b) ignition delay times c) and d) concentration profiles, e) and f) show laminar burning velocities

Biofuels

- Furans e.g. 2-methylfuran (MF),
- Long chain alcohols e.g. octanol
- Ethers (DME, DEE, DBE)
- Levulinates (esters of levulinic acid)
- Biofuel blends
- Not generally at a high technology ready level, except for DME.
- DME (CH_3OCH_3) Potential biodiesel or biodiesel component - high cetane number (≥55) and its combustion produces very low gaseous and particulate emissions.
- DME's energy density is lower than diesel, but overall engine thermal efficiency is same or higher.
- Can be produced from lignocellulosic biomass.
  - Gasification to produce syngas.
  - Syngas to methanol.
  - Dehydration of methanol. $2\ CH_3OH \rightarrow (CH_3)_2O + H_2O$.
- Can also be produced from wind- or PV-based electrolytic hydrogen and captured carbon dioxide (air capture or ethanol fermentation process) .
- Experiments and modeling for DME are in a comparatively advanced state, including details on its important low-temperature chemistry

Key Chemical Kinetic Steps in Reaction Mechanisms for Fuels from Biomass: A Perspective. Westbrook et al, Energy Fuels, 2021, 35, 15339

Low-temperature reactivity reaction pathways for hydrocarbon fuel
(a reminder - see Topic 7)

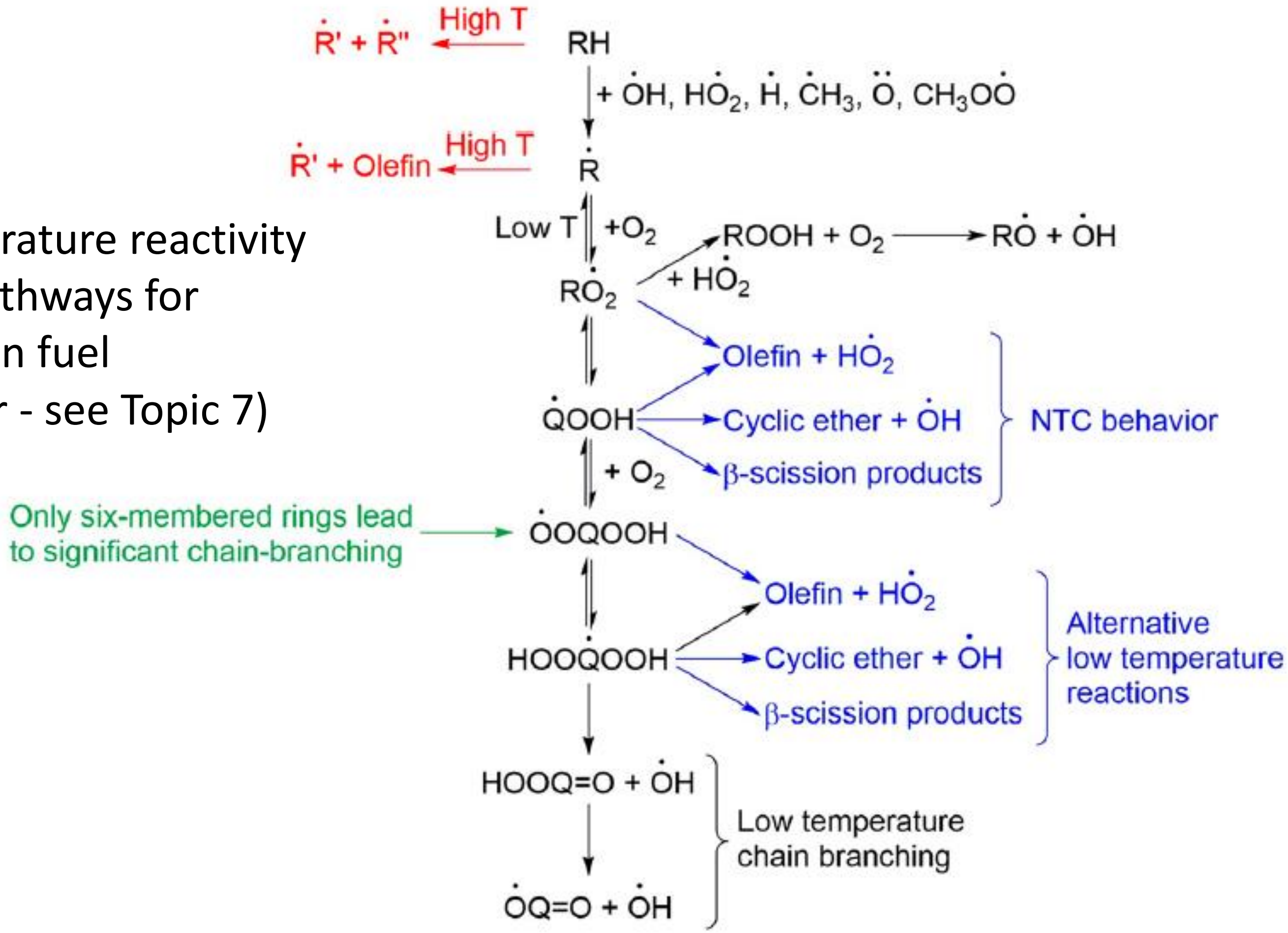

Reminder: Routes to branching: $CH_3OCH_2 + O_2$ (+ O_2)

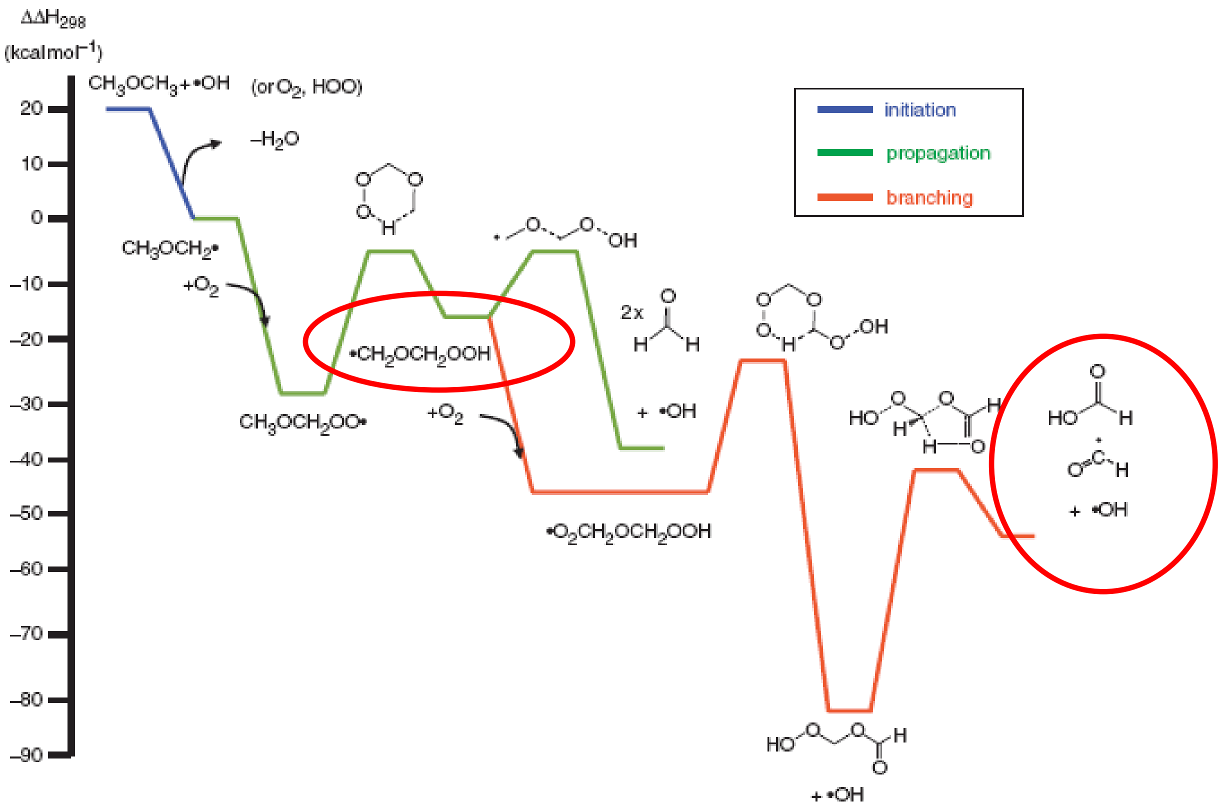

- Anderson and Carter: Molecular Physics 2008, 106, 367-396

An ignition delay and kinetic modeling study of dimethyl ether at high pressures, Burke et al, Combustion and Flame 162 (2015) 315-330

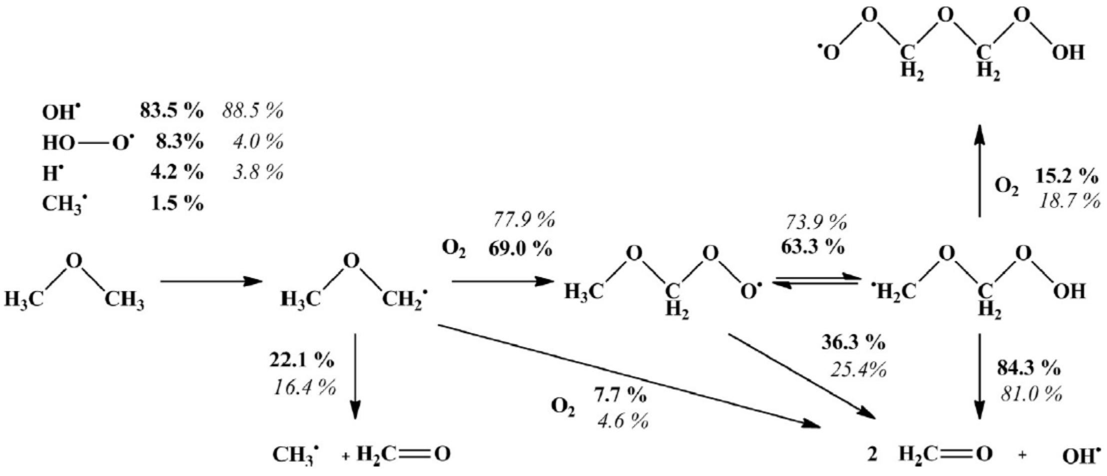

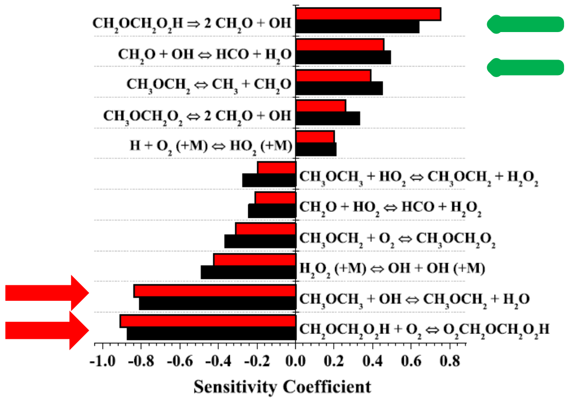

Sensitivity analysis at 827 K and ϕ = 0.50: 12.4 atm (black); 24.7 atm (red)

Flux analyses at 827 K and ϕ = 0.50, 12.4 atm – bold font, 24.7 atm – italic font

Pressure dependent rate constants in DME oxidation

Low-temperature DME reactions treated as pressure dependent.

$CH_3O\dot{C}H_2 \rightleftarrows \dot{C}H_3 + CH_2O$

$CH_3O\dot{C}H_2 + O_2 \rightleftarrows CH_3OCH_2\dot{O}_2$

$CH_3O\dot{C}H_2O_2 \rightleftharpoons \dot{C}H_2OCH_2O_2H$

$\dot{C}H_2OCH_2O_2H \rightarrow CH_2O + CH_2O + \dot{O}H$

$\dot{C}H_2OCH_2O_2H + O_2 \rightleftarrows \dot{O}_2CH_2OCH_2O_2H$

$\dot{O}_2CH_2OCH_2O_2H \rightleftharpoons HO_2CH_2OCHO + \dot{O}H$

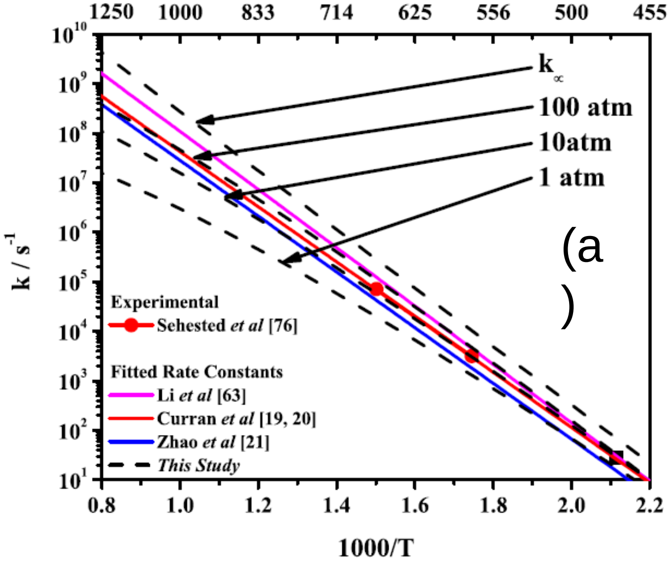

Fig. 3. Rate constants for $CH_3O\dot{C}H_2 \rightleftharpoons \dot{C}H_3 + CH_2O$.

- Burke et al, Combustion and Flame 162 (2015) 315–330
- Key reaction is CH_3OCH_2 dissociation. Pressure dependence is significant at all p. (a)
- (b) shows ignition delay times over p = 11.5 – 39.5 atm (lower τ at higher p). Full lines – full pressure dependence, other lines neglect full p dependence (see paper for details)

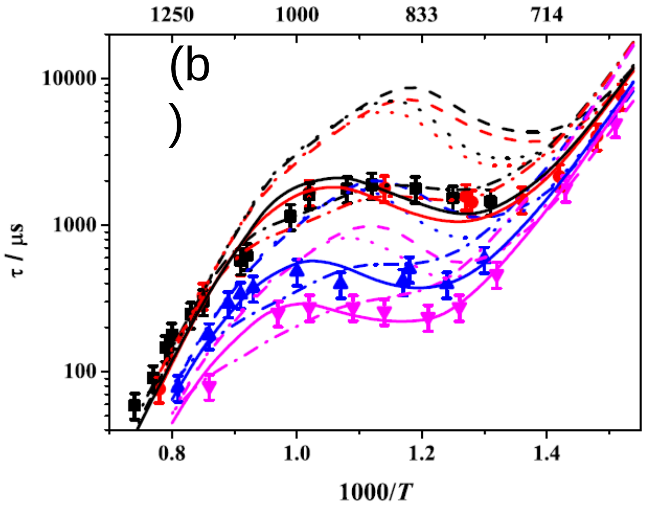

Challenges to modelling biofuels generally

- DME combustion is better characterized than other biofuels
- Mechanisms are large: far too many reactions to assemble using fundamental kinetics experiments.
- Measurements of branching fractions for abstractions are scarce. HO2 + RH particularly challenging and few exp. exist for biofuels.
- Theory becomes expensive for larger molecules, but increasingly feasible
- Thermochemistry for radicals QOOH, RO2, O2QQOH are central to the mechanisms
- Estimates of rate constants essential but rate rules and structure-activity relationships were originally developed for alkanes.
- Different functional groups not always present (or well supported by data) in automatic mechanism generators.
- Wide range of experiments required for validation and for improving mechanisms – but needs to be done quickly

A comparison of GHG emissions from a range of fuels

(Al Breiki Journal of Cleaner Production 279 (2021) 123481)

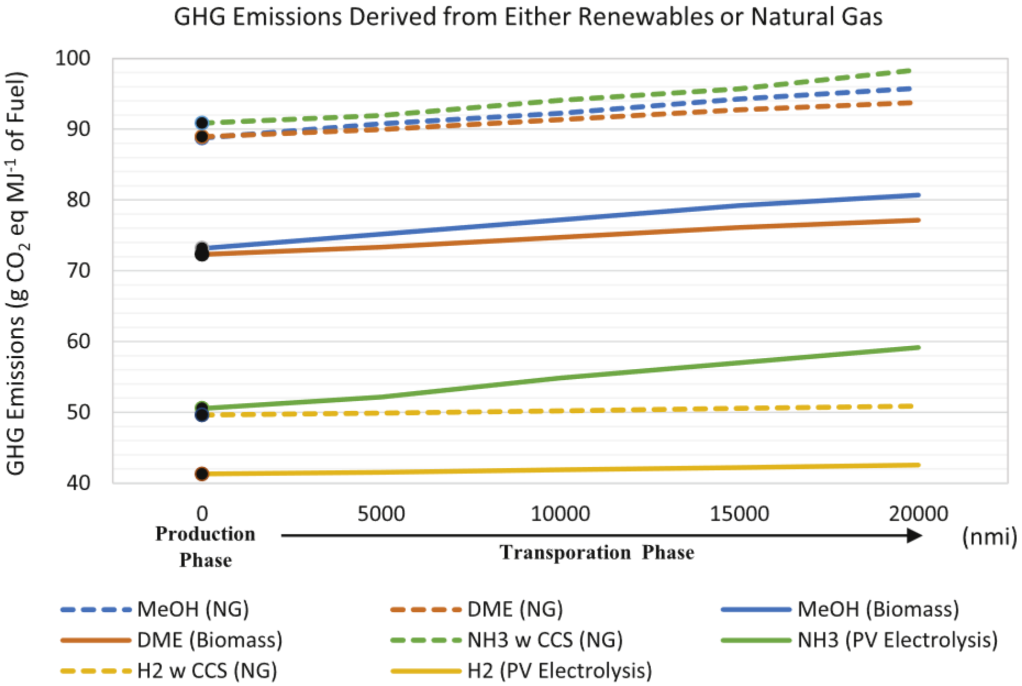

Shows the total GHG emissions from production, transportant (vs distance transported by ship in nautical miles) and utilization. Emissions for DME shown for production from natural gas and from biomass. NH_3 is shown with hydrogen formed from natural gas, with CCS, and with hydrogen formed by electrolysis with electricity from photovoltaics.

Hydrogen and Methane Combustion in high pressure Supercritical CO_2

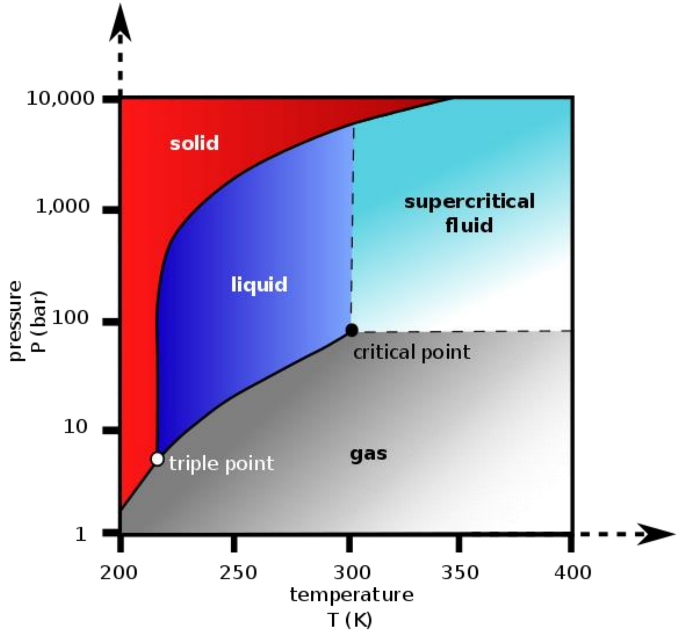

- Critical point for CO2:

  304 K

  74 bar

- Oxy-fuel combustion (no nitrogen), high CO_2 dilution - combustion products mainly to CO2 and H2O, which can be recirculated into the feed.
- Can eliminate CO_2 emissions to the atmosphere. No NOx emissions
- Potential of higher overall efficiency and downsizing in equipment size because of the higher energy density of sCO2 fluids.
- Typical turbine inlet temperature:

  1400 K

  300 bar

Netpower uses Allam-Fetvedt sCO2 cycle.

Energy Procedia 37 (2013) 1135 – 1149; https://netpower.com/

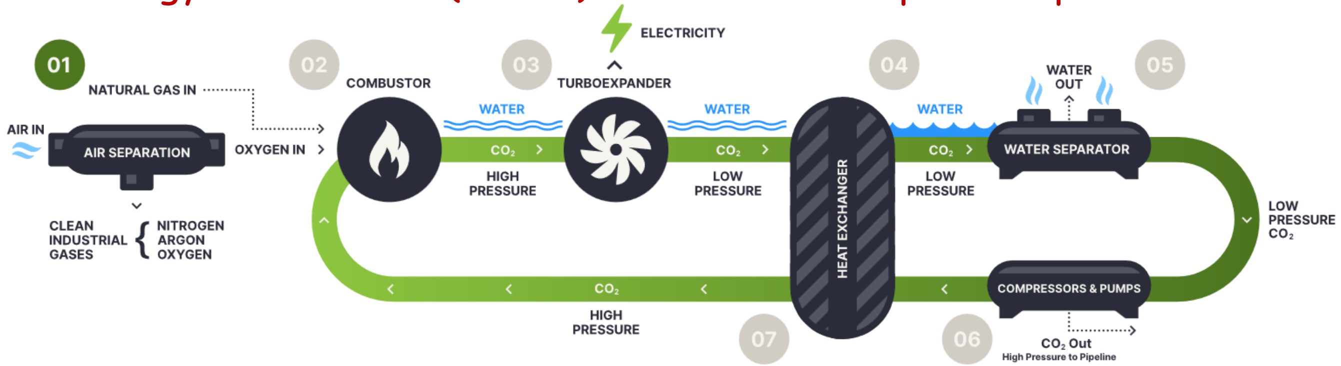

1. Air separated into components (N_2, O_2, Ar)
2. Natural gas and O_2 combust giving CO_2 and H_2O (No NOx)
3. Mixture expands and turns turboexpander to generate electricity
4. Mixture enters heat exchanger to cool.
5. Water removed from CO_2
6. CO_2 repressurized; captured CO_2 exported for storage or commercial use
7. Recirculated CO_2 reheated to be used in process again

~300 MW power stations, based on this methodology, under construction in USA and UK

High pressure combustion mechanisms

- Shao et al. (Proc Comb Inst. 37 (2019) 4555-4562). Ignition delay times of methane and hydrogen highly diluted in carbon dioxide at high pressures up to 300 atm
- Monitored OH emission. 1045 – 1578 K; 27 – 286 atm (CH4); 37 – 311 atm (H2)

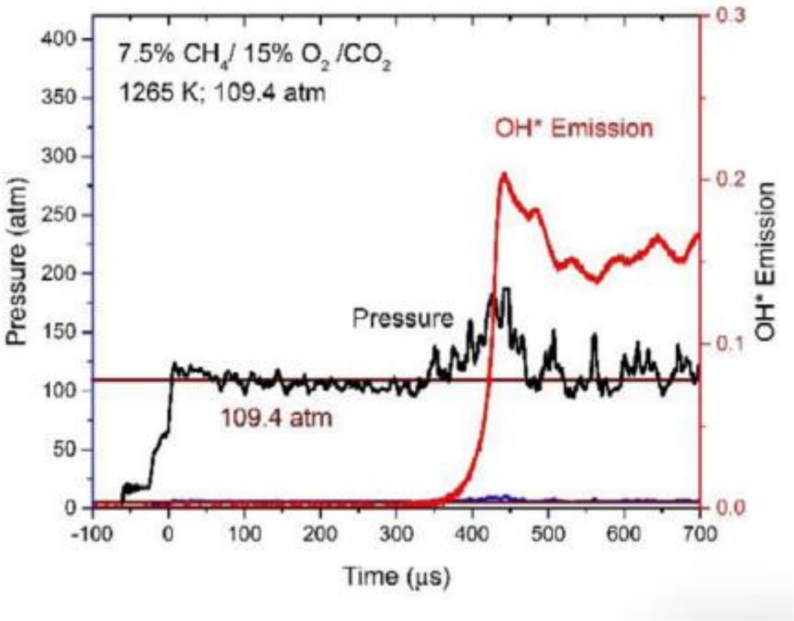

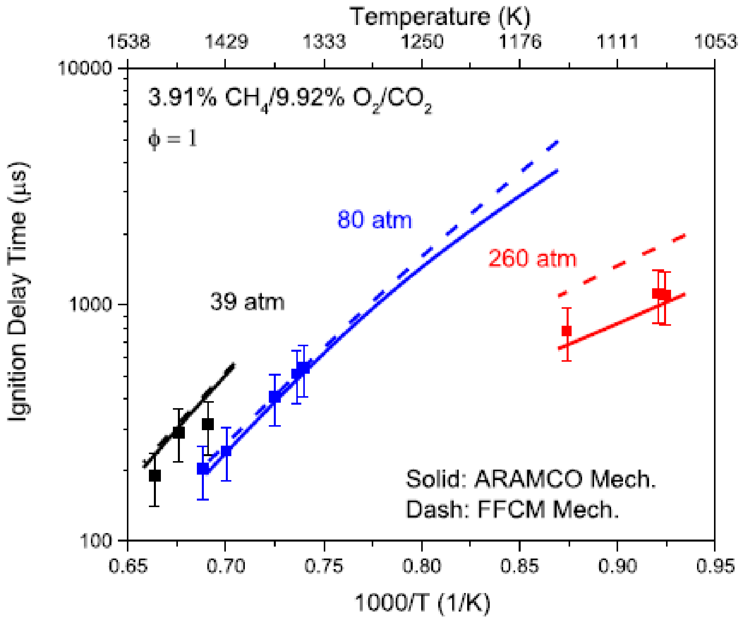

SYNGAS: Shock tube ignition delay times in high pressure CO_2

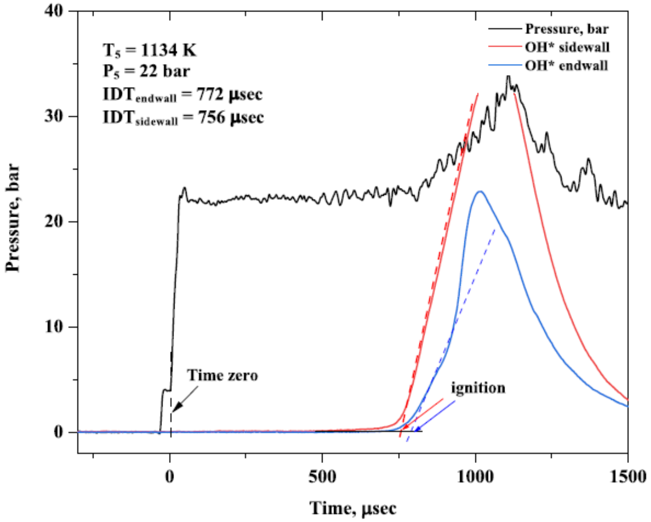

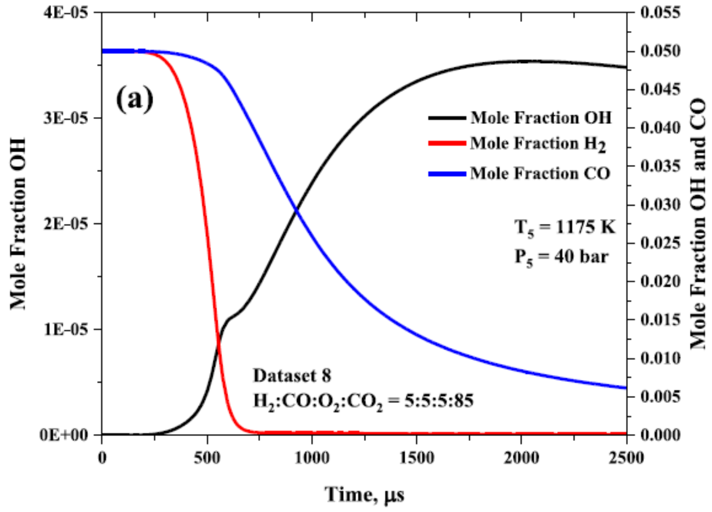

- Shock Tube, KAUST; mechanism, Sheffield (Energy 2022, 255, 124490).
- Two phases of OH formation.
- Importance of $H + CO_2 \rightarrow OH + CO$ in high pressure CO_2
- Normally, OH + CO is the dominant reaction, but the reverse can become important under high $[CO_2]$ conditions
- Harman-Thomas et al. Fuel, 2023, 342, 127685

Key reactions at 1200 K, 110 atm for methane combustion

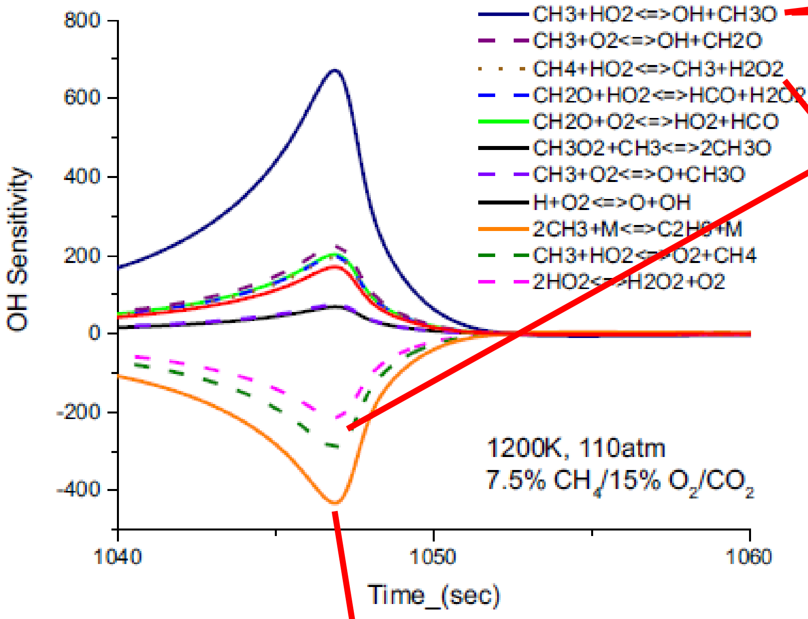

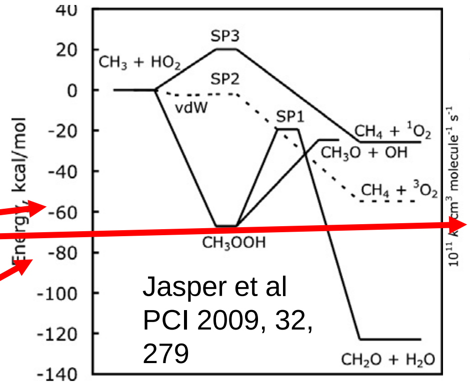

Jasper et al
PCI 2009, 32,
279

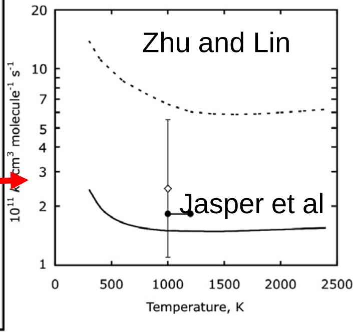

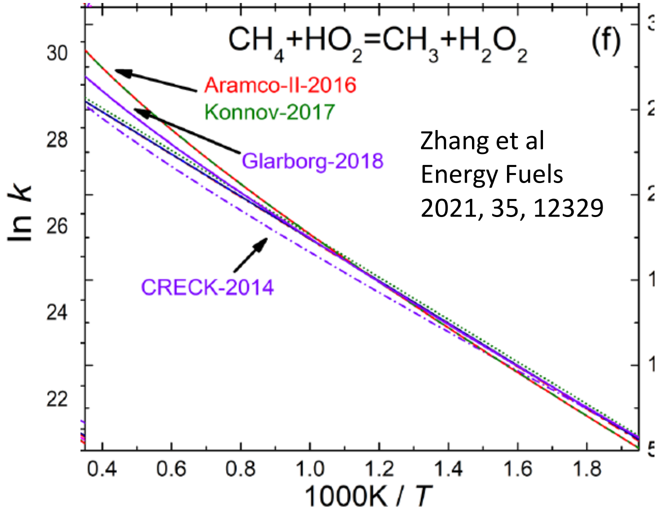

Zhang et al
Energy Fuels
2021, 35, 12329

OH sensitivity FFCM (Wang et al)
$2CH_3$ + M – p dependence
important

Comparison of sensitivities for two mechanisms, methane, 1100 K, 110, 250 atm

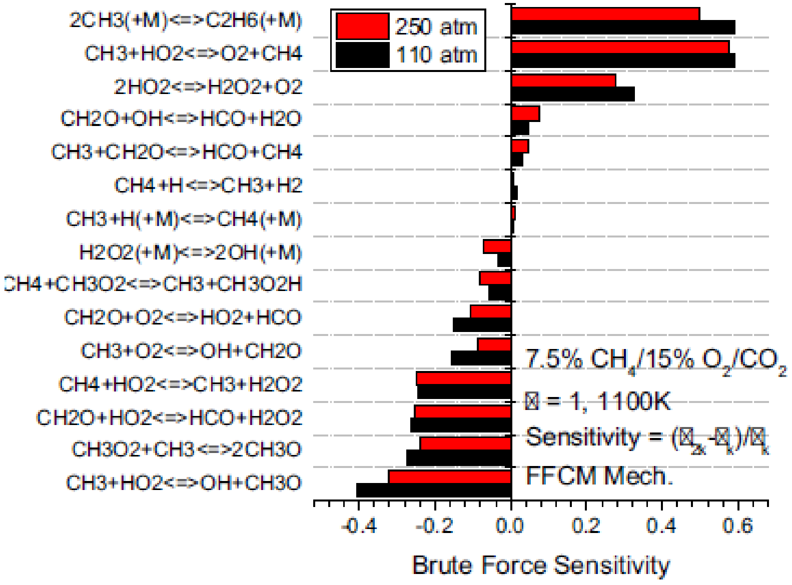

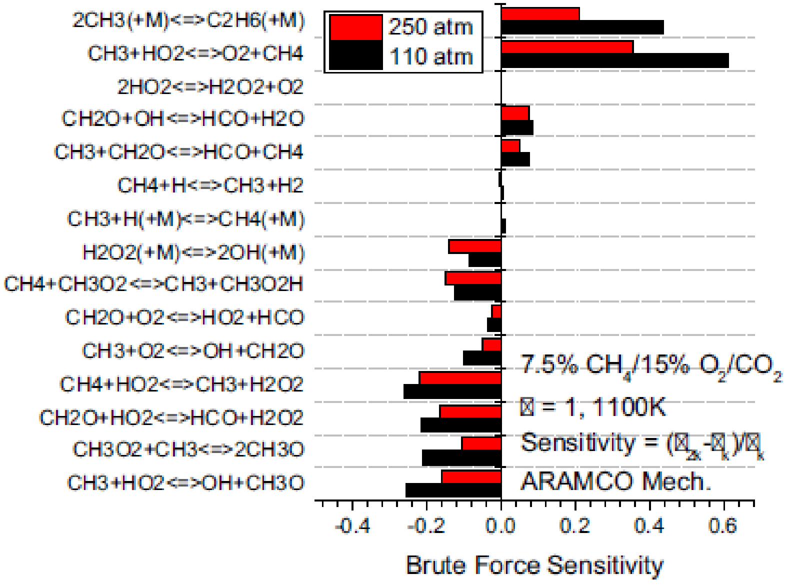

Compare
CH_3 + CH_3, vs CH_3 + HO_2
HO_2 + HO_2

Some concluding remarks

- Chemical kinetics – rate constants as a function of T and, if appropriate, p form central components of chemical mechanisms for use in combustion modelling.
- Experiment was once the main source of such data and remains a key source.
- There have been dramatic developments in the accuracy of theories of rate constants and channel yields and theory is now a key component, sometimes in conjunction with experiment, sometimes as the sole source of data.
- Chemical mechanism construction has also advanced substantially, both for manual and for automatic generation. Evaluation against measurements of combustion systems is essential.
- The combination of chemical mechanisms and combustion measurements enables statistically-based refinement of rate data for elementary reactions and can lead to substantial improvements in the quality of the fits. This approach provides a big improvement over manual tuning of rate data.

清华大学燃烧能源中心
Center for Combustion Energy